"PROGRAM Thales – University of the Aegean – Determination of the Sources and the Physicochemical Properties of Fine and Ultrafine Particulate Matter (Aerosol) that affect the Climate of Greece"

ΠΡΑΞΗ «Θαλής - Πανεπιστήμιο Αιγαίου - Προσδιορισμός των Πηγών και των Φυσικοχημικών Ιδιοτήτων των Λεπτοκόκκων και Υπερλεπτοκόκκων Αιωρούμενων Σωματιδίων του Ατμοσφαιρικού Αερολύματος που επηρεάζουν το κλίμα της Ελλάδας»

FINAL REPORT
ΤΕΛΙΚΗ ΕΚΘΕΣΗ

European Union
European Social Fund
OPERATIONAL PROGRAMME
EDUCATION AND LIFELONG LEARNING
investing in knowledge society
MINISTRY OF EDUCATION & RELIGIOUS AFFAIRS
MANAGING AUTHORITY
NSRF 2007-2013
EUROPEAN SOCIAL FUND
Co-financed by Greece and the European Union

INTRODUCTION

The purpose of the project is to identify and determine the sources and physicochemical processes through which the particulate matter (PM) produced / found in major cities of Greece and the Aegean region affect the climate. The aims of the project are:

1. The creation of a continuous network monitoring basic physicochemical properties using plethora of 'state of the art' instruments.
2. The identification of sources, concentrations and size of suspended particles in two large cities of Greece (Athens and Patras) and the Aegean (Crete).
3. The assessment of the chemical composition of particulate matter, and how it changes during its stay in the atmosphere (AMS measurements and chemical analysis AS1).
4. The determination of the physicochemical properties of aerosols that affect the climate directly and indirectly (field measurements - Tandem DMA CCNC).
5. Perform measurements of the physicochemical properties of laboratory generated particles that simulate those observed in field measurements (laboratory measurements - Tandem DMA CCNC).
6. The development of parametric models (Theory Kohler, ISSOROPIA) and their comparison with the field measurements and laboratory experiments.
7. The identification and quantification of heterogeneous physicochemical processes between suspended particles, water vapor and air pollutants (NOx, HNO3, O3) with the help of laboratory experiments and theoretical calculations.
8. The use of a new generation of 3D-CTMs for both the identification of area and the rate of production of new particles by nucleation, and to determine the number distribution and the chemical composition of aerosols.
9. Determination the physicochemical characteristics of aerosols that contribute most to the optical properties associated with the greenhouse effect.
10. Comparison of surface measurements with remote sensing measurements (MODIS).

European Union
European Social Fund
OPERATIONAL PROGRAMME
EDUCATION AND LIFELONG LEARNING
investing in knowledge society
MINISTRY OF EDUCATION & RELIGIOUS AFFAIRS
MANAGING AUTHORITY
NSRF 2007-2013
programme for development
EUROPEAN SOCIAL FUND
Co-financed by Greece and the European Union

The project includes seven actions, of which the first is the coordination of the project by the Professor of the Department of Environment Christodoulos Pilinis, while the last includes the external evaluation of the program. The other actions have pure scientific content.

ΕΙΣΑΓΩΓΗ

Σκοπός του έργου είναι η διερεύνηση και ο προσδιορισμός των πηγών και των φυσικοχημικών διεργασιών μέσω των οποίων τα Αιωρούμενα Σωματίδια (ΑΣ) που παράγονται/συναντώνται σε μεγάλες πόλεις της Ελλάδας και στην περιοχή του Αιγαίου επηρεάζουν το κλίμα. Οι επιδιωκόμενοι στόχοι του έργου είναι:

1. Η δημιουργία σταθερού δικτύου παρακολούθησης βασικών φυσικοχημικών ιδιοτήτων με χρήση πληθώρας 'state of the art' οργάνων.
2. Ο προσδιορισμός των πηγών, συγκεντρώσεων και μεγέθους των αιωρούμενων σωματιδίων δύο μεγάλες πόλεις της Ελλάδας (Αθήνα και Πάτρα) και στην περιοχή του Αιγαίου (Κρήτη).
3. Η εκτίμηση της χημικής σύστασης των αιωρούμενων σωματιδίων, και πώς αυτή μεταβάλλεται κατά την παραμονή τους στην ατμόσφαιρα (μετρήσεις AMS και χημική ανάλυση ΑΣ1).
4. Ο προσδιορισμός των φυσικοχημικών ιδιοτήτων των αιωρούμενων σωματιδίων που επηρεάζουν το κλίμα με άμεσο και έμμεσο τρόπο (μετρήσεις πεδίου Tandem DMA και CCNC).
5. Η διεξαγωγή μετρήσεων των φυσικοχημικών ιδιοτήτων εργαστηριακά παραγόμενων σωματιδίων που θα προσομοιώνουν αυτά που παρατηρούνται στις μετρήσεις πεδίου (εργαστηριακές μετρήσεις Tandem DMA και CCNC).
6. Η ανάπτυξη παραμετρικών μοντέλων (Θεωρεία Kohler, ISSOROPIA) και σύγκριση με μετρήσεις πεδίου και εργαστηριακά πειράματα.
7. Ο ποιοτικός και ποσοτικός προσδιορισμός των ετερογενών φυσικοχημικών διεργασιών μεταξύ αιωρούμενων σωματιδίων, υδρατμών και ατμοσφαιρικών

European Union
European Social Fund
OPERATIONAL PROGRAMME
EDUCATION AND LIFELONG LEARNING
investing in knowledge society
MINISTRY OF EDUCATION & RELIGIOUS AFFAIRS
MANAGING AUTHORITY
NSRF 2007-2013
EUROPEAN SOCIAL FUND
Co-financed by Greece and the European Union

ρύπων (NOx, HNO3, O3) με την διεξαγωγή εργαστηριακών πειραμάτων και θεωρητικών υπολογισμών.

8. Η χρήση νέας γενιάς 3D-CTM τόσο για τον προσδιορισμό των περιοχών και την ένταση παραγωγής νέων σωματιδίων με πυρηνοποίηση (nucleation), όσο και για τον προσδιορισμό του αριθμού της κατανομής και της χημικής σύστασης των αερολυμάτων.
9. Η εύρεση των φυσικοχημικών χαρακτηριστικών των αερολυμάτων που συνεισφέρουν περισσότερο στις οπτικές ιδιότητες που έχουν σχέση με το φαινόμενο του θερμοκηπίου.
10. Η σύγκριση των επίγειων μετρήσεων με τηλεπισκοπικές μετρήσεις (MODIS).

Το έργο περιλαμβάνει επτά δράσεις, εκ των οποίων η πρώτη αφορά τον συντονισμό από τον Καθηγητή του Τμήματος Περιβάλλοντος Χ. Πηλίνη και η τελευταία την εξωτερική αξιολόγηση του προγράμματος. Οι υπόλοιπες δράσεις είναι καθαρά επιστημονικού περιεχομένου.

European Union
European Social Fund
OPERATIONAL PROGRAMME
EDUCATION AND LIFELONG LEARNING
investing in knowledge society
MINISTRY OF EDUCATION & RELIGIOUS AFFAIRS
MANAGING AUTHORITY
NSRF 2007-2013
EUROPEAN SOCIAL FUND
Co-financed by Greece and the European Union

Activity 1: Coordination

During this coordination activity the following important actions took place during the project:

- Using legal procedures all the chemicals needed for the measurement campaigns were purchased.
- Organized four formal meetings (one in Mytilene, two in Heraklion and one in Athens)
- Organized all the experimental campaigns.
- Organized two press-conferences in Athens, in order to inform the public on the effects of fireplace usage on fine aerosol concentrations. Both of them were extremely successful and they were covered by major TV channels, radio stations and newspapers.

Activity 2: Development and calibration of a Hygroscopic Tandem Differential Mobility Analyzer (HTDMA)

The interaction of airborne nanoparticles with water vapor can change their physicochemical properties (e.g., their size, scattering efficiency, etc.) while suspended in the atmosphere. As a result, the optical properties of the particles may vary with time, thereby changing their contribution to local and regional climate. A custom-made HTDMA system (Rader and McMurry, 1986) was developed for the measurements of the hygroscopic behavior of atmospheric particles in the framework of this Thalis project. The instrument was designed to be employed in all the field campaigns of the project for measurements in Athens, Patras, and on Crete (at Finokalia). The paragraphs below give a brief description of the whole system together with some calibration tests.

European Union
European Social Fund
OPERATIONAL PROGRAMME
EDUCATION AND LIFELONG LEARNING
investing in knowledge society
MINISTRY OF EDUCATION & RELIGIOUS AFFAIRS
MANAGING AUTHORITY
NSRF 2007-2013
programme for development
EUROPEAN SOCIAL FUND
Co-financed by Greece and the European Union

A1. Experimental Setup and Procedure

The layout of the HTDMA system is shown in Figure A1. It consists of two Differential Mobility Analyzers (DMAs; Knutson and Whitby, 1975), and a Condensation Particle Counter (CPC, TSI Model 3772; Stolzenburg and McMurry, 1991). The first DMA (DMA-1, TSI 3080) includes a ^{85}Kr aerosol neutralizer and a closed-loop system for recirculating the sheath flow. The second DMA (DMA-2) employs a custom-made system for the sheath flow recirculation (cf. Biskos et al., 2006). The system also uses two nafion-tube humidity exchangers (Perma Pure Model MD-110), three humidity/temperature sensors (two Rotronic Model SC-05 and one Rotronic Model HC2-C05), two multi input-output data acquisition cards (National Instruments models NI USB 6211 and 6008), two Mass Flow Controllers (Sierra Mass-Trak 810), one air pump and one laptop computer.

To measure the hygroscopicity of airborne particles, the sample air is first passed through a drying system in order to reduce its relative humidity (RH) and ensure that particles are in a dry state before classification. This is important because particles can retain some amount of water even in low RH due to their acidity (cf. Biskos et al. 2009) and/or their organic content (cf. Marcolli et al., 2004). The drying method could be either a silica gel diffusion dryer or a nafion tube dryer combined with a system that provides dry air. The RH of the sample after the drying process is constantly monitored by a temperature/RH sensor (Rotronic Model HC2-C05). The sensor signals (0-1 volts analog signal for both RH and temperature) are recorded along with all the other parameters of the experimental setup.

European Union
European Social Fund
OPERATIONAL PROGRAMME
EDUCATION AND LIFELONG LEARNING
investing in knowledge society
MINISTRY OF EDUCATION & RELIGIOUS AFFAIRS
MANAGING AUTHORITY
NSRF 2007-2013
EUROPEAN SOCIAL FUND
Co-financed by Greece and the European Union

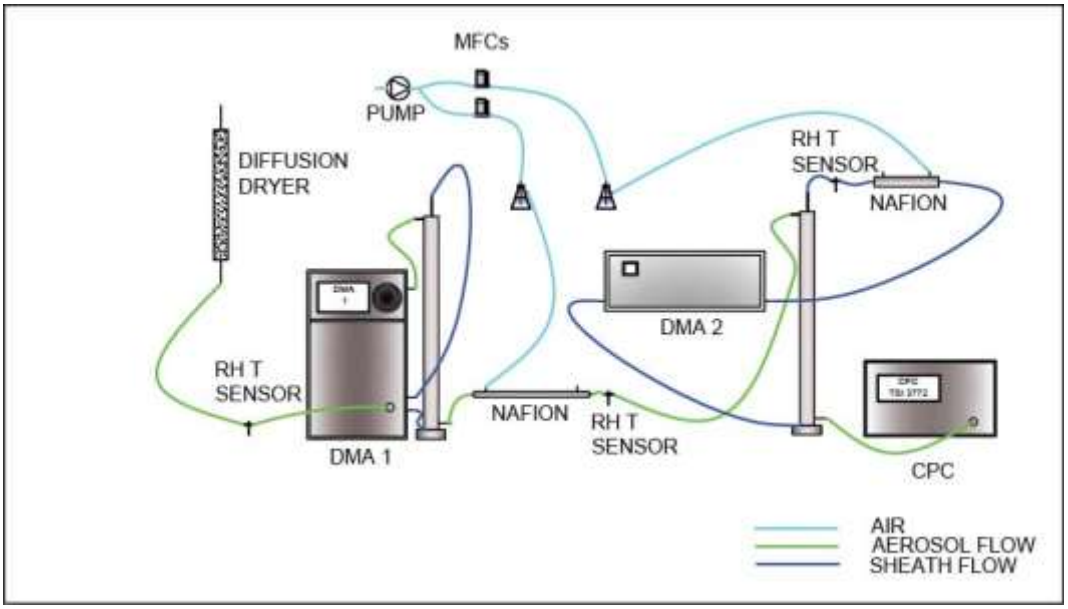

Figure A1: Layout of the HTDMA. The system is mainly composed of two DMAs, one CPC and two RH conditioning systems.

The dried aerosol particles downstream the dryer are passed through a ^{85}Kr aerosol neutralizer in order to established an equilibrium charge distribution before entering DMA-1. DMA-1 (TSI 3081) is used to select dry aerosol particles having mobility diameters within a very narrow range. Due to geometrical/operational limitations of the DMA, particles having slightly smaller or higher mobility diameters from the one selected are obtained, leading to an aerosol with a narrow mobility diameter distribution (monodisperse aerosol). The broadening of the monodisperse aerosol distribution is affected by the sheath to aerosol flow ratio. Monodisperse aerosol particles of a specific mobility diameter are obtained at the exit of DMA-1 by properly adjusting its voltage and sheath flow. The voltage on DMA-1 could be adjusted either by using the onboard control panel or alternatively through the computer. The later is achieved by sending an analog signal (0-5 Volts) from the data acquisition card to the high voltage controller of DMA-1. In that way we can select particles of different mobility diameters for specific time intervals (e.g., running a cycle of particles having dry mobility diameters of 40, 60, 80, 100 and 120 nm every 30 min).

European Union
European Social Fund
OPERATIONAL PROGRAMME
EDUCATION AND LIFELONG LEARNING
investing in knowledge society
MINISTRY OF EDUCATION & RELIGIOUS AFFAIRS
MANAGING AUTHORITY
NSRF 2007-2013
EUROPEAN SOCIAL FUND
Co-financed by Greece and the European Union

The quasi monodisperse particles downstream of DMA-1 are then conditioned within a single nafion-tube humidity exchanger (Perma Pure Model MD-110) to a constant RH. The size distribution of the humidified particles is then measured by DMA-2 and the CPC. DMA-2 is operated in a scanning mode (SMPS; Wang and Flagan, 1989), thereby allowing particles with different mobility diameters to be counted by the CPC. Combining the information of the particle size selected by DMA-2 during the scan and the recorded signal of the CPC, we obtain the size distribution of the humidified monodisperse particles.

An important requirement for the HTDMA measurements is to adjust the RH of the aerosol flow downstream the humidifier and the sheath flow of DMA-2 to the same value. This can be achieved by passing the sheath flow of DMA-2 through a multi nafion tube humidity exchanger (Perma Pure Model MD-110). Humidification of aerosol and sheath flow is achieved by properly adjusting the flows of two parallel streams of very high RH (ca. 100%) on the outer annulus of the nafion-tube humidity exchangers. The highly humidified air streams (RH ca. 100%) used for humidifying the aerosol and the sheath flows in DMA-2 is made by passing air, provided by the systems air-pump, through bottles containing de-ionized water. Their flow rates are independently adjusted using two Mass Flow Controllers (Sierra, Mass-Trak 810).

The RH and temperature of the aerosol flow as well as the sheath flow in DMA-2 are measured by two humidity/temperature sensors (Rotronic, Model SC-05) located downstream the nafion tube humidity exchangers. Two software Proportional-Integral-Derivative (PID) controllers are used to control the RH in the two streams. The closed-loop controllers use as inputs the signals from the two RH sensors located downstream both nafion tube humidity exchangers. These signals (0-1 Volts analog signals) are acquired by the data acquisition card. The output signals from the PID controllers are used to control the flows through the two Mass Flow Controllers (Sierra, Mass-Trak 810), thereby regulating the highly humidified air flow rates at the outer annulus of each nafion-tube humidity exchanger.

In the setup described above the nominal aerosol and the sheath flows for both DMAs is 0.3 and 3.0 lpm, respectively. Because the CPC (TSI 3772) is capable of sampling

European Union
European Social Fund
OPERATIONAL PROGRAMME
EDUCATION AND LIFELONG LEARNING
investing in knowledge society
MINISTRY OF EDUCATION & RELIGIOUS AFFAIRS
MANAGING AUTHORITY
NSRF 2007-2013
programme for development
EUROPEAN SOCIAL FUND
Co-financed by Greece and the European Union

only at 1.0 lpm, a T-junction is used in order for only 0.3 lpm to be sampled through the HTDMA system. The rest 0.7 lpm needed by the CPC are added by a filtered air flow. A regulator valve is used to fine-adjust the above flow ratio. Both DMA sheath flows and the CPC sample flow were calibrated using an inline bubble flow meter (Sensidyne Gilibrator). During these tests sheath flows were both set at 3000 cm^3 min^{-1}, while the sample flow was set at 300 cm^3 min^{-1}. Typical flow measurements with this system are shown in Figure A2. The error of the flows is within less than 2% of the set-point.

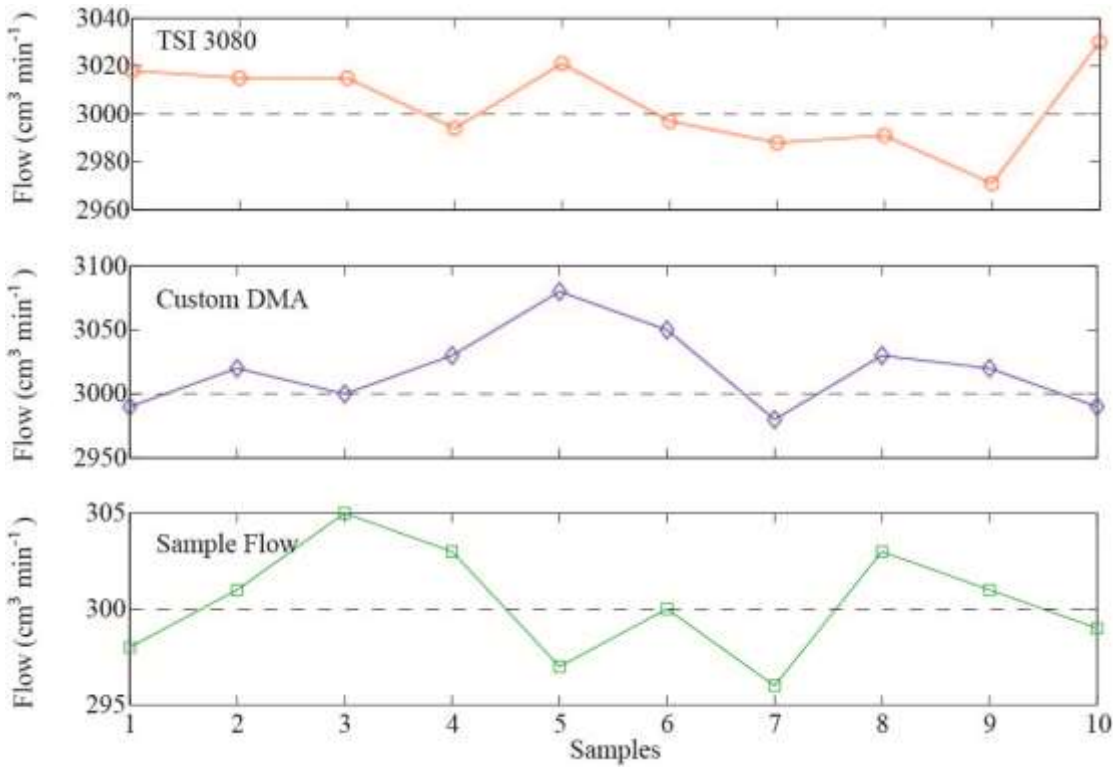

Figure A2: Measurements of aerosol sample flow (top graph) and the sheath flows in DMA-1 (TSI 3080; middle graph), DMA-2 (Custom; bottom graph). Dashed lines represent the flow set-points.

A2. Tests and Calibrations

The performance of both DMAs was tested using monodisperse polysterene latex (PSL) spheres having diameters, reported by the manufacturer of 173, 262, 492 nm. PSL sphere particles were produced by atomization in pure N_2 gas (AirLiquide, 99.9%). The

European Union
European Social Fund
OPERATIONAL PROGRAMME
EDUCATION AND LIFELONG LEARNING
investing in knowledge society
MINISTRY OF EDUCATION & RELIGIOUS AFFAIRS
MANAGING AUTHORITY
NSRF 2007-2013
EUROPEAN SOCIAL FUND
Co-financed by Greece and the European Union

resulting particles were subsequently dried through a nafion tube dryer and then charge-neutralized by a ^{85}Kr neutralizer prior measuring their size distribution by either of the two DMAs and the CPC, operated in SMPS mode. The experimental setup for testing the DMAs using the PSL spheres is shown in Figure A3.

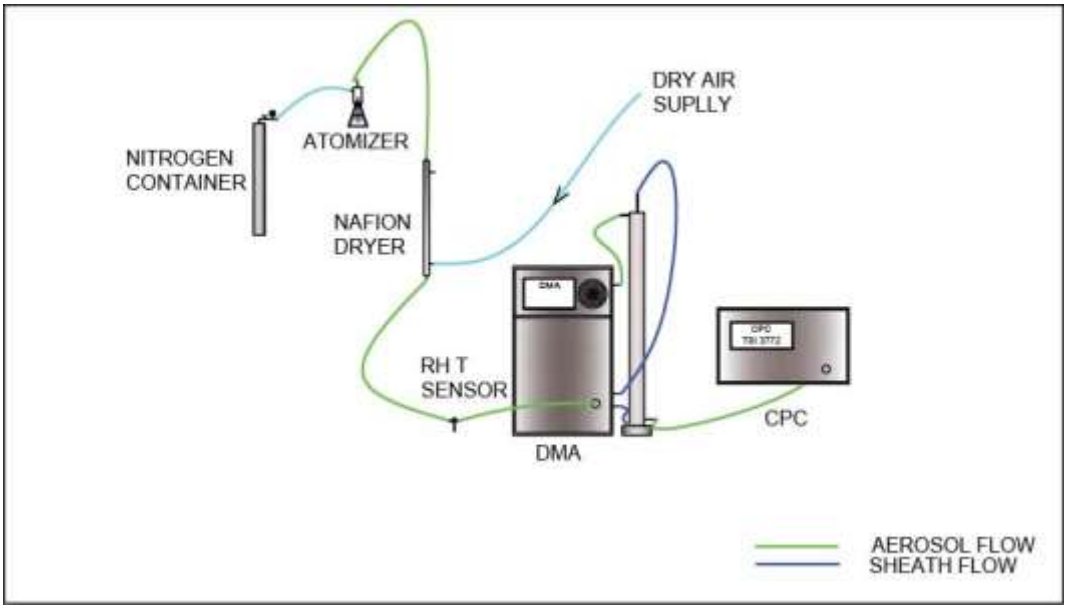

Figure A3: Experimental setup for testing the two DMAs with monodisperse PSL spheres. In these tests PSL spheres having nominal diameters of 173, 262, and 492 nm were produced by atomization, and subsequently dried and measured by each DMA and the CPC.

Figure A4 shows the results with the PSL spheres using custom DMA (Fig 4a) and TSI 3080 (Fig. 4b) operated in SMPS mode. The measurements with PSL spheres having diameters of 173 and 262 nm were well within the 3% accuracy (shaded area) reported for PSL spheres tests when measured with the custom-DMA. Measuring PSL spheres having diameters of 492 nm with the custom DMA showed almost 4% higher measured diameter. With the TSI 3080 DMA, measurements with PSL spheres having of 173 and 492 nm were well within the 3% accuracy (shaded area). For the 262-nm PSL spheres, however the measured diameter was almost 4.5% higher to their diameter. These test results were taken into account when measuring laboratory-generated and/or atmospheric particles.

European Union
European Social Fund
OPERATIONAL PROGRAMME
EDUCATION AND LIFELONG LEARNING
investing in knowledge society
MINISTRY OF EDUCATION & RELIGIOUS AFFAIRS
MANAGING AUTHORITY
NSRF
2007-2013
EUROPEAN SOCIAL FUND
Co-financed by Greece and the European Union

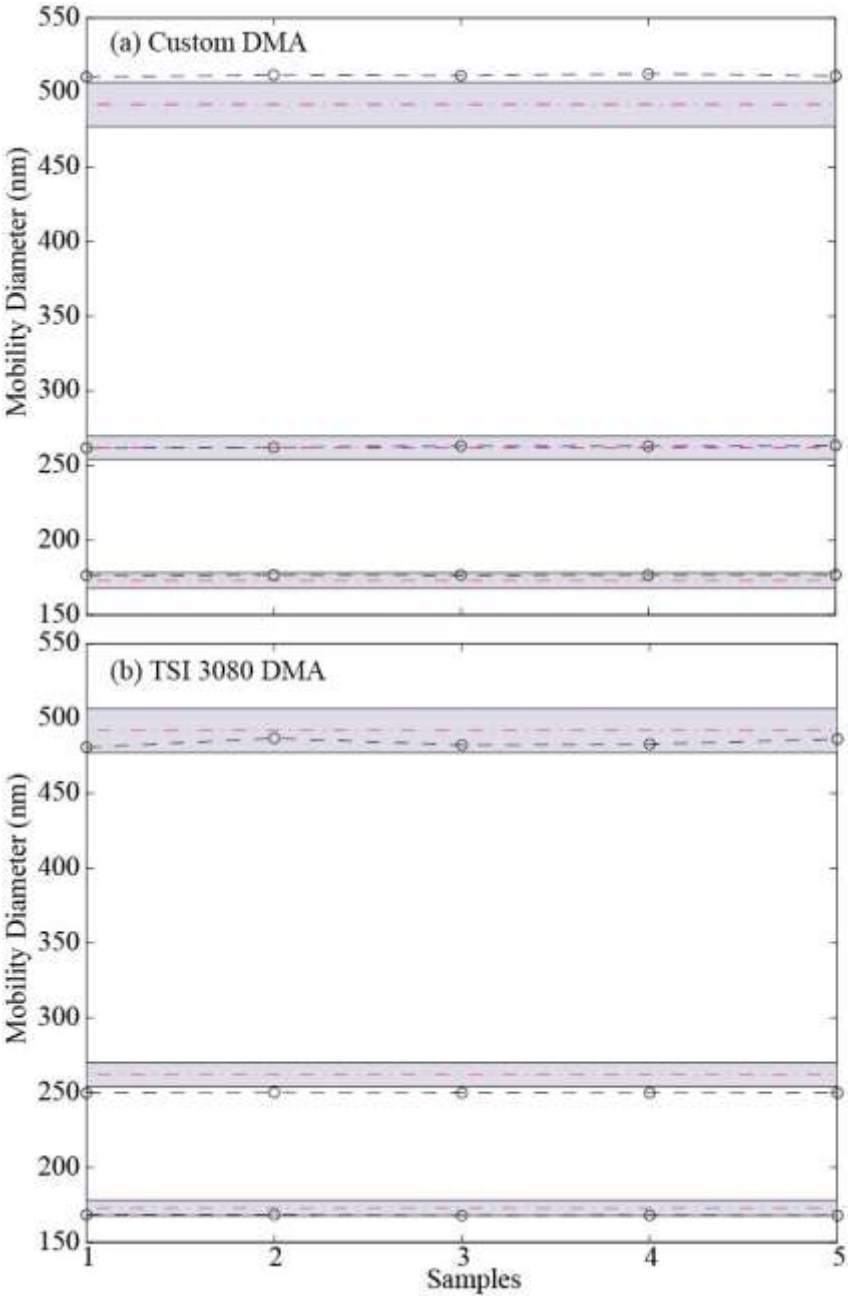

Figure A4: PSL-sphere tests conducted with the custom-made DMA (a) and the TSI 3080 DMA (b). Black circles represent the geometric mean diameters of PSL particles as measured by the DMA and the CPC. Dashed-doted magenta lines represent their nominal size. A 3% difference in PSL spheres nominal size, which is common for PSL spheres, is shown as shaded area.

The performance of the RH conditioning system was tested by instantly raising the RH set-point from 80 to 85%. For this test the system was set up as an HTDMA system (cf.

European Union
European Social Fund
OPERATIONAL PROGRAMME
EDUCATION AND LIFELONG LEARNING
investing in knowledge society
MINISTRY OF EDUCATION & RELIGIOUS AFFAIRS
MANAGING AUTHORITY
NSRF 2007-2013
EUROPEAN SOCIAL FUND
Co-financed by Greece and the European Union

Fig. A1). Sheath flows were set at 3.0 lpm for both DMAs, while the sample flow was set at 0.3 lpm. Results of this test are shown in Figure A5.

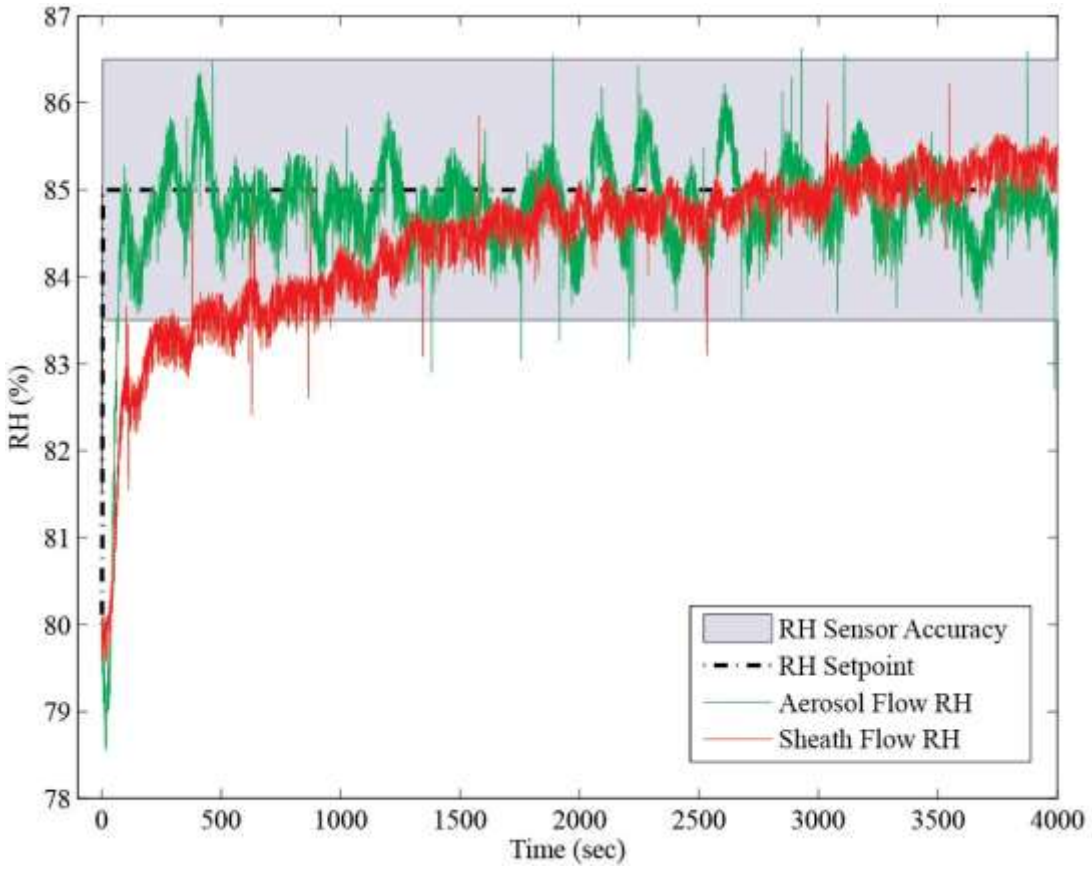

Figure A5: RH control system response and stability test. During this test the RH set-point was increased from 80 to 85%. The RH of the sample (green) and the sheath (red) flow were measured just before DMA-2 column. The shaded area represents the ±1.5% accuracy, claimed by the RH sensor manufacturer.

The sheath flow RH conditioning system has a slower response mainly due to the slow dynamics of the nafion tube humidity exchanger and the recirculation of the sheath. The parameters of this PID controller were set to combine the fastest response time with the smallest overshoot. After reaching their set-points, both PID controllers were able to maintain the RH well within their sensors accuracy.

European Union
European Social Fund
OPERATIONAL PROGRAMME
EDUCATION AND LIFELONG LEARNING
investing in knowledge society
MINISTRY OF EDUCATION & RELIGIOUS AFFAIRS
MANAGING AUTHORITY
NSRF 2007-2013
EUROPEAN SOCIAL FUND
Co-financed by Greece and the European Union

The hygroscopic growth factor, g, determined by the HTDMA measurements is given by

$$g(\mathrm{RH}) = \frac{d_m(\mathrm{RH})}{d_{m,dry}}, \qquad (1)$$

where d_m(RH) and $d_{m,dry}$ are the geometric mean mobility diameters of the sampled particles at the hydrated state (i.e., RH = 85%) measured by DMA-2 and the CPC, and at the dry state (i.e., the mobility diameter selected by DMA-1), respectively.

Once all the individual components of the HTDMA system were calibrated, its overall performance was investigated with ammonium sulfate and sodium chloride particles produced by atomization. The experimental setup was identical to the one shown in Figure 1, with the addition of an atomizer upstream the diffusion drier. Pure N_2 gas (99.9% purity) was used to run the atomizer. The resulting particles were subsequently dried through a nafion tube dryer and then neutralized by a ^{85}Kr neutralizer. Particles having 100-nm dry mobility diameter were selected by DMA-1. The monodisperse aerosol flow was then exposed to different RH conditions and subsequently measured by DMA-2 and the CPC. DMA-2 sheath flow was conditioned at the same RH as the aerosol flow. The sheath flows in both DMAs were set to 3.0 lpm, while the sample flow was set to 0.3 lpm.

Figure A6 shows the results of these tests, compared with theoretical predictions. The hygroscopic growth factor measurements of ammonium sulfate particles are well compared with the theory, while the measured hygroscopic growth factor of the sodium chloride particles appears to be smaller than the theoretically predicted. This is due to the change of the cubical shape of sodium chloride particles when they are in the dry/crystal state (i.e., when selected by DMA-1) to the spherical shape of the droplets (i.e., when measured by DMA-2). Considering that the shape factor cubic particles have an average value of 1.14 (cf. Wang et al., 2010), the HTDMA measuremets agree well with the predicted values.

European Union
European Social Fund
OPERATIONAL PROGRAMME
EDUCATION AND LIFELONG LEARNING
investing in knowledge society
MINISTRY OF EDUCATION & RELIGIOUS AFFAIRS
MANAGING AUTHORITY
NSRF 2007-2013
programme for development
EUROPEAN SOCIAL FUND
Co-financed by Greece and the European Union

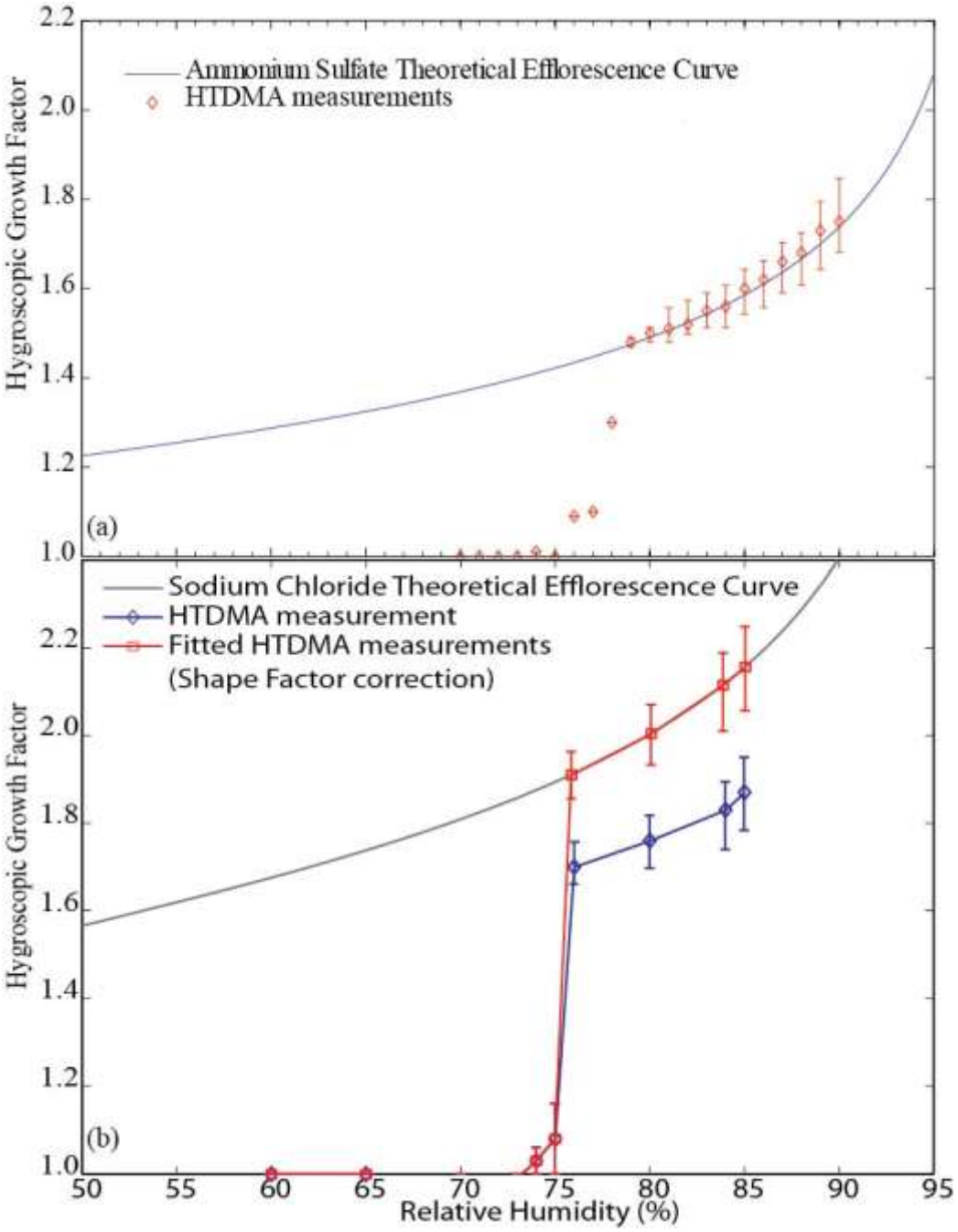

Figure A6: HTDMA measurements of ammonium sulfate (a) and sodium chloride (b) particles, having dry mobility diameter of 100 nm. The curves represents the theoretical Efflorescence curves of the ammonium sulfate and sodium chloride particles. Error bars correspond to ±2% accuracy in the RH measurement.

European Union
European Social Fund
OPERATIONAL PROGRAMME
EDUCATION AND LIFELONG LEARNING
investing in knowledge society
MINISTRY OF EDUCATION & RELIGIOUS AFFAIRS
MANAGING AUTHORITY
NSRF 2007-2013
EUROPEAN SOCIAL FUND
Co-financed by Greece and the European Union

The calibration tests showed that the HTDMA system can very accurately measure the hygroscopic properties of aerosol particles. The instrument has been designed and built to be deployed in long-term field measurements with minor attendance by automating almost all its operating procedures. Pictures A1 and A2 show the actual instrument during operation.

Picture A1: The HTDMA system during calibration and testing. The main components of the system (DMAs, CPC) are located in the metal frame (center of the photograph). The atomizer that was used is also visible on the left.

Picture A2: The HTDMA system during campaign measurements. The HTDMA system (on the left) was combined with one Cloud Condensation Nuclei (CCN) counter (located in the center) in order to provide fine and ultrafine particles hygroscopicity measurements in sub/super- saturation conditions

European Union
European Social Fund
OPERATIONAL PROGRAMME
EDUCATION AND LIFELONG LEARNING
investing in knowledge society
MINISTRY OF EDUCATION & RELIGIOUS AFFAIRS
MANAGING AUTHORITY
NSRF 2007-2013
EUROPEAN SOCIAL FUND
Co-financed by Greece and the European Union

A3. References

Biskos, G., Russel, L.M., Buseck, P.R., Martin, S.T., (2006b), "Nanosize effect on the hygroscopic growth factor of aerosol particles", Geophysical Research Letters, 33, L07801.

Biskos, G., Buseck, P.R., Martin, S.T., (2009), "Hygroscopic Growth of Nucleation-mode Acidic Sulfate Particles", Journal of Aerosol Science, 40, 338-347.

Knutson, E.O., Whitby, K.T., (1975), "Aerosol classification by electric mobility: Apparatus, theory, and applications", Journal of Aerosol Science, 6, 443-451.

Marcolli, C., Luo, B. P. and Peter, T., (2004). "Mixing of the organic aerosol fractions: liquids as the thermodynamically stable phases", The Journal of Physical Chemistry A, 108, 2216–2224.

Rader, D.J., McMurry P.H., (1986), "Application of the tandem differential mobility analyzer to studies of droplet growth or evaporation", Journal of Aerosol Science 17, 771-787.

Stolzenburg, M.R. & McMurry, P.H., (1991), "An ultrafine aerosol Condensation Nucleus Counter", Aerosol Science and Technology, 14, 48-65.

Wang, C.S., Flagan C.R., (1989), "Scanning Electrical Mobility Spectrometer", Aerosol Science and Technology, 13, 230-240.

Wang, Z., King, S.M., Freney, E., Rosenoern, T., Smith, M.L., Chen, Q., Kuwata, M., Lewis, E.R., Pöschl, U., Wang, W., Buseck, P.R., and Martin, S. T., (2010), "The dynamic shape factor of sodium chloride nanoparticles as regulated by drying rate", Aerosol Science and Technology, 44(11), 939-953.

European Union
European Social Fund

OPERATIONAL PROGRAMME
EDUCATION AND LIFELONG LEARNING
investing in knowledge society
MINISTRY OF EDUCATION & RELIGIOUS AFFAIRS
MANAGING AUTHORITY

NSRF 2007-2013
programme for development
EUROPEAN SOCIAL FUND

Co-financed by Greece and the European Union

Activity 3: Variability of concentrations and size distributions of fine atmospheric aerosol

A1. Introduction

Atmospheric aerosol is generated by natural and anthropogenic processes and its lifetime is ranging from a few hours for resuspended coarse dust to several days for fine primary and secondary aerosol (e.g. black carbon, sulphate) (K. Eleftheriadis et al, 2006). It is characterised by marked differences in chemical composition and physical properties. Its composition may be directly influenced by anthropogenic emissions of primary particles, condensation of gaseous precursors of anthropogenic or natural origin and natural sources such as the sea and erodible soils (Seinfeld and Pandis, 1998). Atmospheric aerosols have multiple effects on climate, air quality, human health and atmospheric visibility (e.g. Laden et al., 2006; Lohmann and Feichter, 2005; Pope and Dockery 2006). To understand the effects of aerosol particles on climate and health, measurements of their size distributions and chemical composition in the atmosphere, are needed. The climate effects of the particle number concentration of aerosols with dry diameters larger than 50 nm are divided into two groups. The direct effect represents the ability of the particle population to absorb and scatter short-wave radiation and thus directly to affect the radiation balance. These direct effects depend primarily on the aerosol optical properties and particle size distribution (Bond et al, 2013). The indirect effect is due to aerosol particles acting as condensation Nuclei in cloud formation which subsequently results in cloud albedo effect and cloud lifetime effect. The cloud albedo effect is the resulting change in cloud radiative properties due to changes in cloud droplet number concentration (CDNC) and the lifetime effect is connected to the changes in cloud properties and in drizzle.

Particles with diameters smaller than 100 nm have been widely acknowledged to have adverse health effects. The particle deposition to alveolar region of lungs is assumed to be especially efficient for particles of diameters between 10 - 50 nm (Oberdörster et al., 2005). Another reason to study the sub-50 nm particles is related to aerosol particle

European Union
European Social Fund
OPERATIONAL PROGRAMME
EDUCATION AND LIFELONG LEARNING
investing in knowledge society
MINISTRY OF EDUCATION & RELIGIOUS AFFAIRS
MANAGING AUTHORITY
NSRF 2007-2013
programme for development
EUROPEAN SOCIAL FUND
Co-financed by Greece and the European Union

dynamics in atmosphere. By providing a parameter for the smaller size ranges in the atmosphere, we can take into account smaller particles generated from new particle formation and combustion sources. This provides an additional parameter for model-measurement comparisons and a larger part of the particle spectrum and additional particle processes can be taken into account.

A2 Urban, urban background and regional background stations.

Simultaneous particle size distribution measurements were performed in Patra, Thessaloniki, Athens and Finokalia during the summer of 2012. The datasets are described in Table A1 below:

Table A1: Available datasets of particle size distribution measurements

Data set	ICE–HT Patra	Patra City Center	Finokalia, Crete, (GAW/ACTRIS)	Thessaloniki (Eptapyrgion)	Demokritos, Athens (GAW/ACTRIS)
Dates	8/6/2012-21/7/2012	8/6/2012-26/7/2012	1/6/2012-31/7/2012	9/6/2012-22/7/2012	1/6/2012-2/8/2012
Site type	Urban background 12 km from Patra city center, 1 km from national road, 2 km from the sea.	Urban, on the roof of a 7-storey building, on central city square, near the harbour, traffic influenced	Mediterranean background, 50 km from nearest urban area, 150 m above sea level	Urban background, 2.5 km from city center, 1km from city ring road, 175 m above sea level	Urban background, 10 km from city center, 1 km from city ring road, 270 m above sea level
Data coverage	89%	95%	94%	99%	82%
Instrument	SMPS, TSI	SMPS, TSI	Custom	SMPS, TSI	SMPS, TSI
Characterisation	Urban background	Urban	Regional background	Urban background	Urban background

Patra is located at the foothills of a 2 km mountain, at the Gulf of Patra. It is an urban area with a population of around 300,000 inhabitants. The measurements were conducted simultaneously at two sites. The first station (Patra City Center) was located at the central square of Patra (38° 14′ 46″ N, 21° 44′ 08″ E) on the roof of a seven-floor

European Union
European Social Fund
OPERATIONAL PROGRAMME
EDUCATION AND LIFELONG LEARNING
investing in knowledge society
MINISTRY OF EDUCATION & RELIGIOUS AFFAIRS
MANAGING AUTHORITY
NSRF 2007-2013
EUROPEAN SOCIAL FUND
Co-financed by Greece and the European Union

building (Michael Pikridas et al., 2013). A Scanning Mobility Particle Sizer (SMPS, model 3936, TSI) measured the number size distribution in the 10-500 nm range. The sheath flow rate was 4 L min^{-1} and the sample flow rate was 1 L min^{-1}. The second site (ICE–HT Patra) was at the ICE-HT Institute (38° 17′ 52″ N, 21° 48′ 31″ E), 8 km north-east from Patra city center and 1 km south from the Patra-Athens highway. This site is a suburban area surrounded by olive tree fields, while some small settlements are in a distance of 1 km. A Scanning Mobility Particle Sizer (SMPS, classifier model 3080, DMA model 3081, CPC model 3787, TSI) was deployed for the measurement of the number size distribution in the 10-500 nm range. The SMPS operated at a sheath flow rate of 5 L min^{-1} and a sample flow rate of 1 L min^{-1}.

Finokalia station (http://finokalia.chemistry.uoc.gr/) is a European supersite for aerosol research, part of the ACTRIS (Aerosols, Clouds, and Trace gases Research Infrastructure) Network (35˚20′N, 25˚40′E, 250m a.s.l). The station is on the north east part of the island of Crete, facing the Mediterranean Sea in the wide north sector, located on the top of a hill over the coastline. Finokalia site is representative for the background marine conditions of Eastern Mediterranean (Lelieveld et al., 2002), with little anthropogenic influence. The nearest city is Heraklion with approximately 170,000 inhabitants, located about 50 km west of Finokalia. A detailed description of the Finokalia station and the climatology of the area can be found in Mihalopoulos et al., (1997). The particle number size distributions were measured in the diameter range 9−848 nm using a custom-built Scanning Mobility Particle Sizer (SMPS, Kalivitis et al., 2015). It is a closed-loop system, at 5:1 ratio between the aerosol and sheath flow and it is operated following the recommendations by Wiedensohler et al. (2012).

Thessaloniki is a densely populated (16,000 inhabitants km^{-2}) coastal city in Northern Greece. The city is located NE of the Thermaikos Gulf, and is surrounded by residential communities and an industrial zone situated on the NW. The daily mean air temperature and relative humidity (RH) vary from 5.5 to 28.1ºC and from 47 to 80%, respectively (Voutsa et al. 2002). The prevailing winds have SW and NW directions (~75%) and are

European Union
European Social Fund
OPERATIONAL PROGRAMME
EDUCATION AND LIFELONG LEARNING
investing in knowledge society
MINISTRY OF EDUCATION & RELIGIOUS AFFAIRS
MANAGING AUTHORITY
NSRF 2007-2013
EUROPEAN SOCIAL FUND
Co-financed by Greece and the European Union

mainly weak, while the sea breeze (SW direction) has an important effect on the local ambient climate. Wind conditions are calm for the rest of the time (~25%).The station (urban-background station) is located on Agrafon Street at Eptapyrgio (40° 38' N, 22° 57' E, and 174.3 asl) next to small residences, a park on the West, and the city's ring road 1 km away on the East. A Scanning Mobility Particle Sizer (TSI, Model 3034) was employed to measure the size distributions of the particles having diameters in the range of 10-487 nm.

In Athens, because of its high population (3.75 million in the metropolitan area) and the concentration of commercial and industrial activities in a relatively small area (approximately 450 km^2), severe environmental degradation has taken place characterized by high loadings of atmospheric pollutants (Chaloulakou et al., 2005; Kambezidis et al., 1998; Progiou and Ziomas, 2011). The urban aerosol is strongly affected by the local air-circulation in the basin and the sea-breeze effects developing between the Attica peninsula and the surrounding sea. The wind speed increases during the day and subsides in the night (Bjarke Mølgaard et al, 2013). Combustion processes used for transportation, power generation and other human activities produces a mixture of thousands chemical pollutants (Cohen et al., 2004).

Demokritos Athens (37.995°N 23.816° E at 270 m a.s.l.,) is situated on the foot of Mount Hymettus in Aghia Paraskevi and covers an area of 600 acres in a forest of pine trees. At about 12 km to the north from downtown Athens, the NCSR Demokritos monitoring site is representative of the atmospheric suburban background of Athens. The location of all the sites are depicted in Figure A1.

European Union
European Social Fund
OPERATIONAL PROGRAMME
EDUCATION AND LIFELONG LEARNING
investing in knowledge society
MINISTRY OF EDUCATION & RELIGIOUS AFFAIRS
MANAGING AUTHORITY
NSRF 2007-2013
EUROPEAN SOCIAL FUND
Co-financed by Greece and the European Union

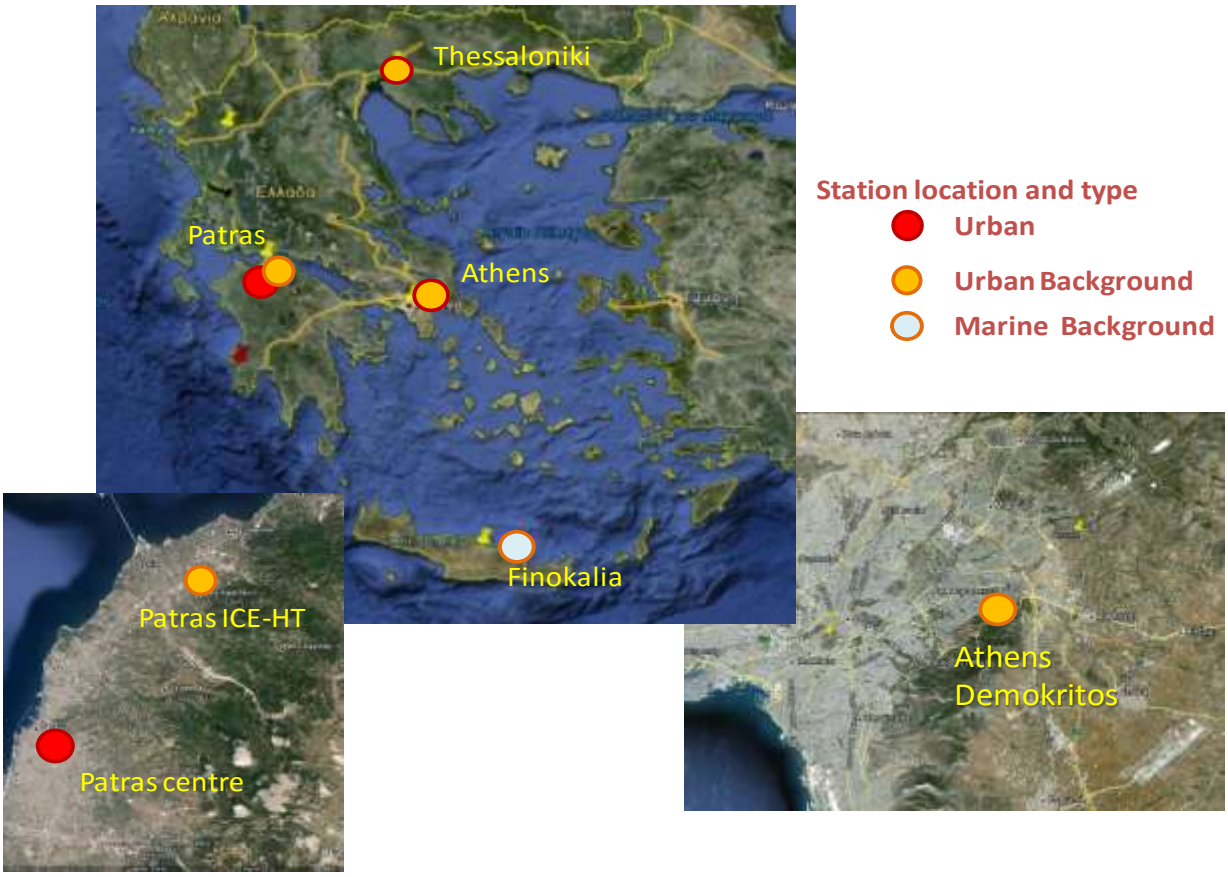

Figure A1: Urban, urban background and regional background stations Measurement sites.

A2 Concentration levels and size distributions at each site

Particle size distribution measurements were conducted, using a scanning mobility particle sizer (SMPS), consisting of an Electrostatic Classifier model 3080, a DMA column model 3081 and a Condensation Particle Counter (CPC 3022A, TSI Inc). Each measurement had duration of five minutes (including 15 s down scan time). Flows within the DMA were checked and adjusted if necessary every week, with the sheath and inlet flows set at 3 and 0.3 l/min respectively.

The inverted particle number size distributions were then analyzed using a curve-fitting algorithm similar to that described in Hussein et al. (2005). This algorithm employed the least squares method to fit the sum of up to 4 lognormal distributions to the

European Union
European Social Fund
OPERATIONAL PROGRAMME
EDUCATION AND LIFELONG LEARNING
investing in knowledge society
MINISTRY OF EDUCATION & RELIGIOUS AFFAIRS
MANAGING AUTHORITY
NSRF 2007-2013
EUROPEAN SOCIAL FUND
Co-financed by Greece and the European Union

measurements. The algorithm starts by fitting a uni-modal lognormal distribution, and successively tests the possibility of increasing it to a bi-, a tri- and finally a tetramodal distribution based on the RMSE, the estimated number concentration of each mode, the geometric mean diameter, and the geometric standard deviation of the neighboring modes. After the fit, the modes were classified to 6 subcategories (N1-C2), based on their geometric mean diameter (d_g). A graphical example of the fitting process is shown in Figure A2, while the terminology of the subcategories and the rest of the statistical variables are shown in Table A2.

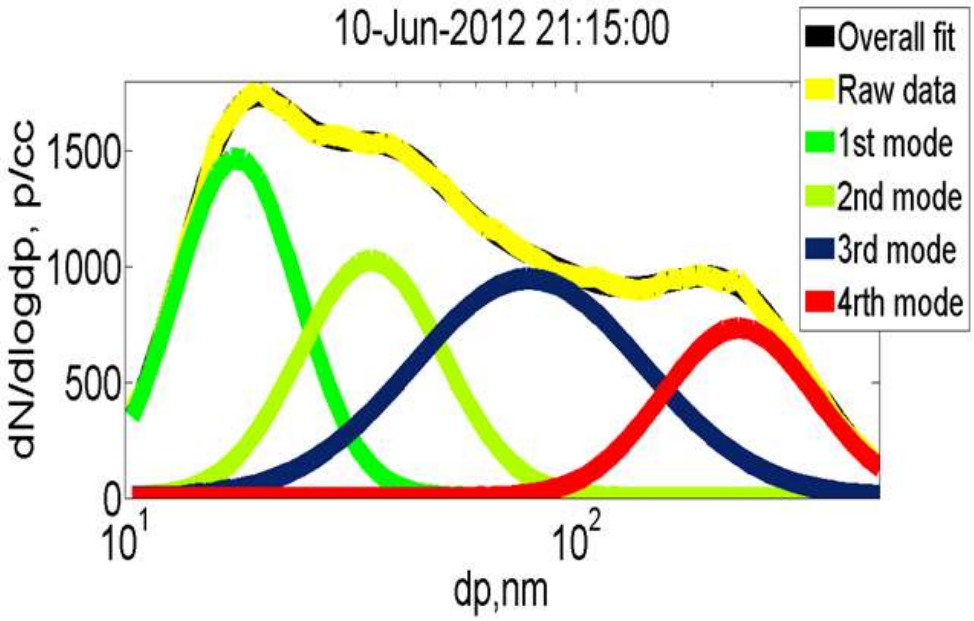

Figure A2: Example of least square fitting of 4 lognormal distributions on experimentally measured particle size distributions.

European Union
European Social Fund
OPERATIONAL PROGRAMME
EDUCATION AND LIFELONG LEARNING
investing in knowledge society
MINISTRY OF EDUCATION & RELIGIOUS AFFAIRS
MANAGING AUTHORITY
NSRF 2007-2013
EUROPEAN SOCIAL FUND
Co-financed by Greece and the European Union

Table A2: Terminology used in the algorithm

σg	geometric standard deviation of mode
dg	geometric mean diameter of mode, referring to dry electrical mobility diameter
N	Total number of mode
n	number of size bins of the SMPS particle size distribution
RMSE	$\mathrm{RMSE} = \frac{100}{\sqrt{n}} * \langle \sum_{j=1}^{n} [\text{SMPS measured number size distribution} - \text{SMPS number fitted distribution}]^2 \rangle^{0.5}$
Mode N1	d_g<15 nm, photochemically induced particle formation, gas to particle conversion
Mode N2	15<d_g<30 nm, related to traffic and growth of nucleated particles
Mode A1	30<d_g<60 nm, related to vehicle emissions, central heating
Mode A2	60<d_g<90 nm, related to vehicle emissions, central heating
Mode C1	90<d_g<120 nm, related to coagulation of ultrafine particles
Mode C2	d_g>120 nm , related to coagulation of ultrafine particles
Frequency %	% percentage of mode combination occurrence per total number of all mode combinations

Figures A3 and A4 illustrate the geometric mean (Gm), 16th and 84th percentile size distribution at the five stations for the time periods indicated earlier. In Thessaloniki station we have an elongated size distribution shape, indicating multiple mixed sources. A well aged accumulation mode is observed, as well as freshly emitted road traffic exhaust. Demokritos Athens and ICE–HT Patra stations have their main peak at 100 nm, with a maximum G_m concentration close to 5,000 dN/dlogdp cm^{-3}. At the 84th percentile at Demokritos Athens we observe the new particle formation influence, as concentration increases for size ranges close to 10 nm. An aged accumulation mode is dominating both sites. Finokalia displays a peak approximately at 100 nm and has the lowest particle concentration values. It probably represents aerosol of intermediate aging (D. C. S. Beddows et al., 2014). The Patra City Center station displays its peak approximately at 60 nm, indicating a domination of freshly emitted road traffic exhaust and it has the highest peak values (twice as high as ICE–HT Patra). Its 84th percentile

European Union
European Social Fund
OPERATIONAL PROGRAMME
EDUCATION AND LIFELONG LEARNING
investing in knowledge society
MINISTRY OF EDUCATION & RELIGIOUS AFFAIRS
MANAGING AUTHORITY
NSRF 2007-2013
programme for development
EUROPEAN SOCIAL FUND
Co-financed by Greece and the European Union

displays an increase of concentration very close to 10 nm which might be attributed to gas to particle conversion (N. Ma et al, 2015).

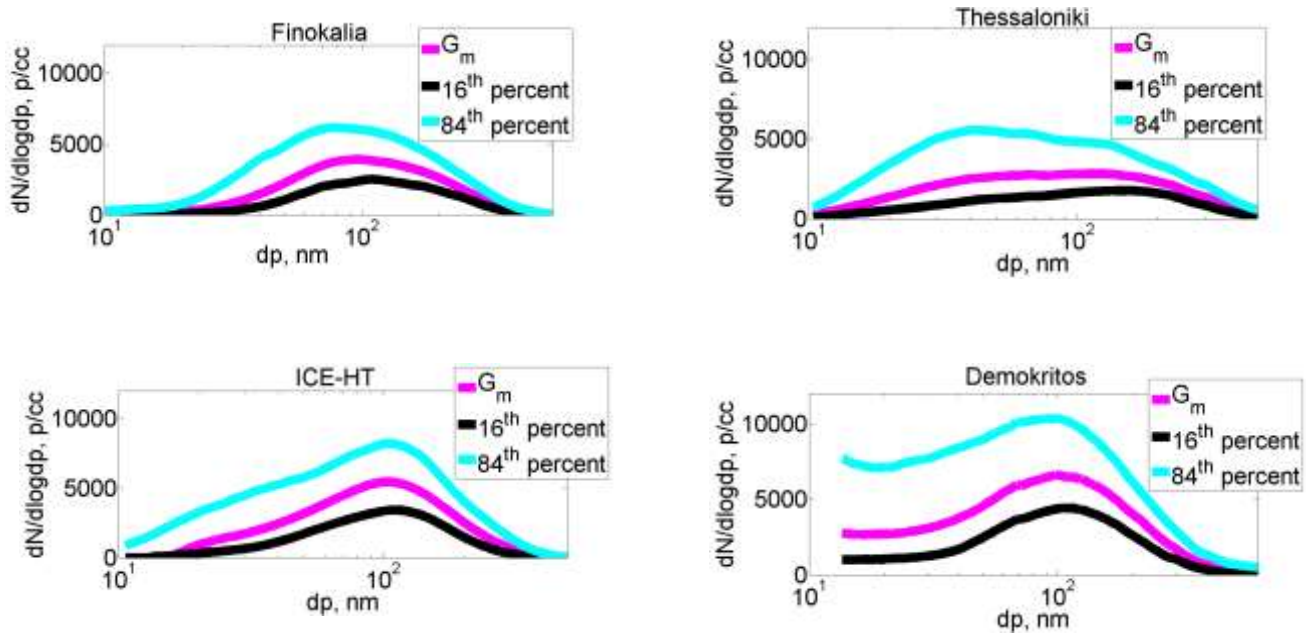

Figure A3: Overview of Particle Size Distribution statistics for each size bin: geometric mean (Gm), the 16th and 84th percentiles of the measured concentrations. Finokalia station is a regional background station, while the three other stations are urban background. The dotted black line depicts dN/dlogdp 1000 particles/cm-3 to help the eye.

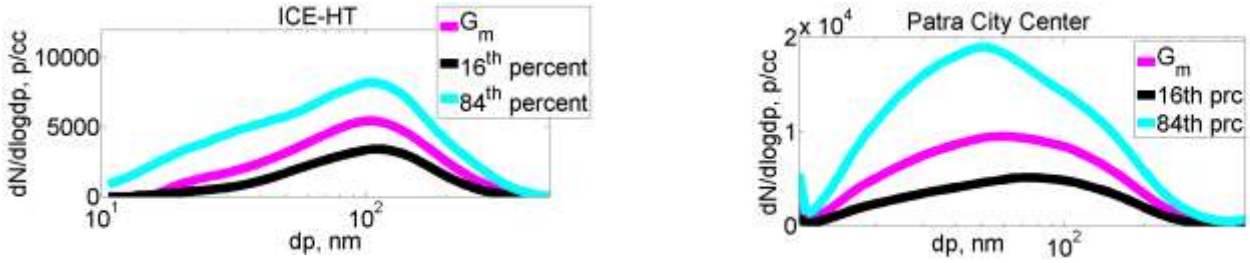

Figure A4: Comparison between the urban background and the city center size distributions for Patra.

European Union
European Social Fund
OPERATIONAL PROGRAMME
EDUCATION AND LIFELONG LEARNING
investing in knowledge society
MINISTRY OF EDUCATION & RELIGIOUS AFFAIRS
MANAGING AUTHORITY
NSRF 2007-2013
EUROPEAN SOCIAL FUND
Co-financed by Greece and the European Union

ATHENS

Demokritos station is situated in a background suburban area. Earlier studies (F. Amato et al, 2015) indicate that the vehicle exhaust source yearly average concentration values are 2 μg/m3 during 2013 in PM2.5 filter samples. This low value is attributed to the distance from avenues with high traffic load.

It was found by a summertime study that katabatic wind dominated the airflow at 18 m above ground for 27% and 9% of night hours, respectively (H. A. Flocas et al, 1998). During katabatic winds, air masses from mount Hymettus (1024 m) are brought to Demokritos Athens station. Also, nocturnal boundary layer (NBL) height is resulting in an increase in particle number concentration, even in the absence of aerosol particle sources. Figure A5 shows the summer 2012 frequency spider plots for Demokritos Athens. A1 mode has a maximum frequency of 37% from 20:00-22:00 and 2:00-4:00. N2 has a maximum of 37% and it has high frequency from 14:00- 02:00. N1 has a maximum frequency of 50% at 6:00-8:00 and 45% at 12:00-14:00. The most frequent mode is C2 with maximum of 55% in the interval 14:00- 20:00, C1 has a maximum of 45% at 06:00-08:00 and A2 has a frequency of 15% during the daytime and 30% during 04:00- 06:00.

A1 has a maximum of 6,000 p/cc from 12:00-14:00, N2 has a maximum of 9,700 p/cc and it has high values from 14:00-16:00 and N1 has a maximum of 11,000 p/cc at 12:00-14:00. C2 has a maximum of 4,000 p/cc in the interval 12:00-16:00, always between 3-4,000 p/cc, C1 has a maximum of 6,000 p/cc at 22:00-00:00 and is always between 5-6,000 p/cc. A2 has a maximum of 9,000 p/cc during 22:00-02:00.

Overall, N1 has its maximum frequency and number concentration at 6:00-8:00 and at 12:00-14:00. These maximums could be attributed to early morning traffic as exhaust gas nucleation particles, consisting of hydrocarbons and sulfate, are forming by

European Union
European Social Fund
OPERATIONAL PROGRAMME
EDUCATION AND LIFELONG LEARNING
investing in knowledge society
MINISTRY OF EDUCATION & RELIGIOUS AFFAIRS
MANAGING AUTHORITY
NSRF 2007-2013
programme for development
EUROPEAN SOCIAL FUND
Co-financed by Greece and the European Union

nucleation during dilution and cooling of the exhaust, and photochemically induced new particle formation at noon (N. Ma et al, 2015). N2 has its maximum number average at 14-16:00, and this may be attributed to the growing of N1 particles. The Aitken mode (A1 and A2) dominates in number and frequency at night (20:00-04:00). The accumulation mode is stable more or less at all hours in number and frequency. Table A3 shows the Demokritos site most frewuent mode combination.

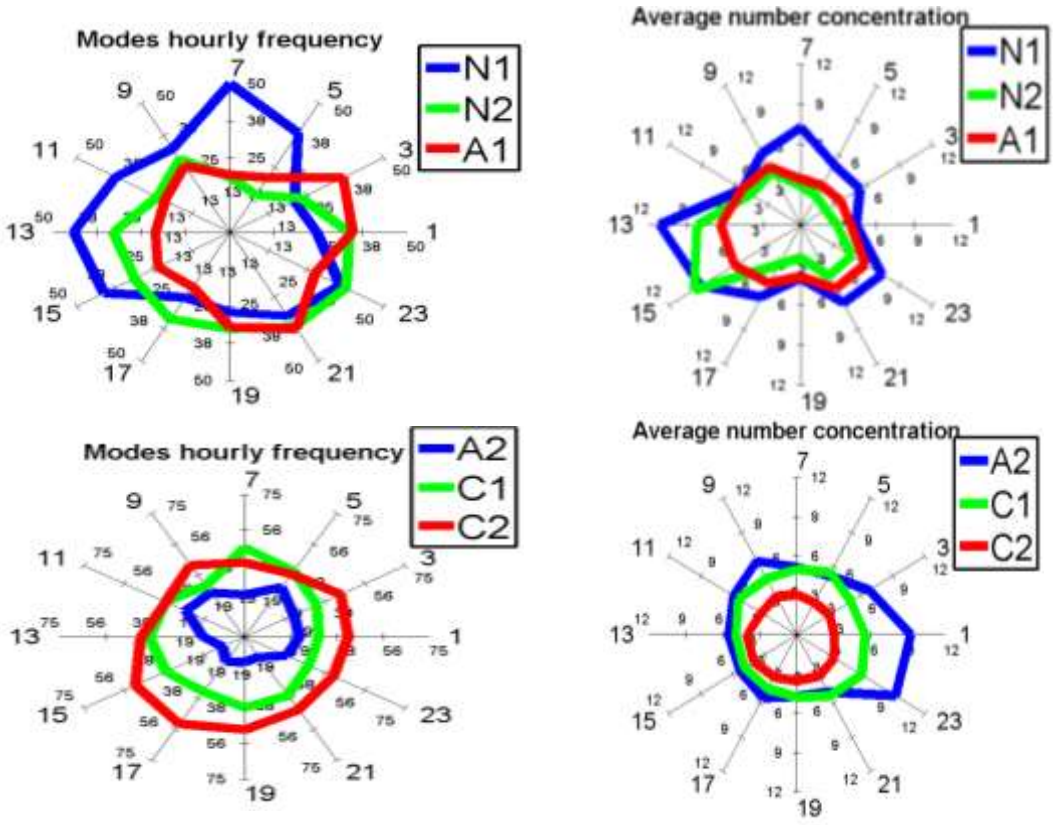

Figure A5: Summer 2012 frequency spider plots for Demokritos Athens. On the left side: the frequency of occurrence for N1 – C2 modes. The numbers 1, 3, 5 correspond to hours of day, while the smaller numbers 50, 38, 25 correspond to frequency of occurrence. On the right side: the average number concentration depending on the hour of the day, for all modes in thousands of particles/cm^{-3}.

.

European Union
European Social Fund
OPERATIONAL PROGRAMME
EDUCATION AND LIFELONG LEARNING
investing in knowledge society
MINISTRY OF EDUCATION & RELIGIOUS AFFAIRS
MANAGING AUTHORITY
NSRF 2007-2013
EUROPEAN SOCIAL FUND
Co-financed by Greece and the European Union

Table A3: Demokritos Athens most frequent mode combination

	N1_C1	A1_C2	N2_C2	N2_C1	N1_C2	N1_A2
	Median	Median	Median	Median	Median	Median
N1-σg	2.5	-	-	-	2.9	1.8
N1-dg	10	-	-	-	10	12
N1-N	4,541	-	-	-	4,368	4,086
N2-σg	-	-	2.9	1.9	-	-
N2-Dg	-	-	23	19	-	-
N2-N	-	-	2,922	2,795	-	-
A1-σg	-	2.4	-	-	-	-
A1-Dg	-	42	-	-	-	-
A1-N	-	3,147	-	-	-	-
A2-σg	-	-	-	-	-	2.1
A2-Dg	-	-	-	-	-	79
A2-N	-	-	-	-	-	7,372
C1-σg	1.9	-	-	1.8	-	-
C1-Dg	106	-	-	107	-	-
C1-N	4,762	-	-	4,698	-	-
C2-σg	-	1.7	1.7	-	1.8	-
C2-Dg	-	141	132	-	128	-
C2-N	-	2,,812	3,660	-	4,335	-
Frequency %	11	10	10	8	8	7

This table demonstrates the most frequent mode combinations: 4 out of 6 of the most frequent combinations are Nuclei mode-Accumulation mode (there is no Aitken mode to act as sink to deposit vapors, and new particles are formed at the time).

European Union
European Social Fund
OPERATIONAL PROGRAMME
EDUCATION AND LIFELONG LEARNING
investing in knowledge society
MINISTRY OF EDUCATION & RELIGIOUS AFFAIRS
MANAGING AUTHORITY
NSRF 2007-2013
EUROPEAN SOCIAL FUND
Co-financed by Greece and the European Union

CRETE-FINOKALIA

Nucleation events are infrequent during summer months in Finokalia (Pikridas et al, 2012). The small Nuclei mode observed (N1) could be attributed to particles formed elsewhere and transported to the site during nighttime. The site is probably influenced by katabatic and anabatic winds. Figure A6 shows the summer 2012 frequency spider plots for Finokalia.

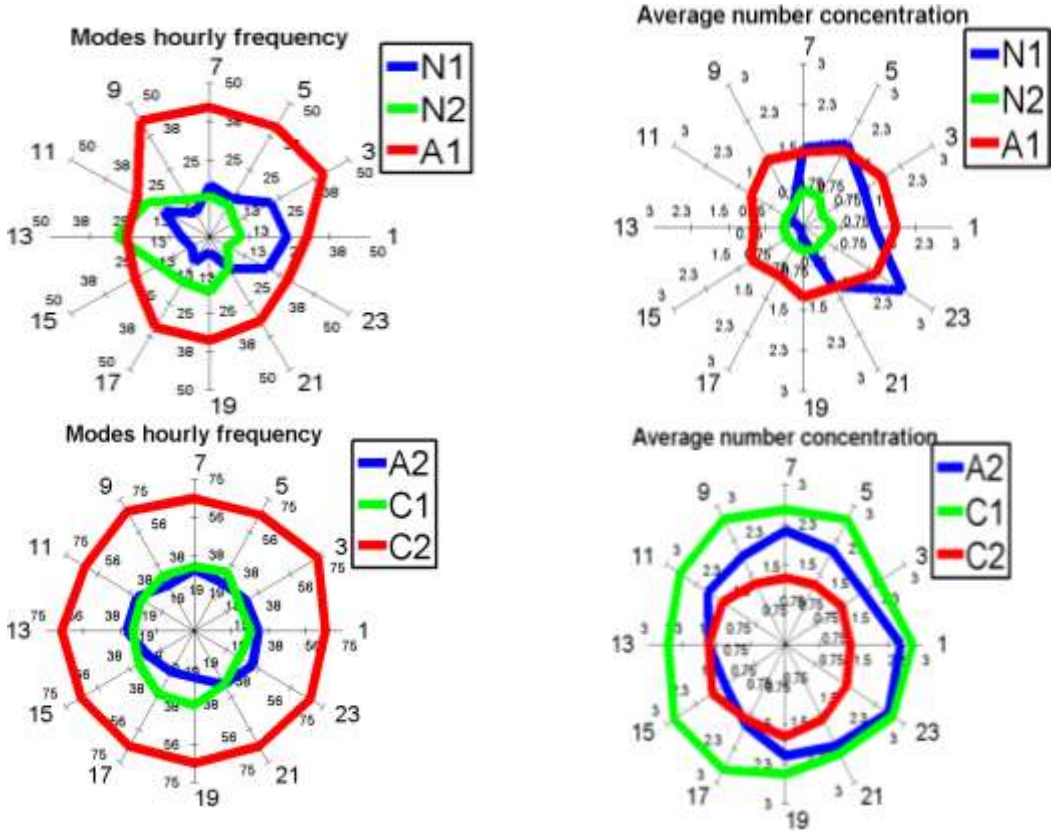

Figure A6: Summer 2012 frequency spider plots for Finokalia. On the left: frequency of occurrence for N1–C2 modes. The numbers 1, 3, 5 correspond to hours of day, while the smaller numbers 50, 38, 25 correspond to frequency of occurrence. On the right side: the average number concentration for all modes in thousands of particles/cm^{-3}.

A1 has a maximum frequency of 44% from 02:00-10:00, N2 has a maximum of 29% and it has its highest values from 10:00-4:00 and N1 has a maximum of 24% at 22:00-4:00. The most frequent mode is C2 which has a maximum of 72% in the interval 2:00-

European Union
European Social Fund
OPERATIONAL PROGRAMME
EDUCATION AND LIFELONG LEARNING
investing in knowledge society
MINISTRY OF EDUCATION & RELIGIOUS AFFAIRS
MANAGING AUTHORITY
NSRF 2007-2013
EUROPEAN SOCIAL FUND
Co-financed by Greece and the European Union

04:00 and its minimum frequency is 64%, C1 has a maximum of 37% at 18:00-20:00, with frequency always above 26% and A2 has its maximum frequency at 22:00-02:00 (34%) and 10:00-14:00.

A1 has a maximum of 1,800 p/cc and it has high values from 22:00-06:00, N2 has a maximum of 700p/cc at 6:00-8:00, N1 has a maximum of 2,300 p/cc at 22:00-24:00. C2 is always between 1,200-1,800 p/cc and C1 is always between 2,300-2,800 p/cc. A2 has a maximum of 2,500 p/cc during 22:00-02:00. Overall, Accumulation and Aitken modes dominate in frequency and number. The particle concentration for N1 is decreasing later at night as coagulation of particles advances. S. Bezantakos et al (2013) reports that above 1,000 meters height over Crete there are aerosol particles mainly consisting of ammonium sulphate and organics. This indicates that katabatic winds, a significant influence to the size distribution can be observed.

Previous studies at Finokalia (A. Asmi et al) reports that the aerosol number size distributions were bimodal for winter with an Aitken mode around 50 nm and Accumulation mode 150 nm. Spring and summer were dominated by strong accumulation mode at around 100 nm. Table A4 demonstrates that both situations exist on the dataset.

European Union
European Social Fund
OPERATIONAL PROGRAMME
EDUCATION AND LIFELONG LEARNING
investing in knowledge society
MINISTRY OF EDUCATION & RELIGIOUS AFFAIRS
MANAGING AUTHORITY
NSRF 2007-2013
EUROPEAN SOCIAL FUND
Co-financed by Greece and the European Union

Table A4: Finokalia most frequent mode combination

	A1_C2	C1	A2_C2	C2	N2_A2_C2	N1_A2_C2
	Median	Median	Median	Median	Median	Median
N1-σg	-	-	-	-	-	1.5
N1-dg	-	-	-	-	-	11
N1-N	-	-	-	-	-	229
N2-σg	-	-	-	-	1.3	-
N2-dg	-	-	-	-	23	-
N2-N	-	-	-	-	244	-
A1-σg	1.5	-	-	-	-	-
A1-dg	46	-	-	-	-	-
A1-N	989	-	-	-	-	-
A2-σg	-	-	1.7	-	1.5	1.6
A2-dg	-	-	73	-	73	78
A2-N	-	-	1,655	-	1,274	1,439
C1-σg	-	1.8	-	-	-	-
C1-dg	-	106	-	-	-	-
C1-N	-	3,480	-	-	-	-
C2-σg	1.5	-	1.5	1.8	1.5	1.4
C2-dg	152	-	169	129	180	190
C2-N	1,809	-	1,202	3,012	843	912
Frequency %	20.2	11.5	10.9	8.5	8.1	6.2

As a conclusion, Accumulation and Aitken modes dominate at the regional background site of Finokalia.

THESSALONIKI

Eptapyrgio site is a typical urban background site at an elevated location. Figure A7 shows the summer 2012 frequency spider plots for Thessaloniki. A1 has a maximum of 3,300 p/cc at 08:00-14:00 and it has another peak from 22:00-24:00 of 3,000p/cc while N2 has a maximum of 2,300p/cc at 10:00-14:00. Nuc1 has a maximum of 1,600 p/cc at 12:00-14:00. C2 is always between 900-1700 p/cc, with its maximum at 10:00-

European Union
European Social Fund
OPERATIONAL PROGRAMME
EDUCATION AND LIFELONG LEARNING
investing in knowledge society
MINISTRY OF EDUCATION & RELIGIOUS AFFAIRS
MANAGING AUTHORITY
NSRF 2007-2013
EUROPEAN SOCIAL FUND
Co-financed by Greece and the European Union

12:00, C1 is always between 1500-3200 p/cc, has a peak at 8:00-10:00 of 3,200p/cc and A2 has a maximum of 3,400 p/cc during 10:00-12:00 and 00:00-02:00 with 3,000 p/cc. A1 has a maximum frequency of 75% at 18:00-20:00, and it appears mostly at day time. N2 has a maximum of 62% and it has high values from 10:00-14:00. The most frequent mode is C2 which is present almost at all times with a maximum of 72% in the interval 2:00-04:00, always above 64%. C1 has a maximum frequency of 30% at 10:00-12:00. A2 has its maximum frequency at 4:00-06:00 (38%), and it has high values mostly at night. We also observe a peak of A2 at 23:00, similar to the situation in Demokritos Athens and Finokalia. Overall we observe that the large Nuclei mode N2, Aitken and the small Accumulation mode have a peak during morning to noon (8:00 to 14:00, probably due to traffic) and 20:00-02:00 (probably due to NBL or katabatic wind). The small Nuclei mode N1 has a peak at the hours with maximum solar radiation, and therefore are attributed to new particle formation. The large accumulation mode is stable throughout the day. Aitken mode is dominant at Thessaloniki station, as it is present at 5 out of 6 most frequent mode combinations. Table A5 shows the Thessaloniki most frequent mode combination

European Union
European Social Fund
OPERATIONAL PROGRAMME
EDUCATION AND LIFELONG LEARNING
investing in knowledge society
MINISTRY OF EDUCATION & RELIGIOUS AFFAIRS
MANAGING AUTHORITY
NSRF 2007-2013
programme for development
EUROPEAN SOCIAL FUND
Co-financed by Greece and the European Union

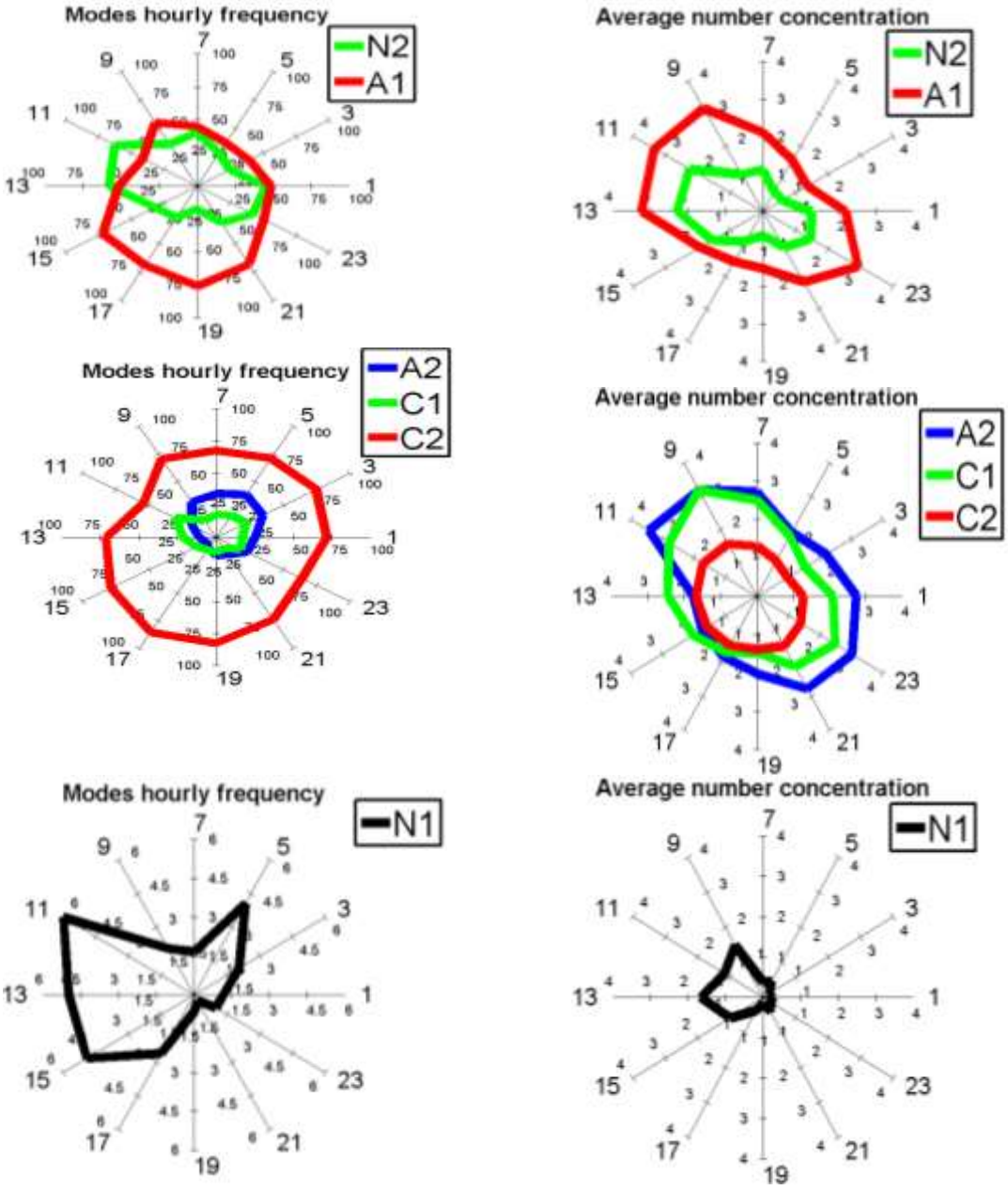

Figure A7: Summer 2012 frequency spider plots for Thessaloniki. On the left: frequency of occurrence for N1–C2 modes. The numbers 1, 3, 5 correspond to hours of day, while smaller numbers 100, 75, 50, 25 correspond to frequency of occurrence. On the right side: the average number concentration for all modes in thousands of particles/cm^{-3}.

European Union
European Social Fund
OPERATIONAL PROGRAMME
EDUCATION AND LIFELONG LEARNING
investing in knowledge society
MINISTRY OF EDUCATION & RELIGIOUS AFFAIRS
MANAGING AUTHORITY
NSRF 2007-2013
programme for development
EUROPEAN SOCIAL FUND
Co-financed by Greece and the European Union

Table A5: Thessaloniki most frequent mode combination

	A1_C2	N2_A1_C2	N2_A2_C2	N2_C2	A2_C2	A2
	Median	Median	Median	Median	Median	Median
N2-σg	-	1.4	1.6	1.6	-	-
N2-Dg	-	21	23	26	-	-
N2-N	-	853	729	1,326	-	-
A1-σg	1.9	1.5	-	-	-	-
A1-Dg	41	48	-	-	-	-
A1-N	1,782	1,561	-	-	-	-
A2-σg	-	-	1.5	-	2.3	2.4
A2-Dg	-	-	69	-	68	77
A2-N	-	-	1,179	-	2,040	3,694
C1-σg	-	-	-	-	-	-
C1-Dg	-	-	-	-	-	-
C1-N	-	-	-	-	-	-
C2-σg	1.6	1.7	1.5	1.9	1.5	-
C2-Dg	175	158	197	140	208	-
C2-N	1,387	1,834	994	1,763	805	-
Frequency %	35	11	8	8	7	6

European Union
European Social Fund
OPERATIONAL PROGRAMME
EDUCATION AND LIFELONG LEARNING
investing in knowledge society
MINISTRY OF EDUCATION & RELIGIOUS AFFAIRS
MANAGING AUTHORITY
NSRF 2007-2013
EUROPEAN SOCIAL FUND
Co-financed by Greece and the European Union

PATRAS

The analysis for Patras includes a central urban and a suburban background site. Figure A8 shows the summer 2012 frequency spider plots for Patra City Center.

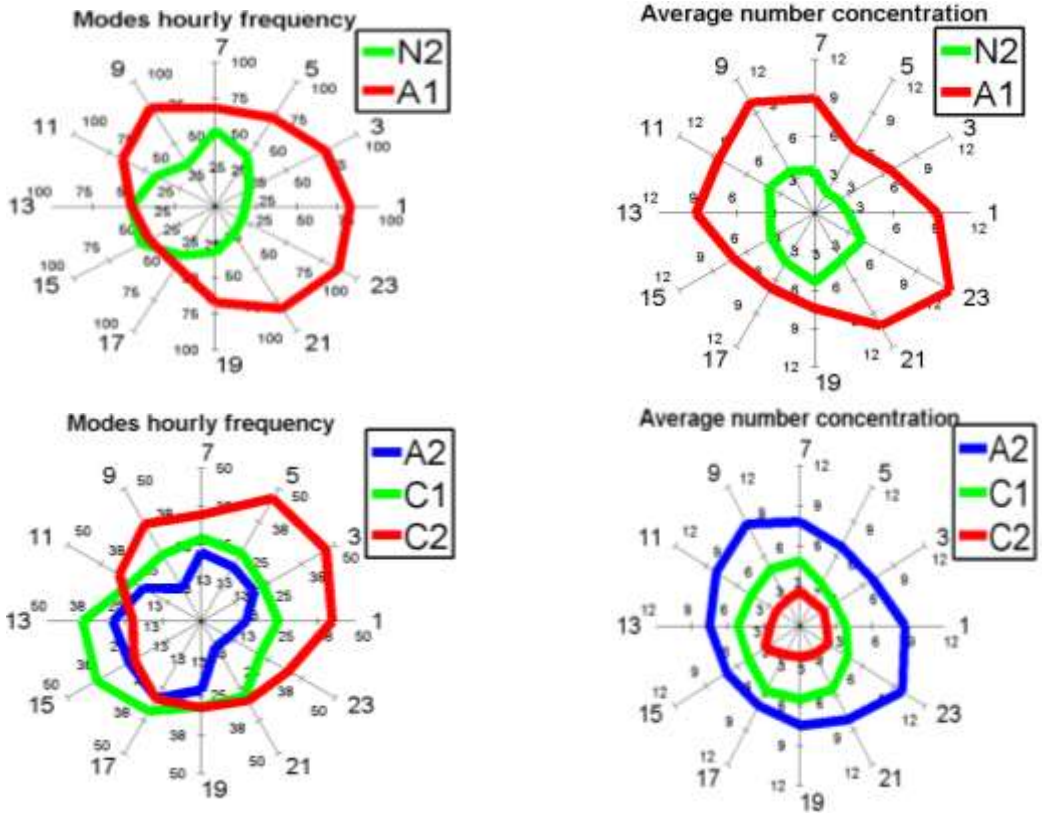

Figure A8: Summer 2012 frequency spider plots for Patra City Center. On the left: frequency of occurrence for N1–C2 modes. The numbers 1, 3, 5 correspond to hours of day, while smaller numbers 100, 75, 50 correspond to frequency of occurrence. On the right side: the average number concentration for all modes in thousands of particles/cm^{-3}.

A1 has a maximum of 12,000 p/cc from 22:00-24:00, N2 has a maximum of 5,400 p/cc and it has high values from 18:00-20:00. C2 has a maximum of 3,400 p/cc in the interval 14:00-16:00, always between 2,000-3,400 p/cc, C1 has a maximum of 5,500 p/cc at 16:00-18:00, always between 3,300-5,300 p/cc, A2 has a maximum of 9,800 p/cc

European Union
European Social Fund
OPERATIONAL PROGRAMME
EDUCATION AND LIFELONG LEARNING
investing in knowledge society
MINISTRY OF EDUCATION & RELIGIOUS AFFAIRS
MANAGING AUTHORITY
NSRF 2007-2013
EUROPEAN SOCIAL FUND
Co-financed by Greece and the European Union

during 22:00-00:00A1 is the most frequent mode with two peak hour intervals: 87%-from 22-24:00 and 80% at 8:00-10:00, N2 has a maximum of 53% and it has high values from 6:00-08:00 and 12:00-16:00, C2 has a maximum of 47% in the interval 22:00-06:00, C1 has a maximum of 39% at 12:00-16:00 and A2 has a frequency of 29% during 12:00-18:00. N1 mode could not be distinguished, although we observe an increase of particle number as we approach the mobility diameter of 10 nm in Figure A8. This could be attributed to the fact that larger particles at high concentrations act as sink, adsorbing gaseous pollutants and not allowing very small particles to grow significantly enough. Table A6 depicts the Patra city center most frequent mode combination Overall, N2, A1 and A2 modes have morning to noon (06:00-14:00) and late evening peaks (20:00-02:00) while modes C1, C2 are stable throughout the day. Aitken mode dominates Patra City Center station, as it is present at 5 out of 6 most frequent mode combinations

Table A6: Patra city center most frequent mode combination

	A1_C2	A1	A1_C1	N2_A2	N2_Ac1	N2_A1
	Median	Median	Median	Median	Median	Median
N2-σg	-	-	-	1.49	1.61	1.34
N2-Dg	-	-	-	24	27	23
N2-N	-	-	-	2,503	3,492	2,460
A1-σg	2.01	2.04	1.87	-	-	2.08
A1-Dg	43	50	37	-	-	52
A1-N	7,175	10,300	5,870	-	-	7,862
A2-σg	-	-	-	1.86	-	-
A2-Dg	-	-	-	77	-	-
A2-N	-	-	-	6,592	-	-
C1-σg	-	-	1.61	-	1.72	-
C1-Dg	-	-	109	-	101	-

European Union
European Social Fund
OPERATIONAL PROGRAMME
EDUCATION AND LIFELONG LEARNING
investing in knowledge society
MINISTRY OF EDUCATION & RELIGIOUS AFFAIRS
MANAGING AUTHORITY
NSRF 2007-2013
EUROPEAN SOCIAL FUND
Co-financed by Greece and the European Union

C1-N	**-**	**-**	**3,627**	**-**	**5,026**	**-**
C2-σg	**1.45**	**-**	**-**	**-**	**-**	**-**
C2-Dg	**137**	**-**	**-**	**-**	**-**	**-**
C2-N	**1,972**	**-**	**-**	**-**	**-**	**-**
Frequency %	**27**	**15**	**15**	**13**	**9**	**5**

Figure A9 shows the summer 2012 frequency spider plots for ICE–HT Patra. C2 has a maximum frequency of 50% in the interval 4:00-10:00, C1 is close to 50% frequency from 13:00 to 01:00 and A2 has a frequency of 41% during 04:00-06:00. A1 has high frequency from 08:00-12:00 and 20:00-02:00.

A1 has a maximum of 3,000 p/cc from 20:00-00:00 and 10:00-12:00. N2 has a maximum of 4,000 p/cc and it has high values from 12:00-14:00. N1 has a maximum of 5,000 p/cc at 6:00-12:00, but it also has a peak at 22:00-24:00 at 6,000 p/cc. The situation is similar to Finokalia and Demokritos Athens. C2 is always between 2,000-3,000 p/cc. C1 has a maximum of 6,000 p/cc at 8:00-12:00, always between 3,000-6,000 p/cc. A2 has a maximum of 11,000 p/cc during 8:00-10:00, the rest of the time it lies between 3,000-6,000 p/cc, with a small maximum at 21:00.

The number concentration is increasing for Aitken mode in morning traffic hours (around 9 o' clock) and at around 22:00 at night, probably due to NBL. We observe the same pattern for the small Nuclei mode which is very infrequent, while the large Nuclei mode (N2) has its maximum particle number at 13:00. Aitken and accumulation modes dominate in ICE–HT Patra station, as it is shown in Table A7.

European Union
European Social Fund
OPERATIONAL PROGRAMME
EDUCATION AND LIFELONG LEARNING
investing in knowledge society
MINISTRY OF EDUCATION & RELIGIOUS AFFAIRS
MANAGING AUTHORITY
NSRF 2007-2013
EUROPEAN SOCIAL FUND
Co-financed by Greece and the European Union

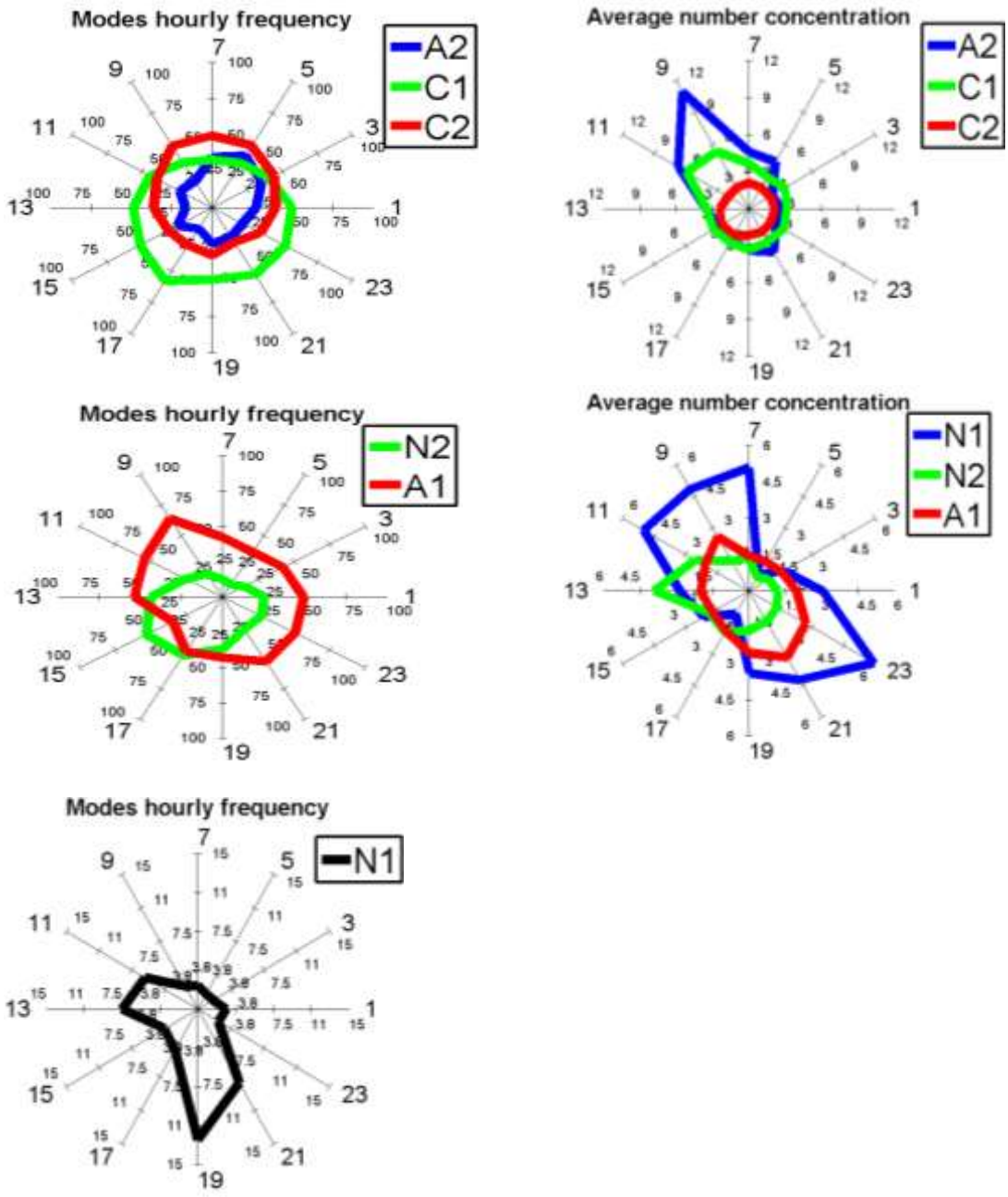

Figure A9: Summer 2012 frequency spider plots for ICE–HT Patra. On the left: frequency of occurrence for N1–C2 modes. The numbers 1, 3, 5 correspond to hours of day, while smaller numbers 100, 75, 50 correspond to frequency of occurrence. On the right side: the average number concentration for all modes in thousands of particles/cm^{-3}.

European Union
European Social Fund
OPERATIONAL PROGRAMME
EDUCATION AND LIFELONG LEARNING
investing in knowledge society
MINISTRY OF EDUCATION & RELIGIOUS AFFAIRS
MANAGING AUTHORITY
NSRF 2007-2013
EUROPEAN SOCIAL FUND
Co-financed by Greece and the European Union

Table A7: ICE-HT PATRA most frequent mode combination

	A1_C2 Median	A1_C1 Median	N2_C1 Median	A2_C2 Median	C1 Median	A2 Median
N2-σg	-	-	1.5	-	-	-
N2-dg	-	-	24	-	-	-
N2-N	-	-	938	-	-	-
A1-σg	1.9	1.9	-	-	-	-
A1-dg	46	39	-	-	-	-
A1-N	1,635	1,560	-	-	-	-
A2-σg	-	-	-	1.9	-	1.9
A2-dg	-	-	-	71	-	77
A2-N	-	-	-	1,878	-	3,999
C1-σg	-	1.6	1.7	-	1.7	-
C1-dg	-	111	105	-	102	-
C1-N	-	2,770	3,311	-	4,037	-
C2-σg	1.6	-	-	1.5	-	-
C2-dg	134	-	-	142	-	-
C2-N	2,312	-	-	1,402	-	-
Frequency %	20	16	12	12	9	6

A3. Conclusions

SMPS particle number concentrations at 5 stations in Greece during the summer of 2012 were investigated.

At Demokritos Athens and ICE–HT Patra Urban Background stations, the number concentration is almost twice as high as Finokalia with a peak at 100 nm. After modal analysis, the diurnal variability of the concentrations in Demokritos Athens indicate that during night time, the katabatic wind is frequently bringing to the ground air from layers with high particle concentration, especially in Nuclei and the small Aitken mode. The Aitken mode dominates in number and frequency at night (20:00-04:00). An aged accumulation mode is dominating both sites, being stable throughout day and night. At

European Union
European Social Fund
OPERATIONAL PROGRAMME
EDUCATION AND LIFELONG LEARNING
investing in knowledge society
MINISTRY OF EDUCATION & RELIGIOUS AFFAIRS
MANAGING AUTHORITY
NSRF 2007-2013
EUROPEAN SOCIAL FUND
Co-financed by Greece and the European Union

Demokritos Athens the most frequent combinations are Nuclei mode - Accumulation mode.

ICE-HT shows a number concentration increase for the Aitken mode in morning traffic hours (around 9:00) and at 22:00 at night. Nucleation mode is not frequent and we observe increased frequency of Aitken and Accumulation modes. The same pattern is observed for the small Nuclei mode which is very infrequent, while the large Nuclei mode (N2) has its maximum particle number at 13:00.

In Finokalia we also observe an infrequent small Nuclei mode (N1), especially at night. The large Aitken mode has increased number concentration at night. The mechanism for the above mentioned observations needs to be investigated. Finokalia particle size distribution geometric mean diameter displays a peak approximately at 100 nm and the lowest particle number concentration values. It probably represents aerosol of intermediate aging. Accumulation and Aitken modes dominate at the regional background site of Finokalia.

At Thessaloniki a well aged accumulation mode is observed, as well as freshly emitted road traffic exhaust. The diurnal variation in Thessaloniki shows an increase in frequency for the large Nuclei mode, the Aitken mode and the small Accumulation mode during 22:00-02:00. The small nuclei mode has low frequency and particle number concentration. Aitken mode is dominant at Thessaloniki station, as it is present at 5 out of 6 most frequent mode combinations observed. Overall, an increase in particle number concentration is observed at 08:00-14:00 and 20:00-02:00.

The Patra City Center station has the highest peak values. It displays its peak approximately at 60 nm, indicating a domination of freshly emitted road traffic exhaust. In Patra City Center we have increased frequency in the morning hours for N2, A1 and A2 modes. The A1 mode has the highest contribution to particle number especially in the morning traffic hours (8:00-14:00), but also at night (22:00-00:00). Overall, Aitken

European Union
European Social Fund
OPERATIONAL PROGRAMME
EDUCATION AND LIFELONG LEARNING
investing in knowledge society
MINISTRY OF EDUCATION & RELIGIOUS AFFAIRS
MANAGING AUTHORITY
NSRF 2007-2013
programme for development
EUROPEAN SOCIAL FUND
Co-financed by Greece and the European Union

mode dominates Patra City Center station, as it is present at 5 out of 6 most frequent mode combinations. The frequency of occurrence and number concentration of the Accumulation mode is stable throughout the day, even though we would expect it to increase at night time due to particle removal processes (C2 has higher frequency but smaller number concentration).

The 95th percentile highest values in all 5 sites often occur simultaneously for the Nucleation and less frequently for the Accumulation modes. This indicates favorable conditions for their potential sources at a wide regional scale or common origin of air mass transported from Northern or Eastern Europe and Turkey.

European Union
European Social Fund
OPERATIONAL PROGRAMME
EDUCATION AND LIFELONG LEARNING
investing in knowledge society
MINISTRY OF EDUCATION & RELIGIOUS AFFAIRS
MANAGING AUTHORITY
NSRF 2007-2013
EUROPEAN SOCIAL FUND
Co-financed by Greece and the European Union

A4. References

Asmi A., A. Wiedensohler, P. Laj, A.-M. Fjaeraa, K. Sellegri, W. Birmili, E.Weingartner, U. Baltensperger,V. Zdimal, N. Zikova, J.-P. Putaud, A. Marinoni, P. Tunved, H.-C. Hansson, M. Fiebig, N. Kivekäs,H. Lihavainen, E. Asmi, V. Ulevicius, P. P. Aalto, E. Swietlicki, A. Kristensson, N. Mihalopoulos,N. Kalivitis, I. Kalapov, G. Kiss, G. de Leeuw,17, B. Henzing, R. M. Harrison, D. Beddows, C. O'Dowd,S. G. Jennings, H. Flentje, K. Weinhold, F. Meinhardt, L. Ries, and M. Kulmala: Number size distributions and seasonality of submicron particles in Europe 2008–2009, Atmos. Chem. Phys., 11, 5505–5538, 2011.

Beddows D. C. S., M. Dall'Osto, R. M. Harrison, M. Kulmala, A. Asmi, A. Wiedensohler, P. Laj,
A.M. Fjaeraa, K. Sellegri, W. Birmili, N. Bukowiecki, E.Weingartner, U. Baltensperger, V. Zdimal,
N. Zikova, J.-P. Putaud, A. Marinoni, P. Tunved, H.-C. Hansson, M. Fiebig, N. Kivekäs, E. Swietlicki,
H. Lihavainen, E. Asmi, V. Ulevicius, P. P. Aalto, N. Mihalopoulos, N. Kalivitis, I. Kalapov, G. Kiss,
G. de Leeuw, B. Henzing, C. O'Dowd, S. G. Jennings, H. Flentje, F. Meinhardt, L. Ries, H. A. C. Denier van der Gon, and A. J. H. Visschedijk: Variations in tropospheric submicron particle size distributions across the European continent 2008–2009, Atmos. Chem. Phys., 14, 4327–4348, 2014.

European Union
European Social Fund
OPERATIONAL PROGRAMME
EDUCATION AND LIFELONG LEARNING
investing in knowledge society
MINISTRY OF EDUCATION & RELIGIOUS AFFAIRS
MANAGING AUTHORITY
NSRF 2007-2013
programme for development
EUROPEAN SOCIAL FUND
Co-financed by Greece and the European Union

Bezantakos S., K. Barmpounis, M. Giamarelou, E. Bossioli, M. Tombrou, N. Mihalopoulos, K. Eleftheriadis, J. Kalogiros, J. D. Allan, A. Bacak, C. J. Percival, H. Coe, and G. Biskos: Chemical composition and hygroscopic properties of aerosol particles over the Aegean Sea, Atmos. Chem. Phys., 13, 11595–11608, 2013

Bond, T. C., Doherty, S. J., Fahey, D. W., Forster, P. M., Berntsen, T., DeAngelo, B. J., Flanner, M. G., Ghan, S., Kärcher, B., Koch, D., Kinne, S., Kondo, Y., Quinn, P. K., Sarofim, M. C., Schultz, M. G., Schulz, M., Venkataraman, C., Zhang, H., Zhang, S., Bellouin, N., Guttikunda, S. K., Hopke, P. K., Jacobson, M. Z., Kaiser, J. W., Klimont, Z., Lohmann, U., Schwarz, J. P., Shindell, D., Storelvmo, T., Warren, S. G. and Zender, C. S.: Bounding the role of black carbon in the climate system: A scientific assessment, J. Geophys. Res. Atmospheres, 118(11), 5380–5552, doi:10.1002/jgrd.50171, 2013.

Chaloulakou, A., Kassomenos, P., Grivas, G. and Spyrellis, N.: Particulate matter and black smoke concentration levels in central Athens, Greece, Environ. Int., 31(5), 651–659, doi:10.1016/j.envint.2004.11.001, 2005.

Cohen, A. J., Anderson, H. R., Ostro, B., Pandey, K. D., Krzyzanowski, M., Künzli, N., Gutschmidt, K., Pope III, C. A., Romieu, I., Samet, J. M. and others: Urban air pollution, Comp. Quantif. Health Risks, 2, 1353–1433, 2004.

European Union
European Social Fund
OPERATIONAL PROGRAMME
EDUCATION AND LIFELONG LEARNING
investing in knowledge society
MINISTRY OF EDUCATION & RELIGIOUS AFFAIRS
MANAGING AUTHORITY
NSRF 2007-2013
EUROPEAN SOCIAL FUND
Co-financed by Greece and the European Union

Eleftheriadis K., I. Colbeck, C. Housiadas, M. Lazaridis, N. Mihalopoulos, C. Mitsakou, J. Smolík, V. Ždímal: Size distribution, composition and origin of the submicron aerosol in the marine boundary layer during the eastern Mediterranean "SUB-AERO" experiment, Atmospheric Environment Volume 40, Issue 32, October 2006, Pages 6245–6260

Flocas H. A., C. G. Helmis, S. N. Blikas, D. N. Asimakopoulos, J. G. Bartzis, and D. G. Deligiorgi: Mean Characteristics of the Katabatic Flow of a 1024m High Knife Edge Mountain, Theor. Appl. Climatol. 59, 237-249 (1998).

Haywood, J. and Boucher, O.: Estimates of the direct and indirect radiative forcing due to tropospheric aerosols: A review, Rev. Geophys., 38, 513–543, 2000

Hussein, T., Dal Maso, M., Petäjä, T., Koponen, I. K., Paatero, P.,Aalto, P. P., Hämeri, K., and Kulmala, M.: Evaluation of an automatic algorithm for fitting the particle number size distributions, Boreal Environ. Res., 10, 337–355, 2005.

Kalivitis, N., Kerminen, V.-M., Kouvarakis, G., Stavroulas, I., Bougiatioti, A., Nenes, A., Manninen, H. E., Petäjä, T., Kulmala, M., and Mihalopoulos, N.: Atmospheric new particle formation as source of CCN in the Eastern Mediterranean marine boundary layer, Atmos. Chem. Phys. Discuss., 15, 11143-11178, doi:10.5194/acpd-15-11143-2015, 2015.

European Union
European Social Fund
OPERATIONAL PROGRAMME
EDUCATION AND LIFELONG LEARNING
investing in knowledge society
MINISTRY OF EDUCATION & RELIGIOUS AFFAIRS
MANAGING AUTHORITY
NSRF 2007-2013
programme for development
EUROPEAN SOCIAL FUND
Co-financed by Greece and the European Union

Kambezidis, H. D., Weidauer, D., Melas, D. and Ulbricht, M.: Air quality in the Athens basin during sea breeze and non-sea breeze days using laser-remote-sensing technique, Atmos. Environ., 32(12), 2173–2182, doi:10.1016/S1352-2310(97)00409-3, 1998.

Laden, F., Schwartz, J., Speizer, F. E., and Dockery, D. W.: Reduction in Fine Particulate Air Pollution and Mortality: Extended Follow-up of the Harvard Six Cities Study, Am. J. Respir. Crit. Care Med., 173, 667–672, doi:10.1164/rccm.200503-443OC, 2006.

Lelieveld, J., Berresheim, H., Borrmann, S., Crutzen, P., Dentener, F., Fischer, H., Feichter, J., Flatau, P., Heland, J., Holzinger, R., Korrmann, R., Lawrence, M., Levin, Z., Markowicz, K., Mihalopoulos, N., Minikin, A., Ramanathan, V., de Reus, M., Roelofs, G., Scheeren, H., Sciare, J., Schlager, H., Schultz, M., Siegmund, P., Steil, B., Stephanou, E., Stier, P., Traub, M., Warneke, C., Williams, J., and Ziereis, H.: Global air pollution crossroads over the Mediterranean, Science, 298, 794–799, doi: 10.1126/science.1075457, 2002.

Lohmann, U. and Feichter, J.: Global indirect aerosol effects: a review, Atmos. Chem. Phys., 5, 715–737, doi:10.5194/acp-5-715-2005, 2005.

Ma N.,W. Birmili: Estimating the contribution of photochemical particle formation to ultrafine particle number averages in an urban atmosphere, Science of the Total Environment 512–513 (2015) 154–166.

European Union
European Social Fund
OPERATIONAL PROGRAMME
EDUCATION AND LIFELONG LEARNING
investing in knowledge society
MINISTRY OF EDUCATION & RELIGIOUS AFFAIRS
MANAGING AUTHORITY
NSRF 2007-2013
EUROPEAN SOCIAL FUND
Co-financed by Greece and the European Union

Mihalopoulos, N., Stephanou, E., Kanakidou, M., Pilitsidis, S., and Bousquet, P.: Tropospheric aerosol ionic composition in the Eastern Mediterranean region, Tellus B, 49, 314–326, 1997.

Mølgaard Bjarke, WolframBirmili, SamClifford, AndreasMassling, KostasEleftheriadis, MichaelNorman, StergiosVratolis, Birgit Wehner, Jukka Corander, KaarleHämeri, TareqHussein: Evaluation of a statistical forecast model for size-fractionated urban particle number concentrations using data from five European cities, Journal of AerosolScience66(2013) 96–110.

Oberdörster, G., Oberdörster, E., and Oberdörster, J.: Nanotoxicology: An Emerging Discipline Evolving from Studies of Ultrafine Particles, Environ. Health Persp., 113, 7, doi:10.1289/ehp.7339,
2005.

Pikridas, M., Riipinen, I., Hildebrandt, L., Kostenidou, E.., Manninen, H., Mihalopoulos, N., Kalivitis, N., Burkhart, J.F., Stohl, A., Kulmala, M., Pandis, S.N.:New particle formation at a remote site in the eastern Mediterranean, Journal of Geophysical Research: Atmospheres, Volume 117, Issue 12, 2012, Article number D12205

European Union
European Social Fund
OPERATIONAL PROGRAMME
EDUCATION AND LIFELONG LEARNING
investing in knowledge society
MINISTRY OF EDUCATION & RELIGIOUS AFFAIRS
MANAGING AUTHORITY
NSRF 2007-2013
EUROPEAN SOCIAL FUND
Co-financed by Greece and the European Union

Pikridas Michael,Antonios Tasoglou, Kalliopi Florou, Spyros N. Pandis: Characterization of the origin of fine particulate matter in a medium size urban area in the Mediterranean, Atmospheric Environment 80 (2013) 264e274

Pope, C. A. I. and Dockery, D. W.: Health Effects of Fine Particulate Air Pollution: Lines that Connect, JAPCA J. Air Waste Ma., 56, 709–742, 2006.

Progiou, A. and Ziomas, I.: Twenty-Year Road Traffic Emissions Trend in Greece, Water. Air. Soil Pollut., 223(1), 305–317, doi:10.1007/s11270-011-0859-9, 2011.

Seinfeld, J. H. and Pandis, S. N.: Atmospheric chemistry and physics: from air pollution to climate change, John Wiley & Sons. [online] Available from: http://books.google.fr/books?hl=fr&lr=&id=YH2K9eWsZOcC&oi=fnd&pg=PA1991&dq=senfield+pandis&ots=hJbxOo3YFs&sig=eVwjRAF1La4JPCjeYEhePZeKHxg (Accessed 5 May 2014), 2012.

Voutsa D., C. Samara, Th. Kouimtzis, K. Ochsenkühn: Elemental composition of airborne particulate matter in the multi-impacted urban area of Thessaloniki, Greece, Atmospheric Environment 36 (2002) 4453–4462.

Wiedensohler, A., Birmili, W., Nowak, A., Sonntag, A., Weinhold, K., Merkel, M., Wehner, B., Tuch, T., Pfeifer, S., Fiebig, M., Fjäraa, A. M., Asmi, E., Sellegri, K., Depuy, R., Venzac, H., Villani, P., Laj, P., Aalto, P., Ogren, J. A., Swietlicki, E.,

European Union
European Social Fund
OPERATIONAL PROGRAMME
EDUCATION AND LIFELONG LEARNING
investing in knowledge society
MINISTRY OF EDUCATION & RELIGIOUS AFFAIRS
MANAGING AUTHORITY
NSRF 2007-2013
programme for development
EUROPEAN SOCIAL FUND
Co-financed by Greece and the European Union

Williams, P., Roldin, P., Quincey, P., Hüglin, C., Fierz-Schmidhauser, R., Gysel, M., Weingartner, E., Riccobono, F., Santos, S., Grüning, C., Faloon, K., Beddows, D., Harrison, R., Monahan, C., Jennings, S. G., O'Dowd, C. D., Marinoni, A., Horn, H.-G., Keck, L., Jiang, J., Scheckman, J., McMurry, P. H., Deng, Z., Zhao, C. S., Moerman, M., Henzing, B., de Leeuw, G., Löschau, G., and Bastian, S.: Mobility particle size spectrometers: harmonization of technical standards and data structure to facilitate high quality long-term observations of atmospheric particle number size distributions, Atmos. Meas. Tech., 5, 657-685, doi:10.5194/amt-5-657-2012, 2012.

European Union
European Social Fund
OPERATIONAL PROGRAMME
EDUCATION AND LIFELONG LEARNING
investing in knowledge society
MINISTRY OF EDUCATION & RELIGIOUS AFFAIRS
MANAGING AUTHORITY
NSRF 2007-2013
programme for development
EUROPEAN SOCIAL FUND
Co-financed by Greece and the European Union

Activity 4: Variability of chemical composition of atmospheric aerosol

A. Spatial distribution of summertime particulate matter and its composition in Greece

A1 Experimental Description

An intensive field campaign was conducted from June 8 to July 26, 2012 at seven different sampling sites distributed across Greece. In this section, a brief description of each sampling site and its surroundings is provided along with details of the instrumentation deployed at each site, followed by a summary of sample analysis and the analytical methodologies used in this study.

A1.1. Sampling sites and instrumentation

The location of each of the seven sampling sites is shown in suuplure A1 while a summary of the instrumentation used in each site is given in Table A1. The sampling sites are characterized as remote, rural, suburban or urban based on criteria suggested by the European Environment Agency (Larssen et al., 1999).

Patras: city center (PAT-C): The sampling station was located in the city center of Patras (38° 15' N, 21° 44' E), the third largest city in Greece with a population of around 250 thousand inhabitants. Patras is situated in the western part of Greece at the foothills of mountain Panachaikon overlooking the Gulf of Patras. The sampling site, referred as PAT-C here after, was located on the roof of a building in the center of the city at an elevation of 30 m above ground. PAT-C is characterized as an urban background site with possible local air pollution sources being road traffic close to the sampling station.

European Union
European Social Fund
OPERATIONAL PROGRAMME
EDUCATION AND LIFELONG LEARNING
investing in knowledge society
MINISTRY OF EDUCATION & RELIGIOUS AFFAIRS
MANAGING AUTHORITY
NSRF 2007-2013
EUROPEAN SOCIAL FUND
Co-financed by Greece and the European Union

Also, a small industrial zone is situated 16 km southwest of the city centre which contains some facilities (food and beverages, pharmaceuticals, timber) with low impact on air quality. The port of Patras is approximately 1 km away from the site and is one of the largest ones in Greece with heavy ship traffic throughout the year, especially during summer.

From June 9 to July 26 2012, a Partisol Federal Reference Method (FRM) air sampler (Rupprecht & Patashnick Co., Inc) operated at a flow of 16.7 L min^{-1} was used to collect $PM_{2.5}$ samples every 24 h on PTFE filters (Whatman, PTFE, White Plain,1 μm 47 mm). The $PM_{2.5}$ scattering coefficient at a wavelength of 530 nm was measured continuously using a nephelometer (Aurora - 1000F, Ecotech). The nephelometer inlet incorporated a heating element to dry the aerosol sample.

Patras: Rio suburb (PAT-S): The sampling station was located 7 km northeast of the city centre (38° 18' N, 21° 47' E) in the Institute of Chemical Engineering Science (ICEHT/FORTH) at an elevation of 85 m above the sea surface level. The area is surrounded by olive trees while the coast is approximately 3 km away. A major road is at a distance of 1 km.

From June 9 to July 26, 2012 a Super Speciation Air Sampling System Sampler (Met One SuperSASS^{TM}) operated at a flow rate of 6.7 L min^{-1} was used to collect $PM_{2.5}$ samples every 24 h, both on PTFE (Whatman, PTFE, White Plain, 0.2 μm 47 mm) and on quartz (Pall 2500 QAO-UP 47 mm) filters. Also, a Tandem Element Oscillating Microbalance (TEOM) monitor (Thermo model 1405-DF) (Patashnick et al., 1991) operated at a flow rate of 3 L min^{-1} was used to measure continuously dried $PM_{2.5}$ and PM_{10} mass concentrations. The size-resolved chemical composition of aerosol (non-refractory PM_1 species) was monitored using a High-Resolution Time-of-Flight Aerosol Mass Spectrometer (HR-ToF-AMS, Aerodyne) from June 9 to 26. The aerosol absorption was monitored continuously by a Multi Angle Absorption Photometer (MAAP, Thermo model 5012). The MAAP measure the amount of light at 670 nm that

European Union
European Social Fund
OPERATIONAL PROGRAMME
EDUCATION AND LIFELONG LEARNING
investing in knowledge society
MINISTRY OF EDUCATION & RELIGIOUS AFFAIRS
MANAGING AUTHORITY
NSRF 2007-2013
programme for development
EUROPEAN SOCIAL FUND
Co-financed by Greece and the European Union

is transmitted and scattered back from a particle laden glass fibre filter (Petzold et al., 2004)). A suite of gas monitors for the continuous measurements of SO_2 (Teledyne Monitor 100EU), NO_x (Teledyne Monitor 201E), O_3 (Teledyne Monitor 400E) were used throughout the sampling period. Finally, a Proton Transfer Reaction Mass Spectrometer (PTR-MS 500, Ionicon Analytik) was used for the measurement of the concentrations of tens of volatile organic compounds (VOCs) from June 9 to 26.

Thessaloniki: (THES-S): The sampling station was located at Eptapyrgio a suburb of Thessaloniki (40° 37' N, 23° 02' E), the second largest city in Greece with a population of 1.1 million inhabitants. THES-S is situated in the northern part of Greece. The sampling site was 5 km northeast of the city center at an elevation of 174 m above sea level. THES-S is characterized as a suburban background site with possible local air pollution sources being a major road at a distance of approximately 1 km and an industrial region (food industries, structural raw materials, iron, steel and aluminium industries, petrochemical facilities) located at a distance of approximately 12 km.

During June 9 to July 22 2012, a Speciation Air Sampling System Sampler (Met One SASS^{TM}) operated at a flow of 6.7 L min^{-1} was used to collect $PM_{2.5}$ samples every 24 h, either on PTFE (Whatman, PTFE, White Plain, 0.2 μm 47 mm) or quartz (Pall 2500 QAO-UP 47 mm) filters.

Athens: Demokritos suburbs (ATH-S): The sampling station was located 12 km from the city centre of Athens (37° 59' N, 23° 49' E) the capital and the largest city of Greece with a population of around 3.8 million people. The basin is surrounded by four mountains: mountain Aegaleo (469 m) to the west, Parnitha (1413 m) to the north, Penteli (1109 m) to the northeast and Hymettus (1026 m) to the east. The sampling site, referred as ATH-S hereafter, was on the premises of the National Center for Scientific Research Demokritos located at the foothills of mountain Hymettus, at an elevation of 280 m above sea level and surrounded by pine trees. ATH-S is characterized as a

European Union
European Social Fund
OPERATIONAL PROGRAMME
EDUCATION AND LIFELONG LEARNING
investing in knowledge society
MINISTRY OF EDUCATION & RELIGIOUS AFFAIRS
MANAGING AUTHORITY
NSRF 2007-2013
programme for development
EUROPEAN SOCIAL FUND
Co-financed by Greece and the European Union

suburban background site with possible local air pollution sources being a major road at a distance of 500 m.

During July 3 to 26 2012, a low volume custom-made sampler operated at a flow of 2.3 m^3 hr^{-1}, was used to collect $PM_{2.5}$, $PM_{2.5-10}$ and PM_{10} samples every 24 h, on PTFE (Zefluor 2.0 μm, 47 mm supported PTFE, PALL) filters. The aerosol absorption was monitored continuously by Magee Scientific Aethalometer (Model AE-31) operated at 880 nm wavelength. A nephelometer was also used (Aurora - 1000F, Ecotech) connected to a diffusion drier. The PM_{10} scattering coefficient was measured at 3 wavelengths: 450, 520 and 700 nm. Continuous measurements of O_3 and NO_x using high-sensitivity gas analyzers were also conducted. A Proton Transfer Reaction Mass Spectrometer (PTR-MS 500, Ionicon Analytik) was used for the characterization of the volatile organic compounds (VOCs). Finally, the size-resolved chemical composition of aerosol (non-refractory PM_1 species) was monitored using HR-ToF-AMS (Aerodyne) during July 12 to 26.

Athens Penteli: (ATH-B): The sampling station was located 17 km from the center of Athens (38° 3' N, 23° 52' E) in the premises of the National Observatory of Athens (NOA) in Penteli, at an elevation of 495 m above the sea surface level. ATH-B is characterized as a suburban background site with local air pollution sources being vehicular emissions and resuspension of mineral dust due to the traffic on the nearby dust roads (Kanakidou et al., 2011).

During June 9 to July 26 2012, a Dichotomous Partisol sampler (R&P Co), operated at a flow of 15 L min^{-1}, was used to collect $PM_{2.5}$ samples every 24 h, on quartz fiber (4.7 cm, Whatman QMA) filters. Aerosol absorption was monitored continuously by a Particle Soot Absorption Photometer (Radiance Research) operated at 3 wavelengths (470, 522, 660 nm). PM_{total} aerosol scattering was measured at 530 nm using a nephelometer (M903 Radiance Research). Continuous measurements of O_3 by a Thermo Ozone analyzer were also conducted.

European Union
European Social Fund
OPERATIONAL PROGRAMME
EDUCATION AND LIFELONG LEARNING
investing in knowledge society
MINISTRY OF EDUCATION & RELIGIOUS AFFAIRS
MANAGING AUTHORITY
NSRF 2007-2013
programme for development
EUROPEAN SOCIAL FUND
Co-financed by Greece and the European Union

Navarino Environmental Observatory (NEO): The sampling station was located in the Costa Navarino resort in Messinia (37° 19' N, 21° 6' E), in the southwest part of Peloponnese. The sampling site, referred as NEO, was located in the area of Navarino, 52 km away from the capital of Messinia and at an elevation of 65 m above the sea surface level. NEO is characterized as a rural site with the nearby Costa Navarino resort being a possible local air pollution source.

During June 9 to July 26 2012, a Sequential Sampler (Derenda PNS 16T, Comde-Derenda GmbH) operated at a flow of 2.3 m^3 h^{-1}, was used to collect PM_{10} samples every 24 h on quartz fiber (4.7 cm, Whatman QMA) filters. The aerosol absorption was monitored by a Magee Scientific aethalometer (model AE-16) operated at 880 nm. O_3 (Ozone analyzer Dasibi 1008 AH), CO and NO_x (HORIBA Ambient Air Pollution analyzers) were also used to measure the corresponding pollutants throughout the sampling period.

Finokalia (FIN): The sampling station was located in Finokalia in Crete (35° 20' N, 25° 40' E) the largest Greek island, in the southeast part of Greece. The sampling site, referred as FIN hereafter, is located in the remote coastal area of Finokalia, 50 km away from the nearest large city center of Heraklion (150 thousand inhabitants) and at an elevation of 230 m above the sea surface level. FIN is characterized as a remote background site without human activity within a radius of approximately 15 km (Mihalopoulos et al., 1997; Kouvarakis et al., 2000; Bardouki et al., 2003; Gerasopoulos et al., 2006).

During June 9 to July 26 2012, a high volume custom-made sampler and a low volume sampler (SEQ Leckel 47/50) operated at a flow of 80 L min^{-1} and 2.3 m^3 hr^{-1} respectively, were used to collect PM_1 samples every 24 h, on quartz fiber (4.7 cm, Whatman QMA) filters. A particulate monitor (FH 62 I-R, Eberline Instruments GmbH) operated at a flow rate of 1 m^3 h^{-1} was used to collect PM_{10} samples

European Union
European Social Fund
OPERATIONAL PROGRAMME
EDUCATION AND LIFELONG LEARNING
investing in knowledge society
MINISTRY OF EDUCATION & RELIGIOUS AFFAIRS
MANAGING AUTHORITY
NSRF 2007-2013
EUROPEAN SOCIAL FUND
Co-financed by Greece and the European Union

(Gerasopoulos et al., 2006). High-temporal-resolution measurements were performed with an Aerodyne Research ACSM (Ng et al., 2011), which measures the chemical composition of non refractory PM_1 in real time. The PM_1 aerosol scattering coefficient at 530 nm was monitored continuously by two instruments: Radiance Research nephelometer (model M903 at ambient RH) and an Aurora 1000 (Ecotech) nephelometer that was connected to a diffusion drier. Aerosol absorption was also measured by a Magee Scientific Aethalometer (Model AE-31) at seven-wavelengths. Continuous measurements of O_3 (Thermo Electron, model 49C, 49i) were also conducted.

These measurements were performed by several groups including collaborators from the Demokritos Research Center, the University of Crete, the National observatory of Athens and the Aegean University. A complete list of instrumentation, sampling resolution and operation period is given in Table 1.

A2. Results and Discussion

A2.1. Temporal variation of PM main chemical components

All sites had similar mean concentrations of sulfate while the concentrations of organics exhibited significant variability. The mean daily sulfate and OA concentrations are illustrated in Figure A2. This OA temporal variability could be attributed to the different air masses that are mainly originating from, based on FLEXPART model simulation (Figure A3). It reveals a long term prevalence of air masses over the Aegean Sea that arrived to ATH and FIN sites, while the air masses that leaded to Patras were across the continental of Greece and to THES from Balkans.

A2.2. PM_1 concentration

A2.2.1. Chemical composition

The mean mass concentration of non refractory PM_1 for the different sampling sites is presented in Figure A4. The measurements in the three sites were conducted in different

European Union
European Social Fund
OPERATIONAL PROGRAMME
EDUCATION AND LIFELONG LEARNING
investing in knowledge society
MINISTRY OF EDUCATION & RELIGIOUS AFFAIRS
MANAGING AUTHORITY
NSRF 2007-2013
programme for development
EUROPEAN SOCIAL FUND
Co-financed by Greece and the European Union

periods due to instrumentation limitations. So the campaign was divided in two periods in order to compare the measurements in the same days.

In the first period, from June 9 to 26 the mean mass concentration was 8 μg m^{-3} for PAT-S and 7.5 μg m^{-3} for FIN. The average organic aerosol mass concentration for FIN was 2.3 μg m^{-3} and 3.8 μg m^{-3} for PAT-S. The average sulfate concentration at the remote site of FIN was 3.8 μg m^{-3}, almost equal to the suburban PAT-S site (3.3 μg m^{-3}). The average concentrations of ammonium were 1.1 μg m^{-3} and 0.9 μg m^{-3}, respectively. The similarity of the fine PM levels between the third biggest Greek city and a remote area with no inhabitants shows the importance of regional pollution during summertime in Greece.

In the second period from July 13 to 26 the mean concentration of non refractory PM_1 in FIN was 6 μg m^{-3} and in ATH-S was 14 μg m^{-3}. The average organic aerosol mass concentration for FIN was 2.1 μg m^{-3} and for ATH-S 6.6 μg m^{-3}, while sulfate was 2.5 μg m^{-3} and 5.3 μg m^{-3}, respectively. The average concentration of ammonium was 0.9 μg m^{-3} and 1.4 μg m^{-3}. These results suggest that Athens (as expected) is characterized by higher OA levels, but also higher sulfate.

A2.2.2. Diurnal profiles

The average diurnal profile for the NR PM_1 components based on the HR-AMS and ACSM in three of the measurements sampling sites are shown in Figures A5, A6.
Sulfate in ATH-S was found to increase at 8:00 reaching its peak at 20:00 while the sulfate profile in other areas was almost flat. This indicates that the contribution of local production does play an important role in ATH-S. For Patras and Finokalia it appears that most of the sulfate was just transported to the sites and there was negligible local production. According to the particle dispersion model FLEXPART in backward mode, the sulfate concentration in FIN during first period was quite higher when the air masses were coming from the west Turkey region, while in the second period were flat with

European Union
European Social Fund
OPERATIONAL PROGRAMME
EDUCATION AND LIFELONG LEARNING
investing in knowledge society
MINISTRY OF EDUCATION & RELIGIOUS AFFAIRS
MANAGING AUTHORITY
NSRF 2007-2013
programme for development
EUROPEAN SOCIAL FUND
Co-financed by Greece and the European Union

lower average concentration when air masses were coming from marine (Figure A3). The behavior of ammonium in all area is similar in general to those of sulfate. The two react to form ammonium sulfate or bisulfate.

The diurnal profiles for organic aerosol in three areas also suggest a strong regional character with significant contribution of local sources in ATH-S. The Athens profile exhibited two peaks, the first from 8:00 to 11:00 corresponding to morning traffic and the second from 19:00 to 22:00. The impact of local OA emissions, originating from traffic and other sources does not have a significant effect on the other two areas. This is consistent with the remote character of Finokalia and the conclusions of Pikridas et al. (2013) for Patras. More detail about OA sources are given by Kostenidou et al. (2015).

Nitrate in ATH-S presented two peaks one in the morning 8:00 to 11:00 and the other at night 19:00 to 22:00 but the levels were quite low. On the other hand, the diurnal profile of nitrate in PAT-S was rather flat, with two small peaks one during 7:00 to 9:00 and the other from 21:00 to 23:00. The behavior of nitrate concentration in all three sites is similar to that of organic aerosol. This indicates that nitrate and organics had at least to some extent, similar sources. The average nitrate levels were quite low (<0.2 μg m^{-3}) in all areas. According to the AMS analysis the nitrate concentration in both regions was mainly due to organonitrates: 89% in ATH-S and 91% in PAT-S. This does explain the correlation of the two in all sites (Kostenidou et al., 2015).

The diurnal average profile of black carbon concentration in PAT-S showed two peaks one during 6:00 to 11:00 and the other from 18:00 to midnight. The average concentration was 0.5 μg m^{-3} with the peak value being close to 0.7 μg m^{-3}. In ATH-S the diurnal profile presented an increase in the concentrations between 08:00 to 11:00 in the morning and in the afternoon from 19:00 to midnight. The more pronounced variation of black carbon, in both Athens and Patras suggest that local sources contributed a significant fraction of the observed concentrations.

European Union
European Social Fund
OPERATIONAL PROGRAMME
EDUCATION AND LIFELONG LEARNING
investing in knowledge society
MINISTRY OF EDUCATION & RELIGIOUS AFFAIRS
MANAGING AUTHORITY
NSRF 2007-2013
EUROPEAN SOCIAL FUND
Co-financed by Greece and the European Union

A2.3. $PM_{2.5}$ Composition

The results of the chemical mass closure for $PM_{2.5}$ are shown in Figure A7. In the first period from June 9 to July 26 average $PM_{2.5}$ was in the range from 12 to 15 μg m^{-3}, while in the second (July 3 to 26) the mean mass concentrations varied in the range 16 μg m^{-3} to 20 μg m^{-3}. The masses match quite well with the sum of ionic mass, POM, EC and dust components in all sites. The main contributors to $PM_{2.5}$ levels at different sites were OM (25-55%), followed by SO_4^{2-} (25-30%), mineral dust (10-35%) and NH_4^+ (5-10%). Particulate water accounted for the remaining 3%.

A2.3.1. Carbonaceous Compounds

Elemental carbon (EC) or black carbon is a primary pollutant formed in combustion processes, whereas OA is a complex mixture of numerous organic compounds originating from a large variety of sources and atmospheric processes (Turpin et al., 1995). The mean OA concentration in $PM_{2.5}$ in the different site was quite variable.

The OA was the largest component at all the sites, except for ATH-B. In the first period, from June 9 to July 26 the $PM_{2.5}$ mass concentration was lower in all areas due to the meteorological conditions. The average organic mass for PAT-C and PAT-S was 5 μg m^{-3} (39%, 43%) and for ATH-B was 2.7 μg m^{-3} (22%). In the second period, from July 13 to 26 the average OA mass concentration for PAT-C was 10 μg m^{-3} (48%). This value is estimated as the difference between the average $PM_{2.5}$ and the average sum of components, because OC was not measured in PAT-C. Also for PAT-S OA was 9.3 μg m^{-3} (52%), for ATH-S was 5.7 μg m^{-3} (33%) and for ATH-B 4.0 μg m^{-3} (23%). The reported concentrations were corrected for the filter blanks levels.

European Union
European Social Fund
OPERATIONAL PROGRAMME
EDUCATION AND LIFELONG LEARNING
investing in knowledge society
MINISTRY OF EDUCATION & RELIGIOUS AFFAIRS
MANAGING AUTHORITY
NSRF 2007-2013
programme for development
EUROPEAN SOCIAL FUND
Co-financed by Greece and the European Union

A2.3.2. Secondary Inorganic $PM_{2.5}$ components

Secondary $PM_{2.5}$ components (sulfate, ammonium, nitrate) are formed in the atmosphere from the precursor gases (SO_2, NH_3 and NO_x) through gas-to-particle conversion. Sulfate was the dominant anion in all stations. Similar levels of sulfate in all sampling sites were observed. In the first period the average sulfate concentration was for PAT-C 3.9 μg m^{-3} (27%), for PAT-S 3.1 μg m^{-3} (30%) and for ATH-B 3.5 μg m^{-3}(25%). In the second period, the mean organic concentration for PAT-C was 10 μg m^{-3} (27%), for PAT-S was 9.3 μg m^{-3} (22%), ATH-S was 5.7 μg m^{-3} (31%) and ATH-B 4.7 μg m^{-3} (27%). The mean nitrate concentration and its contribution to $PM_{2.5}$ were low during the sampling campaign in all stations. Finally, the average concentration of ammonium was quite similar during the two periods. More specifically, from June 9 to 26 for PAT-C it was 1.4 μg m^{-3}, for PAT-S was 1.2 μg m^{-3} (10%) and for ATH-B was 0.75 (6%). In the second period, the average ammonium concentration in PAT-C and PAT-S was 1.7 μg m^{-3} (11%), in ATH-S was 1.2 μg m^{-3} (7%) and in ATH-B 1.1 μg m^{-3} (6%).

A2.3.3. Soil-derived fine particles

Calcium is a reliable tracer of crustal sources in atmospheric PM and its concentration was multiplied by 11 to estimate the mass concentration of dust (Vrekoussis et al., 2005; Seinfeld and Pandis, 2006). $PM_{2.5}$ dust was estimated to be 1.7 μg m^{-3} (9%) for PAT-C, 1.8 μg m^{-3} (16%) for PAT-S and 5.5 μg m^{-3} (27%) for ATH-B. The higher values for both ATH-B and ATH-S most probably originate from resuspension of dust from roads due to traffic. The unpaved roads in Penteli are apparently a major source of ATH-B.

A2.3.4. Water content

The water content of $PM_{2.5}$ samples at the RH of weighting was estimated from their chemical composition. The thermodynamic Aerosol Inorganics Model (AIM) (Carslaw et al., 1995; Clegg et al., 1998; Massucci et al., 1999) (http://www.aim.env.uea.ac.uk/aim/aim.php) for the $H^+ - NH_4^+ - SO_4^{2-} - NO_3^- - Cl^- -$

European Union
European Social Fund
OPERATIONAL PROGRAMME
EDUCATION AND LIFELONG LEARNING
investing in knowledge society
MINISTRY OF EDUCATION & RELIGIOUS AFFAIRS
MANAGING AUTHORITY
NSRF 2007-2013
EUROPEAN SOCIAL FUND
Co-financed by Greece and the European Union

H_2O system was used to calculate the water content associated with the inorganic salts, assuming that the particles on the filters were in equilibrium with their environment.

A2.4. Ionic balance

During the summer, the aerosol is periodically acidic because insufficient ammonium is available to neutralize the sulfate aerosol present. Ionic balance was calculated fine fractions of the aerosol particles for each station. The ion balance was performed by the ratio of the equivalent cations sum (the sum of NH_4^+, K^+, Na^+, Mg^{2+}, Ca^2+ in neq m^{-3}) to the equivalent anion sum (the sum of NO_3^-, Cl^-, SO_4^- in neq m^{-3}). A plot of total cations equivalents against total anion equivalents is presented in Figure A8. The slope of the regression line indicates a value higher than unity (slope = 1.0 to 1.5) in the first period. Similarly, in the second period the slope of the regression line for fine particles is higher than unity (slope= 1.1 to 1.2), accept the ATH-S station (slope= 0.8).

A2.5. Relationship between PM_1 and $PM_{2.5}$ concentration

Figures A9, A10 show sulfate, ammonium, organic and nitrate comparison between $PM_{2.5}$ filters and the PM_1 mass concentration, as measured by HR-ToF-AMS, in ATH-S and PAT-S. AMS sulfate measurements agree well with the $PM_{2.5}$ filter data. The correlation was good in both sites (R^2 = 0.98 in PAT-S and R^2 = 0.92 in ATH-S). A good correlation was found between ammonium with those from $PM_{2.5}$ filters in PAT-S (R^2=0.83) while in ATH-S the correlation was lower. There are discrepancies for some of the measurements of organics in both Athens and Patras that need to be investigated further.

A2.6. PM_{10}

The results of the chemical mass closure for PM_{10} are shown in Figure A11. In the first period from June 9 to 26 varied in the range from 23 to 37 μg m^{-3}. In the second period from July 3 to 26 the mean PM_{10} concentrations were between 26 μg m^{-3} and 35 μg m^{-3}. The masses match quite well with the sum of components with the exception of Finokalia. The main PM_{10} contributors were mineral dust (40-55%), OA (18-22%),

European Union
European Social Fund
OPERATIONAL PROGRAMME
EDUCATION AND LIFELONG LEARNING
investing in knowledge society
MINISTRY OF EDUCATION & RELIGIOUS AFFAIRS
MANAGING AUTHORITY
NSRF 2007-2013
EUROPEAN SOCIAL FUND
Co-financed by Greece and the European Union

SO_4^{2-} (16-20%), NO_3^- (4-6%) and NH_4^+ (1-4%). In this particulate size range the chemical composition were measured only in 3 sites: ATH-S, NEO and FIN.

The chemical composition between the 3 sites was quite similar throughout the campaign in two periods. The average dust concentration during the measurement period in NEO was reaching as high as 15.3 μg m^{-3}, with lower values in ATH-S (12.6 μg m^{-3}) and in FIN (11 μg m^{-3}). Additionally, the estimated organic concentrations were accounted in average 4 μg m^{-3} in NEO and 4.6 μg m^{-3} in FIN for the first period while in the second were 4.4 μg m^{-3} and 5.7 μg m^{-3}. Finally, both coastal sampling sites in FIN and NEO had higher concentrations of sea salt 3 μg m^{-3} and 2 μg m^{-3} respectively.

A3. Summary and Conclusions

This study presents a summary of air pollution during summertime in Greece as observed during an extensive field campaign. Measurements were carried out at seven sites in order to characterize PM chemical composition, temporal and spatial variability.

The non-refractory PM_1 mainly consisted of OA (30-50%) with an important fraction of secondary inorganic aerosols (50-70%). The main constituents of $PM_{2.5}$ in all sites were organics and sulfate. In Penteli, the mineral dust was also a significant component of $PM_{2.5}$. The PM_{10} fraction contained as expected more mineral dust (40-55%) than $PM_{2.5}$. The dust was due to local sources mainly resuspension from car traffic.

The highest average non-refractory PM_1 mass concentration was in the suburban area of Demokritos in Athens, while the lowest was observed in Finokalia. The similarity of the PM_1 levels between suburban Patras and a remote area Greece (Finokalia) with no inhabitants shows the importance of regional pollution during summertime in Greece. Also, major regional pollution contributions for fine PM even in the biggest cities in the country were observed. On the other hand, the pronounced average diurnal variation

European Union
European Social Fund
OPERATIONAL PROGRAMME
EDUCATION AND LIFELONG LEARNING
investing in knowledge society
MINISTRY OF EDUCATION & RELIGIOUS AFFAIRS
MANAGING AUTHORITY
NSRF 2007-2013
programme for development
EUROPEAN SOCIAL FUND
Co-financed by Greece and the European Union

of black carbon in both Athens and Patras suggests that local sources contribute significant fraction of the observed black carbon concentrations.

The FLEXPART model was used to investigate the trajectories of the air masses which traveled and arrived at Patras, Thessaloniki, Athens, NEO and Finokalia during the study. The corresponding results suggest that during days with low wind speed (stagnation) the contribution of local sourced increased for all PM species.

A4 References

Andreae, M. O. and P. Merlet (2001) Emission of trace gases and aerosols from biomass burning, Global Biogeochemical Cycles 15, 955-966.

Bardouki, H., H. Liakakou, C. Economou, J. Sciare, J. Smolık, V. Ždímal, K. Eleftheriadis, M. Lazaridis, C. Dye and N. Mihalopoulos (2003) Chemical composition of size-resolved atmospheric aerosols in the eastern Mediterranean during summer and winter, Atmospheric Environment 37, 195-208.

Bezantakos, S., A. Bougiatioti, E. Kostenidou, K. Florou, M. Giamarelou, S. Vratolis, K. Eleftheriadis, N. Mihalopoulos, A. Nenes, S. Pandis, and G. Biskos (2015) Hygroscopic properties and mixing state of ultrafine aerosol particles in urban background sites, *to be submited.*

Bougiatioti, A., P. Zarmpas, E. Koulouri, M. Antoniou, C. Theodosi, G. Kouvarakis, S. Saarikoski, T. Mäkelä, R. Hillamo and N. Mihalopoulos (2013) Organic, elemental and water-soluble organic carbon in size segregated aerosols, in the marine boundary layer of the Eastern Mediterranean, Atmospheric Environment 64, 251-262.

European Union
European Social Fund
OPERATIONAL PROGRAMME
EDUCATION AND LIFELONG LEARNING
investing in knowledge society
MINISTRY OF EDUCATION & RELIGIOUS AFFAIRS
MANAGING AUTHORITY
NSRF 2007-2013
programme for development
EUROPEAN SOCIAL FUND
Co-financed by Greece and the European Union

Carslaw, K. S., S. L. Clegg and P. Brimblecombe (1995) A thermodynamic model of the system HCl-HNO_3-H_2SO_4-H_2O, including solubilities of HBr, from less-than-200 to 328 K, Journal of Physical Chemistry 99, 11557-11574.

Clegg, S. L., P. Brimblecombe and A. S. Wexler (1998) Thermodynamic model of the system H^+-NH_4^+-SO_4^{2-}-NO_3^--H_2O at tropospheric temperatures, The Journal of Physical Chemistry A 102, 2137-2154.

Danalatos, D. and S. Glavas (1999) Gas phase nitric acid, ammonia and related particulate matter at a Mediterranean coastal site, Patras, Greece, Atmospheric Environment 33, 3417-3425.

DeCarlo, P. F., J. R. Kimmel, A. Trimborn, M. J. Northway, J. T. Jayne, A. C. Aiken, M. Gonin, K. Fuhrer, T. Horvath and K. S. Docherty (2006) Field-deployable, high-resolution, time-of-flight aerosol mass spectrometer, Analytical chemistry 78, 8281-8289.

Dockery, D. W. and C. A. Pope (1994) Acute respiratory effects of particulate air pollution, Annual review of public health 15, 107-132.

Gerasopoulos, E., G. Kouvarakis, P. Babasakalis, M. Vrekoussis, J.-P. Putaud and N. Mihalopoulos (2006) Origin and variability of particulate matter (PM_{10}) mass concentrations over the Eastern Mediterranean, Atmospheric Environment 40, 4679-4690.

Glavas, S. D., P. Nikolakis, D. Ambatzoglou and N. Mihalopoulos (2008) Factors affecting the seasonal variation of mass and ionic composition of $PM_{2.5}$ at a central Mediterranean coastal site, Atmospheric Environment 42, 5365-5373.

European Union
European Social Fund
OPERATIONAL PROGRAMME
EDUCATION AND LIFELONG LEARNING
investing in knowledge society
MINISTRY OF EDUCATION & RELIGIOUS AFFAIRS
MANAGING AUTHORITY
NSRF 2007-2013
programme for development
EUROPEAN SOCIAL FUND
Co-financed by Greece and the European Union

Grivas, G., S. Cheristanidis and A. Chaloulakou (2012) Elemental and organic carbon in the urban environment of Athens. Seasonal and diurnal variations and estimates of secondary organic carbon, Science of the Total Environment 414, 535-545.

Jayne, J. T., D. C. Leard, X. Zhang, P. Davidovits, K. A. Smith, C. E. Kolb and D. R. Worsnop (2000) Development of an aerosol mass spectrometer for size and composition analysis of submicron particles, Aerosol Science & Technology 33, 49-70.

Jimenez, J. L., J. T. Jayne, Q. Shi, C. E. Kolb, D. R. Worsnop, I. Yourshaw, J. H. Seinfeld, R. C. Flagan, X. Zhang and K. A. Smith (2003) Ambient aerosol sampling using the aerodyne aerosol mass spectrometer, Journal of Geophysical Research: Atmospheres 108, 1984–2012.

Kaltsonoudis, C., E. Kostenidou, K. Florou, M. Psichoudaki and S. N. Pandis (2015) Temporal Variability of VOCs in the Eastern Mediterranean, *to be submitted*.

Kanakidou, M., N. Mihalopoulos, T. Kindap, U. Im, M. Vrekoussis, E. Gerasopoulos, E. Dermitzaki, A. Unal, M. Koçak, K. Markakis, D. Melas, G. Kouvarakis, A. F. Youssef, A. Richter, N. Hatzianastassiou, A. Hilboll, F. Ebojie, F. Wittrock, C. von Savigny, J. P. Burrows, A. Ladstaetter-Weissenmayer and H. Moubasher (2011) Megacities as hot spots of air pollution in the East Mediterranean, Atmospheric Environment 45, 1223-1235.

Kanakidou, M., J. Seinfeld, S. Pandis, I. Barnes, F. Dentener, M. Facchini, R. V. Dingenen, B. Ervens, A. Nenes and C. Nielsen (2005) Organic aerosol and global climate modelling: a review, Atmospheric Chemistry and Physics 5, 1053-1123.

European Union
European Social Fund
OPERATIONAL PROGRAMME
EDUCATION AND LIFELONG LEARNING
investing in knowledge society
MINISTRY OF EDUCATION & RELIGIOUS AFFAIRS
MANAGING AUTHORITY
NSRF 2007-2013
EUROPEAN SOCIAL FUND
Co-financed by Greece and the European Union

Koçak, M., N. Mihalopoulos and N. Kubilay (2007) Chemical composition of the fine and coarse fraction of aerosols in the northeastern Mediterranean, Atmospheric Environment 41, 7351-7368.

Kostenidou, E., K. Florou, C. Kaltsonoudis, M. Tsiflikiotou, K. Eleftheriadis and S. Pandis (2015) Sources and chemical characterization of organic aerosol during the Summer in the Eastern Mediterranean, *to be submitted.*

Koulouri, E., S. Saarikoski, C. Theodosi, Z. Markaki, E. Gerasopoulos, G. Kouvarakis, T. Mäkelä, R. Hillamo and N. Mihalopoulos (2008) Chemical composition and sources of fine and coarse aerosol particles in the Eastern Mediterranean, Atmospheric Environment 42, 6542-6550.

Kouvarakis, G., Y. Doukelis, N. Mihalopoulos, S. Rapsomanikis, J. Sciare and M. Blumthaler (2002) Chemical, physical, and optical characterization of aerosols during PAUR II experiment, Journal of Geophysical Research: Atmospheres 107, 1984–2012.

Kouvarakis, G., K. Tsigaridis, M. Kanakidou and N. Mihalopoulos (2000) Temporal variations of surface regional background ozone over Crete Island in the southeast Mediterranean, Journal of Geophysical Research: Atmospheres 105, 1984–2012.

Kouvarakis, G., M. Vrekoussis, N. Mihalopoulos, K. Kourtidis, B. Rappenglueck, E. Gerasopoulos and C. Zerefos (2002) Spatial and temporal variability of tropospheric ozone (O_3) in the boundary layer above the Aegean Sea (eastern Mediterranean), Journal of Geophysical Research: Atmospheres, 1984–2012.

Larssen, S., R. Sluyter and C. Helmiss (1999). Criteria for EUROAIRNET: The EEA air quality monitoring and information network, European Environment Agency.

European Union
European Social Fund
OPERATIONAL PROGRAMME
EDUCATION AND LIFELONG LEARNING
investing in knowledge society
MINISTRY OF EDUCATION & RELIGIOUS AFFAIRS
MANAGING AUTHORITY
NSRF 2007-2013
programme for development
EUROPEAN SOCIAL FUND
Co-financed by Greece and the European Union

Massucci, M., S. L. Clegg and P. Brimblecombe (1999) Equilibrium partial pressures, thermodynamic properties of aqueous and solid phases, and Cl_2 production from aqueous HCl and HNO_3 and their mixtures, The Journal of Physical Chemistry A 103, 4209-4226.

Mihalopoulos, N., E. Stephanou, M. Kanakidou, S. Pilitsidis and P. Bousquet (1997) Tropospheric aerosol ionic composition in the Eastern Mediterranean region, Tellus B 49, 314-326.

Ng, N., M. Canagaratna, J. Jimenez, P. Chhabra, J. Seinfeld and D. Worsnop (2011) Changes in organic aerosol composition with aging inferred from aerosol mass spectra, Atmospheric Chemistry and Physics 11, 6465-6474.

Ng, N. L., S. C. Herndon, A. Trimborn, M. R. Canagaratna, P. Croteau, T. B. Onasch, D. Sueper, D. R. Worsnop, Q. Zhang and Y. Sun (2011) An Aerosol Chemical Speciation Monitor (ACSM) for routine monitoring of the composition and mass concentrations of ambient aerosol, Aerosol Science and Technology 45, 780-794.

Paraskevopoulou, D., E. Liakakou, E. Gerasopoulos, C. Theodosi and N. Mihalopoulos (2014) Long term characterization of organic and elemental carbon in the $PM_{2.5}$ fraction: the case of Athens, Greece, Atmospheric Chemistry and Physics Discussions 14, 17161-17196.

Patashnick, H. and E. G. Rupprecht (1991) Continuous PM_{10} measurements using the tapered element oscillating microbalance, Journal of the Air & Waste Management Association 41, 1079-1083.

Pateraki, S., V. Assimakopoulos, A. Bougiatioti, G. Kouvarakis, N. Mihalopoulos and C. Vasilakos (2012) Carbonaceous and ionic compositional patterns of fine

European Union
European Social Fund
OPERATIONAL PROGRAMME
EDUCATION AND LIFELONG LEARNING
investing in knowledge society
MINISTRY OF EDUCATION & RELIGIOUS AFFAIRS
MANAGING AUTHORITY
NSRF 2007-2013
programme for development
EUROPEAN SOCIAL FUND
Co-financed by Greece and the European Union

particles over an urban Mediterranean area, Science of the Total Environment 424, 251-263.

Petzold, A. and M. Schönlinner (2004) Multi-angle absorption photometry—a new method for the measurement of aerosol light absorption and atmospheric black carbon, Journal of Aerosol Science 35, 421-441.

Pikridas, M., A. Bougiatioti, L. Hildebrandt, G. Engelhart, E. Kostenidou, C. Mohr, A. Prévôt, G. Kouvarakis, P. Zarmpas and J. Burkhart (2010) The Finokalia aerosol measurement experiment–2008 (FAME-08): an overview, Atmospheric Chemistry and Physics 10, 6793-6806.

Pikridas, M., L. Hildebrandt, E. Kostenidou, G. Engelhart, B. Lee, N. Mihalopoulos and S. Pandis (2013). Properties of Aged Aerosols in the Eastern Mediterranean. Advances in Meteorology, Climatology and Atmospheric Physics, 1181-1187.

Pikridas, M., A. Tasoglou, K. Florou and S. N. Pandis (2013) Characterization of the origin of fine particulate matter in a medium size urban area in the Mediterranean, Atmospheric Environment 80, 264-274.

Pikridas, M., A. Tasoglou, K. Florou and S. N. Pandis (2013) Characterization of the origin of fine particulate matter in a medium size urban area in the Mediterranean, Atmospheric Environment 80, 264-274.

Pope, C. A., M. Ezzati and D. W. Dockery (2009) Fine-particulate air pollution and life expectancy in the United States, New England Journal of Medicine 360, 376-386.

Rader, D. and P. McMurry (1986) Application of the tandem differential mobility analyzer to studies of droplet growth or evaporation, Journal of Aerosol Science 17, 771-787.

European Union
European Social Fund
OPERATIONAL PROGRAMME
EDUCATION AND LIFELONG LEARNING
investing in knowledge society
MINISTRY OF EDUCATION & RELIGIOUS AFFAIRS
MANAGING AUTHORITY
NSRF 2007-2013
programme for development
EUROPEAN SOCIAL FUND
Co-financed by Greece and the European Union

Rees, S. L., A. L. Robinson, A. Khlystov, C. O. Stanier and S. N. Pandis (2004) Mass balance closure and the Federal Reference Method for $PM_{2.5}$ in Pittsburgh, Pennsylvania, Atmospheric Environment 38, 3305-3318.

Remoundaki, E., P. Kassomenos, E. Mantas, N. Mihalopoulos and M. Tsezos (2013) Composition and mass closure of $PM_{2.5}$ in urban environment (Athens, Greece), Aerosol Air Qual. Res 13, 72-82.

Roberts, G. and A. Nenes (2005) A continuous-flow streamwise thermal-gradient CCN chamber for atmospheric measurements, Aerosol Science and Technology 39, 206-221.

Seinfeld, J. H. and S. N. Pandiss (2006). Atmospheric Chemistry and Physics: From Air Pollution to Climate change, John Wiley & Sons.

Sillanpää, M., R. Hillamo, S. Saarikoski, A. Frey, A. Pennanen, U. Makkonen, Z. Spolnik, R. Van Grieken, M. Braniš and B. Brunekreef (2006) Chemical composition and mass closure of particulate matter at six urban sites in Europe, Atmospheric Environment 40, 212-223.

Stohl, A., C. Forster, A. Frank, P. Seibert and G. Wotawa (2005) Technical note: The Lagrangian particle dispersion model FLEXPART version 6.2, Atmospheric Chemistry and Physics 5, 2461-2474.

Stohl, A., H. Sodemann, S. Eckhardt, A. Frank, P. Seibert and G. Wotawa (2011) The Lagrangian particle dispersion model FLEXPART version 8.2

European Union
European Social Fund
OPERATIONAL PROGRAMME
EDUCATION AND LIFELONG LEARNING
investing in knowledge society
MINISTRY OF EDUCATION & RELIGIOUS AFFAIRS
MANAGING AUTHORITY
NSRF 2007-2013
programme for development
EUROPEAN SOCIAL FUND
Co-financed by Greece and the European Union

Terzi, E., G. Argyropoulos, A. Bougatioti, N. Mihalopoulos, K. Nikolaou and C. Samara (2010) Chemical composition and mass closure of ambient PM_{10} at urban sites, Atmospheric Environment 44, 2231-2239.

Theodosi, C., G. Grivas, P. Zarmpas, A. Chaloulakou and N. Mihalopoulos (2011) Mass and chemical composition of size-segregated aerosols (PM_1, $PM_{2.5}$, PM_{10}) over Athens, Greece: local versus regional sources, Atmospheric Chemistry and Physics 11, 11895-11911.

Tsitouridou, R., D. Voutsa and T. Kouimtzis (2003) Ionic composition of PM_{10} in the area of Thessaloniki, Greece, Chemosphere 52, 883-891.

Turpin, B. J. and J. J. Huntzicker (1995) Identification of secondary organic aerosol episodes and quantitation of primary and secondary organic aerosol concentrations during SCAQS, Atmospheric Environment 29, 3527-3544.

Viidanoja, J., M. Sillanpää, J. Laakia, V.-M. Kerminen, R. Hillamo, P. Aarnio and T. Koskentalo (2002) Organic and black carbon in $PM_{2.5}$ and PM_{10}: 1 year of data from an urban site in Helsinki, Finland, Atmospheric Environment 36, 3183-3193.

Voutsa, D. and C. Samara (2002) Labile and bioaccessible fractions of heavy metals in the airborne particulate matter from urban and industrial areas, Atmospheric Environment 36, 3583-3590.

Vrekoussis, M., E. Liakakou, M. Kocak, N. Kubilay, K. Oikonomou, J. Sciare and N. Mihalopoulos (2005) Seasonal variability of optical properties of aerosols in the Eastern Mediterranean, Atmospheric Environment 39, 7083-7094.

Yannopoulos, P. C. (2008) Long-term assessment of airborne particulate concentrations in Patras, Greece, Fresenius Environmental Bulletin 17, 608-616.

European Union
European Social Fund
OPERATIONAL PROGRAMME
EDUCATION AND LIFELONG LEARNING
investing in knowledge society
MINISTRY OF EDUCATION & RELIGIOUS AFFAIRS
MANAGING AUTHORITY
NSRF 2007-2013
programme for development
EUROPEAN SOCIAL FUND
Co-financed by Greece and the European Union

Table A1. Summary of summertime measurements in Greece.

Observable		Method/Manufacturer	Resolution	Sampling period (2012)
		PAT-C		
Aerosol mass	$PM_{2.5}$ mass	Partisol FRM Dichotomous	24 h	9/6 - 26/7
Chemical composition	$PM_{2.5}$ inorganic ion	IC analysis	20 min	9/6 - 26/7
Optical characteristics	Light Extinction at 530 nm in $PM_{2.5}$	Nephelometer Aurora 1000F Ecotech Dry	5 min	9/6 - 26/7
		RAT-S		
Aerosol mass	$PM_{2.5}$ mass	Super-SASS MetOne	24 h	9/6 - 26/7
	PM_{10} mass	Thermo model TEOM-DF 1405	10 min	1/7 - 27/7
Chemical composition	$PM_{2.5}$ inorganic ions	IC analysis	20 min	9/6 - 26/7
	$PM_{2.5}$ organic and elemental carbon	Sunset Laboratory Carbon analyzer	20 min	9/6 - 26/7
	$PM_{1.0}$ size resolved composition	Aerodyne Mass spectrometer (AMS)	6 min	9/6 - 26/6
Optical characteristics	Light absorption at 670 nm in $PM_{2.5}$	MAAP	5 min	9/6 - 26/6
Gaseous Species	VOCs	PTRMS	5 min	9/6 - 26/6
	SO_2	Teledyne 100EU Monitor	5 min	9/6 - 26/7
	O_3	Teledyne 400E Monitor	5 min	9/6 - 26/7
	NO_x	Teledyne 201E Monitor	5 min	9/6 - 26/7
		THES-S		
Aerosol mass	$PM_{2.5}$ mass	SASS MetOne	24 h	9/6 - 22/7
Chemical composition	$PM_{2.5}$ inorganic ions	IC analysis	20 min	9/6 - 22/7
	$PM_{2.5}$ organic and elemental carbon	Sunset Laboratory Carbon analyzer	20 min	9/6 - 22/7
Optical characteristics	Light Extinction at 450, 550, 700 nm in PM_{total}	Nephelometer 3563d TSI	5 min	9/6 - 26/7
		ATH-S		
Aerosol mass	$PM_{2.5}$ mass	Low volume custom	24 h	3/7 - 26/7
	PM_{10} mass			
Chemical composition	$PM_{2.5}$, $PM_{2.5-10}$, PM_{10} inorganic ions	IC analysis	20 min	3/7 - 26/7
	$PM_{2.5}$ organic and elemental carbon	Sunset field analyzer (Sunset Lab, Inc.)	3 h	3/7 - 26/7
	$PM_{1.0}$ size resolved composition	Aerodyne Mass spectrometer (AMS)	6 min	12/7 - 26/7

European Union
European Social Fund
OPERATIONAL PROGRAMME
EDUCATION AND LIFELONG LEARNING
investing in knowledge society
MINISTRY OF EDUCATION & RELIGIOUS AFFAIRS
MANAGING AUTHORITY
NSRF 2007-2013
EUROPEAN SOCIAL FUND
Co-financed by Greece and the European Union

Observable		Method/Manufacturer	Resolution	Sampling period (2012)
Optical characteristics	Light Extinction at 450, 520, 700 nm in PM_{10}	Nephelometer Aurora 3000 Ecotech, DRY	5 min	3/7 - 26/7
	Light Absorption at 880 nm in PM_{10}	Aethalometer AE-31 Maggee Scientific	5 min	9/7 - 26/7
Gaseous Species	VOCs	PTRMS	5 min	3/7 - 26/7
	NO_x	Monitor	5 min	3/7 - 26/7
ATH-B				
Aerosol mass	$PM_{2.5}$ mass	Dichotomous Partisol (R&P Co)	24 h	9/6 - 26/7
Chemical composition	$PM_{2.5}$ inorganic ions	IC analysis	20 min	9/6 - 26/7
	$PM_{2.5}$ organic and elemental carbon	Sunset Laboratory Carbon analyzer	20 min	9/6 - 26/7
Optical characteristics	Light Absorption at 470, 522, 660 nm in PM_{total}	PSAP Radiance Research	5 min	9/6 - 26/7
	Light Extinction at 530 nm in PM_{total}	Nephelometer M903 Radiance Research	5 min	9/6 - 26/7
Gaseous Species	O_3	Thermo Ozone analyzer	5 min	9/6 - 26/7
NEO				
Aerosol mass	PM_{10} mass	PNS 16T Derenda	24 h	9/6 - 26/7
Chemical composition	PM_{10} inorganic ions	IC analysis	20 min	9/6 - 26/7
	$PM_{2.5}$ organic and elemental carbon	Sunset Laboratory Carbon analyzer	20 min	9/6 - 26/7
Optical characteristics	Light Absorption 880 nm in PM_{10}	Aethalometer AE-16 Magee Scientific	5 min	9/6 - 26/7
Gaseous Species	O_3	analyzer Dasibi 1008 AH	5 min	9/6 - 18/7
	CO	HORIBA Ambient Air Pollution analyzers	5 min	9/6 - 12/7
	NO_x		5 min	9/6 - 12/7
FIN				
Aerosol mass	PM_1 mass	Aerosol sampler	24 h	9/6 - 26/7
	PM_{10} mass	Leckel SEQ 47/50	24 h	9/6 - 26/7
		FH 62 I-R thermo	5 min	9/6 - 26/7
Chemical composition	PM_1 inorganic ions	IC analysis	20 min	9/6 - 26/7
	PM_{10} inorganic ions		20 min	9/6 - 26/7
	PM_1 organic and elemental carbon	Sunset Laboratory Carbon analyzer	20 min	9/6 - 26/7
	$PM_{1.0}$ size resolved composition	Aerosol Chemical Speciation Monitor (ACSM)	5 min	9/6 - 26/7
Optical characteristics	Light Extinction at 530 nm in PM_1	Nephelometer WET M903 Radiance Research,	5 min	9/6 - 26/7
		Nephelometer DRY Aurora 1000 Ecotech	5 min	9/6 - 26/7
	Light Absorption ABS 7 in PM_{10}	Aethalometer A-31 MAGEE SCI	5 min	9/6 - 26/7
Gaseous Species	O_3	Thermo 49C, 49i	5 min	9/6 - 26/7

European Union
European Social Fund
OPERATIONAL PROGRAMME
EDUCATION AND LIFELONG LEARNING
investing in knowledge society
MINISTRY OF EDUCATION & RELIGIOUS AFFAIRS
MANAGING AUTHORITY
NSRF 2007-2013
EUROPEAN SOCIAL FUND
Co-financed by Greece and the European Union

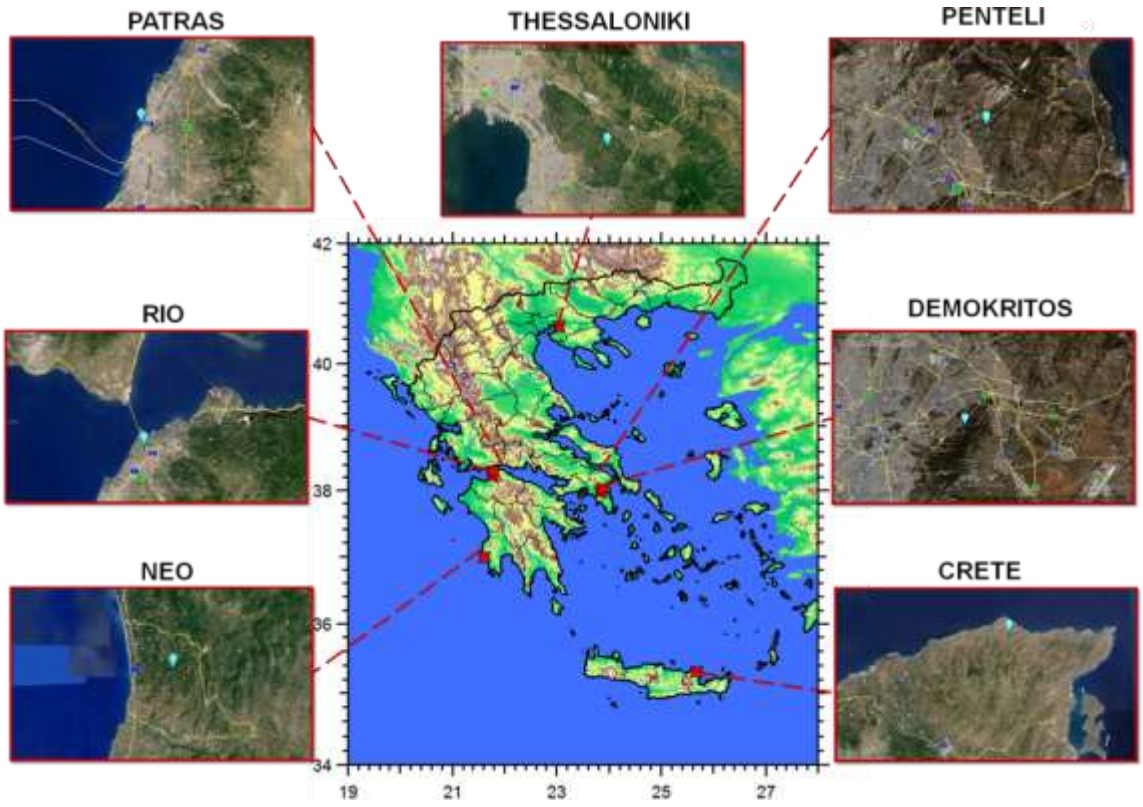

Figure A1. Geographical location of the seven sampling sites distributed across Greece.

European Union
European Social Fund
OPERATIONAL PROGRAMME
EDUCATION AND LIFELONG LEARNING
investing in knowledge society
MINISTRY OF EDUCATION & RELIGIOUS AFFAIRS
MANAGING AUTHORITY
NSRF 2007-2013
EUROPEAN SOCIAL FUND
Co-financed by Greece and the European Union

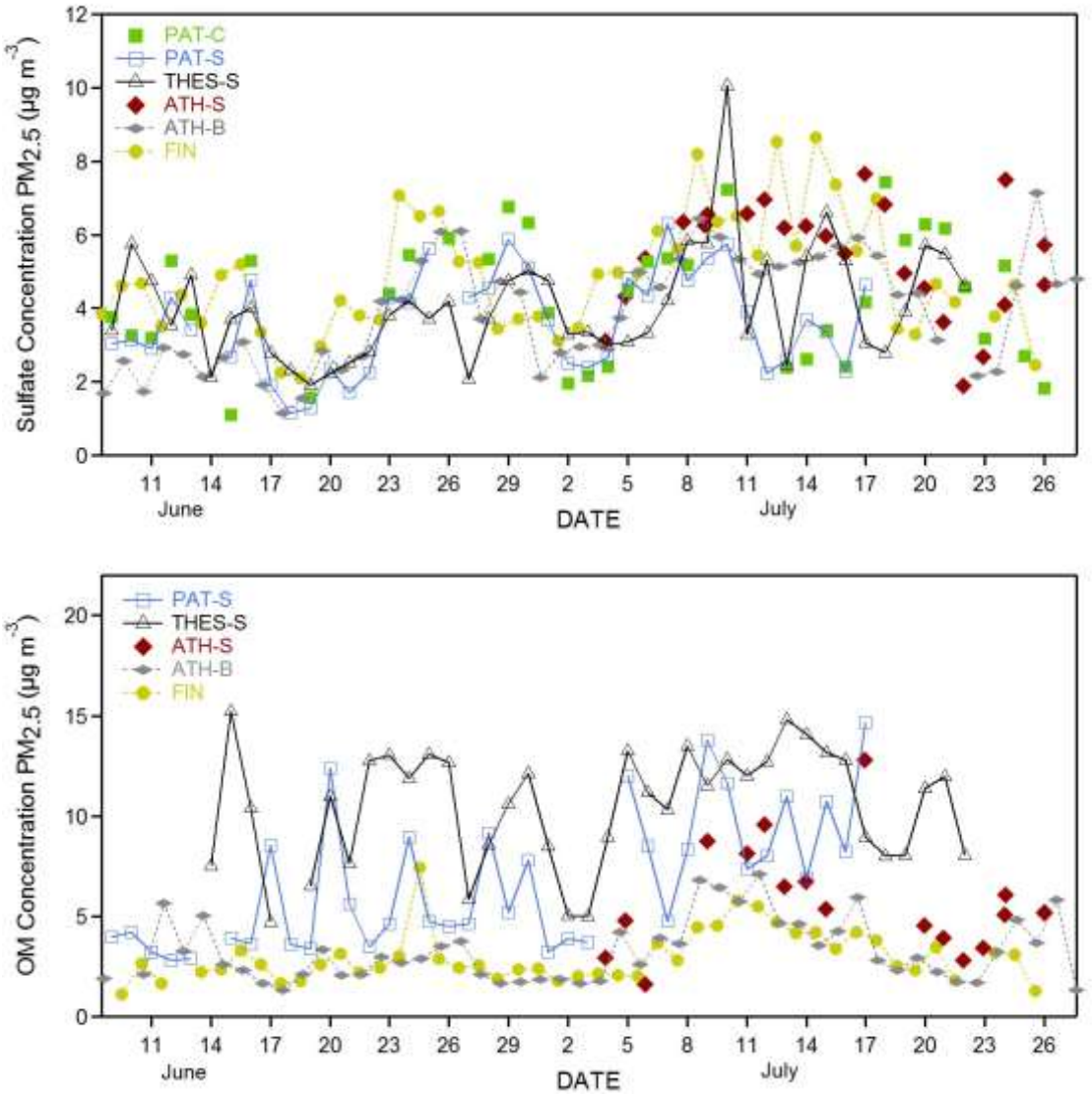

Figure A2. Temporal variations of $PM_{2.5}$ sulfate (top) and organics (bottom). For FIN the PM_1 concentrations are presented. All data are based on filter samples.

European Union
European Social Fund
OPERATIONAL PROGRAMME
EDUCATION AND LIFELONG LEARNING
investing in knowledge society
MINISTRY OF EDUCATION & RELIGIOUS AFFAIRS
MANAGING AUTHORITY
NSRF 2007-2013
EUROPEAN SOCIAL FUND
Co-financed by Greece and the European Union

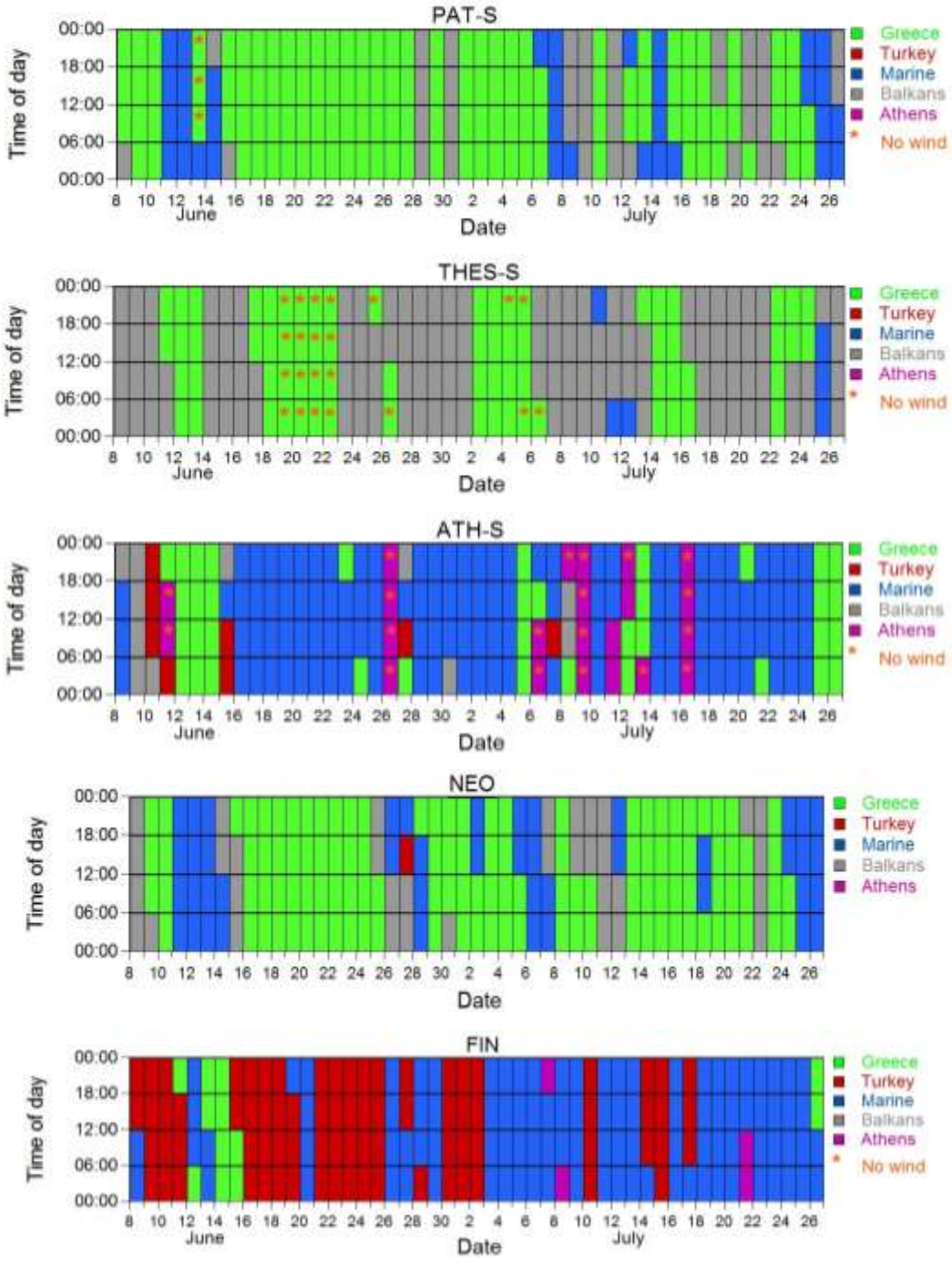

Figure A3. Source regions analysis based on FLEXPART footprint plots for the seven different areas. Back trajectories showing the transport of air masses to the sampling sites from June 9 to July 26 2012. A trajectory was attributed to a category if the source region had a PES value above 0.9 ns kg^{-1} in the corresponding footprint plot.

European Union
European Social Fund
OPERATIONAL PROGRAMME
EDUCATION AND LIFELONG LEARNING
investing in knowledge society
MINISTRY OF EDUCATION & RELIGIOUS AFFAIRS
MANAGING AUTHORITY
NSRF 2007-2013
EUROPEAN SOCIAL FUND
Co-financed by Greece and the European Union

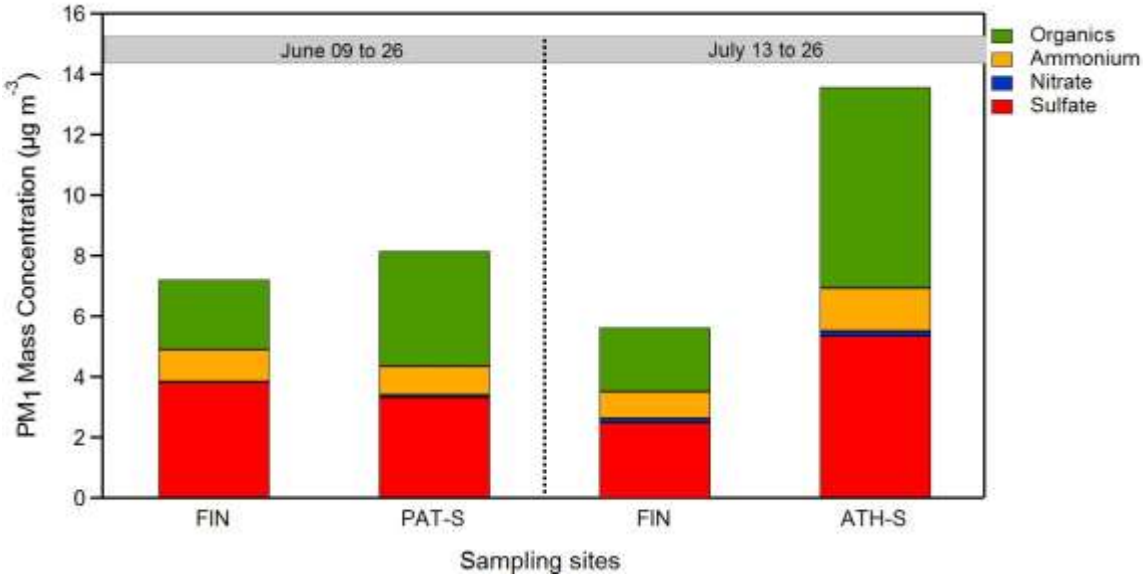

Figure A4. PM_1 mean mass concentration and chemical composition (in μg m^{-3}). Note the two different sampling periods for the different sites (FIN, PAT-S: June 9 to 26 and FIN, ATH-S: July 12 to 26).

European Union
European Social Fund
OPERATIONAL PROGRAMME
EDUCATION AND LIFELONG LEARNING
investing in knowledge society
MINISTRY OF EDUCATION & RELIGIOUS AFFAIRS
MANAGING AUTHORITY
NSRF 2007-2013
EUROPEAN SOCIAL FUND
Co-financed by Greece and the European Union

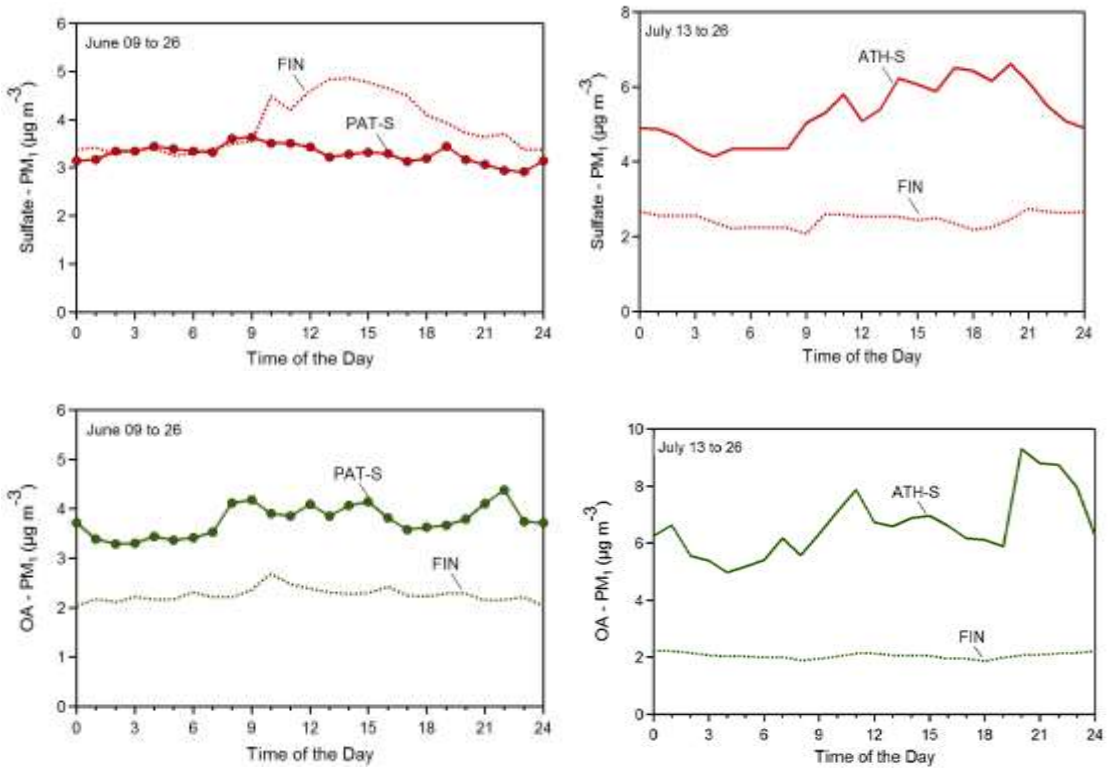

Figure A5. Average diurnal profiles of PM_1 sulfate and organics components in FIN, ATH-S, PAT-S from June 9 to 26 and July 13 to 26. Diurnal values were based on HR-ToF-AMS in PAT-S and ATH-S and on the ACSM in FIN.

European Union
European Social Fund
OPERATIONAL PROGRAMME
EDUCATION AND LIFELONG LEARNING
investing in knowledge society
MINISTRY OF EDUCATION & RELIGIOUS AFFAIRS
MANAGING AUTHORITY
NSRF 2007-2013
EUROPEAN SOCIAL FUND
Co-financed by Greece and the European Union

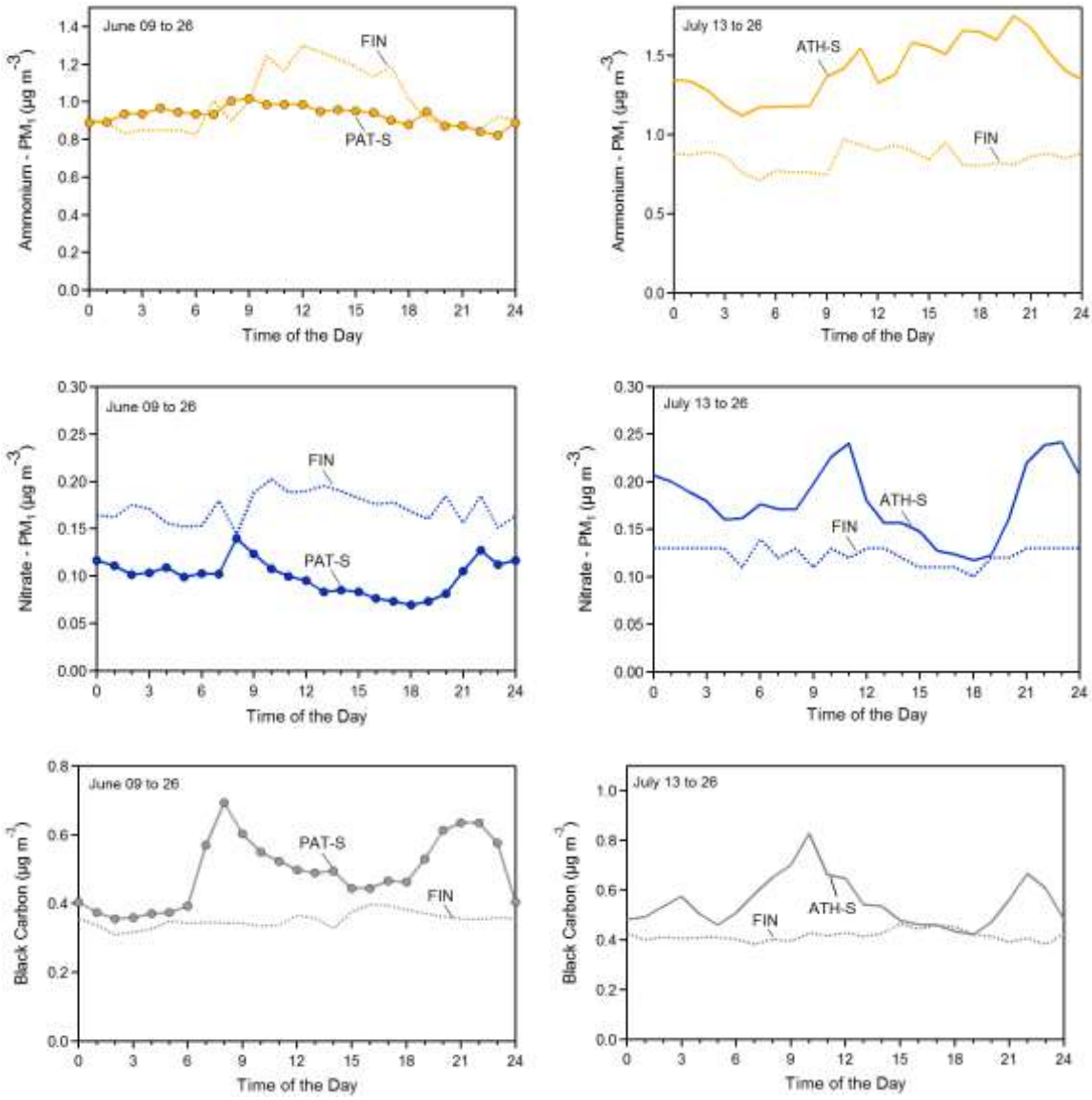

Figure A6. Average diurnal profiles of PM_1 ammonium, nitrate and black carbon components in FIN, ATH-S, PAT-S from June 9 to 26 and July 13 to 26. Diurnal values were based of HR-ToF-AMS in PAT-S and ATH-S and on the ACSM in FIN, while black carbon measurements were carried out with MAAP and aethalometers.

European Union
European Social Fund
OPERATIONAL PROGRAMME
EDUCATION AND LIFELONG LEARNING
investing in knowledge society
MINISTRY OF EDUCATION & RELIGIOUS AFFAIRS
MANAGING AUTHORITY
NSRF 2007-2013
EUROPEAN SOCIAL FUND
Co-financed by Greece and the European Union

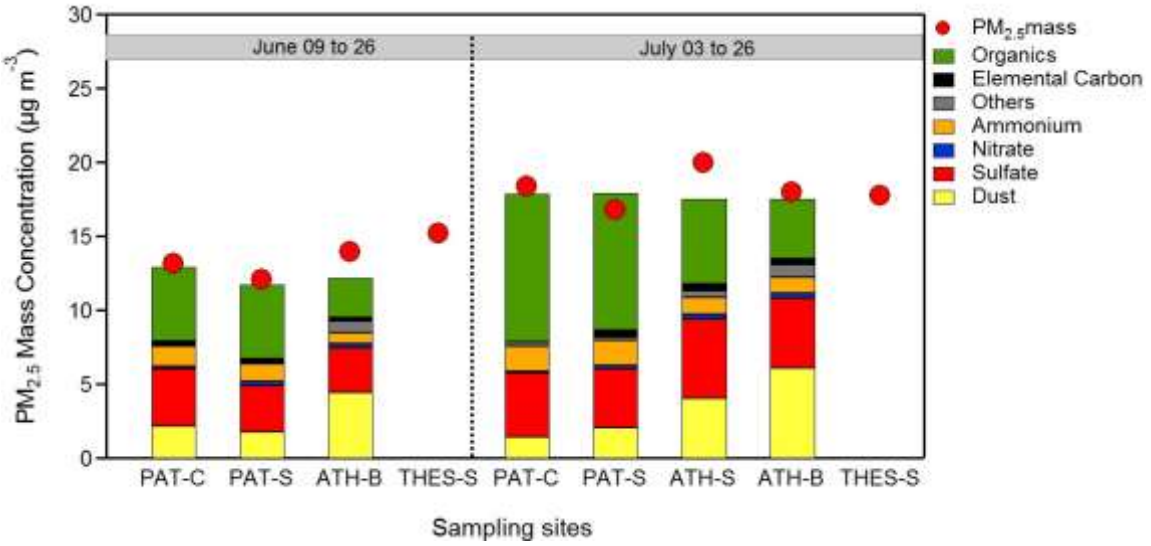

Figure A7. Mean mass concentration and chemical composition of $PM_{2.5}$ during the two campaign periods in PAT-C, PAT-S, ATH-S and ATH-B. The "Others" indicates the sum of potassium, sodium and chloride.

European Union
European Social Fund
OPERATIONAL PROGRAMME
EDUCATION AND LIFELONG LEARNING
investing in knowledge society
MINISTRY OF EDUCATION & RELIGIOUS AFFAIRS
MANAGING AUTHORITY
NSRF 2007-2013
EUROPEAN SOCIAL FUND
Co-financed by Greece and the European Union

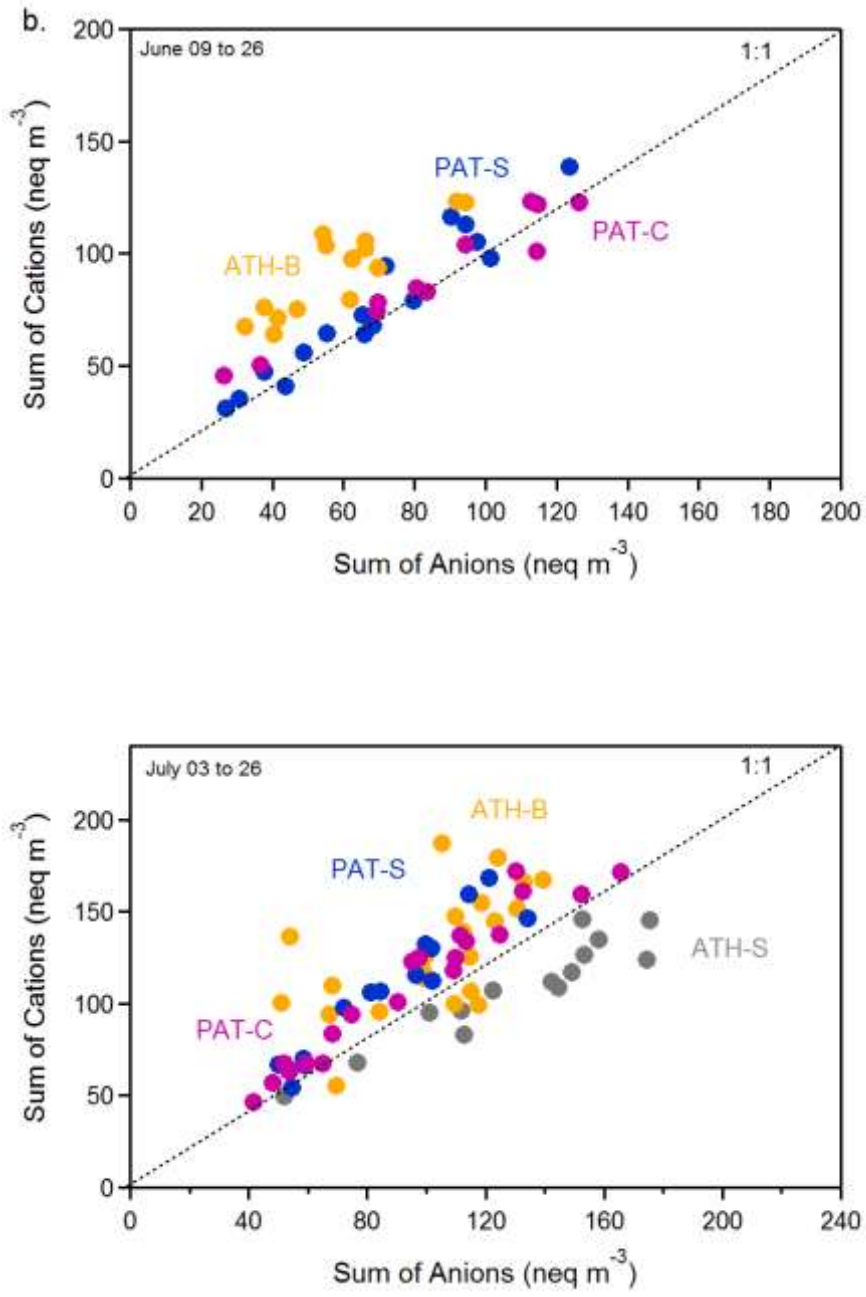

Figure A8. Ionic balance in neq m^{-3} for PAT-C, PAT-S, ATH-B and ATH-B in $PM_{2.5}$ from June 9 to 26 and July 3 to 26.

European Union
European Social Fund
OPERATIONAL PROGRAMME
EDUCATION AND LIFELONG LEARNING
investing in knowledge society
MINISTRY OF EDUCATION & RELIGIOUS AFFAIRS
MANAGING AUTHORITY
NSRF 2007-2013
EUROPEAN SOCIAL FUND
Co-financed by Greece and the European Union

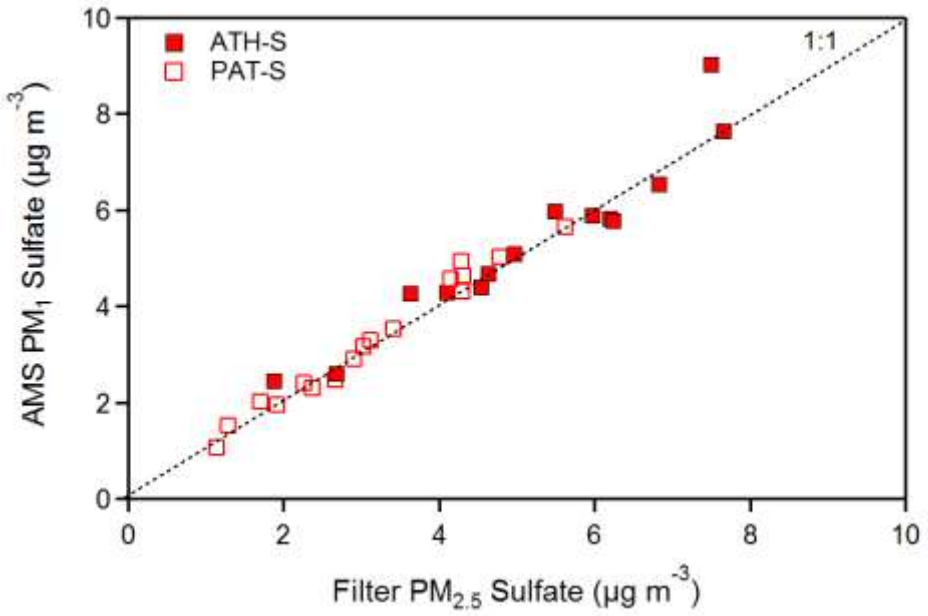

Figure A9. Correlation between HR-ToF-AMS and $PM_{2.5}$ filters for sulfate in ATH-S and PAT-S.

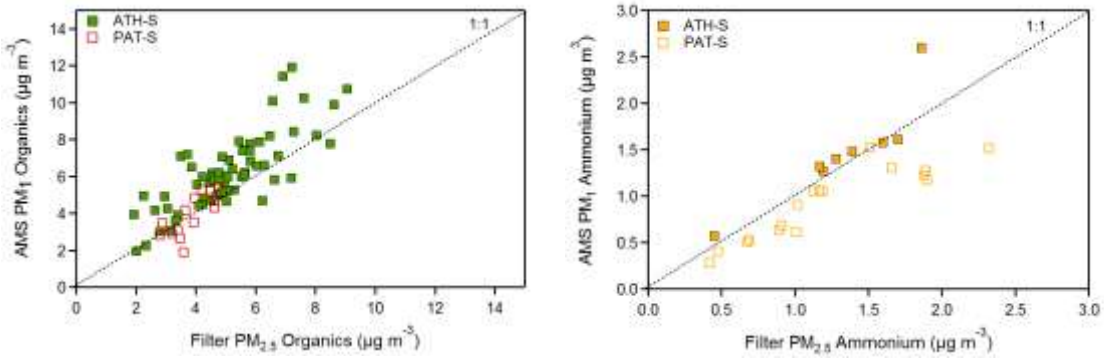

Figure A10. Correlation between HR-ToF-AMS and $PM_{2.5}$ filters for organics and ammonium, in ATH-S and PAT-S.

European Union
European Social Fund
OPERATIONAL PROGRAMME
EDUCATION AND LIFELONG LEARNING
investing in knowledge society
MINISTRY OF EDUCATION & RELIGIOUS AFFAIRS
MANAGING AUTHORITY
NSRF 2007-2013
EUROPEAN SOCIAL FUND
Co-financed by Greece and the European Union

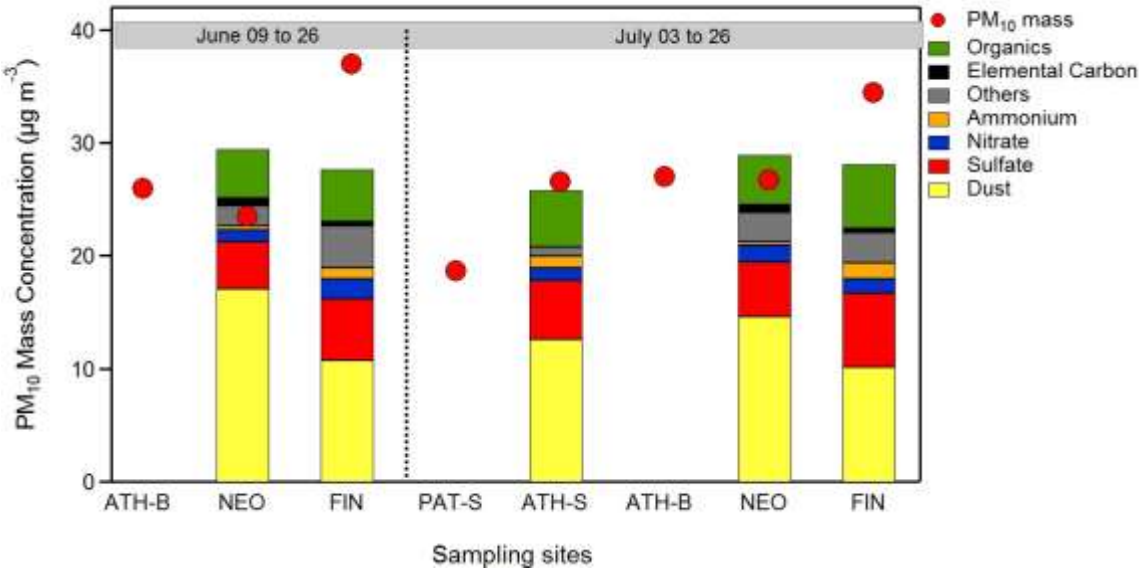

Figure A11. Mean mass concentration and chemical composition of PM_{10} during two periods in PAT-S, ATH-S, ATH-B, NEO and FIN from June 9 to 26 and July 3 to 26. The "Others" indicates the sum of potassium, sodium and chloride.

European Union
European Social Fund
OPERATIONAL PROGRAMME
EDUCATION AND LIFELONG LEARNING
investing in knowledge society
MINISTRY OF EDUCATION & RELIGIOUS AFFAIRS
MANAGING AUTHORITY
NSRF 2007-2013
EUROPEAN SOCIAL FUND
Co-financed by Greece and the European Union

B. Sources and Chemical Characterization of Organic Aerosol during the Summer in the Eastern Mediterranean

B1 Experimental

B1.1 Measurement campaign

The measurements presented here were part of a larger study, which involved measurements in several areas in Greece (Patras, Athens, Thessaloniki, and Finokalia) both in summer and winter. In this work we will focus on the summer HR-ToF-AMS measurements in Patras and Athens. More information about the summer study is provided in Tsiflikiotou et al. (in preparation).

B1.2 Sampling Sites in Patras

Patras has approximately 300,000 inhabitants and is located at the Gulf of Patras, at the foothills of a 2 km high mountain. The major anthropogenic activities include a small industrial zone about 16 km southwest of the city center and a harbor around 2.5 km southwest of the city. The nearest major city is Athens, around 220 km to the east. Measurements in Patras were performed simultaneously at two locations: in the center of the city (38° 14' 46" N, 21° 44' 08" E) and at the Institute of Chemical Engineering Sciences, ICE-HT (38° 17' 52" N, 21° 48' 31" E), which is 8 km (north-east) away from the city center and 1 km (south) from the Patras-Athens highway. The site is surrounded by olive tree fields. A few small settlements are located in a distance of 1 km (southwest and north-east). Most of the instrumentation was deployed at the ICE-HT Institute due to space limitations in the city center station. This paper focuses only on the ICE-HT measurements.

B1.3 Instrumentation in Patras

A HR-ToF-AMS from Aerodyne Research Inc. (DeCarlo et al., 2006) was measuring the size-resolved chemical composition of the NR-PM_1 aerosol species. The tungsten filament for electron ionization was run at an accelerating voltage of 70 eV, while the vaporizer temperature was set at 600^{o}C. Alternative runs between V-mode (single stage

European Union
European Social Fund
OPERATIONAL PROGRAMME
EDUCATION AND LIFELONG LEARNING
investing in knowledge society
MINISTRY OF EDUCATION & RELIGIOUS AFFAIRS
MANAGING AUTHORITY
NSRF 2007-2013
programme for development
EUROPEAN SOCIAL FUND
Co-financed by Greece and the European Union

reflectron) and W-mode (double stage reflectron) were performed with 3 min of measuring time for each mode. In this paper the V-mode data are presented.

A Proton Transfer Reaction Mass Spectrometer (PTR-MS, Ionicon Analytik) was used for the characterization of the volatile organic compounds (VOCs). More details about the VOC measurements are presented in Kaltsonoudis et al. (in preparation). A Scanning Mobility Particle Sizer, (SMPS, classifier model 3080, DMA model 3081, CPC model 3787, TSI) was operated at a sheath flow rate of 5 L min^{-1} and a sample flow rate of 1 L min^{-1}. The SMPS measured the number size distribution in the 10 - 500 nm range. A Multiple-Angle Absorption Photometer (MAAP, Thermo Scientific Inc.) (Petzold and Schönlinner, 2004) was used for the BC measurement. NO_x, SO_2, O_3 and CO concentrations were measured by the corresponding monitors (Teledyne, models T201, 100E, 400E and 300E respectively).

A filter sampler (MetOne SAASS) was used to collect $PM_{2.5}$ samples for inorganic and organic chemical composition analysis. The sampling resolution was 24 h and the flow rate of each filter was 6.7 L min^{-1}. Teflon filters (Whatman 7582 004, 0.2 μm pore size) were used for the measurement of the inorganic anion and cation mass concentrations, using two ion chromatography systems (Metrohm 761 Compact IC). Pre-baked Quartz filters were used for the EC/OC measurement using a laboratory EC/OC analyzer (Sunset Laboratory Inc). More details about the filter extraction procedure are given by Pikridas et al. (2013) and Tsiflikiotou et al. (in preparation). The HR-ToF-AMS and the PTR-MS measurements covered the period from 8 to 27 of June 2012, while the rest of the instrumentation provided measurements from June 8 to July 26, 2012. All the above mentioned instruments were located at the ICE-HT campus.

B1.4 Sampling Site in Athens

Athens is the most densely populated city in Greece with around 4 million inhabitants. The sampling site was at Demokritos National Center for Scientific Research, NCRS (37° 59' 43" N, 23° 48' 57" E), at the municipality of Agia Paraskevi. This is a suburban

European Union
European Social Fund
OPERATIONAL PROGRAMME
EDUCATION AND LIFELONG LEARNING
investing in knowledge society
MINISTRY OF EDUCATION & RELIGIOUS AFFAIRS
MANAGING AUTHORITY
NSRF 2007-2013
programme for development
EUROPEAN SOCIAL FUND
Co-financed by Greece and the European Union

background site 10 km from the city center located at the foothills of Ymittos mountain and is surrounded by pine trees. This site is close (0.5 km) to the ring highway of Ymittos and approximately 1.5 km away from the Mesogion highway to the north-west. The closest residences are 0.5 km away.

B1.5 Instrumentation in the Athens site

For the measurements in Athens we used our mobile laboratory as a fixed station, in which the HR-ToF-AMS, PTR-MS and SMPS (same models as described in session 2.3) were placed. An aethalometer (Magee Scientific, AE31) provided the BC concentrations at 880 nm. An SMPS (classifier model 3080 TSI, custom DMA, CPC model 3022, TSI) was operated at a sheath flow rate of 3 L min^{-1} and a sample flow rate of 0.3 L min^{-1} and measured the number size distribution in the 10 - 660 nm range. $PM_{2.5}$ was collected on Teflon filters every 24 h for the inorganic composition characterization, while a semi-continuous OC/EC analyzer (Field Instrument, Model 4F, Sunset Laboratory Inc) equipped with a $PM_{2.5}$ inlet and an activated carbon denuder was used for the $PM_{2.5}$ EC/OC measurements with a 3 hr resolution. The sampling period was from 8 to 26 of July 2012. Due to technical problems the HR-ToF-AMS started measuring on the July 12, 2012.

B1.6 Data Analysis

For HR-ToF-AMS data analysis SQUIRREL v1.51C and PIKA v1.10C (Sueper, 2014) with Igor Pro 6.22A (Wavemetrics) were used. For the HR-ToF-AMS organic mass spectra, we used the fragmentation table of Aiken et al. (2009). PMF and ME-2 analysis (Paatero and Tapper, 1994; Lanz et al., 2007; Lanz et al., 2008; Ulbrich et al., 2009; Canonaco et al., 2013) were performed using the HR-ToF-AMS organic mass spectra in order to investigate the different organic aerosol sources. High resolution PMF was performed using as inputs the *m/z's* 12-200 and following the procedure of Ulbrich et al. (2009).

European Union
European Social Fund
OPERATIONAL PROGRAMME
EDUCATION AND LIFELONG LEARNING
investing in knowledge society
MINISTRY OF EDUCATION & RELIGIOUS AFFAIRS
MANAGING AUTHORITY
NSRF 2007-2013
EUROPEAN SOCIAL FUND
Co-financed by Greece and the European Union

The Patras HR-ToF-AMS data were corrected for the collection efficiency CE using the algorithm of Kostenidou et al. (2007) with a 2-hour resolution throughout the campaign. A shape factor (χ) of 1 was found to be the most appropriate for this dataset. The average CE was 0.91±0.10 and it was significant higher compared to other studies, which often use a CE of 0.5. One reason could be that the particles entering the HR-ToF-AMS were not dried. Drying the particles usually decreases the CE because the particles bounce on the vaporizer (Matthew et al., 2008). The R^2 between the 2-hour resolution CE and the 2-hour average ambient relative humidity (RH) was very low (0.02). This low correlation and the high CE values can be explained by the fact that the particles were acidic most of the time (see section 3.1) and probably contained water during all the campaign. Comparing the PM_1 HR-ToF-AMS sulphate (after CE corrections) to the $PM_{2.5}$ filter sulphate measurements a slope of 1.05 and a high correlation (R^2=0.98) were found. This could indicate that most of the $PM_{2.5}$ sulfate was in the submicrometer particles. The $PM_{2.5}$ sodium concentration was below the detection limit, so there was practically no sodium sulphate present. The average OA density estimated from the above algorithm was 1.34±0.21 g cm^{-3}, which is very close to the organic density calculated for Finokalia during the summer of 2008 (1.35±0.22 g cm^{-3}, Lee et al., 2010).

For Athens the aerosol was not dried before it entered the HR-ToF-AMS, but the particles entering the SMPS were dried to maintain compatibility with long term measurements performed at the site. Thus we modified the algorithm of Kostenidou et al. (2007) converting the ambient HR-ToF-AMS mass distributions to dry mass distributions using the relative humidity (RH) inside the sampling line and calculating the inorganic aerosol water content using the Extended Aerosol Inorganic Model II (E-AIM, Carslaw et al., 1995; Clegg et al., 1998; Massucci et al., 1999). As inputs to the E-AIM model we used the inorganic concentrations of sulphate, ammonium and nitrate and the temperature and RH at the entrance of the HR-ToF-AMS line. The algorithm was run for shape factors 1-1.4 and the optimum solution was selected (i.e. the minimum of the minimum error scores) which corresponded to the optimum CE,

European Union
European Social Fund
OPERATIONAL PROGRAMME
EDUCATION AND LIFELONG LEARNING
investing in knowledge society
MINISTRY OF EDUCATION & RELIGIOUS AFFAIRS
MANAGING AUTHORITY
NSRF 2007-2013
EUROPEAN SOCIAL FUND
Co-financed by Greece and the European Union

organic density, and shape factor. The average CE was 0.63±0.13. After applying CE corrections, the PM_1 HR-ToF-AMS sulphate correlated well with the $PM_{2.5}$ filter sulphate (R^2=0.91, slope=0.98), once more suggesting that the sulphate in the 1-2.5 μm range was a small fraction of the $PM_{2.5}$ sulfate. The average organic density was 1.15±0.36 g cm^{-3}, lower than in Patras, and the average shape factor was 1.16±0.1 suggesting that a lot of the particles were not spherical.

The angle theta (θ) between the mass spectra vectors was used as a measure of their similarity (Kostenidou et al., 2009). The mass spectra are treated as vectors and the angle θ is calculated by using their internal product. The lower the angle θ is the higher the similarity between the two spectra.

B2 Results and Discussion

B2.1 Patras

The time series of the mass concentration of the NR-PM_1 components measured by the HR-ToF-AMS and the BC in Patras are shown in Figure B1a. The average PM_1 mass concentration (not including dust) was 8.6 μg m^{-3}. On average, the organic mass concentration was 3.8 μg m^{-3}, sulphate 3.3 μg m^{-3}, ammonium 0.9 μg m^{-3} and BC 0.5 μg m^{-3}. Nitrate was very low around 0.1 μg m^{-3}.

The average OM:OC ratio was 1.80±0.10. The average diurnal profile of O:C is depicted in Figure B2. O:C increased in the early morning hours (2:00-7:00 LT) and during the afternoon (15:00-17:00). The OA average diurnal profile exhibited 3 peaks, 2 of them (around 8:00-10:00 and 21:00-23:00) were associated with primary sources as the BC increased the same time as well. The OA increase at 11:00-16:00 is related to the formation of secondary species as the solar intensity peaks the same time. The fragments of *m/z* 44 and 57 represented 0.14 and 0.01 of the organic signal correspondingly.

European Union
European Social Fund
OPERATIONAL PROGRAMME
EDUCATION AND LIFELONG LEARNING
investing in knowledge society
MINISTRY OF EDUCATION & RELIGIOUS AFFAIRS
MANAGING AUTHORITY
NSRF 2007-2013
EUROPEAN SOCIAL FUND
Co-financed by Greece and the European Union

The PM_1 aerosol as measured by the HR-ToF-AMS was always acidic with an average inorganic cations/anions equivalent ratio of 0.75±0.07. This indicates that there was no available ammonia to fully neutralize the sulphate and thus the formation of PM_1 ammonium nitrate (from ammonia and nitric acid) in the PM_1 was not thermodynamically favorable. In order to estimate the organic nitrate mass (ONit) contribution to the total nitrate mass (TotNit) we followed the procedure of Farmer et al. (2010):

$$\frac{\text{ONit}}{\text{TotNit}} = \frac{(1+R_{\text{ONit}})\times\left(R_{[NO_2^+/NO^+]\text{meas}} - R_{[NO_2^+/NO^+]\text{cal}}\right)}{\left(1+R_{[NO_2^+/NO^+]\text{meas}}\right)\times\left(R_{\text{ONit}} - R_{[NO_2^+/NO^+]\text{cal}}\right)} \quad (1)$$

where $R_{[NO_2^+/NO^+]\text{meas}}$ is the measured ratio of NO_2^+/NO^+ ions as a function of time, $R_{[NO_2^+/NO^+]\text{cal}}$ is the ratio of NO_2^+/NO^+ ions obtained during NH_4NO_3 calibrations (0.58 on average) and R_{ONit} is a fixed value set to 0.05, as the minimum ratio of NO_2^+/NO^+ observed in this campaign was 0.05. The average organic nitrate fraction was 0.91±0.05, which suggests that most of the nitrate was in the form of organic nitrate. The correlation between OA and nitrate was moderate (R^2=0.38).

B2.2 Athens (Demokritos Station)

On average the PM_1 mass concentration in Athens (not including dust) was 14.2 μg m^{-3}. This is a different period than the one in Patras so direct comparisons could result in erroneous conclusions. A detailed description and intercomparison of the various measurements (including filter samples) performed in Athens and Patras is given in the companion paper by Tsiflikiotou et al. (in preparation). Briefly, these authors found that for the July period the mean concentrations of $PM_{2.5}$ sulphate in Patras and Athens were similar, while $PM_{2.5}$ organics were higher in Patras than in Athens. Figure B1b shows the time series of the concentration of the NR-PM_1 components measured by the HR-ToF-AMS in Athens and the BC measured by the aethalometer. The average organic concentration was 6.6 μg m^{-3}, sulphate 5.3 μg m^{-3}, ammonium 1.4 μg m^{-3} and BC 0.7 μg m^{-3}. Similarly to Patras nitrate levels were low, 0.2 μg m^{-3} on average.

European Union
European Social Fund
OPERATIONAL PROGRAMME
EDUCATION AND LIFELONG LEARNING
investing in knowledge society
MINISTRY OF EDUCATION & RELIGIOUS AFFAIRS
MANAGING AUTHORITY
NSRF 2007-2013
programme for development
EUROPEAN SOCIAL FUND
Co-financed by Greece and the European Union

The average O:C mass ratio was 0.47±0.11, lower than in Patras (0.50), because of the higher contribution of primary emissions (Section 3.3.1 and 3.3.2). The average OM:OC ratio was 1.76±0.14. The diurnal cycle of O:C is shown in Figure B2 and is similar to the one in Patras. The O:C exhibited two peaks one in the early morning around 3:00-5:00 LT and a second in the late afternoon 17:00-20:00 LT. The OM based on the $PM_{2.5}$ semi-continuous OC/EC measurements was calculated using the OM:OC ratio provided by the HR-ToF-AMS. The measurements are in reasonable agreement (R^2=0.48), with the HR-ToF-AMS providing slightly higher concentrations. The scatter observed when comparing the corresponding measurements is due to a number of factors including the positive and negative artifacts of filter measurements, the uncertainties of the corresponding measurements and the different size ranges. The negative artifacts of the filter measurements due to evaporation of the collected OA can explain the occurrence of some measurements in which the $PM_{2.5}$ filter-based OA is less than the PM_1 HR-ToF-AMS OA. The equivalent ratio of PM_1 cations to anions (measured by the HR-ToF-AMS) was on average 0.70±0.09 and thus the aerosol was acidic. Again free ammonia was not enough to neutralize the sulphate and thus there was no ammonium nitrate observed in the PM_1 fraction. Applying equation (1) to the Athens data set (with an average $R_{[NO_2^+/NO^+]cal}$=0.68, and R_{ONit} = 0.12), the organic nitrate fraction was 0.89±0.08, indicating that most of the nitrate was actually organic nitrate. The coefficient of determination between OA and nitrate was R^2=0.62.

B2.3 OA sources

B2.3.1 Patras

For the PMF analysis both PMF Evaluation Tool, PET, (Lanz et al., 2008; Ulbrich et al., 2009) and ME-2 (Lanz et al., 2008; Canonaco et al., 2013) solutions were examined and evaluated using the HR organic mass spectra. A five factor solution was chosen as the best to describe the major sources of OA in Patras. The factors corresponded to very oxygenated OA (V-OOA, 19%), moderately oxygenated OA (M-OOA, 38%), biogenic oxygenated OA (b-OOA, 21%), HOA-1 (7%) and HOA-2 (15%). The V-OOA factor corresponds to the Low Volatility OOA (LV-OOA) and the M-OOA to Semivolatile

European Union
European Social Fund
OPERATIONAL PROGRAMME
EDUCATION AND LIFELONG LEARNING
investing in knowledge society
MINISTRY OF EDUCATION & RELIGIOUS AFFAIRS
MANAGING AUTHORITY
NSRF 2007-2013
programme for development
EUROPEAN SOCIAL FUND
Co-financed by Greece and the European Union

OOA (SV-OOA) factors reported in previous work. The lack of a direct determination of the volatility of these factors makes the assignment of names based on their oxygen content preferable. The assignment of the factors to specific sources was based on their mass spectra and diurnal profile characteristics: V-OOA had a high contribution of *m/z* 44, M-OOA had a moderate *m/z* 44 contribution. b-OOA was characterized by both biogenic and oxidized OA signatures, HOA-1 was similar to the literature HOA factor related to traffic emissions and HOA-2 included primary cooking and aged traffic emissions. Overall, the oxygenated OA was the dominant component (78%) and the primary OA accounted for only 22%. The HR mass spectrum of each factor is illustrated in Figure B3a, while their time series are shown in Figure B4a and their average diurnal profiles in Figure B5a.

V-OOA was characterized by a high *m/z* 44 (~22%) with an O:C= 0.81 and is related to aged aerosol (Figure B3a). The V-OOA factor correlated well with sulphate (R^2=0.48) and ammonium (R^2=0.51), which is typical for highly oxygenated OA. Its correlation with nitrate was low (R^2=0.09). The V-OOA diurnal profile was almost flat (Figure B5a). R^2 between V-OOA and individual VOCs measured by the PTR-MS were all less than 0.13.

M-OOA had a pronounced but of lower intensity *m/z* 44 (~16%) and an O:C=0.54 implying aged but less oxidized particles (Figure B3a). Nitrate has been suggested as a tracer for the less oxygenated species (e.g. Lanz et al., 2007; Mohr et al., 2012), however there was very little nitrate during our measurements and most of it was organic nitrate resulting in a weak correlation between the M-OOA and nitrate (R^2=0.04). M-OOA had a very similar pattern with the solar radiation peaking at around 14:00 (local time). M-OOA had low correlation with methyl vinyl ketone (MVK) and methacrolein (MACR) (*m/z* 71, R^2=0.31), hydroxyacetone (*m/z* 75, R^2=0.29), C_5 carbonyls/2-methyl-butene-2-ol (MBO)/methacrylic acid (*m/z* 87, R^2=0.29), terpene oxidation products (*m/z* 113, R^2=0.30) and nopinone (*m/z* 139, R^2=0.28), (Table 1). Comparing the M-OOA spectrum to the α-pinene SOA spectrum of Heringa et al.

European Union
European Social Fund
OPERATIONAL PROGRAMME
EDUCATION AND LIFELONG LEARNING
investing in knowledge society
MINISTRY OF EDUCATION & RELIGIOUS AFFAIRS
MANAGING AUTHORITY
NSRF 2007-2013
programme for development
EUROPEAN SOCIAL FUND
Co-financed by Greece and the European Union

(2012) the angle theta was quite high (θ=35°), while the similarity between the M-OOA and the toluene photo-oxidation SOA spectrum (Kostenidou et al., not published data) was greater (θ=16°). Thus this factor may include contributions by both anthropogenic and biogenic sources.

The biogenic OOA factor had an f_{44}=0.13 and O:C=0.48 (Figure B3a) which indicates a relatively moderate degree of oxygenation. It was characterized by a distinct *m/z* 82 (mainly composed of $C_5H_6O^+$), an elevated *m/z* 53 (mostly $C_4H_5^+$) and a significant contribution at *m/z* 39 (5%, mainly CH_3O^+). These characteristics were similar to those found at a rural area in Ontario, Canada (Slowik et al., 2011), downtown Atlanta, Georgia, USA (Budisulistiorini et al., 2013), in tropical rainforests in the central Amazon Basin (Chen et al., 2014) and in Borneo, Malaysia (Robinson et al., 2011) and in Centreville in rural Alabama (Xu et al., 2014) which were associated to secondary OA produced by isoprene photooxidation. Using the HYSPLIT back trajectory model (Draxler and Rolph, 2013), the mass concentration of b-OOA was almost zero when the air masses were coming from the west (e.g. Ionian Sea, 11-15 June), while M-OOA and V-OOA were still high. However, the b-OOA increased in periods (e.g. 10-11 June, 16-17 and 24-26 June) when the air masses passed over the forested mountains of Central Greece, which is an area characterized by high terpene and isoprene emissions (Karl et al., 2009). This supports the biogenic character of this factor. The highest concentration of b-OOA was at 6:00 in the morning on June 16th (5.4 μg m^{-3}). b-OOA exhibited low correlation with isoprene (*m/z* 69, R^2=0.13), isoprene peroxides (*m/z* 101, R^2=0.28) and the first generation isoprene products such as MVK and MACR (*m/z* 71, R^2=0.21) (Table 1). However, it correlated better with acetone (*m/z* 59, R^2=0.35), hydroxyl-acetone (*m/z* 75, R^2=0.41), PAN (*m/z* 77, R^2=0.37), nopinope (*m/z* 139, R^2=0.39) and pinonaldehyde (*m/z* 151, R^2=0.30), which are products of terpenes ozonolysis (Matsunaga et al., 2003; Holzinger et al., 2005; Lee et al., 2006).

HOA-1 was characterized mainly by the *m/z's* 39, 41, 43, 55, 57, 67, 69 and 81 (Figure B3a) which are typical hydrocarbon fragments of fresh traffic emissions (Zhang et al.,

European Union
European Social Fund
OPERATIONAL PROGRAMME
EDUCATION AND LIFELONG LEARNING
investing in knowledge society
MINISTRY OF EDUCATION & RELIGIOUS AFFAIRS
MANAGING AUTHORITY
NSRF 2007-2013
EUROPEAN SOCIAL FUND
Co-financed by Greece and the European Union

2005; Aiken et al., 2009). Its O:C was 0.1 which is in the range found in literature (the HOA factor of Mohr et al. (2012) had an O:C=0.03, while the HOA factor of Ulbrich et al. (2009) had an O:C=0.18). HOA-1 had a medium correlation with BC (R^2=0.38) and nitrate (R^2=0.27). The HOA-1 diurnal profile was characterized by two peaks during the morning (8:00) and evening rush hours (21:00) (Figure B5a). HOA-1 correlated moderately with benzene (*m/z* 79, R^2=0.36), toluene (*m/z* 93, R^2=0.35), xylenes (*m/z* 107, R^2=0.37), C_9 aromatic compounds (*m/z* 121, R^2=0.45). The correlation with NO_x was relatively low (R^2=0.26).

The HOA-2 O:C was 0.21. The HOA-2 spectrums were characterized among others by the *m/z's* 39, 41, 43, 44, 55, 57 and 67 (Figure B3a) which are features of cooking organic aerosol, COA (Ge et al., 2011a, b; Crippa et al., 2013a, b). However, the reported COA spectra (e.g. Ge et al., 2011a, b; Crippa et al., 2013a, b) have lower contributions at *m/z* 44 (0.011-0.022), indicating less oxygenation. The f_{44} in the HOA-2 mass spectrum was 0.034 which implies that this factor may also contain species that have been oxidized to some degree. The HOA-2 diurnal profile had a small peak around 14:00 and a higher one around 22:00, which are consistent with the Greek lunch and dinner periods (Figure B5a). Thus, the HOA-2 in Patras is mainly due to charbroiling of meat cooking OA. The correlation between HOA-2 and BC, nitrate, benzene, toluene, xylenes and C_9 aromatic compounds was moderate (R^2=0.38, 0.38, 0.33, 0.30, 0.33 and 0.43 correspondingly). During June 16-23 the wind speed was relatively high (average 5.3 m s^{-1}) compared to the rest of the sampling days (average 2.5 m s^{-1}). The contribution of the local sources (HOA-1 and HOA-2) was less than 9% of the OA during that windy period compared to 28% during the remaining days (Figure B4a).

B2.3.2 Athens

Four OA factors could be identified in the Athens HR-ToF-AMS data set: V-OOA (35%), M-OOA (30%), HOA-1 (18%) and HOA-2 (17%). The corresponding mass spectra are provided in Figure B3b. The time series of the four PMF factors are shown in Figure B4b, while their diurnal cycles in Figure B5b. Similarly, to Patras the

European Union
European Social Fund
OPERATIONAL PROGRAMME
EDUCATION AND LIFELONG LEARNING
investing in knowledge society
MINISTRY OF EDUCATION & RELIGIOUS AFFAIRS
MANAGING AUTHORITY
NSRF 2007-2013
programme for development
EUROPEAN SOCIAL FUND
Co-financed by Greece and the European Union

contribution of the oxygenated OA in Athens was high (65%), while the primary sources contributed 35%.

The very oxidized OA (V-OOA) had an f_{44}=0.18 and O:C=0.68 and showed a good correlation with sulphate (R^2=0.53) and ammonium (R^2=0.50) consistent with the aged character of this factor. The diurnal profile of the V-OOA (Figure B5b) was characterized by a peak around 15:00-18:00, which is probably associated with production of this component in the afternoon over the region. At the same time M-OOA decreased, which indicates that V-OOA is a product of photochemical processing. V-OOA correlated with formic acid (*m/z* 47, R^2=0.47), hexenal (*m/z* 99, R^2=0.42), isoprene peroxides (*m/z* 101, R^2=0.35), terpene oxidation products (*m/z* 113, R^2=0.40), and heptanal (*m/z* 115, R^2=0.42) (Table B1).

The moderately oxidized OA (M-OOA) was characterized by an f_{44}=0.14 and O:C=0.56 and exhibited a weak correlation with sulphate, ammonium and nitrate (R^2=0.17, 0.17 and 0.13 respectively). M-OOA increased during the day with a maximum at 12:00-14:00, following the diurnal profile of solar radiation, which implies relatively fast photochemical reactions. M-OOA had a second peak during the night around midnight, which could be an indication of nighttime production or condensation due to the change in temperature between day and night (the average temperature at noon was 32^{o}C, while during the night it decreased to around 21^{o}C). M-OOA did not show any correlation (R^2 less than 0.07) with the measured VOCs.

The HOA-1 O:C was 0.07. Surprisingly it had a rather weak correlation with BC (R^2=0.05) and it also showed a low correlation with nitrate (R^2=0.13). The HOA-1 diurnal profile had 2 peaks, a small increase during the morning (7:00) and a larger peak in the evening hours (20:00), consistent with the contribution of traffic emissions. HOA-1 did not correlate with VOCs characteristic of traffic such as benzene, toluene and xylenes (the R^2 values were correspondingly 0.15, 0.13 and 0.16) and inorganic gases as NO_x (R^2= 0.06). The HOA-1 mass spectrum and time series were very stable

European Union
European Social Fund
OPERATIONAL PROGRAMME
EDUCATION AND LIFELONG LEARNING
investing in knowledge society
MINISTRY OF EDUCATION & RELIGIOUS AFFAIRS
MANAGING AUTHORITY
NSRF 2007-2013
EUROPEAN SOCIAL FUND
Co-financed by Greece and the European Union

for 2 to 5 factorial solutions and for f_{peaks} values from -1 to 1. The R^2 between the HOA-1 of the selected solution and the HOA-1 of the solutions of 2, 3 and 5 factors was always greater than 0.973 (both for the time series and the mass spectra). This weak correlation between the HOA-1 factor and other primary organic pollutants indicates that their concentrations were not dominated by the same sources. For example, HOA-1 possibly originated mostly from passenger cars and scooters. In Greece the car-to-scooter ratio is around 3 to 1 and using the Platt et al. (2014) primary OA emissions from two-stroke engines the scooter emissions are expected to be a significant OA source. BC mainly originated from diesel vehicles. Another potential BC source could be shipping emissions from Piraeus (15 km south-west of the sampling site) and Rafina (17 km east) ports. However, during high BC concentration periods (around 10:00 LT) the wind was from the north. Thus, the main source of BC was probably diesel vehicles.

The location of the sampling site and the inhomogeneity of the surrounding areas, in combination with the wind direction changes have confounded these effects. The rose plots of HOA-1, BC, NO_x and benzene for wind speeds greater than 1 m s^{-1} indicated that BC, NO_x and benzene had the same origin, while HOA-1 did not. For example, at 8:00 LT the HOA-1 was on average coming from southwest, likely from the ring highway of Ymittos, while BC, NO_x and benzene from the north probably influenced by the Mesogion highway. HOA-2 had an O:C=0.24 and exhibited a good correlation with BC (R^2=0.57). HOA-2 also correlated well with nitrate (R^2=0.75) implying that organic nitrate compounds were possibly emitted or produced along with this OA type. The HOA-2 profile had 2 peaks at around 11:00 and 22:00. The second peak is characteristic of Greek dinner period; thus part of HOA-2 could be attributed to meat cooking OA. However, the first peak cannot be explained by the Greek lunch period. Although it could contain cooking emissions from canteens or caterings which start cooking earlier than the typical Greek lunchtime, it still does not explain the good correlation with BC. Greek cooking emissions have a low BC/OA ratio (unpublished measurements). Thus HOA-2 may include sources other than cooking. The correlation with the BC implies that HOA-2 and BC had the same origin. Comparing the HOA-2

European Union
European Social Fund
OPERATIONAL PROGRAMME
EDUCATION AND LIFELONG LEARNING
investing in knowledge society
MINISTRY OF EDUCATION & RELIGIOUS AFFAIRS
MANAGING AUTHORITY
NSRF 2007-2013
programme for development
EUROPEAN SOCIAL FUND
Co-financed by Greece and the European Union

mass spectrum with aged POA or SOA emissions from other sources such as α-pinene, wood burning, scooter and diesel (Heringa et al., 2012) the angles θ were 19, 19, 28, 17° respectively. This indicates that HOA-2 could include aged diesel emissions since α-pinene is not associated with BC and there were no observed biomass burning events during the sampling period. The HOA-2 factor correlated with the *m/z* 43 (R^2=0.43), acetone (*m/z* 59, R^2=0.44), methyl ethyl ketone (MEK, *m/z* 73, R^2=0.49), benzene (*m/z* 79, R^2=0.62), toluene (*m/z* 93, R^2=0.54), xylenes (*m/z* 107, R^2=0.56), C_9 aromatic compounds (*m/z* 121, R^2=0.58) and C_{10} aromatic compounds (*m/z* 135, R^2=0.55). It also had a good correlation with NO_x (R^2=0.58).

Trying rotations in the f_{peak} range -1 to 1 the correlations between the factors HOA-1 and HOA-2 and traffic markers such as BC and toluene practically did not change. In addition, using a fixed HOA spectrum (the HOA mass spectrum of Aiken et al. (2009) and the HOA mass spectrum found in Athens during winter, unpublished results) with *a*=0.1 the correlation between HOA-1 and BC did not improve. All these suggest that our conclusions are robust to the details of the PMF process. Our explanation is that the correlations are affected also by the locations of the various sources around the receptor site and the corresponding wind directions. The fact that these area sources (gasoline cars, diesel cars, cooking activities) did not have a homogeneous spatial distribution can lead to these rather unexpected results.

B2.3.3 Comparison of the PMF factors in the two cities

The mass spectra of the V-OOA factors in the two cities were almost the same (θ=6.7°). However, Athens V-OOA exhibited lower f_{44} and O:C ratio (0.18 and 0.68 correspondingly) compared to Patras V-OOA (0.22 and 0.81 respectively). This difference could be partially due to the different periods of the two measurements. The two M-OOA mass spectra were even more similar to each other (θ=5.4°). A high correlation was also observed between the two HOA-2 mass spectra (θ=5.9°). The Athens HOA-2 was slightly more oxygenated (O:C=0.24), as the oxygenated part of *m/z* 43 was more elevated, 65%, compared to 51% observed in Patras HOA-2 and the

European Union
European Social Fund
OPERATIONAL PROGRAMME
EDUCATION AND LIFELONG LEARNING
investing in knowledge society
MINISTRY OF EDUCATION & RELIGIOUS AFFAIRS
MANAGING AUTHORITY
NSRF 2007-2013
programme for development
EUROPEAN SOCIAL FUND
Co-financed by Greece and the European Union

f_{44} was just slightly higher (0.07), while in Patras HOA-2 was 0.06. The two HOA-1 factors exhibited a lower correlation with each other (θ=22.8º). The main differences were at *m/z* 41, 43, 55, 57, 69, 71, 81, 83 and 85 which were more abundant in the Athens HOA-1 spectrum, while in the Patras spectrum the f_{44} was higher (0.04) compared to Athens (0.02). In Patras HOA-1 spectrum *m/z* 57 was lower in comparison with *m/z* 55. The O:C in Athens HOA-1 was a little lower (0.07) than in Patras HOA-1 (0.10).

B2.3.4 Comparing the PMF factors with other studies

Table B2 shows comparisons of the mass spectra of the factors found in the two cities with selected PMF factors from the literature (Aiken et al., 2009; Docherty et al., 2011; Sun et al., 2011; Robinson et al., 2011; Heringa et al., 2012; Mohr et al., 2012, Ge et al., 2012a, b; Crippa et al., 2013a, b; Budisulistiorini et al., 2013; Xu et al., 2014) that have all been extracted using the fragmentation table of Aiken et al. (2009). The two V-OOA factors were quite similar with LV-OOA at Riverside (Docherty et al., 2011), θ=8-10º, and with LV-OOA at New York City (Sun et al., 2011), θ=11-14º. They also showed good correlation with LV-OOA measured in Barcelona (Mohr et al., 2012) and Paris (Crippa et al., 2013a, b) θ=13-19º.

M-OOA had moderate to low agreement with the majority of the literature profiles. The lowest angle θ (around 22-24º) corresponded to the comparison with the SV-OOA found in Mexico City (Aiken et al., 2009). It did however resemble (θ=13-16º) the toluene SOA spectrum (Kostenidou et al., not published data). The b-OOA factor in Patras correlated moderately with α-pinene SOA, θ=29º, (Heringa et al., 2012) and the isoprene factor found in Alabama, θ=28º, (Xu et al., submitted). However, it had low correlation with the Factor 82, θ=47º, found in Malaysia (Robinson et al., 2011) and the IEPOX OA factor extracted in Atlanta, θ=76º, (Budisulistiorini et al., 2013).

The HOA-1 factors correlated well with most of the literature HOA profiles, θ=10-25º.The highest angles (24 and 25º) corresponded to the comparison with Paris during

European Union
European Social Fund
OPERATIONAL PROGRAMME
EDUCATION AND LIFELONG LEARNING
investing in knowledge society
MINISTRY OF EDUCATION & RELIGIOUS AFFAIRS
MANAGING AUTHORITY
NSRF 2007-2013
programme for development
EUROPEAN SOCIAL FUND
Co-financed by Greece and the European Union

the winter (Crippa et al., 2013b). The major differences were in the *m/z's* 44 and 28 which were higher than in Paris, *m/z's* 29 and 43 which were lower compared to Paris and *m/z* 39 which was absent in Paris probably due to the unit mass resolution spectra used as input for the Crippa et al. (2013) PMF analysis. The HOA-2 mass spectra resembled the COA factor extracted in New York City, θ=11-14º, (Sun et al., 2011) and the SOA from diesel VOCs emissions, θ=17º, (Heringa et al., 2012).

B2.4 Discussion

In both cities the composition of NR-PM_1 was surprisingly similar. Organic contributions in Patras and Athens were around 45%, which is similar to other areas in Europe: London (UK) 46%, mountain Taunus (Germany) 59%, Melpitz (Germany) 59%, Mace Head (Ireland) 39%, Po Valley (Italy) 33%, and Paris (France) 50% (Cubison et al., 2006; Hings et al., 2007; Poulain et al., 2011; Dall'Osto et al., 2010; Saarikoski et al., 2012; Crippa et al., 2013a). With 38%, sulphate made a larger contribution compared to other studies in Europe during the summer: London 31%, mountain Taunus 24%, Mace Head 32%, Melpitz 22%, Po Valley 9%, and Paris 25% (Cubison et al., 2006; Hings et al., 2007; Dall'Osto et al., 2010; Poulain et al., 2011; Saarikoski et al., 2012; Crippa et al., 2013a). Nitrate contributed very little (less than 2%) and was mostly attributed to organonitrate compounds, in contrast with other European studies where nitrate ranged from 6% (Melpitz) to 39% (Po Valley) (Poulain et al., 2011; Saarikoski et al., 2012) and mainly was ammonium nitrate. The absence of particulate nitrate in PM_1 was also observed at Finokalia (Hildebrandt et al., 2010) and is characteristic of the Eastern Mediterranean. Ammonia levels in this region are quite low (Wichink Kruit et al., 2012) to fully neutralize the existing relatively high sulphate.

The O:C ratios (0.50 for Patras and 0.47 for Athens) were moderately high. The O:C ratio at Finokalia was 0.8 (Hildebrandt et al., 2010), at Cape Corsica 0.9 (Nicolas, 2013), while in Paris 0.38 (Crippa et al., 2013a). In both cities the OOA was the dominant OA component (78% in Patras and 65% in Athens). This fraction is within the range that has been measured in previous summer studies in the Mediterranean. For

European Union
European Social Fund
OPERATIONAL PROGRAMME
EDUCATION AND LIFELONG LEARNING
investing in knowledge society
MINISTRY OF EDUCATION & RELIGIOUS AFFAIRS
MANAGING AUTHORITY
NSRF 2007-2013
EUROPEAN SOCIAL FUND
Co-financed by Greece and the European Union

example, the OOA at Finokalia was 100% of the OA (Hildebrandt et al., 2010), in Marseille accounted for 80% (El Haddad et al., 2013), at Cape Corsica 80-85% (Nicolas, 2013), while in Po Valley 61% (Saarikoski et al., 2012).

In Athens 35% of the OA was V-OOA, while in Patras only 19% of the OA was attributed to V-OOA. In addition the V-OOA in Athens was increasing in the afternoon, suggesting its production either locally or regionally. In Patras V-OOA had an almost flat diurnal profile. This difference could be attributed to the different air masses that arrive to each site. According to back trajectory analysis, based on FLEXPART (Stohl et al., 2005) and HYSPLIT (Draxler and Rolph 2013) during most of the sampling days in Athens the air masses had spent considerable time over the source-poor Aegean Sea, while the majority of the air masses that arrived in Patras were continental and passed over the mountains of Central Greece.

Given the location of the two sites, one would expect to find a marine OA (MOA) factor. The S:C ratio estimated by the AMS is often underestimated in the presence of organosulfates (Farmer et al., 2010; Docherty et al., 2011). To avoid such artifacts, we investigated the contribution of MOA applying a constrained solution in the ME-2 using the MOA mass spectrum of Crippa et al. (2013) with a=0.1. For Patras the average MOA concentration for 4, 5, and 6 factors was around 0.04 μg m^{-3} corresponding to 1 percent of the OA mass. For Athens the MOA concentration for the 3, 4 and 5 factor solutions was approximately 0.25 μg m^{-3} (3.7 percent of the OA mass). So if MOA was indeed present its contribution to OA was quite low.

B3 Conclusions

During the summer of 2012 the air pollution in Patras (June) and Athens (July) was monitored continuously. The sum of the NR-PM_1 and BC concentration was on average 8.6 μg m^{-3} in Patras and 14.2 μg m^{-3} in Athens. However, the aerosol composition was quite similar in both areas: 45% OA, 38% sulphate, 11% ammonium, 1% nitrate (mostly organic) and 5% BC indicating the importance of regional sources. In both

European Union
European Social Fund
OPERATIONAL PROGRAMME
EDUCATION AND LIFELONG LEARNING
investing in knowledge society
MINISTRY OF EDUCATION & RELIGIOUS AFFAIRS
MANAGING AUTHORITY
NSRF 2007-2013
programme for development
EUROPEAN SOCIAL FUND
Co-financed by Greece and the European Union

cities the fine aerosol was acidic, which is consistent with the low ammonia levels in the Eastern Mediterranean.

For Patras the average O:C ratio was 0.50±0.08, while in Athens 0.47±0.11. In both cities oxygenated OA was the major component of organic aerosol (78% in Patras and 65% in Athens), indicating the impact of regional pollution in Mediterranean. OOA included a moderately oxygenated OA and a very oxygenated OA component. In Patras a biogenic oxidized OA factor could be identified, which was related to air masses passing over the forests of Central Greece. A primary OA factor (HOA-2) was found in both cities attributed to primary emissions such as meat cooking. This factor may also contain oxygenated primary emissions (e.g., aged diesel emissions). Hydrocarbon-like OA mainly from traffic emissions was also indentified, accounting only for 7-18% of the OA and indicating that new emission control technologies applied to vehicles during the last decade have reduced dramatically the levels of the corresponding primary OA.

B4 References

Aiken, A. C., Salcedo, D., Cubison, M. J., Huffman, J. A., DeCarlo, P. F., Ulbrich, I. M., Docherty, K. S., Sueper, D., Kimmel, J. R., Worsnop, D. R., Trimborn, A., Northway, M., Stone, E. A., Schauer, J. J., Volkamer, R. M., Fortner, E., de Foy, B., Wang, J., Laskin, A., Shutthanandan, V., Zheng, J., Zhang, R., Gaffney, J., Marley, N. A., Paredes-Miranda, G., Arnott, W. P., Molina, L. T., Sosa, G., and Jimenez, J. L.: Mexico City aerosol analysis during MILAGRO using high resolution aerosol mass spectrometry at the urban supersite (T0) – Part 1: Fine particle composition and organic source apportionment, Atmos. Chem. Phys., 9, 6633-6653, 2009.

Bougiatioti, A., Stavroulas, I., Kostenidou, E., Zarmpas, P., Theodosi, C., Kouvarakis, G., Canonaco, F., Prévôt, A. S. H., Nenes, A., Pandis, S. N., and

European Union
European Social Fund
OPERATIONAL PROGRAMME
EDUCATION AND LIFELONG LEARNING
investing in knowledge society
MINISTRY OF EDUCATION & RELIGIOUS AFFAIRS
MANAGING AUTHORITY
NSRF 2007-2013
EUROPEAN SOCIAL FUND
Co-financed by Greece and the European Union

Mihalopoulos, N.: Processing of biomass-burning aerosol in the eastern Mediterranean during summertime, Atmos. Chem. Phys., 14, 4793-4807, 2014.

Budisulistiorini, S. H., Canagaratna, M. R., Croteau, P. L., Marth, W. J., Baumann, K., Edgerton, E. S., Shaw, S. L., Knipping, E. M., Worsnop, D. R., Jayne, J. T., Gold, A., and Surratt, J. D.: Real-time continuous characterization of secondary organic aerosol derived from isoprene epoxydiols in downtown Atlanta, Georgia, using the Aerodyne Aerosol Chemical Speciation Monitor, Environ. Sci. Technol., 47, 5686–5694, doi: 10.1021/es400023n, 2013.

Canonaco, F., Crippa, M., Slowik, J. G., Baltensperger, U., and Prévôt, A. S. H.: SoFi, an IGOR-based interface for the efficient use of the generalized multilinear engine (ME-2) for the source apportionment: ME-2 application to aerosol mass spectrometer data, Atmos. Meas. Tech., 6, 3649-3661, 2013.

Carslaw, K. S., Clegg, S. L., and Brimblecombe, P.: A thermodynamic model of the system HCl-HNO_3-H_2SO_4-H_2O, including solubilities of HBr, from <200K to 328 K, J. Phys. Chem., 99, 11557–11574, 1995.

Chaloulakou A., Kassomenos, P., Spyrellis, N., Demokritou, P., and Koutrakis, P.: Measurements of PM_{10} and $PM_{2.5}$ particle concentrations in Athens, Greece, Atmos. Environ., 37, 649–660, 2003.

Chen, Q., Farmer, D. K., Rizzo, L. V., Pauliquevis, T., Kuwata, M., Karl, T. G., Guenther, A., Allan, J. D., Coe, H., Andreae, M. O., Pöschl, U., Jimenez, J. L., Artaxo, P., and Martin, S. T.: Fine-mode organic mass concentrations and sources in the Amazonian wet season (AMAZE-08), Atmos. Chem. Phys. Discuss., 14, 16151-16186, 2014.

European Union
European Social Fund
OPERATIONAL PROGRAMME
EDUCATION AND LIFELONG LEARNING
investing in knowledge society
MINISTRY OF EDUCATION & RELIGIOUS AFFAIRS
MANAGING AUTHORITY
NSRF 2007-2013
programme for development
EUROPEAN SOCIAL FUND
Co-financed by Greece and the European Union

Chirico, R., DeCarlo, P. F., Heringa, M. F., Tritscher, T., Richter, R., Prévôt, A. S. H., Dommen, J., Weingartner, E., Wehrle, G., Gysel, M., Laborde, M., and Baltensperger, U.: Impact of aftertreatment devices on primary emissions and secondary organic aerosol formation potential from in-use diesel vehicles: results from smog chamber experiments, Atmos. Chem. Phys., 10, 11545–11563, 2010.

Chrysikou L.P. and Samara C.: Seasonal variation of the size distribution of urban particulate matter and associated organic pollutants in the ambient air, Atmos. Environ., 43, 4557- 4569, 2009.

Clegg, S., Brimblecombe, L., P. and Wexler, A. S.: A thermodynamic model of the system H^+-NH_4^+-SO_4^{2-}-NO_3^--H_2O at tropospheric temperatures. J. Phys. Chem. A102, 2137–2154, doi: 10.1021/jp973043j, 1998.

Crippa M., El Haddad I., Slowik J., G., DeCarlo P. F., Mohr, C., Heringa, M., F, Chirico, R., Marchand, N., Sciare, J., Urs, B., and Prévôt, A. S. H.: Identification of marine and continental aerosol sources in Paris using high resolution aerosol mass spectrometry, J. Geophys. Res, doi: 118, 1950-1963, doi: 10.1002/jgrd.50151, 2013a.

Crippa, M., DeCarlo, P. F., Slowik, J. G., Mohr, C., Heringa, M. F., Chirico, R., Poulain, L., Freutel, F., Sciare, J., Cozic, J., Di Marco, C. F., Elsasser, M., Jose, N., Marchand, N., Abidi, E., Wiedensohler, A., Drewnick, F., Schneider, J., Borrmann, S., Nemitz, E., Zimmermann, R., Jaffrezo, J.-L., Prévôt, A. S. H., and Baltensperger, U.: Wintertime aerosol chemical composition and source apportionment of the organic fraction in the metropolitan area of Paris, Atmos. Chem. Phys., 13, 961–981, 2013b.

Cubison, M. J., Alfarra, M. R., Allan, J., Bower, K. N., Coe, H., McFiggans, G. B., Whitehead, J. D., Williams, P. I., Zhang, Q., Jimenez, J. L., Hopkins, J., and Lee, J.: The characterization of pollution aerosol in a changing photochemical environment, Atmos. Chem. Phys., 6, 5573-5588, 2006.

European Union
European Social Fund
OPERATIONAL PROGRAMME
EDUCATION AND LIFELONG LEARNING
investing in knowledge society
MINISTRY OF EDUCATION & RELIGIOUS AFFAIRS
MANAGING AUTHORITY
NSRF 2007-2013
programme for development
EUROPEAN SOCIAL FUND
Co-financed by Greece and the European Union

Dall'Osto, M., Ceburnis, D., Martucci, G., Bialek, J., Dupuy, R., Jennings, S. G., Berresheim, H., Wenger, J., Healy, R., Facchini, M. C., Rinaldi, M., Giulianelli, L., Finessi, E., Worsnop, D., Ehn, M., Mikkilä, J., Kulmala, M., and O'Dowd, C. D.: Aerosol properties associated with air masses arriving into the North East Atlantic during the 2008 Mace Head EUCAARI intensive observing period: an overview, Atmos. Chem. Phys., 10, 8413-8435, 2010.

Davidson, C. I., Phalen, R. F., and Solomon, P. A.: Airborne particulate matter and human health: A review, Aerosol Sci. Tech., 39, 737–749, 2005.

DeCarlo, P.F., Kimmel, J. R., Trimborn, A., Northway, M. J., Jayne, J. T., Aiken, A. C., Gonin, M., Fuhrer, K., Horvath, T., Docherty, K., Worsnop, D. R., and Jimenez, J. L.: Field-Deployable, High-Resolution, Time-of-Flight Aerosol Mass Spectrometer, Analytical Chemistry, 78, 8281-8289, 2006.

Docherty, K. S., Aiken, A. C., Huffman, J. A., Ulbrich, I. M., DeCarlo, P. F., Sueper, D., Worsnop, D. R., Snyder, D. C., Peltier, R. E., Weber, R. J., Grover, B. D., Eatough, D. J., Williams, B. J., Goldstein, A. H., Ziemann, P. J., and Jimenez, J. L.: The 2005 Study of Organic Aerosols at Riverside (SOAR-1): Instrumental intercomparisons and fine particle composition, Atmos. Chem. Phys., 11, 12387-12420, 2011.

Draxler, R. R., and Rolph, G. D., 2013. HYSPLIT (HYbrid Single-Particle Lagrangian Integrated Trajectory) Model access via NOAA ARL READY Website (http://ready.arl.noaa.gov/HYSPLIT.php). NOAA Air Resources Laboratory, Silver Spring, MD.

El Haddad, I., D'Anna, B., Temime-Roussel, B., Nicolas, M., Boreave, A., Favez, O., Voisin, D., Sciare, J., George, C., Jaffrezo, J.-L., Wortham, H., and Marchand, N.:

European Union
European Social Fund
OPERATIONAL PROGRAMME
EDUCATION AND LIFELONG LEARNING
investing in knowledge society
MINISTRY OF EDUCATION & RELIGIOUS AFFAIRS
MANAGING AUTHORITY
NSRF 2007-2013
programme for development
EUROPEAN SOCIAL FUND
Co-financed by Greece and the European Union

Towards a better understanding of the origins, chemical composition and aging of oxygenated organic aerosols: case study of a Mediterranean industrialized environment, Marseille, Atmos. Chem. Phys., 13, 7875-7894, 2013.

Farmer, D.K., Matsunaga, A., Docherty, K. S., Surratt, J. D., Seinfeld, J. H., Ziemann P. J., and Jimenez, J. L., Response of an aerosol mass spectrometer to organonitrates and organosulfates and implications for atmospheric chemistry. Proceedings of the National Academy of Sciences, 107, 6670-6675, doi: 10.1073/pnas.0912340107, 2010.
Ge, X., Setyan, A., Sun, Y., and Zhang, Q.: Primary and secondary organic aerosols in Fresno, California during wintertime: Results from high resolution aerosol mass spectrometry, J. Geophys. Res., 117, D19301, 10.1029/2012JD018026, 2012a.

Ge, X., Zhang, Q., Sun, Y., Ruehl, C. R., and Setyan, A.: Effect of aqueous-phase processing on aerosol chemistry and size distribution in Fresno, California, during wintertime, Environ. Chem., 9, 221-235, 10.1071/EN11168, 2012b.

Grivas, G., Chaloulakou, A, Samara, C., and Spyrellis, N.: Spatial and temporal variation of PM_{10} mass concentrations within the greater area of Athens, Greece, Water, Air and Soil Pollution, 158, 357-371, 2004.

Heringa, M. F., DeCarlo, P. F., Chirico, R., Tritscher, T., Clairotte, M., Mohr, C., Crippa, M., Slowik, J. G., Pfaffenberger, L., Dommen, J., Weingartner, E., Prévôt, A. S. H., and Baltensperger, U.: A new method to discriminate secondary organic aerosols from different sources using high-resolution aerosol mass spectra, Atmos. Chem. Phys., 12, 2189-2203, 2012.

Hildebrandt, L., Engelhart, G. J., Mohr, C., Kostenidou, E., Lanz, V. A., Bougiatioti, A., DeCarlo, P. F., Prévôt, A. S. H., Baltensperger, U., Mihalopoulos, N., Donahue, N. M., and Pandis, S. N.: Aged organic aerosol in the Eastern Mediterranean: the Finokalia Aerosol Measurement Experiment – 2008, Atmos. Chem. Phys., 10, 4167–4186, 2010.

European Union
European Social Fund
OPERATIONAL PROGRAMME
EDUCATION AND LIFELONG LEARNING
investing in knowledge society
MINISTRY OF EDUCATION & RELIGIOUS AFFAIRS
MANAGING AUTHORITY
NSRF 2007-2013
programme for development
EUROPEAN SOCIAL FUND
Co-financed by Greece and the European Union

Hildebrandt, L., Kostenidou, E., Lanz, V. A., Prévôt, A. S. H., Baltensperger, U., Mihalopoulos, N., Laaksonen, A., Donahue, N. M., and Pandis, S. N.: Sources and atmospheric processing of organic aerosol in the Mediterranean: insights from aerosol mass spectrometer factor Analysis, Atmos. Chem. Phys., 11, 12499–12515, 2011.

Hings S.S., Walter, S., Schneider, J., Borrmann, S., and Drewnick, F.: Comparison of a Quadrupole and a Time-of-Flight Aerosol Mass Spectrometer during the Feldberg Aerosol Characterization Experiment 2004, Aerosol Science and Technology, 41, 679 - 691, 2007.

Holzinger, R., Lee, A., Paw, K. T., and Goldstein, U. A. H.: Observations of oxidation products above a forest imply biogenic emissions of very reactive compounds, Atmos. Chem. Phys., 5, 67-75, doi: 10.5194/acp-5-67-2005, 2005.

IPCC: Climate Change 2013 – The Physical Science Basis, Contribution of Working Group I to the Fourth Assessment Report of the IPCC, Cambridge University Press, Cambridge, 2013.

Jimenez, J. L., Canagaratna, M. R., Donahue, N. M., Prévôt, A. S. H., Zhang, Q., Kroll, J. H., DeCarlo, P. F., Allan, J. D., Coe, H., Ng, N. L., Aiken, A. C., Docherty, K. S., Ulbrich, I. M., Grieshop, A. P., Robinson, A. L., Duplissy, J., Smith, J. D., Wilson, K. R., Lanz, V. A., Hueglin, C., Sun, Y. L., Tian, J., Laaksonen, A., Raatikainen, T., Rautiainen, J., Vaattovaara, P., Ehn, M., Kulmala, M., Tomlinson, J. M., Collins, D. R., Cubison, M. J., Dunlea, E. J., Huffman, J. A., Onasch, T. B., Alfarra, M. R., Williams, P. I., Bower, K., Kondo, Y., Schneider, J., Drewnick, F., Borrmann, S., Weimer, S., Demerjian, K., Salcedo, D., Cottrell, L., Griffin, R., Takami, A., Miyoshi, T., Hatakeyama, S., Shimono, A., Sun, J. Y., Zhang, Y. M., Dzepina, K., Kimmel, J. R., Sueper, D., Jayne, J. T., Herndon, S. C., Trimborn, A. M., Williams, L. R., Wood, E.

European Union
European Social Fund
OPERATIONAL PROGRAMME
EDUCATION AND LIFELONG LEARNING
investing in knowledge society
MINISTRY OF EDUCATION & RELIGIOUS AFFAIRS
MANAGING AUTHORITY
NSRF 2007-2013
EUROPEAN SOCIAL FUND
Co-financed by Greece and the European Union

C., Middlebrook, A. M., Kolb, C. E., Baltensperger, U., and Worsnop, D. R.: Evolution of organic aerosols in the atmosphere, Science, 326, 1525–1529, 2009.

Holzinger, R., Lee, A., Paw, K. T., and Goldstein, U. A. H.: Observations of oxidation products above a forest imply biogenic emissions of very reactive compounds, Atmos. Chem. Phys., 5, 67-75, 2005.

Kanakidou, M., Seinfeld, J. H., Pandis, S. N., Barnes, I., Dentener, F. J., Facchini, M. C., Van Dingenen, R., Ervens, B., Nenes, A., Nielsen, C. J., Swietlicki, E., Putaud, J. P., Balkanski, Y., Fuzzi, S., Horth, J., Moortgat, G. K., Winterhalter, R., Myhre, C. E. L., Tsigaridis, K., Vignati, E., Stephanou, E. G., and Wilson, J.: Organic aerosol and global climate modeling: a review, Atmos. Chem. Phys., 5, 1053–1123, 2005.

Kaltsonoudis, C., Kostenidou, E., Florou, K., Psichoudaki, M., and Pandis, S. N.: Temporal variability of VOCs in the Eastern Mediterranean (in preparation).

Karanasiou, A. A., Sitaras, I. E., Siskos, P. A., and Eleftheriadis, K.: Size distribution and sources of trace metals and n-alkanes in the Athens urban aerosol during summer, Atmos. Environ., 41, 2368–2381, 2007.

Karl, M., Guenther, A., Köble, R., Leip, A., and Seufert, G.: A new European plant-specific emission inventory of biogenic volatile organic compounds for use in atmospheric transport models, Biogeosciences, 6, 1059-1087, 2009.

Kostenidou, E., Pathak, R. K., and Pandis, S. N.: An algorithm for the calculation of secondary organic aerosol density combining AMS and SMPS data, Aerosol Sci. Technol., 41, 1002–1010, 2007.

European Union
European Social Fund
OPERATIONAL PROGRAMME
EDUCATION AND LIFELONG LEARNING
investing in knowledge society
MINISTRY OF EDUCATION & RELIGIOUS AFFAIRS
MANAGING AUTHORITY
NSRF 2007-2013
EUROPEAN SOCIAL FUND
Co-financed by Greece and the European Union

Kostenidou, E., Lee, B. H., Engelhart, G. J., Pierce, J. R., and Pandis, S. N.: Mass spectra deconvolution of low, medium and high volatility biogenic secondary organic aerosol, Environ. Sci. Technol., 43, 4884–4889, 2009.

Koulouri, E., Saarikoski, S., Theodosi, C., Markaki, Z., Gerasopoulos, E., Kouvarakis, G., Makela, T., Hillamo, R., and Mihalopoulos, N.: Chemical composition and sources of fine and coarse aerosol particles in the Eastern Mediterranean, Atmos. Environ., 42, 6542–6550, 2008.

Lanz, V. A., Alfarra, M. R., Baltensperger, U., Buchmann, B., Hueglin, C., and Prévôt, A. S. H.: Source apportionment of submicron organic aerosols at an urban site by factor analytical modeling of aerosol mass spectra, Atmos. Chem. Phys., 7, 1503–1522, 2007.

Lanz, V. A., Alfarra, M. R., Baltensperger, U., Buchmann, B., Hueglin, C., Szidat, S., Wehrli, M. N., Wacker, L., Weimer, S., Caseiro, A., Puxbaum, J., and Prévôt, A. S. H.: Source attribution of submicron organic aerosols during wintertime inversions by advanced factor analysis of aerosol mass spectra, Environ. Sci. Technol., 42, 214-220, 2008.

Lee, A., Goldstein, A. H., Keywood, M. D., Gao, S.,Varutbangkul, V., Bahreini, R., Ng, N. L., Flagan, R. C., and Seinfeld, J. H.: Gas-phase products and secondary aerosol yields from the ozonolysis of ten different terpenes, J. Geophys. Res., 111, D07302, doi: 10.1029/2005JD006437, 2006.

Lee, B. H., Kostenidou, E., Hildebrandt, L., Riipinen, I., Engelhart, G. J., Mohr, C., DeCarlo, P. F., Mihalopoulos, N., Prévôt, A. S. H., Baltensperger, U. and Pandis S. N.: Measurement of the ambient organic aerosol volatility distribution: application during

European Union
European Social Fund
OPERATIONAL PROGRAMME
EDUCATION AND LIFELONG LEARNING
investing in knowledge society
MINISTRY OF EDUCATION & RELIGIOUS AFFAIRS
MANAGING AUTHORITY
NSRF 2007-2013
programme for development
EUROPEAN SOCIAL FUND
Co-financed by Greece and the European Union

the Finokalia Aerosol Measurement Experiment (FAME-2008), Atmos. Chem. Phys., 10, 12149–12160, 2010.

Manoli E., Voutsa D. and Samara C.: Chemical characterization and source identification/apportionment of fine and coarse air particles in Thessaloniki, Greece, Atmos. Environ., 36, 949-961, 2002.

Massucci, M., Clegg, S. L., and Brimblecombe, P.: Equilibrium partial pressures, thermodynamic properties of aqueous and solid phases, and Cl_2 production from aqueous HCl and HNO_3 and their mixtures, J. Phys. Chem. A 103, 4209 4226, doi: 10.1021/jp9847179, 1999.

Matsunaga, S., Mochida, M., and Kawamura, K.: Growth of organic aerosols by biogenic semi-volatile carbonyls in the forest atmosphere, Atmos. Environ., 37, 2045–2050, 2003.

Matthew, B. M., Middlebrook, A. M., and Onasch, T. B.: Collection efficiencies in an Aerodyne Aerosol Mass Spectrometer as a function of particle phase for laboratory generated aerosols, Aerosol Sci. Technol., 42, 884–898, 2008.

Mohr, C., DeCarlo, P. F., Heringa, M. F., Chirico, R., Slowik, J. G., Richter, R., Reche, C., Alastuey, A., Querol, X., Seco, R., Peñuelas, J., Jimenez, J. L., Crippa, M., Zimmermann, R., Baltensperger, U., and Prévôt, A. S. H.: Identification and quantification of organic aerosol from cooking and other sources in Barcelona using aerosol mass spectrometer data, Atmos. Chem. Phys., 12, 1649–1665, 2012.

Nicolas, J. : Caractérisation physico-chimique de l'aérosol troposphérique en Méditerranée : Sources et Devenir, Ph.D. thesis, Université de Versailles Saint-Quentin-en-Yvelines, Ecole Doctorale des Sciences de l'Environnement d'Ile-de-France, Paris, France, 2013.

European Union
European Social Fund
OPERATIONAL PROGRAMME
EDUCATION AND LIFELONG LEARNING
investing in knowledge society
MINISTRY OF EDUCATION & RELIGIOUS AFFAIRS
MANAGING AUTHORITY
NSRF 2007-2013
programme for development
EUROPEAN SOCIAL FUND
Co-financed by Greece and the European Union

Ng, N.L., Canagaratna, M. R., Zhang, Q., Jimenez, J. L., Tian, J., Ulbrich, I. M., Kroll, J. H., Docherty, K. S., Chhabra, P. S., Bahreini, R., Murphy, S. M., Seinfeld, J. H., Hildebrandt, L., Donahue, N. M., DeCarlo, P. F., Lanz, V. A., Prévôt, A. S. H., Dinar, E., Rudich, Y., and Worsnop D. R.: Organic aerosol components observed in northern hemispheric datasets measured with Aerosol Mass Spectrometry. Atmos. Chem. Phys, 10, 4625-4641, 2010.

Paatero, P. and Tapper, U.: Positive matrix factorization – a nonnegative factor model with optimal utilization of error-estimates of data values, Environmetrics, 5, 111–126, 1994.

Pandolfi, M., Querol, X., Alastuey, A., Jimenez, J. L., Jorba, O., Day, D., Ortega, A., Cubison, M. J., Comerón, A., Sicard, M., Mohr, C., Prévôt, A. S. H., Minguillón, M. C., Pey, J., Baldasano, J. M., Burkhart, J. F., Seco, R., Peñuelas, J., van Drooge, B. L., Artiñano, B., Di Marco, C., Nemitz, E., Schallhart, S., Metzger, A., Hansel, A., Llorente, J., Ng, S., Jayne, J., and Szidat, S.: Effects of sources and meteorology on particulate matter in the Western Mediterranean Basin: An overview of the DAURE campaign, J. Geophys. Res. Atmos., 119, 4978–5010, doi: 10.1002/2013JD021079, 2014.

Papaefthymiou, H., Kritidis, P., Anousis, J., and Sarafidou, J.: Comparative assessment of natural radioactivity in fallout samples from Patras and Megalopolis, Greece, J. of Environomental Radioactivity, 78, 249-265, 2005.

Pérez, N., Pey, J., Castillo, S., Viana, M., Alastuey, A., and Querol, X.: Interpretation of the variability of levels of regional background aerosols in the Western Mediterranean, Science of the Total Environment, 407, 527-540, 2008.

European Union
European Social Fund
OPERATIONAL PROGRAMME
EDUCATION AND LIFELONG LEARNING
investing in knowledge society
MINISTRY OF EDUCATION & RELIGIOUS AFFAIRS
MANAGING AUTHORITY
NSRF 2007-2013
programme for development
EUROPEAN SOCIAL FUND
Co-financed by Greece and the European Union

Petzold, A., and Schönlinner, M: Multi-angle absorption photometry – a new method for the measurement of aerosol light absorption and atmospheric black carbon, J. Aerosol Sci., 35, 421-441, 2004.

Pey, J., Pérez, N., Querol, X., Alastuey, A., Cusack, M., and Reche, C.: Intense winter atmospheric pollution episodes affecting the Western Mediterranean, Science of the Total Environment, 408, 1951-1959, 2010.
Pikridas, M., Tasoglou, A., Florou, K., and Pandis, S. N.: Characterization of the origin of fine particulate matter in a medium size urban area in the Mediterranean, Atmos. Environ., 80, 264–274, 2013.

Platt, S. M., El Haddad, I., Zardini, A. A., Clairotte, M., Astorga, C., Wolf, R., Slowik, J. G., Temime-Roussel, B., Marchand, N., Ježek, I., Drinovec, L., Močnik, G., Möhler, O., Richter, R., Barmet, P., Bianchi, F., Baltensperger, U., and Prévôt, A. S. H.: Secondary organic aerosol formation from gasoline vehicle emissions in a new mobile environmental reaction chamber, Atmos. Chem. Phys., 13, 9141-9158, 2013.

Platt, S.M., El Haddad, I., Pieber, S. M., Huang, R-J., Zardini, A. A., Clairotte, M., Suarez-Bertoa, R., Barmet, P., Pfaffenberger, L., Wolf, R., Slowik, J.G., Fuller, S. J., Kalberer, M., Chirico, R., Domme, J., Astorga, C., Zimmermann, R., Marchand, N., Hellebust, S., Temime-Roussel, B., Baltensperger U., and. Prévôt A.S.H.: Two-stroke scooters are a dominant source of air pollution in many cities, Nature Communications, 5, doi: 10.1038/ncomms4749, 2014.

Pope, C. A. and Dockery, D. W.: Health effects of fine particulate air pollution: Lines that connect, J. Air Waste Manage., 56, 709–742, 2006.

European Union
European Social Fund
OPERATIONAL PROGRAMME
EDUCATION AND LIFELONG LEARNING
investing in knowledge society
MINISTRY OF EDUCATION & RELIGIOUS AFFAIRS
MANAGING AUTHORITY
NSRF 2007-2013
programme for development
EUROPEAN SOCIAL FUND
Co-financed by Greece and the European Union

Poulain, L., Spindler, G., Birmili, W., Plass-Dülmer, C., Wiedensohler, A., and Herrmann, H.: Seasonal and diurnal variations of particulate nitrate and organic matter at the IfT research station Melpitz, Atmos. Chem. Phys., 11, 12579-12599, 2011.

Robinson, N. H., Hamilton, J. F., Allan, J. D., Langford, B., Oram, D. E., Chen, Q., Docherty, K., Farmer, D. K., Jimenez, J. L., Ward, M. W., Hewitt, C. N., Barley, M. H., Jenkin, M. E., Rickard, A. R., Martin, S. T., McFiggans, G., and Coe, H.: Evidence for a significant proportion of secondary organic aerosol from isoprene above a maritime tropical forest, Atmos. Chem. Phys., 11, 1039–1050, 2011.

Saarikoski, S., Carbone, S., Decesari, S., Giulianelli, L., Angelini, F., Canagaratna, M., Ng, N. L., Trimborn, A., Facchini, M. C., Fuzzi, S., Hillamo, R., and Worsnop, D.: Chemical characterization of springtime submicrometer aerosol in Po Valley, Italy, Atmos. Chem. Phys., 12, 8401-8421, 2012.

Schmale, J., Schneider, J., Nemitz, E., Tang, Y. S., Dragosits, U., Blackall, T. D., Trathan, P. N., Phillips, G. J., Sutton, M., and Braban C. F.: Sub-Antarctic marine aerosol: significant contributions from biogenic sources, Atmos. Chem. Phys., 13, 8669–8694, 2013.

Slowik, J. G., Brook, J., Chang, R. Y.-W., Evans, G. J., Hayden, K., Jeong, C.-H., Li, S.-M., Liggio, J., Liu, P. S. K., McGuire, M., Mihele, C., Sjostedt, S., Vlasenko, A., and Abbatt, J. P. D.: Photochemical processing of organic aerosol at nearby continental sites: contrast between urban plumes and regional aerosol, Atmos. Chem. Phys., 11, 2991–3006, 2011.

Stohl, A., Forster, V., Frank, A., Seibert, P., & Wotawa, G.: Technical Note: The Lagrangian particle dispersion model FLEXPART version 6.2, Atmos. Chem. Phys., 5, 2461–2474, 2005.

European Union
European Social Fund
OPERATIONAL PROGRAMME
EDUCATION AND LIFELONG LEARNING
investing in knowledge society
MINISTRY OF EDUCATION & RELIGIOUS AFFAIRS
MANAGING AUTHORITY
NSRF 2007-2013
programme for development
EUROPEAN SOCIAL FUND
Co-financed by Greece and the European Union

Sueper, D.: ToF-AMS High Resolution Analysis Software – Pika, online available at: http://cires.colorado.edu/jimenez-group/ ToFAMSResources/ToFSoftware, last access: 1 December 2014.

Sun, Y. L., Zhang, Q., Schwab, J. J., Demerjian, K. L., Chen, W. N., Bae, M. S., Hung, H. M., Hogrefe, O., Frank, B., Rattigan, O. V., and Lin, Y. C.: Characterization of the sources and processes of organic and inorganic aerosols in New York city with a high-resolution time-of-flight aerosol mass spectrometer, Atmos. Chem. Phys., 11, 1581–1602, 2011.

Tsiflikiotou, T., Papanastasiou, D., Zarmpas, P., Paraskevopoulou, D., Diapouli, E., Kostenidou, E., Kaltsonoudis, C., Bougiatioti, A., Theodosi, C., Kouvarakis, G., Liakakou, E., Vassilatou, V., Siakavaras, D., Biskos, G., Eleftheriadis, K., Gerasopoulos, E., Mihalopoulos, N., and Pandis, S. N.: Spatial distribution of summertime particulate matter and its composition in Greece (in preparation).

Ulbrich, I. M., Canagaratna, M. R., Zhang, Q., Worsnop, D. R., and Jimenez, J. L.: Interpretation of organic components from Positive Matrix Factorization of aerosol mass spectrometric data, Atmos. Chem. Phys., 9, 2891–2918, 2009.

Vardoulakis S. and Kassomenos P.: Sources and factors affecting PM10 levels in two European cities: Implications for local air quality management, Atmos. Environ., 4142, 3949-3963, 2008.

Viana, M., Pérez, C., Querol, X., Alastuey, A., Nickovic, S., and Baldasano J. M.: Spatial and temporal variability of PM levels and composition in a complex summer atmospheric scenario in Barcelona (NE Spain), Atmos. Environ., 39, 5343-5361, 2005.

Watson, J. G.: Visibility: Science and regulation, J. Air Waste Manage., 52, 628–713, 2002.

European Union
European Social Fund
OPERATIONAL PROGRAMME
EDUCATION AND LIFELONG LEARNING
investing in knowledge society
MINISTRY OF EDUCATION & RELIGIOUS AFFAIRS
MANAGING AUTHORITY
NSRF 2007-2013
programme for development
EUROPEAN SOCIAL FUND
Co-financed by Greece and the European Union

Wichink Kruit, R. J., Schaap, M., Sauter, F. J., van Zanten, M. C., and van Paul, W. A. J.: Modeling the distribution of ammonia across Europe including bi-directional surface-atmosphere exchange, Biosciences, 9, 5261–5277, 2012.

Yannopoulos, P.C.: Long-term assessment of airborne particulate concentrations in Patras, Greece, Fresenius Environ. Bull., 17, 608-616, 2008.

Xu, L., Guo, H., Boyd, C. M., Klein, M., Bougiatioti, A., Cerully, K, M., Hite, J. R., Isaacman-VanWertz, G., Kreisberg, N. M., Knote, C., Olson, K., Koss, A., Goldstein, A. H., Hering, S. V., de Gouw, J., Baumann, K., Lee, S-H., Nenes, A., Weber, R. J., Ng, N. L.: Effects of anthropogenic emissions on aerosol formation from isoprene and monoterpenes in the Southeastern United States, P. Natl. Acad. Sci., 112, 37-42, doi: 10.1073/pnas.1417609112, 2014.

Zhang, Q., Alfarra, M. R., Wornsop, D. R., Allan, J. D., Coe, H., Canagaratna, M., and Jimenez, J. L.: Deconvolution and quantification of hydrocarbon-like and oxygenated organic aerosols based on aerosol mass spectrometry, Environ. Sci. Technol., 39, 4938-4952, 2005.

Zhang, Q., Jimenez, J. L., Canagaratna, M. R., Allan, J. D., Coe, H., Ulbrich, I., Alfarra, M. R., Takami, A., Middlebrook, A. M., Sun, Y. L., Dzepina, K., Dunlea, E., Docherty, K., De- Carlo, P. F., Salcedo, D., Onasch, T., Jayne, J. T., Miyoshi, T., Shimono, A., Hatakeyama, S., Takegawa, N., Kondo, Y., Schneider, J., Drewnick, F., Borrmann, S., Weimer, S., Demerjian, K., Williams, P., Bower, K., Bahreini, R., Cottrell, L., Griffin, R. J., Rautiainen, J., Sun, J. Y., Zhang, Y. M., and Worsnop, D. R.: Ubiquity and dominance of oxygenated species in organic aerosols in anthropogenically-influenced Northern Hemisphere midlatitudes, Geophys. Res. Lett., 34, L13801, doi: 10.1029/2007gl029979, 2007.

European Union
European Social Fund
OPERATIONAL PROGRAMME
EDUCATION AND LIFELONG LEARNING
investing in knowledge society
MINISTRY OF EDUCATION & RELIGIOUS AFFAIRS
MANAGING AUTHORITY
NSRF 2007-2013
programme for development
EUROPEAN SOCIAL FUND
Co-financed by Greece and the European Union

Zhang, Q., Jimenez, J., Canagaratna, M., Ulbrich, I., Ng, N., Worsnop, D., and Sun, Y.: Understanding atmospheric organic aerosols via factor analysis of aerosol mass spectrometry: a review, Anal. Bioanal.Chem., 401, 3045-3067, 2011.

Table B1. Correlations[a] of the M-OOA and b-OOA factors (Patras) and the V-OOA factor (Athens) with various VOCs measured by the PTR-MS.

R^2	Patras M-OOA	Patras b-OOA	Athens V-OOA
m/z 43	0.29	0.13	0.39
m/z 47 (formic acid)	0.21	0.09	0.47
m/z 59 (acetone, glyoxal)	0.21	0.35	0.32
m/z 71 (MVK, MACR)	0.31	0.21	0.20
m/z 73 (MEK)	0.24	0.25	0.29
m/z 75 (hydroxyacetone)	0.29	0.41	0.30
m/z 77 (PAN)	0.16	0.37	0.16
m/z 81 (terpenes)	0.19	0.26	0.12
m/z 87 (MBO, C5, methacrylic acid)	0.29	0.31	0.38
m/z 95 (2 vinyl furan, phenol)	0.17	0.31	0.36
m/z 99 (hexenal)	0.19	0.30	0.42
m/z 101 (isoprene hyperoxides,hexanal)	0.17	0.28	0.35
m/z 103 (MPAN)	0.23	0.28	-
m/z 113 (chlorobenzene, terpenes +O_3)	0.30	0.37	0.40
m/z 115 (heptanal)	0.16	0.32	0.42
m/z 137 (monoterpenes)	0.20	0.24	0.1
m/z 139 (nopinone)	0.28	0.39	0.19
m/z 151 (pinonaldehyde)	0.17	0.30	0.17

[a]All correlations are significant at the p=0.05 level.

European Union
European Social Fund
OPERATIONAL PROGRAMME
EDUCATION AND LIFELONG LEARNING
investing in knowledge society
MINISTRY OF EDUCATION & RELIGIOUS AFFAIRS
MANAGING AUTHORITY
NSRF 2007-2013
EUROPEAN SOCIAL FUND
Co-financed by Greece and the European Union

Table B2. Correlations between PMF factors from Patras and Athens and PMF factors from selected studies using both the angle theta and R^2 (in parenthesis).

	Angle in degrees (and R^2) **with V-OOA Patras**	**Angle in degrees** (and R^2) **with V-OOA Athens**
LV-OOA Mexico City[1]	21 (0.86)	20 (0.87)
LV-OOA Riverside[2]	10 (0.97)	8 (0.98)
LV-OOA Barcelona[3]	18 (0.90)	16 (0.92)
LV-OOA Paris (SIRTA) summer[4]	19 (0.89)	15 (0.93)
OOA Paris (SIRTA), winter[5]	13 (0.95)	15 (0.93)
LV-OOA New York City[6]	14 (0.94)	11 (0.96)
LV-OOA Fresno[7,8]	36 (0.64)	30 (0.73)

	Angle in degrees (and R^2) **with M-OOA Patras**	**Angle in degrees** (and R^2) **with M-OOA Athens**
SV-OOA Mexico City[1]	24 (0.81)	22 (0.84)
SV-OOA Riverside [2]	42 (0.48)	39 (0.53)
SV-OOA Barcelona[3]	33 (0.66)	31 (0.69)
SV-OOA Paris (SIRTA) summer[4]	42 (0.48)	39 (0.53)
SV-OOA New York City[6]	30 (0.73)	27 (0.77)
α-pinene ozonolysis SOA aged[9]	35 (0.62)	32 (0.67)
Toluene photooxidation (HONO) SOA[10]	16 (0.93)	13 (0.95)

	Angle in degrees (and R^2) **with HOA-1 Patras**	**Angle in degrees** (and R^2) **with HOA-1 Athens**
HOA Mexico City[1]	13 (0.94)	14 (0.93)
HOA Riverside [2]	20 (0.86)	10 (0.96)
HOA Barcelona[3]	22 (0.84)	11 (0.96)
HOA Paris (SIRTA) summer[4]	16 (0.92)	18 (0.90)
HOA Paris (SIRTA), winter[5]	25 (0.79)	24 (0.81)
HOA New York City[6]	12 (0.95)	10 (0.97)
HOA Fresno[7,8]	11 (0.96)	11 (0.96)

	Angle in degrees (and R^2) **with HOA-2 Patras**	**Angle in degrees** (and R^2) **with HOA-2 Athens**
COA Barcelona[3]	77 (0.01)	77 (0.01)
COA Paris (SIRTA), summer[4]	30 (0.68)	34 (0.6)
COA Paris (SIRTA), winter[5]	30 (0.74)	28 (0.70)
COA Paris (LHVP), winter[5]	27 (0.76)	31 (0.70)
COA New York City[6]	11 (0.96)	14 (0.93)
COA Fresno[7,8]	28 (0.72)	33 (0.64)
Aged VOCs diesel emissions[9]	17 (0.90)	17 (0.90)
α-pinene ozonolysis SOA aged[9]	20 (0.86)	19 (0.87)
Toluene photooxidation (HONO) SOA[10]	26 (0.79)	23 (0.84)

European Union
European Social Fund
OPERATIONAL PROGRAMME
EDUCATION AND LIFELONG LEARNING
investing in knowledge society
MINISTRY OF EDUCATION & RELIGIOUS AFFAIRS
MANAGING AUTHORITY
NSRF 2007-2013
programme for development
EUROPEAN SOCIAL FUND
Co-financed by Greece and the European Union

	Angle in degrees (and R^2) **with b-OOA Patras**
α-pinene ozonolysis SOA aged[9]	29 (0.73)
Factor 82[11]	47 (0.40)
IEPOX OA[12]	76 (0.01)
Isoprene-OA[13]	28 (0.75)

[1]Aiken et al. (2009), [2]Docherty et al. (2011), [3]Mohr et al. (2012), [4]Crippa et al. (2013a), [5]Crippa et al. (2013b), [6]Sun et al. (2011), [7,8]Ge et al. (2012a,b), [9]Heringa et al. (2012), [10]Kostenidou et al., (not published data),[11]Robinson et al. (2011), [13]Budisulistiorini et al. (2013), [13]Xu et al., (2014).

European Union
European Social Fund
OPERATIONAL PROGRAMME
EDUCATION AND LIFELONG LEARNING
investing in knowledge society
MINISTRY OF EDUCATION & RELIGIOUS AFFAIRS
MANAGING AUTHORITY
NSRF 2007-2013
EUROPEAN SOCIAL FUND
Co-financed by Greece and the European Union

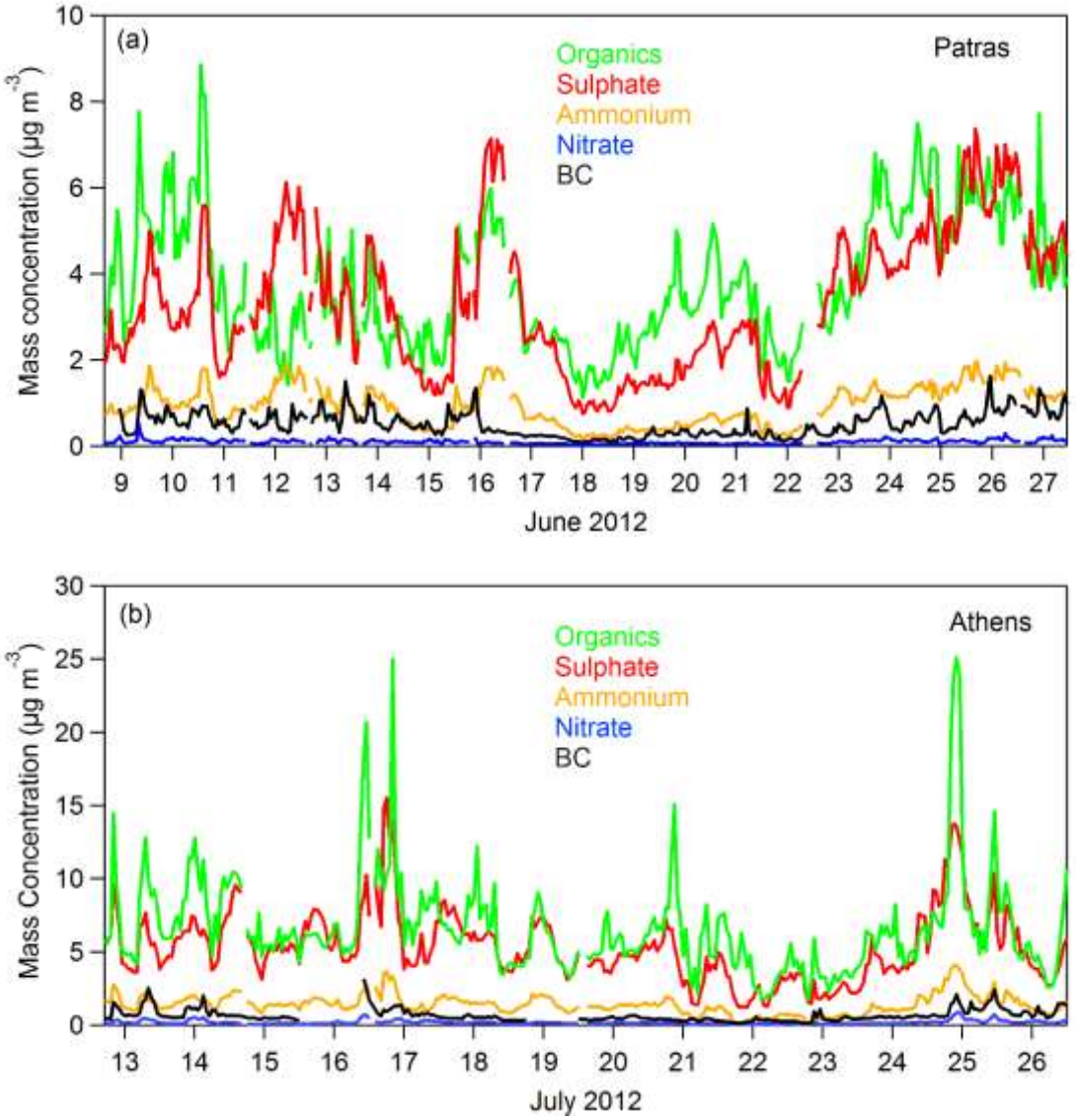

Figure B1. Time series of organics, sulphate, ammonium and nitrate mass concentration measured by the HR-ToF-AMS (corrected for the CE) and BC a) for Patras and b) for Athens. The BC was provided by MAAP for Patras measurements and by an aethalometer for Athens.

European Union
European Social Fund
OPERATIONAL PROGRAMME
EDUCATION AND LIFELONG LEARNING
investing in knowledge society
MINISTRY OF EDUCATION & RELIGIOUS AFFAIRS
MANAGING AUTHORITY
NSRF 2007-2013
EUROPEAN SOCIAL FUND
Co-financed by Greece and the European Union

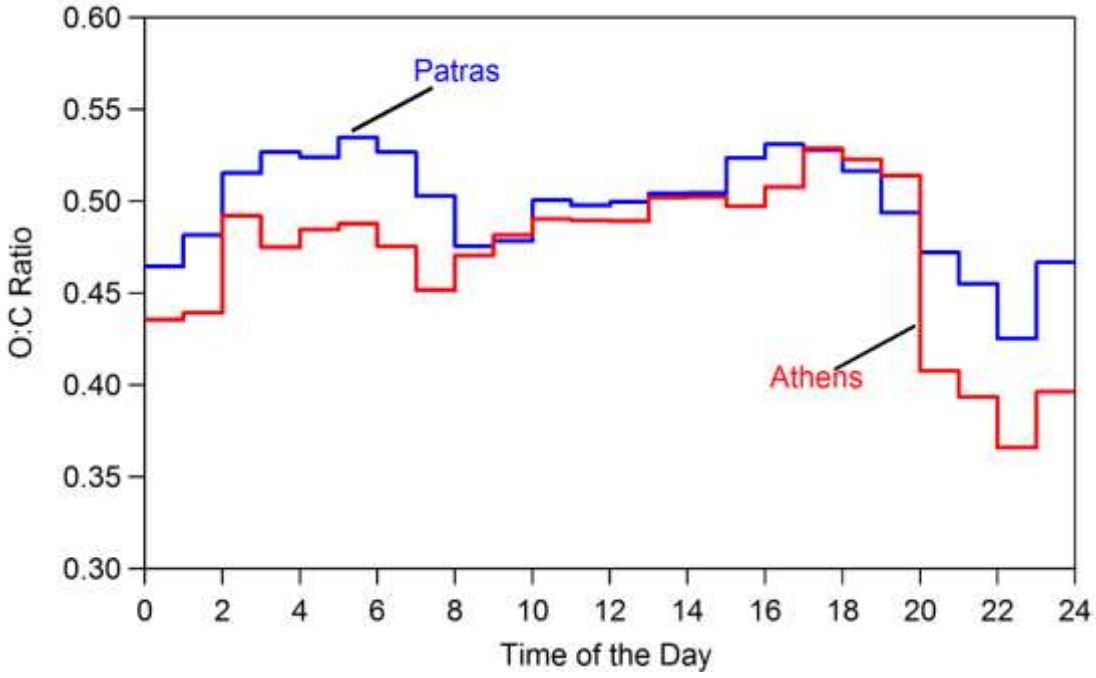

Figure B2. Diurnal profile of O:C ratio for Patras (blue line) and Athens (red line) data set. The O:C was calculated with the Aiken et al. (2009) fragmentation table.

European Union
European Social Fund
OPERATIONAL PROGRAMME
EDUCATION AND LIFELONG LEARNING
investing in knowledge society
MINISTRY OF EDUCATION & RELIGIOUS AFFAIRS
MANAGING AUTHORITY
NSRF 2007-2013
EUROPEAN SOCIAL FUND
Co-financed by Greece and the European Union

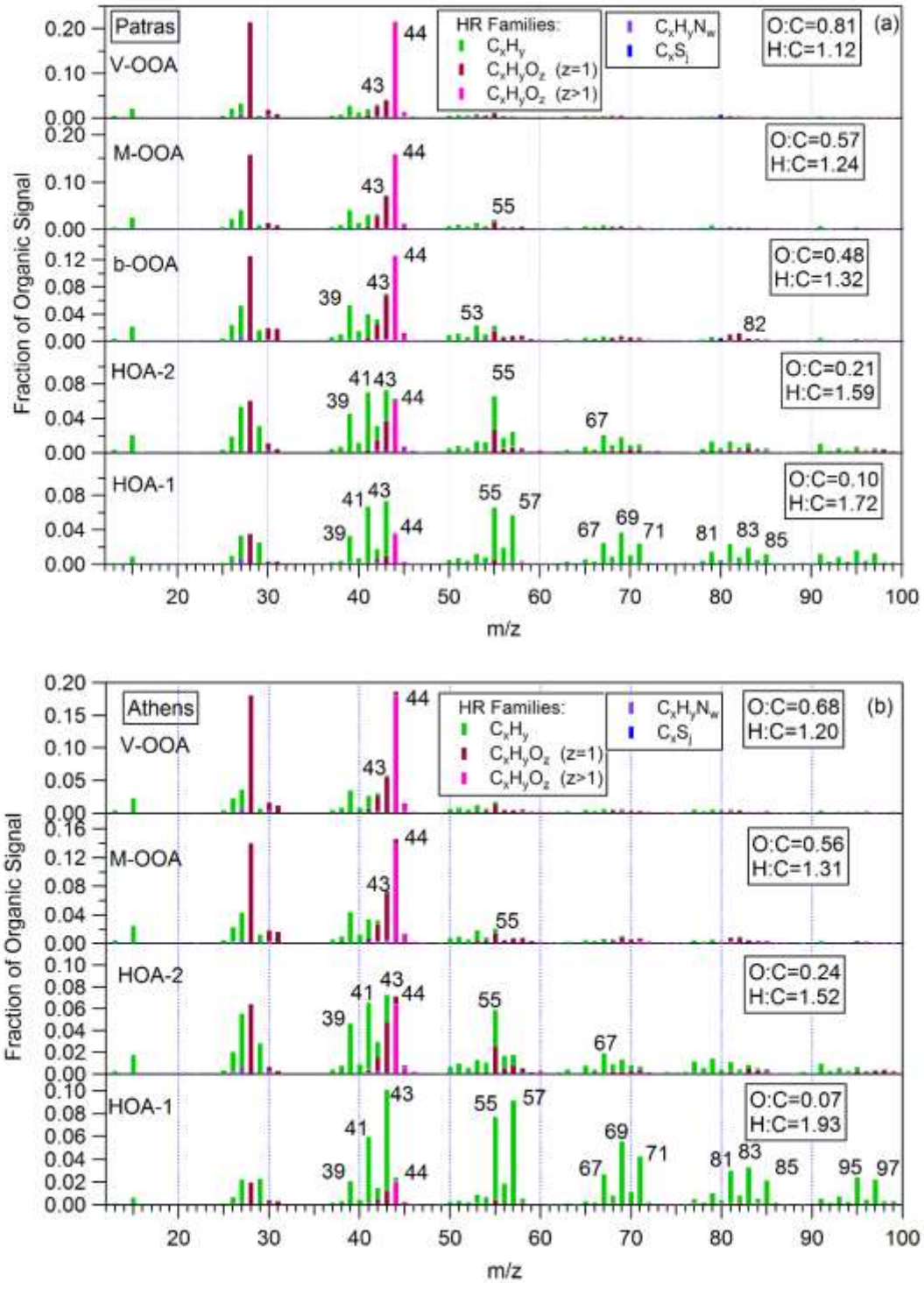

Figure B3. HR mass spectra profiles of the sources found a) in Patras and b) in Athens.

European Union
European Social Fund
OPERATIONAL PROGRAMME
EDUCATION AND LIFELONG LEARNING
investing in knowledge society
MINISTRY OF EDUCATION & RELIGIOUS AFFAIRS
MANAGING AUTHORITY
NSRF 2007-2013
EUROPEAN SOCIAL FUND
Co-financed by Greece and the European Union

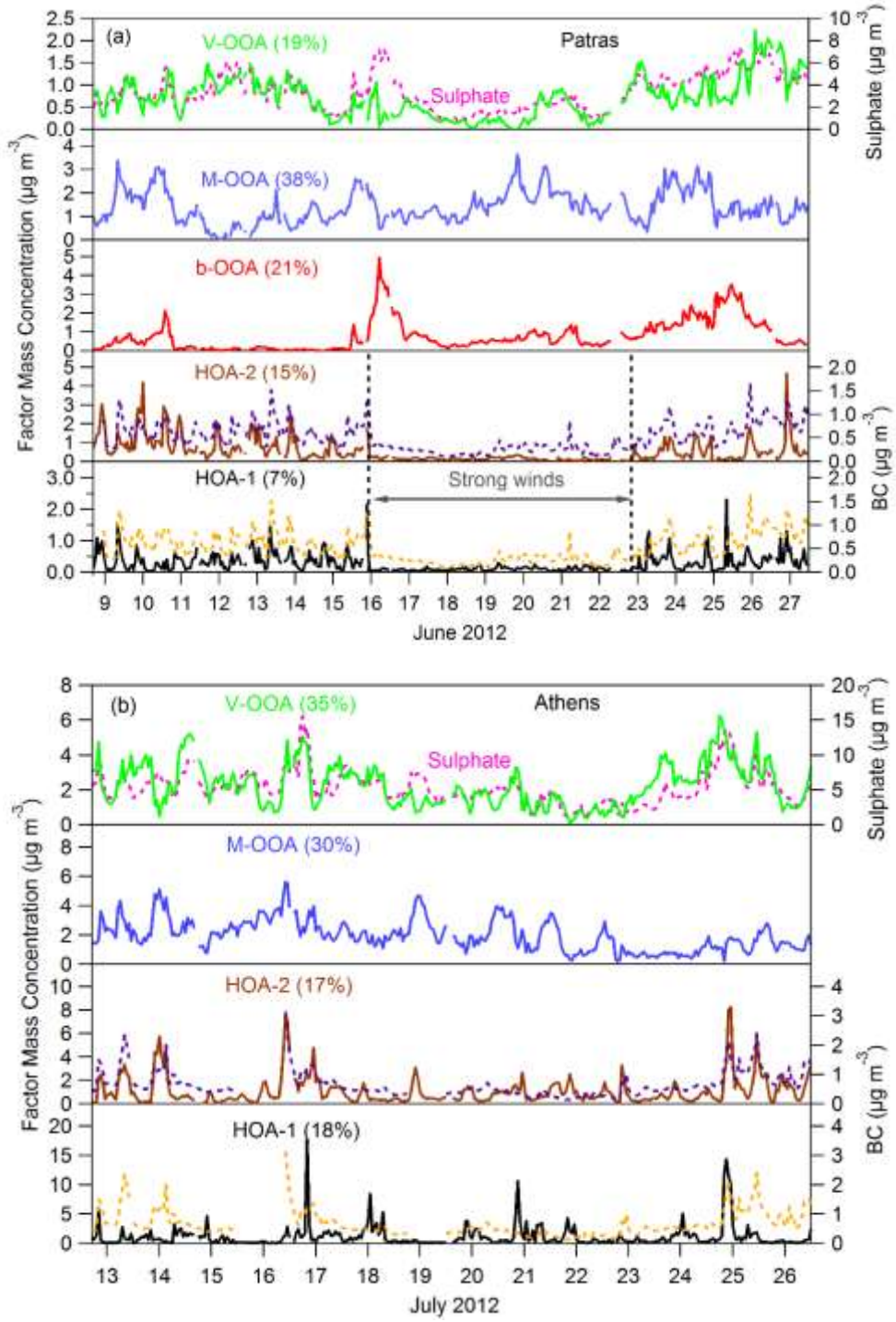

Figure B4. Time series a) of the five PMF factors using HR organic mass spectra for Patras and b) of the four PMF factors found in Athens. For the Patras measurements the HOA-1 and HOA-2 contribution was very low between the 16th and 23rd of June 2012 due to the high wind speed during that period.

European Union
European Social Fund
OPERATIONAL PROGRAMME
EDUCATION AND LIFELONG LEARNING
investing in knowledge society
MINISTRY OF EDUCATION & RELIGIOUS AFFAIRS
MANAGING AUTHORITY
NSRF 2007-2013
EUROPEAN SOCIAL FUND
Co-financed by Greece and the European Union

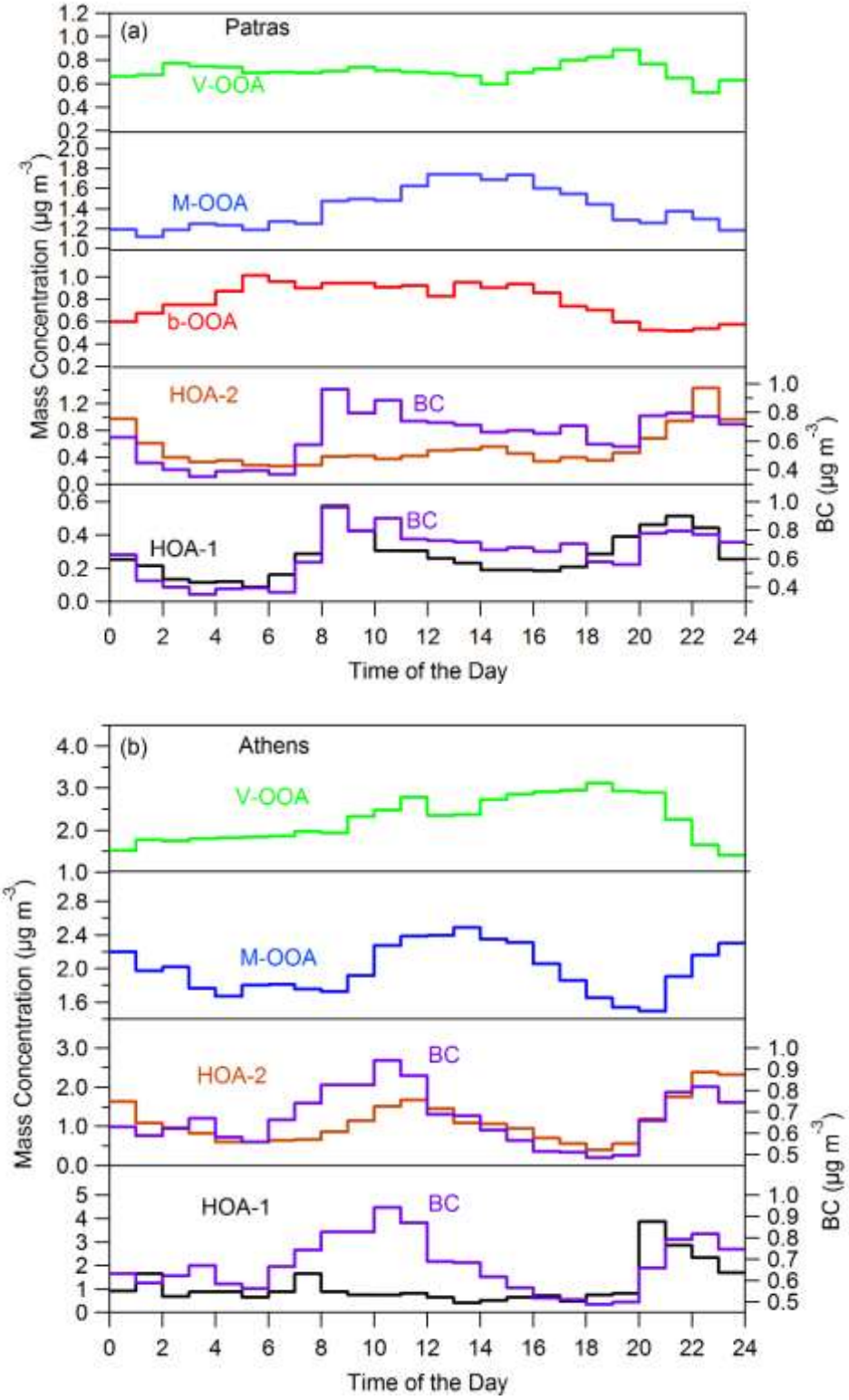

Figure B5. Diurnal cycles of the PMF factors a) in Patras and b) in Athens.

European Union
European Social Fund
OPERATIONAL PROGRAMME
EDUCATION AND LIFELONG LEARNING
investing in knowledge society
MINISTRY OF EDUCATION & RELIGIOUS AFFAIRS
MANAGING AUTHORITY
NSRF 2007-2013
EUROPEAN SOCIAL FUND
Co-financed by Greece and the European Union

C. Sources, seasonality and oxidation state of organic aerosol in the Eastern Mediterranean

C1. Experimental Methods

C1.1 Sampling site and period

The measurements were performed for a period of 16 months, between June 2012 and December 2013 at the remote background station of Finokalia, Crete (35º32'N, 25º67'E; http://finokalia.chemistry.uoc.gr), which is a European supersite for aerosol research, part of the ACTRIS (Aerosols, Clouds, and Trace gases Research Infrastructure Network). The station is situated in the northeastern part of the island of Crete, and is representative for background conditions of the Eastern Mediterranean as it is merely influenced by direct, local anthropogenic sources. The closest major civic centre is the city of Heraklion with 170000 inhabitants, situated approximately 50 km to the west of the measurement site. Detailed climatology and description of the area can be found in Mihalopoulos et al. (1997) and Sciare et al. (2003).

C1.2 Instruments and Methods

Measurements were performed with the use of an Aerosol Chemical Speciation Monitor (ACSM) by Aerodyne Research (Ng et al. 2011a), measuring PM_1 aerosol mass and chemical composition of non-refractory aerosol particles in real-time. During the first 6 months of the measurement period (June-November 2012) ambient air was drawn into the ACSM by the multiple PM_{10} aerosol inlet operating at Finokalia, without prior drying, with a temporal resolution of 30 minutes. During the rest of the measurement period the ACSM was sampling on its own directly from a PM_1 Sharp Cut Cyclone (BGI Inc.) using a nafion dryer before the instrument inlet (MD-110-12S-2, Perma Pure LLC). The ACSM was not operating at the Finokalia station between mid-December

European Union
European Social Fund
OPERATIONAL PROGRAMME
EDUCATION AND LIFELONG LEARNING
investing in knowledge society
MINISTRY OF EDUCATION & RELIGIOUS AFFAIRS
MANAGING AUTHORITY
NSRF 2007-2013
programme for development
EUROPEAN SOCIAL FUND
Co-financed by Greece and the European Union

and 2012-mid-February 2013, as it participated in an intensive measurement campaign in Athens, Greece. Finally, mass concentrations are calculated with a recommended collection efficiency of 0.5 for all constituents, verified by calibration and comparison with external measurements (daily PM_1 filters). More details about the quality control/quality assurance of the obtained data can be found in Stavroulas et al. (2015).

Back carbon (BC) absorption measurements were performed with the use of a 7-wavelength aethalometer (Magee Scientific, AE31) where ambient air was drawn into the aethalometer by the same multiple PM_{10} aerosol inlet as mentioned above, but after passing through a diffusional silica dryer. Values were obtained every 5 min, which were then averaged to 30 min in order to coincide with the ACSM time intervals. During winter 2012-2013 the aethalometer was not operating for the whole period because of maintenance therefore BC measurements during that period are limited. Finally, wavelength dependent source apportionment of the BC load was performed providing a fossil fuel (BC_{ff}) and a wood combustion (BC_{wb}) generated factor using an absorption exponent of 1.1 for fossil fuel combustion and 1.86 for pure wood burning based on the approach of Sandradewi et al. (2008).

C1.3 Additional measurements

Daily PM_1 filter samples were collected concurrently at the measurement station on pre-combusted quartz fiber filters. Samples were analyzed for organic and elemental carbon using the OC/EC analyzer (SUNSET Laboratory Inc.) as well as for water-soluble ions after extraction in ultrasonic bath with nanopure water. The solutions obtained were analyzed by ion chromatography (IC) for anions (Cl^-, Br^-, NO_3^-, SO_4^{2-}, $C_2O_4^{2-}$) and cations (K^+, Na^+, NH_4^+, Mg^{2+}, Ca^{2+}) using the procedure described by Bardouki et al. (2003). Results for organic carbon (OC), sulfate and ammonium were compared to concentrations derived from the ACSM for quality control/quality assurance of the results. As the ACSM provides organic matter (OM) concentrations, the measured OC concentrations from the filter samples were compared with the OM

European Union
European Social Fund
OPERATIONAL PROGRAMME
EDUCATION AND LIFELONG LEARNING
investing in knowledge society
MINISTRY OF EDUCATION & RELIGIOUS AFFAIRS
MANAGING AUTHORITY
NSRF 2007-2013
EUROPEAN SOCIAL FUND
Co-financed by Greece and the European Union

concentrations of the ACSM and the slope was then compared to the estimated OM/OC mass ratio calculated from the ACSM f_{44} measurements (Aiken et al. 2008). Auxiliary particle number distribution was monitored using a scanning mobility particle sizer (SMPS) in 5-min time resolution, chemical measurements (O_3) and meteorological parameters (wind speed and direction, pressure, temperature, relative humidity) were also continuously monitored.

C1.4 Source apportionment using Positive Matrix Factorization analysis

The source apportionment of the organic fraction was achieved with the use of the graphical interface SoFi (Source Finder) within the bilinear model of the multilinear engine (ME-2), developed at PSI, Zurich (Canonaco et al., 2013). Briefly, the organic mass spectra measured by the ACSM are represented as a matrix X, with columns representing the different m/z's and rows the time series of the mass spectrum. Then the measured matrix X is approximated by the product of F and G, added to E (X=GF+E) where each column of matrix G represents the time series of a factor and each row of F represents the profile (mass spectrum) of this factor and E is the model residual. The entries in F and G are then fit using a least squares algorithm that iteratively minimizes the quantity Q^m, which is the sum of the squared residuals weighted by their uncertainties. Finally, at each step of the solution process, outliers are defined based on the ratio of residuals to uncertainties (Canonaco et al., 2013). The input organics and organics' error matrices are derived automatically from the ACSM data analysis software, using a simple automated procedure (latest version, acsm_local_1553). All PMF runs are realized using SoFi version 4.8, without any spectral restraints.

European Union
European Social Fund
OPERATIONAL PROGRAMME
EDUCATION AND LIFELONG LEARNING
investing in knowledge society
MINISTRY OF EDUCATION & RELIGIOUS AFFAIRS
MANAGING AUTHORITY
NSRF 2007-2013
EUROPEAN SOCIAL FUND
Co-financed by Greece and the European Union

C2. Results and Discussion

C2.1 PM_1 Composition and seasonality

We divided the measurement period into the corresponding seasons for each year and calculated the median concentrations of the different species. The seasonal variability of the main measured species, along with the median PM_1 concentration calculated from the ACSM+BC measurements can be found in Figures C1a,b. It can be seen that mass concentrations exhibit a clear seasonal cycle with maximum values during summer and minimum during winter. It can also be seen that mass concentrations between the years 2012 and 2013 are comparable. This is also the case for the two main aerosol components, organics and sulfate. Sulfate is the main constituent of PM_1 with an average contribution of 39.5±1.5%, having a clear seasonal cycle with maximum values during autumn and minimum during spring. Organics are the second most abundant species in ultrafine aerosol, with an average contribution of 33.7±2.2% and seasonality with maximum concentrations during summer and minimum during autumn and winter. Organics exhibit also relatively high concentrations during winter, probably due to additional sources such as domestic heating. For both species also there is not significant intra-annual difference. Figure C1b portrays the rest of the most abundant species of PM_1 aerosol; ammonium exhibits also a clear seasonal cycle, having maximum concentrations during spring and a mean contribution of 16.7±2.2%, exhibiting somewhat higher concentrations in 2013 than 2012. BC has maximum concentrations during summer and winter and minimum concentrations during spring. The interesting feature about BC is the significantly lower concentrations during 2013, especially during summertime. The opposite trend is observed for nitrate, which shows approximately two times higher contribution during 2013.

European Union
European Social Fund
OPERATIONAL PROGRAMME
EDUCATION AND LIFELONG LEARNING
investing in knowledge society
MINISTRY OF EDUCATION & RELIGIOUS AFFAIRS
MANAGING AUTHORITY
NSRF 2007-2013
EUROPEAN SOCIAL FUND
Co-financed by Greece and the European Union

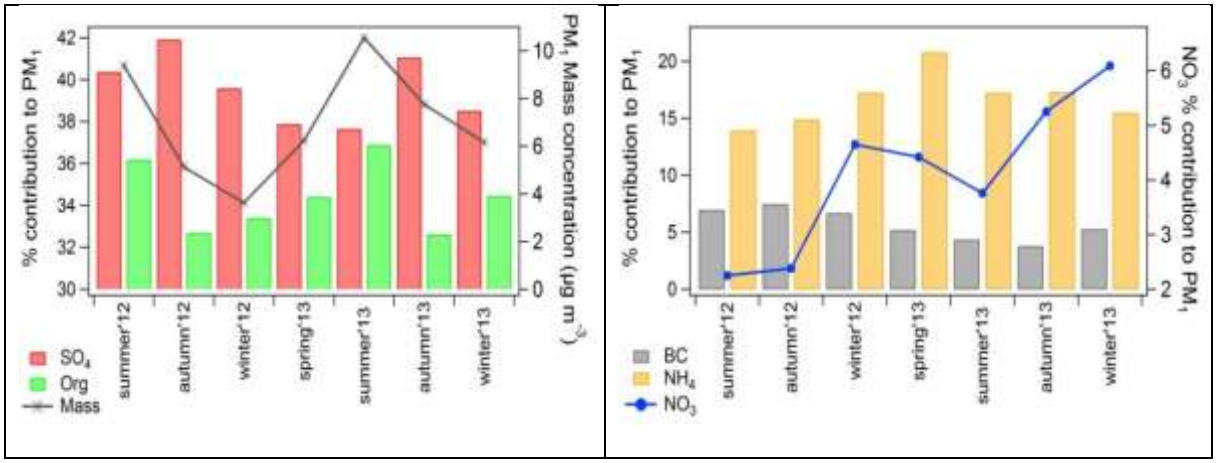

Figure C1: Interannual variability of mass, sulfate and organics (a) and BC, NO_3^- and NH_4^+ during the measuring period.

C2.2 Source apportionment of organic aerosol using PMF

Positive Matrix Factorization (PMF) analysis was performed on the organics mass spectra matrix in order to deconvolve the acquired PM_1 organic fraction to its possible sources. The SoFi toolkit (version 4.8; Canonaco et al., 2013) was used executing the PMF algorithm without applying any constraints to the generated outcome in terms of reference mass spectra. The algorithm was applied exploring solutions from two to five factors and having as a first estimated the results from Bougiatioti et al. (2014) from summer 2012, and the three-factor solution was selected for each one of the seasons. First of all the solutions were selected based on their low Q/Q_{exp} value and their residuals analysis, making sure that there is as little diurnal variability in the residuals as possible. Also an important selection criterion was the sanity of the mass spectra and the distinct time series and diurnal variability of each factor. In that aspect, the selection of the solution was based on the good correlation of the resulting factors with tracer species and factors that have MS features that compare well to reference mass spectra. An additional test for the sanity of the outcome was the stability of the solution, by verifying that the results exhibit very little variability when initializing the algorithm from 10 different starting points ("seed runs"). PMF solutions with four and five factors were rejected as having a splitting behavior of the resulting factors, without identifying

European Union
European Social Fund
OPERATIONAL PROGRAMME
EDUCATION AND LIFELONG LEARNING
investing in knowledge society
MINISTRY OF EDUCATION & RELIGIOUS AFFAIRS
MANAGING AUTHORITY
NSRF 2007-2013
EUROPEAN SOCIAL FUND
Co-financed by Greece and the European Union

a unique factor profile and for having mass spectra that appear to be split between factors. Correlations with tracer species and reference mass spectra were also significantly lower for 4- and 5-factor solutions with at least one timeseries exhibiting extremely low mass concentrations.

In the following section the PMF solutions for spring, summer, autumn and winter 2013 are presented, complimenting the results from summer 2012 already presented by Bougiatioti et al. (2014). Figure C2 (a-c) represents the mass spectra of the three-factor solution for spring, the time series of each factor associated with external reference time series, as well as the average diurnal profile for each factor. The three factors correspond to fresh BBOA, and OOA component associated with biomass burning (OOA-BB) and a more oxidized OOA. The BBOA, OOA-BB and OOA accounted on average for 20.3, 27.8 and 36.2% of the organic mass, respectively, together with 14.4% of unexplained mass. BBOA has characteristic markings of fresh aerosol associated with biomass burning and an estimated O/C of 0.26 and an H/C of 1.26, which is consistent with other BBOA found in the literature. The BBOA-factor time series showed good correlation with both the estimated BC originating from wood burning ($R_{pearson}^2$=0.59) as well as with the two fragments of levoglucosan, associated to biomass burning, namely m/z 60 and m/z 73 ($R_{pearson}^2$=0.79 and 0.74, respectively) and poor correlation with sulfate and ammonium. Its diurnal profile does not show any significant variability, which can be explained by the relatively low concentrations and limited fluctuations. Finally, as far as similarity with other BBOA found in the literature is concerned (expressed as theta angle between the spectra; Kostenidou et al., 2009), the identified BBOA correlates well with the average BBOA of Ng et al. (2011) (θ=18.4). The difference between the specific mass spectra and other "traditional" BBOA spectra is the similar intensities of m/z 43 and 44 and the lower intensity of m/z 60. This characteristic has been reported for the burning of olive tree branches by Kostenidou et al. (2013) and also can be seen in secondary organic aerosol from monoterpenes. Therefore, it correlates well with the reference olive-tree branch burning BBOA (θ=15.1 degrees; Kostenidou et al., 2013), $SOA_{a\text{-pinene}}$ (θ=20 degrees; Bahreini

European Union
European Social Fund
OPERATIONAL PROGRAMME
EDUCATION AND LIFELONG LEARNING
investing in knowledge society
MINISTRY OF EDUCATION & RELIGIOUS AFFAIRS
MANAGING AUTHORITY
NSRF 2007-2013
programme for development
EUROPEAN SOCIAL FUND
Co-financed by Greece and the European Union

et al., 2005). Finally, it also has some similarities with the BBOA spectrum obtained at the same site during summer 2012 (θ=23 degrees; Bougiatioti et al., 2014).

The OOA-BB mass spectrum has characteristics of oxygenated OA with enhanced signals at m/z 18, 29 and 44 but also has enhanced signal at m/z 43, implying its provenance from primary OA. Its O/C is 0.59 and its H/C 1.2, indicating its processed nature. OOA-BB correlates well with BC from wood burning and with nitrate ($R_{pearson}$=0.63 and 0.69, respectively) and lower correlation with sulfate and ammonium ($R_{pearson}$=0.57 and 0.61). Its diurnal profile does not show any diurnal variability as well. In terms of similarity with other spectra found in the literature, OOA-BB correlates very well to the OOA-BB identified at Finokalia during summer 2012 (θ=8.9 degrees) (Bougiatioti et al., 2014) and has some similarity with the less oxygenated OOA reported for the same sampling site during late spring (θ=18.9 degrees; Hildebrandt et al., 2010) and the average OOA of Ng et al. (2011) (θ=16.7 degrees).

Finally, the OOA component has the markings of a very oxidized organic aerosol with very pronounced relative intensity of m/z 18 and 44, which is also supported by its elevated O/C (1.43) and the presence of very little of other fragments in its spectrum. This factor correlates very well with both sulfate and ammonium ($R_{pearson}$=0.72 and 0.73, respectively). The coincidence of peaks in the OOA time series in the same time as in both BBOA and OOA is an indication that apart from other multiple possible source origins of OOA, it can also originate as a chemical processing product of BBOA in the atmosphere. The OOA diurnal profile, having somewhat higher concentration during higher insolation periods suggests that there is still chemistry and production of OOA near the site. The identified OOA profile is almost identical with the very oxidized OOA reported by Bougiatioti et al. (2014) (θ=4 degrees) and very similar to the more oxidized OOA found for the same location in the previous study of Hildebrandt et al. (2010) (θ=17.7 degrees).

European Union
European Social Fund
OPERATIONAL PROGRAMME
EDUCATION AND LIFELONG LEARNING
investing in knowledge society
MINISTRY OF EDUCATION & RELIGIOUS AFFAIRS
MANAGING AUTHORITY
NSRF 2007-2013
programme for development
EUROPEAN SOCIAL FUND
Co-financed by Greece and the European Union

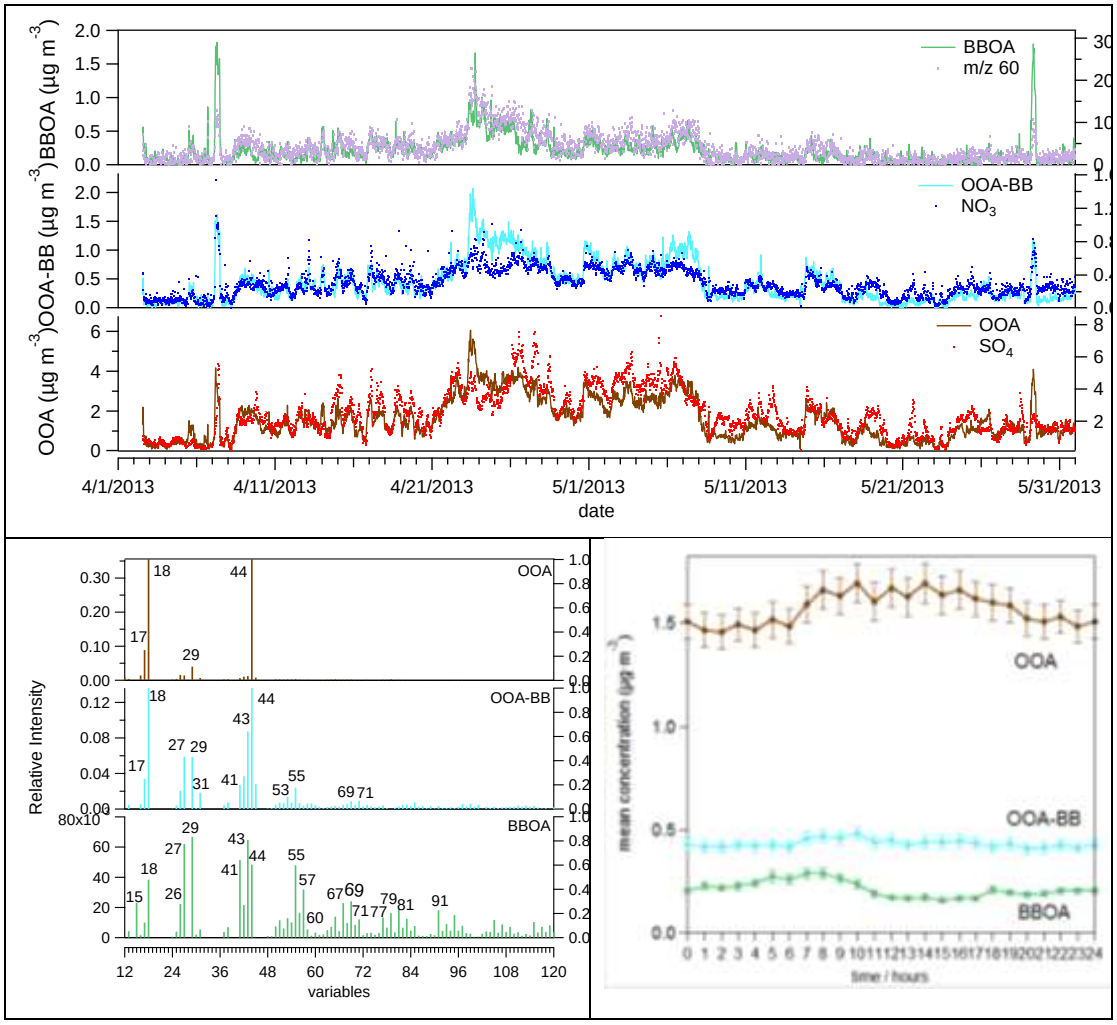

Figure C2: Mass spectra of the three-factor solution for spring(a), the time series of each factor associated with external reference time series(b), as well as the average diurnal profile for each factor(c)

Figure C3 (a-c) shows the time series, mass spectra and diurnal profile of the three-factor selected solution for summer 2013. Once more the three factors correspond to BBOA, OOA-BB and OOA having a mean contribution of 15.4, 27.9 and 45% to the total organic mass, respectively, with 11.7% of unexplained variation in mass. During summer 2013 the BBOA has once more the characteristic markings associated with biomass burning and an estimated O/C of 0.39 and an H/C of 1.38. Once more the

European Union
European Social Fund
OPERATIONAL PROGRAMME
EDUCATION AND LIFELONG LEARNING
investing in knowledge society
MINISTRY OF EDUCATION & RELIGIOUS AFFAIRS
MANAGING AUTHORITY
NSRF 2007-2013
EUROPEAN SOCIAL FUND
Co-financed by Greece and the European Union

BBOA spectrum exhibits similar intensities of m/z 43 and 44 and lower intensity of m/z 60. Therefore, it correlates well with the BBOA observed during spring (θ=20.4 degrees), $SOA_{a\text{-}pinene}$ (θ=19 degrees; Bahreini et al., 2005) and has some similarities with the average BBOA of Ng et al. (2011) (θ=24 degrees). The BBOA-factor time series correlated very well with the two fragments m/z 60 and 73 associated with biomass burning ($R_{pearson}^2$=0.78 and 0.72) and to a lesser extent with nitrate ($R_{pearson}^2$=0.52). Finally, its diurnal profile does not show any significant variability, only somewhat lower concentrations during the highest insolation period, when it may be oxidized and consumed.

The resulting OOA-BB for summer 2013 is more oxidized than the respective spring one, having more elevated relative intensity of m/z 18 and 44, and estimated atomic ratios of O/C and H/C of 1.07 and 1.24, respectively. Its time series correlates well with the fragments from levoglucosan m/z 60 and 73, as well as with nitrate ($R_{pearson}^2$=0.79, 0.73 and 0.65, respectively). Its diurnal variability shows relatively lower concentrations during early afternoon, similarly to BBOA, possibly due to its atmospheric processing. As far as similarity with other reference mass spectra is concerned, OOA-BB is very similar to the OOA-BB from summer 2012 (θ=9.8 degrees; Bougiatioti et al., 2014), correlates well to the OOA-BB from the same site observed during spring 2013 (θ=14 degrees) and has similarities with the average OOA of Ng et al. (2011) (θ=20 degrees).

Finally, the resulting OOA once more is the most oxygenated component having an elevated O/C and the lowest H/C (1.31 and 1.16, respectively). It correlates well with both sulfate and ammonium ($R_{pearson}^2$=0.72 and 0.73, respectively). The OOA mass spectrum is identical to the respective one from spring 2013 (θ=2.3 degrees) and to the one from summer 2012 reported by Bougiatioti et al. (2014) (θ=3.1 degrees). Its diurnal variability shows once more that there are chemical processes and consequent production of OOA near the site.

European Union
European Social Fund
OPERATIONAL PROGRAMME
EDUCATION AND LIFELONG LEARNING
investing in knowledge society
MINISTRY OF EDUCATION & RELIGIOUS AFFAIRS
MANAGING AUTHORITY
NSRF 2007-2013
programme for development
EUROPEAN SOCIAL FUND
Co-financed by Greece and the European Union

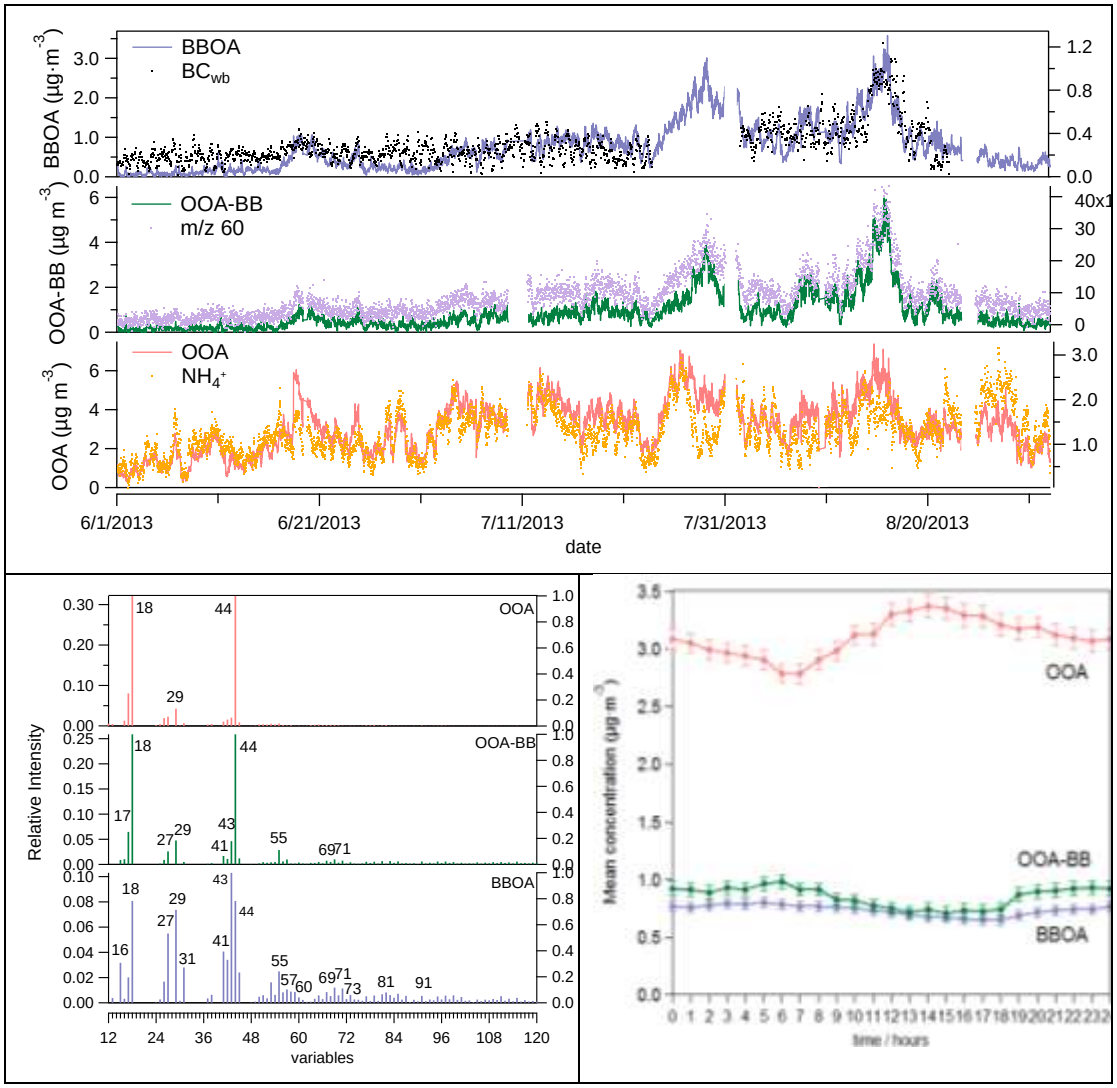

Figure C3: Time series (a), mass spectra (b) and diurnal profile of the three-factor selected solution for summer 2013(c).

For autumn and winter 2013 once more the resulting 3-factor solution was selected. Overall it can be seen that the observed organics concentrations are significantly lower during autumn. The three-factor solution for autumn 2013 with the time series, mass spectra and diurnal variability is presented in Figure C4 (a-c). The three factors correspond once more to BBOA, OOA-BB and OOA, with a mean contribution of 23.5, 23.9 and 38.6% to the total organic mass, respectively, with 13.9% of the variability in mass being unexplained. BBOA correlates better with the reference average BBOA

European Union
European Social Fund
OPERATIONAL PROGRAMME
EDUCATION AND LIFELONG LEARNING
investing in knowledge society
MINISTRY OF EDUCATION & RELIGIOUS AFFAIRS
MANAGING AUTHORITY
NSRF 2007-2013
EUROPEAN SOCIAL FUND
Co-financed by Greece and the European Union

(θ=13.2 degrees; Ng et al., 2011) and $SOA_{a\text{-}pinene}$ (θ=20.5 degrees; Bahreini et al., 2005) while it also correlates well with the BBOA identified during summer 2012 and 2013 (θ=21.3 and 20.9 degrees, respectively). It has an O/C of 0.27 and H/C of 1.26, which are similar to the typical values observed for BBOA. The BBOA-factor time series correlated well with the two fragments of levoglucosan, m/z 60 and 73 ($R_{pearson}^2$=0.75 and 0.7), with BC associated with wood burning ($R_{pearson}^2$=0.54) and with nitrate ($R_{pearson}^2$=0.57). Finally, its diurnal profile does not show any significant variability, only somewhat lower concentrations during the maximum insolation period.

The resulting OOA-BB for autun 2013 is as oxidized as the respective spring one, having estimated atomic ratios of O/C and H/C of 1.05 and 1.21, respectively. Its time series correlates well with the fragments from levoglucosan m/z 60 and 73, as well as with nitrate ($R_{pearson}^2$=0.79, 0.82 and 0.62, respectively). Its diurnal variability shows relatively higher concentrations during early afternoon, possibly due to the atmospheric processing of its precursor, BBOA. As far as similarity with other reference mass spectra is concerned, OOA-BB is very similar to the OOA-BB from summer 2012 (θ=6.4 degrees; Bougiatioti et al., 2014), has many similarities with the average OOA of Ng et al. (2011) (θ=17.7 degrees) and correlates very well to the OOA-BB from the same site observed during summer 2013 (θ=6.3 degrees).

The OOA for autumn 2013 once more is very oxidized, with an O/C equal to 1.44 and H/C equal to 1.19. It correlates very well with sulfate ($R_{pearson}^2$=0.73) and ammonium ($R_{pearson}^2$=0.74). Its diurnal variability shows maximum values during early afternoon, consistent with earlier observation concerning existing chemistry and production of OOA close to the site. As observed before for the OOA factors, the OOA mass spectrum remains quite "stable", being almost identical to the OOA from summer 2012 and 2013 (θ=4.8 and 3.7 degrees, respectively).

European Union
European Social Fund
OPERATIONAL PROGRAMME
EDUCATION AND LIFELONG LEARNING
investing in knowledge society
MINISTRY OF EDUCATION & RELIGIOUS AFFAIRS
MANAGING AUTHORITY
NSRF 2007-2013
EUROPEAN SOCIAL FUND
Co-financed by Greece and the European Union

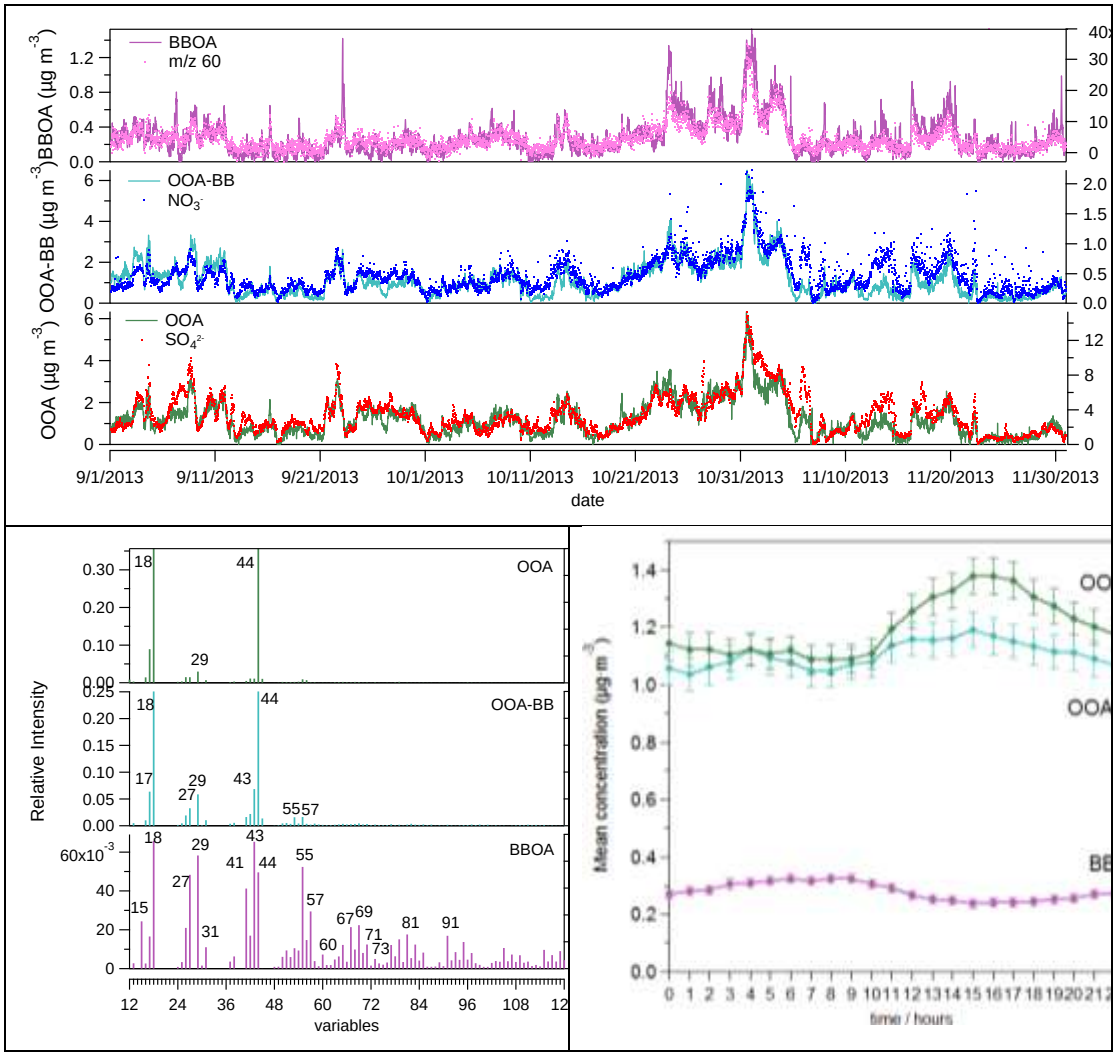

Figure C4: The three-factor solution for autumn 2013 with the time series (a), mass spectra (b) and diurnal variability (c).

Finally, the obtained results for winter 2013 are presented in Figure C5, with the corresponding time series, mass spectra and diurnal variability. Once more the overall organics concentrations are relatively low, even lower than the ones observed during autumn. The three resulting factors represent a BBOA, an OOA-BB and an OOA, with mean contributions of 20.2, 24.9 and 38.5% to the total organic mass, respectively and 12.6% of the mass remaining unexplained. BBOA has an O/C and H/C of 0.33 and 1.3, respectively and the time series correlates well with BC associated with wood burning ($R_{pearson}^2$=0.57) and with nitrate ($R_{pearson}^2$=0.64) as well as with the fragments of

European Union
European Social Fund
OPERATIONAL PROGRAMME
EDUCATION AND LIFELONG LEARNING
investing in knowledge society
MINISTRY OF EDUCATION & RELIGIOUS AFFAIRS
MANAGING AUTHORITY
NSRF 2007-2013
EUROPEAN SOCIAL FUND
Co-financed by Greece and the European Union

levoglucosan associated with biomass burning, m/z 60 and 73 ($R_{pearson}^2$=0.72 and 0.77, respectively). Its diurnal profile does not show any variability. During winter, from November to February, burning of olive tree branches after pruning of the trees is a common agricultural waste management technique (Kostenidou et al., 2013). Therefore, it is "expected" that the BBOA identified during winter 2013 correlates very well with the reference olive-tree branch burning BBOA (θ=13.7 degrees; Kostenidou et al., 2013). It also has similarities with the reference of $SOA_{a\text{-}pinene}$ (θ=19.5 degrees; Bahreini et al., 2005), the BBOA identified during spring (θ=18.9 degrees) and with the average BBOA of Ng et al. (2011) (θ=22.9 degrees).

OOA-BB is less oxygenated than the respective ones during summer and autumn, expressed both by the lower relative intensities of the prevalent fragments, but also by the lower O/C and higher H/C (0.92 and 1.28, respectively). The diurnal profile of OOA-BB does not exhibit significant variability, nevertheless shows somewhat lower values during nighttime. Once more the OOA-BB at this site is very similar to the respective one observed during other seasons (θ=8.3 degrees; Bougiatioti et al., 2014; θ=6.4 degrees with $OOA\text{-}BB_{autumn}$) and also correlates well with the average OOA of Ng et al. (2011) (θ=13.7 degrees). Finally its time series correlates very well with m/z 60 and 73 ($R_{pearson}^2$=0.74 and 0.81, respectively) and with nitrate ($R_{pearson}^2$=0.68).

OOA has an O/C of 1.45 and H/C of 1.19 and correlates very well with both sulfate and ammonium ($R_{pearson}^2$=0.79 and 0.75, respectively) and has some correlation with nitrate ($R_{pearson}^2$=0.61). The OOA diurnal profile does not show significant diurnal variability, apart from relatively higher values during early afteroon. The limited diurnal variability might be associated with limited photochemical activity during wintertime as well as with the significantly lower concentrations during this period. Finally, the resulting OOA mass spectrum is again almost identical to the OOA spectra of the other seasons (θ=1.3 degrees with $OOA_{autumn13}$, 3.1 degrees with $OOA_{summer13}$ and 5.6 degrees with $OOA_{summer12}$). This underlines the fact that OOA at the site is quite uniform throughout

European Union
European Social Fund
OPERATIONAL PROGRAMME
EDUCATION AND LIFELONG LEARNING
investing in knowledge society
MINISTRY OF EDUCATION & RELIGIOUS AFFAIRS
MANAGING AUTHORITY
NSRF 2007-2013
programme for development
EUROPEAN SOCIAL FUND
Co-financed by Greece and the European Union

the year, regardless of whether part of it originates from oxidative processes of BBOA or other types of primary OA.

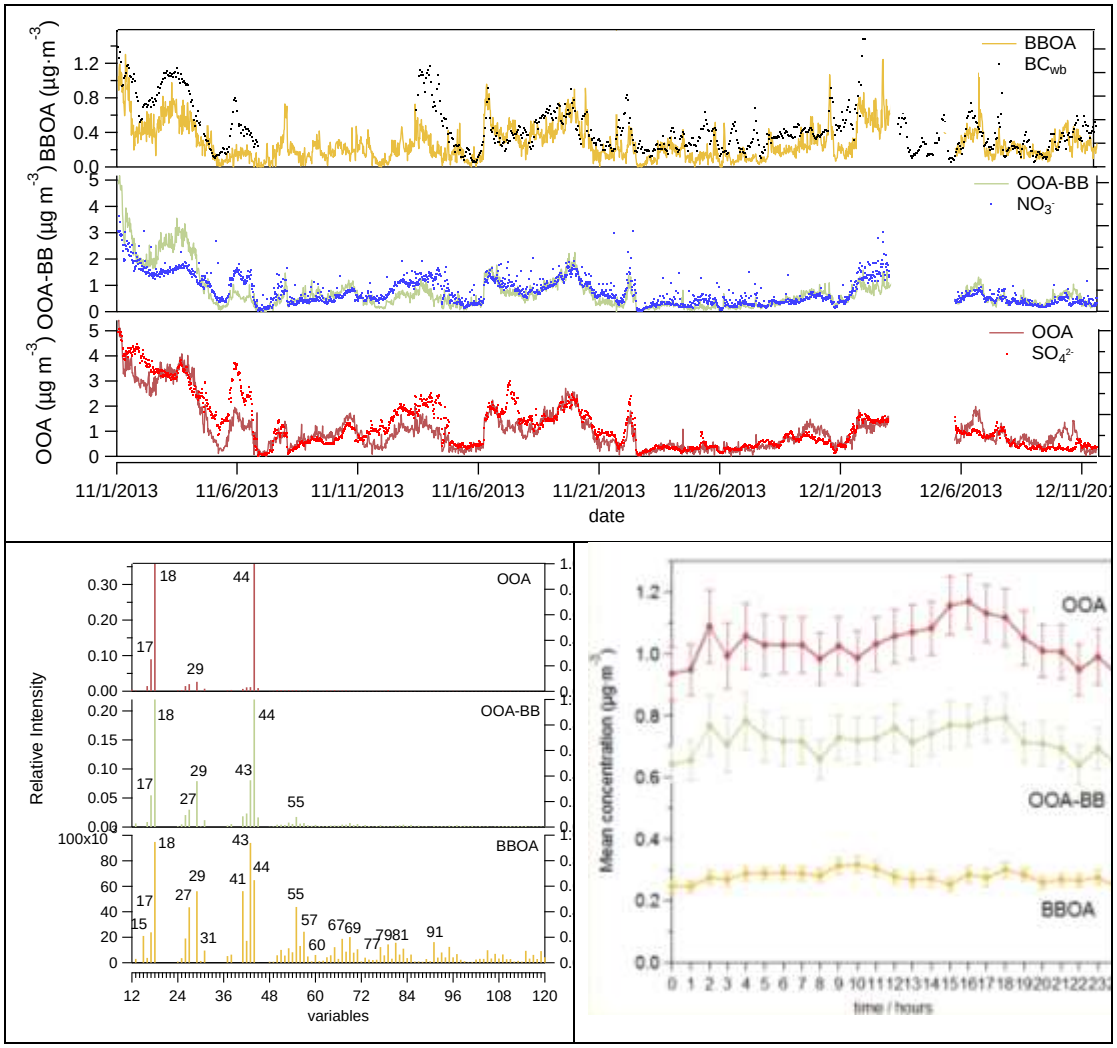

Figure C5: The three-factor solution for winter 2013 with the time series (a), mass spectra (b) and diurnal variability (c).

C2.3 Seasonal variability of organic aerosol sources

Based on the analysis of the PMF resulting factors for each season, after normalizing the contribution of each factor to 100% when removing the unexplained mass, we calculated the seasonal variability of the different OA fractions. The seasonal variability of the three identified factors, namely BBOA, OOA-BB and OOA can be seen in Figure C6. On average BBOA accounts for 22.5±3.8% of the total organic fraction of the

European Union
European Social Fund
OPERATIONAL PROGRAMME
EDUCATION AND LIFELONG LEARNING
investing in knowledge society
MINISTRY OF EDUCATION & RELIGIOUS AFFAIRS
MANAGING AUTHORITY
NSRF 2007-2013
EUROPEAN SOCIAL FUND
Co-financed by Greece and the European Union

aerosol, OOA-BB for 28.8±2.2% and OOA for 45.3±4.1%. There are not enough data available for autumn 2012 for the PMF run because of instrumental issues with the ACSM and clogging of the critical orifice before installing the PM_1 inlet.

It can be seen that during the warm seasons when photochemical activity is maximum in the area, the contribution of BBOA together with OOA-BB can add up to almost 50% of the sampled organic aerosol. At the same time, BBOA exhibits minimum contribution during summertime, and maximum concentrations during spring and autumn. This observation is consistent with the finding of Sciare et al. (2008) who found that long-range transport of agricultural waste burning from Southeastern Europe and countries around the Black Sea has each year two periods, one during March-April and one during July-September. During the cold seasons, when photochemical processes are limited, OOA-BB has minimum contribution. Concurrently OOA also has its minimum contribution during the same seasons. On the contrary, it exhibits maximum contribution during summer, and so does OOA-BB, probably because of increased atmospheric processing.

It is therefore clear that throughout the year and regardless of the season, biomass burning is an important source of organic matter in the area. Having in mind that the BBOA mass spectrum most of the time exhibits significant similarities with the mass spectrum of BBOA from olive-tree branches and at the same time, olive tree branches burning is a common agricultural waste management practice in the whole Mediterranean area after the annual pruning of olive trees, this gives another dimension to this source. Especially when this activity takes place during the cold periods when there is no rainfall and wind speeds are low, burning of olive tree branches can be an important source of organic matter, and particulate matter as well, in all the Mediterranean area where the most olive-oil producing countries are.

European Union
European Social Fund
OPERATIONAL PROGRAMME
EDUCATION AND LIFELONG LEARNING
investing in knowledge society
MINISTRY OF EDUCATION & RELIGIOUS AFFAIRS
MANAGING AUTHORITY
NSRF 2007-2013
programme for development
EUROPEAN SOCIAL FUND
Co-financed by Greece and the European Union

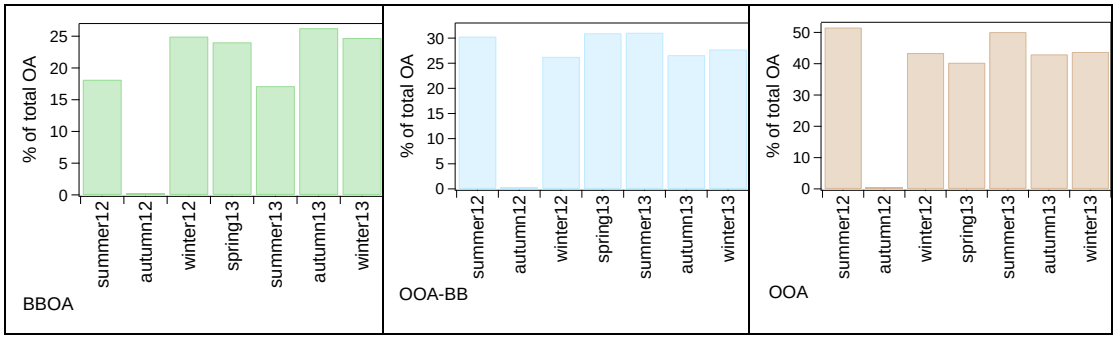

Figure C6: Seasonal variability of the three identified factors, namely BBOA, OOA-BB and OOA.

C3. References

Aiken, A.C., DeCarlo, P.F., Kroll, J.H., Worsnop, D.R., Huffman, J.A., Docherty, K.S., Ulbrich, I.M., Mohr, C., Kimmel, J.R., Sueper, D., Sun, Y., Zhang, Q., Trimborn, A., Northway, M., Ziemann, P.J., Canagaratna, M.R., Onasch, T.B., Alfarra, M.R., Prevot, A.S.H., Dommen, J., Duplissy, J., Metzger, A., Baltensperger, U., and Jinemez, J.L..: O/C and OM/OC ratios of primary, secondary, and ambient organic aerosols with high-resolution time-of-flight Aerosol Mass Spectrometry, *Environ. Sci. Technol.*, **42**, 4478-4485, 2008.

Aiken, A.C., Salcedo, D., Cubison, M.J., Huffman, J.A., DeCarlo, P.F., Ulbrich, I.M., Docherty, K.S., Sueper, D., Kimmel, J.R., Worsnop, D.R., Trimborn, A., Northway, M., Stone, E.A., Schauer, J.J., Volkamer, R.M., Fortner, E., de Foy, B., Wang, J., Laskin, A., Shutthanandan, V., Zheng, J., Zhang, R., Gaffeny, J., Marley, N.A., Paredes-Miranda, G., Arnott, W.P., Molina, L.T., Sosa, G., and Jimenez, J.L.: Mexico City aerosol analysis during MILAGRO using high-resolution mass spectrometry at the urban supersite (T0)- Part 1: Fine particle composition and organic source apportionment, *Atmos. Chem. Phys.*, **9**, 6633-6653, 2009.

Alfarra, M. R., Prevot, A. S. H., Szidat, S., Sandradewi, J., Weimer, S., Lanz, V. A., Schreiber, D., Mohr, M., and Baltensperger, U.: Identification of the mass spectral signature of organic aerosols from wood burning emissions, *Environ. Sci. Technol.*, **41**, 5770-5777, 2007.

European Union
European Social Fund
OPERATIONAL PROGRAMME
EDUCATION AND LIFELONG LEARNING
investing in knowledge society
MINISTRY OF EDUCATION & RELIGIOUS AFFAIRS
MANAGING AUTHORITY
NSRF 2007-2013
EUROPEAN SOCIAL FUND
Co-financed by Greece and the European Union

Allan, J.D., Williams, P.I., Morgan, W.T., Martin, C.L., Flynn, M.J., Lee, J., Nemitz, E., Phillips, G.J., Gallagher, M.W., and Coe, H.: Contributions from Transport, Solid Fuel Burning and Cooking to Primary Organic Aerosols in two UK cities, *Atmos. Chem. Phys.*, **10** (2), 647-668, 2010.

Bardouki, H., Liakakou, E., Economou, C., Sciare, J., Smolik, J., Zdimal, V., Eleftheriadis, K., Lazaridis, M., Dye, C., and Mihalopoulos, N.: Chemical composition of size-resolved atmospheric aerosols in the Eastern Mediterranean during summer and winter, *Atmos. Environ.*, **37**, 195-208, 2003.

Bahreini, R., Keywood, M.D., Ng. N.L., Varutbangkul, V., Gao., S., Flagan, R.C., Seinfeld, J.H., Wornsop, D.R., and Jimenez, J.L.: Measurements of Secondary Organic Aerosol from Oxidation of cycloalkenes, terpenes and m-xylene using an Aerodyne Aerosol Mass Spectrometer, *Environ. Sci. Technol.* 39, 5674-5688, 2005.

Bougiatioti, A., Zarmpas, P., Koulouri, E., Antoniou, M., Theodosi, C., Kouvarakis, G., Saarikoski, S., Mäkelä, T., Hillamo, R., and Mihalopoulos, N.: Organic, elemental and water-soluble organic carbon in size segregated aerosols, in the marine boundary layer of the Eastern Mediterranean, *Atmos. Environ.*, **64**, 251-262, 2013.

Capes, G., Johnson, B., McFiggans, G., Williams, P.I., Haywood, J., and Coe, H.: Aging of biomass burning aerosols over West Africa: Aircraft measurements of chemical composition, microphysical properties, and emission ratios, *J. Geophys. Res.*, **113**, D00C15, doi:10.1029/2008JD009845, 2008.

Cottrell, L.D., Griffin, R.J., Jimenez, J.L., Zhang, Q., Ulbrich, I., Ziembra, L.D., Beckman, P.J., Sive, B.C., and Talbot, R.W.: Submicron particles at Thompson Farm during ICARTT measured using aerosol mass spectrometry, *J. Geophys. Res.*, **113**, D08212, doi:10.1029/2007JD009192, 2008.

Crippa, M., DeCarlo, P.F., Slowik, J.G., Mohr, C., Heringa, M.F., Chirico, R., Poulain, L., Freutel, F., Sciare, J., Cozic, J., Di Marco, C.F., Elsasser, M., José, N., Marchand, N., Abidi, E., Wiedensohler, A., Drewnick, F., Schneider, J., Borrmann, S., Nemitz, E., Zimmermann, Jaffrezo, J.-L., Prévôt, A.S.H., and Baltensperger, U.: Wintertime aerosol chemical composition and source apportionment of the organic fraction in the metropolitan area of Paris, *Atmos. Chem. Phys.*, **13**, 961-981, 2013.

European Union
European Social Fund
OPERATIONAL PROGRAMME
EDUCATION AND LIFELONG LEARNING
investing in knowledge society
MINISTRY OF EDUCATION & RELIGIOUS AFFAIRS
MANAGING AUTHORITY
NSRF 2007-2013
programme for development
EUROPEAN SOCIAL FUND
Co-financed by Greece and the European Union

Cristofanelli, P., Fierli, F., Marinoni, A., Calzolari, F., Duchi, R., Burkhart, J., Stohl, A., Maione, M., Arduini, J., and Bonasoni, P. : Influence of biomass burning and anthropogenic emissions on ozone, carbon monoxide and black carbon at the Mt. Cimone GAW_WMO global station (Italy, 2165 m a.s.l.), *Atmos. Chem. Phys.*, **13**, 15-30, 2013.

Cubison, M.J., Ortega, A.M., Hayes, P.L., Farmer, D.K., Day, D., Lechner, M.J., Brune, W.H., Apel, E., Diskin, G.S., Fisher, J.A., Fuelberg, H.E., Hecobian, A., Knapp, D.J., Mikoviny, T., Riemer, D., Sachse, G.W., Sessions, W., Weber, R.J., Weinheimer, A.J., Wisthaler, A., and Jimenez, J.L.: Effects of aging on organic aerosol from open biomass burning smoke in aircraft and laboratory studies, *Atmos. Chem. Phys.*, **11**, 12049-12064, 2011.

He, L.-Y., Lin, Y., Huang, X.-F., Guo, S., Xue, L., Su, Q., Luan, S.-J., and Zhang, Y.-H.: Characterization of high-resolution aerosol mass spectra of primary organic aerosol emissions from Chinese cooking and biomass burning, *Atmos. Chem. Phys.*, **10**, 11535-11543, 2010.

He., L.-Y., Huang, X.-F., Xue, L., Hu, M., Lin, Y., Zheng, J., Zhang, R., and Zhang, Y.-H.: Submicron aerosol analysis and organic source apportionment in an urban atmosphere in Pearl River Delta of China using high-resolution aerosol mass spectrometry, *J. Geophys. Res.*, **116**, D12304, doi:10.1029/2010JD014566, 2011.

Huang, X.-F., He, L.-Y., Hu, M., Canagaratna, M.R., Kroll, J.H., Ng, N.L., Zhang, Y.-H., Lin, Y., Xue, L., Sun, T.-L., Liu, X.-G., Shao, M., Jayne, J.T., and Worsnop, D.R.: Characterization of submicron aerosols at a rural site in Pearl River Delta of China using an Aerodyne High-Resolution Aerosol Mass Spectrometer, *Atmos. Chem. Phys.*, **11**, 1865-1877, 2011.

Hildebrandt, L., Engelhart, G.J., Mohr, C., Kostenidou, E., Lanz, V.A., Bougiatioti, A., DeCarlo, P.F., Prevot, A.S.H., Baltensperger, U., Mihalopoulos, N., Donahue, N.M., and Pandis, S.N.: Aged organic aerosol in the Eastern Mediterranean: the Finokalia Aerosol Measurement Experiment-2008, *Atmos. Chem. Phys.*, **10**, 4167-4186, 2010a.

European Union
European Social Fund
OPERATIONAL PROGRAMME
EDUCATION AND LIFELONG LEARNING
investing in knowledge society
MINISTRY OF EDUCATION & RELIGIOUS AFFAIRS
MANAGING AUTHORITY
NSRF 2007-2013
programme for development
EUROPEAN SOCIAL FUND
Co-financed by Greece and the European Union

Hildebrandt, L., Kostenidou, E., Mihalopoulos, N., Worsnop, D. R., Donahue, N. M., and Pandis, S. N.: Formation of highly oxygenated organic aerosol in the atmosphere: Insights from the Finokalia Aerosol Measurement Experiments, Geophys. Res. Lett., 37, L23801, doi:10.1029/2010GL045193, 2010b.

Hildebrandt, L., Kostenidou, E., Lanz, V.A., Prevot, A.S.H., Baltensperger, U., Mihalopoulos, N., Laaksonen, A., Donahue, N.M., and Pandis, S.N.: Sources and atmospheric processing of organic aerosol in the Mediterranean: insights from aerosol mass spectrometer factor analysis, *Atmos. Chem. Phys.*, **11**, 12499-12515, 2011.

Huffman, J. A., Docherty, K. S., Mohr, C., Cubison, M. J., Ulbrich, I. M., Ziemann, P. J., Onasch, T. B., and Jimenez, J. L.: Chemically-Resolved Volatility Measurements of Organic Aerosol from Different Sources, *Environ. Sci. Technol.*, **43**, 5351–5357, doi:10.1021/es803539d, 2009.

Jayne, J.: Aerosol Chemical Speciation Monitor Data Acquisition Software Manual, Aerodyne Research, May 2011a.

Jayne, J.: Aerosol Chemical Speciation Monitor Data Analysis Software Manual, Aerodyne Research, 2011b.

Jimenez, J. L., Canagaratna, M. R., Donahue, N. M., Prevot, A. S. H., Zhang, Q., Kroll, J. H., DeCarlo, P. F., Allan, J. D., Coe, H., Ng, N. L., Aiken, A. C., Docherty, K. D., Ulbrich, I. M., Grieshop, A. P., Robinson, A. L., Duplissy, J., Smith, J. D., Wilson K. R., Lanz, V. A., Hueglin, C., Sun, Y. L., Tian, J., Laaksonen, A., Raatikainen, T., Rautiainen, J., Vaattovaara, P., Ehn, M., Kulmala, M., Tomlinson, J. M., Collins, D. R., Cubison, M. J., Dunlea, E. J., Huffman, J. A., Onasch, T. B., Alfarra, M. R., Williams, P. I., Bower, K., Kondo, Y., Schneider, J., Drewnick, F., Borrmann, S., Weimer, S., Demerjian, K., Salcedo, D., Cottrell, L., Griffin, R., Takami, A., Miyoshi, T., Hatakeyama, S., Shimono, A., Sun, J. Y., Zhang, Y. M., Dzepina, K., Kimmel, J. R., Sueper, D., Jayne, J. T., Herndon, S. C., Trimborn, A. M., Williams, L. R.,Wood, E. C., Kolb, C. E., Baltensperger, U., and Worsnop, D. R.: Evolution of organic aerosol in the atmosphere, *Science*, **326**, 1525–1529, doi:10.1126/science.1180353, 2009.

European Union
European Social Fund
OPERATIONAL PROGRAMME
EDUCATION AND LIFELONG LEARNING
investing in knowledge society
MINISTRY OF EDUCATION & RELIGIOUS AFFAIRS
MANAGING AUTHORITY
NSRF 2007-2013
EUROPEAN SOCIAL FUND
Co-financed by Greece and the European Union

Kalivitis, N., Bougiatioti, A., Kouvarakis, G., and Mihalopoulos, N.: Long term measurements of atmospheric aerosol optical properties in the Eastern Mediterranean, *Atmos. Res.*, **102**, 351-357, 2011.

Kanakidou, M., Tsigaridis, K., Dentener, F.J., and Crutzen, P.J.: Human-activity-enhanced formation of organic mass fraction of aerosols by biogenic hydrocarbon oxidation, *J. Geophys. Res.*, **105** (D7), 9243-9254, 2000.

Kostenidou, E., Pathank, R.K., and Pandis,S.N.: An algorithm for the calculation of secondary organic aerosol density combining AMS and SMPS data, *Aerosol Sci. Technol.*, **41**, 1002-1010, 2007.

Kostenidou, E., Kaltsonoudis, C., Tsiflikiotou, M., Louvaris, E., Russell, L.M., and Pandis, S.N.: Burning of olive tree branches: a major organic aerosol source in the Mediterranean, *Atmos. Chem. Phys. Discuss.*, **13**, 7223-7266, 2013.

Kuwata, M., Shao, W., Lebouteiller, R., and Martin, S.T.: Classifying organic materials by oxygen-to-carbon elemental ratio to predict the activation regime of cloud condensation nuclei (CCN), *Atmos. Chem. Phys. Discuss.*, **12**, 31829-31870, 2012.

Lanz, V.A., Alfarra, M.R., Baltensperger, U., Buchmann, B., Hueglin, C., and Prévôt, A.S.H.: Source apportionment of submicron organic aerosols at an urban site by factor analytical modeling of aerosol mass spectra, *Atmos. Chem. Phys.*, **7**, 1503-1522, 2007.

Lanz, V. A., Alfarra, M. R., Baltensperger, U., Buchmann, B., Hueglin, C., Szidat, S., Wehrli, M. N., Wacker, L., Weimer, S., Caseiro, A., Puxbaum, H., and Prevot, A. S. H.: Source attribution of submicron organic aerosols during wintertime inversions by advanced factor analysis of aerosol mass spectra, *Environ. Sci. Technol.*, **42**, 214–220, 2008.

Lathem, T.L., Beyersdorf, A.J., Thornhill, K.L., Winstead, E.L., Cubison, M.J., Hecobian, A., Jimenez, J.L., Weber, R.J., Anderson, B.E., and Nenes, A.: Analysis of CCN activity of Arctic aerosol and Canadian biomass burning during summer 2008, *Atmos. Chem. Phys. Disc.*, **12**, 24677-24733, 2012.

Lee, T., Sullivan, A. P., Mack, L., Jimenez, J. L., Kreidenweis, S. M., Onasch, T. B., Worsnop, D. R., Malm, W., Wold, C. E., Hao, W. M., and Collett, J. L.: Variation

European Union
European Social Fund
OPERATIONAL PROGRAMME
EDUCATION AND LIFELONG LEARNING
investing in knowledge society
MINISTRY OF EDUCATION & RELIGIOUS AFFAIRS
MANAGING AUTHORITY
NSRF 2007-2013
EUROPEAN SOCIAL FUND
Co-financed by Greece and the European Union

of chemical smoke marker emissions during flaming vs. smoldering phases of laboratory open burning of wildland fuels, *Aerosol Sci. Technol.*, **44**, 1–5, doi:10.1080/02786826.2010.499884, 2010.

Mihalopoulos, N., Stephanou, E., Kanakidou,M., Pilitsidis, S., and Bousquet, P.: Troposheric aerosol ionic composition above the eastern Mediterranean area, *Tellus B*, **49**, 314–326, 1997.

Mohr, C., Huffman, J.A., Cubison, M.J., Aiken, A.C., Docherty, K.S., Kimmel, J.R., Ulbrich, I.M., Hannigan, M., and Jimenez, J.L.: Characterization of Primary Organic Aerosol Emissions from Meat Cooking, Trash Burning, and Motor Vehicles with High-Resolution Aerosol Mass Spectrometry and Comparison with Ambient and Chamber Observations, *Environ. Sci. Technol.*, **43**, 2443-2449, 2009.

Mohr, C., DeCarlo, P.F., Heringa, M.F., Chirico, R., Slowik, J.G., Richter, R., Reche, C., Alastuey, A., Querol, X., Seco, R., Peñuelas, J., Jiménez, J.L., Crippa, M., Zimmermann, R., Baltensperger, U., and Prévôt, A.S.H.: Identfication and quantification of organic aerosol from cooking and other sources in Barcelona using aerosol mass spectrometer data, *Atmos. Chem. Phys.*, **12**, 1649-1665, 2012.

Moore, R.H., Bahreini, R., Brock, C.A., Froyd, K.D., Cozic, J., Holloway, J.S., Middlebrook, A.M., Murphy, D.M., and Nenes, A.: Hygroscopicity and composition of Alaskan Arctic CCN during April 2008, *Atmos. Chem. Phys.*, **11**, 11807-11825, 2011.

Ng, N. L., Canagaratna, M. R., Zhang, Q., Jimenez, J. L., Tian, J., Ulbrich, I. M., Kroll, J. H., Docherty, K. S., Chhabra, P. S., Bahreini, R., Murphy, S. M., Seinfeld, J. H., Hildebrandt, L., Donahue, N. M., DeCarlo, P. F., Lanz, V. A., Pr´evˆot, A. S. H., Dinar, E., Rudich, Y., and Worsnop, D. R.: Organic aerosol components observed in Northern Hemispheric datasets from Aerosol Mass Spectrometry, *Atmos. Chem. Phys.*, **10**, 4625–4641, doi:10.5194/acp-10-4625-2010, 2010.

Ng, N.L., Herndon, S.C., Trimborn, A., Canagaratna, M.R., Croteau, P.L., Onasch, T.B., Sueper, D., Worsnop, D.R., Zhang, Q., Sun, Y.L., and Jayne, J.T.: An Aerosol Chemical Speciation Monitor (ACSM) for routine monitoring of the composition

European Union
European Social Fund
OPERATIONAL PROGRAMME
EDUCATION AND LIFELONG LEARNING
investing in knowledge society
MINISTRY OF EDUCATION & RELIGIOUS AFFAIRS
MANAGING AUTHORITY
NSRF 2007-2013
EUROPEAN SOCIAL FUND
Co-financed by Greece and the European Union

and mass concentration of ambient aerosol., *Aerosol Sci. Technol.*, **45** (7), 780-794, 2011a.

Ng, N.L., Canagaratna, M.R., Jimenez, J.L., Zhang, Q., Ulbrich, I.M., and Worsnop, D.R.: Real-time methods for estimating organic component mass concentrations from aerosol mass spectrometer data, *Environ. Sci. Technol.*, **45**, 910-916, 2011b.

Ng, N.L., Canagaratna, M.R., Jimenez, J.L., Chhabra, P.S., Seinfeld, J.H., and Worsnop, D.R.: Changes in organic aerosol composition with aging inferred from aerosol mass spectra, *Atmos. Chem. Phys.*, **11**, 6465-6474, 2011c.

Paatero, P., and Tapper, U.: Positive Matrix Factorization – a Nonnegative Factor Model with Optimal Utilization of Error-Estimates of Data Values, *Environmetrics*, **5**, 111-126, 1994.

Putaud, J.-P., Raes, F., Van Dingenen, R., Bruggemann, E., Facchini, M.C., Decesari, S., Fuzzi, S., Gehrig, R., Huglin, C., Laj, P., Lorbeer, G., Maenhaut, W., Mihalopoulos, N., Muller, K., Querol, X., Rodriguez, S., Schneider, J., Spindler, G., Ten Brink, H., Torseth, K., and Wiedensohler, A.: A European aerosol phenomenology-2: chemical characteristics of particulate matter at kerbside, urban, rural and background sites in Europe, *Atmos. Environ.*, **38**, 2579-2595, 2004.

Saarikoski, S., Carbone, S., Decessari, S., Giulianelli, L., Angelini, F., Canagaratna, M., Ng, N.L., Trimborn, A., Facchini, M.C., Fuzzi, S., Hillamo, R., and Worsnop, D.: Chemical characterization of springtime submicrometer aerosol in Po Valley, *Atmos. Chem. Phys.*, **12**, 8401-8421, 2012.

Sciare, J., Bardouki, H., Moulin, C., and Mihalopoulos, N.: Aerosol sources and their contribution to the chemical composition of aerosols in the Eastern Mediterranean Sea during summertime, *Atmos. Chem. Phys.*, **3**, 291-302, doi:10.5194/acp-3-291-2003, 2003.

Sciare, J., Oikonomou, K., Cachier, H., Mihalopoulos, N., Andreae, M.O., Maenhaut, W., and Sarda-Estève, R. : Aerosol mass closure and reconstruction of the light scattering coefficient over the Eastern Mediterranean Sea during the MINOS campaign, *Atmos. Chem. Phys.*, **5**, 2253-2265, 2005.

European Union
European Social Fund
OPERATIONAL PROGRAMME
EDUCATION AND LIFELONG LEARNING
investing in knowledge society
MINISTRY OF EDUCATION & RELIGIOUS AFFAIRS
MANAGING AUTHORITY
NSRF 2007-2013
programme for development
EUROPEAN SOCIAL FUND
Co-financed by Greece and the European Union

Sciare, J., Oikonomou, K., Favez, O., Liakakou, E., Markaki, Z., Cachier, H., and Mihalopoulos, N.: Long-term measurements of carbonaceous aerosols in the Eastern Mediterranean: evidence of long-range transport of biomass burning, *Atmos. Chem. Phys.*, **8**, 5551-5563, 2008.

Schneider, J., Weimer, S., Drewnick, F., Borrmann, S., Helas, G., Gwaze, P., Schmid, O., Andreae, M. O. and Kirchner, U.: Mass spectrometric analysis and aerodynamic properties of various types of combustion-related aerosol particles, Int. J. Mass. Spec., 258, 37–49, 2006.

Ulbrich, I.M., Canagaratna, M.R., Zhang, Q., Worsnop, D.R., and Jimenez, J.L.: Interpretation of organic components from Positive Matrix Factorization of aerosol mass spectrometric data, *Atmos. Chem. Phys.*, **9**, 2891-2918, 2009.

Van Dingenen, R., Putaud, J.-P., Martins-Dos Santos, S., and Raes, F.: Physical aerosol properties and their relation to air mass origin at Monte Cimone (Italy) during the first MINATROC campaign, *Atmos. Chem. Phys.*, **5**, 2203-2226, 2005.

Vrekoussis, M., Liakakou, E., Koçak, M., Kubilay, N., Oikonomou, K., Sciare, J., and Mihalopoulos, N.: Seasonal variability of optical properties of aerosol in the Eastern Mediterranean, *Atmos. Environ.*, **39**, 7083-7094, 2005.

Zhang, Q., Jimenez, J. L., Canagaratna, M. R., Allan, J. D., Coe, H., Ulbrich, I., Alfarra, M. R., Takami, A., Middlebrook, A. M., Sun, Y. L., Dzepina, K., Dunlea, E., Docherty, K., De- Carlo, P. F., Salcedo, D., Onasch, T., Jayne, J. T., Miyoshi, T., Shimono, A., Hatakeyama, S., Takegawa, N., Kondo, Y., Schneider, J., Drewnick, F., Borrmann, S., Weimer, S., Demerjian, K., Williams, P., Bower, K., Bahreini, R., Cottrell, L., Griffin, R. J., Rautiainen, J., Sun, J. Y., Zhang, Y. M., and Worsnop, D. R.: Ubiquity and dominance of oxygenated species in organic aerosols in anthropogenically-influenced Northern Hemisphere midlatitudes, *Geophys. Res. Lett.*, **34**, L13801, doi:10.1029/2007gl029979, 2007.

European Union
European Social Fund
OPERATIONAL PROGRAMME
EDUCATION AND LIFELONG LEARNING
investing in knowledge society
MINISTRY OF EDUCATION & RELIGIOUS AFFAIRS
MANAGING AUTHORITY
NSRF 2007-2013
programme for development
EUROPEAN SOCIAL FUND
Co-financed by Greece and the European Union

D. Long term chemical characterization of fine particulate matter over the Eastern Mediterranean at high temporal resolution

D1. Experimental and Methods

D1.1 Sampling Site

Measurements were held at the remote coastal atmospheric monitoring station of the Environmental Chemical Processes Laboratory (ECPL) at Finokalia (35º 20' N, 25º 40' E). The station is situated on the north coast of the island of Crete, 70 km to the east of the region's largest city, Heraklion, measuring roughly 170.000 inhabitants. It is located on a hill at 230 m a.s.l. overlooking the Cretan Sea. Very little human activity, mainly agriculture, is observed at a range of approximately 15km (Kouvarakis et al., 2000). Details on the meteorology and prevailing atmospheric conditions of the site can be found in Mihalopoulos et al. (1997). The measuring period spans over roughly 32 months, starting on 18 May 2012 and ending on 31 December 2014, during which a variety of different atmospheric attributes was recorded.

D1.2 Instrumentation

An Aerodyne Aerosol Chemical Speciation Monitor (ACSM) (Ng et al., 2011) was deployed in Finokalia in late May 2012. The ACSM provides measurements of aerosol mass and chemical composition at a high temporal resolution making it ideal for atmospheric monitoring purposes. To be more specific, the ACSM, practically an online quadrupole mass spectrometer, built on the same operating principle as the widely acknowledged Aerosol Mass Spectrometer (AMS) (Jayne et al., 2000), measures the non-refractory part of the PM_1 ambient aerosol, providing mass concentrations of Organics, $SO_4^{=}$, NO_3^{-}, NH_4^{+} and Chloride. Temporal resolution of the measurements was set to 30 minutes, thus giving clear information and detail on the variation of these species in the aerosol population over Finokalia.

The instrument sampled through a PM_1 sharp cut cyclone (BGI Inc.) at 3.5 lt/min. The inlet was positioned 3.5 meters above ground level. For a first period, starting on 18

European Union
European Social Fund
OPERATIONAL PROGRAMME
EDUCATION AND LIFELONG LEARNING
investing in knowledge society
MINISTRY OF EDUCATION & RELIGIOUS AFFAIRS
MANAGING AUTHORITY
NSRF 2007-2013
EUROPEAN SOCIAL FUND
Co-financed by Greece and the European Union

May 2012, when the instrument was deployed and until 1 October 2013, sampled air was not dried before entering the instrument. During this period several cases in which the instrument's 50 μm critical orifice was clogged, were observed. Thereafter a naphion drier was installed (TROPOS custom built), resulting to the elimination of this kind of behavior. Data were collected using software provided by Aerodyne (DAQ version 1.4.3.8) while data analysis was performed using the ACSM Panel package built for the Wavemetrics Igor Pro software (version 1.5.5.3).

A constant Collection Efficiency (CE) of 0.5 was selected for all measured species. Relative Ionization Efficiency (RIE) for NH_4^+ was set to 5.15, derived from the monodisperse ammonium nitrate aerosol calibration process proposed by the instrument's manufacturer. RIE for $SO_4^=$ was set to 0.6, estimated following the fitting approach proposed by Budisulistiorni et al. 2014. The default values of RIE was used for the rest of the species, namely 1.4 for Organics, 1.1 for NO_3^- and 1.3 for Chloride.

Black Carbon (BC) concentrations were measured at a 5-minute temporal resolution using a Magee Scientific Aethalometer (AE-31). Optical attenuation was obtained at seven different wavelengths and the correction proposed by Weingartner et al., 2003 was applied, in order to determine the concentration, taking into account the collection filter's shadowing effect. Moreover, two distinct components of BC particles, attributed to different sources, namely wood burning (BC_{wb}) and fossil fuel combustion (BC_{ff}), were determined, using the model proposed by Sandradewi et al. 2007.

A TROPOS built, custom made Scanning Mobility Particle Sizer (SMPS) was used to determine aerosol number size distributions in the size range 8 – 850 nm. Number size distributions were then used to derive surface and volume distributions and concentrations. Using the particle volume concentration, assuming that the PM_1 population is dominated by particles consisting of ammonium sulfate and organic compounds, thus applying density derived from the following equation

$$\rho = \left\{\frac{x_{as}}{\rho_{as}} + \frac{x_{org}}{\rho_{org}}\right\}^{-1}$$

European Union
European Social Fund
OPERATIONAL PROGRAMME
EDUCATION AND LIFELONG LEARNING
investing in knowledge society
MINISTRY OF EDUCATION & RELIGIOUS AFFAIRS
MANAGING AUTHORITY
NSRF 2007-2013
EUROPEAN SOCIAL FUND
Co-financed by Greece and the European Union

Were x_{as} is the ammonium sulfate mass fraction calculated by the ACSM measurements, ρ_{as} is the ammonium sulfate concentration, namely 1.77 g cm^{-3}, x_{org} is the organics mass fraction while ρ_{org} is the average 1.35 g cm^{-3} density for organic aerosols determined by Lee et al. 2010. We must note out here, that a factor of 0.4 was applied to the volume distributions, regarding size bins above 600 nm and up to 850 nm, in order to comply with the ACSM's aerodynamic lens transmission efficiency above this size threshold which is calculated at 0.4 for 600 nm and drops to 0.2 at 1 μm. (Liu et al. 2007).

An automatic aerosol sampler (Derenda) was used to sample PM_{10} aerosol loadings on pre combusted quartz fiber filters. Filters were subsequently analyzed for water soluble ions following extraction in an ultrasonic bath with nanopure water. The solutions were subsequently analyzed using ion chromatography in order to determine loadings of several anions (Cl^-, Br^-, NO_3^- , $SO_4^=$, $C_2O_4^=$) and cations (K^+, Na^+, NH_4^+, Mg^{2+}, Ca^{2+}). Furthermore, the filters were analyzed in order to determine organic (OC) and elemental carbon (EC), using a Sunset OC/EC aerosol analyzer.

In order to gain insight on the history of air masses arriving at Finokalia and furthermore categorize in detail the source region of the aerosol population, two different tools were utilized. In order to implement a categorization of the whole period in terms of air mass origin the NOAA ARL's HYSPLIT model (Draxler and Hess, 1997; Draxler and Rolph, 2015) was used. 72 hour backward trajectories of the air masses arriving at Finokalia at midday were calculated for each day of the period. In order to acquire more detailed information on the sources affecting Finokalia, in some cases which will be thoroughly presented, the footprint potential emission sensitivity (PES) from retroplume calculations from the particle dispersion model FLEXPART in backward mode (Stohl et al., 2005) was used.

European Union
European Social Fund
OPERATIONAL PROGRAMME
EDUCATION AND LIFELONG LEARNING
investing in knowledge society
MINISTRY OF EDUCATION & RELIGIOUS AFFAIRS
MANAGING AUTHORITY
NSRF 2007-2013
programme for development
EUROPEAN SOCIAL FUND
Co-financed by Greece and the European Union

D2 Results and discussion

D2.1 Comparison of ACSM data with collocated measurements

Two main components of the aerosol population over the Eastern Mediterranean, namely $SO_4^=$ and Organics, were selected in order to assess the ACSM's performance. According to Koulouri et al. 2008, the bulk of these two species mass concentration lies within the PM_1 size range. Actually for $SO_4^=$ 80% of the PM_{10} mass lies in the PM_1 size range while for Organic Carbon (OC) this percentage is determined at 70%. Furthermore, OC was multiplied by a factor of 2.1 in order to determine total organic mass and to achieve consistency with the Organics measured by the ACSM. Daily mean values were calculated from the ACSM measurements, for these two components, so that they are in temporal accordance to the daily sampling on the PM_{10} filters.

In Figure D1 a) and b) these comparisons are presented, and in order to assess their correlation, linear regression forced through (0, 0) was performed. For $SO_4^=$ a slope of 0.88 was determined, while for Organics the slope was 0.71, pretty close to the percentages expected between these two components when comparing PM_1 and PM_{10} population. Correlation was indeed satisfactory for those two comparisons, as R^2 was 0.61 for $SO_4^=$ and 0.63 for Organics, thus providing confidence to the dataset.

Linear regression was also performed between total mass acquired by the ACSM and mass derived from SMPS measurements as described above in order to assess both instruments' performance. As shown in Figure D1 c) R^2 was calculated to be 0.67, indicating good correlation, while a slope of 0.96 further supports the claim of good accordance between the two measuring techniques.

D2.2 PM_1 chemical composition throughout the period. Annual and diurnal trends.

The nearly three-year period's PM_1 chemical composition time series, along with each species overall relative contribution, in the form of an embedded pie chart, is presented in Figure D2. The average PM_1 concentration, i.e. the non-refractory species measured

European Union
European Social Fund
OPERATIONAL PROGRAMME
EDUCATION AND LIFELONG LEARNING
investing in knowledge society
MINISTRY OF EDUCATION & RELIGIOUS AFFAIRS
MANAGING AUTHORITY
NSRF 2007-2013
EUROPEAN SOCIAL FUND
Co-financed by Greece and the European Union

by the ACSM plus BC concentration, was found to be 6.53 ± 3.79 μgr m^{-3}. PM_1 population was clearly dominated by $SO_4^=$ which contributes up to 42.1% of total mass, with a mean value of 2.81 ± 1.75 μgr m^{-3}. Organics come second exhibiting a contribution of 36.5% and mean value of 2.44 ± 2.05 μgr m^{-3}, while the remaining 21.4% is distributed among the rest of the measured species, namely NO_3^-, NH_4^+ and BC at 5%, 11.7% and 4.4% respectively. The mean values obtained are 0.33 ± 0.30, 0.78 ± 0.70 and 0.29 ± 0.16 μgr m^{-3} for these species. Chloride contributes a mere 0.3% while its concentration (average of 0.02 ±0.01) throughout the measuring period was pretty close, and mostly bellow the ACSM's detection limit.

Statistically significant correlation between the mentioned components was also investigated. In that manner we calculated the Pearson product moment correlation coefficients (R) for each pair of the measured parameters. P-values were then calculated in order to test whether the null hypothesis, in this case that the pairs are totally uncorrelated, would be rejected or not. The confidence level for this decision, the α-value, was set at 0.01. Significant correlations were found between $SO_4^=$ and NH_4^+ ($R_{Pearson}$ = 0.87), Organics and NH_4^+ ($R_{Pearson}$ = 0.76), Organics and $SO_4^=$ ($R_{Pearson}$ = 0.71) and finally Organics and BC ($R_{Pearson}$ = 0.65). The remaining components' correlations are shown in Table D1. P-values were well below the determined confidence level for all correlations, apart from those related to Chloride which was not significantly correlated to any of the other species. Chloride exhibited a low P-value and some poor correlation only to BC ($R_{Pearson}$ = 0.20), while P-values were close or even larger than the α-value for the rest of the combinations.

After calculating monthly averages and keeping in mind the time series of Figure D2, three facts become evident. First of all a clear annual cycle can be observed and will be further analyzed. Secondly a domination of Organics versus $SO_4^=$ in 2013 during summertime, probably related to combustion episodes such as wildfires, taking place in the Balkans and continental Europe, and thirdly an evident decrease on the

European Union
European Social Fund
OPERATIONAL PROGRAMME
EDUCATION AND LIFELONG LEARNING
investing in knowledge society
MINISTRY OF EDUCATION & RELIGIOUS AFFAIRS
MANAGING AUTHORITY
NSRF 2007-2013
EUROPEAN SOCIAL FUND
Co-financed by Greece and the European Union

summertime maxima during the year 2014, possibly related with the remarkable decline of the strong northerly winds (Etesians) reported by Tyrlis et al., 2015.

The annual cycle observed is depicted in Figure D3 a). PM_1 mass concentration peaks during the summer, in accordance to previous observations in the region, probably explained by the lack of removal processes during this period of the year, exhibiting a maximum in August of 10.8 μgr m^{-3}. Furthermore, the, already mentioned, Etesians prevail during summertime, making long range transport from continental Europe a key process determining the aerosol population according to earlier studies (Mihalopoulos et al. 1997; Sciare et al.,2003). Each one of the measured species concentrations, comply with this trend. In Figure D3 b) the annual behavior of Organics, Sulfate and Ammonium are depicted, since these are the prevailing constituents over the region. Besides the maximum during August, Organics exhibit a small peak in March, while for Ammonium elevated concentrations are present throughout spring time.

BC along with its components, BC_{ff} and BC_{wb} are shown in Figure D3 c). BC annual pattern is characterized not solely by the summer maximum, but also by the evident activity during spring. Unfortunately, due to the aethalometer's malfunction over some periods of time, there are no March data available throughout the campaign. The figure is filled out for March with EC measurements from concurrent filter sampling, thus some uncertainty is present. This activity during springtime could be related to local biomass burning, during agricultural activity, since March is the period when olive trees are pruned and the byproducts are incinerated. The small lump in the Organics annual trend at this time could further support this assumption. One more case of local contribution, should be evident by the peak in BC at November, as the simultaneous maximum in BC_{ff} suggests.

Two ratios, giving some insight on the chemical behavior of the PM_1 aerosol population are also investigated. Acidity, on the one hand, is defined as the ratio of ammonium, measured by the ACSM, to sulfate plus nitrate, in molar equivalents.

European Union
European Social Fund
OPERATIONAL PROGRAMME
EDUCATION AND LIFELONG LEARNING
investing in knowledge society
MINISTRY OF EDUCATION & RELIGIOUS AFFAIRS
MANAGING AUTHORITY
NSRF 2007-2013
EUROPEAN SOCIAL FUND
Co-financed by Greece and the European Union

Acidity was measured to an average of 0.70 ± 0.16 meq/meq. An annual cycle is also observed for this attribute and is shown in Figure D3 d). Maximum acidity is observed during April, coinciding to the relatively higher contribution of Ammonium during the spring months. A steady decline follows this maximum over the next months, from May to January, before it rises again in February and March.

On the other hand, we calculated the Sulfate to Organics ratio for the entire period. The average Sufate to Organics ratio was found to be 1.28 ± 0.53, confirming Sulfate dominance in the region. Its annual cycle, depicted on the right axis in Figure D3 d) exhibits two maxima, one in May and the other, a bit less pronounced, in September. Organics seem to be dominant, on an average, only during January and March, when the ratio seems to drop slightly below one, possibly due to contribution of local sources, in combination with clean air masses arriving from regions with pronounced removal mechanisms, thus smaller Sulfate load.

Diurnal variability of the measured species and some calculated attributes is illustrated in Figure D4. Figures D4 a) and 4 b) host the non-refractory components measured by the ACSM, excluding Chloride which exhibits no distinct diurnal variability. A similar pattern is observed for all species, which is probably related to the boundary layer development within the day, given the absence of major local sources. Almost all species reach their maximum values in the early afternoon. To be more precise, Organics and NO_3^- exhibit maximum values at 14:00 local time (UTC + 02:00), while Sulfate and Ammonium, confirming their close correlation, reach their maximum two hours later, at 16:00. Organics decrease rapidly after their maximum value is reached, while Sulfate, Ammonium and Nitrate tend to maintain their presence for a couple of hours more, until 19:00. This behavior is reported also by Minguillon et al. 2015 for the regional background site of Montseny in Spain. Probably the same explanation applies in our case, i.e. ammonium sulfate exhibits a clear regional character, while Organics seem to be more influenced by smaller scale phenomena

.

European Union
European Social Fund
OPERATIONAL PROGRAMME
EDUCATION AND LIFELONG LEARNING
investing in knowledge society
MINISTRY OF EDUCATION & RELIGIOUS AFFAIRS
MANAGING AUTHORITY
NSRF 2007-2013
programme for development
EUROPEAN SOCIAL FUND
Co-financed by Greece and the European Union

In Figure D4 c) daily development of BC and its two distinct components, BC_{ff} and $BC_{wb,}$ are illustrated. We must note here that the pattern provided for BC_{wb} is the product of the days when biomass burning episodes occurred, meaning that BC_{wb} is in fact absent in the majority of the measured days. BC and BC_{ff} share the same pattern, since the second is the major component, reaching maximum at noon, e.g. 12:00 local time. On the other hand, BC_{wb} exhibits two distinct peaks within the day, the primary maximum at 10:00 in the morning and a secondary at 17:00 in the afternoon, both probably related to local combustion habits. Furthermore, the BC_{wb} peak could be related to the Biomass Burning Organic aerosol component peak, observed by Bougiatioti et al., 2014 for wildfire events in the Eastern Mediterranean region and the Balkans.

Finally Figure D4 d) depicts the diurnal variation of the two already mentioned ratios, namely acidity and $SO_4^=$/Organics. Acidity reaches minimum values during noon and early afternoon, related to the Sulfate reaching its maximum at this period in the day, a fact also depicted to the $SO_4^=$/Organics pattern peaking at 15:00. It is clear that the aerosol phase is acidic throughout the day while some neutralization takes place in the night time.

D2.3 An inter-annual approach

Finokalia is the longest standing atmospheric sampling site in Greece and the Eastern Mediterranean in general. Almost 20 years of consecutive measurements of several atmospheric attributes including aerosol chemical composition, are up to now depicted in the ECPL's datasets and numerous publications. In this section the inter-annual variability of Non Sea Salt Sulfate (nss-$SO_4^=$), the submicron fraction of Sulfate, measured by different off line techniques, will be presented. Since the ACSM measures in the size range 75 – 650 nm, the Sulfate measured by the instrument is actually nss-$SO_4^=$, thus the ACSM dataset can be combined with the previously existing datasets.

European Union
European Social Fund
OPERATIONAL PROGRAMME
EDUCATION AND LIFELONG LEARNING
investing in knowledge society
MINISTRY OF EDUCATION & RELIGIOUS AFFAIRS
MANAGING AUTHORITY
NSRF 2007-2013
EUROPEAN SOCIAL FUND
Co-financed by Greece and the European Union

As shown in Figure D5, where annual mean values are illustrated, three distinct periods can be pointed out. A first, early period, consisting of the years 1994 and 1995 exhibiting really elevated concentrations in the order above 7 μgr m^{-3}. A second, stable period, following a sharp decline in concentrations through the year 1996 and consisting of the years 1997 through 2008 and finally a third, recession period, consisting of the years 2009 to 2014, exhibiting a further decline in Sulfate concentrations. Mean values for the early period stand at 7.6 μgr m^{-3}, for the stable period at 3.93 μgr m^{-3}, while for the recession period at 2.98 μgr m^{-3}.

This further decline could be the outcome of the 2008 eruption of the global financial crisis that occurred during that year, which might have led to a decrease in activities related to the production of anthropogenic Sulfate particles both in Greece and the rest of Europe. This assumption is further supported, when comparing to earlier experiments held at the Finokalia station, where it can be observed that not only Sulfate, but the entire aerosol population was affected downwards. In Table D2, a comparison regarding aerosol chemical composition, between the FAME-08 (Pikridas et al., 2010) experiment held at Finokalia during May 2008, and the corresponding periods of 2012, 2013 and 2014, is presented. It is evident that besides Sulfate, the rest of the non-refractory fraction of the submicron aerosol is also affected since a decrease in Organics and Ammonium is depicted. Acidity did not show any consistent behavior or pattern during these last years, implying that it is the overall mass that is decreasing rather than individual components.

D2.4 Aerosol chemical composition related to air mass origin.

Air masses arriving at Finokalia were categorized according to their origin. Back trajectories produced by the HYSPLIT model were examined for each day and were categorized, according to their path, in ten different geographical sectors. These sectors were selected not only according to strict rules concerning each trajectory's orientation and path, but also based on expected sources found in each path. These sectors, namely

European Union
European Social Fund
OPERATIONAL PROGRAMME
EDUCATION AND LIFELONG LEARNING
investing in knowledge society
MINISTRY OF EDUCATION & RELIGIOUS AFFAIRS
MANAGING AUTHORITY
NSRF 2007-2013
programme for development
EUROPEAN SOCIAL FUND
Co-financed by Greece and the European Union

the North, N-West, West, S-West, South, S-East, East and N-East are presented in Figure D6. The remaining two, are the so called Mixed sector, meaning that trajectories passed clearly over more than one of the previous eight, and the Local sector, implying that the trajectory lied mainly in the region of close vicinity to the island of Crete. Some of these sectors are represented by a small number of trajectories, hence days of data, making the extraction of safe conclusions a bit harsher. Nevertheless, all sectors are all illustrated here but our focus will be the sectors represented by more than forty days.

It is evident that the air masses over Finokalia in the majority of the days presented in this study, originated from the wider North sector, i.e. from N-East to N-West, accounting for a total number of 642 days, in other words for roughly two thirds of the period. These days were characterized by elevated concentrations in comparison to the wider West to South sectors. Especially air masses connected to the N-East sector, highly influenced by industrial and urban emissions from Eastern Europe, the Balkans and Turkey exhibit the highest loadings with a mean concentration of 9.26 ± 3.65 μgr m^{-3}. On the contrary air masses originating from the West and S-West were found to be loaded with much less particulate mass (3.98 ± 1.72 and 3.40 ± 1.84 μgr m^{-3} respectively) implying clean air masses in no interaction with human activity. Organic contribution is also at its lowest (30%) when the West and S-West air masses prevail while Sulfate exhibits the highest contributions in the order of 44-46%. This behavior could imply secondary aerosols originating from emissions of marine origin, or aerosols highly affected by ship circulation related emissions.

Diurnal patterns for the six major sectors and regarding Organics and Sulfate are shown in Figure D7. Similar patterns for Sulfate can be noticed for the wider North sector. The range of the variation decreases though from roughly 1 μgr m^{-3} concerning the N-East sector, to almost 0.6 μgr m^{-3} concerning the North and N-West sectors, further supporting the dominance of the N-East sector as to bearing the largest amounts of pollutants. The West and S-West sectors are characterized by insignificant diurnal variation, implying well mixed aerosols, and concentrations close to the regions natural

European Union
European Social Fund
OPERATIONAL PROGRAMME
EDUCATION AND LIFELONG LEARNING
investing in knowledge society
MINISTRY OF EDUCATION & RELIGIOUS AFFAIRS
MANAGING AUTHORITY
NSRF 2007-2013
programme for development
EUROPEAN SOCIAL FUND
Co-financed by Greece and the European Union

background. Aerosols coming from the islands mainland, probably affected by minor anthropogenic activity seem to enrich air masses arriving from the south contributing to the significant Organics variation in days belonging to the South sector, which covariates pretty close to the Sulfate component.

D2.5 Megacities direct influence

A very clear example of the direct influence of the neighboring megacities, namely Istanbul and Athens, to the Eastern Mediterranean's aerosol load, especially in the submicron fraction, was evident during late April, early May in 2013. Probably following a period of pronounced removal processes, mainly precipitation, a sharp increase was observed in the loadings over Finokalia in 21/04/2013. The elevated concentrations, with some variability, lasted until 08/05/2013 when a sudden decrease occurred.

In Figure D8, the timeseries of non-refractory components along with BC is illustrated for April and May, while two pie charts with each component's relative contribution, one concerning the mentioned elevation period and the other concerning the whole two-month period, are embedded. Mean values in the elevation period are higher, by a factor of roughly 1.5 for all components. Nevertheless, each components relative contribution during this episode is mostly the same when comparing to the entire two-month period. Organics contribution rises by almost 2%, a 1% decrease is observed for BC while Sulfate, Nitrate and Ammonium practically remain unchanged.

In order to investigate the different sources influence on the site's aerosol load we performed retroplume analysis and distinguished four separate scenarios of influence. Retroplumes were provided by implementing the FLEXPART model and defining Finokalia as the receptor of the plumes. The threshold for characterizing each plume was PES values above 0.2 ns/kg. In the first scenario, air masses and aerosol load were directly affected by Istanbul (Ist IN), in the second Athens was part of the retroplume's path (Ath IN), in the third scenario air masses did not get affected by any of the two

European Union
European Social Fund
OPERATIONAL PROGRAMME
EDUCATION AND LIFELONG LEARNING
investing in knowledge society
MINISTRY OF EDUCATION & RELIGIOUS AFFAIRS
MANAGING AUTHORITY
NSRF 2007-2013
EUROPEAN SOCIAL FUND
Co-financed by Greece and the European Union

large cities (NONE) and finally in the fourth, both cities lied within the plumes path (BOTH).

In Figure D9 this analysis is illustrated in the form of a color scale, where red corresponds to the Ist IN scenario, green to the Ath IN scenario, cyan to the NONE scenario and purple to the BOTH scenario. In Figure D9 a) this color scale is applied to Organics concentration, in 9 b) to Sulfate and in 9 c) to the particles' acidity. It is pretty clear that when the plumes originated from regions that did not include the two cities, i.e. the NONE scenario, a decrease in concentrations occurred. These plumes mainly were of local character, exhibiting large PES values above Asia Minor and the Aegean Sea, they covered in principal a much smaller area, pointing to rather stagnant conditions in the area. Acidity was found to be slightly larger during the NONE scenario, related to the fact that Sulfate declined by a factor of 2.5 while Ammonium just lost half of its concentration, suggesting different sources for the two species.

European Union
European Social Fund
OPERATIONAL PROGRAMME
EDUCATION AND LIFELONG LEARNING
investing in knowledge society
MINISTRY OF EDUCATION & RELIGIOUS AFFAIRS
MANAGING AUTHORITY
NSRF 2007-2013
EUROPEAN SOCIAL FUND
Co-financed by Greece and the European Union

	Organics	$SO_4^=$	NO_3^-	NH_4^+	Chl	BC
Organics	1	0.712735	0.505963	0.759604	-0.13801	0.649286
$SO_4^=$	0.712735	1	0.434214	0.866046	-0.11642	0.534549
NO_3^-	0.505963	0.434214	1	0.567357	-0.04632	0.407825
NH_4^+	0.759604	0.866046	0.567357	1	-0.26859	0.493545
Chl	-0.13801	-0.11642	-0.04632	-0.26859	1	0.200478
BC	0.649286	0.534549	0.407825	0.493545	0.200478	1

Table D1: Pearson's R for each pair of chemical constituents for the entire measuring period

	Org	$SO_4^=$	NO_3^-	NH_4^+	acidity
May-12	1.4	3.02	0.16	0.71	0.62
May-13	1.74	2.13	0.25	0.82	0.93
May-14	1.67	2.58	0.54	0.8	0.71
Fame 2008*	2.6	5.64	0.08	1.68	0.82

Table D2: Mean mass concentrations for non-refractory species concerning May 2008 and the FAME-08 experiment opposed to measurements during May in the years of the ACSM operation in Finokalia.

European Union
European Social Fund
OPERATIONAL PROGRAMME
EDUCATION AND LIFELONG LEARNING
investing in knowledge society
MINISTRY OF EDUCATION & RELIGIOUS AFFAIRS
MANAGING AUTHORITY
NSRF 2007-2013
EUROPEAN SOCIAL FUND
Co-financed by Greece and the European Union

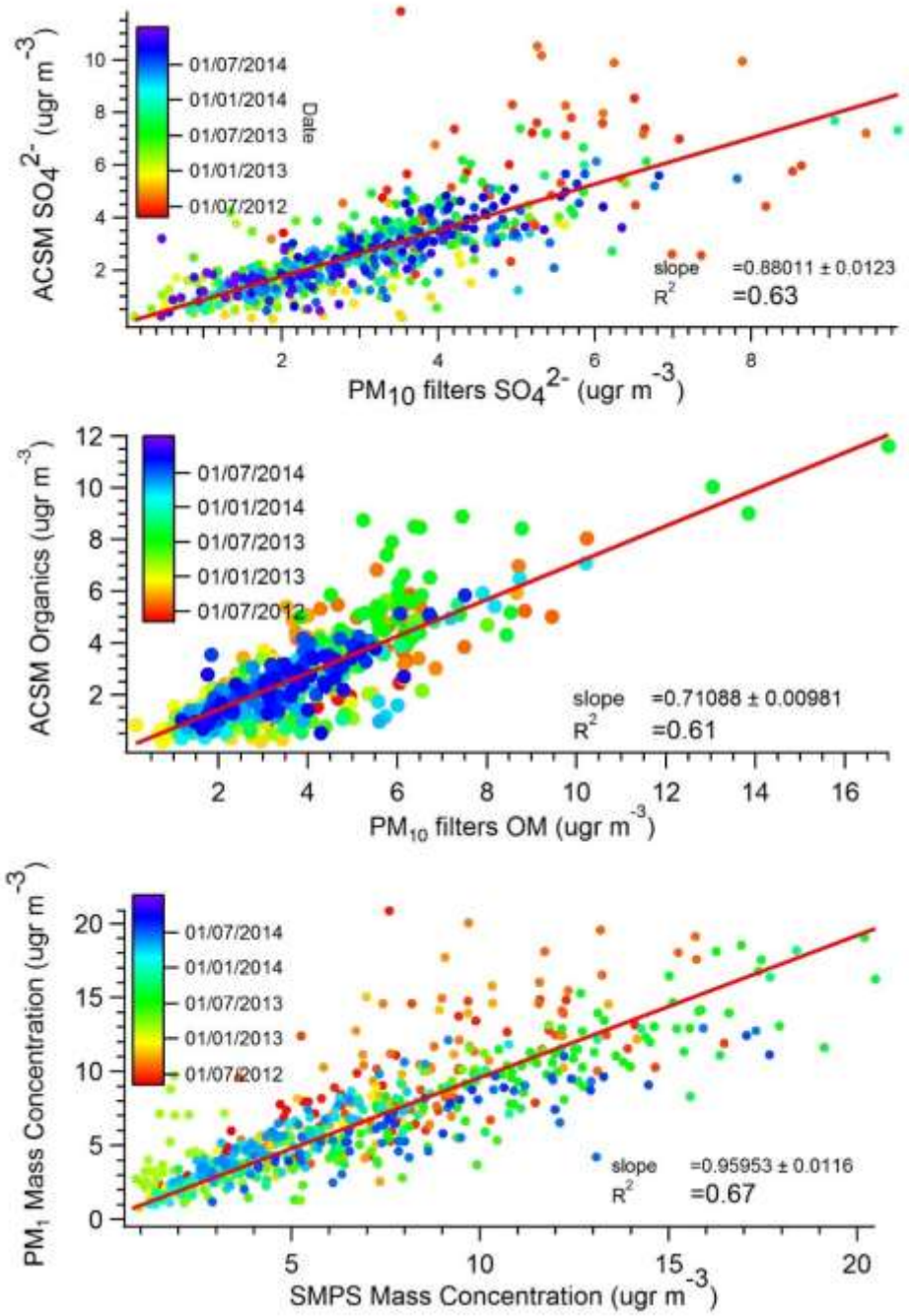

Figure D1: Quality control of the ACSM operation. a) Sulfate measured by the ACSM versus PM_{10} Sulfate collected on filters, b) Organics versus reconstructed PM_{10} Organic Matter (OM) and c) total mass measured by the ACSM plus BC concentrations versus mass derived from SMPS volume distributions.

European Union
European Social Fund
OPERATIONAL PROGRAMME
EDUCATION AND LIFELONG LEARNING
investing in knowledge society
MINISTRY OF EDUCATION & RELIGIOUS AFFAIRS
MANAGING AUTHORITY
NSRF 2007-2013
EUROPEAN SOCIAL FUND
Co-financed by Greece and the European Union

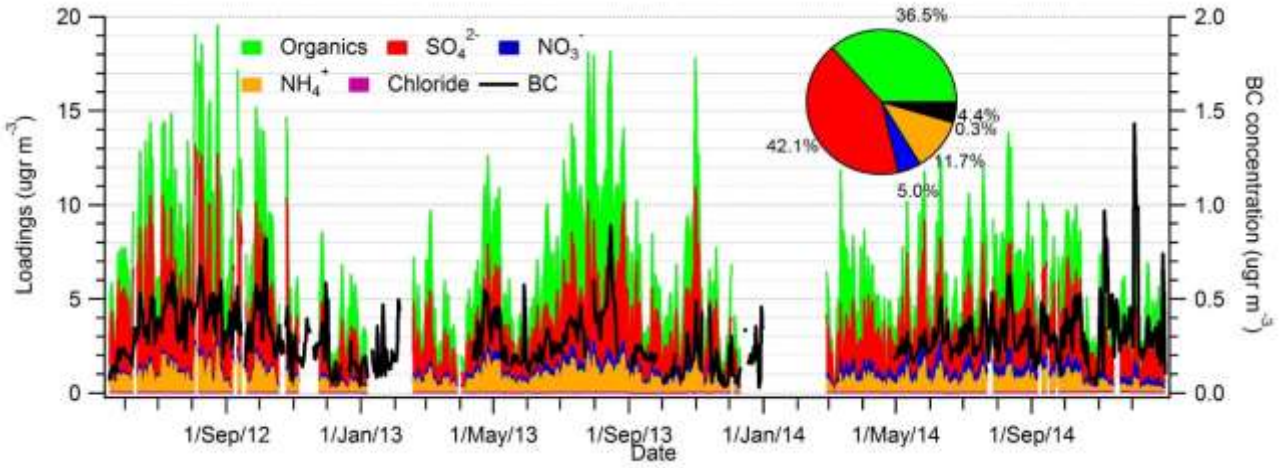

Figure D2: Timeseries of non-refractory species measured by the ACSM and BC concentrations for the entire measuring period. Relative contribution of each species depicted in the embedded pie chart.

European Union
European Social Fund
OPERATIONAL PROGRAMME
EDUCATION AND LIFELONG LEARNING
investing in knowledge society
MINISTRY OF EDUCATION & RELIGIOUS AFFAIRS
MANAGING AUTHORITY
NSRF 2007-2013
EUROPEAN SOCIAL FUND
Co-financed by Greece and the European Union

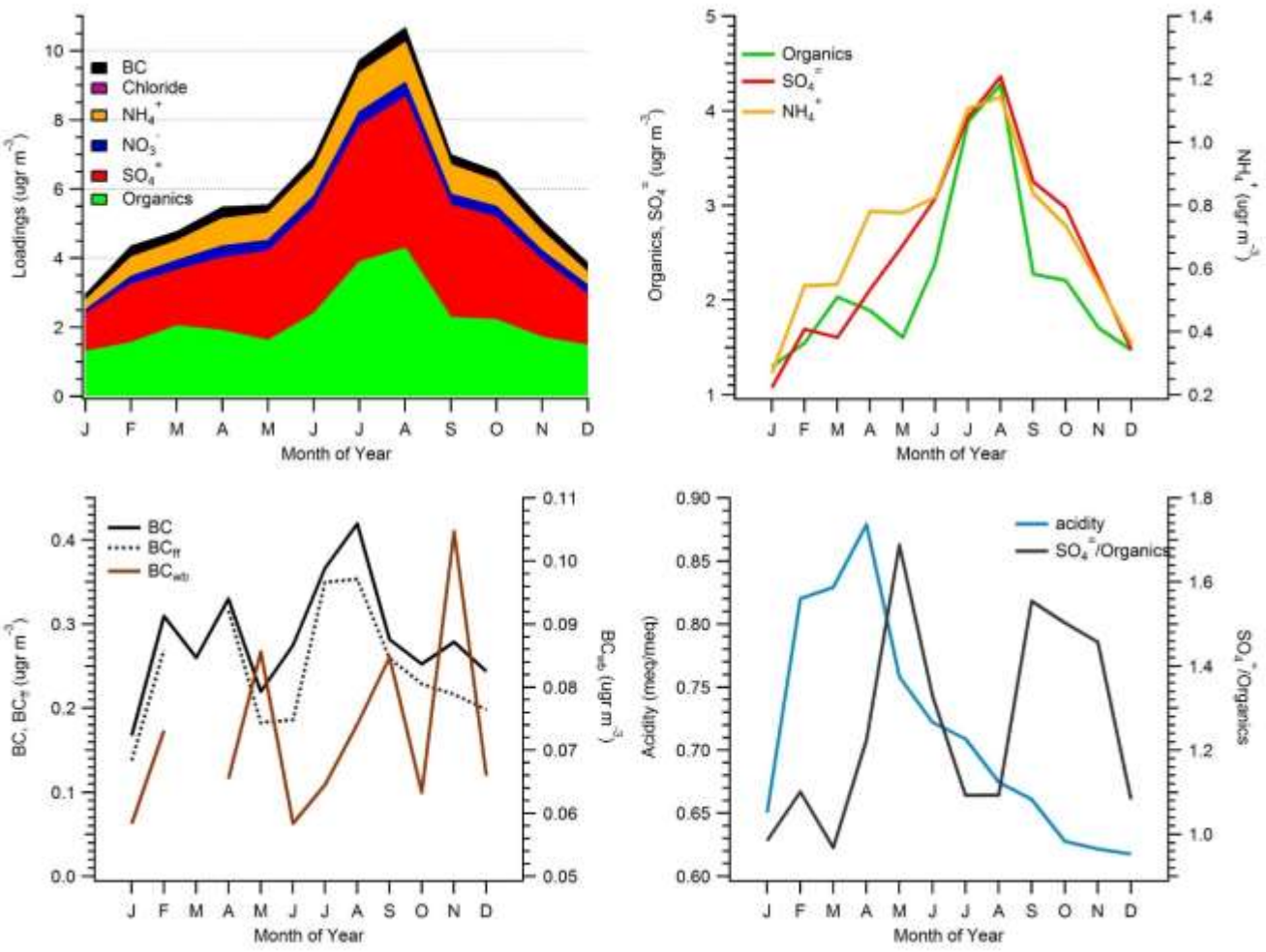

Figure D3: Annual cycle of PM (a), sulfate, organics and ammonium (b), BC and its components (ff and wb; c) and acidity (d) during the measuring period.

European Union
European Social Fund
OPERATIONAL PROGRAMME
EDUCATION AND LIFELONG LEARNING
investing in knowledge society
MINISTRY OF EDUCATION & RELIGIOUS AFFAIRS
MANAGING AUTHORITY
NSRF 2007-2013
EUROPEAN SOCIAL FUND
Co-financed by Greece and the European Union

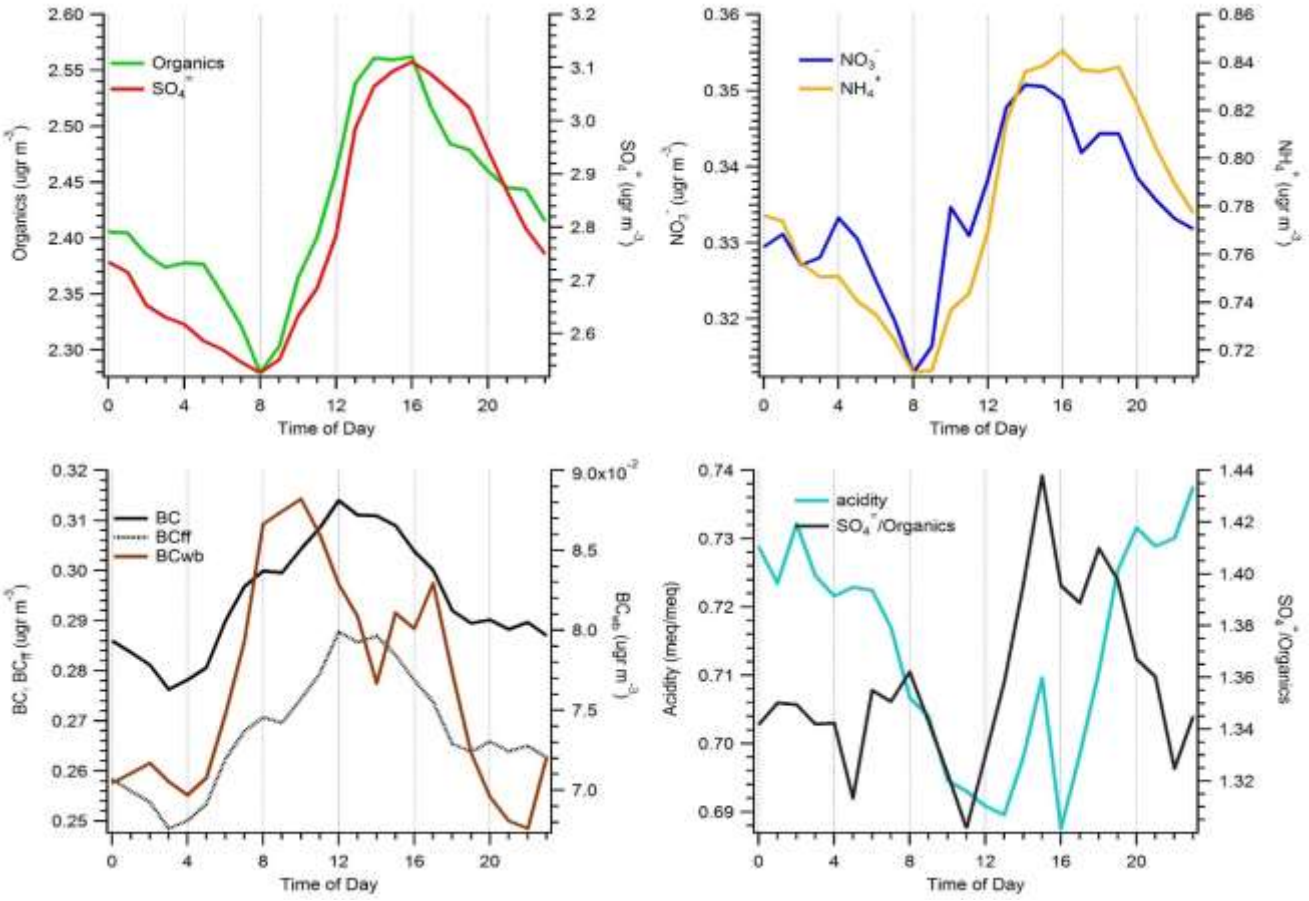

Figure D4: Diurnal variability of sulfate and organics (a), nitrate and ammonium (b), BC and its components (ff and wb; c) and acidity along with sulfate/organics ratio (d) during the measuring period.

European Union
European Social Fund
OPERATIONAL PROGRAMME
EDUCATION AND LIFELONG LEARNING
investing in knowledge society
MINISTRY OF EDUCATION & RELIGIOUS AFFAIRS
MANAGING AUTHORITY
NSRF 2007-2013
programme for development
EUROPEAN SOCIAL FUND
Co-financed by Greece and the European Union

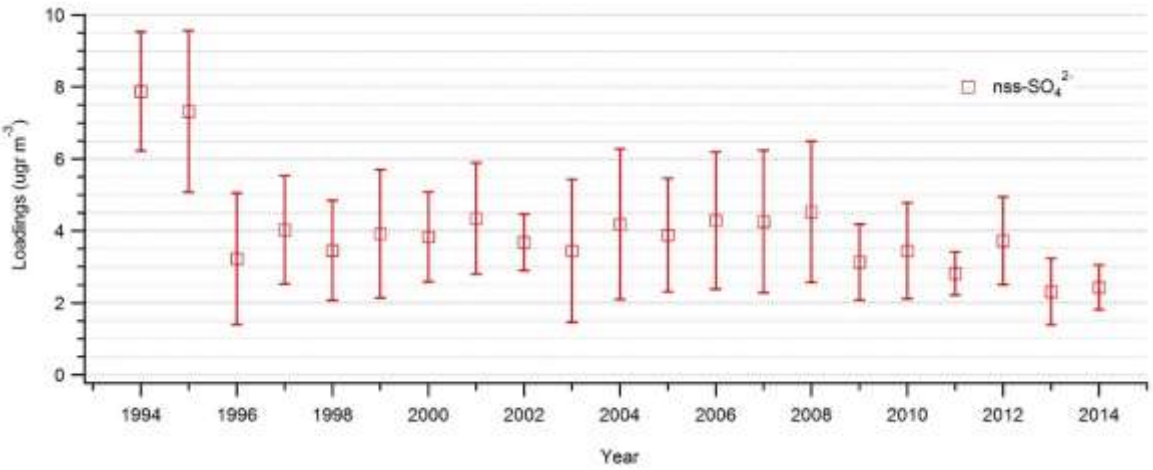

Figure D5: Interannual variability of sulfate at Finokalia (1994-2014).

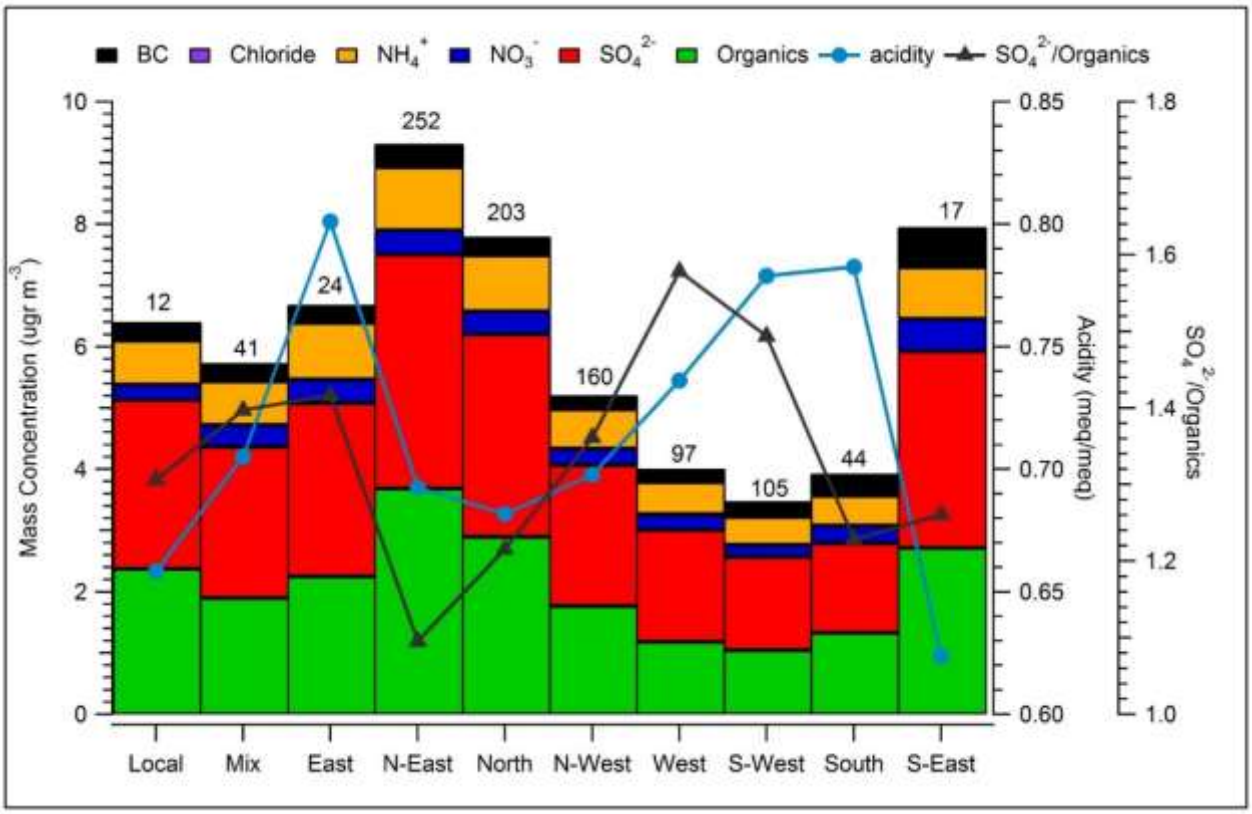

Figure D6: Variability of fine aerosol chemical composition as a function of air masses origin.

European Union
European Social Fund
OPERATIONAL PROGRAMME
EDUCATION AND LIFELONG LEARNING
investing in knowledge society
MINISTRY OF EDUCATION & RELIGIOUS AFFAIRS
MANAGING AUTHORITY
NSRF 2007-2013
EUROPEAN SOCIAL FUND
Co-financed by Greece and the European Union

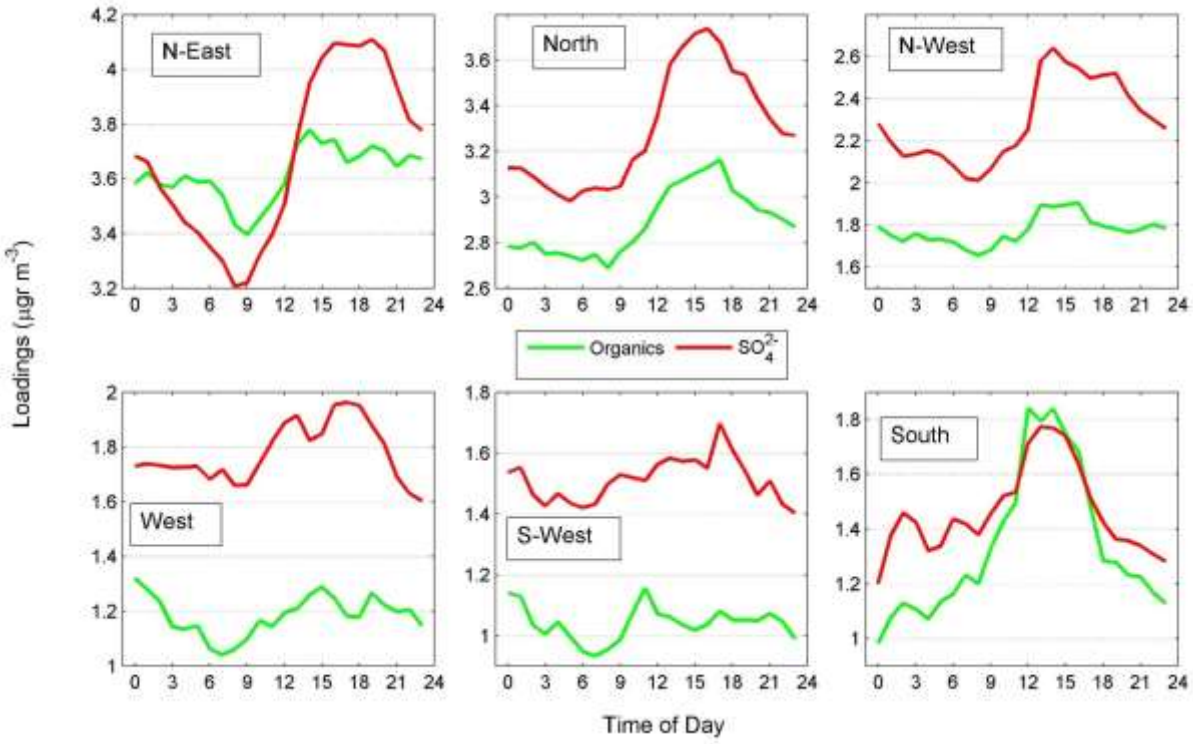

Figure D7: Diurnal variability of sulfate and organics as a function of air masses origin.

European Union
European Social Fund
OPERATIONAL PROGRAMME
EDUCATION AND LIFELONG LEARNING
investing in knowledge society
MINISTRY OF EDUCATION & RELIGIOUS AFFAIRS
MANAGING AUTHORITY
NSRF 2007-2013
EUROPEAN SOCIAL FUND
Co-financed by Greece and the European Union

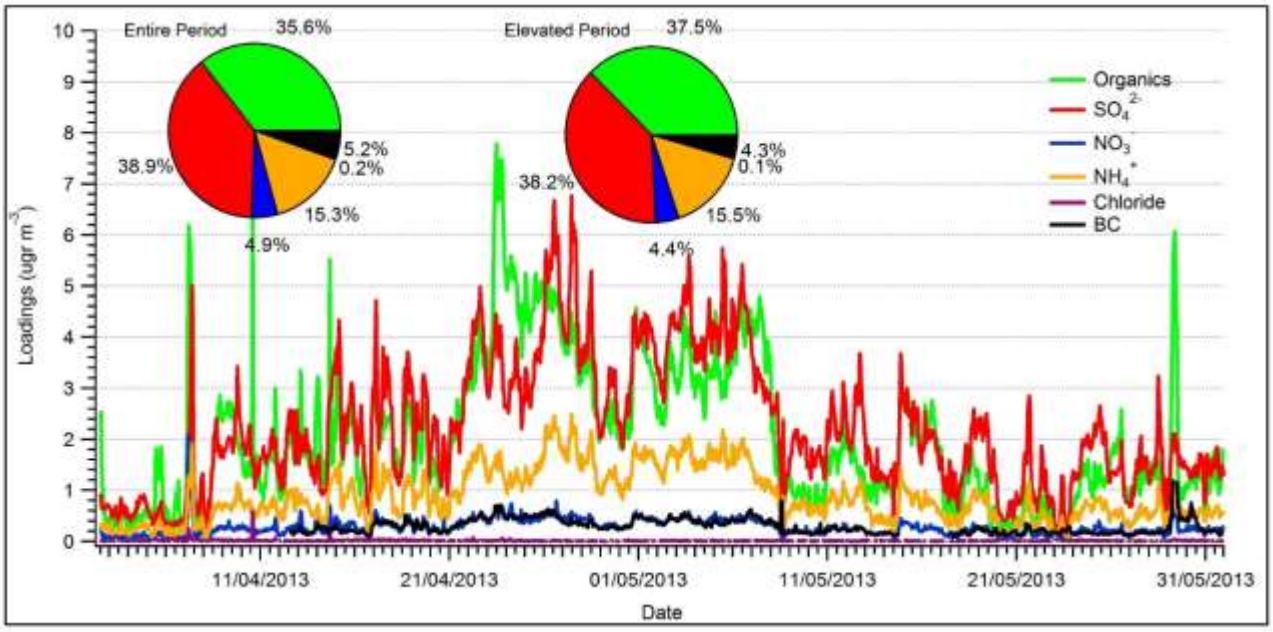

Figure D8: Time series of the aerosol chemical composition during April and May 2013. The elevated concentrations period is evident. Pie charts depict relative compound contribution for the elevated and the entire period.

European Union
European Social Fund
OPERATIONAL PROGRAMME
EDUCATION AND LIFELONG LEARNING
investing in knowledge society
MINISTRY OF EDUCATION & RELIGIOUS AFFAIRS
MANAGING AUTHORITY
NSRF 2007-2013
EUROPEAN SOCIAL FUND
Co-financed by Greece and the European Union

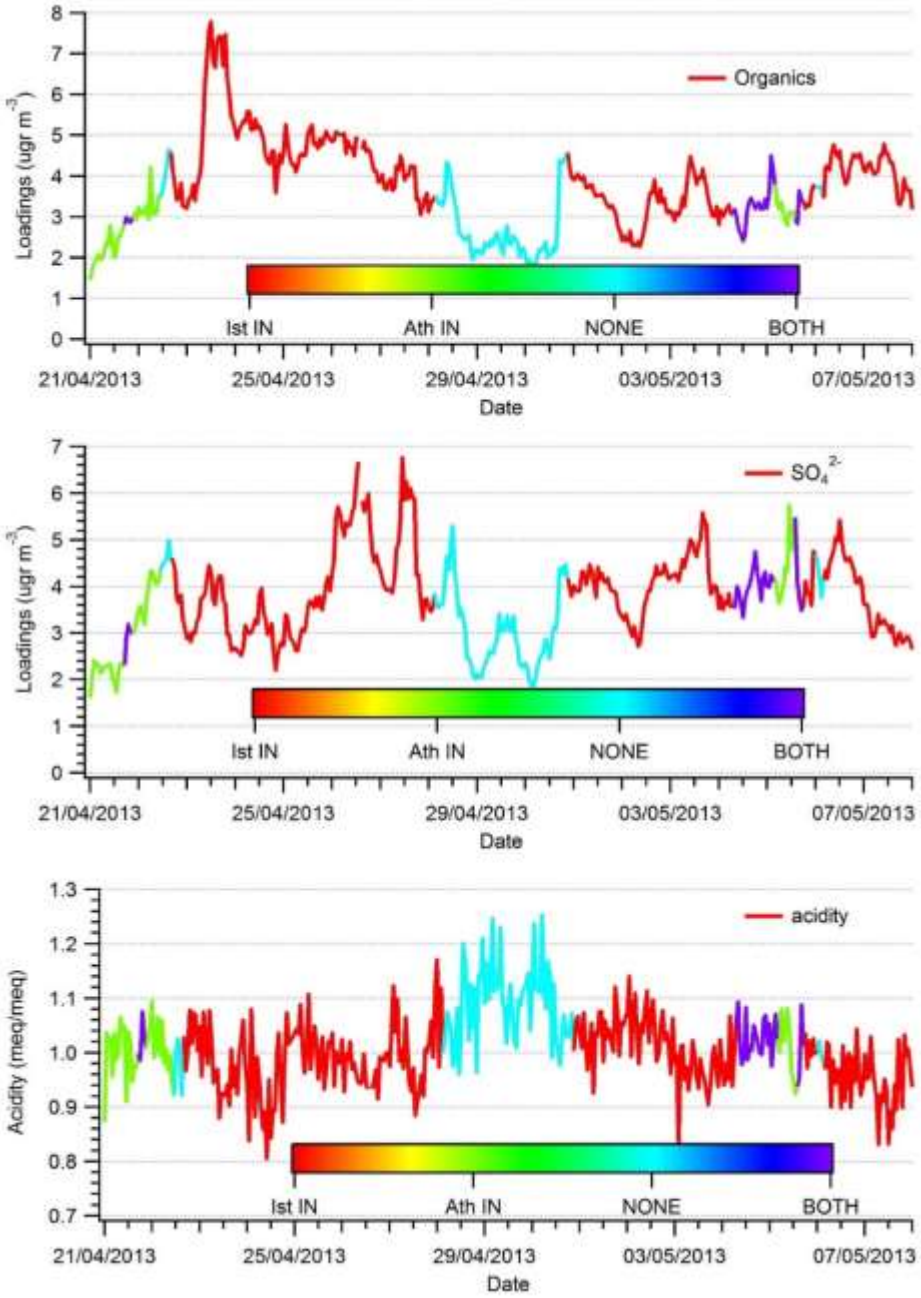

Figure D9: Color scale analysis illustrating the influence of various cities in organics, sulfate and aerosol acidity measured at Finokalia. Red corresponds to the Istanbul IN scenario, green to the Athens IN scenario, cyan to the NONE scenario and purple to the BOTH scenario.

European Union
European Social Fund
OPERATIONAL PROGRAMME
EDUCATION AND LIFELONG LEARNING
investing in knowledge society
MINISTRY OF EDUCATION & RELIGIOUS AFFAIRS
MANAGING AUTHORITY
NSRF 2007-2013
EUROPEAN SOCIAL FUND
Co-financed by Greece and the European Union

D3. References

Jayne, J. T., Leard, D. C., Zhang, X., Davidovits, P., Smith, K. A., Kolb, C. E., & Worsnop, D. R. (2000). Development of an aerosol mass spectrometer for size and composition analysis of submicron particles. *Aerosol Science & Technology*, *33*(1-2), 49-70.

Koulouri, E., Saarikoski, S., Theodosi, C., Markaki, Z., Gerasopoulos, E., Kouvarakis, G., ... & Mihalopoulos, N. (2008). Chemical composition and sources of fine and coarse aerosol particles in the Eastern Mediterranean.*Atmospheric Environment*, *42*(26), 6542-6550.

Weingartner, E., Saathoff, H., Schnaiter, M., Streit, N., Bitnar, B., & Baltensperger, U. (2003). Absorption of light by soot particles: determination of the absorption coefficient by means of aethalometers. *Journal of Aerosol Science*, *34*(10), 1445-1463.

Budisulistiorini, S., Canagaratna, M. R., Croteau, P. L., Baumann, K., Edgerton, E. S., Kollman, M. S., ... & Surratt, J. D. (2014). Intercomparison of an Aerosol Chemical Speciation Monitor (ACSM) with ambient fine aerosol measurements in downtown Atlanta, Georgia. *Atmospheric Measurement Techniques*, *7*(7), 1929-1941.

Lee, B. H., Kostenidou, E., Hildebrandt, L., Riipinen, I., Engelhart, G. J., Mohr, C., DeCarlo, P. F., Mihalopoulos, N., Prevot, A. S. H., Baltensperger, U., and Pandis, S. N.: Measurement of the ambient organic aerosol volatility distribution: application during the Finokalia Aerosol Measurement Experiment (FAME- 2008), Atmos. Chem. Phys., 10, 12149-12160, doi:10.5194/acp- 10-12149-2010, 2010

Liu, P. S., Deng, R., Smith, K. A., Williams, L. R., Jayne, J. T., Canagaratna, M. R., ... & Deshler, T. (2007). Transmission efficiency of an aerodynamic focusing lens system: Comparison of model calculations and laboratory measurements for the Aerodyne Aerosol Mass Spectrometer. *Aerosol Science and Technology*, *41*(8), 721-733.

Draxler, R.R., and G.D. Hess, 1997: Description of the HYSPLIT_4 modeling system. NOAA Tech. Memo. ERL ARL-224, NOAA Air Resources Laboratory, Silver Spring, MD, 24 pp.

European Union
European Social Fund
OPERATIONAL PROGRAMME
EDUCATION AND LIFELONG LEARNING
investing in knowledge society
MINISTRY OF EDUCATION & RELIGIOUS AFFAIRS
MANAGING AUTHORITY
NSRF 2007-2013
programme for development
EUROPEAN SOCIAL FUND
Co-financed by Greece and the European Union

Draxler, R.R. and Rolph, G.D., 2015. HYSPLIT (HYbrid Single-Particle Lagrangian Integrated Trajectory) Model access via NOAA ARL READY Website (http://ready.arl.noaa.gov/HYSPLIT.php). NOAA Air Resources Laboratory, Silver Spring, MD.

Stohl, A., Forster, C., Frank, A., Seibert, P., & Wotawa, G. (2005). Technical note: The Lagrangian particle dispersion model FLEXPART version 6.2.*Atmospheric Chemistry and Physics*, *5*(9), 2461-2474.

Sandradewi, Jisca, et al. "Using aerosol light absorption measurements for the quantitative determination of wood burning and traffic emission contributions to particulate matter." *Environmental science & technology* 42.9 (2008): 3316-3323.

Gerasopoulos, E., Kouvarakis, G., Babasakalis, P., Vrekoussis, M., Putaud, J. P., & Mihalopoulos, N. (2006). Origin and variability of particulate matter (PM 10) mass concentrations over the Eastern Mediterranean. *Atmospheric Environment*, *40*(25), 4679-4690.

Kanakidou M., Mihalopoulos N., Kindap T., Im U., Vrekoussis M., Gerasopoulos E., Dermitzaki E., Unal A., Kocak M., Markakis K., Melas D., Kouvarakis G., Youssef A.F., Richter A., Hatzianastassiou N., Hilboll A., Ebojie F., Wittrock F, von Savigny C., Burrows J.P., Megacities as hot spots of air pollution in the East Mediterranean, Atmospheric Environment, 45, 1223-1235, 2011.

Pikridas, M., A. Bougiatioti, Lea Hildebrandt, G. J. Engelhart, Evangelia Kostenidou, C. Mohr, A. S. H. Prévôt et al. "The Finokalia Aerosol Measurement Experiment–2008 (FAME-08): an overview." *Atmospheric Chemistry and Physics* 10, no. 14 (2010): 6793-6806.

Sciare, J., H. Bardouki, C. Moulin, and N. Mihalopoulos. "Aerosol sources and their contribution to the chemical composition of aerosols in the Eastern Mediterranean Sea during summertime." *Atmospheric Chemistry and Physics*3, no. 1 (2003): 291-302.

Minguillón, M. C., A. Ripoll, N. Pérez, A. S. H. Prévôt, F. Canonaco, X. Querol, and A. Alastuey. "Chemical characterization of submicron regional background aerosols in the Western Mediterranean using an Aerosol Chemical Speciation Monitor." *Atmospheric Chemistry and Physics Discussions* 15, no. 1 (2015): 965-1000.

Ng, Nga L., Scott C. Herndon, Achim Trimborn, Manjula R. Canagaratna, P. L. Croteau, Timothy B. Onasch, Donna Sueper et al. "An Aerosol Chemical Speciation Monitor (ACSM) for routine monitoring of the composition and mass concentrations of ambient aerosol." *Aerosol Science and Technology* 45, no. 7 (2011): 780-794.

Bardouki, H., H. Liakakou, C. Economou, J. Sciare, J. Smolık, V. Ždímal, K. Eleftheriadis, M. Lazaridis, C. Dye, and N. Mihalopoulos. "Chemical composition of size-resolved atmospheric aerosols in the eastern Mediterranean during summer and winter." *Atmospheric Environment* 37, no. 2 (2003): 195-208.

Vrekoussis, M., E. Liakakou, M. Kocak, N. Kubilay, K. Oikonomou, J. Sciare, and N. Mihalopoulos. "Seasonal variability of optical properties of aerosols in the Eastern Mediterranean." *Atmospheric Environment* 39, no. 37 (2005): 7083-7094.

Tyrlis, Evangelos, Filippos S. Tymvios, Christos Giannakopoulos, and Jos Lelieveld. "The role of blocking in the summer 2014 collapse of Etesians over the eastern Mediterranean." *Journal of Geophysical Research: Atmospheres*(2015).

European Union
European Social Fund
OPERATIONAL PROGRAMME
EDUCATION AND LIFELONG LEARNING
investing in knowledge society
MINISTRY OF EDUCATION & RELIGIOUS AFFAIRS
MANAGING AUTHORITY
NSRF 2007-2013
programme for development
EUROPEAN SOCIAL FUND
Co-financed by Greece and the European Union

E. The contribution of wood burning and other sources to wintertime organic aerosol levels in two Greek cities

E1 Experimental Section

E1.1 Measurement Sites

Patras: Patras is the third biggest city of Greece with 300,000 inhabitants and is situated at the foothills of Mount Panachaikon, overlooking the Gulf of Patras, 220 km west of Athens. The instruments were housed inside the campus of the Technological Educational Institute (TEI) of Patras ($38^0$13' N, $21^0$45' E) and were monitoring from February 26 to March 5, 2012. The TEI is in the southwest of the city, surrounded by moderate traffic streets and houses and is considered as an urban site (Fig. E1). Measurements of black carbon (BC) were made at the center of the city ($38^0$14' N, $21^0$44' E), approximately 4 km away from the main site. During the campaign, the ambient temperature ranged from 4 ^{o}C to 16 ^{o}C, with an average of 11 ^{o}C. The average RH was 75% (ranging from 40 to 90%).

Athens: Athens is the capital and largest city of Greece, with approximately 5million inhabitants within the Greater Athens Metropolitan area, which represents almost half of the country's population (Fig. E1). A second and more extensive campaign was conducted a year later in the center of Athens from January 10 till February 9, 2013. The measurements took place at the National Observatory premises at Thiseio ($37^0$58' N, $23^0$43' E, and 100 m above sea level) at the historic center of the city. The average ambient temperature was 12.5 ^{0}C (ranging from 6 ^{0}C to 19 ^{0}C), while the average RH was 71% (ranging from 25 to 95%).

E1.2 Instrumentation

HR-ToF-AMS: The Aerodyne Aerosol Mass Spectrometer (AMS) developed by Jayne et al. (2000), can provide continuous quantitative size and composition information for the non-refractory (NR) components of submicron atmospheric aerosol in real time. The

European Union
European Social Fund
OPERATIONAL PROGRAMME
EDUCATION AND LIFELONG LEARNING
investing in knowledge society
MINISTRY OF EDUCATION & RELIGIOUS AFFAIRS
MANAGING AUTHORITY
NSRF 2007-2013
EUROPEAN SOCIAL FUND
Co-financed by Greece and the European Union

chemical composition of NR-PM_1 organic and inorganic (nitrate, sulfate, ammonium and partially potassium) aerosol particles were monitored using a High Resolution Time of Flight AMS (HR-ToF-AMS) described in detail in the literature (Drewnick et al., 2005; DeCarlo et al., 2006; Canagaratna et al., 2007). Briefly, aerosols are sampled in the AMS through an aerodynamic lens, where they are focused into a narrow beam and accelerated to a velocity inversely related to their aerodynamic size. The sample during this study was not dried, and the vaporizer surface temperature was set at 600 ^{0}C. The HR-ToF-AMS measurements during both campaigns alternated between V- and W-mode every 3 min, but only V-mode data were used to obtain the aerosol mass concentrations presented here. The HR-ToF-AMS can further determine the elemental ratios (e.g., oxygen-to-carbon ratio, O:C) of organics (Aiken et al., 2008; Canagaratna et al., 2015).

SMPS: The aerosol particle number distribution, for not dried particles smaller than 500 nm in diameter, was measured by a TSI Scanning Mobility Particle Sizer (SMPS) (model 3081) coupled with a Condensation Particle Counter (CPC) (model 3775). The system operated at a sheath flow rate of 5 L min^{-1} and a sample flow rate of 1 L min^{-1}.

MAAP: $PM_{2.5}$ aerosol absorption was monitored continuously during the two campaigns by a Multi Angle Absorption Photometer (MAAP, Thermo Scientific Inc. model 5012). The MAAP estimates black carbon (BC) mass loadings based on aerosol optical absorption (Petzold and Schönlinner, 2004). The MAAP was set at a wavelength of 637 nm during the measurements and its inlet was heated to 70 ^{0}C.

TEOM: The Tapered Element Oscillating Microbalance (TEOM, Thermo model, 1405-DF) is composed of two Filter Dynamics Measurement Systems (FDMS) and two TEOM mass sensors, which account for volatile and nonvolatile PM fractions. Ambient air is drawn in the instrument through the two filters at a constant flow rate (16.7 L min^{-1}). TEOM continuously weighs the filters calculating near real-time mass concentrations. TEOM monitors continuously and simultaneously the $PM_{2.5}$ (fine) and PM_{Coarse} ($PM_{10-2.5}$) mass concentrations, while by adding the concentrations, the PM_{10} mass

European Union
European Social Fund
OPERATIONAL PROGRAMME
EDUCATION AND LIFELONG LEARNING
investing in knowledge society
MINISTRY OF EDUCATION & RELIGIOUS AFFAIRS
MANAGING AUTHORITY
NSRF 2007-2013
EUROPEAN SOCIAL FUND
Co-financed by Greece and the European Union

concentration is acquired. During the Athens campaign TEOM encountered many technical problems, and its results will not be presented.

PTR-MS: The VOCs during the Athens campaign were measured by a PTR-MS (Ionicon Analytik Inc.). The operation principles and application details can be found in Steinbacher et al. (2004). Additional information and analysis about these VOC measurements during the sampling period, are presented in Kaltsonoudis et al. (2015).

Thermodenuder: The thermodenuder of An et al. (2007) was used to separate the aerosol based on its volatility. It consists of a heated vaporizer section in which particles are volatilized, followed by a denuder section containing activated charcoal to remove the vapors. The air mass passed alternately through the bypass line and the heated section. The thermodenuder operated in the range from 25 to 400 ^{0}C with a centerline residence time of 15.8 s. A detailed analysis of the thermodenuder measurements is presented in Louvaris et al. (2015) and Gkatzelis et al. (2015).

Gas monitors: The concentrations of CO, CO_2, NO_x and O_3 were measured by Teledyne monitors (models 300E, T360, T201 and 400E, respectively).

Filters: Three different filter samplers were used in order to collect $PM_{2.5}$ samples for the measurement of organic carbon (OC), elemental carbon (EC), water-soluble organic carbon (WSOC) and the main ions. The Met One SuperSASS (Speciation Air Sampler System) was deployed during the Patras campaign, while a dichotomous partisol sampler (Rupprecht & Patashnick Co., Inc.) and a Partisol FRM (Federal Reference Method) Model 2000 were used in Athens. Both teflon and quartz fiber filters were used in Athens and Patras. Daily, 12-hour and 6-hour collection of samples was applied during the campaigns. Details about the filter extraction procedure and chemical analysis can be found in Pikridas et al. (2013), Paraskevopoulou et al. (2014) and Tsifikiotou et al. (2015).

European Union
European Social Fund
OPERATIONAL PROGRAMME
EDUCATION AND LIFELONG LEARNING
investing in knowledge society
MINISTRY OF EDUCATION & RELIGIOUS AFFAIRS
MANAGING AUTHORITY
NSRF 2007-2013
programme for development
EUROPEAN SOCIAL FUND
Co-financed by Greece and the European Union

E1.3 AMS Data analysis

All HR-ToF-AMS data were analyzed using the standard AMS software toolkit (SQUIRREL v1.53) while the high-resolution data were processed using the Peak Integration by Key Analysis (PIKA v1.10C, Sueper, 2011) software within Igor Pro 6.34A (Wave Metrics). For the determination of the elemental ratios measured by the HR-AMS, the empirical method by Aiken et al. (2008) was used. An Improved-Ambient (I-A) calculation of the elemental ratios was proposed by Canagaratna et al. (2015), suggesting that ambient OA has a higher relative oxygen content. Both Aiken and I-A elemental ratios were calculated and are presented for this study. In order to calculate the collection efficiency (CE) of the HR-ToF-AMS, we combined the HR-ToF-AMS mass distributions and the SMPS volume distributions (for particles between 10 and 500 nm) applying the algorithm of Kostenidou et al. (2007), every two hours. The algorithm was modified to take into account the BC mass loadings measured by the MAAP. We assumed that the BC had the same size distribution as the OA.

PMF analysis (Paatero and Tapper, 1994; Lanz et al., 2007; Ulbrich et al., 2009) was performed using as input the HR-AMS organic mass spectra (m/z's 12-200) in order to determine the different OA sources. The mass spectra of the identified factors and those in the literature have been compared using the theta angle (θ) between the corresponding vectors (Kostenidou et al., 2009). A low value of the theta angle (less than 10^o) is indicating high similarity between the two spectra. The corresponding spectra of the same factors for the two cities were expected to be relatively similar but not identical, as these refer to two different time periods (2012 and 2013). For the comparison of the OOA and HOA spectra with the ones in literature, only HR spectra using the fragmentation table by Aiken et al. (2009) were used from the HR-database. The BBOA and COA spectra have been compared with almost all the corresponding spectra found in database (both HR and UMR), resulting in higher theta values due to immense differences at *m/z* 18, 28, and 39.

European Union
European Social Fund
OPERATIONAL PROGRAMME
EDUCATION AND LIFELONG LEARNING
investing in knowledge society
MINISTRY OF EDUCATION & RELIGIOUS AFFAIRS
MANAGING AUTHORITY
NSRF 2007-2013
EUROPEAN SOCIAL FUND
Co-financed by Greece and the European Union

E2. Results and Discussion

E2.1 PM_1 chemical composition

The concentrations (in μg m^{-3}) of OA, sulfate, nitrate, ammonium, chloride, and BC are depicted in Fig. E2. The dominant component of PM_1 for both sites was organic matter (60-75%).

Athens: The average AMS CE during the campaign calculated by the Kostenidou et al. (2007) algorithm was 0.85±0.23. The density of organics calculated by the same algorithm was 1.29±0.21 g cm^{-3}, which is comparable to the organic density calculated for Athens during the summer of 2012 (1.15±0.36 g cm^{-3}, Kostenidou et al., 2015). During the wintertime campaign in Athens, the average total PM_1 mass concentration (not including crustal elements) was approximately 10 μg m^{-3} (of which, 2 μg m^{-3} BC), while the maximum value was 140 μg m^{-3} (of which, 120 μg m^{-3} OA). OA was the major component of PM_1 with frequent nighttime (after 18:00, Local Standard Time, LST) peaks exceeding 40 μg m^{-3} (Figure E2a). During most of the days of the campaign, the PM_1 mass was lower than 20 μg m^{-3} due to frequent rain events and strong winds. The BC mass concentration during the nighttime was as high as 15 μg m^{-3}, while the corresponding morning rush hour maximum was up to 8 μg m^{-3}. Average ammonium was low and around 0.4 μg m^{-3}, while average sulfate was 0.96 μg m^{-3}. Nitrate was on average 0.48 μg m^{-3} but its maximum value was up to 3.4 μg m^{-3}. The correlation between OA and nitrate was moderate (R^2=0.59).

Particulate organonitrates (ON) are important in ambient air but their quantification remains a challenge (Fry et al., 2009; Farmer et al., 2010). In order to estimate their fraction to nitrate, the NO_x^+ ratio (NO_2^+/NO^+) is used. Typical values of this ratio for pure NH_4NO_3 are 1:1.18 to 1:2.7 (Alfarra et al., 2006; Cottrell et al., 2008; Fry et al., 2009) and 1:10 to 1:15 for organonitrates (Hao et al., 2014). In this work, the ON fraction was estimated using the equation suggested by Farmer et al. (2010):

$$\frac{ON}{NO_2} = \frac{(R_{obs} - R_{NH_4NO_3})(1 + R_{ON})}{(R_{ON} - R_{NH_4NO_3})(1 - R_{obs})} \qquad (1)$$

European Union
European Social Fund
OPERATIONAL PROGRAMME
EDUCATION AND LIFELONG LEARNING
investing in knowledge society
MINISTRY OF EDUCATION & RELIGIOUS AFFAIRS
MANAGING AUTHORITY
NSRF 2007-2013
programme for development
EUROPEAN SOCIAL FUND
Co-financed by Greece and the European Union

where, R_{obs} is the observed average NO_x^+ ratio during the campaign, $R_{NH_4NO_3}$ is the NO_x^+ ratio with pure NH_4NO_3 during the AMS calibrations (0.59 on average), and R_{ON} is a fixed value (0.04) equal to the minimum NO_x^+ ratio observed during the campaign. The average ON fraction was 42±25%. During nighttime peaks (20:00 till 2:00 LST) the average ON fraction was 19±10%. In this study, the NO^+/NO_2^+ ratio of ON was 4, close to the values of ON by other studies.

The average size distributions of the different aerosol species (sulfate, organics, ammonium, chloride and nitrate) as a function of the vacuum aerodynamic diameter are depicted in Fig. E3a. Sulfate peaked at 310 nm, whereas OA at 250 nm. Nitrate's size distribution peaked at the same diameter (250 nm) as OA.

Back trajectory analysis for the sampling period, based on FLEXPART (Stohl et al., 2005) showed that air masses arrived mainly from Sahara desert and sea (70%). Four distinct categories were found for the period of measurements. In the first group air masses originated from Africa and passed aloft Mediterranean Sea. The second category was characterized by air masses of marine origin from the west (Sicilia). The third group contained air masses from the Aegean Sea, but originating from NE Europe. Finally, the fourth category included air masses from central Greece and Balkans. Even if there was a transfer of air masses from the Sahara desert during January 16 to 17, the heavy rains of the January 16 and the high levels of humidity on the January 17 did not favor the increase of PM concentrations.

Patras: The estimated mean value of the CE during the wintertime campaign in Patras was 0.77±0.05, higher than the standard CE of 0.5 often used. One reason for this difference may be that, in other studies, the aerosol is often dried before sampling with the AMS. The density of organics estimated by the same algorithm was 1.45±0.04 g cm^{-3}, which is close to the one for Patras during the summer of 2012 (1.34±0.21 g cm^{-3}, Kostenidou et al., 2015). The one-hour averaged mass concentration of the PM_1 measured by the AMS and the MAAP varied from a few μg m^{-3} up to 100 μg m^{-3} (Figure E2b). The average $PM_{2.5}$ mass concentration measured by the TEOM was 28 μg m^{-3} and

European Union
European Social Fund
OPERATIONAL PROGRAMME
EDUCATION AND LIFELONG LEARNING
investing in knowledge society
MINISTRY OF EDUCATION & RELIGIOUS AFFAIRS
MANAGING AUTHORITY
NSRF 2007-2013
EUROPEAN SOCIAL FUND
Co-financed by Greece and the European Union

reached levels up to 160 μg m^{-3}. During this campaign, the average PM_1 mass concentration was approximately 25 μg m^{-3} (of which, 2 μg m^{-3} BC and 18 μg m^{-3} OA). OA mass concentration increased dramatically during the evening hours, reaching levels up to 85 μg m^{-3}. The OA also increased during morning rush hour (7:00-10:00, LST), but the corresponding concentrations were less than 25 μg m^{-3}. BC concentrations followed closely the variation of OA, with maximum BC mass concentration of approximately 8 μg m^{-3} during nighttime, and 4 μg m^{-3} during rush hour in the mornings. Average BC levels in Patras were nearly 50% lower than those in Athens. Nitrates followed a similar trend with OA with significant peaks occurring both during the morning and evening hours. Nitrates were on average 1 μg m^{-3}, but higher values up to 5 μg m^{-3} were measured during the second half of the campaign. Sulfate concentration was on average 2.6 μg m^{-3} and had smaller fluctuations during the campaign, indicating a different source origin. Chloride's average concentration was 0.4 μg m^{-3}, but reached values up to 7 μg m^{-3}. Ammonium's behavior was affected by those of sulfate, chloride and nitrates, indicating the formation of the corresponding ammonium salts.

The average campaign size distributions of the different aerosol species versus the aerodynamic diameter are depicted in Fig. E3b. Sulfate peaked at 340 nm, whereas OA peaked at 140 nm, implying that the PM_1 particles during the sampling period had different composition at different size ranges. The size distribution of nitrate, which was a minor component of PM_1 (4 %), followed the same trend as organics due to the fact that a significant fraction of the nitrate signal came from ON (45%), while that of ammonium mainly followed the trend of sulfate. In comparison to Athens' distributions sulfate peaks at around the same aerodynamic diameter for both campaigns, whereas OA in Patras seems fresher, as it peaked in lower diameter.

Back trajectory analysis using FLEXPART showed that air masses in Patras arrived mainly from the north, while there was no transfer from the Sahara desert. Three main groups were found during the sampling period: the days 25/26-02 and 3/4-03 were characterized by air masses coming predominantly from the western Greece but also

European Union
European Social Fund
OPERATIONAL PROGRAMME
EDUCATION AND LIFELONG LEARNING
investing in knowledge society
MINISTRY OF EDUCATION & RELIGIOUS AFFAIRS
MANAGING AUTHORITY
NSRF 2007-2013
programme for development
EUROPEAN SOCIAL FUND
Co-financed by Greece and the European Union

originating from the sea (44% of the air masses), during the 26/27-02 and 5-03 the air masses had marine origin but were approaching from Italy and Sicilia (14%), whilst air masses of the third group, for the days 28-02 till the 2-03 were originating from central Greece and Balkans (42%).

E2.2 Elemental ratios and OS_C

The O:C ratio of OA is a useful metric of its extent of oxygenation, which increases as the aerosol is exposed to atmospheric oxidants (Grieshop et al., 2009; Sage et al., 2008). In Athens, the mean "Aiken-ambient" $O:C_{A-A}$ ratio was equal to 0.26±0.09, ranging from 0.03 to 0.85 (Figure E5) and the $H:C_{A-A}$ was 1.59±0.11. The improved ambient (I-A) $O:C_{I-A}$ ratio was 0.32±0.11 while the $H:C_{I-A}$ was 1.72±0.11. In Patras, the average $O:C_{A-A}$ ratio was 0.33±0.07, and ranged from 0.07 to 0.61. The $O:C_{I-A}$ was 0.42±0.09 and the $H:C_{I-A}$ was 1.71±0.06. The low average values of $O:C_{A-A}$ for both Athens and Patras are consistent with the organic aerosol being heavily dominated by primary emissions (Allan et al., 2010). The corresponding $O:C_{A-A}$ ratios during summertime for Athens and Patras were 0.47 and 0.50, respectively (Kostenidou et al., 2015). Another metric for the extent of oxidation of atmospheric OA, is the average carbon oxidation state OS_C, a value that increases upon oxidation (Kroll et al., 2011). The OS_C for both cities was calculated by applying the equation proposed by Kroll et al. (2011):

$$OS_C = 2(O:C)-(H:C) \qquad (2)$$

In Athens, the OS_C was -1.11±0.1, but varied from -2.1 to 0.09. In Patras, the corresponding OS_C was -0.88±0.22, ranging from -1.72 to -0.08.

E2.3 Average diurnal concentration profiles

The average diurnal profiles of the main PM_1 species during the two campaigns are shown in Fig. E4. In Athens, both OA and BC concentrations increased during the evening hours, peaking at around 23:00 LST. BC also exhibited a strong morning peak at 8:00 LST, which is attributed to the morning rush hour. Sulfates, ammonium, and chloride exhibited a rather flat average diurnal profile. Nitrates also displayed two peaks

European Union
European Social Fund
OPERATIONAL PROGRAMME
EDUCATION AND LIFELONG LEARNING
investing in knowledge society
MINISTRY OF EDUCATION & RELIGIOUS AFFAIRS
MANAGING AUTHORITY
NSRF 2007-2013
EUROPEAN SOCIAL FUND
Co-financed by Greece and the European Union

during the day, one in the morning (9:00 LST) coinciding with the peak traffic hours, and another one in the late evening (23:00 LST).

Similarly, to Athens, the OA and BC concentrations in Patras demonstrated two major peaks during the day. The first one appeared at around 8:00 LST, and coincides with the morning rush hour traffic, while the second one, which was significantly higher, at 20:00 LST. During the evening the OA and BC concentrations increased considerably, and were responsible for almost 90% of the total PM_1 mass, until around midnight. Sulfate had a reasonably smooth profile during the day, while nitrates, like in Athens, had two peaks, which coincided with those of OA and BC. This suggests for one more time, that nitrates and OA had at least to some extent, similar sources. The diurnal variation of chloride had a major morning peak at around 7:00 LST, which could be due to two Olympic-size swimming pools, located in a major athletic center, less than 1 km from the sampling site. There was also an evening chloride peak.

The average diurnal profiles of $O:C_{A-A}$ for both cities are shown in Fig. E5. In Athens, the $O:C_{A-A}$ increased during the early morning hours and after 10:00 LST. In Patras, the $O:C_{A-A}$ ratio increased significantly during the early morning hours (2:00 to 7:00 LST), during midday (peak at around 10:00 LST), and also at around 15:00 in the afternoon. The mean OA/OC ratio for Athens was 1.50±0.1, and varied between 1.2 and 2.2 during the measurement period. The OA/OC ratio in Patras was 1.59±0.1, ranging from 1.3 to 2. In Athens, the average $H:C_{A-A}$ ratio was 1.59±0.11, and N:C ratio 0.019±0.005. In Patras, the corresponding values were 1.53±0.05, and 0.018±0.003, respectively.

E2.4 Organic aerosols sources

Positive matrix factorization (Paatero and Tapper, 1994) (PMF) was applied to the HR-ToF-AMS OA data, using the PMF Evaluation Tool, PET (Lanz et al., 2008; Ulbrich et al., 2009). The PMF analysis deconvoluted the OA spectra into different factors for both campaigns. Biomass burning was the dominant source of OA, and was responsible for 40-60% of the total OA. The major results for both sites are summarized in Figure E6,

European Union
European Social Fund
OPERATIONAL PROGRAMME
EDUCATION AND LIFELONG LEARNING
investing in knowledge society
MINISTRY OF EDUCATION & RELIGIOUS AFFAIRS
MANAGING AUTHORITY
NSRF 2007-2013
EUROPEAN SOCIAL FUND
Co-financed by Greece and the European Union

where the PM_1 chemical composition obtained from the AMS and the organic source apportionment are depicted.

Four sources were identified in Athens: BBOA (43%), OOA (24%), HOA (17%) and COA (16%). Their time series and contribution to PM_1 OA are depicted in Fig. E7. BBOA, HOA and COA factors correspond to primary sources, whereas the OOA factor to atmospheric processing (secondary OA). In Patras a five-factor solution was selected (see Supplementary Information for more details, Section 9). The OOA factor accounted on average for 18% of the OA, while HOA and COA represented 12% and 11%, respectively. Two biomass burning-related OA (BBOA and BBOA-I) factors dominated the measured OA composition (almost 60%) during the observed period. The PMF factors' time series and contribution to PM_1 OA are depicted in Fig. E8. Figure E9 displays the mass spectra of the OA components, identified by the PMF analysis for the two campaigns. These factors are analyzed below.

E2.4.1 Oxygenated Organic Aerosol (OOA)

OOA is a surrogate for secondary OA and represents the chemically aged OA and can be due to both local production processes and long range transport from other areas. In contrast to other measurement datasets in Athens, in which two OOA types were deconvoluted by PMF (a very-oxidized OOA, V-OOA, and a moderate-oxygenated, M-OOA) (Kostenidou et al., 2015), only one type was clearly present in Athens during the winter. The OOA factor dominated OA during the daytime and its mass concentration increased after the January 28, when air masses originated from the Balkans and not from the Mediterranean Sea, and there was little rain (See Supplementary material, Sections2 and 4). The average OOA concentration was 1.3 μg m^{-3}, with a maximum value of 9.7 μg m^{-3}. OOA was correlated with NH_4^+ (R^2=0.65), SO_4^{2-} (R^2=0.58), and NO_3^- (R^2=0.67). The average diurnal concentration of OOA decreased smoothly during morning hours, reaching a minimum at around 15:00 LST, and increased again during the afternoon and evening, peaking at midnight (Fig. E10). This maximum could be related to nighttime SOA production.

European Union
European Social Fund
OPERATIONAL PROGRAMME
EDUCATION AND LIFELONG LEARNING
investing in knowledge society
MINISTRY OF EDUCATION & RELIGIOUS AFFAIRS
MANAGING AUTHORITY
NSRF 2007-2013
programme for development
EUROPEAN SOCIAL FUND
Co-financed by Greece and the European Union

The OOA factor dominated daytime OA in Patras and its mass concentration increased during the last days of measurements. The OOA was correlated reasonably well with particulate ammonium (R^2=0.61) and sulfate (R^2=0.56), while the correlation to nitrate was moderate (R^2=0.38). Its mean value was 3.2 μg m^{-3}, while its maximum value occurred around midday of March 5, and was equal to 10.8 μg m^{-3}. For comparison, during summertime, OOA in Patras accounted for almost 80% of OA due to the higher photochemical activity (Kostenidou et al., 2015). The average diurnal pattern of OOA was relatively stable in Patras (Fig. E10), which is consistent with a regional source and domination by atmospheric transport rather than local sources and processes. There were minor peaks during the morning hours (at 8:00 and 11:00 LST), while it decreased after 18:00 (LST).

In Athens, the O:C ratio for OOA during the winter of 2013 was equal to 0.47 (Fig. E9a). The corresponding values of O:C during summertime in Athens, for V-OOA and M-OOA were 0.68 and 0.56, respectively (Kostenidou et al., 2015). In Patras, the O:C ratio during the measurement period was 0.65, while the OM:OC ratio was equal to 2.01. The O:C ratio for V-OOA, M-OOA and b-OOA during the summer campaign of 2012 in Patras, were 0.81, 0.54 and 0.48, respectively (Kostenidou et al., 2015).
Both OOA spectra are characterized by a strong peak at m/z 44 (mostly due to CO_2^+), related to the thermal decomposition of organic acids (Alfarra, 2004), a lower one at 43 (mostly due to $C_2H_3O^+$), and another one at *m/z* 28, all consistent with bibliography. They do not contain important contributions from marker peaks of other organic aerosol classes (Fig. E9). The identified spectra of the OOA factors in the two cities were quite similar (θ=11.3º) to each other, with the bigger differences corresponding to *m/z* 28 and 44. The OOA in Athens exhibited lower f_{44} (0.12) compared to the one in Patras (0.15).

The spectrum of OOA in Athens was similar to both moderate oxygenated OA (M-OOA) (θ=8º) identified in Athens and Patras (θ=10.6º) during summer (Kostenidou et al., 2015). It was also similar with the proposed biogenic OOA factor (b-OOA) (θ=10.5º) in

European Union
European Social Fund
OPERATIONAL PROGRAMME
EDUCATION AND LIFELONG LEARNING
investing in knowledge society
MINISTRY OF EDUCATION & RELIGIOUS AFFAIRS
MANAGING AUTHORITY
NSRF 2007-2013
programme for development
EUROPEAN SOCIAL FUND
Co-financed by Greece and the European Union

Patras for the same summer period. A strong similarity (θ=11-13 ^{o}) was exhibited between OOA in Athens with all the OOA (OOA-a, OOA-b, OOA-c) factors for Po Valley measurements (Saarikoski et al., 2012).

The spectrum of OOA in Patras was quite similar to the OOAa and OOAb (θ=7^{o}) for Po Valley (Saarikoski et al., 2012).Aa great similarity (θ=10^{o}) was also exhibited with the mass spectra of M-OOA in Athens and Patras (Kostenidou et al., 2015).The LV-OOA spectra from both DAURE and SOAR campaigns (Mohr et al., 2012; Docherty et al., 2011) were quite similar (θ=11^{o}) to the spectrum of OOA in Patras. Higher theta angles (θ=20^{o}-40^{o}) were derived for the spectra of SV-OOA from different studies, implying that OOA in Patras campaign was more likely in the form of LV-OOA instead of SV-OOA.

E2.4.2 Hydrocarbon-Like Organic Aerosol (HOA)

The HOA mean value in Athens was 0.95 μg m^{-3}, and its hourly maximum value was 34 μg m^{-3}. HOA was correlated with CO (R^2=0.69) and NO_x (R^2=0.74) suggesting that traffic was a major source. HOA was also correlated to AMS chloride (R^2=0.75), and VOCs, such as methacrolein (MACR) (PTR-MS, *m/z* 71) (R^2=0.74), naphthalene (PTR-MS, *m/z* 129) (R^2=0.73), benzene (PTR-MS, *m/z* 79) (R^2 =0.65), and the xylenes (PTR-MS, *m/z* 107) (R^2 =0.7). The HOA correlation with BC for the whole campaign was low (R^2=0.15). However, splitting the time series into two periods, one during the day (6:00-18:00 LST) and another one during the night (18:00-6:00 LST), led to high correlation during daytime (R^2 =0.78) and low during the nighttime (R^2 =0.15). This can be explained, as BC originated mainly from diesel combustion sources during the day, while during the night was associated with both traffic and wood burning. However, the MAAP cannot distinguish the different origin of BC. The diurnal pattern of HOA in Athens was the same as that of BC, and exhibited strong morning (8:00-9:00 LST) and evening peaks (20:00-23:00 LST) consistent with increased traffic during morning and evening rush hours.

European Union
European Social Fund
OPERATIONAL PROGRAMME
EDUCATION AND LIFELONG LEARNING
investing in knowledge society
MINISTRY OF EDUCATION & RELIGIOUS AFFAIRS
MANAGING AUTHORITY
NSRF 2007-2013
programme for development
EUROPEAN SOCIAL FUND
Co-financed by Greece and the European Union

In Patras, HOA contributed on average approximately 10% to the total OA, while the corresponding HOA contribution during summer was 7% (Kostenidou et al., 2015). HOA's mean value was 2.14 μg m^{-3}, and its hourly maximum value was 15.8 μg m^{-3}. The strongest peak in the average diurnal cycle occurred in the morning (06:00–09:00 LST) and was probably associated with traffic emissions (Fig. E10). A peak in the afternoon (17:00–22:00 LST) was also present, but was often smaller. The time series of HOA shows poor correlation with NO_x (R^2 = 0.2), and BC (R^2 = 0.16), as the MAAP was monitoring 4 km away from the HR-ToF-AM.

In Athens, the O:C for HOA was equal to 0.13, while its H:C ratio was 1.74. In Patras, the O:C ratio was 0.1, while the H:C ratio was equal to 1.83. The corresponding values of O:C during summertime of 2012 were 0.07 (Athens) and 0.1 (Patras) (Kostenidou et al., 2015). The two HOA spectra were also quite similar to each other (θ=13º). Their major differences were observed at *m/z* 28, 43, 44, 57, 69, and 71, which were generally higher in the Patras HOA spectrum, while the f_{44} in the Athens spectrum was two times higher (0.04) compared to the Patras one. The HOA spectrum was characterized by ions with the general types $C_nH_{2n+1}^+$ and $C_nH_{2n-1}^+$. As a result, the HOA spectrum had characteristic peaks at *m/z* 41, 43, 55, 57, 69, 71, 83 and 85 etc., with little signal at *m/z* 44 (Fig. E9a). The mass spectra of HOA are often similar to those of diesel exhaust (Canagaratna et al., 2004; Schneider et al., 2005), and other incomplete combustion sources. For both spectra, the largest peaks were at *m/z* 43 ($C_3H_7^+$) and *m/z* 57 ($C_4H_9^+$), consistent with literature (Zhang et al., 2014).

Comparing the identified HOA spectra with literature, the spectrum of HOA in Athens was similar (θ=6º) with the corresponding one from HOA in Patras (Kostenidou et al., 2015) during summertime (2012), and relatively similar with the majority of HOA in literature (θ=10-15º). The spectrum of HOA in Patras was very similar (θ=5-8 º) with the spectra of HOA in New York City (Sun et al., 2011), Fresno (Ge et al., 2012), and MILAGRO campaign (Aiken et al., 2009).

European Union
European Social Fund
OPERATIONAL PROGRAMME
EDUCATION AND LIFELONG LEARNING
investing in knowledge society
MINISTRY OF EDUCATION & RELIGIOUS AFFAIRS
MANAGING AUTHORITY
NSRF 2007-2013
EUROPEAN SOCIAL FUND
Co-financed by Greece and the European Union

E2.4.3 Cooking Organic Aerosol (COA)

In Athens, COA exhibited strong night peaks at around 23:00 LST, with values up to 15 μg m^{-3}. Its mean value was 0.87 μg m^{-3}. COA correlated moderately with BC (R^2=0.32), and CO (R^2=0.27), while the correlation between COA and individual VOCs measured by the PTR-MS was poor, with R^2 varying from 0.01 to 0.32. The temporal trend of COA in Athens is different from those in previous studies. Contrary to what was expected, no peak was demonstrated during lunch hours (12:00-15:00 LST). However, no other factor displayed a peak during these hours. A large nighttime peak, clearly affected by the decrease of the planetary boundary layer is present at around 23:00 LST (Fig. E10). This late peak is consistent with the late dinner hours of Greeks.

A COA factor was also identified during the Patras campaign, with a mean value of 2.05 μg m^{-3}, and an hourly maximum value of 33.6 μg m^{-3}. The diurnal profile of COA in Patras exhibited two major peaks during the day: the mahor peak occurred in the late evening (18:00–24:00 LST) probably modulated by the boundary layer height, and a second significant peak around midday (10:00–15:00 LST), both corresponding to typical Greek mealtimes (Fig. E10). Compared to traffic, organic aerosol from cooking activities was equally responsible, confirming its importance to local pollution sources.

In Athens, the O:C ratio was equal to 0.11, while the H:C ratio was 1.68. In Patras, the O:C ratio was 0.14, while the H:C ratio was equal to 1.71. The corresponding values of O:C during summertime of 2012 were 0.21 (Athens) and 0.24 (Patras) (Kostenidou et al., 2015). The COA spectrum, like the HOA one was characterized by the ion series: $C_nH_{2n+1}^+$ and $C_nH_{2n-1}^+$, but also by $C_mH_{2m-1}CO^+$ (*m/z* 41, 55, 69, 83...) and $C_mH_{2m+1}CO^+$ (*m/z* 29, 43, 57, 71, 85...) (Crippa et al., 2013; He et al., 2010) (Fig. E9a). The COA spectrum in both cities had some similarity to that of the HOA but was dominated by *m/z* 41 ($C_3H_5^+$) and 55 ($C_4H_7^+$ and $C_3H_3O^+$) instead of *m/z* 43 and 57. The signal of *m/z* 55 of COA mass spectrum in Patras was almost twice that of the *m/z* 57. This characteristic of the COA spectra was first reported by Lanz et al. (2007) and is related with charbroiling

European Union
European Social Fund
OPERATIONAL PROGRAMME
EDUCATION AND LIFELONG LEARNING
investing in knowledge society
MINISTRY OF EDUCATION & RELIGIOUS AFFAIRS
MANAGING AUTHORITY
NSRF 2007-2013
programme for development
EUROPEAN SOCIAL FUND
Co-financed by Greece and the European Union

(Allan et al., 2010). The two COA mass spectra were very similar to each other with a theta angle of 8º, and minor differences at *m/z* 27, 28, 39, 41 and 43.

The COA spectrum in Athens and Patras were quite similar to the COA spectra reported in Fresno (Ge et al., 2012), New York City (Sun et al., 2011) and Paris (Crippa et al., 2013) with theta angle values varying between 11-17º.

E2.4.4 Biomass Burning-related Organic Aerosol

In Athens, biomass burning OA (BBOA) was the dominant factor (43%) of OA. BBOA reached levels up to 80 μg m^{-3} during the evening hours of the first day of the campaign, which coincides with the coldest day during the period of measurements. The average BBOA concentration was 2.3 μg m^{-3}. However, when meteorological conditions allowed it (no rain events), BBOA sharply increased during the evening hours (after 17:00 LST), frequently reaching values greater than 20 μg m^{-3}. BBOA and gas-phase acetonitrile (*m/z* 42, CH_3CN^+) measured by the PTR-MS were strongly correlated (R^2 =0.81). BBOA was also well correlated with AMS chloride (R^2=0.88), while there was low correlation with markers of biomass burning (Zhang et al., 2010; Hudson et al., 2005), such as the AMS K^+ (R^2 =0.40). A moderate correlation was observed between BBOA and other species, like CO (R^2=0.58), while its correlation with NO_x (R^2=0.29), and BC (R^2=0.33%) was rather low. A surprisingly high correlation was also observed between BBOA and biogenic VOCs, such as 2-methyl-3-buten-2-ol (MBO) (PTR-MS, *m/z* 87) (R^2=0.93) which is related with emissions from pine trees (Vlasenko et al., 2009), isoprene and furan at *m/z* 69 (C_5H^+ and $C_4H_5O^+$) (R^2=0.88), methacrolein ($C_4H_7O^+$) or/and methyl vinyl ketone (MVK, $C_4H_7O^+$) at *m/z* 71 (R^2=0.81), and *m/z* 85 (among possible candidates, ethyl vinyl ketone) (R^2=0.9), results consistent with previous works for VOCs which are described to have wood burning as a main source (Akagi et al., 2011). In the average diurnal cycle of BBOA mass concentration increased significantly in the afternoon (17:00 LST) reaching its maximum value at 23:00 LST (Fig. E10). These hours correspond to the prime wood combustion period for domestic heating. An early morning peak was also observed between 1:00 and 4:00 (LST), and was similar to the peak

European Union
European Social Fund
OPERATIONAL PROGRAMME
EDUCATION AND LIFELONG LEARNING
investing in knowledge society
MINISTRY OF EDUCATION & RELIGIOUS AFFAIRS
MANAGING AUTHORITY
NSRF 2007-2013
programme for development
EUROPEAN SOCIAL FUND
Co-financed by Greece and the European Union

presented in the diurnal profile of the AMS K^+, implying a common source between the two. During daytime no significant peak was observed and its mass concentration was lower than 1 μg m^{-3}.

In Patras, the OA was dominated (60%) by biomass burning-related OA. The detection of a biomass burning OA factor is often driven by a prominent contribution of characteristic mass fragments such as *m/z* 60 and 73, attributed to $C_2H_4O_2^+$ and $C_3H_5O_2^+$, respectively, which are regarded as tracer ions of biomass burning aerosols (Alfarra et al., 2007; Aiken et al., 2009). The OA in Patras deconvoluted in two BBOA-like factors: the BBOA (f_{60}=0.025) and the BBOA-I (f_{60}=0.009). These factors had different mass spectra (θ=32°), and displayed distinct diurnal variation, with poor correlation to each other (R^2=0.2). For those reasons, they were considered as separate factors by the PMF analysis (See Supplementary Material). By summing up the mass concentration of the two biomass burning-related factors in Patras, their contribution to the total OA was on average 60% and as high as 90% during evenings, indicating the major contribution of biomass burning to the OA levels. Similar contribution of BBOA to OA (up to 94%) was noted, in the Swiss village of Roveredo, during the cold periods of 2005 (Alfarra et al., 2007).

The BBOA in Patras was by far the most important component of PM_1 OA (40%) and specifically during the evening periods represented up to 75% on the total OA. BBOA concentrations were remarkably higher than those of Athens campaign, with a mean value of 7 μg m^{-3}. Like in Athens, BBOA increased in the afternoon, after 16:00 LST, with daily values higher than 20 μg m^{-3}, and even greater than 35 μg m^{-3} after the February 29. The BBOA factor correlated well with the AMS K^+ (R^2=0.76), even if no precise correlation was expected as AMS K^+ is only a portion of ambient K^+, due to the incomplete vaporization of KCl and K_2SO_4. BBOA demonstrated a modest correlation with AMS particulate nitrate (R^2=0.55), and a low one with CO (R^2=0.40), and BC (R^2=0.27). The average BBOA concentration during the day, increased in the evening (16:00 LST), reaching its maximum value (25 μg m^{-3}) three hours earlier than the BBOA

European Union
European Social Fund
OPERATIONAL PROGRAMME
EDUCATION AND LIFELONG LEARNING
investing in knowledge society
MINISTRY OF EDUCATION & RELIGIOUS AFFAIRS
MANAGING AUTHORITY
NSRF 2007-2013
EUROPEAN SOCIAL FUND
Co-financed by Greece and the European Union

in Athens (20:00 LST) (Fig. E10). During daytime, the observed BBOA mass was less than 5 μg m^{-3}.

BBOA-I was the second biomass burning-related factor, which contributed 19% to the total OA in Patras. Its contribution was higher during the first days of the campaign reaching values up to 40% of the total OA. Its mean value was equal to 3.3 μg m^{-3}, and its hourly maximum value almost 21 μg m^{-3}. BBOA-I correlated poorly with all the major AMS species (R^2<0.1), and BC (R^2=0.26). Its diurnal cycle exhibited two evening peaks, one at 18:00 (LST) and a smaller one at 22:00 (LST) related to domestic heating needs. Its mass concentration during daytime was less than 3 μg m^{-3}, and close to the corresponding one of BBOA (Fig. E10).

The O:C ratio in Athens for BBOA was 0.27, while its OM:OC ratio was equal to 1.50. In Patras, the O:C ratio of BBOA was 0.30, while its OM:OC ratio was equal to 1.55, and the O:C ratio of BBOA-I and its OM:OC ratio were 0.26 and 1.47, respectively (Fig. E9). The spectrum of BBOAin Athens had prominent peaks at *m/z* 39 ($C_3H_3^+$), 60 ($C_2H_4O_2^+$) and 73 ($C_3H_5O_2^+$). A really high contribution to the total organic signal in BBOA spectrum, was also observed at *m/z* 29 (mostly due to CHO^+, and $C_2H_5^+$), consistent with Alfarra et al. (2007). BBOA spectrum displayed a major contribution of C_xH_y and $C_xH_yO_z$ (where, z=1) families. The BBOA high resolution (HR) spectra, with the dominant ion families are represented in Fig. E9a.

In Patras, the BBOA and BBOA-I spectra are shown in Fig. E9b. The BBOA spectrum had strong signal at *m/z* 29 (CHO^+, $C_2H_4O_2^+$ and $C_3H_5O_2^+$), 43 ($C_2H_3O^+$), 60 ($C_2H_4O_2^+$) and 73 ($C_3H_5O_2^+$), while the AMS spectrum of BBOA-I factor was characterized by lower signal in *m/z* attributed to fresh OA, like *m/z* 43, 55 and 57, and a stronger peak at *m/z* 44 (C_xH_yO family), which is related to aged organic aerosol (f_{44} equal to 0.043). Furthermore, *m/z* 60 in BBOA-I spectrum was still present but lower (67% less) compared to the one in BBOA spectrum, implying the reaction of levoglucosan. In BBOA-I mass spectrum, the *m/z* 39 ($C_3H_3^+$) displayed a prominent peak, while of

European Union
European Social Fund
OPERATIONAL PROGRAMME
EDUCATION AND LIFELONG LEARNING
investing in knowledge society
MINISTRY OF EDUCATION & RELIGIOUS AFFAIRS
MANAGING AUTHORITY
NSRF 2007-2013
programme for development
EUROPEAN SOCIAL FUND
Co-financed by Greece and the European Union

particular interest is the peak at *m/z* 91, which can be indicative of aromatic species such as benzyl ions (Allan et al., 2003, 2004; Trainer et al., 2012). This peak was also present in the spectrum of the BBOA factor from the burning of olive tree branches in Greece (Kostenidou et al., 2013).

The mass spectra of BBOA in Athens and Patras were quite similar (θ=14º) with small differences at *m/z* 29, 39, 43, 57, 60 and 73. Their f_{44} were close to each other (0.02). The mass spectra of BBOA in Athens and BBOA-I in Patras were quite different (θ=25.1º). Their major differences were presented at *m/z* 26, 28, 29, 39, 41, 43, 44, 55, 57, 60, and 73.

By comparing the BBOA spectra to those of literature, the spectrum of BBOA in Athens presented great similarity (θ=12º) to the BBOA factor in Fresno (Ge et al., 2012), and slighter ones with the ponderosa pine duff (θ=21º) and the Alaska core Tundra duff spectra (θ=22º) both from FLAME-1 measurements (Sullivan et al., 2008). For the rest of the database spectra, the theta angle values were above 20º .

BBOA in Patras, was similar to the Fresno spectrum (θ=11º), but also to the BBOA from MILAGRO campaign (θ=14º) (Aiken et al., 2009). The BBOA-I spectrum in Patras and bibliography spectra, demonstrated the higher values of theta angle, varying from 24º for BBOA factor (Crippa et al., 2013) to 67º for Beech Smouldering (Weimer et al., 2008). Smouldering of different types of wood, presented higher theta values (θ=38-66º) with BBOA-I, while the theta values for flaming types of wood were lower (θ=37-43º) (Weimer et al., 2008). Further calculation of theta angle between BBOA-I and HR spectra of OOA factors revealed lower theta values (θ=28-48º) between these two types of spectra . The theta angle was found lower than 30º for the spectra of OOA in Fresno (Ge et al., 2012), New York (Sun et al., 2011), and SV-OOA from SOAR (Docherty et al., 2011), indicating a moderate resemblance of BBOA-I and chemically aged aerosol. Nevertheless, more investigations are necessary to better enlighten the nature of BBOA-I factor.

European Union
European Social Fund
OPERATIONAL PROGRAMME
EDUCATION AND LIFELONG LEARNING
investing in knowledge society
MINISTRY OF EDUCATION & RELIGIOUS AFFAIRS
MANAGING AUTHORITY
NSRF 2007-2013
programme for development
EUROPEAN SOCIAL FUND
Co-financed by Greece and the European Union

Wood burning was not expected to be such an important source of aerosols in Athens and Patras, as measurements were conducted during relatively warm Greek wintertime periods. The average ambient temperature for both campaigns was close to 12°C, ranging from 6-19 °C in Athens, and 4-16°C in Patras. The contribution of wood burning is expected to be even higher for lower temperatures.

E3 Conclusions

An aerosol mass spectrometer (HR-ToF-AMS), as well as a number of other techniques was deployed for the measurement of the chemical composition of the PM_1, in two of the biggest cities in Greece (Athens and Patras), during two consecutive winters (2012 and 2013). The carbonaceous PM (BC+OA) accounted for about 80% of the PM_1 during the two field campaigns, and up to 95% during morning (5:00-10:00 LST) and evening (16:00-24:00 LST) hours. PMF was applied to the HR-ToF-AMS organic matrix and four- and five-factor solutions were found for Athens and Patras, respectively.

During both wintertime campaigns, domestic wood burning was in general more significant than traffic in both sites. The PM_1 consisted of principally biomass burning-related OA (23-42%), a contribution from traffic (BC =7-20% and HOA=9-10%), cooking activities (COA= 8-9%), and also oxygenated OA (OOA=13-14%). Sulfates, ammonium and nitrate accounted for 10%, 4% and 5%, respectively, of the total PM_1 in both cities. The OA O:C ratio for the Athens campaign was equal to 0.26, while in Patras 0.33, suggesting that air masses in Patras were to some extent more oxidized.

OOA factor dominated daytime OA in both sites and correlated reasonably well with inorganic compounds. In comparison to summertime campaigns in the same cities during 2012, only one type of OOA was noticeably present during wintertime. The detected spectra of OOA were quite similar (θ=11 ^{0}) to each other, and were quite comparable (θ=8-11^0) to moderate oxygenated OA (M-OOA) identified during the summertime

European Union
European Social Fund
OPERATIONAL PROGRAMME
EDUCATION AND LIFELONG LEARNING
investing in knowledge society
MINISTRY OF EDUCATION & RELIGIOUS AFFAIRS
MANAGING AUTHORITY
NSRF 2007-2013
programme for development
EUROPEAN SOCIAL FUND
Co-financed by Greece and the European Union

study. By comparing the OOA spectrum in Patras campaign to those of literature, it was more likely to be in the form of LV-OOA instead of SV-OOA. In Athens (2013), the O:C ratio of OOA was equal to 0.47, while in Patras (2012), 0.65.

In both sites the HOA factor peaked during both day (8:00-9:00 LST) and evening (20:00-23:00 LST) hours. Its diurnal pattern followed closely the diurnal cycle of BC, exhibiting strong peaks consistent with increased traffic during morning and evening rush hours. The two HOA spectra were also quite similar to each other ($\theta=13^o$), and by comparing them to HOA spectra of literature, they presented a high correlation with the corresponding spectra in New York City, Fresno, and MILAGRO campaigns. In Athens, the HOA O:C ratio was equal to 0.12, while in Patras was 0.1.

The diurnal profile of COA in Athens exhibited strong peaks only during the night at around 23:00 LST, while COA in Patras exhibited two major peaks during the day (13:00 and 22:00 LST). In Athens, the O:C ratio was equal to 0.11, while in Patras the corresponding ratio was 0.14. The two COA mass spectra were very similar to each other with a theta angle of 8^o, and also quite similar to COA spectra in Fresno, New York City and Paris.

BBOA factors in both sites were the dominant source (40%) of OA, and presented quite similar ($\theta=13.2^o$) spectra to each other. In the average diurnal profile, they both sharply increased during the evening hours (after 16:00 LST), and BBOA in Patras reached its maximum value at 8:00 LST, three hours earlier than the BBOA in Athens. Both BBOA spectra were quite similar to the literature spectra of BBOA in Fresno. A second biomass burning-related factor (BBOA-I) was identified in Patras. The BBOA-I (19% of OA) displayed quite different spectra to the dominant BBOA factor. In Patras, the two BBOA factors (BBOA and BBOA-I) exhibited different diurnal profiles, but comparable O:C ratios. The O:C ratio of BBOA was 0.30, while the corresponding ratio of BBOA-I was equal to 0.26.

European Union
European Social Fund
OPERATIONAL PROGRAMME
EDUCATION AND LIFELONG LEARNING
investing in knowledge society
MINISTRY OF EDUCATION & RELIGIOUS AFFAIRS
MANAGING AUTHORITY
NSRF 2007-2013
programme for development
EUROPEAN SOCIAL FUND
Co-financed by Greece and the European Union

E4 References

Aiken, A. C., DeCarlo, P. F., Kroll, J. H., Worsnop, D. R., Huffman, J. A., Docherty, K. S., Ulbrich, I. M., Mohr, C., Kimmel, J. R., Sueper, D., Sun, Y., Zhang, Q., Trimborn, A., Northway, M., Ziemann, P. J., Canagaratna, M. R., Onasch, T. B., Alfarra, M. R., Prevot, A. S. H., Dommen, J., Duplissy, J., Metzger, A., Baltensperger, U., and Jimenez, J. L. (2008). O/C and OM/OC ratios of primary, secondary, and ambient organic aerosols with high-resolution time-of-flight aerosol mass spectrometry, Environ. Sci. Technol., 42, 4478-4485, doi:10.1021/es703009q.

Aiken, A. C., Salcedo, D., Cubison, M. J., Huffman, J. A., DeCarlo, P. F., Ulbrich, I. M., Docherty, K. S., Sueper, D., Kimmel, J. R., Worsnop, D. R., Trimborn, A., Northway, M., Stone, E. A., Schauer, J. J., Volkamer, R. M., Fortner, E., de Foy, B., Wang, J., Laskin, A., Shutthanandan, V., Zheng, J., Zhang, R., Gaffney, J., Marley, N. A., Paredes-Miranda, G., Arnott, W. P., Molina, L. T., Sosa, G., and Jimenez, J. L. (2009). Mexico City aerosol analysis during MILAGRO using high resolution aerosol mass spectrometry at the urban supersite (T0) – Part 1: Fine particle composition and organic source apportionment, Atmos. Chem. Phys., 9, 6633-6653.

Akagi, S. K., Yokelson, R. J., Wiedinmyer, C., Alvarado, M. J., Reid, J. S., Karl, T., Crounse, J. D., and Wennberg, P. O. (2011). Emission factors for open and domestic biomass burning for use in atmospheric models. Atmospheric Chemistry and Physics, 11:4039–4072.

Alfarra, M. R., Paulsen, D., Gysel, M., Garforth, A. A., Dommen, J., Prevot, A. S. H.,Worsnop, D. R., Baltensperger, U., and Coe, H. (2006). A mass spectrometric study of secondary organic aerosols formed from the photooxidation of anthropogenic and biogenic precursors in a reaction chamber., Atmos. Chem. Phys., 6, 5279– 5293.

Alfarra, M. R., Prevot, A. S. H., Szidat, S., Sandradewi, J., Weimer, S., Lanz, V. a., Schreiber, D., Mohr, M., and Baltensperger, U. (2007). Identification of the mass

spectral signature of organic aerosols from wood burning emissions. Environmental Science & Technology, 41:5770–7.

Allan, J. D., Alfarra, M. R., Bower, K. N., Williams, P. I., Gallagher, M. W., Jimenez, J. L., McDonald, A. G., Nemitz, E., Canagaratna, M. R., Jayne, J. T., Coe, H., and Worsnop, D. R. (2003). Quantitative Sampling Using an Aerodyne Aerosol Mass Spectrometer 2.Measurements of Fine Particulate Chemical Composition in Two U.K. Cities, J. Geophys. Res., 108, 4091–4112.

Allan, J. D., Delia, A. E., Coe, H., Bower, K. N., Alfarra, M., Jimenez, J. L., Middlebrook, A. M., Drewnick, F., Onasch, T. B., Canagaratna, M. R., Jayne, J. T., and Worsnop, D. R. (2004). A generalised method for the extraction of chemically resolved mass spectra from Aerodyne aerosol mass spectrometer data. Journal of Aerosol Science, 35:909–922.

Allan, J. D., Williams, P. I., Morgan, W. T., Martin, C. L., Flynn, M. J., Lee, J., Nemitz, E., Phillips, G. J., Gallagher, M. W., and Coe, H. (2010). Contributions from transport, solid fuel burning and cooking to primary organic aerosols in two UK cities. Atmospheric Chemistry and Physics, 10(2):647–668.

An, W. J., Pathak, R. K., Lee, B.-H., and Pandis, S. N. (2007). Aerosol volatility measurement using an improved thermodenuder: Application to secondary organic aerosol. Journal of Aerosol Science, 38(3):305–314.

Argyropoulos, G., Manoli, E., Kouras, A., and Samara, C. (2012). Concentrations and source apportionment of PM10 and associated major and trace elements in the Rhodes Island, Greece, Sci. Total Environ., 432, 12–22.

Bond, T. C. (2004). A technology-based global inventory of black and organic carbon emissions from combustion. Journal of Geophysical Research, 109:D14203.

Bougiatioti, A., Stavroulas, I., Kostenidou, E., Zarmpas, P., Theodosi, C., Kouvarakis, G., Canonaco, F., Prévôt, A. S. H., Nenes, A., Pandis, S. N., and Mihalopoulos, N. (2014). Processing of biomass-burning aerosol in the eastern Mediterranean during summertime, Atmos. Chem. Phys., 14, 4793-4807.

Canagaratna, M. R., Jayne, J. T., Ghertner, D. a., Herndon, S., Shi, Q., Jimenez, J. L., Silva, P. J., Williams, P., Lanni, T., Drewnick, F., Demerjian, K. L., Kolb, C. E.,

European Union
European Social Fund
OPERATIONAL PROGRAMME
EDUCATION AND LIFELONG LEARNING
investing in knowledge society
MINISTRY OF EDUCATION & RELIGIOUS AFFAIRS
MANAGING AUTHORITY
NSRF 2007-2013
programme for development
EUROPEAN SOCIAL FUND
Co-financed by Greece and the European Union

and Worsnop, D. R. (2004). Chase Studies of Particulate Emissions from in-use New York City Vehicles. Aerosol Science and Technology, 38(6):555–573.

Canagaratna, M. R., Jayne, J. T., Jimenez, J. L., Allan, J. D., Al- farra, M. R., Zhang, Q., Onasch, T. B., Drewnick, F., Coe, H., Middlebrook, A., Delia, A., Williams, L. R., Trimborn, A. M., Northway, M. J., Kolb, C. E., Davidovits, P., and Worsnop, D. R. (2007). Chemical and microphysical characterization of ambient aerosols with the aerosol mass spectrometer, Mass. Spectrom. Rev., 26, 185–222.

Canagaratna, M. R., Jimenez, J. L., Kroll, J. H., Chen, Q., Kessler, S. H., Massoli, P., Hildebrandt Ruiz, L., Fortner, E., Williams, L. R., Wilson, K. R., Surratt, J. D., Donahue, N. M., Jayne, J. T., and Worsnop, D. R. (2015). Elemental ratio measurements of organic compounds using aerosol mass spectrometry: characterization, improved calibration, and implications, Atmos. Chem. Phys., 15, 253-272, doi:10.5194/acp-15-253-2015.

Chaloulakou A., Kassomenos, P., Spyrellis, N., Demokritou, P., and Koutrakis, P. (2003). Measurements of PM10 and $PM_{2.5}$ particle concentrations in Athens, Greece, Atmos. Environ., 37, 649–660.

Cottrell, L. D., Griffin, R. J., Jimenez, J. L., Zhang, Q., Ulbrich, I., Ziemba, L. D., Beckman, P. J., Sive, B. C., and Talbot, R. W. (2008). Submicron particles at Thompson Farm during ICARTT mea- sured using aerosol mass spectrometry, J. Geophys. Res. Atmos., 113, D08212, doi:10.1029/2007JD009192.

Crippa, M., DeCarlo, P. F., Slowik, J. G., Mohr, C., Heringa, M. F., Chirico, R., Poulain, L., Freutel, F., Sciare, J., Cozic, J., Di Marco, C. F., Elsasser, M., Jose, N., Marchand, N., Abidi, E., Wiedensohler, A., Drewnick, F., Schneider, J., Borrmann, S., Nemitz, E., Zimmermann, R., Jaffrezo, J.-L., Prévôt, A. S. H., and Baltensperger, U. (2013b). Wintertime aerosol chemical composition and source apportionment of the organic fraction in the metropolitan area of Paris, Atmos. Chem. Phys., 13, 961–98.

Dall'Osto, M. and Harrison, R. M. (2006). Chemical characterization of single airborne particles in Athens (Greece) by ATOFMS, At- mos. Environ., 40, 7614–7631.

European Union
European Social Fund
OPERATIONAL PROGRAMME
EDUCATION AND LIFELONG LEARNING
investing in knowledge society
MINISTRY OF EDUCATION & RELIGIOUS AFFAIRS
MANAGING AUTHORITY
NSRF 2007-2013
EUROPEAN SOCIAL FUND
Co-financed by Greece and the European Union

DeCarlo, P.F., Kimmel, J. R., Trimborn, A., Northway, M. J., Jayne, J. T., Aiken, A. C., Gonin, M., Fuhrer, K., Horvath, T., Docherty, K., Worsnop, D. R., and Jimenez, J. L. (2006). Field-Deployable, High-Resolution, Time-of-Flight Aerosol Mass Spectrometer, Analytical Chemistry, 78: 8281-8289.

Docherty, K. S., Aiken, A. C., Huffman, J. A., Ulbrich, I. M., DeCarlo, P. F., Sueper, D., Worsnop, D. R., Snyder, D. C., Peltier, R. E., Weber, R. J., Grover, B. D., Eatough, D. J., Williams, B. J., Goldstein, A. H., Ziemann, P. J., and Jimenez, J. L. (2011) The 2005 Study of Organic Aerosols at Riverside (SOAR-1): Instrumental intercomparisons and fine particle composition, Atmos. Chem. Phys., 11, 12387-12420.

Drewnick, F., Hings, S. S., DeCarlo, P., Jayne, J. T., Gonin, M., Fuhrer, K., Weimer, S., Jimenez, J. L., Demerjian, K. L., Borrmann, S., and Worsnop, D. R. (2005). A New Time-of-Flight Aerosol Mass Spectrometer (TOF-AMS) Instrument Description and First Field Deployment. Aerosol Science and Technology, 39:637–658.

Farmer, D.K., Matsunaga, A., Docherty, K. S., Surratt, J. D., Seinfeld, J. H., Ziemann P. J., and Jimenez, J. L. (2010). Response of an aerosol mass spectrometer to organonitrates and organosulfates and implications for atmospheric chemistry. Proceedings of the National Academy of Sciences, 107, 6670-6675.

Favez, O., El Haddad, I., Piot, C., Boreave, A., Abidi, E., Marchand, N., Jaffrezo, J.-L., Besombes, J.-L., Personnaz, M.-B., Sciare, J., Wortham, H., George, C., and D'Anna, B. (2010). Inter-comparison of source apportionment models for the estimation of wood burning aerosols during wintertime in an Alpine city (Grenoble, France), Atmos. Chem. Phys., 10, 5295–5314, doi:10.5194/acp-10-5295- 2010.

Fry, J. L., Kiendler-Scharr, A., Rollins, A. W., Wooldridge, P. J., Brown, S. S., Fuchs, H., Dube, W., Mensah, A., dal Maso, M., Tillmann, R., Dorn, H.-P., Brauers, T., and Cohen, R. C. (2009). Organic nitrate and secondary organic aerosol yield from NO_3 oxidation of β-pinene evaluated using a gas-phase kinetics/aerosol partitioning model, Atmos. Chem. Phys., 9, 1431– 1449.

European Union
European Social Fund
OPERATIONAL PROGRAMME
EDUCATION AND LIFELONG LEARNING
investing in knowledge society
MINISTRY OF EDUCATION & RELIGIOUS AFFAIRS
MANAGING AUTHORITY
NSRF 2007-2013
EUROPEAN SOCIAL FUND
Co-financed by Greece and the European Union

Fuller, G.W., Sciare, J., Lutz, M., Moukhtar, S., Wagener, S., (2013). New Directions: time to tackle urban wood burning? Atmos. Environ. 68, 295-296.

Fuller, G.W., Tremper, A.H., Baker, T.D., Yttri, K.E., Butterfield, D., (2014). Contribution of wood burning to PM_{10} in London. Atmos. Environ., 87,87–94.

Gaidajis G., Angelakoglou K., Aktsoglou D., (2014). Wintertime particulate mass concentrations in urban environment and the impact of economic crisis – Evidence from Greece, Journal of Environmental Science and Health, Part A, Vol. 49, 1653-1660.

Gkatzelis, G. I., Papanastasiou, D. K., Florou, K., Kaltsonoudis, C., Louvaris, E., and Pandis, S. N., (2015). Measurement of non-volatile particle number size distribution, Atmos. Meas. Tech. Discuss., 6355-6393.

Grantz, D. a., Garner, J. H. B., and Johnson, D. W. (2003). Ecological effects of particulate matter. Environment international, 29:213–39.

Grieshop, A. P., Donahue, N. M., and Robinson, A. L. (2009). Laboratory investigation of photochemical oxidation of organic aerosol from wood fires 2: analysis of aerosol mass spectrometer data. Atmospheric Chemistry and Physics, 9:2227–2240.

Hallquist, M., Wenger, J. C., Baltensperger, U., Rudich, Y., Simpson, D., Claeys, M., Dommen, J., Donahue, N. M., George, C., Goldstein, A. H., Hamilton, J. F., Herrmann, H., Hoffmann, T., Iinuma, Y., Jang, M., Jenkin, M. E., Jimenez, J. L., Kiendler-Scharr, A., Maenhaut, W., Mc- Figgans, G., Mentel, T. F., Monod, A., Prevot, A. S. H., Seinfeld, J. H., Surratt, J. D., Szmigielski, R., and Wildt, J. (2009). The formation, prop- erties and impact of secondary organic aerosol: current and emerging is- sues. Atmospheric Chemistry and Physics, 9:5155–5236.

Hao, L. Q., Kortelainen, A., Romakkaniemi, S., Portin, H., Jaatinen, A., Leskinen, A., Komppula, M., Miettinen, P., Sueper, D., Pajunoja, A., Smith, J. N., Lehtinen, K. E. J., Worsnop, D. R., Laaksonen, A., and Virtanen, A. (2014). Atmospheric submicron aerosol composition and particulate organic nitrate formation in a boreal forestland–urban mixed region, Atmos. Chem. Phys., 14, 13483-13495, doi:10.5194/acp-14-13483-2014.

European Union
European Social Fund
OPERATIONAL PROGRAMME
EDUCATION AND LIFELONG LEARNING
investing in knowledge society
MINISTRY OF EDUCATION & RELIGIOUS AFFAIRS
MANAGING AUTHORITY
NSRF 2007-2013
programme for development
EUROPEAN SOCIAL FUND
Co-financed by Greece and the European Union

He, L.-Y., Lin, Y., Huang, X.-F., Guo, S., Xue, L., Su, Q., Hu, M., Luan, S.-J., and Zhang, Y.-H. (2010). Characterization of high-resolution aerosol mass spectra of primary organic aerosol emissions from Chinese cooking and biomass burning. Atmospheric Chemistry and Physics, 10:11535– 11543.

Herndon, S. C., Jayne, J. T., Lobo, P., Onasch, T. B., Fleming, G., Hagen, D. E., Whitefield, P. D., and Miake-Lye, R. C. (2008). Commercial aircraft engine emissions characterization of in-use aircraft at Hartsfield- Jackson Atlanta International Airport. Environmental Science & Technology, 42:1877–83.

Huang, M., Carmichael, G. R., Spak, S. N., Adhikary, B., Kulkarni, S., Cheng, Y., Wei, C., Tang, Y., D'Allura, a., Wennberg, P. O., Huey, G. L., Dibb, J. E., Jimenez, J. L., Cubison, M. J., Weinheimer, a. J., Kaduwela, a., Cai, C., Wong, M., Bradley Pierce, R., Al-Saadi, J. a., Streets, D. G., and Zhang, Q. (2011). Multi-scale modeling study of the source con- tributions to near-surface ozone and sulfur oxides levels over California during the ARCTAS-CARB period. Atmospheric Chemistry and Physics, 11:3173–3194.

Hudson, P.K., Murphy, D.M., Cziczo, D.J., Thomson, D.S., de Gouw, J.A., Warneke, C., Holloway, J., Jost, H.-J., Hubler, G. (2005). Biomass-Burning Particle Measurements: Characteristic Composition and Chemical Processing, J. Geophys. Res. 2005, 109, D23S27.

Jayne, J. T., Leard, D. C., Zhang, X., Davidovits, P., Smith, K. A., Kolb, C. E., and Worsnop, D. R. (2000). Development of an Aerosol Mass Spectrometer for Size and Composition Analysis of Submicron Particles. Aerosol Science and Technology, 33:49–70.

Jimenez, J. L. (2003). Ambient aerosol sampling using the Aerodyne Aerosol Mass Spectrometer. Journal of Geophysical Research, 108(D7):8425.

Jimenez, J. L., Canagaratna, M. R., Donahue, N. M., Prevot, a. S. H., Zhang, Q., Kroll, J. H., DeCarlo, P. F., Allan, J. D., Coe, H., Ng, N. L., Aiken, a. C., Docherty, K. S., Ulbrich, I. M., Grieshop, a. P., Robinson, a. L., Du- plissy, J., Smith, J. D., Wilson, K. R., Lanz, V. a., Hueglin, C., Sun, Y. L., Tian, J., Laaksonen, a., Raatikainen, T., Rautiainen, J., Vaattovaara, P., Ehn, M., Kulmala, M., Tomlinson,

European Union
European Social Fund
OPERATIONAL PROGRAMME
EDUCATION AND LIFELONG LEARNING
investing in knowledge society
MINISTRY OF EDUCATION & RELIGIOUS AFFAIRS
MANAGING AUTHORITY
NSRF 2007-2013
EUROPEAN SOCIAL FUND
Co-financed by Greece and the European Union

J. M., Collins, D. R., Cubison, M. J., Dunlea, E. J., Huffman, J. a., Onasch, T. B., Alfarra, M. R., Williams, P. I., Bower, K., Kondo, Y., Schneider, J., Drewnick, F., Borrmann, S., Weimer, S., Demerjian, K., Salcedo, D., Cottrell, L., Griffin, R., Takami, a., Miyoshi, T., Hatakeyama, S., Shimono, a., Sun, J. Y., Zhang, Y. M., Dzepina, K., Kimmel, J. R., Sueper, D., Jayne, J. T., Herndon, S. C., Trimborn, a. M., Williams, L. R., Wood, E. C., Middlebrook, a. M., Kolb, C. E., Baltensperger, U., and Worsnop, D. R. (2009). Evolution of organic aerosols in the atmosphere. Science (New York, N.Y.), 326(5959):1525–9.

Kaltsonoudis, C., Kostenidou, E., Florou, K., Psichoudaki, M., and Pandis, S. N.: Temporal Variability of VOCs in the Eastern Mediterranean. In preparation.

Kanakidou, M., Seinfeld, J. H., Pandis, S. N., Barnes, I., Dentener, F. J., Facchini, M. C., Van Dingenen, R., Ervens, B., Nenes, a., Nielsen, C. J., Swietlicki, E., Putaud, J. P., Balkanski, Y., Fuzzi, S., Horth, J., Moort- gat, G. K., Winterhalter, R., Myhre, C. E. L., Tsigaridis, K., Vignati, E., Stephanou, E. G., and Wilson, J. (2005). Organic aerosol and global climate modelling: a review. Atmospheric Chemistry and Physics, 5:1053– 1123.

Katragkou, E., Kazadzis, S., Amiridis, V., Papaioannou, V., Karathanasis, S. and Melas, D. (2009). PM_{10} regional transport pathways in Thessaloniki, Greece, Atmospheric Environment, 43, 1079-1085.

Kostenidou, E., Pathak, R. K., and Pandis, S. N. (2007). An Algorithm for the Calculation of Secondary Organic Aerosol Density Combining AMS and SMPS Data. Aerosol Science and Technology, 41:1002–1010.

Kostenidou, E., Lee, B. H., Engelhart, G. J., Pierce, J. R., and Pan- dis, S. N. (2009.). Mass spectra deconvolution of low, medium and high volatility biogenic secondary organic aerosol, Environ. Sci. Technol., 43, 4884–4889

Kostenidou, E., Kaltsonoudis, C., Tsiflikiotou, M., Louvaris, E., Russell, L. M., and Pandis S. N. (2013). Burning of olive tree branches: a major organic aerosol source in the Mediterranean, Atmos. Chem. Phys., 13, 8797–8811.

Kostenidou E., Florou K., Kaltsonoudis C., Tsiflikiotou M., Vratolis S., Eleftheriadis K., and Pandis S. N. (2015). Sources and chemical characterization of organic aerosol

European Union
European Social Fund
OPERATIONAL PROGRAMME
EDUCATION AND LIFELONG LEARNING
investing in knowledge society
MINISTRY OF EDUCATION & RELIGIOUS AFFAIRS
MANAGING AUTHORITY
NSRF 2007-2013
programme for development
EUROPEAN SOCIAL FUND
Co-financed by Greece and the European Union

during the summer in the eastern Mediterranean, Atmospheric Chemistry and Physics Discuss., 15, 3455-3491, doi:10.5194/acpd-15-3455-2015.

Koulouri, E., Saarikoski, S., Theodosi, C., Markaki, Z., Gerasopoulos, E., Kouvarakis, G., Makela, T., Hillamo, R., and Mihalopoulos, N. (2008). Chemical composition and sources of fine and coarse aerosol particles in the Eastern Mediterranean, Atmos. Environ., 42, 6542–6550.

Kroll, J. H., Donahue, N. M., Jimenez, J. L., Kessler, S. H., Cana- garatna, M. R., Wilson, K. R., Altieri, K. E., Mazzoleni, L. R., Wozniak, A. S., Bluhm, H., Mysak, E. R., Smith, J. D., Kolb, C. E., and Worsnop, D. R. (2011). Carbon Oxidation State as a Metric for Describing the Chemistry of Atmospheric Organic Aerosol, Nature Chemistry, 3, 133–139.

Lanz, V. A., Alfarra, M. R., Baltensperger, U., Buchmann, B., Hueglin, C., and Pr´evot, A. S. H. (2007). Source apportionment of submicron organic aerosols at an urban site by factor analytical modelling of aerosol mass spectra. Atmospheric Chemistry and Physics, 7:1503–1522.

Lanz, V. A., Alfarra, M. R., Baltensperger, U., Buchmann, B., Hueglin, C., Szidat, S., Wehrli, M. N., Wacker, L., Weimer, S., Caseiro, A., Puxbaum, J., and Prévôt, A. S. H. (2008). Source attribution of submicron organic aerosols during wintertime inversions by advanced factor analysis of aerosol mass spectra, Environ. Sci. Technol., 42, 214-220.

Lelieveld, J., Crutzen, P. J., Ramanathan, V., and Andreae, M. O. (2001). The Indian Ocean Experiment : Widespread Air Pollution from South and Southeast Asia.

Louvaris, E.: Determination of ambient OA volatility in the city of Athens. In preparation.

Mohr, C., Huffman, J. A., Cubison, M. J., Aiken, A. C., Docherty, K. S., Kim- mel, J. R., Ulbrich, I. M., Hannigan, M., and Jimenez, J. L. (2009). Char- acterization of Primary Organic Aerosol Emissions from Meat Cooking, Trash Burning, and Motor Vehicles with High-Resolution Aerosol Mass Spectrometry and Comparison with Ambient and Chamber Observations. Environmental Science & Technology, 43:2443–2449.

European Union
European Social Fund
OPERATIONAL PROGRAMME
EDUCATION AND LIFELONG LEARNING
investing in knowledge society
MINISTRY OF EDUCATION & RELIGIOUS AFFAIRS
MANAGING AUTHORITY
NSRF 2007-2013
EUROPEAN SOCIAL FUND
Co-financed by Greece and the European Union

Mohr, C., DeCarlo, P. F., Heringa, M. F., Chirico, R., Slowik, J. G., Richter, R., Reche, C., Alastuey, A., Querol, X., Seco, R., Peñuelas, J., Jimenez, J. L., Crippa, M., Zimmermann, R., Baltensperger, U., and Prévôt, A. S. H. (2012). Identification and quantification of organic aerosol from cooking and other sources in Barcelona using aerosol mass spectrometer data, Atmos. Chem. Phys., 12, 1649–1665.

Nel, A.: Air pollution-related illness: Effects of particles, Science, 308, 804–806, 2005.

Paatero, P. and Tapper, U. (1994). Positive matrix factorization: A non- negative factor model with optimal utilization of error estimates of data values. Environmetrics, 5:111–126.

Paraskevopoulou, D., Liakakou, E., Gerasopoulos, E., Theodosi, C., and Mi- halopoulos, N. (2014). Long-term characterization of organic and elemental carbon in the $PM_{2.5}$ fraction: the case of Athens, Greece. Atmospheric Chemistry and Physics, 14:13313–13325.

Petrakakis, M.J.; Kelessis, A.G.; Tzoumaka, P.; Samara, C. (2013). In Levels of Suspended Particulate Matter before and after the Economic Crisis in Thessaloniki, Greece, Proceedings of 17th International Symposium on Environmental Pollution and its Impact on Life in the Mediterranean Region, Istanbul, Turkey, Sept 28–Oct 1, 2013. Mediterranean Scientific Association of Environmental Protection (MESAEP).

Petzold, A. and Schönlinner, M. (2004). Multi-angle absorption photometry a new method for the measurement of aerosol light absorption and atmospheric black carbon. Journal of Aerosol Science, 35:421–441.

Pikridas, M., Tasoglou, A., Florou, K., and Pandis, S. N. (2013). Characterization of the origin of fine particulate matter in a medium size urban area in the Mediterranean. Atmospheric Environment, 80:264–274.

Puxbaum, H., Caseiro, A., S´anchez-Ochoa, A., Kasper-Giebl, A., Claeys, M., Gelencser, A., Legrand, M., Preunkert, S., and Pio, C. (2007). Levoglucosan levels at background sites in Europe for assessing the impact of biomass combustion on the

European Union
European Social Fund
OPERATIONAL PROGRAMME
EDUCATION AND LIFELONG LEARNING
investing in knowledge society
MINISTRY OF EDUCATION & RELIGIOUS AFFAIRS
MANAGING AUTHORITY
NSRF 2007-2013
programme for development
EUROPEAN SOCIAL FUND
Co-financed by Greece and the European Union

European aerosol background. Journal of Geophysical Research, 112(D23):D23S05.

Robinson, A. L., Subramanian, R., Donahue, N. M., Bernardo-Bricker, A., and Rogge, W. F. (2006). Source Apportionment of Molecular Markers and Organic Aerosol. 3. Food Cooking Emissions. Environmental Science & Technology, 40:7820–7827.

Saarikoski, S., Carbone, S., Decesari, S., Giulianelli, L., Angelini, F., Canagaratna, M., Ng, N. L., Trimborn, a., Facchini, M. C., Fuzzi, S., Hillamo, R., and Worsnop, D. (2012). Chemical characterization of springtime submicrometer aerosol in Po Valley, Italy. Atmospheric Chemistry and Physics, 12:8401–8421.

Sage, A. M., Weitkamp, E. A., Robinson, A. L., and Donahue, N. M. (2008). Evolving mass spectra of the oxidized component of organic aerosol: results from aerosol mass spectrometer analyses of aged diesel emissions. Atmospheric Chemistry and Physics, 8(5):1139–1152.

Schauer, J. J., and G. R. Cass (2000). Source apportionment of wintertime gas-phase and particle-phase air pollutants using organic compounds as tracers, Environ. Sci. Technol., 34, 1821–1832, doi:10.1021/-s981312t.

Schneider, J., Hock, N., Weimer, S., Borrmann, S., Kirchner, U., Vogt, R., and Scheer, V. (2005). Nucleation particles in diesel exhaust: composition inferred from in situ mass spectrometric analysis. Environmental science & technology, 39:6153–61.

Sciare, J., Oikonomou, K., Favez, O., Liakakou, E., Markaki, Z., Cachier, H., and Mihalopoulos, N. (2008). Long-term measurements of carbonaceous aerosols in the Eastern Mediterranean: evidence of long-range transport of biomass burning, Atmos. Chem. Phys., 8, 5551–5563, doi:10.5194/acp-8-5551-2008.

Steinbacher, M., J. Dommen, C. Ammann, C. Spirig, A. Neftel, and A. S. H. Prevot (2004), Performance characteristics of a proton- transfer-reaction mass spectrometer (PTR-MS) derived from laboratory and field measurement, Int. J. Mass Spectrom., 239, 117–128.

European Union
European Social Fund
OPERATIONAL PROGRAMME
EDUCATION AND LIFELONG LEARNING
investing in knowledge society
MINISTRY OF EDUCATION & RELIGIOUS AFFAIRS
MANAGING AUTHORITY
NSRF 2007-2013
EUROPEAN SOCIAL FUND
Co-financed by Greece and the European Union

Stohl, A., Eckhardt, S., Forster, C., James, P., and Spichtinger, N. (2002). On the pathways and timescales of intercontinental air pollution transport, J. Geophys. Res., 107, 4684, doi:10.1029/2001JD001396.

Stohl, A., Forster, V., Frank, A., Seibert, P., & Wotawa, G. (2005). Technical Note: The Lagrangian particle dispersion model FLEXPART version 6.2, Atmos. Chem. Phys., 5, 2461–2474.

Sullivan, A., Holden, A., Patterson, L., McMeeking, G., Kreidenweis, S., Malm, W., Hao, W., Wold, C., Collett Jr., J., (2008). A method for smoke marker measurements and its potential application for determining the contribution of biomass burning from wildfires and prescribed fires to ambient $PM_{2.5}$ organic carbon. Journal of Geophysical Researche Atmospheres 113. doi:10.1029/ 2008JD010216.

Sueper, D.: ToF-AMS High Resolution Analysis Software – Pika, online available at: http://cires.colorado.edu/jimenez-group/ ToFAMSResources/ToFSoftware, 2011.

Sun, Y. L., Zhang, Q., Schwab, J. J., Chen, W.-N., Bae, M.-S., Hung, H.-M., Lin, Y.-C., Ng, N. L., Jayne, J., Massoli, P., Williams, L. R., and Demerjian, K. L. (2012). Characterization of near-highway submicron aerosols in New York City with a high-resolution aerosol mass spectrometer. Atmospheric Chemistry and Physics, 12:2215–2227.

Theodosi, C., Grivas, G., Zarmpas, P., Chaloulakou, A., Mihalopoulos, N. (2011). Mass and chemical composition of size-segregated aerosols (PM_1,$PM_{2.5}$,PM_{10})over Athens, Greece: local versus regional sources. Atmospheric Chemistry and Physics 11, 11895-11911.

Trainer, M. G., Jimenez, J. L., Yung, Y. L., Toon, O. B., and Tolbert, M. A. (2012). Nitrogen Incorporation in CH_4-N_2 Photochemical Aerosol Produced by Far Ultraviolet Irradiation. Astrobiology. 315-326. doi:10.1089/ast.2011.0754.

Tsiflikiotou, T., Papanastasiou, D., Patoulias, D., Zarmpas, P., Paraskevopoulou, D., Diapouli, E., Kostenidou, E., Kaltsonoudis, C., Bougiatioti, A., Theodosi, C., Kouvarakis, G., Liakakou, E., Vassilatou, V., Siakavaras, D., Biskos, G., Eleftheriadis, K., Gerasopoulos, E., Mihalopoulos, N., and Pandis, S. N.: Spatial

European Union
European Social Fund
OPERATIONAL PROGRAMME
EDUCATION AND LIFELONG LEARNING
investing in knowledge society
MINISTRY OF EDUCATION & RELIGIOUS AFFAIRS
MANAGING AUTHORITY
NSRF 2007-2013
programme for development
EUROPEAN SOCIAL FUND
Co-financed by Greece and the European Union

distribution of summertime particulate matter and its composition in Greece (in preparation).

Turpin, B. J., and J. J. Huntzicker (1995), Identification of secondary organic aerosol episodes and quantification of primary and secondary organic aerosol concentrations during SCAQS, Atmos. Environ., 29, 3527–3544.

Ulbrich, I. M., Canagaratna, M. R., Zhang, Q., Worsnop, D. R., and Jimenez, J. L. (2009). Interpretation of organic components from Positive Matrix Factorization of aerosol mass spectrometric data. Atmospheric Chemistry and Physics, 9:2891–2918.

Vlasenko, a., Slowik, J. G., Bottenheim, J. W., Brickell, P. C., Chang, R. Y.-W., Macdonald, a. M., Shantz, N. C., Sjostedt, S. J., Wiebe, H. a., Leaitch, W. R., and Abbatt, J. P. D. (2009). Measurements of VOCs by proton transfer reaction mass spectrometry at a rural Ontario site: Sources and correlation to aerosol composition. Journal of Geophysical Research, 114(D21):D21305.

Watson, J. G. (2002). Visibility: Science and Regulation. Journal of the Air & Waste Management Association, 52:628–713.

Weimer, S., Alfarra, M.R., Schreiber, D., Mohr, M., Prévôt, A.S.H., Baltensperger, U., (2008). Organic aerosol mass spectral signatures from wood-burning emissions: influence of burning conditions and wood type. Journal of Geophysical Research e Atmospheres 113 (D10). doi:10.1029/2007JD009309.

Wotawa, G. and Trainer, M. (2000). The influence of Canadian forest fires on pollutant concentrations in the United States, Science, 288, 324, doi:10.1126/science.288.5464.324.

Zhang, H. and Ying, Q. (2010). Source apportionment of airborne particulate matter in Southeast Texas using a source-oriented 3D air quality model. Atmospheric Environment, 44:3547–3557.

Zhang, Q., Jimenez, J. L., Canagaratna, M. R., Allan, J. D., Coe, H., Ulbrich, I., Alfarra, M. R., Takami, A., Middlebrook, A. M., Sun, Y. L., Dzepina, K., Dunlea, E., Docherty, K., De- Carlo, P. F., Salcedo, D., Onasch, T., Jayne, J. T., Miyoshi, T., Shimono, A., Hatakeyama, S., Takegawa, N., Kondo, Y., Schneider, J., Drewnick, F., Borrmann, S., Weimer, S., Demerjian, K., Williams, P., Bower, K., Bahreini,

European Union
European Social Fund
OPERATIONAL PROGRAMME
EDUCATION AND LIFELONG LEARNING
investing in knowledge society
MINISTRY OF EDUCATION & RELIGIOUS AFFAIRS
MANAGING AUTHORITY
NSRF 2007-2013
EUROPEAN SOCIAL FUND
Co-financed by Greece and the European Union

R., Cottrell, L., Griffin, R. J., Rautiainen, J., Sun, J. Y., Zhang, Y. M., and Worsnop, D. R., (2007). Ubiquity and dominance of oxygenated species in organic aerosols in anthropogenically-influenced Northern Hemisphere midlatitudes, Geophys. Res. Lett., 34, L13801, doi:10.1029/2007gl029979.

Zhang, Y. M., Zhang, X. Y., Sun, J. Y., Hu, G. Y., Shen, X. J., Wang, Y. Q., Wang, T. T., Wang, D. Z., and Zhao, Y. (2014). Chemical composition and mass size distribution of PM1 at an elevated site in central east China, Atmos. Chem. Phys., 14, 12237-12249, doi:10.5194/acp-14-12237-2014.

European Union
European Social Fund
OPERATIONAL PROGRAMME
EDUCATION AND LIFELONG LEARNING
investing in knowledge society
MINISTRY OF EDUCATION & RELIGIOUS AFFAIRS
MANAGING AUTHORITY
NSRF 2007-2013
programme for development
EUROPEAN SOCIAL FUND
Co-financed by Greece and the European Union

Figure E1. The location of the sampling sites.

(a) The location of Patras and Athens in Greece.

(b) The Technological Educational Institute (TEI) and the city center of Patras.

(c) The National Observatory (Thiseio) in Athens.

European Union
European Social Fund
OPERATIONAL PROGRAMME
EDUCATION AND LIFELONG LEARNING
investing in knowledge society
MINISTRY OF EDUCATION & RELIGIOUS AFFAIRS
MANAGING AUTHORITY
NSRF 2007-2013
programme for development
EUROPEAN SOCIAL FUND
Co-financed by Greece and the European Union

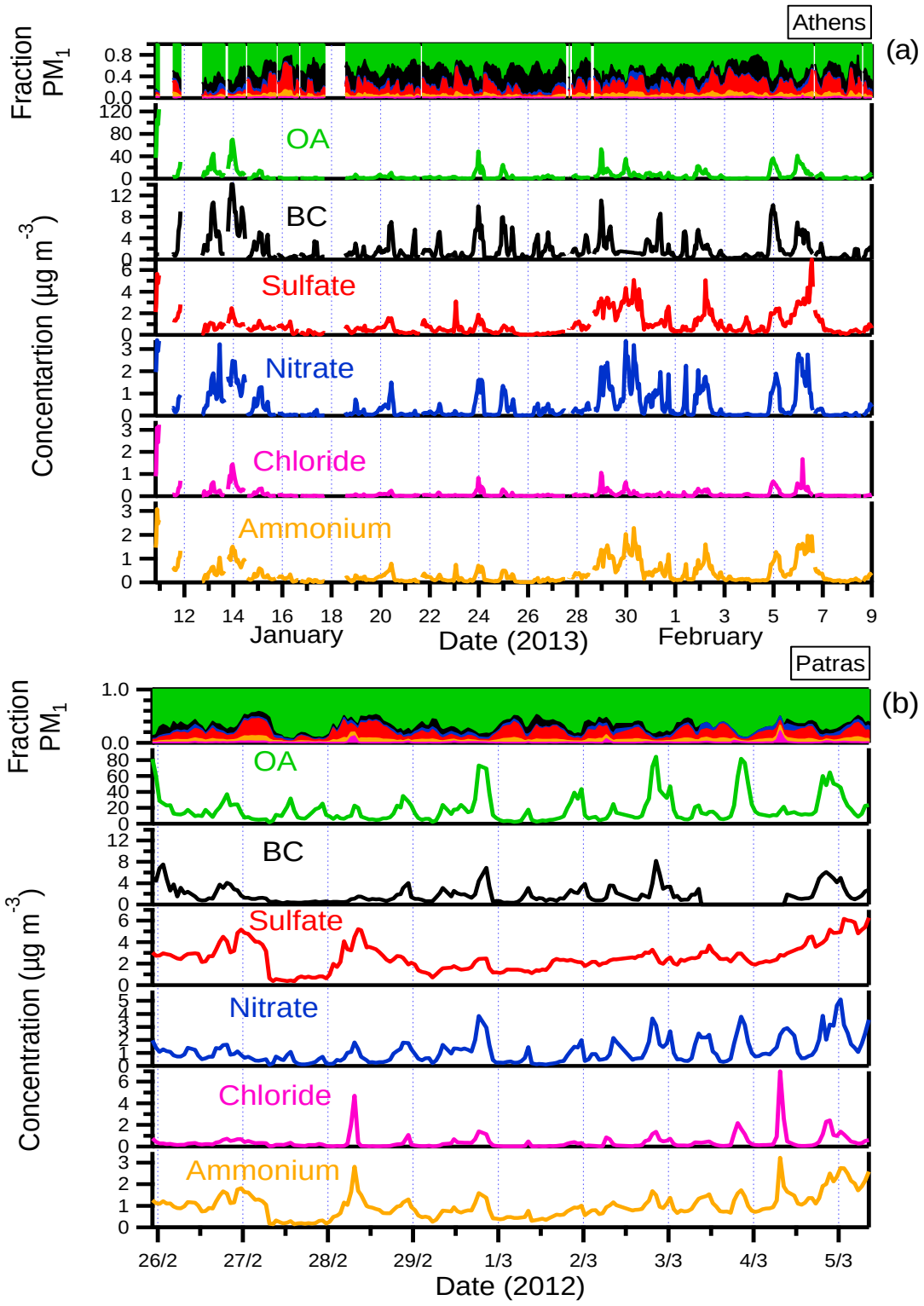

Figure E2. The hourly time series of the main PM_1 species during the (a) Athens and (b) Patras campaigns.

European Union
European Social Fund
OPERATIONAL PROGRAMME
EDUCATION AND LIFELONG LEARNING
investing in knowledge society
MINISTRY OF EDUCATION & RELIGIOUS AFFAIRS
MANAGING AUTHORITY
NSRF 2007-2013
EUROPEAN SOCIAL FUND
Co-financed by Greece and the European Union

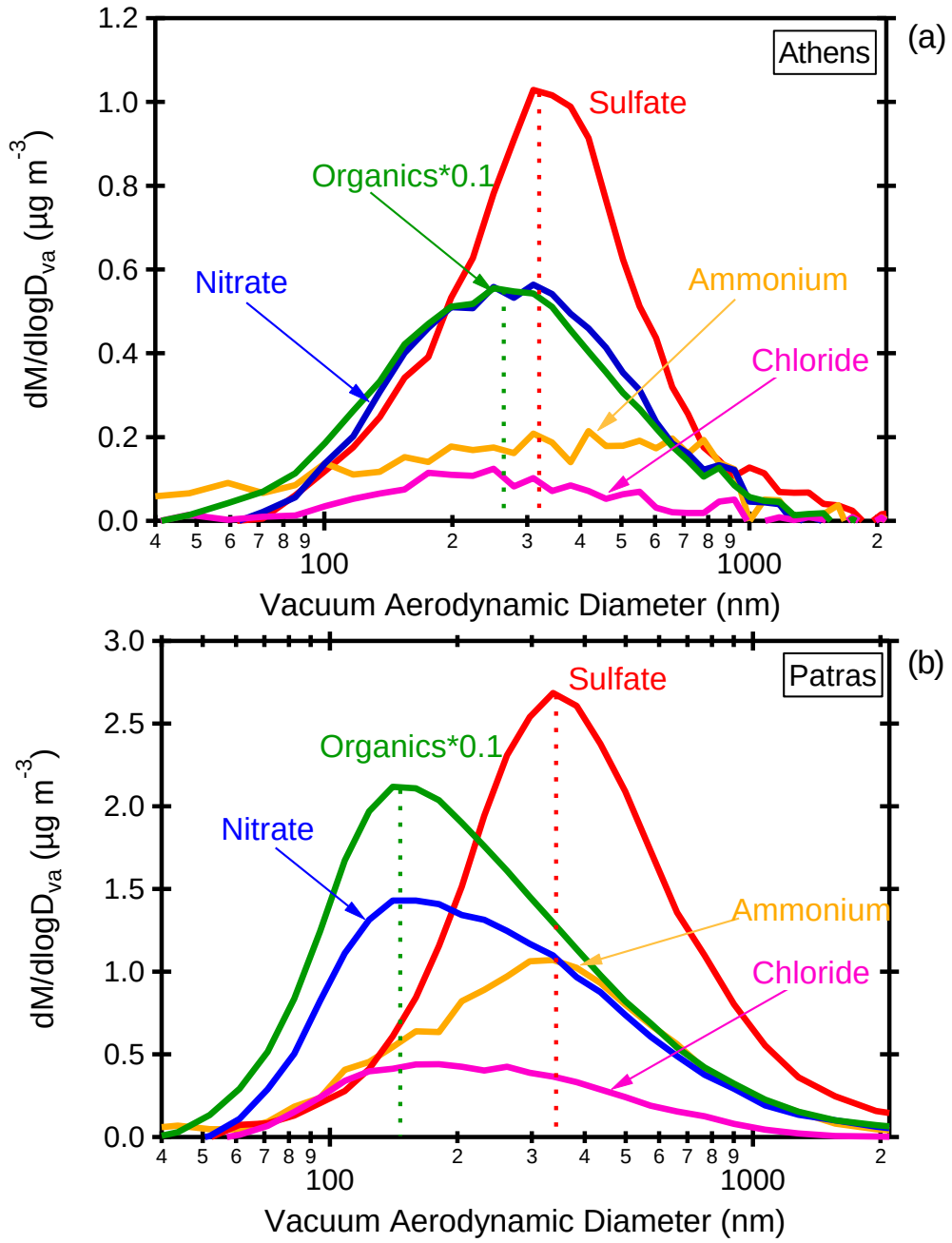

Figure E3. The (a) Athens and (b) Patras size distributions measured by the HR-AMS as a function of the vacuum aerodynamic diameter. The modes of the size distribution of the organics and sulfates are marked with dashed lines.

European Union
European Social Fund
OPERATIONAL PROGRAMME
EDUCATION AND LIFELONG LEARNING
investing in knowledge society
MINISTRY OF EDUCATION & RELIGIOUS AFFAIRS
MANAGING AUTHORITY
NSRF 2007-2013
EUROPEAN SOCIAL FUND
Co-financed by Greece and the European Union

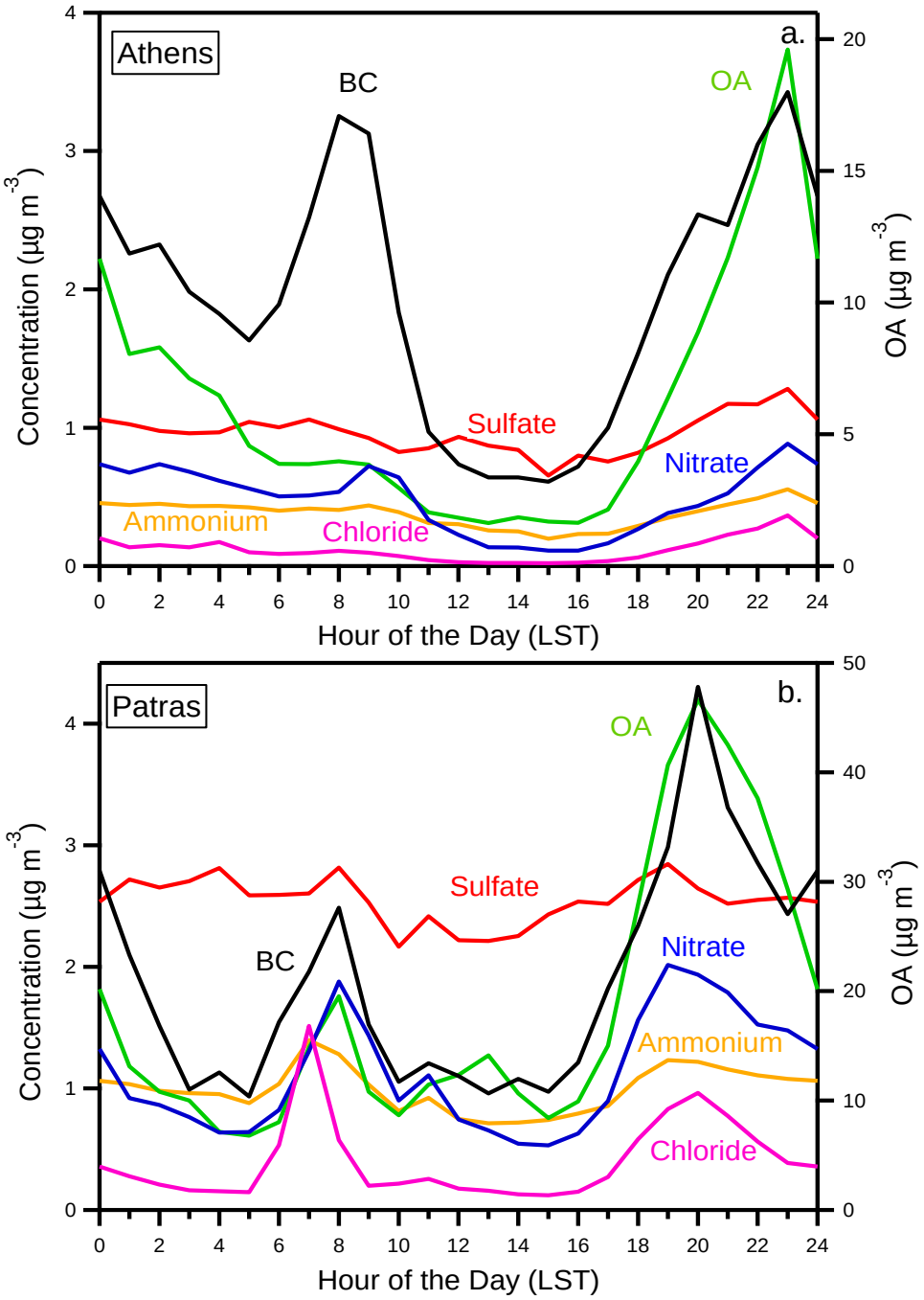

Figure E4. Average diurnal profiles for the main PM_1 species during the (a) Athens and (b) Patras campaigns. The concentration of OA is shown in the right y-axis.

European Union
European Social Fund
OPERATIONAL PROGRAMME
EDUCATION AND LIFELONG LEARNING
investing in knowledge society
MINISTRY OF EDUCATION & RELIGIOUS AFFAIRS
MANAGING AUTHORITY
NSRF 2007-2013
EUROPEAN SOCIAL FUND
Co-financed by Greece and the European Union

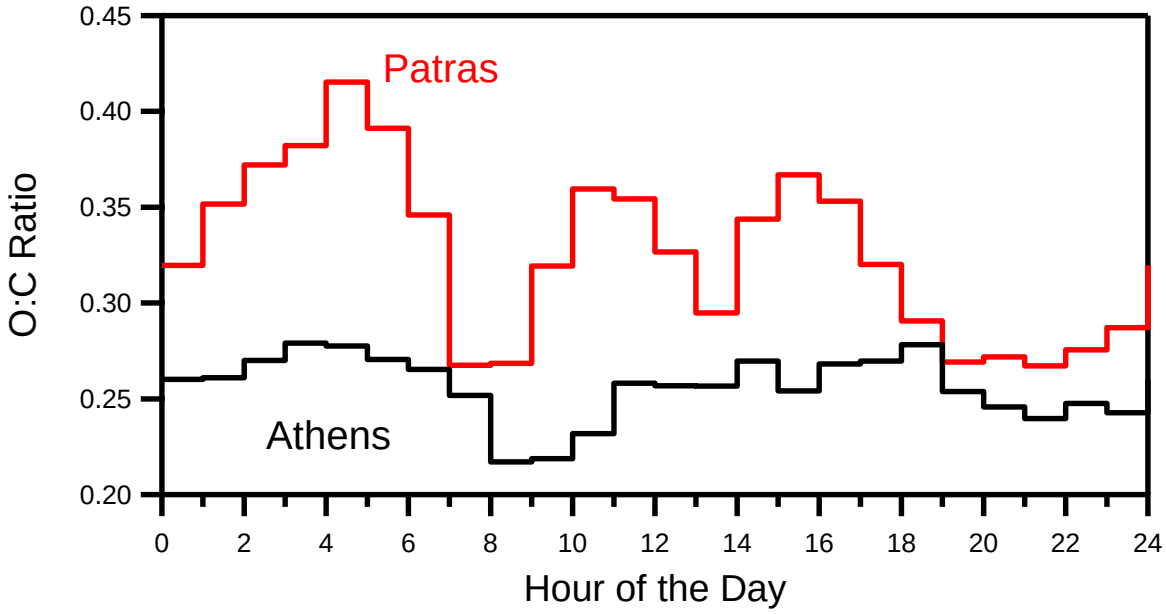

Figure E5. The diurnal profile of the O:C ratio in Athens (black) and Patras (red).

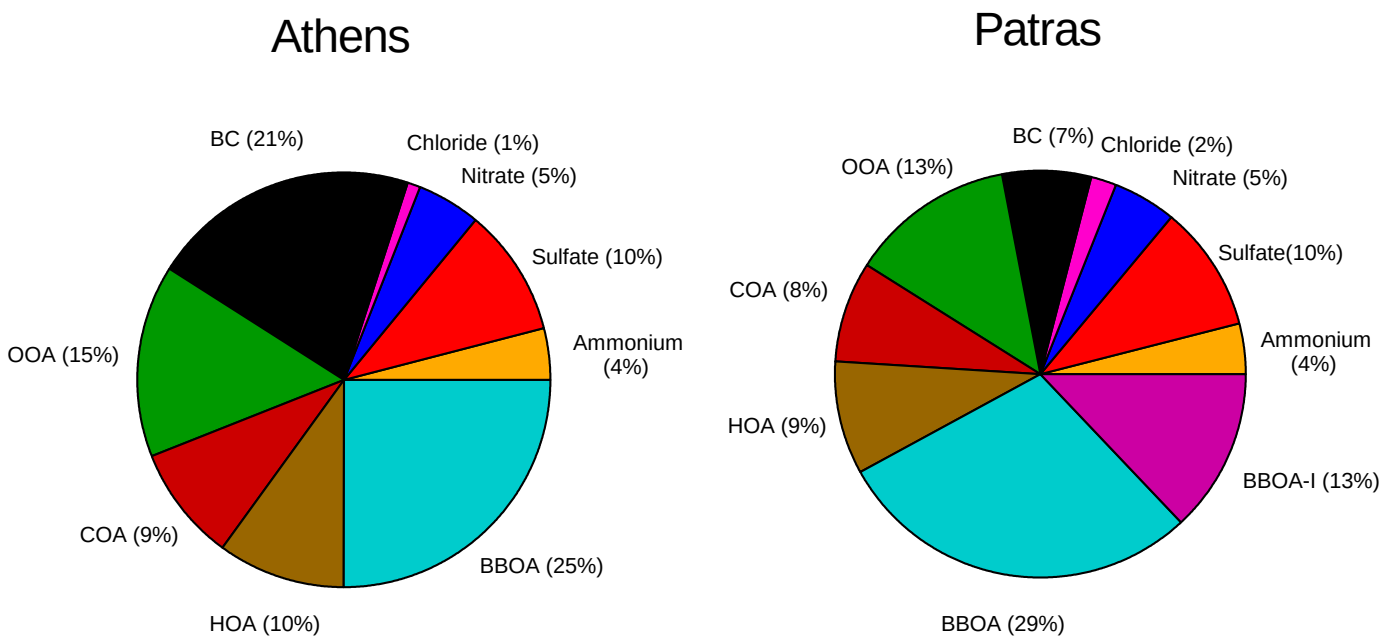

Figure E6. The average PM_1 mass balance and organics source apportionment. The average PM_1 for Athens was 10 μg m^{-3} while for Patras 25 μg m^{-3}.

European Union
European Social Fund
OPERATIONAL PROGRAMME
EDUCATION AND LIFELONG LEARNING
investing in knowledge society
MINISTRY OF EDUCATION & RELIGIOUS AFFAIRS
MANAGING AUTHORITY
NSRF 2007-2013
EUROPEAN SOCIAL FUND
Co-financed by Greece and the European Union

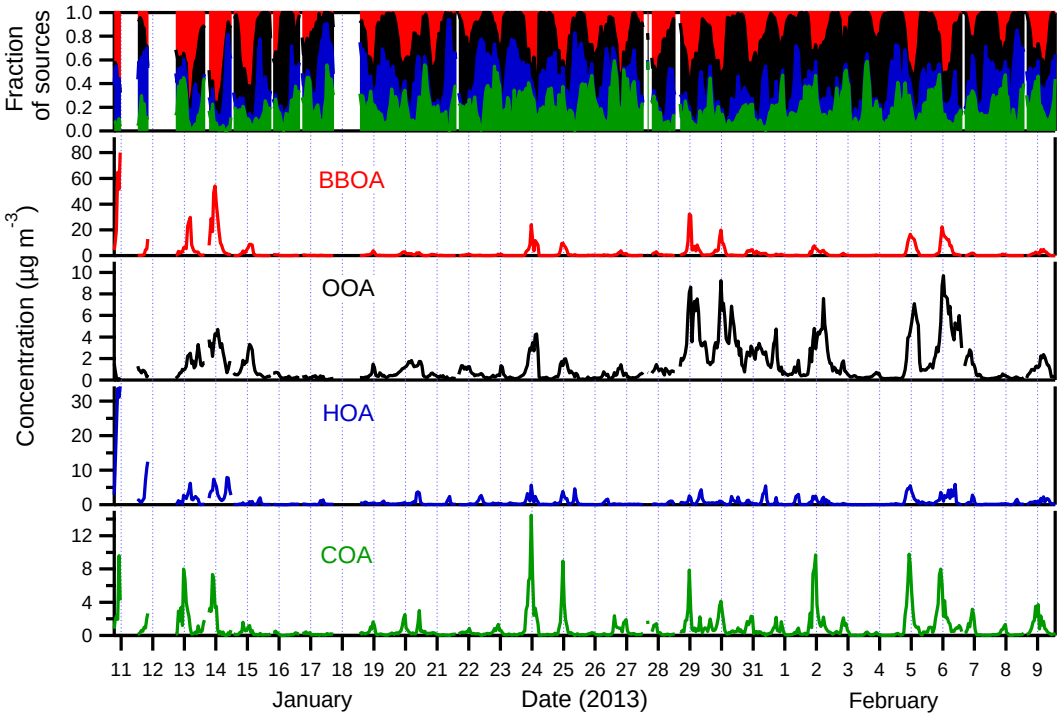

Figure E7. The hourly time series of the PMF factors during the Athens campaign. The PM_1 OA composition is also shown.

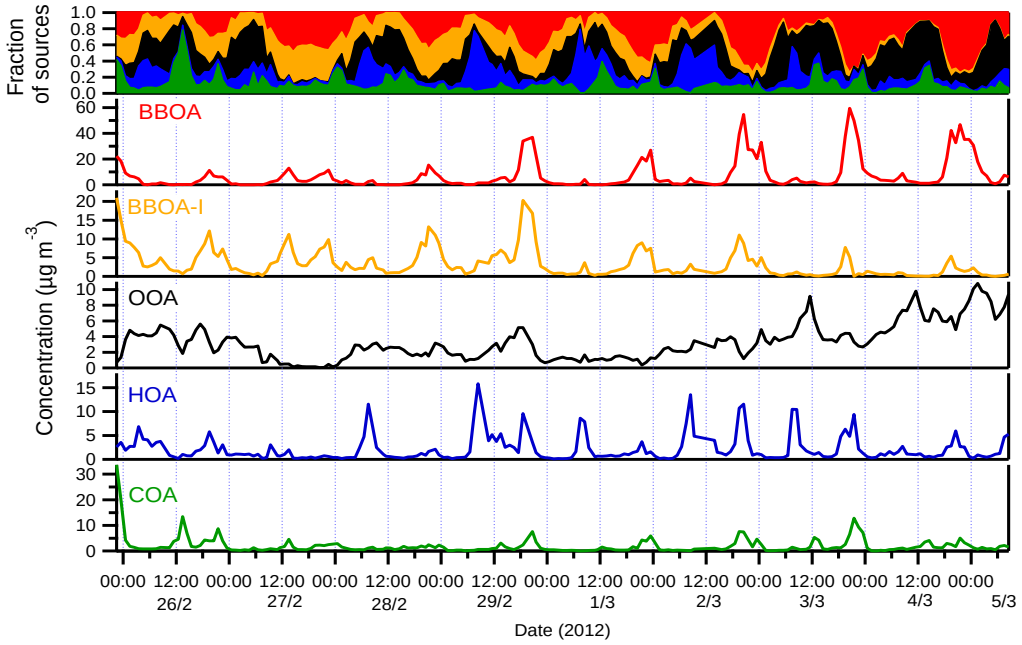

Figure E8. The hourly time series of the PMF factors during the Patras campaign. Their fraction to PM_1 OA is also shown.

European Union
European Social Fund
OPERATIONAL PROGRAMME
EDUCATION AND LIFELONG LEARNING
investing in knowledge society
MINISTRY OF EDUCATION & RELIGIOUS AFFAIRS
MANAGING AUTHORITY
NSRF 2007-2013
EUROPEAN SOCIAL FUND
Co-financed by Greece and the European Union

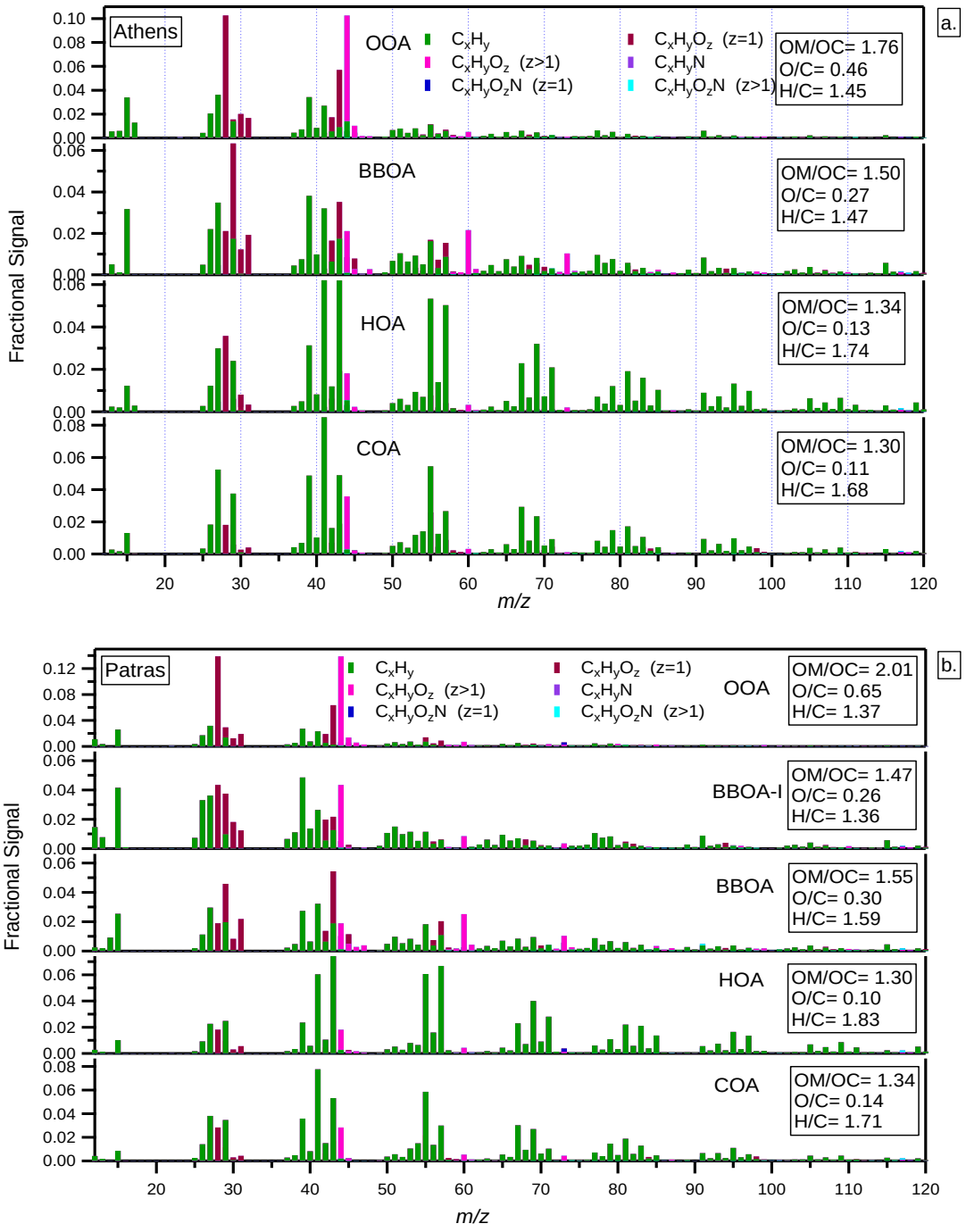

Figure E9. High resolution AMS mass spectra for the factor found in (a) Athens and (b) Patras.

European Union
European Social Fund
OPERATIONAL PROGRAMME
EDUCATION AND LIFELONG LEARNING
investing in knowledge society
MINISTRY OF EDUCATION & RELIGIOUS AFFAIRS
MANAGING AUTHORITY
NSRF 2007-2013
EUROPEAN SOCIAL FUND
Co-financed by Greece and the European Union

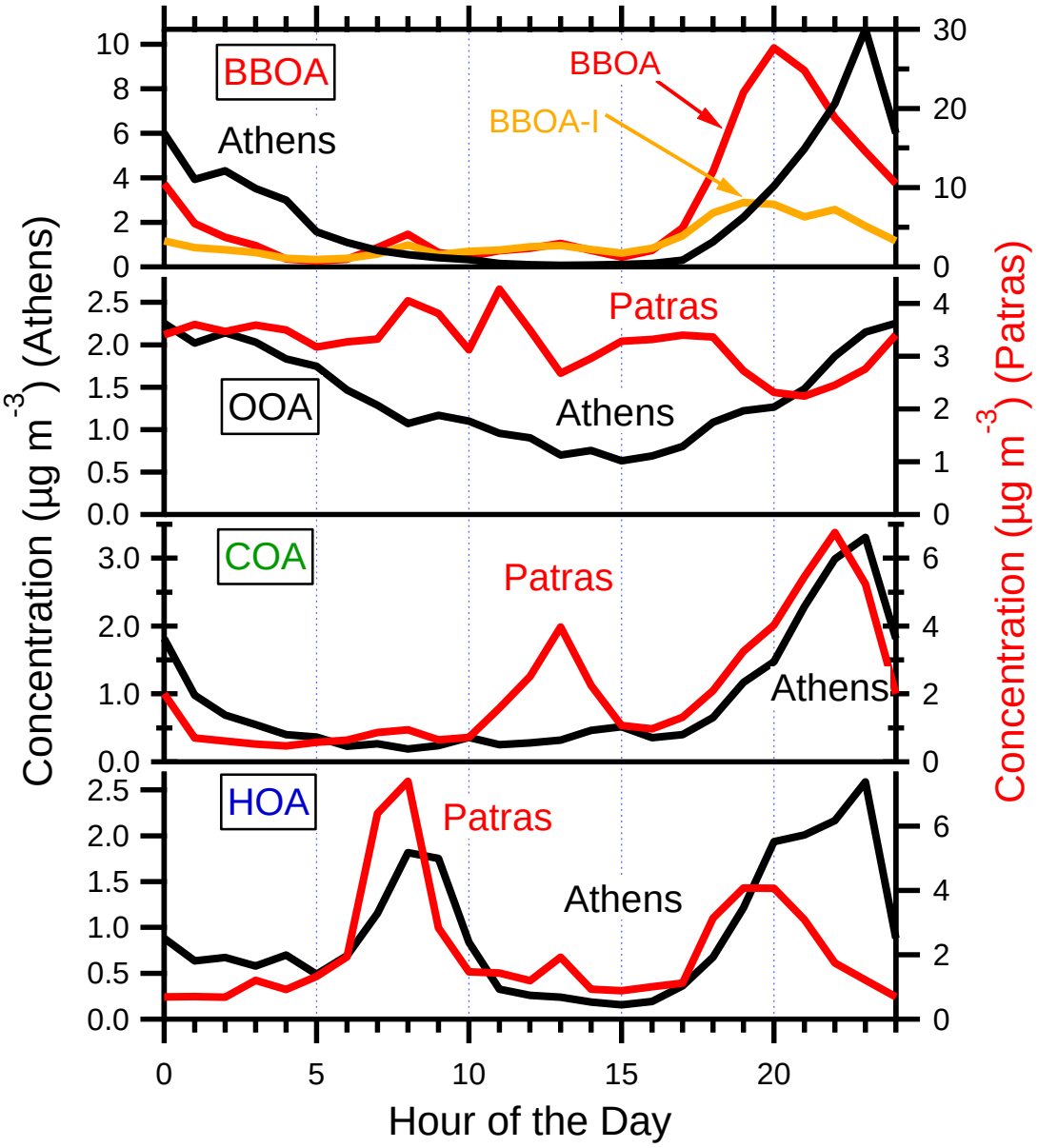

Figure E10. Diurnal profiles of the PMF factors in Athens (black) and Patras (red-yellow). On the left y-axis are the concentrations of Athens' PMF factors, while on the right y-axis those of Patras.

European Union
European Social Fund
OPERATIONAL PROGRAMME
EDUCATION AND LIFELONG LEARNING
investing in knowledge society
MINISTRY OF EDUCATION & RELIGIOUS AFFAIRS
MANAGING AUTHORITY
NSRF 2007-2013
EUROPEAN SOCIAL FUND
Co-financed by Greece and the European Union

Activity 5: Study of the physicochemical properties of atmospheric particulate matter that affect the climate directly and indirectly

A. Hygroscopic properties of atmospheric particles during the winter campaign

A1. Introduction

Atmospheric aerosols play an important role in the Earth's atmosphere, affecting the local and global climate (Vestin et al., 2007). Aerosol particles can affect the global radiation budget by scattering and absorbing solar radiation and thus have a direct effect on climate. On the other hand, depending on their physical and chemical properties, aerosols can serve as cloud droplet condensation nuclei (CCN) becoming cloud droplets and can indirectly affect climate by modifying the cloud reflectivity and lifetime (Kaufman et al., 2002; Cerully et al., 2011 and references therein). The indirect effect of atmospheric particles on climate depends among others on their size and hygroscopic properties (Fors et al., 2010). Increased concentrations of CCN result in the formation of more but smaller cloud droplets (Rose et al., 2005; Vestin et al., 2007) which can lead to suppression of precipitation and increase of cloud lifetimes and cloud cover (Vestin et al., 2007; Rosenfeld et al., 2008; Fors et al., 2010).

Biomass burning emissions are a major source of fine atmospheric particles on a global scale (Andreae and Rosenfeld, 2008). Main sources include forest fires and domestic wood burning for heating and cooking (Martin et al., 2013). These particles represent a significant fraction of global CCN. Some of the highest CCN concentrations have been observed in biomass burning influenced areas (Hennigan et al., 2012). Biomass burning particles consist mainly of organic species and black carbon. They also contain low concentrations of inorganic species, representing usually less than 15% of the

European Union
European Social Fund
OPERATIONAL PROGRAMME
EDUCATION AND LIFELONG LEARNING
investing in knowledge society
MINISTRY OF EDUCATION & RELIGIOUS AFFAIRS
MANAGING AUTHORITY
NSRF 2007-2013
programme for development
EUROPEAN SOCIAL FUND
Co-financed by Greece and the European Union

particulate mass. The extent of the contribution of inorganic components depends on fuel composition and the efficiency of the burning process (Reid et al., 2005). The chemical composition of aerosols originating from biomass burning is in general related to the combustion conditions (Vestin et al., 2007).

Biomass burning organic aerosol (BBOA) mass can be both primarily emitted, but also can be formed by the oxidation of gaseous organic emissions and subsequent condensation, leading to the formation of secondary aerosol. The chemical aging process of BBOA also includes heterogeneous oxidation of the organic aerosol, condensed-phase reactions and cloud-processing. While primary combustion emissions are in general hydrophobic, fresh BBOA is relatively hygroscopic and can serve as CCN (Semeniuk et al., 2007). Atmospheric aging of organic combustion emissions can lead to the increase of their hygroscopicity. In general, the hygroscopicity of organic aerosol increases as it is oxidized in the atmosphere. The organic aerosol O:C (atomic oxygen to carbon) ratio is an indicator of its oxidation state. Water soluble organic carbon (WSOC) represents a large fraction of the BBOA emitted in poor combustion conditions. WSOC is quite hygroscopic and increases the CCN ability of the particles (Vestin et al., 2007).

Biomass burning emissions have also important impacts on regional air quality. The presence of an inversion layer often leads to the trapping of the particles in the lower atmosphere where they can remain for extended periods of time. The contribution of biomass burning to the concentration of the organic aerosols during air pollution episodes was found to be around 40% in Beijing and 70% in a rural site in Austria (Duan et al., 2004; Caseiro et al., 2009). BBOA was also found to be a significant contributor to organic aerosol concentrations in Paris, with a contribution up to 15%, while its contribution in the southeastern US is close to 30% during winter (Zhang et al., 2010; Crippa et al., 2013).

European Union
European Social Fund
OPERATIONAL PROGRAMME
EDUCATION AND LIFELONG LEARNING
investing in knowledge society
MINISTRY OF EDUCATION & RELIGIOUS AFFAIRS
MANAGING AUTHORITY
NSRF 2007-2013
EUROPEAN SOCIAL FUND
Co-financed by Greece and the European Union

In order to understand the impact of biomass burning emissions on climate, the hygroscopic properties of the corresponding particles must be known. The evaluation of the hygroscopic and CCN properties of BBOA is necessary to further understand the role of such particles in cloud formation processes. In this work, we investigate the hygroscopic properties of fresh and aged biomass burning particle emissions in an urban environment, the center of Athens, during winter of 2013, when wood burning in fireplaces for domestic heating was a dominant source.

A2. Experimental

A2.1 Sampling site

Athens is a city of around 4 million residents. The city is surrounded by mountains to the north, west and east. It has significant air quality problems due to its population density, the meteorology and the morphology of the area. Sampling was conducted at the National Observatory of Athens (NOA site, 37°58′23.99″N 23°43′12″E) located on a hill, at the center of Athens, from 12 January to 7 February of 2013. The low concentration data from an almost continuously rainy week were excluded from the analysis in order to focus on the properties of BBOA in the urban atmosphere of Athens. The following results are based on the data collected during 10-15 January and 23 January to 7 February of 2013.

A2.2 Experimental Setup

The hygroscopic properties of the aerosols were measured using a Cloud Condensation Nuclei Counter (CCNC, DMT Technologies, Roberts and Nenes, 2005). Simultaneously, a High-Resolution Time-of-Flight Aerosol Mass Spectrometer (HR-ToF-AMS, Aerodyne Research Inc, De Carlo et al., 2006) was continuously monitoring the chemical composition and size distribution of PM_1 particles.

European Union
European Social Fund
OPERATIONAL PROGRAMME
EDUCATION AND LIFELONG LEARNING
investing in knowledge society
MINISTRY OF EDUCATION & RELIGIOUS AFFAIRS
MANAGING AUTHORITY
NSRF 2007-2013
EUROPEAN SOCIAL FUND
Co-financed by Greece and the European Union

A2.3 Scanning Mobility CCN Analysis (SMCA)

The CCN counter was coupled with a Differential Mobility Analyzer (DMA) and a Condensation Particle Counter (CPC) to provide additional information about the CCN activity of ambient particles. Ambient air was dried by passing through a diffusion drier (RH<5%) and afterwards was introduced in the DMA (TSI 3080). The size-classified aerosol exiting the DMA was split in two, to the CPC (TSI 3787) measuring the total number concentration of particles or Condensation Nuclei (CN) and to the CCN counter (DMT Technologies) which measured the CCN number concentration.

The supersaturation in the column of the CCNC was stepped in increments of ~0.2%, ranging from 0.19 to 0.91% and changed every 12 min, enabling the data collection of at least 4 SMPS scans (total duration 135 sec each) for each supersaturation. The deviation of the CFSTG flow chamber temperature from the nominal was checked for each scan and scans with temperature deviation more than 15% were discarded.

The DMA was running from low to high voltages, enabling a monodisperse aerosol flow to exit the DMA column each time. During a scan (135 sec) the DMA selected particle sizes from 10 to 500 nm. The total number concentration of each size bin was recorded by the CPC and the CCN concentration by the CCNC, thus the total number concentration (CN) and CCN distributions were obtained. Afterwards the two distributions were carefully aligned.

The Aerosol Instrument Manager (AIM) software (TSI, Inc) was used to convert the particle number measurements to size distributions. The same inversion technique was applied to the CCN time series to obtain the CCN size distribution. For constant supersaturation of the instrument and by dividing the CCN number concentration by the total number concentration of particles for each diameter d_p, the corresponding activation fraction CCN/CN versus d_p was obtained. The activation ratio function $R_a(d_p)$ was fit to a sigmoidal function:

$$R_a(d_p) = \frac{CCN(d_p)}{CN(d_p)} = \frac{E}{1+(\frac{d_{p50}}{d_p})^C} \quad (1)$$

where E corresponds to the asymptote of $R_a(d_p)$, d_p is the particle diameter, d_{p50} is the characteristic dry diameter for which 50% of the particles activate (activation diameter) and C an empirical coefficient. A similar fitting can be performed for the measurements at a specific particle size using the supersaturation S as an independent variable. The corresponding activated fraction $R_a(S)$ is expressed by Equation 2:

$$R_a(S) = \frac{CCN(S, d_p = const)}{CN(d_p = const)} = \frac{E^*}{1+(\frac{S}{S^*})^{C^*}} \quad (2)$$

where E^* refers to the asymptote of the sigmoid and expresses the maximum fraction of particles that activate at high supersaturations, S is the instrument supersaturation, S^* is the critical supersaturation, at which half of the particles activate. C^* is a fitting constant which is proportional to the slope of the sigmoid function and expresses the chemical heterogeneity of the activated particles**.** The activation ratio function, $R_a(S)$ represents the cumulative distribution of critical supersaturation of particles with a specific dry diameter d_p.

Petters and Kreidenweis (2007) introduced as a measure of the hygroscopicity of the aerosol the hygroscopicity parameter, κ:

$$\kappa = \frac{4A^3}{27 d_p^3 S^2} \quad (3)$$

where $A=4M_w\sigma_w/(RT\rho_w)$, M_w, σ_w, ρ_w is the molecular weight, surface tension and density of water, R the universal gas constant, and T the average temperature in the CCNC column. Equations 2 and 3 can be combined to provide the hygroscopicity-dependent activation ratio function:

$$R_a(\kappa) = \frac{CCN(\kappa, d_p)}{CN(\kappa, d_p)} \frac{E^*}{1+(\kappa^*/\kappa)^{C^*/2}} \quad (4)$$

The probability distribution function of κ, $p(\kappa)$, can be estimated by differentiating and normalizing Equation 4 (Cerully et al., 2011; Bougiatioti et al., 2011):

European Union
European Social Fund
OPERATIONAL PROGRAMME
EDUCATION AND LIFELONG LEARNING
investing in knowledge society
MINISTRY OF EDUCATION & RELIGIOUS AFFAIRS
MANAGING AUTHORITY
NSRF 2007-2013
EUROPEAN SOCIAL FUND
Co-financed by Greece and the European Union

$$p(\kappa) = \frac{1}{E}\frac{dR_a(\kappa)}{d\kappa} = -\frac{\frac{C}{2\kappa^*}(\kappa/\kappa^*)^{\frac{C}{2}-1}}{(1+(\kappa/\kappa^*)^{C/2})^2} \quad (5)$$

The standard variation of κ, $\sigma(\kappa)$, can be also calculated for the same set of measurements. The dispersion of the hygroscopicity parameter expresses the degree of heterogeneity (chemical dispersion) of particles with a diameter d_p and is calculated as the square root of the variance of the hygroscopicity around κ* (Lance et al., 2007). One value of $\kappa^* \pm \sigma(\kappa)$ every one hour (5 different supersaturations for 12 min each) is obtained:

$$\sigma^2(\kappa) = \frac{\int_0^\infty (\kappa - \kappa^*)^2 p(\kappa) d\kappa}{\int_0^\infty p(\kappa) d\kappa} \quad (6)$$

A2.4 Calibration of the CCN counter

The calibration of the instrument supersaturation was done by the determination of the critical diameter D_{pc} of $(NH_4)_2SO_4$ particles that activate at the nominal supersaturation of the instrument. A dilute ammonium sulfate solution was prepared and used in a syringe pump. The syringe pump provided an atomizer continuously with the solution, producing wet ammonium sulfate particles. The air stream containing the particles afterwards passed through the diffusion drier and the dried particles were introduced to the classifier. As in the measurement mode, total (CN) and activated (CCN) particles were simultaneously measured as the nominal supersaturation of the instrument was changing every 12 minutes, from 0.2 to 1% in increments of 0.2. The activated fraction CCN/CN was then calculated. Repeating the procedure for a wide range of sizes, from 10 to 460 nm, the sigmoidal activation curve was obtained. This curve can provide the characteristic, critical diameter D_{pc} which can be used in the Köhler equation in order to estimate the corresponding supersaturation in the instrument. For the calculation of the supersaturation an $(NH_4)_2SO_4$ solution with a density of 1770 kg m^{-3}, surface tension of the solution of 0.0706 N m^{-1}, molar mass of water 0.018 g mol^{-1} and van't Hoff factor ν equal to 2.5 were used (Brechtel and Kreidenweis, 2000).

European Union
European Social Fund
OPERATIONAL PROGRAMME
EDUCATION AND LIFELONG LEARNING
investing in knowledge society
MINISTRY OF EDUCATION & RELIGIOUS AFFAIRS
MANAGING AUTHORITY
NSRF 2007-2013
EUROPEAN SOCIAL FUND
Co-financed by Greece and the European Union

A3. Results and discussion

The chemical composition and the CCN properties of the aerosols in Athens during the winter 2013 campaign are discussed in the following sections.

A3.1 Particle composition

Organic compounds dominated the PM_1 composition during the campaign representing 58% of the PM_1 mass followed by black carbon (BC) with 20.4%. Sulfate ions contributed 10% to the total PM_1 mass, nitrates 5.1%, ammonium 4.2% and potassium and chloride ions each 1.1%. The corresponding average concentrations were 6.5 μg m^{-3} for organic species, 2.3 μg m^{-3} BC, 1.1 μg m^{-3} sulfates, 0.6 μg m^{-3} nitrates, 0.5 μg m^{-3} ammonium and potassium and chloride 0.1 μg m^{-3} each.

The average diurnal variations of organics and sulfate measured by the AMS, are shown in Figure A1. Organic aerosol concentrations increase after 16:00-17:00 continuously until 23:00 peaking a little before midnight. On the other hand, sulfate had an almost constant average profile with a concentration around 1 μg m^{-3}. This constant profile is characteristic of species that are not produced locally but are transported to the site.

Figure A2 presents the organic aerosol fraction in the total PM_1 mass. The organic compounds dominated PM_1 mass composition throughout the day. A peak was observed in the morning between 7:00-10:00 due to the traffic emissions, a smaller one in the afternoon (14:00-16:00) and a major peak at night with the organic average contribution reaching 80% at 22:00.

European Union
European Social Fund
OPERATIONAL PROGRAMME
EDUCATION AND LIFELONG LEARNING
investing in knowledge society
MINISTRY OF EDUCATION & RELIGIOUS AFFAIRS
MANAGING AUTHORITY
NSRF 2007-2013
EUROPEAN SOCIAL FUND
Co-financed by Greece and the European Union

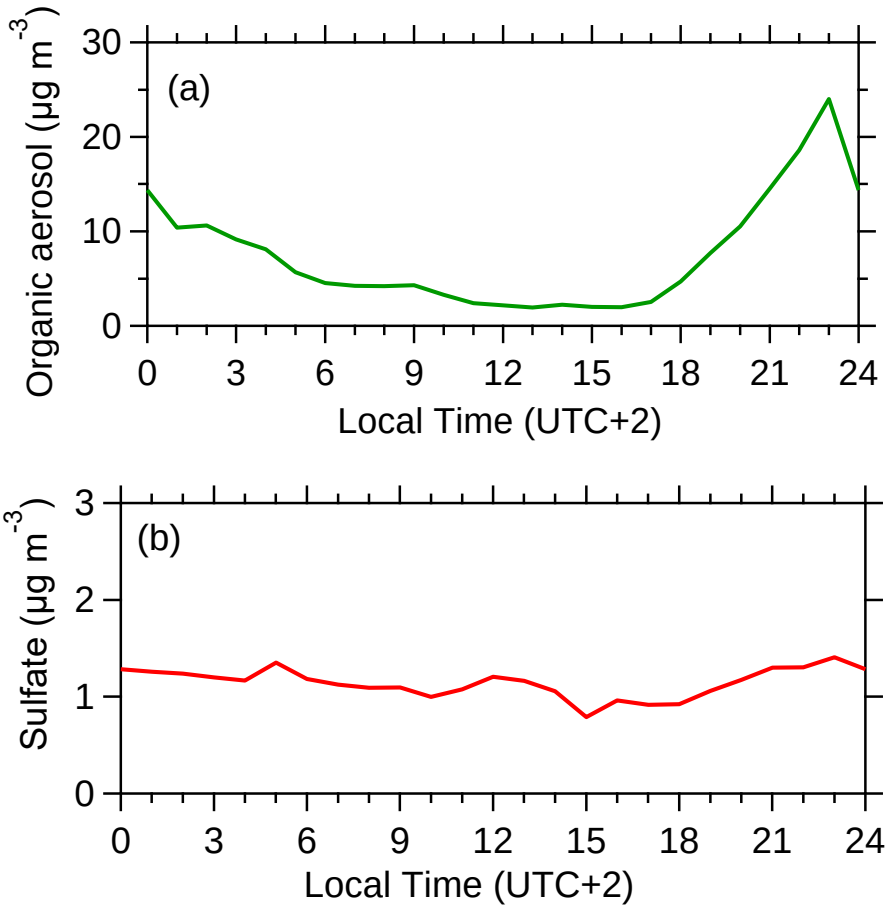

Figure A1: Diurnal profile of (a) organic aerosol and (b) sulfate ions in PM_1 particles in Athens during the winter campaign of 2013.

PMF analysis revealed 4 organic factors (Florou et al., 2014): biomass burning organic aerosol (BBOA), cooking aerosol (COA), hydrocarbon-like organic aerosol (HOA) and oxygenated organic aerosol (OOA).

The average diurnal variations of the factors are shown in Figure A3. Biomass burning particle concentrations were found to increase after 16:00 until 23:00 when a peak of 10 μg m^{-3} was reached. BBOA remained at high levels during all night and dropped to almost zero at noon. HOA concentrations peaked in the morning between 6:00-11:00, and then remained low increasing again from 18:00-23:00. The oxygenated organics which represent aged aerosol transported to the area had an almost constant average

European Union
European Social Fund
OPERATIONAL PROGRAMME
EDUCATION AND LIFELONG LEARNING
investing in knowledge society
MINISTRY OF EDUCATION & RELIGIOUS AFFAIRS
MANAGING AUTHORITY
NSRF 2007-2013
EUROPEAN SOCIAL FUND
Co-financed by Greece and the European Union

diurnal profile. Corresponding to Greek eating periods, cooking organic aerosol was observed from 13:00-16:00 and also increased from 18:00 to 23:00.

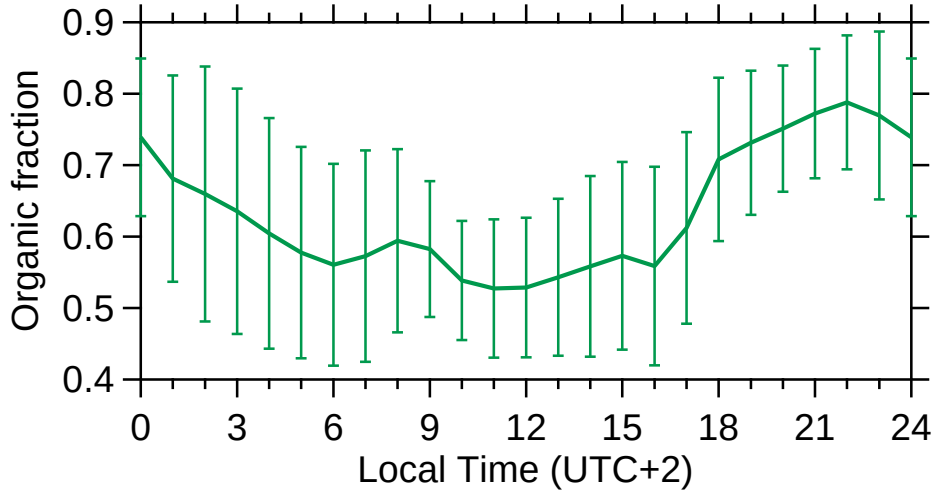

Figure A2: Average mass fraction of organic aerosol in PM_1 particles. The error bars represent ±1σ of the corresponding fractions.

A3.2 Particle CCN activity

The average diurnal variability of the critical supersaturation S_c for different particle sizes is shown in Figure A4. The variability of this parameter for the same particle sizes expresses changes in particle composition. Particles of 40 nm have not been used in the following analysis since their S_c was higher than the instrument's maximum supersaturation (0.91%). Smaller particles activated at higher supersaturation values, as expected from Köhler theory.

European Union
European Social Fund
OPERATIONAL PROGRAMME
EDUCATION AND LIFELONG LEARNING
investing in knowledge society
MINISTRY OF EDUCATION & RELIGIOUS AFFAIRS
MANAGING AUTHORITY
NSRF 2007-2013
EUROPEAN SOCIAL FUND
Co-financed by Greece and the European Union

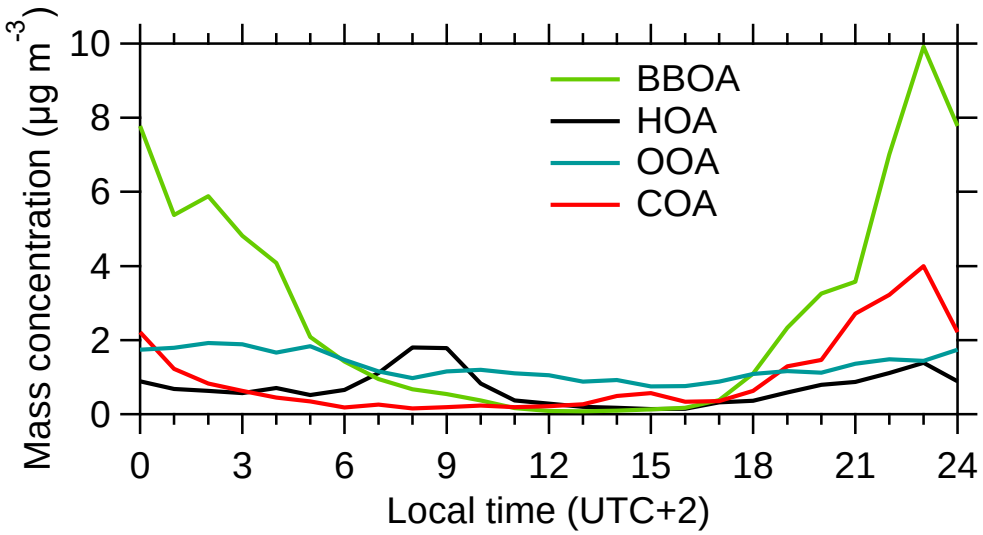

Figure A3: Diurnal variation of the concentration of the four factors: biomass burning (BBOA), traffic (HOA), oxygenated (aged) organics (OOA), and cooking (COA).

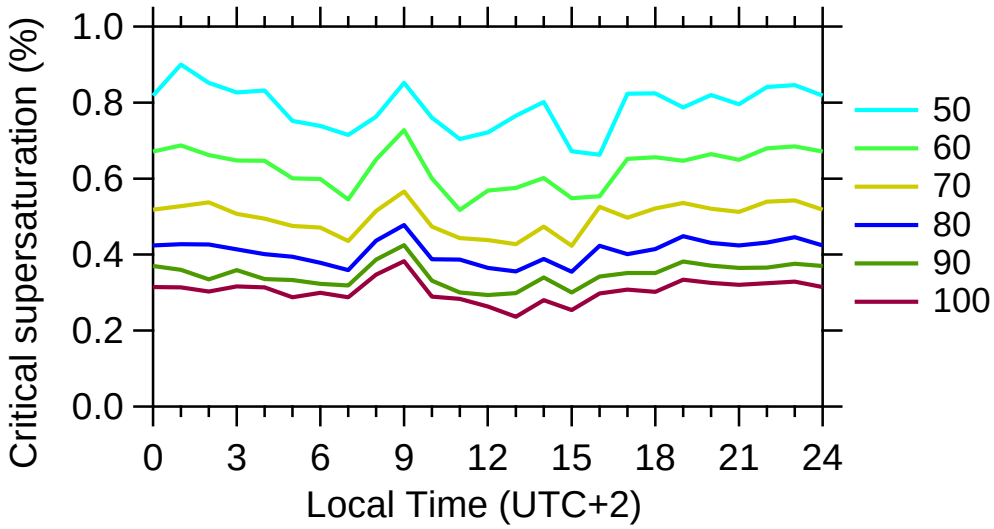

Figure A4: Average variation of critical supersaturation for different particle diameters from 50 to 100 nm.

The main characteristic of the average diurnal profiles of particles S_c is a sharp increase in the morning, between 7:00 and 10:00. During this period there is a significant contribution of HOA traffic emissions to the organic aerosol mass (Figure A3). These

European Union
European Social Fund
OPERATIONAL PROGRAMME
EDUCATION AND LIFELONG LEARNING
investing in knowledge society
MINISTRY OF EDUCATION & RELIGIOUS AFFAIRS
MANAGING AUTHORITY
NSRF 2007-2013
EUROPEAN SOCIAL FUND
Co-financed by Greece and the European Union

results suggest significant HOA contributions to particles in the 50-100 nm range, something expected for traffic in major urban area.

Smaller particles had larger variations of their S_c during the day compared to larger particles (70-100 nm). Such discrepancies of small particles with larger ones could be due to differences in their sources and chemical composition. This suggests that the CCN properties of the small particles may not represent the bulk composition of PM_1 and vice versa. We will analyze this point further in subsequent sections.

The size distribution of the chemical components provided by the AMS showed chemical composition differences in the diameter range targeted by the CCN counter. Figure A5 represents the diurnal variations of the non-refractory inorganic and organic fractions as measured by the AMS estimated for the time period 23 to 25 January for different particle sizes, ranging from 50 to 100 nm. The size distribution of the AMS was rather noisy, especially for the smaller particle diameters. Smaller particles show a different diurnal behavior compared with the larger sizes. Particles of 50 and 60 nm consisted mainly of inorganic compounds during all hours of the day on average. Their average inorganic mass fraction was 65% for the 50 nm and 56% for the 60 nm particles. As particle diameter increased, the diurnal cycle of the organic fraction becomes more similar with the cycle of the total organic fraction (Figure A5). Particles with dry diameters 85 and 100 nm consisted mostly of organics (52 and 68% respectively) and their composition followed the diurnal pattern of the total organic fraction in PM_1.

The hygroscopic properties of the particles are strongly affected by the presence of inorganic compounds which are much more hygroscopic compared to the organics. According to Figure A5, 85 and 100 nm dry particles follow the diurnal trend of OA in PM_1 and also have similar composition as the bulk PM_1. For this reason, the averaged hygroscopic properties of 80, 90 and 100 nm in diameter particles will be used here to approximate the average properties of PM_1 mass.

European Union
European Social Fund
OPERATIONAL PROGRAMME
EDUCATION AND LIFELONG LEARNING
investing in knowledge society
MINISTRY OF EDUCATION & RELIGIOUS AFFAIRS
MANAGING AUTHORITY
NSRF 2007-2013
programme for development
EUROPEAN SOCIAL FUND
Co-financed by Greece and the European Union

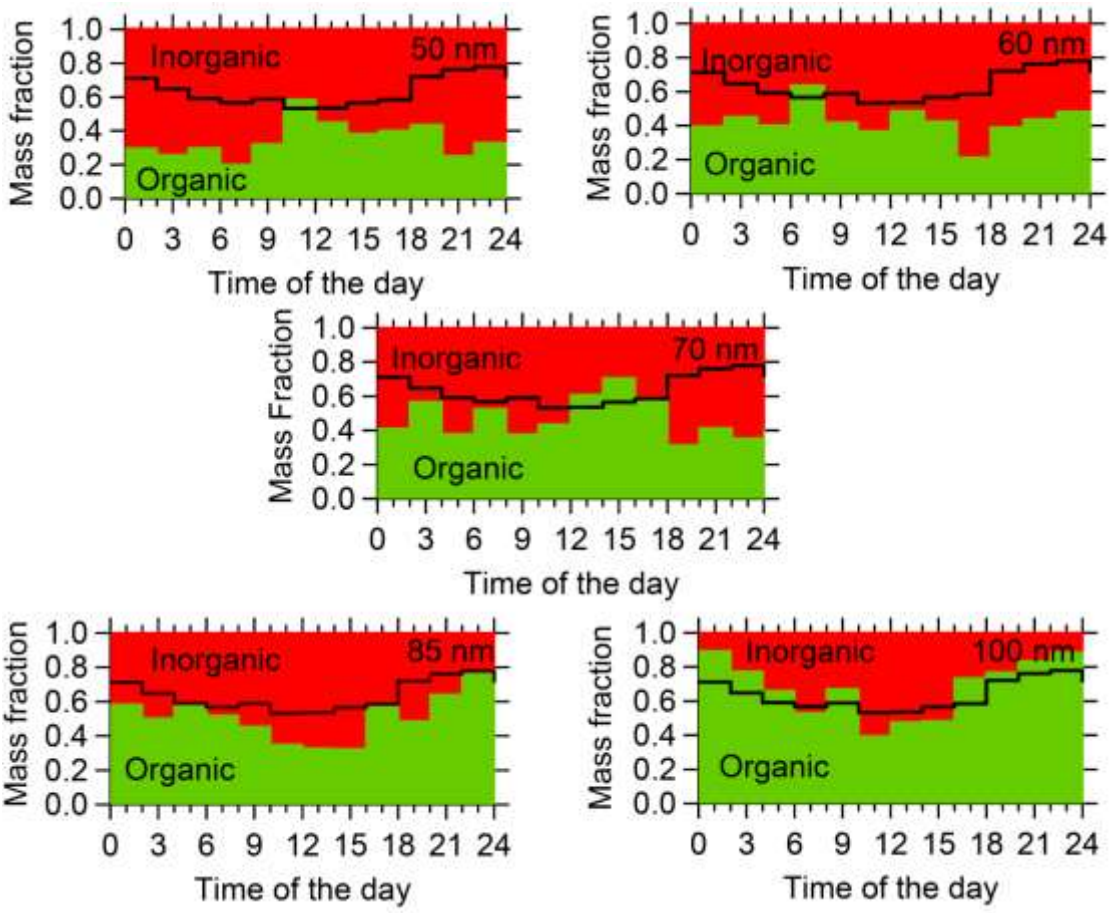

Figure A5: Diurnal profiles of non-refractory organic and inorganic mass fractions for selected particle sizes. The black line indicates the total fraction of organic aerosols in PM_1.

The average diurnal profile of the estimated hygroscopicity factor κ for different particle diameters is shown in Figure A6. The average κ (κ_{av}) of 80 to 100 nm particles was also estimated. The total particle hygroscopicity depends both on the hygroscopicity of the corresponding organic components and on the contribution of the inorganic species to the particle mass. Biomass burning emissions started increasing around 18:00 (Figure A3) and dominated the number and mass concentration of the aerosols until midnight. During that period, the average hygroscopicity was constant with a κ value around 0.15. After midnight κ increased and it started to sharply decrease around 6:00, when the contribution of traffic emissions started becoming significant, according to the HOA diurnal profile. Due to the hydrophobic nature of the HOA

European Union
European Social Fund
OPERATIONAL PROGRAMME
EDUCATION AND LIFELONG LEARNING
investing in knowledge society
MINISTRY OF EDUCATION & RELIGIOUS AFFAIRS
MANAGING AUTHORITY
NSRF 2007-2013
EUROPEAN SOCIAL FUND
Co-financed by Greece and the European Union

particles emitted from traffic, hygroscopicity dropped, increasing again due to dilution of these particles and photochemistry to values close to 0.25 after 12:00. The decrease of κ_{av} from around 0.25 to 0.2 between 13:00-14:00 can be attributed to the presence of HOA particles, together with the relatively hydrophobic cooking emissions that peak at the same time. The κ_{av} values remained high (between 0.2 and 0.25) from noon till the beginning of biomass burning early in the evening (around 17:00) when residents went back to their homes and started using their fireplaces.

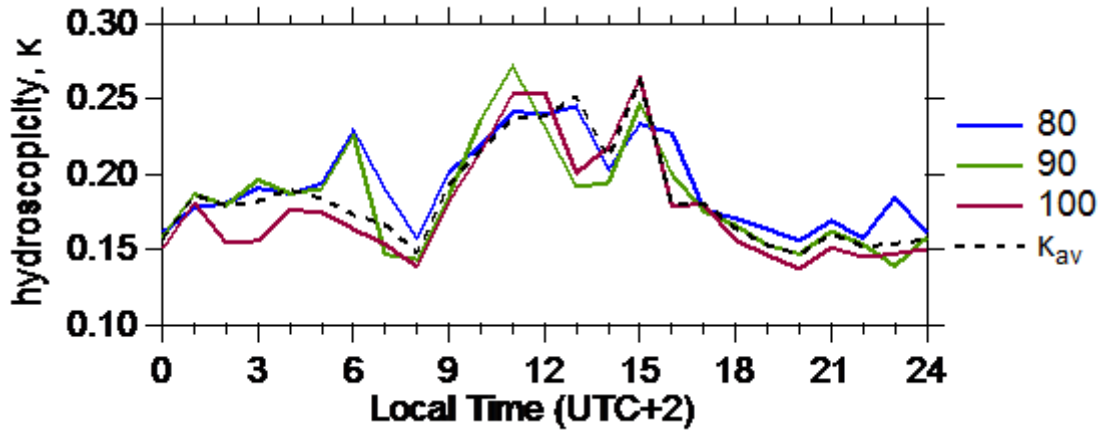

Figure A6: Diurnal profile of hygroscopicity κ of 80, 90 and 100 nm particle diameter. The dashed line indicates the averaged hygroscopicity of 80-100 nm particles.

The 80-100 nm average hygroscopicity factor κ had similar diurnal profile as the O:C ratio (Figure A7). However, the total time series of κ and O:C had a weak correlation (R^2=0.17). This can be explained by the fact that other factors (e.g. inorganic PM_1 contribution) are more important than the organic O:C in determining the average hygroscopicity of particles. Previous work (Massoli et al., 2010; Martin et al., 2012; Lathem et al., 2013) has also suggested that organic hygroscopicity may not be especially sensitive to O:C for the values less than 0.5 encountered in this study.

European Union
European Social Fund
OPERATIONAL PROGRAMME
EDUCATION AND LIFELONG LEARNING
investing in knowledge society
MINISTRY OF EDUCATION & RELIGIOUS AFFAIRS
MANAGING AUTHORITY
NSRF 2007-2013
EUROPEAN SOCIAL FUND
Co-financed by Greece and the European Union

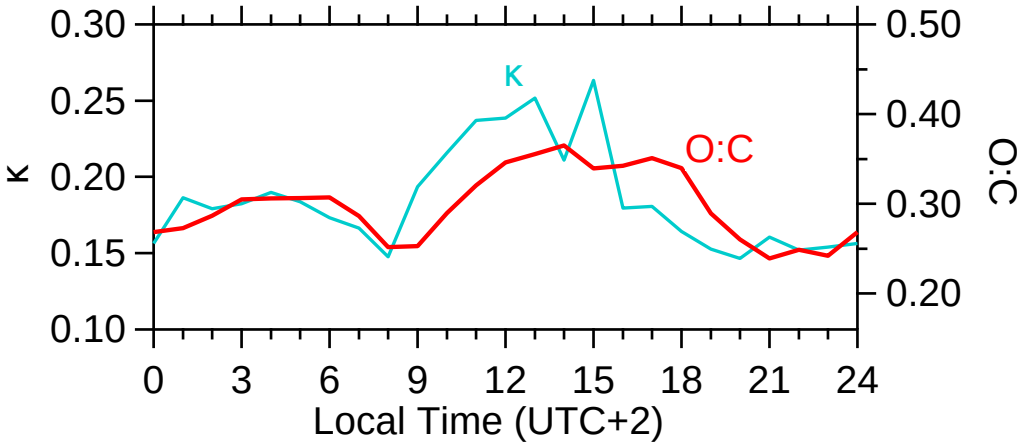

Figure A7: Diurnal profile of average hygroscopicity and O:C ratio.

The degree of heterogeneity of the particles can be expressed by the ratio of the standard deviation (chemical dispersion) of the hygroscopicity, $\sigma(\kappa)$ divided by κ. The diurnal profile of the chemical dispersion $\sigma(\kappa)/\kappa$ is shown in Figure A8. This parameter was found to peak between 7:00 and 11:00, around the same time when average hygroscopicity drops. This can be attributed to the increase of HOA-like traffic contribution to the total aerosol concentration during this period.

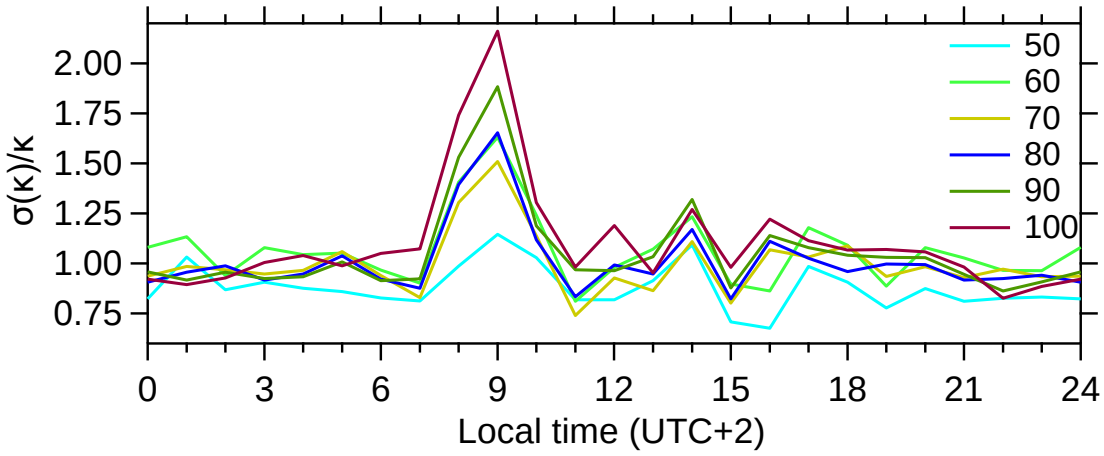

Figure A8: Diurnal profile of the dispersion, σ(κ)/κ, around κ of 50, 60, 70, 80, 90 and 100 nm diameter particles and average hygroscopicity for all particle diameters.

European Union
European Social Fund
OPERATIONAL PROGRAMME
EDUCATION AND LIFELONG LEARNING
investing in knowledge society
MINISTRY OF EDUCATION & RELIGIOUS AFFAIRS
MANAGING AUTHORITY
NSRF 2007-2013
EUROPEAN SOCIAL FUND
Co-financed by Greece and the European Union

This behavior is more pronounced for particles larger than 60 nm while the diurnal profile of the smaller particles presents less variability. The smaller particles were dominated by inorganic species and had more consistent behavior than the larger ones.

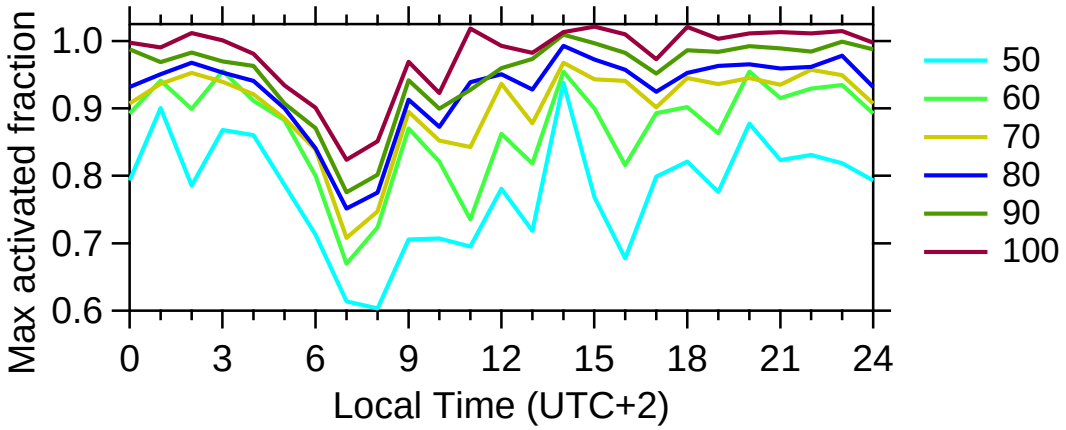

Figure A9: Diurnal profile of the maximum activated fraction E* of 50, 60, 70, 80, 90 and 100 nm diameter particles.

Figure A9 presents the maximum activated fraction E^* (see Equation 2) of particles of different diameters. In general, the smaller the particle size, the lower the corresponding maximum activated fraction. This is consistent with Köhler theory predictions that bigger particles activate easier. This trend is opposite to that suggested by the particle composition with organic fraction increasing with particle size in the range of interest.

A3.3 Organic aerosol hygroscopicity

The particle hygroscopicity parameter is equal to the sum of the hygroscopicity parameters of all components multiplied by their volume fraction (Petters and Kreidenweis, 2007). Despite the low fraction of the inorganic species compared to the organics which dominate, the former significantly affects the average hygroscopicity of the particles. In order to explore the hygroscopic properties of the organic components of the aerosols, the hygroscopicity of organics, κ_{org} was estimated.

European Union
European Social Fund
OPERATIONAL PROGRAMME
EDUCATION AND LIFELONG LEARNING
investing in knowledge society
MINISTRY OF EDUCATION & RELIGIOUS AFFAIRS
MANAGING AUTHORITY
NSRF 2007-2013
EUROPEAN SOCIAL FUND
Co-financed by Greece and the European Union

The model ISORROPIA II (Fountoukis and Nenes, 2007) was used in order to estimate chemical composition of the inorganic fraction. This model requires as input the concentrations of the inorganic ions (relative humidity and temperature conditions and can provide the concentration of the inorganic salts in the aerosol phase (Fountoukis and Nenes, 2007). By dividing the corresponding salt mass concentration by its density, the volume fractions of the inorganic components can be calculated. According to Petters and Kreidenweis, (2007):

$$\Sigma \varepsilon_i \cdot \kappa_i = \kappa \quad (7)$$

where ε_i are the volume fractions of all particle components, κ_i their hygroscopicity and κ the total hygroscopicity measured. By using κ_{av} for κ, and assuming that black carbon (BC) has a κ=0, the hygroscopicity of the organic compounds, κ_{org} was estimated. The average diurnal profile of κ_{org} is presented in Figure A10.

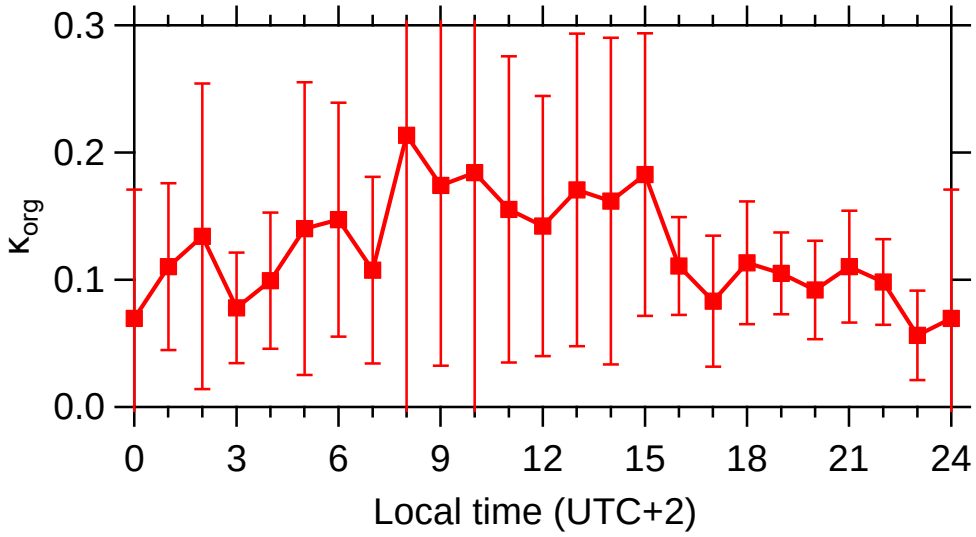

Figure A10: Diurnal profile of the average organic hygroscopicity κ_{org}. The error bars represent ±1σ of the corresponding hygroscopicity.

The estimated κ_{org} varies from 0.06 to 0.21. During the night biomass burning emissions dominate and the corresponding κ is around 0.09. After 3:00 OOA becomes an important OA component so κ_{org} increases. OOA dominated the organic aerosol composition between 10:00-17:00 and is expected to be quite hygroscopic. Its κ values reported in literature are around 0.25-0.3 (Kreidenweis et al., 2008; Chang et al., 2010)

European Union
European Social Fund
OPERATIONAL PROGRAMME
EDUCATION AND LIFELONG LEARNING
investing in knowledge society
MINISTRY OF EDUCATION & RELIGIOUS AFFAIRS
MANAGING AUTHORITY
NSRF 2007-2013
EUROPEAN SOCIAL FUND
Co-financed by Greece and the European Union

justifying the increase of the organic aerosol hygroscopicity at that time. Estimations of κ_{org} from open fires and lab measurements (Jimenez, 2009; Moore et al., 2011; Lathem et al., 2013) also leaded to values around 0.1 for biomass burning organics.

A4. Conclusions

The composition and hygroscopic properties of atmospheric aerosol in Athens during the winter of 2013 were studied. The PM_1 was dominated by organic species during all the sampling period, with an average organic mass fraction of 0.58, followed by black carbon with a corresponding fraction of 0.2. The PMF analysis revealed that the most important contributor to the organic aerosol concentrations was biomass burning which started in the evening and peaked during the night. HOA from traffic peaked during the morning rush hour, affecting the total hygroscopic properties of organic aerosols. During the HOA peak, the critical supersaturation of the particles studied here (50 nm$\leq d_p \leq$100 nm) was lower due to the hydrophobic nature of HOA. The maximum chemical dispersion of the particles is also observed during this period.

Size-resolved chemical composition data provided by the HR-AMS revealed differences in the composition of smaller (50-70 nm) and bigger particles (80-100 nm) and showed that the properties of the PM_1 bulk composition can be represented by the properties of bigger particles. These particles were found to be quite hygroscopic, with the maximum activated fraction reaching almost 1 during most of the day, except for the morning traffic period. The average hygroscopicity of these particles, κ_{av}, ranged roughly from 0.15 to 0.25. The lowest values are observed during the HOA peak, as expected, while the highest were observed between 11:00-16:00 when oxygenated organics dominated the organic mass. The average hygroscopicity κ_{av} of the mixed (organic/inorganic) particles during the night when biomass burning particles prevailed was around 0.15. The diurnal profile of κ_{av} was very similar with the profile of the O:C ratio but no correlation was observed.

Using a thermodynamic model to predict the inorganic chemical composition of the inorganic fraction, the hygroscopicity of the 80-100 nm organic particles was estimated.

European Union
European Social Fund
OPERATIONAL PROGRAMME
EDUCATION AND LIFELONG LEARNING
investing in knowledge society
MINISTRY OF EDUCATION & RELIGIOUS AFFAIRS
MANAGING AUTHORITY
NSRF 2007-2013
EUROPEAN SOCIAL FUND
Co-financed by Greece and the European Union

The organic particles hygroscopicity κ_{org} was on average 0.12 while during the biomass burning period was on average 0.09.

A5. References

Andreae, M.O. and Rosenfeld, D. Aerosol-cloud precipitation interactions. Part 1. The nature and sources of cloud-active aerosols. *Earth-Science Reviews,* **2008**, 89, 13-41.

Bougiatioti, A., Nenes, A., Fountoukis, C., Kalivitis, N., Pandis, S.N., Mihalopoulos, N. Size-resolved CCN distributions and activation kinetics of aged continental and marine aerosol. *Atmos. Chem. Phys.,* **2011**, 11, 8791-8808.

Brechtel, F.J., Kreidenweis, S.M. Predicting particle critical supersaturation from hygroscopic growth measurements in the humidified TDMA. Part I: Theory and sensitivity studies. *J. Atmos. Sci.*, **2000**, 57, 1854-1871.

Cerully, K.M., Raatikainen, T., Lance, S., Tkacik, D., Tiitta, P., Petaja, T., Ehn, M., Kulmala, M., Worsnop, D.R., Laakosonen, A., Smith, J.N., Nenes, A. Aerosol hygroscopicity and CCN activation kinetics in a boreal forest environment during the 2007 EUCAARI campaign. Atmos. Chem. Phys., **2011**, 11, 12369-12386.

Chang, R.Y.-W., Slowik, J.G., Shantz, N.C., Vlasenko, A., Liggio, J., Sjostedt, S.J., Leaitch, W.R., Abbat, J.P.D. The hygroscopicity parameter (κ) of ambient organic aerosol at a field site subject to biogenic and antrhropogenic influences: relationship to degree of aerosol oxidation. *Atmos. Chem. Phys.*, **2010**, 10, 5047-5064.

M. Crippa, De Carlo, P. F., Slowik, J. G., Mohr, C., Heringa, M.F., Chirico, R., Poulain, L., Freutel, F., Sciare, J., Cozic, J., Di Marco, C.F., Elsasser, M., Nicolas, J.B., Marchand, N., Abidi, E., Wiedensohler, A., Drewnick, F., Schneider, J., Borrmann, S., Nemitz, E., Zimmermann, R., Jaffrezo, J.-L., Prevôt, A.S.H., Baltensperger, U. Wintertime aerosol chemical composition and source apportionment of the organic fraction in the Metropolitan area of Paris.*Atmos. Chem. Phys.*, **2013**, 13, 961-981.

European Union
European Social Fund
OPERATIONAL PROGRAMME
EDUCATION AND LIFELONG LEARNING
investing in knowledge society
MINISTRY OF EDUCATION & RELIGIOUS AFFAIRS
MANAGING AUTHORITY
NSRF 2007-2013
programme for development
EUROPEAN SOCIAL FUND
Co-financed by Greece and the European Union

De Carlo, P.F., J.R. Kimmel, J.R., Trimborn, A., Northway, M.J. Jayne, J.T. Aiken, A.C. Gonin, M. Fuhrer, K. Horvath, T. Docherty, K. Worsnop, D.R. Jimenez, J.L. Field-Deployable, High-Resolution, Time-of-Flight Aerosol Mass Spectrometer, *Analytical Chemistry*, **2006**, 78: 8281-8289.

Florou, K., Pikridas, M., Papanastasiou, D.K. Papanastasiou, Louvaris, E.E., Gkatzelis, G.I., Pandis, S.N. Air pollution from airborne particulate matter during wintertime in two Greek cities. In preparation.

Fors, E.O., Rissler, J., Massling, A., Svenningsson, B., Andrae, M.O., Dusek, U., Frank, G.P., Hoffer, A., Bilde, M., Kiss, G., Janitsek, S., Henning, S., Facchini, M.C., Decesari, S., Swietlicki, E. Hygroscopic properties of Amazonian biomass burning and European background HULIS and investigation of thei effects on surface tensxeion with two models linking H-TDMA to CCNC data. *Atmos. Chem. Phys.*, 2010, 10, 5625-5639.

Fountoukis, C., Nenes, A. A computationally efficient thermodynamic equilibrium model for K^+-Ca^{2+}-Mg^{2+}-NH_4^+-SO_4^{2-}-NO_3^--Cl^--H_2O aerosols. *Atmos. Chem. Phys.*, **2007**, 4639-4659.

Hennigan, C.J., Westervelt, D.M., Riipinen, I., Engelhart, G.J., Lee, T., Collet Jr., J.L., Pandis, S.N., Adams, P.J., Robinson, A.L. New particle formation and growth in biomass burning plumes: An important source of cloud condensation nuclei. *Geophys. Res. Let.*, **2012**, 39, L09805, doi:10.1029/2012GL050930.

Kaufman, Y. J., Tanre, D., and Boucher, O. A satellite view of aerosols in the climate system. *Nature*, **2002**, 419, 6903, 215–223.

Lance, S., Raatikainen, T., Onasch, T., Worsnop, D.R., Yu, X.-Y., Alexander, M.L., Stolzenburg, M.R., McMurry, P.H., Smith, J.N., Nenes, A. Aerosol mixing-state, hygroscopic growth and cloud activation efficiency during MIRAGE 2006. *Atmos. Chem. Phys*. **2012**, 12, 15709-15742.

Lathem, T.L., Beyersdorf, A.J., Thornhill, K.L., Winstead, E.L., Cubison, M.L., Hecobian, A., Jimenez, J.L., Weber, R.J., Anderson, B.E., Nenes, A. Analysis of CCN activity of Arctic aerosol and Canadian biomass burning during summer 2008. *Atmos. Chem. Phys.*, **2013**, 13, 2735-2756.

European Union
European Social Fund
OPERATIONAL PROGRAMME
EDUCATION AND LIFELONG LEARNING
investing in knowledge society
MINISTRY OF EDUCATION & RELIGIOUS AFFAIRS
MANAGING AUTHORITY
NSRF 2007-2013
programme for development
EUROPEAN SOCIAL FUND
Co-financed by Greece and the European Union

Lide, D.R. CRC Handbook of chemistry and physics. *CRC Press*, Ann Arbor, MI.

Martin, M., Tritscher, T., Jurányi, Z., Heringa, M.F., Sierau, B., Weingartner, E., Chirico, R., Gyzel, M., Prévôt, A.S.H., Baltensperger, U., Lohmann, U. Hygroscopic properties of fresh and aged wood burning particles. *J. Aerosol Sci.*, **2013**, 56, 15-29.

Massoli, P., Lambe, A.T., Ahern, A.T., Williams, L.R., Ehn, M., Mikkilä, J., Canagaratna, M.R., Brune, W.H., Onasch, T.B., Jayne, J.T., Petäjä, T., Kulmala, M., Laaksonen, A., C. E. Kolb, C.E., Davidovits, P., Worsnop, D.R. Relationship between aerosol oxidation level and hygroscopic properties of laboratory generated secondary organic aerosol (SOA) particles. *Geophys. Res.Lett.*, **2010**, 37, L24801.

Moore, R. H., Nenes, A., Medina, J. Scanning mobility CCN analysis - A method for fast measurements of size-resolved CCN distributions and activation kinetics. *Aerosol. Sci. Technol.*, **2010**, 44:861-871.

Petters, M.D., Kreidenweis, S.M. A single parameter representation of hyroscopic growth and cloud condensation nucleus activity. *Atmos. Chem. Phys.*, **2007**, 7, 1961-1971.

Reid, J. S., Koppmann, R., Eck, T. F., and Eleuterio, D. P. A review of biomass burning emissions part II: Intensive physical properties of biomass burning particles, *Atmos. Chem. Phys*., 5, 799–825, 2005.

Roberts, G.C., Nenes, A. A continuous-flow streamwise thermal-gradient CCN chamber for atmospheric measurements. *Aeros. Sci. Technol.*, **2005**, 39, 206-221.

Rose, D., Novak, A., Achtert, P., Wiedensohler, A., Hu, M., Shao, M., Zhang, Y., Andreae, M.O, Pöschl, U. Cloud condensation nuclei in polluted air and biomass burning smoke near the mega-city Guangzhou, China - Part 1: Size-resolved measurements and implications for the modeling of the aerosol particle hygroscopicity and CCN activity. *Atmos. Chem. Phys.*, **2010**, 10, 3365-3383.

Semeniuk, T. A., Wise, M. E., Martin, S. T., Russell, L. M., Buseck, P. R. Hygroscopic behavior of aerosol particles from biomass burning using environmental transmission electron microscopy. J. Atmos. Chem., **2007**, 56:259-273.

European Union
European Social Fund
OPERATIONAL PROGRAMME
EDUCATION AND LIFELONG LEARNING
investing in knowledge society
MINISTRY OF EDUCATION & RELIGIOUS AFFAIRS
MANAGING AUTHORITY
NSRF 2007-2013
programme for development
EUROPEAN SOCIAL FUND
Co-financed by Greece and the European Union

Slowik, J.G., Staiken, K., Davidovits, P., Williams, L.R., Jayne, J.T., Kolb, C.E., Worsnop, D.R., rudich, Y., DeCarlo, P.F., Jimenez, J.L. Particle morphology and density chatacterization by combined mobility and aerodynamic diameter measurements. Part 2: Application to combustion-generated soot aerosols as a function of fuel equivalence ratio. *Aerosol Sc. Technol.*, **2004**, 38, 1206-1222.

Ulbrich, I.M., Canagaratna, M.R., Zhang, Q., Worsnop, D.R., Jimenez, J.L. Interpretation of organic components from Positive Matrix Factorization of aerosol mass spectrometric data. *Atmos. Chem. Phys.*, 9, **2009**, 2891-2918.

Vestin, A., Rissler, J., Swietlicki, E., Frank, G. P., Andreae, M. O. Cloud-nucleating properties of Amazonian biomass burning aerosol: Cloud condensation nuclei measurements and modeling. *J. Geophys. Res.*, **2007**, Vol. 112, D14201, doi:10.1029/2006JD008104.

Zhang, X., Hecobian, A., Zheng, M., Frank, N.H., Weber, R.J. Biomass burning impact on PM2.5 over the southeastern US during 2007: integrating chemically speciated FRM filter measurements, MODIS fire counts and PMF analysis. *Atmos. Chem. Phys*, **2010**, 10, 6839-6853.

Zuberi, B., Johnson, K.S., Aleks, G.K., Molina, L.T., Molina, M.J., Laskin, A. Hydrophilic properties of aged soot. *Geophys. Res. Let.*, **2005**, 32, L01807.

European Union
European Social Fund
OPERATIONAL PROGRAMME
EDUCATION AND LIFELONG LEARNING
investing in knowledge society
MINISTRY OF EDUCATION & RELIGIOUS AFFAIRS
MANAGING AUTHORITY
NSRF 2007-2013
programme for development
EUROPEAN SOCIAL FUND
Co-financed by Greece and the European Union

B. Hygroscopic properties of atmospheric particles during the summer campaign

B1. Experimental

The hygroscopicity (i.e. ability to take up water) and Cloud Condensation Nuclei (CCN) activity of sub-micrometer aerosol particles were measured in suburban and remote locations, in Greece during the summer of 2012. More specifically, the suburban sites of Patras (FORTH/ICE-HT; 38.297º N, 21.809º E, height 85 m asl) and Athens (Demokritos GAW station 37.995º N, 23.816º E, height 250 m asl) were selected for providing hygroscopicity measurements of both freshly emitted and aged, natural, anthropogenic or mixed particles, as they are influenced by different sources (i.e. local or remote) according to the wind direction. The remote site of Finokalia (35º32'N, 25º67'E; http://finokalia.chemistry.uoc.gr), located on the island of Crete, was selected for studying the hygroscopic properties of long range transport particles originated from Southern Europe and countries surrounding the Black Sea.

A Hygroscopic Tandem Differential Mobility Analyzer (HTDMA; Rader and McMurry, 1986) and a continuous flow streamwise thermal gradient Cloud Condensation Nuclei Counter (CFSTGC; Roberts and Nenes, 2005) were combined to probe the hygroscopic properties of aerosols at both sub- and super-saturation conditions (cf. Fig. B1). In brief, atmospheric particles were sampled with a total flow rate of 1.8 lpm, dried, neutralized and selected based on their electrical mobility diameter by a Differential Mobility Analyzer (DMA-1;TSI Model 3080; Knutson and Whitby, 1975). DMA-1 employed a closed loop sheath flow of 10.8 lpm, while its inner electrode voltage was changed accordingly every 6 minutes for classifying particles having mobility diameters of 60, 80, 100 and 120 nm. The monodisperse aerosol downstream DMA-1 was then split in two streams. The first stream of particles was exposed to sub-saturated relative humidity (RH) conditions (i.e. RH≈87%) before their

European Union
European Social Fund
OPERATIONAL PROGRAMME
EDUCATION AND LIFELONG LEARNING
investing in knowledge society
MINISTRY OF EDUCATION & RELIGIOUS AFFAIRS
MANAGING AUTHORITY
NSRF 2007-2013
EUROPEAN SOCIAL FUND
Co-financed by Greece and the European Union

size distribution to be measured by DMA-2 (custom made, closed loop sheath and RH control; cf. Biskos et al., 2006) and a Condensation Nuclei Counter (CPC, TSI Model 3772; Stolzenburg and McMurry, 1991). The second stream of monodisperse particles was introduced into the CFSTGC to measure the CCN activity of particles. The CFSTGC was operated in Scanning Flow CCN Analysis (SFCA) mode (Moore and Nenes, 2009), in which the flow rate in the growth chamber changes over time, while a constant streamwise temperature difference is applied. This causes supersaturation to change continuously, allowing the rapid and continuous measurement of CCN spectra with high temporal resolution. More details on the HTDMA and CFSTGC can be found in Bezantakos et al., (2013) and Bougiatioti et al., (2009).

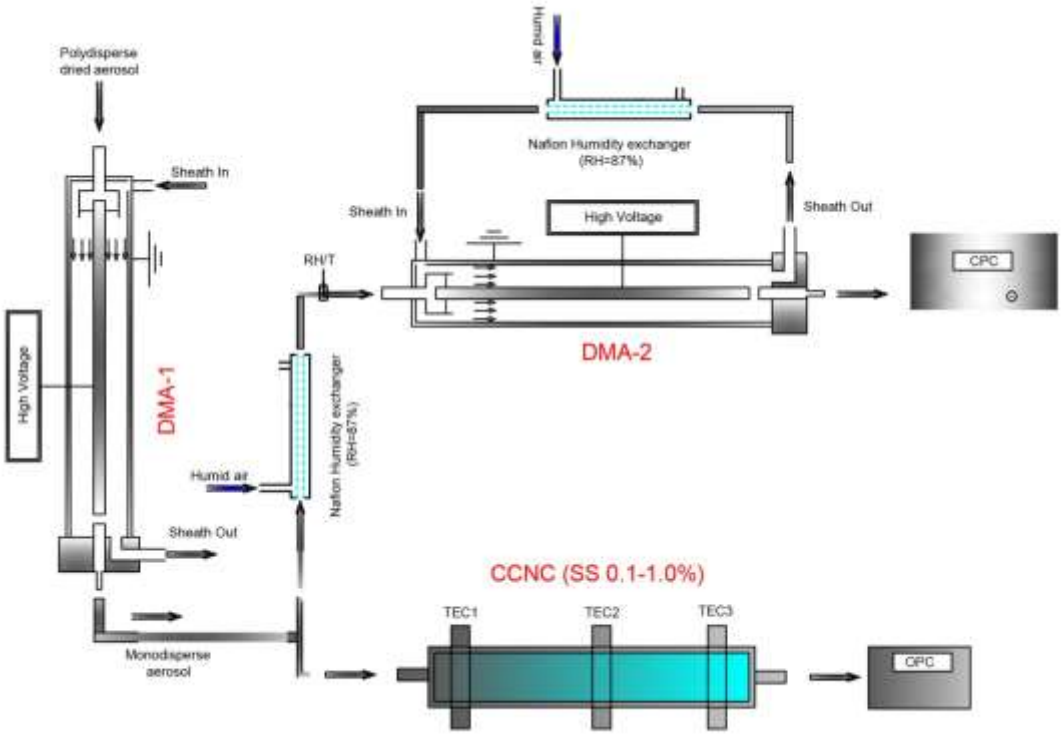

Fig B1. Experimental setup of HTDMA-CCNC combo. In brief, ambient air was sampled at a rate of 1.8 lpm. Particles passed through a drier, a ^{85}Kr neutralizer and DMA-1, where particles of 40, 60, 80, 100 and 120 nm were selected. 0.3 lpm of the monodisperse flow downstream DMA-1 was passed through a nafion humidifier, where its RH was increased to 87 ±2%, before measured by DMA-2 and the CPC. The rest of the monodisperse flow (1.5 lpm) was directed through the CCNC, where it was super-saturated from 0.1 to 1.0% with water vapors. Particles that activated as Cloud Condensation Nuclei were detected downstream by an Optical Particle Counter.

European Union
European Social Fund
OPERATIONAL PROGRAMME
EDUCATION AND LIFELONG LEARNING
investing in knowledge society
MINISTRY OF EDUCATION & RELIGIOUS AFFAIRS
MANAGING AUTHORITY
NSRF 2007-2013
EUROPEAN SOCIAL FUND
Co-financed by Greece and the European Union

B2. Results and Discussion

For expressing particles growth due to water uptake at the sub-saturation regime, we used their hygrosocopic growth factor (g), which is defined as:

$$g(\mathrm{RH}) = \frac{d_m(\mathrm{RH})}{d_{\mathrm{dry}}}, \quad (1)$$

where $d_{\mathrm{m}}(\mathrm{RH})$ and d_{dry} are respectively the geometric mean mobility diameters of the sampled particles at the hydrated state (i.e., at RH ≈ 87%) as measured by DMA-2 and the CPC, and at the dry state as dictated by the settings (i.e., flow rates and voltage) used in DMA-1. The TDMAfit algorithm (Stolzenburg and McMurry, 1988) was employed for inverting the HTDMA measurements and distinguishing between internally and externally mixed aerosols (cf. Bezantakos et al., 2013).

The CCN activity of the particles is characterized by the activation ratio given by:

$$R_a \equiv \frac{CCN}{CN} = a_0 + \frac{a_1 - a_0}{1 + (Q/Q_{50})^{-a_2}}, \quad (2)$$

where CCN and CN are the activated and total particle concentrations, while a_0, a_1, a_2 and Q_{50} are constants that describe the minimum, maximum, slope and inflection point of the sigmoidal, respectively, while Q is the instantaneous volumetric flow rate inside the CFSTGC. Ideally, a_0 is zero and a_1 is expected to be unity; however, values for a_1 varied throughout the measurement period depending on the selected aerosol particle size and the mixing state. The inflection point (i.e. Q_{50} or "critical flow rate"), corresponds to the instantaneous flow rate, that produces a level of super-saturation within the CFSTGC, required to activate the measured monodisperse aerosol.

The κ-Köhler theory (Petters and Kreidenweis 2007) was used for expressing particles hygroscopic properties at both sub- and super-saturation conditions, using a common parameter (κ) and for overcoming the complexities involved in associating their chemical composition with their hygroscopicity. The hygroscopic parameter κ can be determined by the hygroscopic growth factor measured by HTDMA as follows (Kreidenweis et al., 2008):

European Union
European Social Fund
OPERATIONAL PROGRAMME
EDUCATION AND LIFELONG LEARNING
investing in knowledge society
MINISTRY OF EDUCATION & RELIGIOUS AFFAIRS
MANAGING AUTHORITY
NSRF 2007-2013
EUROPEAN SOCIAL FUND
Co-financed by Greece and the European Union

$$\kappa_{\mathrm{HTDMA}} = \frac{\left(g(\mathrm{RH})^3\text{-}1\right)}{a_w/(1\text{-}a_w)}\ , \tag{3}$$

where g(RH) is the measured hygroscopic growth factor (i.e., at ca. 87% RH in our measurements) and aw is the water activity of the solution droplet, which can be calculated by:

$$a_w \approx \frac{\mathrm{RH}}{100}\left(exp\left(\frac{4\sigma_{s/\alpha}\ M_w}{RT\rho_w d_m(RH)}\right)\right)^{-1}. \tag{4}$$

Here $\sigma_{s/a}$ and M_w are the surface tension and molecular weight of pure water (0.072 J m^{-2} and 18^{-3} kg/mol, respectively), R is the universal gas constant, T is the absolute temperature, ρ_w is the density of water and d_m is the diameter of the particles at elevated RH. Note that the exponential term, i.e., the Kelvin term, provides only a small correction for particles larger than 60 nm.

For externally mixed particles κ_{HTDMA} corresponding to each mode can be obtained. An average value of the hygroscopic parameter, which is representative of the hygroscopic properties of the entire particle population, can be also obtained as follows:

$$\overline{\kappa_{\mathrm{HTDMA}}} = \frac{\left(g_{\mathrm{avg}}(\mathrm{RH})^3-1\right)}{a_w/(1-a_w)}. \tag{5}$$

Here g_{avg}(RH) is the average hygroscopic growth factor of the entire monodisperse particle population. The hygroscopic parameter of the particles can also be obtained using the CFSTGC measurements (i.e., critical super-saturation) as follows:

$$\kappa_{\mathrm{CCN}} = \frac{4A^3}{d_{\mathrm{dry}}^3 S_c^2} \tag{6}$$

where S_c is the critical super-saturation at which half of the monodisperse particles activate, d_{dry} is the dry mobility diameter selected by DMA-1, and

$$A = \frac{4M_w\sigma_w}{RT\rho_w} \tag{7}$$

Here M_w, σ_w and ρ_w are the molecular weight, the surface tension and the density of water, while R and T are the universal gas constant and temperature of the system, respectively.

European Union
European Social Fund
OPERATIONAL PROGRAMME
EDUCATION AND LIFELONG LEARNING
investing in knowledge society
MINISTRY OF EDUCATION & RELIGIOUS AFFAIRS
MANAGING AUTHORITY
NSRF 2007-2013
EUROPEAN SOCIAL FUND
Co-financed by Greece and the European Union

The hygroscopic parameter of the particles can be estimated using measurements of their chemical composition as follows:

$$\kappa_{\mathrm{CHEM}} = \sum_{\mathrm{i}} \varepsilon_{\mathrm{i}} \kappa_{\mathrm{i}} \,. \quad (8)$$

Here $\varepsilon_{\mathrm{i}} = V_{\mathrm{si}}/V_{\mathrm{s}}$ and κ_{i} are the volume fraction and the hygroscopic parameter of the *i*th chemical species comprising the particles, with V_{si} being the volume occupied by that species and V_{s} the volume of the dry particle.

Figure B2 shows the κ values together with the activation fractions of particles having dry electrical mobilities of 80 nm at sub- and super-saturated conditions, in Patras suburban site. For the HTDMA measurements $\overline{\kappa_{\mathrm{HTDMA}}}$ (cf. Eq. 5) is reported, giving the average value of particles hygroscopicity in cases that they were externally mixed. Overall, particles of all measured sizes exhibited moderate hygroscopicities in both sub- and super-saturated conditions, which are comparable with the observations provided by Bezantakos et al., (2013) and Bougiatioti et al., (2009) for remote locations in Greece. The observed κ values from both the instruments agreed within ±30 %, which is typical for these kind of measurements. Most of the particles were CCN active with one exception at 17 June, where their activation fraction decreased down to 50%.

Aerosols mixing state was also investigated (i.e., using the HTDMA measurements) and while the majority of them were hygroscopic, an increased fraction of nearly hydrophobic particles was observed when the air-masses that reached the sampling site were passing over the city of Patras. Particles having 60-nm mobility diameters exhibited the highest fraction of nearly hydrophobic particles which combined with the wind direction is indicative of freshly emitted, anthropogenic aerosols.

European Union
European Social Fund
OPERATIONAL PROGRAMME
EDUCATION AND LIFELONG LEARNING
investing in knowledge society
MINISTRY OF EDUCATION & RELIGIOUS AFFAIRS
MANAGING AUTHORITY
NSRF 2007-2013
programme for development
EUROPEAN SOCIAL FUND
Co-financed by Greece and the European Union

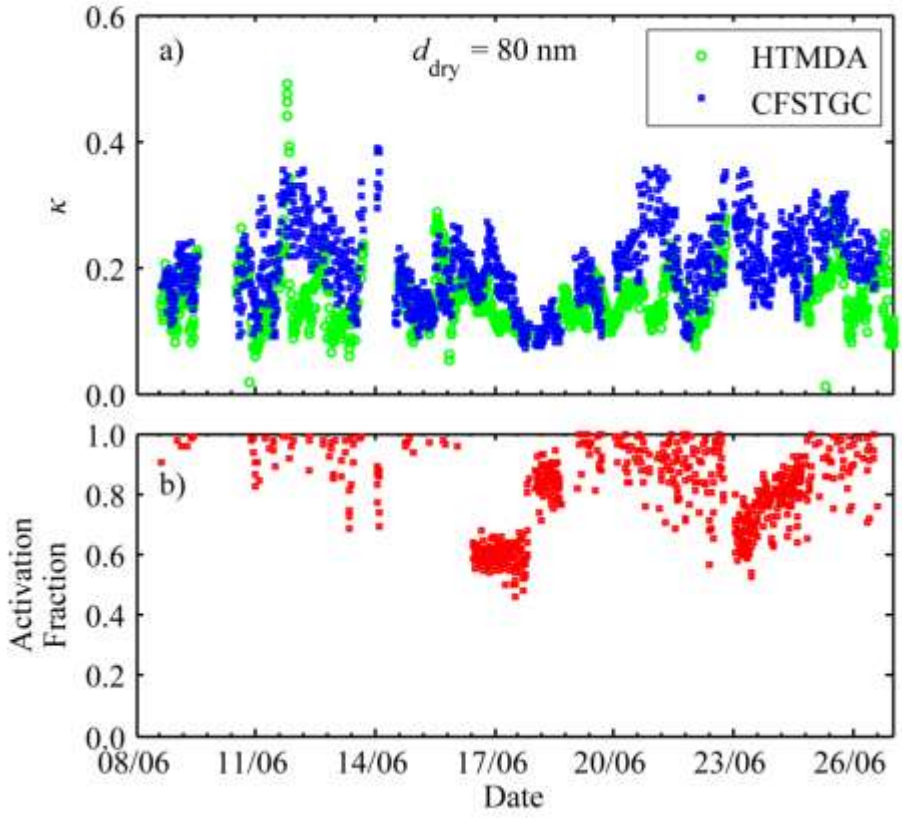

Fig B2. Hygroscopic parameter κ of 80-nm aerosols, obtained from the HTDMA and CFSTGC combined measurements (**a**), together with their activation fraction (**b**), in Patras suburban site.

The κ values together with the activation fractions of particles having dry electrical mobilities of 80 nm at sub- and super-saturated conditions, in Athens suburban site are shown in Fig B3. For the HTDMA measurements $\overline{\kappa_{\mathrm{HTDMA}}}$ (cf. Eq. 5) is reported, giving the average value of particles hygroscopicity in cases that they were externally mixed. In contrast to the measurements conducted in Patras suburban site, in Athens particles were highly hygroscopic, in both sub- and super-saturated conditions. Deviations, which in some cases exceeded 30%, were also observed in the κ values reported from both the instruments. Different particle properties and exposure conditions (i.e. sub- and super-saturation) inside the HTDMA and CFSTGC, could have been contributing to the observed discrepancies between κ_{CCN} and κ_{HTDMA}. For example, κ_{HTDMA} is more sensitive to changes in the particles shape, than κ_{CCN}. On the other hand, κ_{CCN} is affected

European Union
European Social Fund
OPERATIONAL PROGRAMME
EDUCATION AND LIFELONG LEARNING
investing in knowledge society
MINISTRY OF EDUCATION & RELIGIOUS AFFAIRS
MANAGING AUTHORITY
NSRF 2007-2013
EUROPEAN SOCIAL FUND
Co-financed by Greece and the European Union

by changes in droplet surface tension, while κ_{HTDMA} stays practically unaffected (Dusek et al., 2011). Non-idealities of the solution in the particle droplets at sub-saturation conditions (Petters et al., 2009) and limitations posed by organic coating on particles surface, inhibiting particles ability to take up water in sub-saturation conditions (Henning et al., 2012; Chan,M.N. and Chan C.K., 2007), should also be considered.

The activation fraction of the measured aerosols varied more in Athens than in Patras, ranging from 50 to 100 % for 80-nm particles, but overall particles were CCN active.

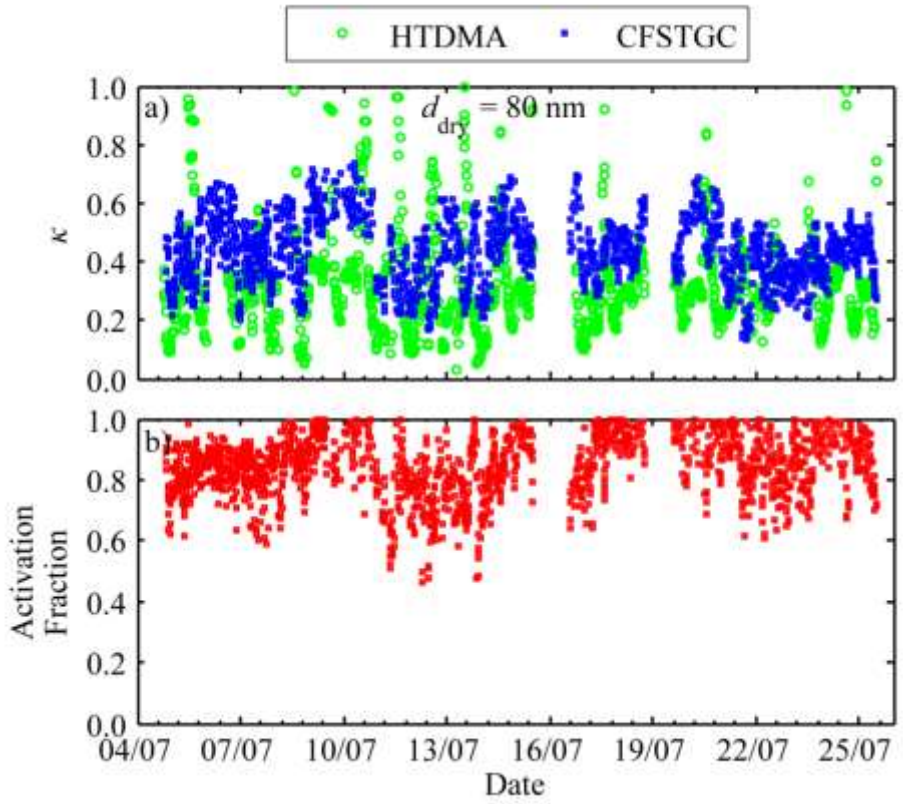

Fig B3. Hygroscopic parameter κ of 80-nm aerosols, obtained from the HTDMA and CFSTGC combined measurements (**a**), together with their activation fraction (**b**), in Athens suburban site.

Aerosols mixing state (i.e., derived from the HTDMA measurements) showed that particles were in most of the cases internally mixed and hygroscopic. However, nearly hydrophobic externally mixed particles were more often observed in Athens than in Patras and their fraction was increased when the air-masses that reached the sampling

European Union
European Social Fund
OPERATIONAL PROGRAMME
EDUCATION AND LIFELONG LEARNING
investing in knowledge society
MINISTRY OF EDUCATION & RELIGIOUS AFFAIRS
MANAGING AUTHORITY
NSRF 2007-2013
EUROPEAN SOCIAL FUND
Co-financed by Greece and the European Union

site were passing over the city of Athens. Particles having 60-nm mobility diameters exhibited the highest fraction of nearly hydrophobic particles, which combined with their highly variable activation fraction, indicates the presence of anthropogenic emitted aerosols.

Hygroscopicity measurements that were conducted during late Summer and Autumn 2012, at the remote site of Finokalia showed that particles were moderately hygroscopic and in most of the cases internally mixed, which is expected for a remote site. However, the site was affected by the plumes of several wildfires during the sampling period, which raised the opportunity of studying the hygroscopic properties of biomass burning particles. More specifically, the site was affected by a severe fire event that burned most of the island of Chios (19–21 August), an extensive wildfire at the Dalmatian Coast in Croatia resulting in smoke plumes that spread across the Balkans during the period 28–30 August, and, less extensive fires on the Greek islands of Euboea (3-5 September) and Andros (12-13 September). During the arrival of the biomass-burning-laden air masses, the hygroscopicity parameters of all particle sizes were decreased in comparison to the other periods. More specifically, the HTDMA derived hygroscopic parameters during the events were half of those measured through other periods, exhibiting values even less than 0.1 (c.f. Fig B4). At super-saturation conditions values of the hygroscopic parameter were in the range of 0.2-0.3 (c.f. Fig. B5). Aerosols activation fractions were overall unaffected during the events, except those of the 60-nm particles, which more probably were consisted of hydrophobic matter in a bigger extend than their larger counterparts.

European Union
European Social Fund
OPERATIONAL PROGRAMME
EDUCATION AND LIFELONG LEARNING
investing in knowledge society
MINISTRY OF EDUCATION & RELIGIOUS AFFAIRS
MANAGING AUTHORITY
NSRF 2007-2013
EUROPEAN SOCIAL FUND
Co-financed by Greece and the European Union

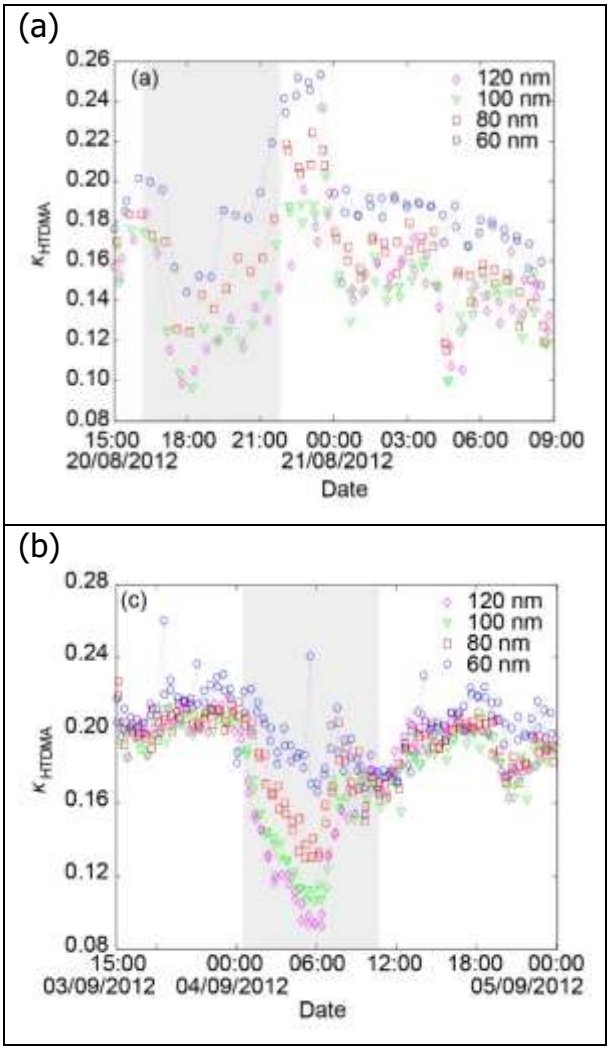

Fig B4. Hygroscopic parameter κ obtained from the HTDMA measurements for the Chios (**a**) and Euboea (**b**), fire events. The shadowed area indicates the arrival of the plume.

European Union
European Social Fund
OPERATIONAL PROGRAMME
EDUCATION AND LIFELONG LEARNING
investing in knowledge society
MINISTRY OF EDUCATION & RELIGIOUS AFFAIRS
MANAGING AUTHORITY
NSRF 2007-2013
EUROPEAN SOCIAL FUND
Co-financed by Greece and the European Union

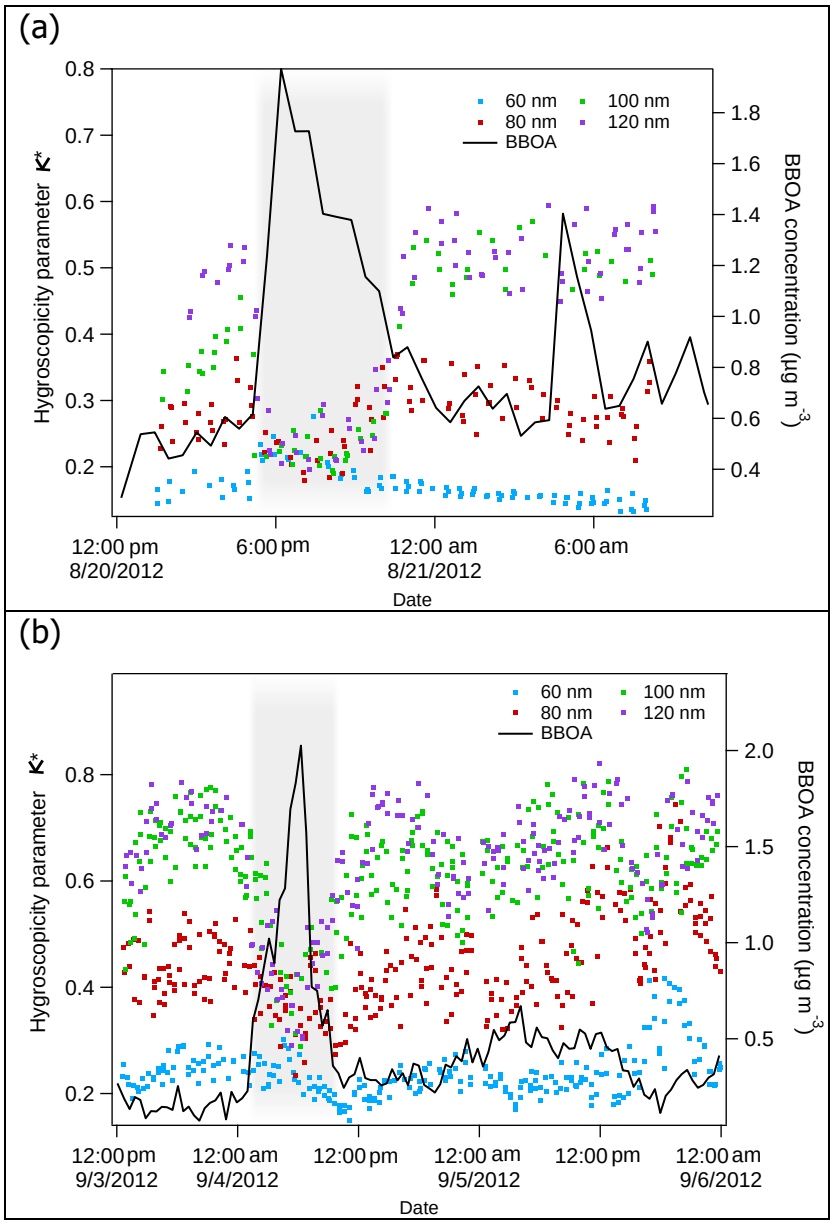

Fig B5. Hygroscopic parameter κ obtained from the CFSTGC measurements for the Chios (**a**) and Euboea (**b**), fire events. The shadowed area indicates the arrival of the plume, while the black line indicates the presence of biomass burning particles.

European Union
European Social Fund
OPERATIONAL PROGRAMME
EDUCATION AND LIFELONG LEARNING
investing in knowledge society
MINISTRY OF EDUCATION & RELIGIOUS AFFAIRS
MANAGING AUTHORITY
NSRF 2007-2013
EUROPEAN SOCIAL FUND
Co-financed by Greece and the European Union

B3. References

Bezantakos, S., Barmpounis, K., Giamarelou, M., Bossioli, E., Tombrou, M., Mihalopoulos, N., Eleftheriadis, K., Kalogiros, J., Allan, J. D., Bacak, A., Percival, C. J., Coe, H. and Biskos, G.: Chemical composition and hygroscopic properties of aerosol particles over the Aegean Sea, Atmos. Chem. Phys., 13, 11595–11608, 2013, doi:10.5194/acp-13-11595-2013.

Biskos, G., Paulsen, D., Russell, L.M., Buseck, P.R., Martin, S.T.: Prompt deliquescence and efflorescence of aerosol nanoparticles. Atmos. Chem. Phys. 6, 4633-4642, 2006a.

Bougiatioti, A., Fountoukis, C., Kalivitis, N., Pandis, S. N., Nenes, A. and Mihalopoulos N.: Cloud condensation nuclei measurements in the marine boundary layer of the eastern Mediterranean: CCN closure and droplet growth kinetics, Atmos. Chem. Phys., 9, 7053–7066, 2009.

Chan, M. N., & Chan, C. K.: Mass transfer effects on the hygroscopic growth of ammonium sulfate particles with a water-insoluble coating. Atmos. Environ., 41(21), 4423-4433, 2007.

Dusek, U., Frank, G. P., Massling, A., Zeromskiene, K., Iinuma, Y., Schmid, O., Helas, G., Hennig, T., Wiedensohler, A., and Andreae, M. O.: Water uptake by biomass burning aerosol at sub-and supersaturated conditions: closure studies and implications for the role of organics. Atmos. Chem.Phys. 11, no. 18, 9519-9532, 2011.

Henning, S., Ziese, M., Kiselev, A., Saathoff, H., Möhler, O., Mentel, T. F., Buchholz, A., Spindler, C., Michaud, V., Monier, M., Sellegri, K., and Stratmann, F.: Hygroscopic growth and droplet activation of soot particles: uncoated, succinic or sulfuric acid coated. Atmos. Chem. Phys., 12, 4525-4537, doi:10.5194/acp-12-4525-2012, 2012.

Knutson, E.O., Whitby, K.T.: Aerosol classification by electric mobility: Apparatus, theory, and applications. J. Aerosol Sci., 6, 443-451, 1975.

Kreidenweis, S.M., Petters, M.D., DeMott, P.J.: Single parameter estimates of aerosol water content, Environ. Res. Lett., 3, 035002, 2008.

European Union
European Social Fund

OPERATIONAL PROGRAMME
EDUCATION AND LIFELONG LEARNING
investing in knowledge society
MINISTRY OF EDUCATION & RELIGIOUS AFFAIRS
MANAGING AUTHORITY

NSRF 2007-2013
programme for development
EUROPEAN SOCIAL FUND

Co-financed by Greece and the European Union

Moore, Richard H., and Nenes, A.: Scanning flow CCN analysis - A method for fast measurements of CCN spectra. Aerosol Sci. Tech. 43.12, 1192-1207, 2009.

Petters, M.D. & Kreidenweis S.M.: A single parameter representation of hygroscopic growth and cloud condensation nucleus activity, Atmos. Chem. Phys., 7, 1961-1971, 2007.

Petters, M. D., Wex, H., Carrico, C. M., Hallbauer, E., Massling, A., McMeeking, G. R., Poulain, L., Wu, Z., Kreidenweis, S. M., and Stratmann, F.: Towards closing the gap between hygroscopic growth and activation for secondary organic aerosol – Part 2: Theoretical approaches, Atmos. Chem. Phys., 9, 3999-4009, doi:10.5194/acp-9-3999-2009, 2009.

Rader, D.J., McMurry P.H.: Application of the tandem differential mobility analyzer to studies of droplet growth or evaporation, J. Aerosol Sci., 17, 771-787, 1986.

Roberts, G. C., and Nenes, A.: A continuous-flow streamwise thermal-gradient CCN chamber for atmospheric measurements. Aerosol Sci. Tech. 39.3, 206-221, 2005.

Stolzenburg, M. R. and McMurry, P.H.: TDMAFIT User's Manual, Particle Technology Laboratory, Department of Mechanical Engineering, Univercity of Minnesota, Minneapolis, 1-61, 1988.

Stolzenburg, M.R. & McMurry, P.H.: An ultrafine aerosol Condensation Nucleus Counter, Aerosol Sci. Technol., 14, 48-65, 1991.

European Union
European Social Fund
OPERATIONAL PROGRAMME
EDUCATION AND LIFELONG LEARNING
investing in knowledge society
MINISTRY OF EDUCATION & RELIGIOUS AFFAIRS
MANAGING AUTHORITY
NSRF 2007-2013
programme for development
EUROPEAN SOCIAL FUND
Co-financed by Greece and the European Union

C. Volatility measurements of ambient organic aerosols in Athens during the winter.

C1 Introduction

Atmospheric particulate matter contains a variety of both inorganic and organic species. Organic compounds contribute 20-90% of the submicrometer mass depending on the location and season making them often the major fraction (Kanakidou et al., 2005). OA is either emitted directly (primary organic aerosol, POA) or formed in the atmosphere by condensation of low vapor pressure products of the oxidation of volatile organic compounds (VOCs) (secondary organic aerosols, SOA). The complexity of oxidation pathways has led to insufficient knowledge of OA formation mechanisms and its properties. One of the most important physical properties of OA is volatility which provides information about its origin, and indirect information about its chemical composition (Jennings and O'Dowd, 1990; Clarke, 1991, 1993; Brock, et al., 1995; Orsini et al., 1999; Sakurai et al., 2003; Philippin et al., 2004; Kalberer et al., 2004; Wehner et al., 2004; Kuhn et al., 2005).

A number of recent studies coupling a TD with an AMS in the field (Faulhaber et al., 2009; Grieshop et al., 2009; Huffman et al., 2009; Kostenidou et al., 2009; Cappa and Jimenez, 2010; Lee et al., 2010; May et al., 2013) have tried to obtain information about the relationship between the OA composition and its volatility. The interpretation of ambient TD-AMS results is however very challenging. Difficulties include how to account for the mass transfer resistances, the changes in the AMS collection efficiency and the particle losses inside the TD during particle evaporation. Due to these challenges and the lack of the appropriate theoretical analysis, comparison between the findings of different studies is difficult.

During the period of 10 January – 9 February 2013 the Laboratory of Air Quality Studies (LAQS) of University of Patras and FORTH-ICEHT conducted an intensive campaign in Athens. This study aimed to investigate the impact of biomass burning OA

European Union
European Social Fund
OPERATIONAL PROGRAMME
EDUCATION AND LIFELONG LEARNING
investing in knowledge society
MINISTRY OF EDUCATION & RELIGIOUS AFFAIRS
MANAGING AUTHORITY
NSRF 2007-2013
programme for development
EUROPEAN SOCIAL FUND
Co-financed by Greece and the European Union

produced mainly from residential heating during the winter months on the atmosphere and human health. The present chapter focuses on measuring the volatility of OA from residential wood burning. A HR-Tof-AMS and an SMPS placed upstream of the TD (the one presented in Chapter 2) in order to measure the volatility of OA at the National Observatory in Thissio were our sampling site was located.

C2 Methods

C2.1 Thermodenuder-AMS-SMPS field operation

The mobile laboratory of FORTH-ICEHT was located at the National Observatory of Athens. Inside the mobile laboratory the TD-AMS-SMPS configuration of Fig. C1 measured continuously the ambient aerosol size-composition distribution both at room temperature and at elevated (TD) temperatures.

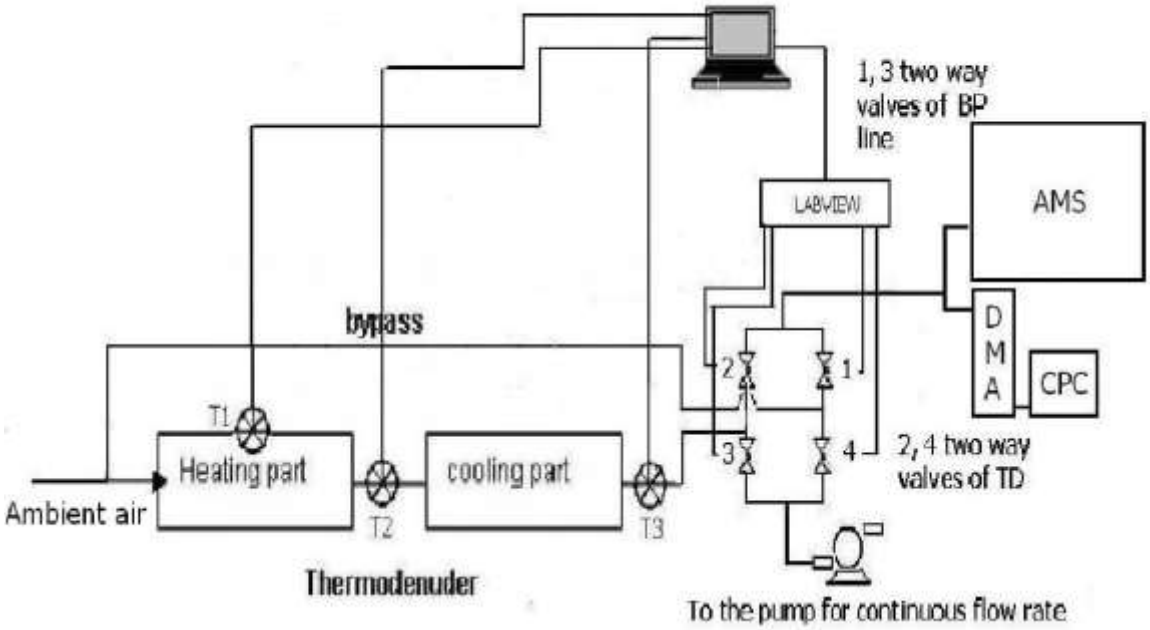

Figure C1 Experimental configuration of TD-AMS-SMPS system inside the mobile laboratory.

European Union
European Social Fund
OPERATIONAL PROGRAMME
EDUCATION AND LIFELONG LEARNING
investing in knowledge society
MINISTRY OF EDUCATION & RELIGIOUS AFFAIRS
MANAGING AUTHORITY
NSRF 2007-2013
EUROPEAN SOCIAL FUND
Co-financed by Greece and the European Union

Ambient air was sampled 6 m above the ground. The incoming total flow rate to our system was 1.1 L min^{-1}. 1 L min^{-1} was needed for the SMPS and 0.1 L min^{-1} for the AMS. The TD was operating at 15.8 s residence time. Temperatures of interest were 25, 40, 60, 80,100, 150, 200, and 300 ºC.

C2.2 TD-AMS-SMPS data analysis

For the present analysis we selected periods during which there were very high concentrations of OA due to wood burning. The criteria for the selection of these periods were a) the concentration of accetonitrile which is a tracer of fire smoke and measured by a Proton Transfer Reaction Mass Spectrometer (PTR-MS) had to be higher than 0.25 ppb. b) the measurements were between 18:00 and 06:00 (nightime), c) the AMS mass concentration exceeded 15 μg m^{-3}. If all these criteria were met, the period characterized as a burning period. For our analysis there were 10 such periods in the 30 days of the campaign.

The calculations were made assuming that the ratio of AMS CE_{BP} to CE_{TD} is unity meaning that there was no difference between the two collection efficiency values. The same assumption was used OA densities ($\rho_{OA,BP}=\rho_{OA,TD}$).

We tested the validity of these assumptions following the consistency test proposed by Lee et al. (2010). A comparison of the predicted and measured number and size distributions at 100ºC is shown in Fig. C2 and C3. The agreement is satisfactory suggesting that our loss corrections and simplifying assumptions are accurate to within 10-20%.

European Union
European Social Fund
OPERATIONAL PROGRAMME
EDUCATION AND LIFELONG LEARNING
investing in knowledge society
MINISTRY OF EDUCATION & RELIGIOUS AFFAIRS
MANAGING AUTHORITY
NSRF 2007-2013
programme for development
EUROPEAN SOCIAL FUND
Co-financed by Greece and the European Union

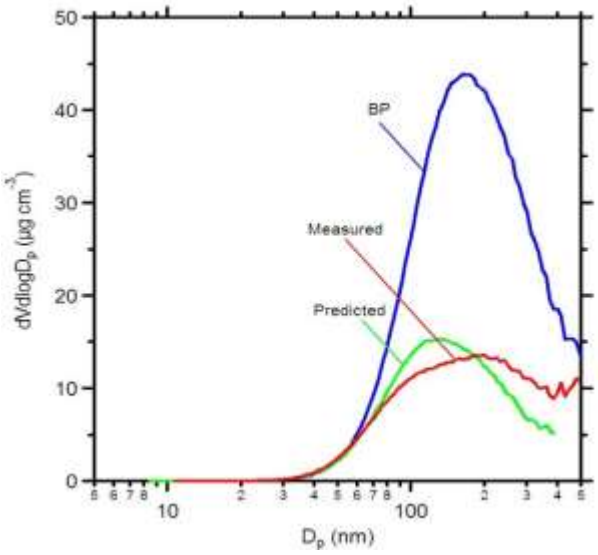

Figure C2. Number distributions comparison at 100 ºC. The blue line corresponds to the ambient SMPS measurements. The red line is the SMPS measurements after the TD. The green line our estimates based on the losses in the system and the AMS measurements.

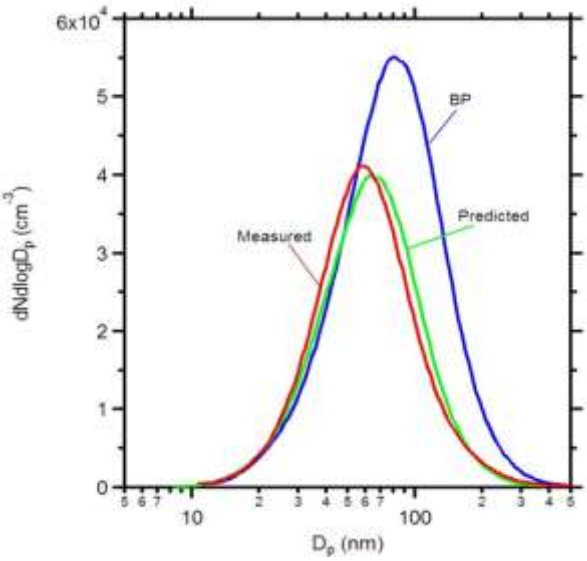

Figure C3. Volume distributions comparison at 100 ºC. The blue line corresponds to the ambient SMPS measurements. The red line is the SMPS measurements after the TD. The green line our estimates based on the losses in the system and the AMS measurements.

European Union
European Social Fund
OPERATIONAL PROGRAMME
EDUCATION AND LIFELONG LEARNING
investing in knowledge society
MINISTRY OF EDUCATION & RELIGIOUS AFFAIRS
MANAGING AUTHORITY
NSRF 2007-2013
EUROPEAN SOCIAL FUND
Co-financed by Greece and the European Union

C2.3 Mass Fraction Remaining (MFR) determination

In order to determine MFR we have calculated the losses (f_{Losses}) for the experimental setup in Athens (Fig. C4). An additional complication was the variability of the ambient OA levels. When the OA concentration changed significantly faster than our timescale for a TD measurement the data point was considered not valid. This elimination of data points is illustrated in Fig. C5.

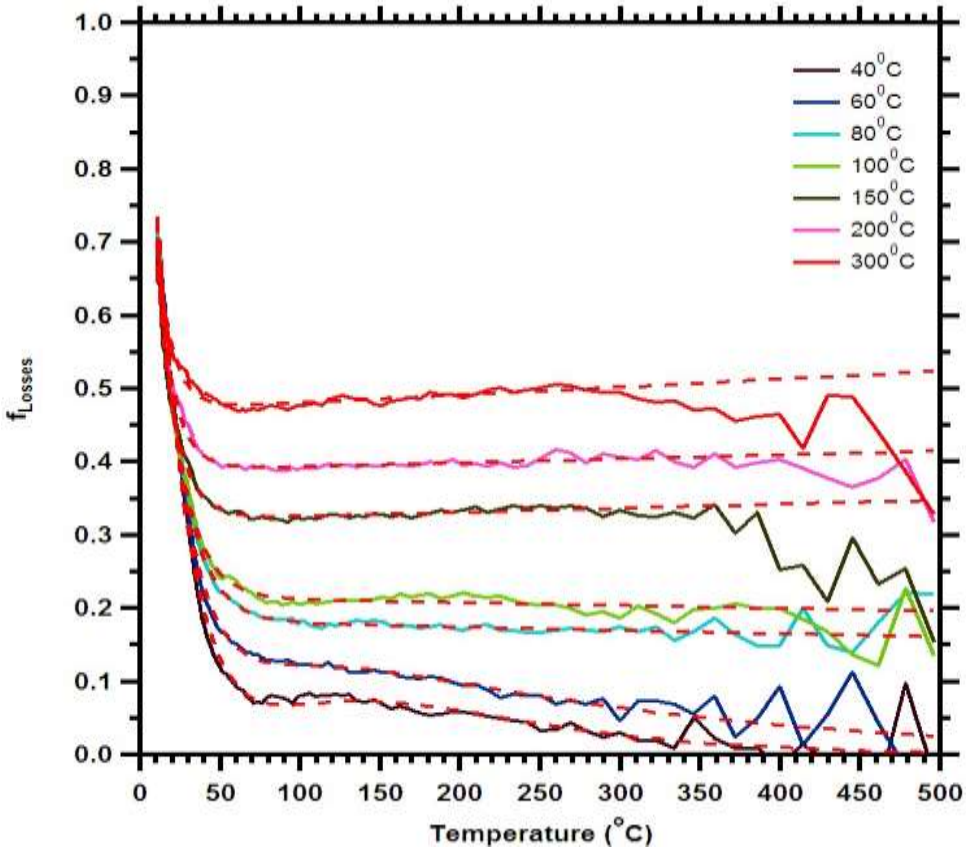

Figure C4. Losses fraction as a function of Temperature for Athens experimental conditions. The red dashed fitted curves are used to guide the eye.

In Fig. C5 not valid data measurements were collected during night hours from 23:15-01:00 and temperatures 40 and 60 ^{o}C and 03:00-05:00 with temperatures 200 and 300 ^{o}C. This cleaning of the dataset has been done for all the days of the campaign (not

European Union
European Social Fund
OPERATIONAL PROGRAMME
EDUCATION AND LIFELONG LEARNING
investing in knowledge society
MINISTRY OF EDUCATION & RELIGIOUS AFFAIRS
MANAGING AUTHORITY
NSRF 2007-2013
EUROPEAN SOCIAL FUND
Co-financed by Greece and the European Union

shown). The MFRs is then calculated with the assumption of equal collection efficiencies for BP and TD measurements. The thermogram of all burning periods is shown in Fig. C6.

The next step was the determination of the average OA MFR for each temperature during the burning period. The thermogram in Fig. C7 shows these average values together with their uncertainty range. From both Fig. C6 and C7 we can see that after 150^{o}C no more evaporation of ambient OA seems to occur.

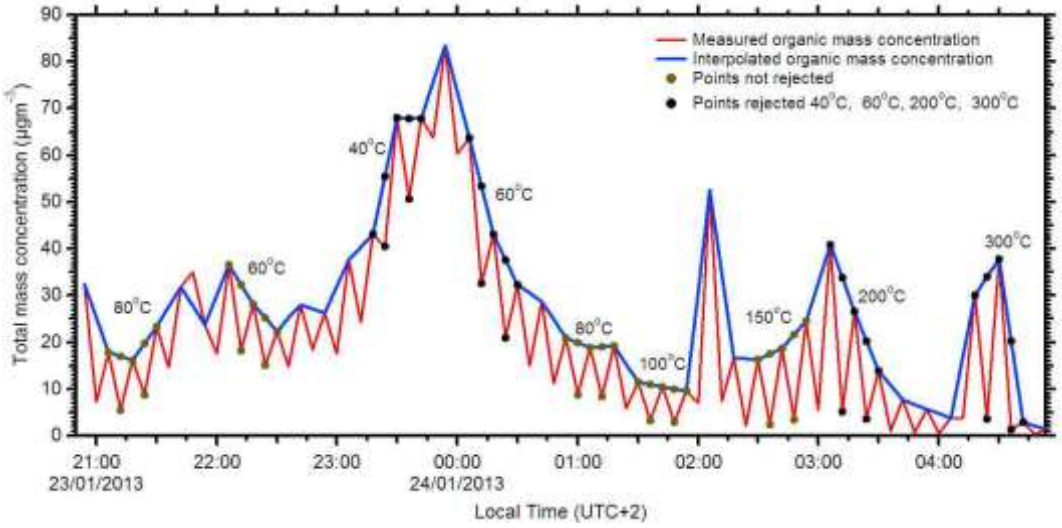

Figure C5. Total mass AMS concentration as a function of time for a day of burning period. Black markers represent the rejected data points and are not taken into account for the MFR calculations since the bypass data which are the upper markers of the red line are not so stable.

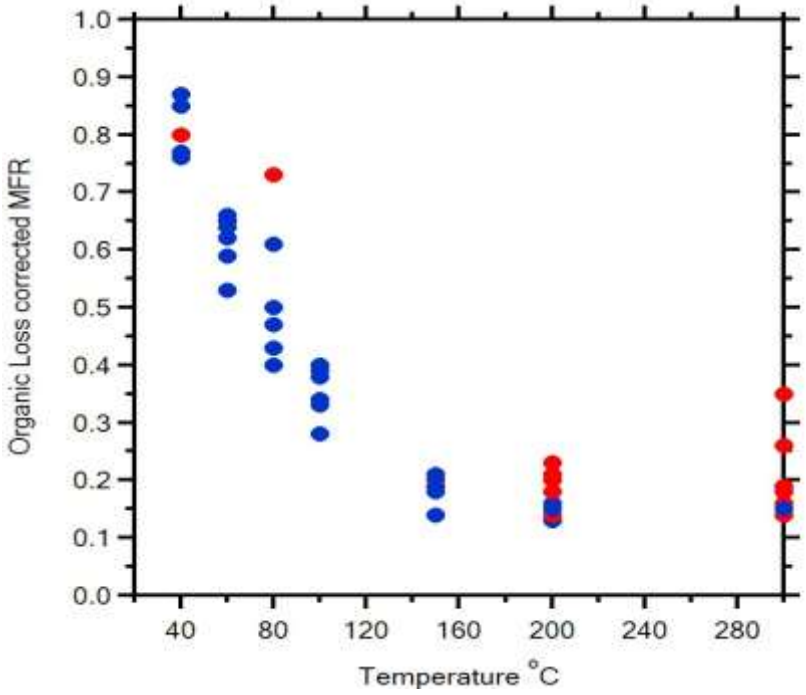

Figure C6. Burning periods OA MFR as function of temperature. Blue symbols are the valid data points and red the ones rejected due to unacceptable OA variability during the measurement period.

European Union
European Social Fund
OPERATIONAL PROGRAMME
EDUCATION AND LIFELONG LEARNING
investing in knowledge society
MINISTRY OF EDUCATION & RELIGIOUS AFFAIRS
MANAGING AUTHORITY
NSRF 2007-2013
EUROPEAN SOCIAL FUND
Co-financed by Greece and the European Union

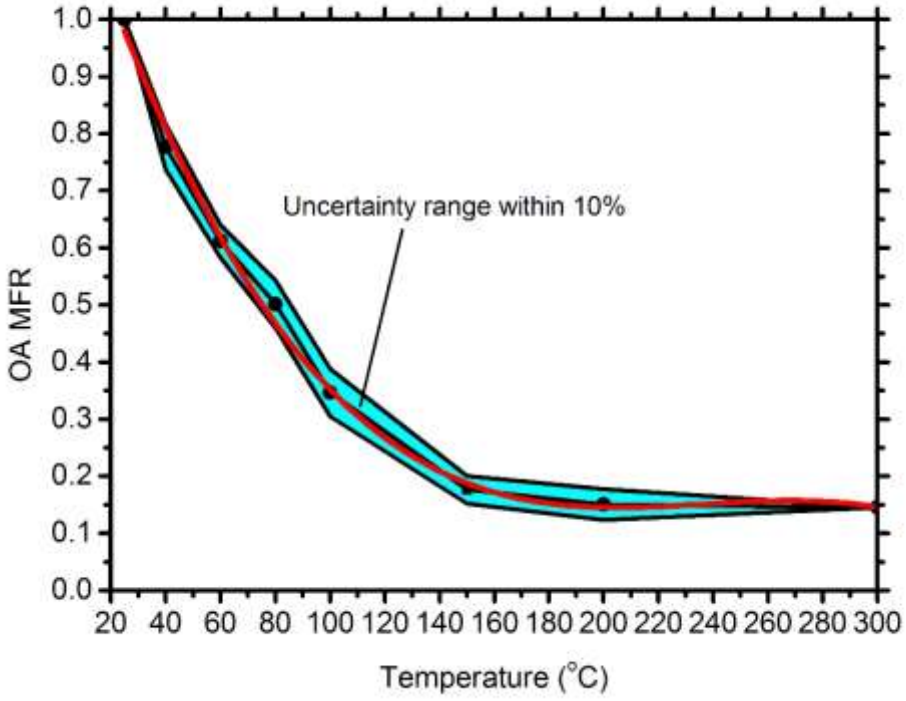

Figure C7. Thermogram of average post corrected experimental OA MFR for all burning periods. The shaded area corresponds to 1 standard deviation. Red line is a fit to guide the eye.

The calculation of mass fraction remaining distribution shows that 23% of the mass evaporated between 25-40 ^{o}C and 18% between 100-150 ^{o}C (Fig. C8). However, 15% of the mass remain at temperature values larger than 300^{o}C. A probable reason for this is that reactions occur inside the TD after 150-200 ^{o}C.

C2.4 Volatility measurement of ambient OA

The volatility distribution is estimated by applying the inverse TD dynamics model presented by Karnezi et al. (2013). Using as inputs the ambient OA MFR values and the geometric characteristics of our TD, the volatility distribution, vaporization enthalpy, and mass accommodation coefficient are estimated.

European Union
European Social Fund
OPERATIONAL PROGRAMME
EDUCATION AND LIFELONG LEARNING
investing in knowledge society
MINISTRY OF EDUCATION & RELIGIOUS AFFAIRS
MANAGING AUTHORITY
NSRF 2007-2013
EUROPEAN SOCIAL FUND
Co-financed by Greece and the European Union

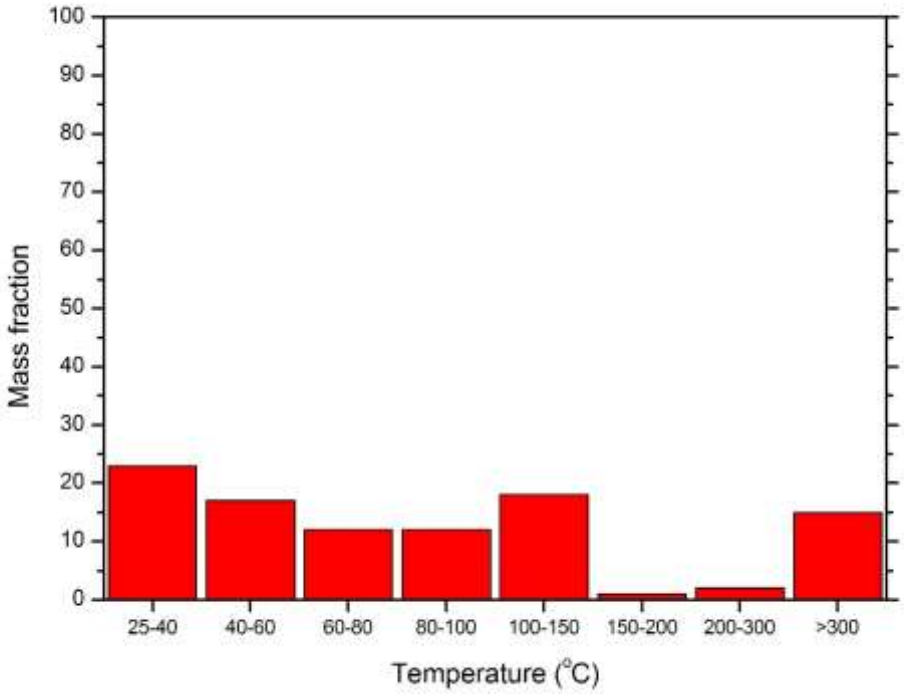

Figure C8. Mass fraction of the OA that evaporated at each temperature during the burning periods.

Using all the measurements we estimated the volatility distribution shown in Fig. C9. This is characterized by a wide range of low volatility and semivolatile compounds but also 15% of OA of extremely low volatility (10^{-7} μg m^{-3}). The corresponding values for the evaporation enthalpies were 85±18 kJ mol^{-1} for the 10^{-2}-10^{2} μg m^{-3} components and 50 kJ mol^{-1} for the 10^{-7} μg m^{-3}. The estimated accommodation coefficients were in the range of 0.12-0.88. The predicted thermogram with these estimated parameter values, is shown in Fig. C10.

The measurements above 150°C are probably affected by reactions in these elevated temperatures and do not reflect to the volatility of the OA. We repeated the fitting exercise using only temperatures up to 150°C. The resulting volatility distribution is shown in Fig. C11.

European Union
European Social Fund
OPERATIONAL PROGRAMME
EDUCATION AND LIFELONG LEARNING
investing in knowledge society
MINISTRY OF EDUCATION & RELIGIOUS AFFAIRS
MANAGING AUTHORITY
NSRF 2007-2013
programme for development
EUROPEAN SOCIAL FUND
Co-financed by Greece and the European Union

.

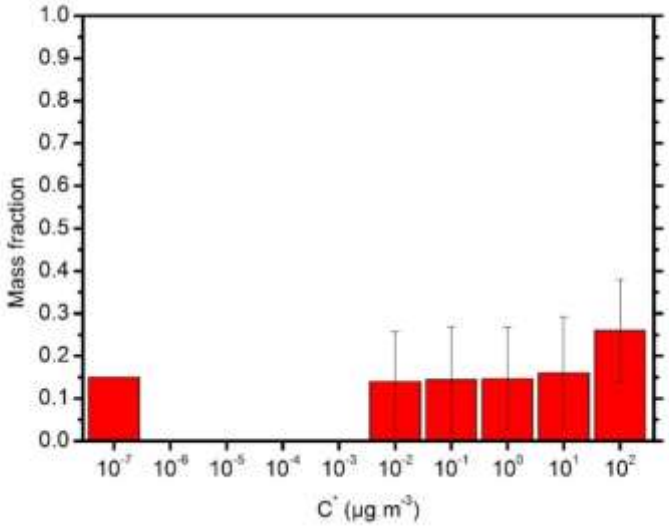

Figure C9. Volatility distribution of ambient OA mass fraction using the measurements at all TD temperatures

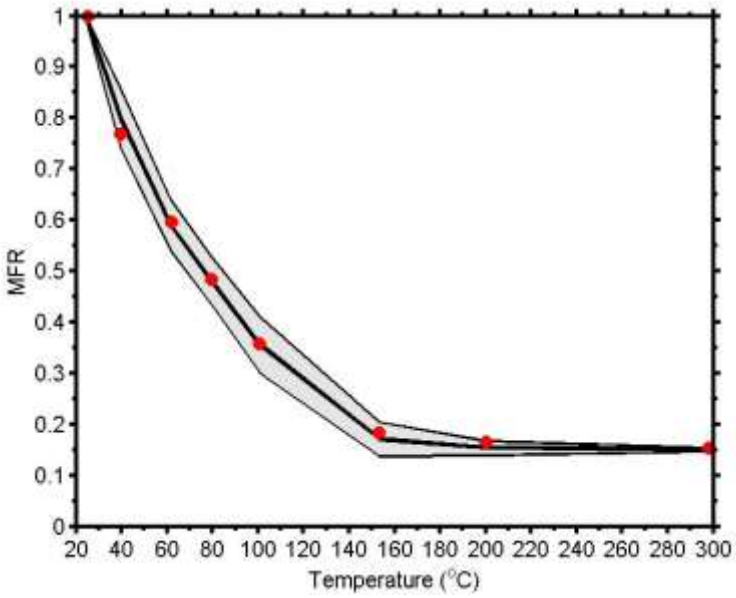

Figure C10. Predicted thermogram of ambient OA using the measurements at all TD temperatures. The symbols correspond to the measurements. The shaded area corresponds to 1 standard deviation.

European Union
European Social Fund
OPERATIONAL PROGRAMME
EDUCATION AND LIFELONG LEARNING
investing in knowledge society
MINISTRY OF EDUCATION & RELIGIOUS AFFAIRS
MANAGING AUTHORITY
NSRF 2007-2013
EUROPEAN SOCIAL FUND
Co-financed by Greece and the European Union

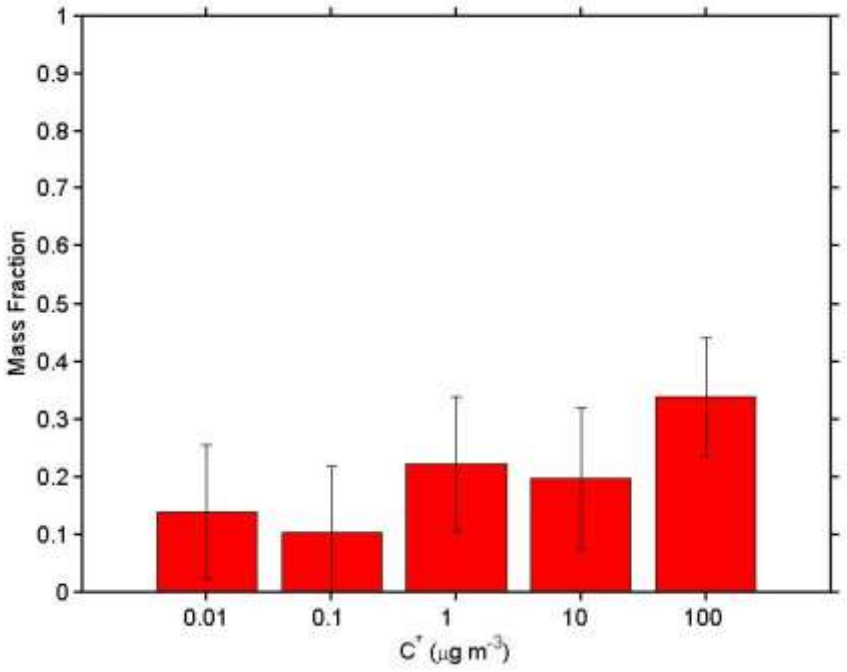

Figure C11 Volatility distribution of ambient OA mass fraction for temperatures up to 150°C and its uncertainty.

Most of the OA (around 80%) is predicted to be semivolatile ($1 \leq C^* \leq 100$ μg m^{-3}) while there is approximately 20% low volatility OA ($C^* \leq 0.1$ μg m^{-3}) (Tsimpidi et al., 2010). The corresponding effective ΔH_{evap} and accommodation coefficients are shown in Fig. C12 and C13 with their corresponding uncertainty ranges. The model predictions with these estimated parameters are compared to the TD measurements in Fig. C14.

European Union
European Social Fund
OPERATIONAL PROGRAMME
EDUCATION AND LIFELONG LEARNING
investing in knowledge society
MINISTRY OF EDUCATION & RELIGIOUS AFFAIRS
MANAGING AUTHORITY
NSRF 2007-2013
EUROPEAN SOCIAL FUND
Co-financed by Greece and the European Union

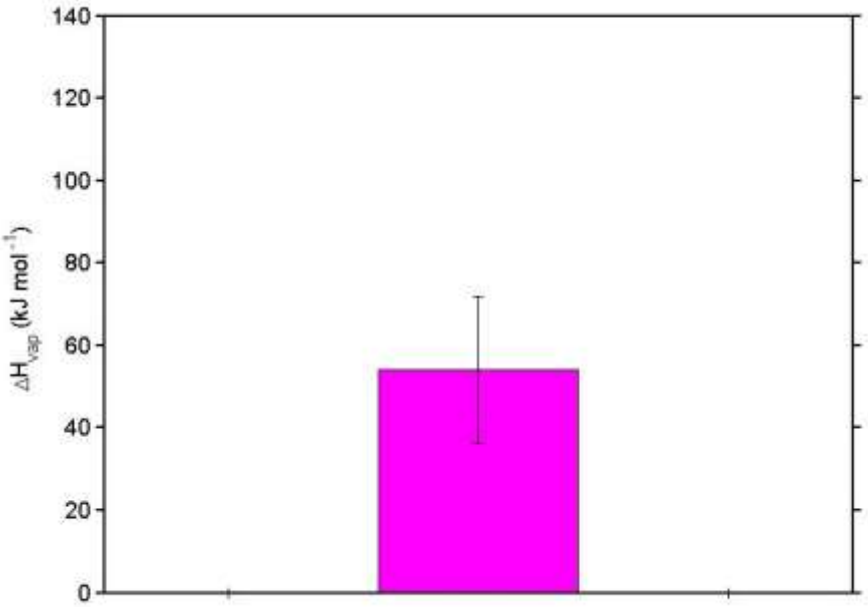

Figure C12. Effective vaporization enthalpy of ambient OA and its uncertainty.

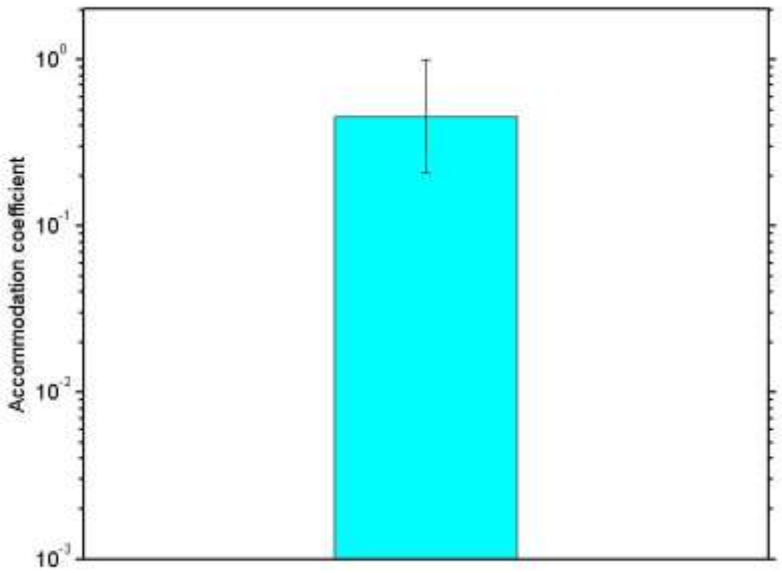

Figure C13. Mass accommodation coefficient of ambient OA and its uncertainty.

European Union
European Social Fund
OPERATIONAL PROGRAMME
EDUCATION AND LIFELONG LEARNING
investing in knowledge society
MINISTRY OF EDUCATION & RELIGIOUS AFFAIRS
MANAGING AUTHORITY
NSRF 2007-2013
EUROPEAN SOCIAL FUND
Co-financed by Greece and the European Union

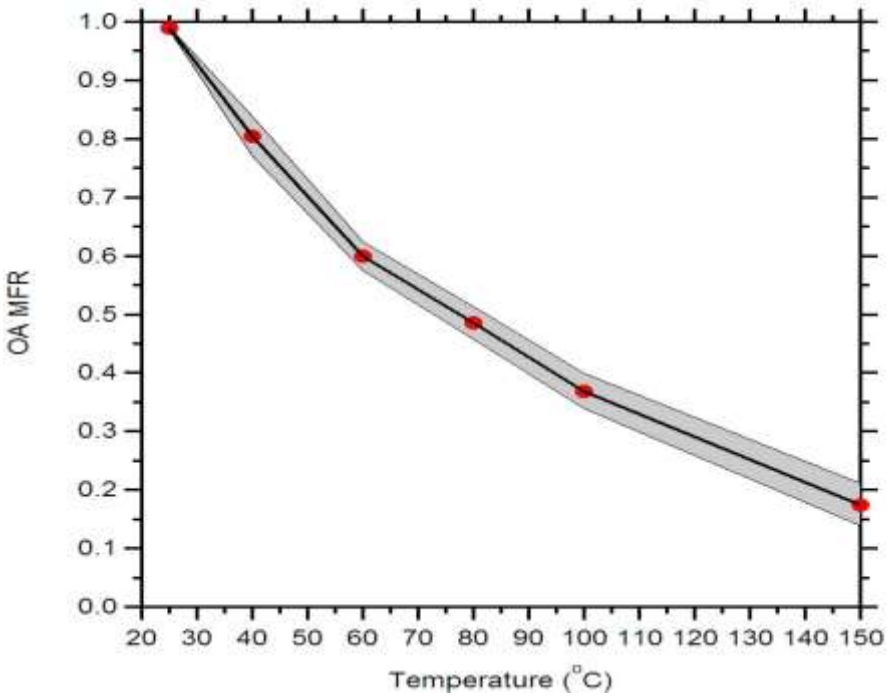

Figure C14. Predicted thermogram of ambient OA for temperatures up to 150ºC. The symbols correspond to the measurements. The shaded area corresponds to 1 standard deviation.

C4.2.5 Gas-to-particle partitioning estimation

The estimated fraction of the organic material that is in the particulate phase as a function of the ambient OA concentration is shown in Fig. C15, C16 and C17. For comparison, we also show our results for the olive-branch burning and the May et al. (2013) results for a wide of US wood types. The results are quite consistent with each other with small differences due to different wood types and combustion conditions.

European Union
European Social Fund
OPERATIONAL PROGRAMME
EDUCATION AND LIFELONG LEARNING
investing in knowledge society
MINISTRY OF EDUCATION & RELIGIOUS AFFAIRS
MANAGING AUTHORITY
NSRF 2007-2013
EUROPEAN SOCIAL FUND
Co-financed by Greece and the European Union

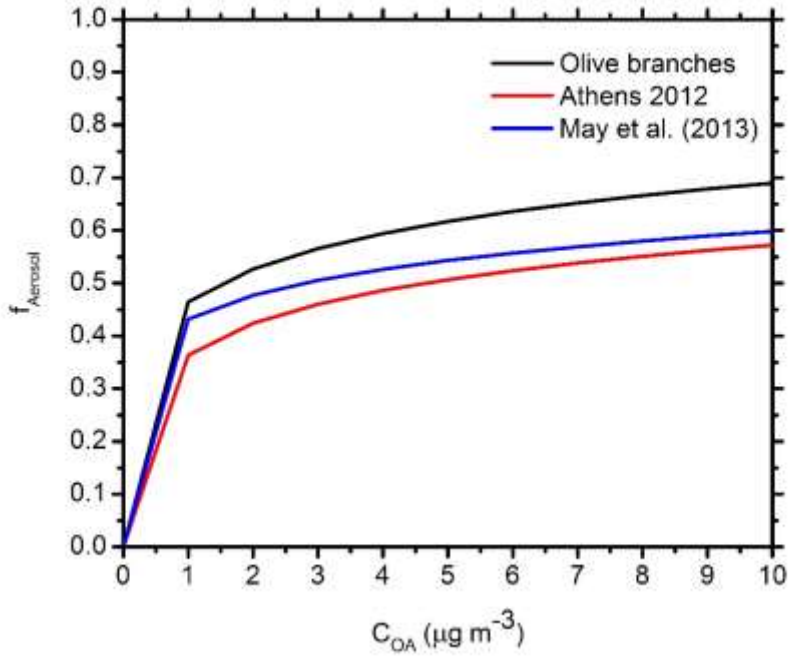

Figure C15 Particulate fractions as a function of OA concentration $0 \leq C_{OA} \leq 10$ μg m^{-3}.

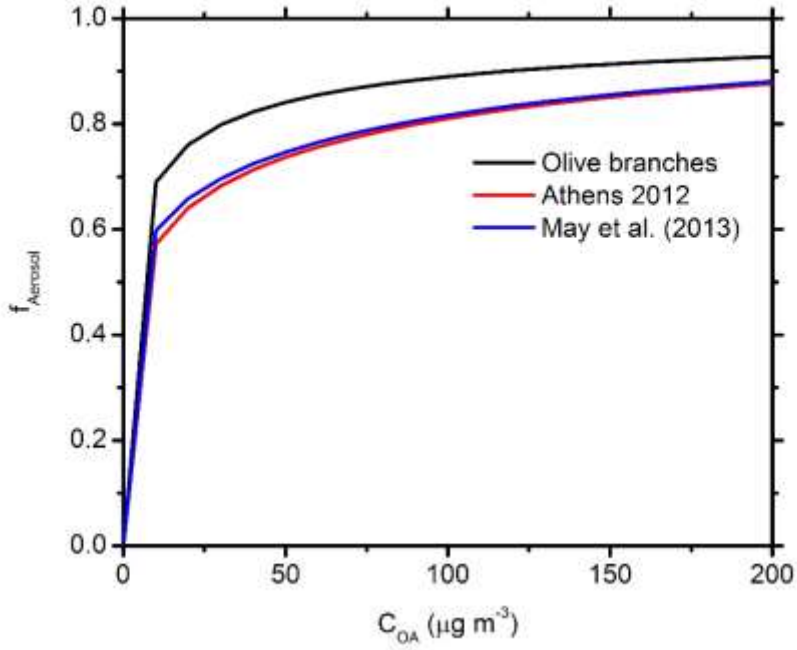

Figure C16. Particulate fractions as a function of OA conc. $0 \leq C_{OA} \leq 200$ μg m^{-3}.

European Union
European Social Fund
OPERATIONAL PROGRAMME
EDUCATION AND LIFELONG LEARNING
investing in knowledge society
MINISTRY OF EDUCATION & RELIGIOUS AFFAIRS
MANAGING AUTHORITY
NSRF 2007-2013
EUROPEAN SOCIAL FUND
Co-financed by Greece and the European Union

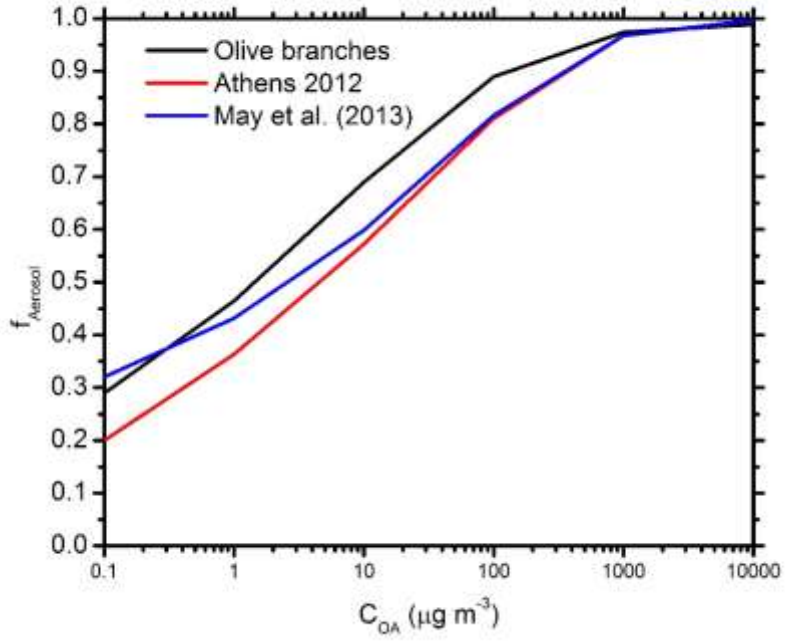

Figure C17. Particulate fractions as a function of OA conc. $0.1 \leq C_{OA} \leq 10^4$ μg m^{-3}.

The corresponding volatility distributions are compared in Fig. C18.

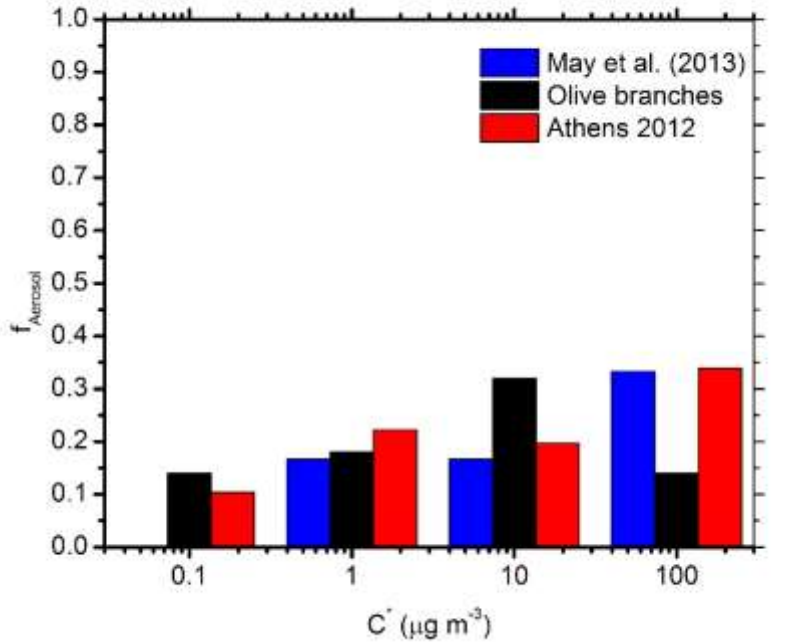

Figure C18. Volatility distributions comparison.

European Union
European Social Fund
OPERATIONAL PROGRAMME
EDUCATION AND LIFELONG LEARNING
investing in knowledge society
MINISTRY OF EDUCATION & RELIGIOUS AFFAIRS
MANAGING AUTHORITY
NSRF 2007-2013
EUROPEAN SOCIAL FUND
Co-financed by Greece and the European Union

C3 Conclusions

Combining a TD with an AMS and an SMPS we estimated the ambient OA volatility during wood burning periods in Athens. The data were corrected for TD wall losses. Overall these corrections increased the MFR values on average by 20%.

A TD dynamic model was used in order to estimate the volatility distribution of ambient OA during the burning periods. Around 80% of the ambient OA during the burning periods can be characterized as semivolatile while the other 20% has low volatility.

The gas-to-particle partitioning determination shows that ambient OA during the burning periods is little more volatile than wild fire OA studies in FLAME-III by May et al. (2013) and also a little more volatile than the BBOA produced during olive tree branches fire during winter of 2012 at ICEHT Patras.

C4 References

Brock, C. A., Hamill, P., Wilson, J. C., Honsson, H. H., and Chan, K. R. (1995). Particle formation in the upper tropical troposphere: A source of nuclei in the stratospheric aerosol. *Science*, 270, 1650–1653.

Clarke, A. D. (1991). A thermo-optic technique for in-situ analysis of size-resolved aerosol physicochemistry. *Atmospheric Environment*, 25, 635–644.

Clarke, A. D. (1993). Atmospheric nuclei in the Pacific mid-troposphere—their nature, concentration, and evolution. *Journal of Geophysical Research*, 98, 20633–20647.

Faulhaber, A. E., Thomas, B. M., J., Jimenez, J. L., and Ziemann, P. J. (2009). Characterization of a thermodenuder-particle beam mass spectrometer system for the study of organic aerosol volatility and composition. *Atmospheric Measurement Techniques*, 2, 15-31.

European Union
European Social Fund
OPERATIONAL PROGRAMME
EDUCATION AND LIFELONG LEARNING
investing in knowledge society
MINISTRY OF EDUCATION & RELIGIOUS AFFAIRS
MANAGING AUTHORITY
NSRF 2007-2013
programme for development
EUROPEAN SOCIAL FUND
Co-financed by Greece and the European Union

Huffman, J. A., Docherty, K. S., Mohr, C., Cubison, M. J., Ulbrich, I. M., Ziemann, P. J., Onasch, T. B., and Jimenez, J. L. (2009). Chemically-resolved volatility measurements of organic aerosol from different source, *Environmental Science and Technology*, 43, 5351-5357.

Jennings, S. G., and O'Dowd, C. D. (1990). Volatility of aerosol at Mace Head on the west coast of Ireland. *Journal of Geophysical Research*, 95, 13937–13948.

Kalberer, M., Paulsen, D., Sax, M., Steinbacher, M., Dommen, J., Prevot, A. S. H., Fisseha, R., Weingartner, E., Frankevich, V., Zenobi, R., and Baltensperger, U. (2004). Identification of polymers as major components of atmospheric organic aerosols, *Science*, 303, 1659–1662.

Kanakidou, M. Seinfeld, J. H., Pandis, S. N., Barnes, I., Dentener, F. J., Facchini, M. C., Van Dingenen, R., Ervens, B., Nenes, A., Nielsen, C. J., Swietlicki, E., Putaud, J. P., Balkanski, Y., Fuzzi, S., Hjorth, J., Moortgat, G. K., Winterhalter, R., Myhre, C. E. L., Tsigaridis, K., Vignati, E., Stephanou, E. and G., Wilson, J. (2005). Organic aerosol and global climate modeling: A review. *Atmospheric Chemistry and Physics*, 5, 1-70.

Karnezi, E., Riipinen, I., Pandis, S., N. (2013). Measuring the atmospheric organic aerosol volatility distribution: A Theoretical Analysis, submitted.

Kostenidou, E., Lee, B. H., Engelhart, G. J., Pierce, J. R., and Pandis, S. N. (2009) Mass spectra deconvolution of low, medium and high volatility biogenic secondary organic aerosol. *Environmental Science and Technology*, 43, 4884-4889.

Kuhn, T., Krudysz, M., Zhu,Y., Fine, P. M., Hinds,W. C., Froines, J., Sioutas, C. (2005). Volatility of indoor and outdoor ultrafine particulate matter near a freeway. *Journal of Aerosol Science*, 36, 291–302.

Lee, B. H., Kostenidou, E., Hildebrandt, L.., Riipinen, I., Engelhart, G. J., Mohr, C., DeCarlo, P. F., Mihalopoulos, N., Prevot, A. S. H., Baltensperger,U. , and Pandis, S. N. (2010). Measurement of the ambient organic aerosol volatility distribution: Application during the Finokalia Aerosol Measurement Experiment (FAME-2008). *Atmosheric Chemistry and Physics*, 10, 12149-121.

European Union
European Social Fund
OPERATIONAL PROGRAMME
EDUCATION AND LIFELONG LEARNING
investing in knowledge society
MINISTRY OF EDUCATION & RELIGIOUS AFFAIRS
MANAGING AUTHORITY
NSRF 2007-2013
programme for development
EUROPEAN SOCIAL FUND
Co-financed by Greece and the European Union

May, A. A., Ezra, Levin,J. T., Hennigan, C. J., Riipinen, I., Lee, T., Collett, J. L. Jr., Jimenez, J. L., Kreidenweis, S. M., Robinson, A. L. (2013). Gas-particle partitioning of primary organic aerosol emissions 3. Biomass burning. *Journal of Geophysical Research Atmospheres*, 118, 11327-11338.

Orsini, D. A.,Wiedensohler, A., and Stratmann, F. (1999). A new volatility tandem differential mobility analyzer to measure the volatile sulfuric acid aerosol fraction. *Journal of Atmospheric and Oceanic Technology*, 16, 760–772.

Philippin, S., Wiedensohler, A., and Stratmann, F. (2004). Measurements of non-volatile fractions of pollution aerosols with an eight-tube volatility tandem differential mobility analyzer (VTDMA-8). *Journal of Aerosol Science*, 35, 185-203.

Robinson, A. L., Subramanian, R., Donahue, N. M., Bernardo-Bricker, A., and Rogge, W. F. (2006). Source apportionment of molecular markers and organic aerosol, 2. Biomass smoke. *Environmental Science and Technology*, 40, 7811–7819.

Sakurai, H., Park, K., McMurry, P. H., Zarling, D. D., Kittelson, D. B., and Ziemann, P. J. (2003). Size-dependent mixing characteristics of volatile and nonvolatile components in diesel exhaust aerosols. *Environmental Science and Technology*, 37, 5487–5495.

Tsimpidi A. P., V. A. Karydis, M. Zavala, L. Molina, I. Ulbrich, J. L. Jimenez, and S. N. Pandis (2010) Evaluation of the volatility basis-set approach for the simulation of organic aerosol formation in the Mexico City metropolitan area, *Atmos. Chem. Phys.*, 10, 525-546.

Wehner, B., Philippin, S.,Wiedensohler, A., Scheer, V., and Vogt, R. (2004). Variability of non-volatile fractions of atmospheric aerosol particles with traffic influence. *Atmospheric Environment*, 38, 6081–6090.

European Union
European Social Fund
OPERATIONAL PROGRAMME
EDUCATION AND LIFELONG LEARNING
investing in knowledge society
MINISTRY OF EDUCATION & RELIGIOUS AFFAIRS
MANAGING AUTHORITY
NSRF 2007-2013
EUROPEAN SOCIAL FUND
Co-financed by Greece and the European Union

Activity 6: Data Analysis and Modeling

A. Simulation of Particulate Matter Concentrations and Composition over Greece

A1. PMCAMx Description

PMCAMx (Murphy and Pandis, 2009; Tsimpidi et al., 2010; Karydis et al., 2010) uses the framework of the CAMx air quality model (Environ, 2003) describing the processes of horizontal and vertical advection, horizontal and vertical dispersion, wet and dry deposition, and gas-phase chemistry. For wet deposition PMCAMx uses a scavenging coefficient approach, in which the local rate of concentration changes within or below a precipitating cloud is equal to the product of the concentration of a pollutant and the corresponding scavenging coefficient. The scavenging coefficient is determined differently for gases and particles, based upon relationships described by Seinfeld and Pandis (2006). For dry deposition, PMCAMx determines a deposition velocity for each land use type, for each given species, particle size, and grid cell, and then linearly combines them according to the fractional distribution of land use in the cell. The deposition flux is used as the lower boundary condition in the vertical diffusion algorithm. For the gas phase species, the resistance model of Wesely (1989) is used, while for aerosol the resistance approach of Slinn and Slinn (1980), as implemented in UAM-AERO (Kumar et al., 1996), has been adopted in PMCAMx. An effective Henry's Law constant, which affects vapor removal processes, of 2700 M atm^{-1} is used for all gas-phase OA species (Murphy and Pandis, 2009). For the aerosol processes, three detailed aerosol modules are used. The approach of Fahey and Pandis (2001) is used for the simulation of aqueous-phase chemistry. The inorganic aerosol growth is described in Gaydos et al. (2003) and Koo et al. (2003), and the secondary organic aerosol (SOA) formation and growth in Koo et al. (2003). These aerosol modules use a sectional approach to dynamically track the size evolution of the aerosol mass across 10 size sections spanning from 40 nm to 40 μm. The aerosol species modeled include

European Union
European Social Fund
OPERATIONAL PROGRAMME
EDUCATION AND LIFELONG LEARNING
investing in knowledge society
MINISTRY OF EDUCATION & RELIGIOUS AFFAIRS
MANAGING AUTHORITY
NSRF 2007-2013
programme for development
EUROPEAN SOCIAL FUND
Co-financed by Greece and the European Union

sulfate, nitrate, ammonium, sodium, chloride, potassium, calcium, magnesium, elemental carbon, primary and secondary organics. The chemical mechanism used in the gas-phase chemistry is based on the SAPRC99 mechanism (Carter, 2000; Environ, 2003). The version of SAPRC99 used here includes 211 reactions of 56 gases and 18 radicals and has five lumped alkanes, two olefins, two aromatics, isoprene, a lumped monoterpene species, and a lumped sesquiterpene species.

Three options are available in PMCAMx for the simulation of inorganic aerosol growth. The most computationally efficient approach is the bulk equilibrium approach, which assumes equilibrium between the bulk inorganic aerosol and gas phase. At a given time step the amount of each species transferred between the gas and aerosol phases is determined by applying the aerosol thermodynamic equilibrium model ISORROPIA (Nenes et al., 1998) and is then distributed over the aerosol size sections by using weighting factors for each size section based on their surface area (Pandis et al., 1993). The second approach (hybrid approach) assumes equilibrium for the fine particles (<1 μm) and solves the mass transfer differential equations for the coarse particles (Capaldo et al., 2000). The most accurate but computationally demanding method is the dynamic approach where mass transfer is simulated explicitly for all particles (Pilinis et al., 2000). In this work we use the bulk equilibrium approach since we are focusing on the model's performance for fine particles.

Based on the approach of Shrivastava et al. (2008), primary organic aerosol in PMCAMx-2008 is assumed to be semivolatile. Nine surrogate POA species are used, with effective saturation concentrations at 298 K ranging from 10^{-2} to 10^{6} μg m^{-3}. POA is simulated in the model in two types, "fresh" (unoxidized) POA and oxidized POA (OPOA). For the intermediate VOC (IVOC) emissions we followed the approach of Tsimpidi et al. (2010) and Shrivastava et al. (2008), in which the IVOC emissions are proportional to the emitted primary OA mass. Emission inventories do not include these compounds because of the difficulty in measuring mass in this volatility range (it is emitted and remains largely in the gas phase), and thus we add an additional 1.5 times

European Union
European Social Fund
OPERATIONAL PROGRAMME
EDUCATION AND LIFELONG LEARNING
investing in knowledge society
MINISTRY OF EDUCATION & RELIGIOUS AFFAIRS
MANAGING AUTHORITY
NSRF 2007-2013
EUROPEAN SOCIAL FUND
Co-financed by Greece and the European Union

the original POA mass emission rate to the intermediate volatility organic gas emission rate following several past studies (Robinson et al., 2007; Murphy and Pandis, 2009; Hodzic et al., 2010; Tsimpidi et al., 2010). In the gas phase, this mass can be oxidized by OH and may go to lower volatility and condense. SOA consists of organic aerosol of anthropogenic (aSOA) and biogenic (bSOA) origin. The SOA volatility basis-set approach (Lane et al., 2008) used in the current version of the model includes four SOA species for each VOC with 4 volatility bins (1, 10, 100, 1000 μg m^{-3}). Laboratory results from recent smog-chamber experiments (Ng et al., 2006; Hildebrandt et al., 2009) have been used to update the SOA module in PMCAMx in order to include anthropogenic aerosol yields. The SOA module incorporates NO_x-dependent SOA yields (Lane et al., 2008b) which are based on an assumed density of 1.5 g cm^{-3}. The model treats all organic species (primary and secondary) as chemically reactive. Chemical aging through gas-phase oxidation of OA vapors is modeled using a gas-phase OH reaction with a rate constant of $k = 1 \times 10^{-11}$ cm^3 $molec^{-1}$ s^{-1} for anthropogenic SOA and $k = 4 \times 10^{-11}$ cm^3 $molec^{-1}$ s^{-1} for the primary OA (Atkinson and Arey, 2003). Each reaction is assumed to decrease the volatility of the vapor material by a factor of 10. The base-case simulation neglects the chemical aging of biogenic SOA. It effectively assumes that the chemical aging reactions of biogenic SOA (leading to both functionalization and fragmentation) do not result in a net increase of the bSOA concentration.

A2 Model application

During June/July 2012 an intensive campaign of measurements was performed in Greece by the partners of the current project. This campaign was coordinated with intensive measurements in Northern Italy as part of the PEGASOS project and also in the rest of Europe as part of the ACTRIS project. The PMCAMx modeling domain covers a 5400 × 5832 km^2 region in Europe with 36 × 36 km grid resolution and 14 vertical layers covering approximately 6 km (Fig. A1). PMCAMx was set to perform simulations on a rotated polar stereographic map projection.

European Union
European Social Fund
OPERATIONAL PROGRAMME
EDUCATION AND LIFELONG LEARNING
investing in knowledge society
MINISTRY OF EDUCATION & RELIGIOUS AFFAIRS
MANAGING AUTHORITY
NSRF 2007-2013
EUROPEAN SOCIAL FUND
Co-financed by Greece and the European Union

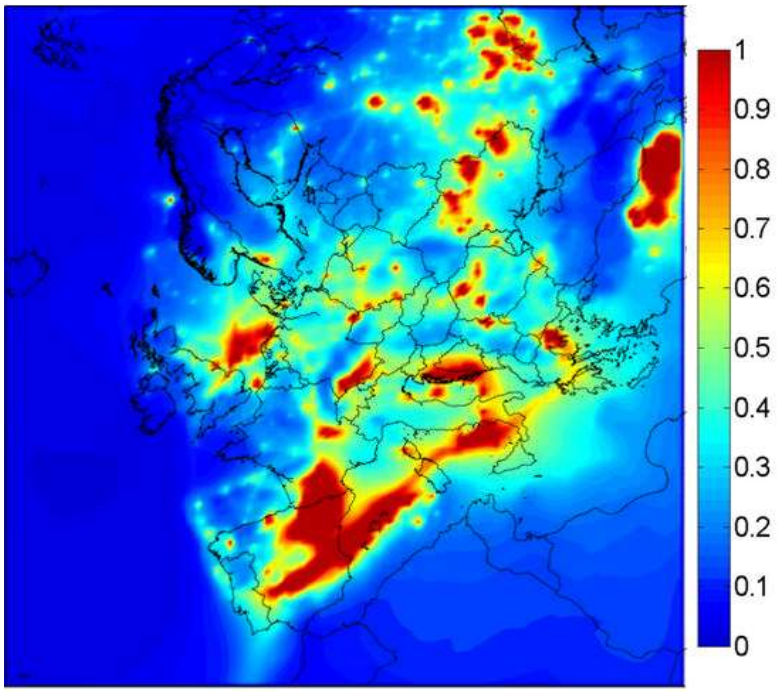

Figure A1. Predicted black carbon average concentration (μg m^{-3}) at the ground level for the simulated summer 2012 period.

The model predictions over Greece were evaluated against the measurements performed in this project in four locations: Athens, Thessaloniki, Patra, and Finokalia (Fig. A2). The first two days of each simulation were excluded from the analysis to limit the effect of the initial conditions on the results. Concentrations of the major PM_1 species at the boundaries of the domain (Table A1) are based on measured average background concentrations in sites close to the boundaries of the domain (e.g. Zhang et al., 2007; Seinfeld and Pandis 2006). The boundary condition organic aerosol (BC-OA) is expected to consist of both SOA and oxidized POA. All concentrations reported here are under ambient temperature and pressure conditions.

European Union
European Social Fund
OPERATIONAL PROGRAMME
EDUCATION AND LIFELONG LEARNING
investing in knowledge society
MINISTRY OF EDUCATION & RELIGIOUS AFFAIRS
MANAGING AUTHORITY
NSRF 2007-2013
programme for development
EUROPEAN SOCIAL FUND
Co-financed by Greece and the European Union

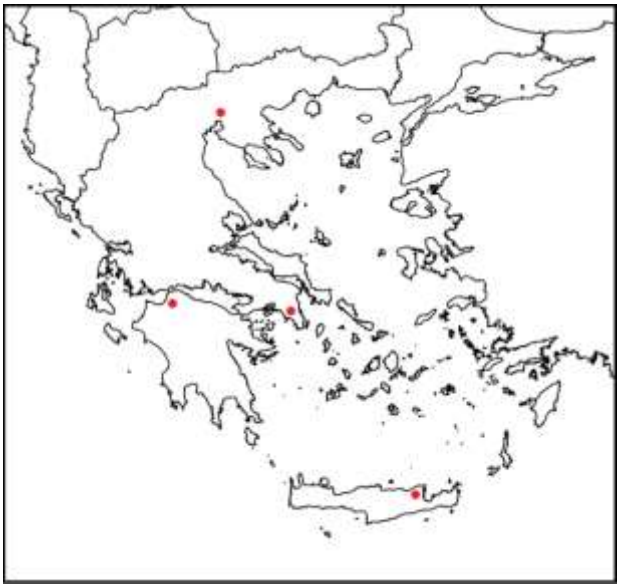

Figure A2: Measurement sites (red circles) used for the evaluation of PMCAMx predictions during June-July 2012.

Table A1. Aerosol concentrations (in μg m^{-3}) at the boundaries of the domain.

	Boundaries[1]			
Species	North	South	West	East
OA	1	0.5	0.5	1
Sulfate	1	1	1	1
Ammonium	0.37	0.37	0.37	0.37
Nitrate	0.1	0.02	0.01	0.1
Sodium	0.001	0.005	0.09	0.03
Chloride	0.002	0.01	0.1	0.05

[1]"North", "South", "West" and "East" here represent the top, bottom, left and right edge, respectively, of our modeling domain as it is depicted in Figure 1.

The necessary inputs to the model include horizontal wind components, vertical diffusivity, temperature, pressure, water vapor, clouds and rainfall. The meteorological model WRF (Weather Research and Forecasting) (Skamarock et al., 2005) was used to

European Union
European Social Fund
OPERATIONAL PROGRAMME
EDUCATION AND LIFELONG LEARNING
investing in knowledge society
MINISTRY OF EDUCATION & RELIGIOUS AFFAIRS
MANAGING AUTHORITY
NSRF 2007-2013
EUROPEAN SOCIAL FUND
Co-financed by Greece and the European Union

create the above inputs. WRF was driven by static geographical data and dynamic meteorological data (near real-time and historical data generated by the Global Forecast System (1x1 deg)). 27 sigma-p layers up to 0.1 bars were used in the vertical dimension. Each layer of PMCAMx-2008 is aligned with the layers used in WRF. The WRF May 2008 run was periodically (every 3 days) re-initialized to ensure accuracy in the corresponding fields that are used as inputs in PMCAMx.

Anthropogenic and biogenic hourly emission gridded fields were developed for the European domain for gases and primary particulate matter. Volatile organic compounds are split based on the speciation approach proposed by Visschedijk et al. (2007). Anthropogenic gas emissions that were used to develop the gridded fields include land emissions from the GEMS dataset (Visschedijk et al., 2007) as well as international shipping emissions. Anthropogenic particulate matter mass emissions of organic and elemental carbon are based on the EUCAARI (Kulmala et al., 2009) Pan-European Carbonaceous Aerosol Inventory. Industrial, domestic, agricultural and traffic emission sources are included in the two inventories. Three different datasets are combined in order to produce the biogenic gridded emissions for the model. Emissions from ecosystems are produced by MEGAN (Model of Emissions of Gases and Aerosols from Nature) (Guenther et al., 2006). MEGAN inputs include the leaf area index, the plant functional type and the emission factors while the weather data needed for MEGAN are provided from the WRF model. The sesquiterpene emissions have been set to 30% of the monoterpene emissions (Helmig et al., 2006). Since sea surface covers a considerable portion of the domain, the marine aerosol emission model developed by O'Dowd et al. (2008) has been used to estimate mass fluxes for both accumulation and coarse mode including the organic aerosol fraction. Wind speed data from WRF and chlorophyll-a concentrations are the inputs needed for the marine aerosol model. Wildfire emissions from June-July 2012 were also included (Sofiev et al., 2008a; 2008b). The OA emissions in PMCAMx were distributed by volatility using the volatility distributions of Tsimpidi et al. (2010).

European Union
European Social Fund
OPERATIONAL PROGRAMME
EDUCATION AND LIFELONG LEARNING
investing in knowledge society
MINISTRY OF EDUCATION & RELIGIOUS AFFAIRS
MANAGING AUTHORITY
NSRF 2007-2013
programme for development
EUROPEAN SOCIAL FUND
Co-financed by Greece and the European Union

A3. Overview of PMCAMx predictions

The average predicted total $PM_{2.5}$ concentrations for Europe during the simulation period are shown in Figure A3. The model suggests that the highest $PM_{2.5}$ during this warm sunny period existed over the Mediterranean due to the intense photochemical activity and the production of secondary particulate matter.

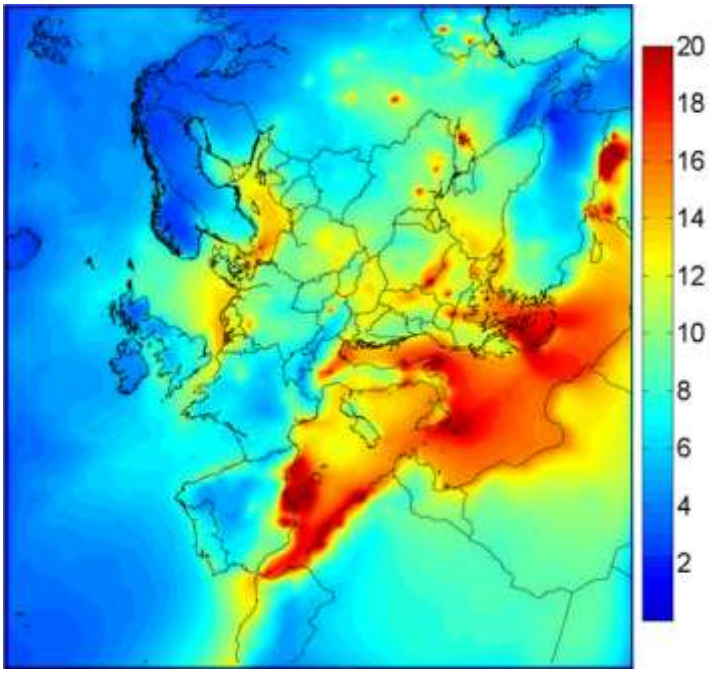

Figure A3. Average ground-level $PM_{2.5}$ (μg m^{-3}) concentrations predicted by PMCAMx for the simulated summer 2012 period.

The high $PM_{2.5}$ levels over the Eastern Mediterranean were to a large extent due to high sulfate levels with concentrations up to 8 μg m^{-3} (Figure A4). These high sulfate levels are due to both the high SO_2 emissions in the area and the high OH radical levels due to the photochemical activity. The situation is different in the Western Mediterranean because the SO_2 emissions in that area are much lower.

Organic particulate matter was the second major component of $PM_{2.5}$ during that period over the Mediterranean (Fig. A5). Most of it was secondary produced from the

European Union
European Social Fund
OPERATIONAL PROGRAMME
EDUCATION AND LIFELONG LEARNING
investing in knowledge society
MINISTRY OF EDUCATION & RELIGIOUS AFFAIRS
MANAGING AUTHORITY
NSRF 2007-2013
EUROPEAN SOCIAL FUND
Co-financed by Greece and the European Union

photooxidation of anthropogenic and biogenic volatile and intermediate volatility organic compounds. Due to the time required for its production its concentration field had a regional character with only slightly higher concentrations over certain urban areas. Black carbon (BC) contributed a relatively small fraction of the $PM_{2.5}$ with average concentrations in general lower than 1 μg m^{-3}. However its climatic effects could be significant because of its ability to absorb sunlight and warm the atmosphere. Figure 1 indicates high BC levels over and downwind of large urban areas and also over the Mediterranean (especially its Western part) due to emissions by shipping.

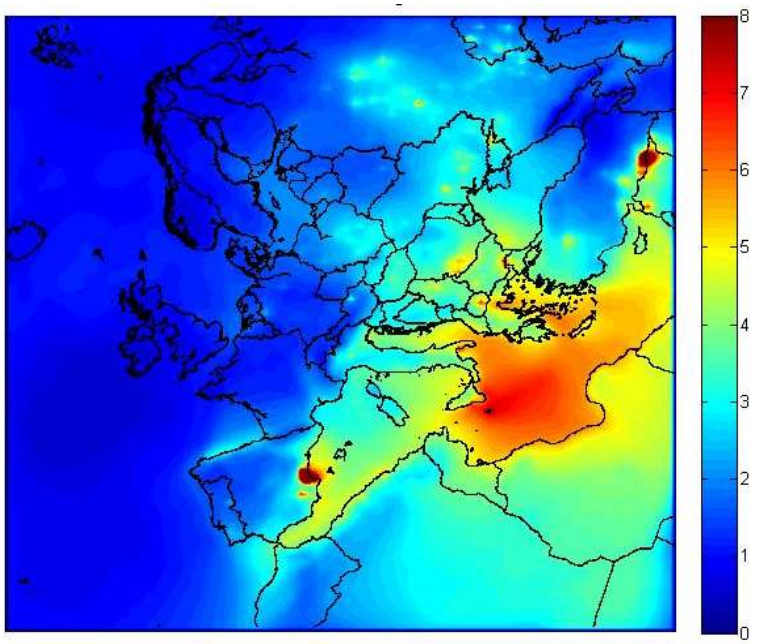

Figure A4. Average ground-level sulfate (μg m^{-3}) concentrations predicted by PMCAMx for the simulated summer 2012 period.

According to the PMCAMx predicted the average total $PM_{2.5}$ concentration over Greece was 16.4 μg m^{-3} with sulfates contributing approximately 40% and organics 30%. The remaining mass consisted of ammonium, nitrates, black carbon, dust and metal oxides, and sea-salt. The highest concentrations are predicted over Athens and in the Aegean downwind of Athens (Fig. A6).

European Union
European Social Fund
OPERATIONAL PROGRAMME
EDUCATION AND LIFELONG LEARNING
investing in knowledge society
MINISTRY OF EDUCATION & RELIGIOUS AFFAIRS
MANAGING AUTHORITY
NSRF 2007-2013
EUROPEAN SOCIAL FUND
Co-financed by Greece and the European Union

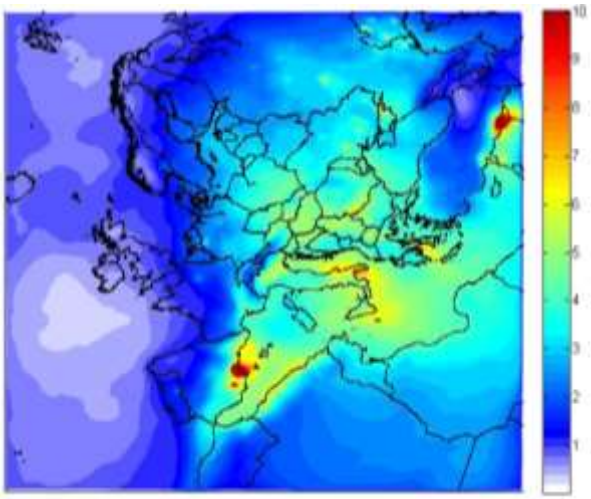

Figure A5. Average ground-level organic aerosol (μg m^{-3}) concentrations predicted by PMCAMx for the simulated summer 2012 period.

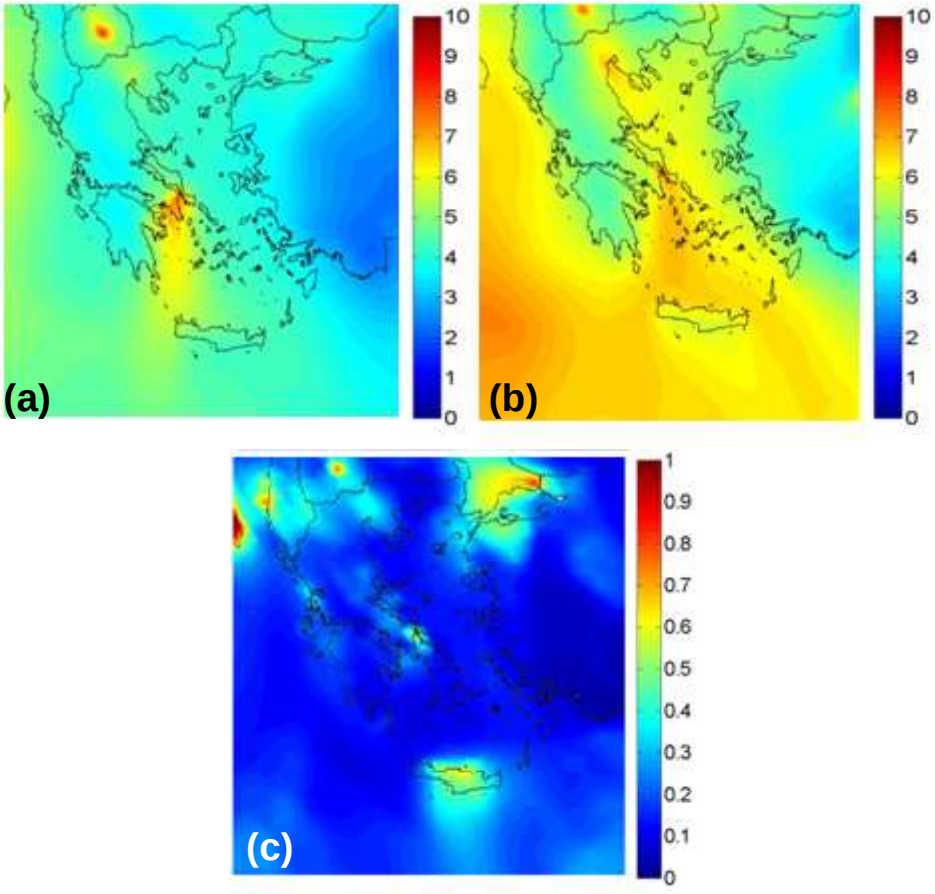

Figure A6. Average ground-level concentrations (μg m^{-3}) predicted by PMCAMx for the simulated summer 2012 period for: (a) organic aerosol; (b) sulfate and (c) nitrate.

European Union
European Social Fund
OPERATIONAL PROGRAMME
EDUCATION AND LIFELONG LEARNING
investing in knowledge society
MINISTRY OF EDUCATION & RELIGIOUS AFFAIRS
MANAGING AUTHORITY
NSRF 2007-2013
EUROPEAN SOCIAL FUND
Co-financed by Greece and the European Union

The organic aerosol concentrations are highest, as expected, in Athens (Fig. A6a) but there is also a high concentration region south of Athens extending almost all the way to western Crete. These high concentrations are due to the transfer of air pollution from Attica and the production of secondary organic particulate matter in the corresponding plume. There is a relatively high background of approximately 5 μg m^{-3} of fine organic aerosol over most of Greece. The sulfate concentrations over Greece (Fig. A6b) are predicted to be higher over the Ionian and southern Aegean seas due to the higher OH levels over the water. Finally, the $PM_{2.5}$ nitrate levels (Fig. A6c) are predicted to be relatively low (less than 1 μg m^{-3}) because the particles are mostly acidic and accounting also for the high temperatures the formation of ammonium nitrate is not favoured thermodynamically.

PMCAMx is also able to predict the contributions of different processes to the organic aerosol levels. The oxidation of the emitted primary organic particulate matter and the intermediate volatility organic compounds is predicted to be the major source of OA for all areas (Fig. A7). The contribution of fresh primary OA is predicted to be important only in Athens contributing approximately 25% to the total OA levels. The model is predicting that most of the OA during the summer in Greece is secondary, something that is consistent with the measurements in this project.

European Union
European Social Fund
OPERATIONAL PROGRAMME
EDUCATION AND LIFELONG LEARNING
investing in knowledge society
MINISTRY OF EDUCATION & RELIGIOUS AFFAIRS
MANAGING AUTHORITY
NSRF 2007-2013
programme for development
EUROPEAN SOCIAL FUND
Co-financed by Greece and the European Union

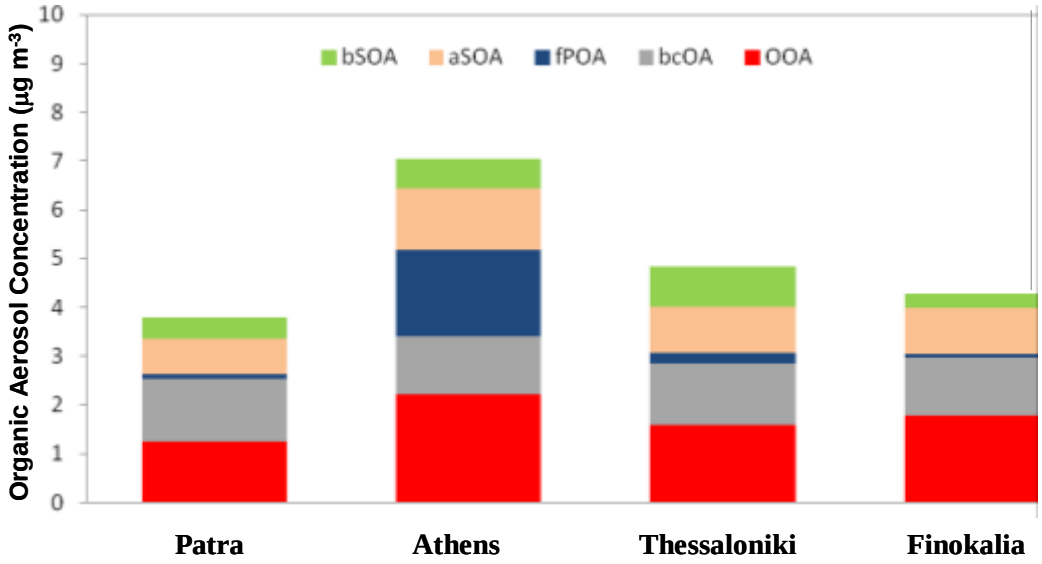

Figure A7. Average organic aerosol ground-level concentrations (μg m^{-3}) predicted by PMCAMx for the simulated summer 2012 period for the four sampling sites where: bSOA is biogenic secondary organic aerosol (OA), aSOA is anthropogenic secondary OA, fPOA is fresh primary OA, bcOA is OA due to long range transport from outside the modeling domain, and OOA is secondary OA from the evaporation/reaction of primary OA and intermediate volatility organic compounds (IVOCs).

A4. Evaluation of PMCAMx predictions

The concentrations of the major $PM_{2.5}$ components predicted by PMCAMx are compared to the corresponding measurements of this project in Fig. A8. The model does a good job in reproducing the very low $PM_{2.5}$ nitrate levels in all areas. Its performance for the sulfates is excellent in Patras but there is a tendency towards overprediction in Athens and Thessaloniki. A potential explanation of this behavior is the decrease in sulfur emissions in Greece during the financial crisis that is not accounted by the model (it is using emissions for 2008 and not 2012). These lead to corresponding overpredictions of ammonium in these areas. The performance for organics is excellent in Patras, satisfactory in Thessaloniki, but the model overpredicts seriously in Penteli. This is due to the coarse resolution used by the model and its inability to separate the relatively clean conditions in Penteli from the average organic aerosol levels in Attica. It is clear that applications of chemical transport models in

European Union
European Social Fund
OPERATIONAL PROGRAMME
EDUCATION AND LIFELONG LEARNING
investing in knowledge society
MINISTRY OF EDUCATION & RELIGIOUS AFFAIRS
MANAGING AUTHORITY
NSRF 2007-2013
EUROPEAN SOCIAL FUND
Co-financed by Greece and the European Union

Athens require much higher spatial resolution than the 36x36 km used here. This will be the topic of future work.

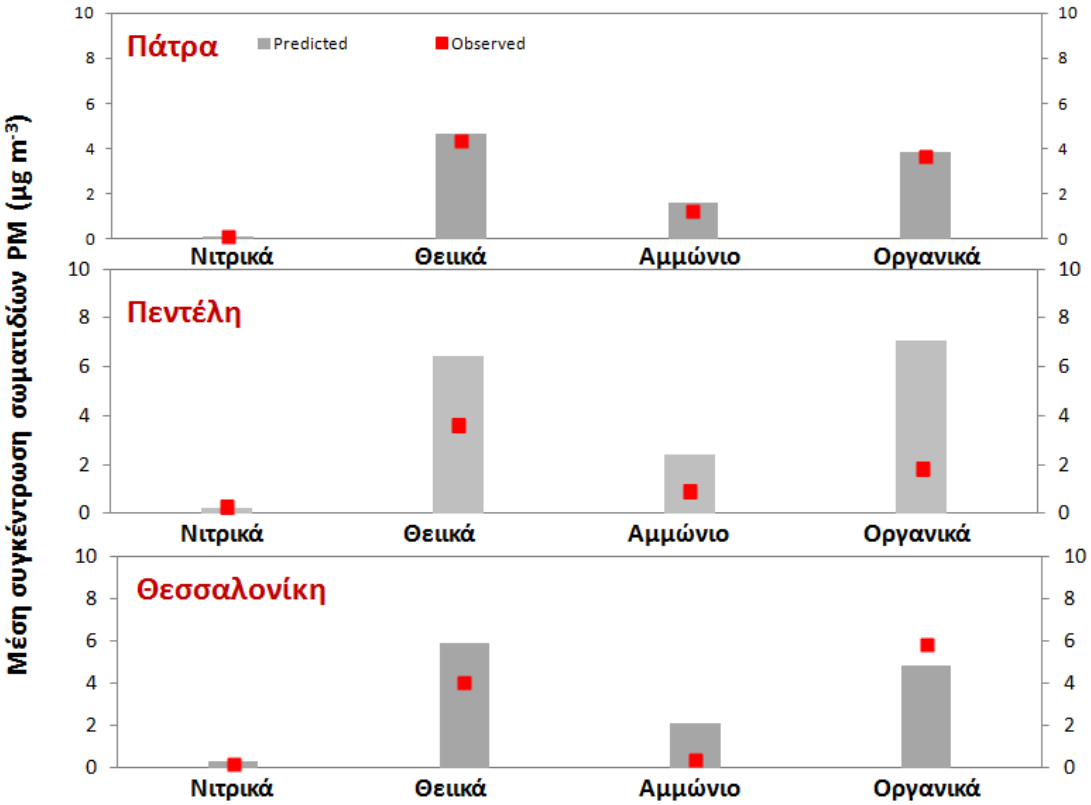

Figure A8. Average concentrations of nitrates, sulfates, ammonium, and organics measured (grey bars) and predicted (red squares) by PMCAMx for the summer 2012 period for Patras, Penteli in Athens, and Thessaloniki.

Figure A9 demonstrates the ability of PMCAMx to reproduce the day-to-day variability of the concentrations of the two major fine PM components using Thessaloniki as an example. The model does a reasonable job of capturing both the range of the

European Union
European Social Fund
OPERATIONAL PROGRAMME
EDUCATION AND LIFELONG LEARNING
investing in knowledge society
MINISTRY OF EDUCATION & RELIGIOUS AFFAIRS
MANAGING AUTHORITY
NSRF 2007-2013
EUROPEAN SOCIAL FUND
Co-financed by Greece and the European Union

corresponding daily average concentrations but also their variation during the period of the measurements.

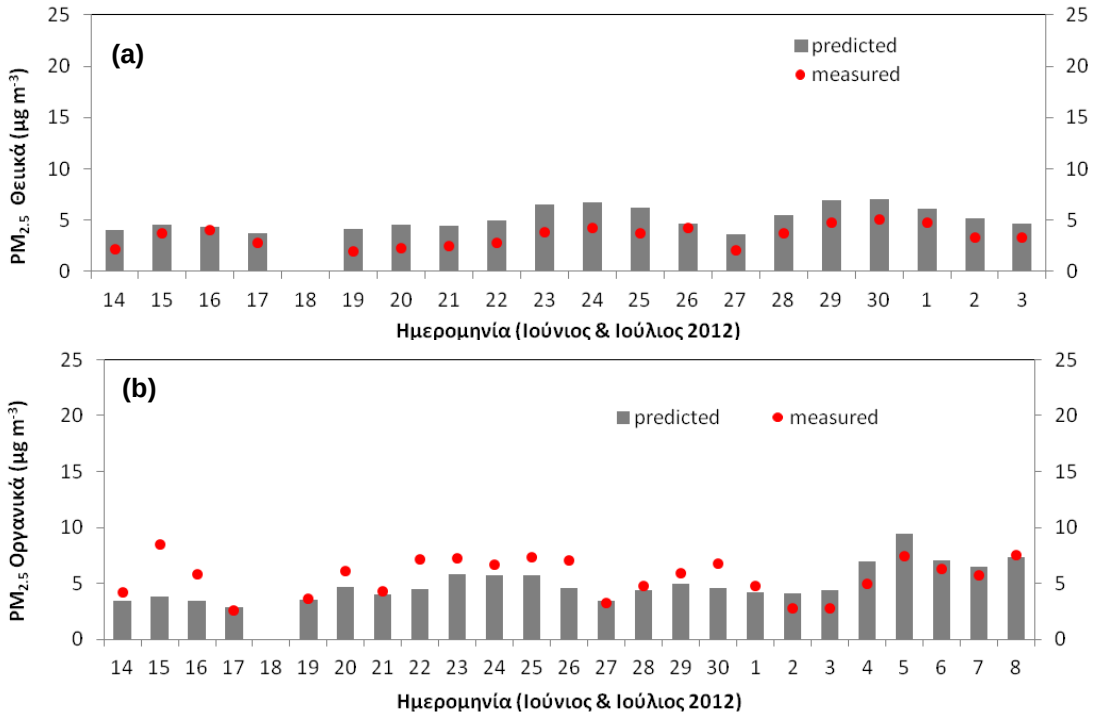

Figure A9. Daily average concentrations of (a) sulfate and (b) organics measured (grey bars) and predicted (red squares) by PMCAMx for the summer 2012 period for Thessaloniki.

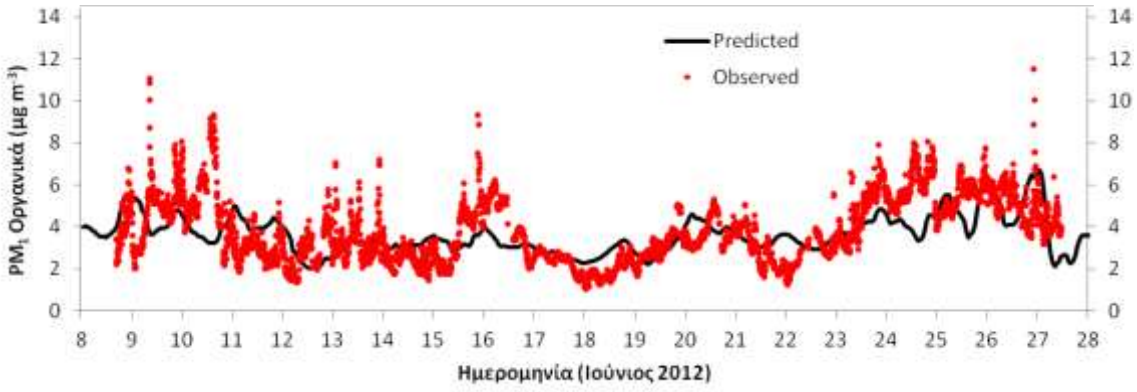

Figure A10. Hourly concentrations of fine organic particulate matter measured (red symbols) and predicted (black line) by PMCAMx for the summer 2012 period for Patra.

European Union
European Social Fund
OPERATIONAL PROGRAMME
EDUCATION AND LIFELONG LEARNING
investing in knowledge society
MINISTRY OF EDUCATION & RELIGIOUS AFFAIRS
MANAGING AUTHORITY
NSRF 2007-2013
EUROPEAN SOCIAL FUND
Co-financed by Greece and the European Union

Figure A10 presents an example of the model to capture the very short time variability of observed concentrations for Patras using the organic aerosol predictions. While overall the model does an excellent job of representing the overall variation of concentrations during the measurement period it cannot capture the short term spikes in the observations. These are due to local changes in the emissions and capturing them requires both much higher grid resolution, but also anthropogenic emission inventories that are day specific.

According to PMCAMx the fine PM levels in Finokalia and Patra were more representative of the background concentrations over Greece. Its ability to reproduce these concentrations on an hourly basis for these two locations is summarized in Table A2. The performance of the model is quite encouraging. The relatively high errors for nitrate are due to the very low (often zero) values and are not a concern.

Table A2. Evaluation metrics[a] for the performance of PMCAMx in Patra and Finokalia.

PM_1	Average Measured ($\mu g\ m^{-3}$)	Average Predicted ($\mu g\ m^{-3}$)	MB ($\mu g\ m^{-3}$)	MAGE ($\mu g\ m^{-3}$)	FBIAS	FERROR
Patra						
OA	3.6	3.8	-0.2	1.04	-0.01	0.28
Θειικά	4.8	4.5	-0.3	1.6	-0.04	0.3
Νιτρικά	0.2	0.15	-0.06	0.2	-0.6	1
Αμμώνιο	1.3	1.6	0.3	0.6	0.3	0.5
Finokalia						
OA	2	4.3	2.3	2.4	0.4	0.6
Θειικά	3.1	5.3	2.2	2.2	0.2	0.7
Νιτρικά	0.1	0.02	-0.08	0.1	-	-
Αμμώνιο	1	1.9	0.9	0.9	0.4	0.6

European Union
European Social Fund
OPERATIONAL PROGRAMME
EDUCATION AND LIFELONG LEARNING
investing in knowledge society
MINISTRY OF EDUCATION & RELIGIOUS AFFAIRS
MANAGING AUTHORITY
NSRF 2007-2013
EUROPEAN SOCIAL FUND
Co-financed by Greece and the European Union

[a]Number of measurements used: Patra 460 and Finokalia 680

$$MB = {}^{1}/_{n}\sum_{i=1}^{n}(P_i - O_i) \qquad MAGE = {}^{1}/_{n}\sum_{i=1}^{n}|P_i - O_i|$$

$$BIAS = {}^{2}/_{n}\sum_{i=1}^{n}{}^{(P_i - O_i)}\Big/_{(P_i + O_i)} \qquad FBIAS = {}^{2}/_{n}\sum_{i=1}^{n}{}^{|P_i - O_i|}\Big/_{(P_i + O_i)}$$

A4. References

Andersson-Skold, Y., and Simpson, D.: Secondary organic aerosol formation in northern Europe: A model study, J. Geophys. Res., 106, D7, 7357-7374, doi: 10.1029/2000JD900656, 2001.

Andreae, M. O. and Crutzen, P. J.: Atmospheric aerosols: biogeochemical sources and role in atmospheric chemistry, Science, 276, 1052-1058, 1997.

Atkinson, R. and Arey, J.: Atmospheric degradation of volatile organic compounds, Chem. Rev., 103, 4605-4638, 2003.

Baltensperger, U., Kalberer, M., Dommen, J., Paulsen, D., Alfarra, M. R., Coe, H., Fisseha, R., Gascho, A., Gysel, M., Nyeki, S., Sax, M., Steinbacher, M., Prevot, A. S. H., Sjogren, S., Weingartner, E., and Zenobi, R.: Secondary organic aerosols from anthropogenic and biogenic precursors, Faraday Discuss., 130, 265-278, 2005.

Bessagnet, B., Menut, L., Curci, G., Hodzic, A., Guillaume, B., Liousse, C., Moukhtar, S., Pun, B., Seigneur, C., and Schulz, M.: Regional modeling of carbonaceous aerosols over Europe-focus on secondary organic aerosols, J. Atmos. Chem., 61, 3, 175-202, doi: 10.1007/s10874-009-9129-2, 2008.

Birmili, W., K. Schepanski, A. Ansmann, G. Spindler, I. Tegen, B. Wehner, A. Nowak, E. Reimer, I. Mattis, K. Müller, E. Brüggemann, T. Gnauk, H. Herrmann, A. Wiedensohler, D. Althausen, A. Schladitz, T. Tuch, and G. Löschau. A case of extreme particulate matter concentrations over Central Europe caused by dust emitted over the southern Ukraine. Atmos. Chem. Phys., 8: 997-1016, 2008.

European Union
European Social Fund
OPERATIONAL PROGRAMME
EDUCATION AND LIFELONG LEARNING
investing in knowledge society
MINISTRY OF EDUCATION & RELIGIOUS AFFAIRS
MANAGING AUTHORITY
NSRF 2007-2013
programme for development
EUROPEAN SOCIAL FUND
Co-financed by Greece and the European Union

Birmili, W., K. Weinhold, S. Nordmann, A. Wiedensohler, G. Spindler, K. Müller, H. Herrmann, T. Gnauk, M. Pitz, J. Cyrys, H. Flentje, C. Nickel, T.A.J. Kuhlbusch, G. Löschau, D. Haase, F. Meinhardt, A. Schwerin, L. Ries, and K. Wirtz. Atmospheric aerosol measurements in the German Ultrafine Aerosol Network (GUAN): Part 1 - soot and particle number size distributions. Gefahrst. Reinh. Luft, 69: 137-145, 2009.

Bougiatioti, B., Fountoukis, C., Kalivitis, N., Pandis, S. N., Nenes, A., and Mihalopoulos, N.: Cloud condensation nuclei measurements in the marine boundary layer of the eastern Mediterranean: CCN closure and droplet growth kinetics, Atmos. Chem. Phys., 9, 7053-7066, 2009.

Burtraw, D., Krupnick, A., Mansur, E., Austin, D., and Farrell, D.: Costs and benefits of reducing air pollutants related to acid rain, Contemporary Economic Policy, 16, 379-400, doi:10.1111/j.1465-7287.1998.tb00527.x, 2007.

Capaldo, K. P., Pilinis, C., and Pandis, S. N.: A computationally efficient hybrid approach for dynamic gas/aerosol transfer in air quality models, Atmos. Environ., 34, 3617-3627, 2000.

Carter, W. P. L.: Programs and Files Implementing the SAPRC-99 Mechanism and its Associates Emissions Processing Procedures for Models-3 and Other Regional Models: http://pah.cert.ucr.edu/~carter/SAPRC99.htm, last access: 31 January 2000.

Dall'Osto, M., Ceburnis, D., Martucci, G., Bialek, J., Dupuy, R., Jennings, S. G., Berresheim, H., Wenger, J. C., Sodeau, J. R., Healy, R. M., Facchini, M. C., Rinaldi, M., Giulianelli, L., Finessi, E., Worsnop, D., and O'Dowd, C. D.: Aerosol properties associated with air masses arriving into the North East Atlantic during the 2008 Mace Head EUCAARI intensive observing period: an overview, Atmos. Chem. Phys., 10, 8413-8435, 2010.

DeCarlo, P. F., Kimmel, J. R., Trimborn, A., Northway, M. J., Jayne, J. T., Aiken, A. C., Gonin M., Fuhrer, K., Horvath, T., Docherty, K. S., Worsnop, D. R., and Jimenez, J. L.: Field-deployable, high-resolution, time-of-flight aerosol mass spectrometer, Anal. Chem., 78, 8281–8289, 2006.

European Union
European Social Fund
OPERATIONAL PROGRAMME
EDUCATION AND LIFELONG LEARNING
investing in knowledge society
MINISTRY OF EDUCATION & RELIGIOUS AFFAIRS
MANAGING AUTHORITY
NSRF 2007-2013
programme for development
EUROPEAN SOCIAL FUND
Co-financed by Greece and the European Union

Donahue, N. M., Robinson, A. L., Stanier, C. O., and Pandis, S. N.: Coupled partitioning, dilution, and chemical aging of semivolatile organics. Environ. Sci. Technol., 40, 2635-2643, 2006.

Dzepina, K., Volkamer, R. M., Madronich, S., Tulet, P., Ulbrich, I. M., Zhang, Q., Cappa, C. D., Ziemann, P. J., and Jimenez, J. L.: Evaluation of recently-proposed secondary organic aerosol models for a case study in Mexico City, Atmos. Chem. Phys., 9, 5681-5709, 2009.

Engler, C., D. Rose, B. Wehner, A. Wiedensohler, E. Brüggemann, T. Gnauk, G. Spindler, T. Tuch, W. Birmili. Size distributions of non-volatile particle residuals (Dp<800 nm) at a rural site in Germany and relation to air mass origin. Atmos. Chem. Phys., 7, 5785-5802, 2007.

ENVIRON: User's Guide to the Comprehensive Air Quality Model with Extensions (CAMx), Version 4.02, Report, ENVIRON Int. Corp., Novato, Calif. Available at: http://www.camx.com, 2003.

Fahey, K. and Pandis, S. N.: Optimizing model performance: variable size resolution in cloud chemistry modeling, Atmos. Environ., 35, 4471–4478, 2001.

Farina, S. C., Adams, P. J., and Pandis, S. N.: Modeling global secondary organic aerosol formation and processing with the volatility basis set: Implications for anthropogenic secondary organic aerosol, J. Geophys. Res., 115, D09202, doi:10.1029/2009JD013046, 2010.

Ganor, E., Foner, H. A., Bingemer, H. G., Udisti, R., and Setter, I.: Biogenic sulphate generation in the Mediterranean Sea and its contribution to the sulphate anomaly in the aerosol over Israel and the Eastern Mediterranean, Atmos. Environ., 36, 929-938, 2000.

Gaydos, T., Koo, B., and Pandis, S. N.: Development and application of an efficient moving sectional approach for the solution of the atmospheric aerosol condensation/evaporation equations. Atmos. Environ., 37, 3303-3316, 2003.

Gelencser, A., May, B., Simpson, D., Sanchez-Ochoa, A., Kasper-Giebl, A., Puxbaum, H., Caseiro, A., Pio, C., and Legrand, M.: Source apportionment of PM2.5 organic aerosol over Europe: Primary/secondary, natural/anthropogenic, and

European Union
European Social Fund
OPERATIONAL PROGRAMME
EDUCATION AND LIFELONG LEARNING
investing in knowledge society
MINISTRY OF EDUCATION & RELIGIOUS AFFAIRS
MANAGING AUTHORITY
NSRF 2007-2013
EUROPEAN SOCIAL FUND
Co-financed by Greece and the European Union

fossil/biogenic origin, J. Geophys. Res., 112, D23S04, doi: 10.1029/2006JD008094, 2007.

Guenther, A., Karl, T., Harvey, P., Wiedinmyer, C., Palmer, P. I., and Geron, C.: Estimates of global terrestrial isoprene emissions using MEGAN (Model of Emissions of Gases and Aerosols from Nature), Atmos. Chem. Phys., 6, 3181-3210, 2006.

Heald, C. L., Jacob, D. J., Park, R. J., Russell, L. M., Huebert, B. J., Seinfeld, J. H., Liao, H., and Weber, R. J.: A large organic aerosol source in the free troposphere missing from current models, Geophys. Res. Lett., 32, L18809, doi:10.1029/2005GL023831, 2005.

Helmig, D., Ortega, J., Guenther, A., Herrick, J. D., and Geron, C.: Sesquiterpene emissions from loblolly pine and their potential contribution to biogenic aerosol formation in the Southeastern US, Atmos. Environ. 40, 4150-4157, 2006.

Hildebrandt, L., Donahue, N. M., and Pandis, S. N.: High formation of secondary organic aerosol from the photo-oxidation of toluene, Atmos. Chem. Phys., 9, 2973-2986, 2009.

Hildebrandt, L., Engelhart, G. J., Mohr, C., Kostenidou, E., Lanz, V. A., Bougiatioti, A., DeCarlo, P. F., Prevot, A. S. H., Baltensperger, U., Mihalopoulos, N., Donahue, N. M., and Pandis, S. N.: Aged organic aerosol in the Eastern Mediterranean: the Finokalia aerosol measurement experiment-2008, Atmos. Chem. Phys., 10, 4167-4186, 2010.

Huffman, J. A., Docherty, K. S., Aiken, A. C., Cubison, M. J., Ulbrich, I. M., DeCarlo, P. F., Sueper, D., Jayne, J. T., Worsnop, D. R., Ziemann, P. J., and Jimenez, J. L.: Chemically-resolved aerosol volatility measurements from two megacity field studies, Atmos. Chem. Phys., 9, 7161–7182, 2009a.

Huffman, J. A., Docherty, K. S., Mohr, C., Cubison, M. J., Ulbrich, I. M., Ziemann, P. J., Onasch, T. B., and Jimenez, J. L.: Chemically-resolved volatility measurements of organic aerosol from different sources, Environ. Sci. Technol., 43, 5351-5357, 2009b.

European Union
European Social Fund
OPERATIONAL PROGRAMME
EDUCATION AND LIFELONG LEARNING
investing in knowledge society
MINISTRY OF EDUCATION & RELIGIOUS AFFAIRS
MANAGING AUTHORITY
NSRF 2007-2013
EUROPEAN SOCIAL FUND
Co-financed by Greece and the European Union

Jayne, J. T., Leard, D. C., Zhang, X. F., Davidovits, P., Smith, K.A., Kolb, C.E., and Worsnop, D.R.: Development of an aerosol mass spectrometer for size and composition analysis of submicron particles, Aerosol Sci. Tech., 33, 49-70, 2000.

Kanakidou, M., Seinfeld, J. H., Pandis, S. N., Barnes, I., Dentener, F. J., Facchini, M. C., Van Dingenen, R., Ervens, B., Nenes, A., Nielsen, C. J., Swietlicki, E., Putaud, J. P., Balkanski, Y., Fuzzi, S., Horth, J., Moortgat, G. K., Winterhalter, R., Myhre, C. E. L., Tsigaridis, K., Vignati, E., Stephanou, E. G., and Wilson, J.:: Organic aerosol and global climate modeling: a review, Atmos. Chem. Phys., 5, 1053-1123, 2005.

Karydis, V. A., Tsimpidi, A. P., Fountoukis, C., Nenes A., Zavala, M., Lei, W., Molina, L. T., and Pandis, S. N.: Simulating the fine and coarse inorganic particulate matter concentrations in a polluted megacity, Atmos. Environ., 44, 608-620, 2010.

Keenan, T., Niinemets, Ü., Sabate, S., Gracia, C., and Peñuelas J.: Process based inventory of isoprenoid emissions from European forests: model comparisons, current knowledge and uncertainties Atmos. Chem. Phys., 9, 4053-4076, 2009.

Koo, B., Pandis, S. N., and Ansari, A.: Integrated approaches to modeling the organic and inorganic atmospheric aerosol components, Atmos. Environ., 37, 4757-4768, 2003.

Koulouri, E., Saarikoski, S., Theodosi, C., Markaki, Z., Gerasopoulos, E., Kouvarakis, G., Makela, T., Hillamo, R., and Mihalopoulos, N.: Chemical composition and sources of fine and coarse aerosol particles in the Eastern Mediterranean, Atmos. Environ., 42, 6542-6550, doi:10.1016/j.atmosenv.2008.04.010, 2008.

Kulmala, M., Asmi1, A., Lappalainen, H. K., Carslaw, K. S., Poschl, U., Baltensperger, U., Hov, Ø., Brenquier, J.-L., Pandis, S. N., Facchini, M. C., Hansson, H.-C., Wiedensohler, A., and O'Dowd, C. D.: Introduction: European Integrated Project on Aerosol Cloud Climate and Air Quality interactions (EUCAARI) – integrating aerosol research from nano to global scales, Atmos. Chem. Phys., 9, 2825-2841, 2009.

Kumar, N., Lurmann, F. W., Wexler, A. S., Pandis, S. N., and Seinfeld, J. H.: Development and Application of a Three Dimensional Aerosol Model. Presented

European Union
European Social Fund
OPERATIONAL PROGRAMME
EDUCATION AND LIFELONG LEARNING
investing in knowledge society
MINISTRY OF EDUCATION & RELIGIOUS AFFAIRS
MANAGING AUTHORITY
NSRF 2007-2013
EUROPEAN SOCIAL FUND
Co-financed by Greece and the European Union

at the A&WMA Specialty Conference on Computing in Environmental Resource Management, Research Triangle Park, NC, December 2-4, 1996.

Lane, T. E., Donahue, N. M., and Pandis, S. N.: Simulating secondary organic aerosol formation using the volatility basis-set approach in a chemical transport model, Atmos. Environ., 42, 7439-7451, 2008a.

Lane, T. E., Donahue, N. M., and Pandis, S. N.: Effect of NOx on secondary organic aerosol concentrations, Environ. Sci. Technol., 42, 6022-6027, 2008b.

Lanz, V. A., Prevot, A. S. H., Alfarra, M. R., Mohr, C., DeCarlo, P. F., Weimer, S., Gianini, M. F. D., Hueglin, C., Schneider, J., Favez, O., D'Anna, B., George, C., and Baltensperger, U.: Characterization of aerosol chemical composition by aerosol mass spectrometry in Central Europe: an overview, Atmos. Chem. Phys. Discuss., 9, 24985-25021, 2009.

Lanz, V. A., Alfarra, M. R., Baltensperger, U., Buchmann, B., Hueglin, C., and Prevot, A. S. H.: Source apportionment of submicron organic aerosols at an urban site by factor analytical modelling of aerosol mass spectra, Atmos. Chem. Phys., 7, 1503-1522, 2007.

Lelieveld, J., Berresheim, H., Borrmann, S., Crutzen, P. J., Dentener, F. J., Fischer, H., Feichter, J., Flatau, P. J., Heland, J., Holzinger, R., Korrmann, R., Lawrence, M. G., Levin, Z., Markowicz, K. M., Mihalopoulos, N., Minikin, A., Ramanathan, V., de Reus, M., Roelofs, G., J., Scheeren, H. A., Sciare, J., Schlager, H., Schultz, M., Siegmund, P., Steil, B., Stephanou, E. G., Stier, P., Traub, M., Warneke, C., Williams, J., and Ziereis, H.: Global Air Pollution Crossroads over the Mediterranean, Science, 298, 794-799, DOI:10.1126/science.1075457, 2002.

Lipsky, E. M. and Robinson, A. L.: Effects of dilution on fine particle mass and partitioning of semivolatile organics in diesel exhaust and wood smoke, Environ. Sci. Technol., 40, 155-162, 2006.

Mihalopoulos, N., Stephanou, E., Kanakidou, M., Pilitsidis, S., and Bousquet, P.: Tropospheric aerosol ionic composition in the Eastern Mediterranean region, Tellus B, 49, 314-326, 1997.

European Union
European Social Fund
OPERATIONAL PROGRAMME
EDUCATION AND LIFELONG LEARNING
investing in knowledge society
MINISTRY OF EDUCATION & RELIGIOUS AFFAIRS
MANAGING AUTHORITY
NSRF 2007-2013
programme for development
EUROPEAN SOCIAL FUND
Co-financed by Greece and the European Union

Morgan, M. T., Allan, J. D., Bower, K. N., Esselborn, M., Harris, B., Henzing, J. S., Highwood, E. J., Kiendler-Scharr, A., McMeeking, G. R., Mensah, A. A., Northway, M. J., Osborne, S., Williams, P. I., Krejci, R., and Coe, H.: Enhancement of the aerosol direct radiative effect by semi-volatile aerosol components: airborne measurements in North-Western Europe, Atmos. Chem. Phys. Discuss., 10, 10653-10705, 2010a.

Morgan, M. T., Allan, J. D., Bower, K. N., Highwood, E. J., Liu, D., McMeeking, G. R., Northway, M. J., Williams, P. I., Krejci, R., and Coe, H.: Airborne measurements of the spatial distribution of aerosol chemical composition across Europe and evolution of the organic fraction, Atmos. Chem. Phys., 10, 4065–4083, 2010b.

Murphy, B. N. and Pandis, S. N.: Simulating the formation of semivolatile primary and secondary organic aerosol in a regional chemical transport model, Environ. Sci. Technol., 43, 4722-4728, 2009.

Murphy, B. N., Donahue, N. M., Fountoukis, C., and Pandis, S. N.: Simulating the oxygen content of ambient organic aerosol with the 2D volatility basis set, Atmos. Chem. Phys., 11, 7859-7873, 2011.

Nenes, A., Pandis, S. N., and Pilinis, C.: ISORROPIA: a new thermodynamic equilibrium model for multiphase multicomponent inorganic aerosols, Aquatic Geochemistry, 4, 123-152, 1998.

Ng, N. L., Canagaratna, M. R., Zhang, Q., Jimenez, J. L., Tian, J., Ulbrich, I. M., Kroll, J. H., Docherty, K. S., Chhabra, P. S., Bahreini, R., Murphy, S. M., Seinfeld, J. H., Hildebrandt, 15 L., DeCarlo, P. F., Lanz, V. A., Prevot, A. S. H., Dinar, E., Rudich, Y., and Worsnop, D. R.: Organic aerosol components observed in Northern hemisphere datasets from aerosol mass spectrometry, Atmos. Chem. Phys., 10, 4625-4641, 2010.

Ng, N. L., Kroll, J. H., Keywood, M. D., Bahreini, R., Varutbangkul, V., Flagan, R. C., and Seinfeld, J. H.: Contribution of first- versus second-generation products to secondary organic aerosols formed in the oxidation of biogenic hydrocarbons, Environ. Sci. Technol., 40, 2283-2297, 2006.

European Union
European Social Fund
OPERATIONAL PROGRAMME
EDUCATION AND LIFELONG LEARNING
investing in knowledge society
MINISTRY OF EDUCATION & RELIGIOUS AFFAIRS
MANAGING AUTHORITY
NSRF 2007-2013
programme for development
EUROPEAN SOCIAL FUND
Co-financed by Greece and the European Union

O'Dowd, C. D., Langmann, B., Varghese, S., Scannell, C., Ceburnis, D., and Facchini, M. C.: A Combined Organic-Inorganic Sea-Spray Source Function, Geophys. Res. Lett., 35, L01801, doi:10.1029/2007GL030331, 2008.

Paatero, P. and Tapper, U.: Positive matrix factorization: a nonnegative factor model with optimal utilization of error estimates of data values, Environmetrics, 5, 111-126, 1994.

Paatero, P.: Least squares formulation of robust non-negative factor analysis, Chemometr. Intell. Lab., 37, 23-35, 1997.

Pandis, S. N., Wexler, A. S., and Seinfeld, J. H.: Secondary organic aerosol formation and transport. 2. Predicting the ambient secondary organic aerosol size distribution, Atmos. Environ., 27A, 2403-2416, 1993.

Pikridas, M., Bougiatioti, A., Hildebrandt, L., Engelhart, G. J., Kostenidou, E., Mohr, C., Prevot, A. S. H., Kouvarakis, G., Zarmpas, P., Burkhart, J. F., Lee, B.-H., Psichoudaki, M., Mihalopoulos, N., Pilinis, C., Stohl, A., Baltensperger, U., Kulmala, M., and Pandis, S. N.: The Finokalia Aerosol Measurement Experiment – 2008 (FAME-08): an overview, Atmos. Chem. Phys., 10, 6793-6806, 2010.

Pilinis, C., Capaldo, K. P., Nenes, A., and Pandis, S. N.: MADM - a new multicomponent aerosol dynamics model. Aerosol Science and Technology, 32, 482–502, 2000.

Pope, C. A., Burnett, R. T., Thun, M. J., Calle, E. E., Krewski, D., Ito, K., and Thurston, G. D.: Lung cancer, cardiopulmonary mortality, and long-term exposure to fine particulate air pollution, Journal of the American Medical Association 287, 1132-1141, 2002.

Presto, A. A. and Donahue, N. M.: Investigation of α-pinene + ozone secondary organic aerosol formation at low total aerosol mass, Environ. Sci. Technol., 40, 3536-3543, 2006.

Pun, B. K., Wu, S. Y., Seigneur, C., Seinfeld, J. H., Griffin, R. J., and Pandis, S. N.: Uncertainties in modeling secondary organic aerosols: Three-dimensional modeling studies in Nashville/Western Tennessee, Environ. Sci. Technol., 37 (16), 3647-3661, doi:10.1021/es0341541, 2003.

European Union
European Social Fund
OPERATIONAL PROGRAMME
EDUCATION AND LIFELONG LEARNING
investing in knowledge society
MINISTRY OF EDUCATION & RELIGIOUS AFFAIRS
MANAGING AUTHORITY
NSRF 2007-2013
programme for development
EUROPEAN SOCIAL FUND
Co-financed by Greece and the European Union

Roberts, G. C., Andreae, M. O., Zhou, J., and Artaxo, P.: Cloud condensation nuclei in the Amazon Basin: "Marine" conditions over a continent?, Geophys. Res. Lett., 28, 2807-2810, 2001.

Robinson, A. L., Donahue, N. M., Shrivastava, M. K., Weitkamp, E. A., Sage, A. M., Grieshop, A. P., Lane, T. E., Pierce, J. R., Pandis, S. N.: Rethinking organic aerosol: semivolatile emissions and photochemical aging, Science, 315, 1259-1262, 2007.

Schwartz, J.: Air pollution and hospital admissions for respiratory disease, Epidemiology, 7, 20-28, 1996.

Sciare, J., Bardouki, H., Moulin, C., and Mihalopoulos, N.: Aerosol sources and their contribution to the chemical composition of aerosols in the Eastern Mediterranean Sea during summertime, Atmos. Chem. Phys., 3, 291–302, 2003.

Seinfeld, J. H. and Pandis, S. N.: Atmospheric chemistry and physics: From air pollution to climate change. 2nd ed.; John Wiley and Sons, Hoboken, NJ, 2006.

Shrivastava, M. K., Lane, T. E., Donahue, N. M., Pandis, S. N., and Robinson, A. L.: Effects of gas-particle partitioning and aging of primary emissions on urban and regional organic aerosol concentrations, J. Geophys. Res., 113, D18301, doi:10.1029/2007JD009735, 2008.

Simpson, D. Yttri, K. E., Klimont, Z., Kupiainen, K., Caseiro, A., Gelencser, A., Pio, C., Puxbaum, H., Legrand, M.: Modeling carbonaceous aerosol over Europe: Analysis of the CARBOSOL and EMEP EC/OC campaigns, J. Geophys. Res., 112, D23S14, doi: 10.1029/2006JD008158, 2007.

Skamarock, W. C., Klemp, J. B., Dudhia, J., Gill, D. O., Barker, D. M., Wang, W., and Powers, J. G.: A Description of the Advanced Research WRF Version 2, NCAR Technical Note (http://www.mmm.ucar.edu/wrf/users/docs/arw_v2.pdf), 2005.

Slinn, S. A. and Slinn, W.G.N.: Predictions for particle deposition on natural waters. Atmos. Environ., 24, 1013-1016, 1980.

Sofiev, M., Vankevich, R., Lanne, M., Koskinen, J., and Kukkonen, J.: On integration of a Fire Assimilation System and a chemical transport model for near-real-time monitoring of the impact of wild-land fires on atmospheric composition and air

European Union
European Social Fund
OPERATIONAL PROGRAMME
EDUCATION AND LIFELONG LEARNING
investing in knowledge society
MINISTRY OF EDUCATION & RELIGIOUS AFFAIRS
MANAGING AUTHORITY
NSRF 2007-2013
programme for development
EUROPEAN SOCIAL FUND
Co-financed by Greece and the European Union

quality, Modelling, Monitoring and Management of Forest Fires, WIT Transactions on Ecology and the Environment, 119, 343-351, 2008a.

Sofiev, M., Lanne, M., Vankevich, R., Prank, M., Karppinen, A., and Kukkonen, J.: Impact of wild-land fires on European air quality in 2006-2008, Modelling, Monitoring and Management of Forest Fires, WIT Transactions on Ecology and the Environment, 119, 353-361, 2008b.

Spindler, G., E. Brüggemann, T. Gnauk, A. Grüner, K. Müller, H. Herrmann, A four-year size-segregated characterization study of particles PM10, PM2.5 and PM1 depending on air mass origin at Melpitz. Atmos. Environ., 44, 164-173, 2010.

Stanier, C. O., Donahue, N. M., and Pandis, S. N.: Parameterization of secondary organic aerosol mass fraction from smog chamber data, Atmos. Environ., 42, 2276-2299, 2008.

Steinbrecher, R., Smiatek, G., Koble, R., Seufert, G., Theloke, J., Hauff, K., Ciccioli, P., Vautard, R., and Curci, G. (2009). Intra- and inter-annual variability of VOC emissions from natural and seminatural vegetation in Europe and neighbouring countries, Atmos. Environ., 43, 1380–1391.

Szidat, S., Jenk, T. M., Synal, H. A., Kalberer, M., Wacker, L., Hajdas, I., Kasper-Giebl, A., and Baltensperger, U.: Contributions of fossil fuel, biomass-burning, and biogenic emissions to carbonaceous aerosols in Zurich as traced by (14)C, J. Geophys. Res., 111, D07206, doi: 10.1029/2005JD006590, 2006.

Takegawa, N., Miyazaki, Y., Kondo, Y., Komazaki, Y., Miyakawa, T., Jimenez, J. L., Jayne, J. T., Worsnop, D. R., Allan, J. D., and Weber, R. J.: Characterization of an Aerodyne Aerosol Mass Spectrometer (AMS): Intercomparison with other aerosol instruments, Aerosol Sci. Tech., 39, 760-770, 2005.

Tsimpidi, A. P., Karydis, V. A., Zavala, M., Lei, W., Bei, N., Molina, L., and Pandis, S. N.: Sources and production of organic aerosol in Mexico City: insights from the combination of a chemical transport model (PMCAMx-2008) and measurements during MILAGRO, Atmos. Chem. Phys., 11, 5153-5168, 2011.

Tsimpidi, A. P., Karydis, V. A., Zavala, M., Lei, W., Molina, L., Ulbrich, I. M., Jimenez, J. L., and Pandis, S. N.: Evaluation of the volatility basis-set approach for

European Union
European Social Fund
OPERATIONAL PROGRAMME
EDUCATION AND LIFELONG LEARNING
investing in knowledge society
MINISTRY OF EDUCATION & RELIGIOUS AFFAIRS
MANAGING AUTHORITY
NSRF 2007-2013
EUROPEAN SOCIAL FUND
Co-financed by Greece and the European Union

the simulation of organic aerosol formation in the Mexico City metropolitan area, Atmos. Chem. Phys., 10, 525-546, 2010.

Visschedijk, A. J. H., Zandveld, P., and Denier van der Gon, H. A. C.: TNO Report 2007 A-R0233/B: A high resolution gridded European emission database for the EU integrated project GEMS, Netherlands, Organization for Applied Scientific Research, 2007.

Wesely, M. L.: Parameterization of Surface Resistances to Gaseous Dry Deposition in Regional-Scale Numerical Models. Atmos. Environ., 23, 1293-1304, 1989.

Zhang, Q., Canagaratna, M. C., Jayne, J. T., Worsnop, D. R., and Jimenez, J. L: Time and size-resolved chemical composition of submicron particles in Pittsburgh Implications for aerosol sources and processes, J. Geophys. Res., 110, D07S09, doi:10.1029/2004JD004649, 2005a.

Zhang, Q., Worsnop, D. R., Canagaratna, M. R., and Jimenez, J. L.: Hydrocarbon-like and oxygenated organic aerosols in Pittsburgh: insights into sources and processes of organic aerosols, Atmos. Chem. Phys., 5, 3289-3311, 2005b.

Zhang, Q., Jimenez, J. L., Canagaratna, M. R., Allan, J. D., Coe, H., Ulbrich, I., Alfarra, M. R., Takami, A., Middlebrook, A. M., Sun, Y. L., Dzepina, K., Dunlea, E., Docherty, K., De-Carlo, P., Salcedo, D., Onasch, T. B., Jayne, J. T., Miyoshi, T., Shimono, A., Hatakeyama, N., Takegawa, N., Kondo, Y., Schneider, J., Drewnick, F., Weimer, S., Demerjian, K. L., Williams, P. I., Bower, K. N., Bahreini, R., Cottrell, L., Griffin, R. J., Rautianen, J., and Worsnop, D. R.: Ubiquity and dominance of oxygenated species in organic aerosols in anthropogenically-influenced Northern Hemisphere midlatitudes, Geophys. Res. Lett., 34, L13801, doi:10.1029/2007GL029979, 2007.

B. Satellite data on aerosol properties and comparison with ground station measurements

It is well known that despite their great accuracy and usefulness, the surface-based aerosol optical properties are unable to ensure the complete geographical coverage of extended areas. This is because of the large spatial variability of these properties and the local character of surface measurements. Instead, such a large spatial coverage is only possible based on satellite measurements. Nevertheless, given that satellites only measure radiances, aerosol optical properties can only be derived from the raw satellite measured radiances using retrieval algorithms and techniques, which however include assumptions. This results in uncertainties associated with the satellite aerosol optical properties, which in turn have to be validated against ground truth.

The present action of the 6th work package focused on the use of satellite based data in order to examine the spatial and temporal distribution of aerosol optical properties over the Greek region, as well as to the comparison of satellite data against available surface measurements. The primary interest was to ensure first of all a large, actually complete, spatial coverage of the study area. At the same time, emphasis was also given to enable an as long as possible temporal coverage, like a climatological-type one. Therefore, the most recent, up to date and accurate relevant satellite aerosol data were selected and used, namely: (i) MODIS (Terra and Aqua), (ii) OMI and (iii) CALIOP-CALIPSO. These data were compared to AERONET corresponding data as well as to surface PM measurements. An overview of the satellite data used, along with their resolution and coverage, is given in the following Table B1. Some of the key aerosol optical data are included, which are relevant to their physical and chemical properties, which are used in radiation, climate and air-quality models. All of the used data are on a daily basis.

European Union
European Social Fund
OPERATIONAL PROGRAMME
EDUCATION AND LIFELONG LEARNING
investing in knowledge society
MINISTRY OF EDUCATION & RELIGIOUS AFFAIRS
MANAGING AUTHORITY
NSRF 2007-2013
EUROPEAN SOCIAL FUND
Co-financed by Greece and the European Union

Table B1: Aerosol optical properties for which data from three satellite databases is used in the action.

	MODIS	OMI	CALIOP	Spatial resolution		Period
Aerosol optical depth at 550nm (AOD_{550nm})	√			1° x 1° 10km 10km	x	1/3/2000-20/1/2014 (Terra) 4/7/2002-2/9/2013 (Aqua)
Aerosol optical depth at 388 and 500nm (AOD_{388nm}, AOD_{500nm})		√		1° x 1° 13km 24km	x	1/10/2004-14/12/2013
Aerosol optical depth at 532nm (AOD_{532nm})			√	1° x 1°		1/7/2006-31/10/2011
Aerosol absorption optical depth at 388 and 550nm ($AAOD_{388nm}$, $AAOD_{500nm}$)		√		1° x 1° 13km 24km	x	1/10/2004-14/12/2013
Aerosol fine mode fraction(FF)	√			1° x 1° 10km 10km	x	1/3/2000-20/1/2014 (Terra) 4/7/2002-2/9/2013 (Aqua)
Ångström exponent (α)	√			1° x 1° 10km 10km	x	1/3/2000-20/1/2014 (Terra) 4/7/2002-2/9/2013 (Aqua)
Single scattering albedo		√		1° x 1° 13km 24km	x	1/10/2004-14/12/2013
Aerosol Index (AI)		√		1° x 1° 13km 24km	x	1/10/2004-14/12/2013

European Union
European Social Fund
OPERATIONAL PROGRAMME
EDUCATION AND LIFELONG LEARNING
investing in knowledge society
MINISTRY OF EDUCATION & RELIGIOUS AFFAIRS
MANAGING AUTHORITY
NSRF 2007-2013
EUROPEAN SOCIAL FUND
Co-financed by Greece and the European Union

Representative results of aerosol optical properties are given in the following paragraphs, organized in three sub-sections dealing with their: (i) geographical distribution and seasonal variability, (ii) inter-annual variability and changes, both on a pixel-level and regional mean terms and (iii) inter-comparison with AERONET and PM surface measurements.

Geographical and seasonal variability of aerosol optical properties over Greece

In Figure B1 the distribution of AOD is displayed, on a long-term annual basis, over the broader Greek region, based on MODIS-Terra and Aqua and CALIOP-CALIPSO data for the periods 2000-2014, 2002-2013 and 2006-2011, respectively.

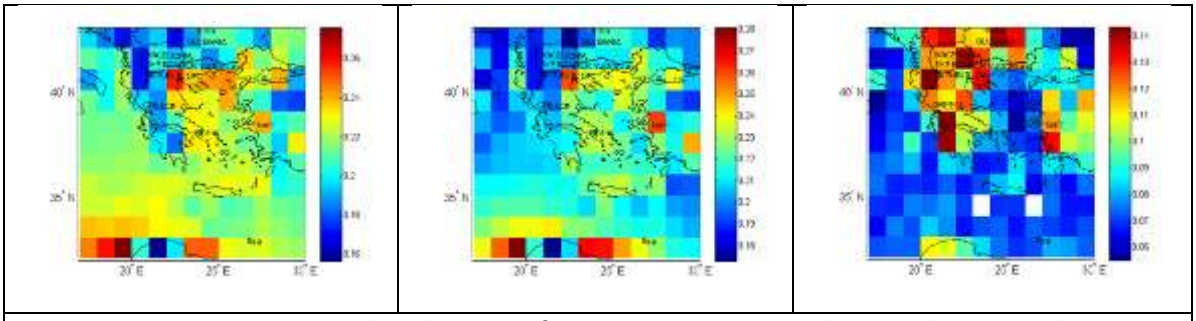

Figure B1: Mean annual distribution of AOD over the broader Greek region, based on satellite: **(i)** MODIS-Terra (2000-2014),**(ii)** MODIS-Aqua (2002-2013), and **(iii)** CALIOP (2006-2011) data at 550nm (MODIS) and 532nm (CALIOP).

A quite large spatial variability of AOD over Greece is apparent, with values ranging from 0.16-0.17 to 0.27-0.28 according to MODIS and from 0.06 to 0.14 according to CALIOP instruments. A great similarity exists between Terra and Aqua both in terms of values and spatial patterns, but some differences are found with CALIOP. Thus, generally smaller AODs are suggested by CALIOP, with clearly larger values over land than sea areas. Although large AODs also appear over continental areas based on MODIS, especially over coastal populated and industrialized areas, relatively high

European Union
European Social Fund
OPERATIONAL PROGRAMME
EDUCATION AND LIFELONG LEARNING
investing in knowledge society
MINISTRY OF EDUCATION & RELIGIOUS AFFAIRS
MANAGING AUTHORITY
NSRF 2007-2013
EUROPEAN SOCIAL FUND
Co-financed by Greece and the European Union

AODs are in the southernmost parts of the region, namely the seas that are close to North Africa, where frequent dust export originates from (Gkikas et al., 2013). The disparity of AOD between MODIS and CALIOP, can be attributed to the infrequent passage of CALIPSO (about every 16 days) satellite, and highlights the role of representativeness and temporal resolution of satellite data. It should be noted, however, that there is also a significant month-to-month (seasonal) AOD variation (not shown here) with larger values in spring and summer.

Apart from AOD, which is a good measure of aerosol particulate matter in the atmospheric column, another important property is their size. This is indicated by the satellite derived FF and α data shown in Fig. B2 on annual basis. Results are given separately over land and sea areas, because of different retrieval algorithms utilized to derive them. Larger FF and α values, up to 0.9 for FF and 1.7 for α, are found over the southern Balkans, indicating the stronger presence of fine aerosols. On the contrary, the smallest values for both parameters, down to 0.5 for FF and 0.6 for α, are observed in the central and southern parts of Aegean Sea, where coarse aerosols, either dust or sea-salt, seem to be predominant. Despite the poorer quality of the two optical properties over land (Levy et al., 2010), there is an agreement with the corresponding products over sea, in an obvious south-to-north increasing gradient. The results confirm the predominance of fine and coarse aerosols over continental and maritime areas of the region. It should be noted that differences between the land and ocean products appear over Asia Minor, where the previous statement is not valid. This is attributed to reported (Levy et al., 2010) problems with the land algorithm, so that only the satellite information over sea should be trusted.

In Fig. B3-i the annual mean distribution of AI over Greece is shown, based on OMI measurements for the 10-year period 2004-2013. The main feature is the occurrence of large values in southern Greece, especially in Libyan Sea down to African coasts, which are associated with the absorbing dust aerosols, whose presence is mostly widespread in spring (Fig. B3-iii). High AI values are also observed on annual basis in the

European Union
European Social Fund
OPERATIONAL PROGRAMME
EDUCATION AND LIFELONG LEARNING
investing in knowledge society
MINISTRY OF EDUCATION & RELIGIOUS AFFAIRS
MANAGING AUTHORITY
NSRF 2007-2013
EUROPEAN SOCIAL FUND
Co-financed by Greece and the European Union

northwestern part of the region as well as in the Black Sea, where fine absorbing aerosols occur originating either from anthropogenic, e.g. urban, or biomass burning (e.g. forest fires) activities.

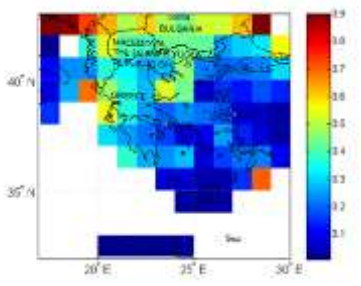
(i-a)

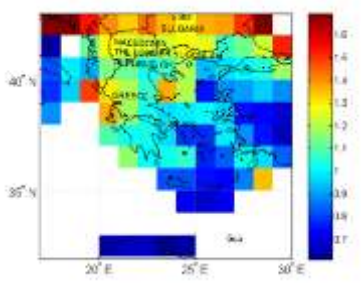
(ii-a)

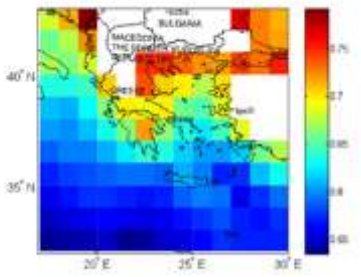
(i-b)

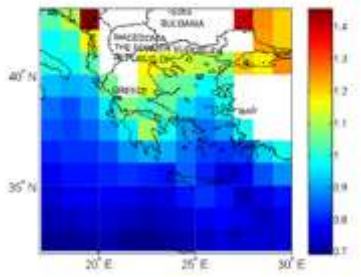
(ii-b)

Figure B2: Mean annual distribution of (i) FM and (ii) α data over (-a) land and (-b) sea surfaces of the broader Greek region, based on MODIS-Terra (2000-2014).

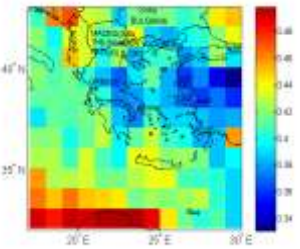
(i)

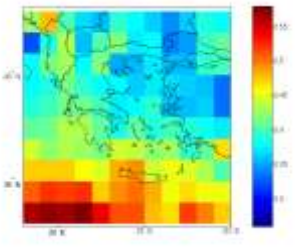
(ii)

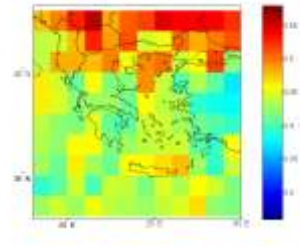
(iii)

Figure B3: Mean distribution of AI over the broader Greek region, based on OMI data for the period 2004-2013. Results are given for: (i) the year, (ii) winter and (iii) spring.

European Union
European Social Fund
OPERATIONAL PROGRAMME
EDUCATION AND LIFELONG LEARNING
investing in knowledge society
MINISTRY OF EDUCATION & RELIGIOUS AFFAIRS
MANAGING AUTHORITY
NSRF 2007-2013
programme for development
EUROPEAN SOCIAL FUND
Co-financed by Greece and the European Union

Inter-annual variability and changes of aerosol optical properties over Greece

The year to year variability and especially the changes of aerosol optical properties is important and relevant to climate (IPCC, 2013) as well as to other aspects, namely to health. Such changes are important not only on global scale, but also on a regional one. Therefore, changes of AOD, which are the most important, have been estimated over the Greek region and are given in Figure B4. Results are given for MODIS-Terra and Aqua as well as for OMI-Aura, referring to the corresponding time periods.

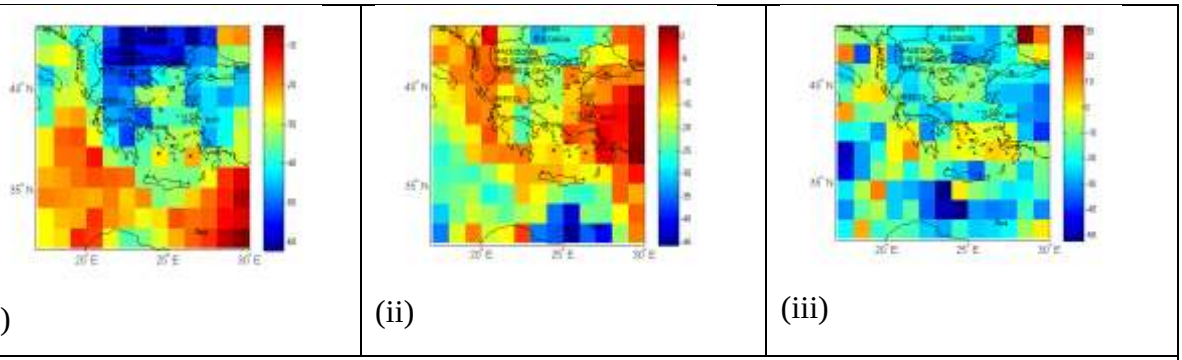

(i) (ii) (iii)

Figure B4: Geographical distribution of percent changes of AOD over the broader Greek region according to: (i) MODIS-Terra for the period 2001-2013, (ii) MODIS-Aqua for the period 2003-2012 and (iii) OMI-Aura for the period 2005-2012.

Irrespectively of the dataset used and the corresponding time period, which is slightly different from one to another, a clear decline of AOD values over the region is apparent for the post-2000 years. It seems that aerosol particulate matter has been decreasing at the beginning of 21st century all over the region, with a few exceptions for OMI. This aerosol loading decline is significant, reaching percentages as high as -50%. This overall decreasing AOD trend is possibly related to taken measures and actions, namely by European Union, aiming at cleaner air conditions over Europe.

In a further step, the causes of the declining AOD over the first decade of 21st century have been examined by looking at the changes of FF and Ångström Exponent.

European Union
European Social Fund
OPERATIONAL PROGRAMME
EDUCATION AND LIFELONG LEARNING
investing in knowledge society
MINISTRY OF EDUCATION & RELIGIOUS AFFAIRS
MANAGING AUTHORITY
NSRF 2007-2013
EUROPEAN SOCIAL FUND
Co-financed by Greece and the European Union

Corresponding data taken from MODIS-Terra (Figure B5) indicate that over the period 2001-2013 relatively small changes of both parameters took place. A positive tendency of both parameters is observed in the northern Ionian and southwestern Black Seas, against a decreasing tendency over the Aegean Sea, especially its southern parts. Over most of continental Greece, a rather positive tendency is found for the two parameters.

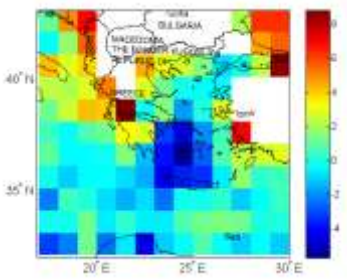

(i-a)

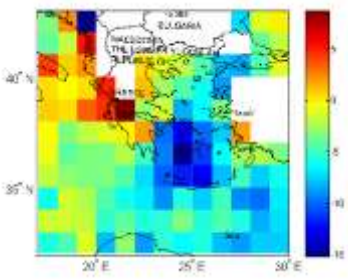

(i-b)

Figure B5: Geographical distribution of percent changes of: (i) FF and (ii) α over the broader Greek region according to MODIS-Terra for the period 2001-2013.

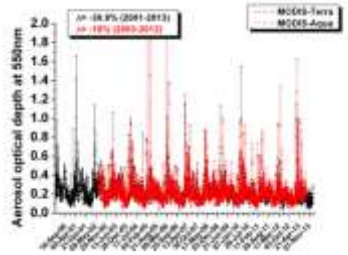

(i-a)

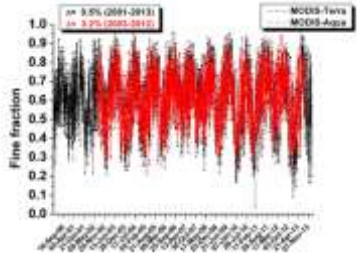

(i-b)

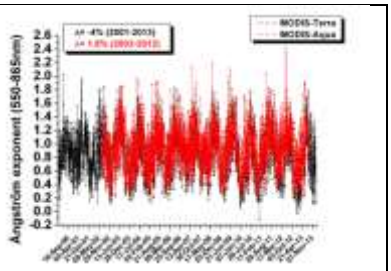

(i-c)

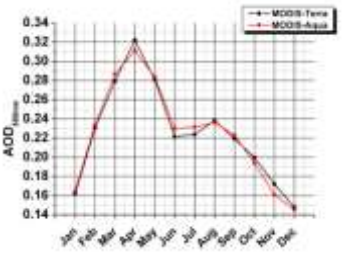

(ii-a)

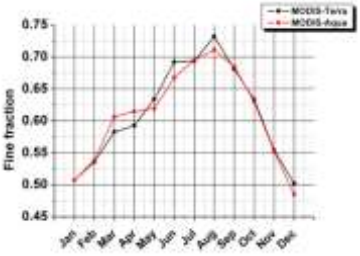

(ii-b)

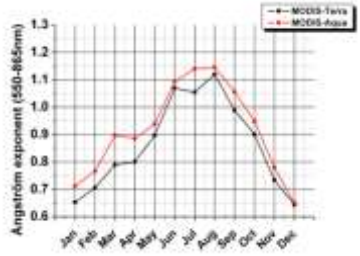

(ii-c)

Figure B6: (i) Inter-annual and (ii) seasonal variation of: (a) AOD, (b) FF and (iii) α over 2001-2013. Values for the three parameters are regional averages, whereas in case (i) percent linear trends are also provided. Results are given for MODIS-Terra and Aqua, separately.

European Union
European Social Fund
OPERATIONAL PROGRAMME
EDUCATION AND LIFELONG LEARNING
investing in knowledge society
MINISTRY OF EDUCATION & RELIGIOUS AFFAIRS
MANAGING AUTHORITY
NSRF 2007-2013
programme for development
EUROPEAN SOCIAL FUND
Co-financed by Greece and the European Union

Figure B6 displays the seasonal and inter-annual cycles of AOD over land and ocean, and of FF and α over ocean. The time series of daily data reveal a significant year-to-year variability of all parameters, with AOD values varying between 0.05 and 2.0, FF values between 0.05 and 0.95, and α values between 0 and 2.4, which suggest that the region can occasionally be dominated by the presence of either fine or coarse aerosols. A clear seasonal cycle is also identified, with primary spring and secondary summer maxima for AOD, and summer maxima for FF and α, highlighting that the two seasonal AOD maxima are attributed to different aerosol types.

Inter-comparison between satellite and surface based data

The satellite based aerosol optical properties were validated against available surface measurements. In Greece, during the period 2000-2013, there were seven (7) operating AERONET stations. Nevertheless, among them, only three stations provided satisfactorily long temporal availability of data, while the others have been operational periodically. Therefore, the comparison was performed for the Heraklion (FORTH-Crete), Athens and Thessaloniki stations. Furthermore, two kinds of comparisons were made, first using the standard 1°x1° (Level-3) satellite data, and secondly the higher resolution (27.5 km, Petrenko et al., 2012) data. In the latter case, the comparisons were performed for the Athens and Heraklion stations.

In Figure B7 we present the overall scatterplot comparison of MODIS-Terra and Aqua AOD at 550 nm against corresponding data from AERONET stations for Athens, Thessaloniki and Heraklion (the AERONET AOD_{550nm} data have been derived from available products at 440 and 870 nm using the Ångström equation). The obtained results reveal a satisfactory agreement, with correlation coefficients (R) close to 0.8 and a relatively small scatter of values (SD smaller than 0.1). The MODIS is found to overestimate AOD with respect to AERONET by up to 0.05 in overall. The

European Union
European Social Fund
OPERATIONAL PROGRAMME
EDUCATION AND LIFELONG LEARNING
investing in knowledge society
MINISTRY OF EDUCATION & RELIGIOUS AFFAIRS
MANAGING AUTHORITY
NSRF 2007-2013
programme for development
EUROPEAN SOCIAL FUND
Co-financed by Greece and the European Union

performance of OMI-Aura AOD against AERONET (not shown here) is found to be inferior to MODIS, with R values ranging from 0.39 (for Athens) to 0.52 (best value for Thessaloniki). The performance of OMI against AERONET is found to be even poorer for aerosol absorption optical depth, with R values not larger than 0.45 (best value for FORTH-Crete). The FF satellite data were compared to those from AERONET, and in this case good results were obtained for the FF products over ocean (R values up to 0.69, Athens-Crete) but not over land (R values up to 0.33) proving thus the insufficient quality of this satellite product over continental areas. The same is valid for the MODIS Ångström Exponent data, which provide a nice comparison against AERONET over sea (R between 0.48 and 0.7) whilst over land the comparison is bad (R between 0.07 and 0.36).

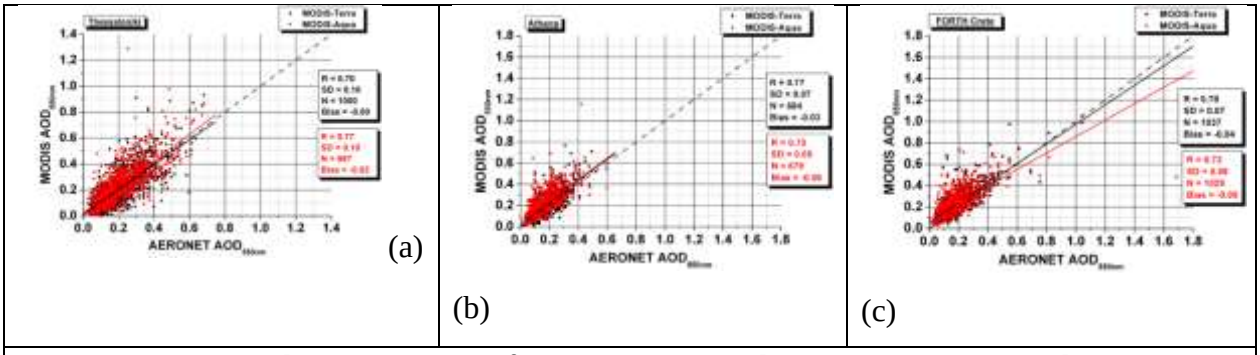

Figure B7: Scatterplot comparison of MODIS-Terra and MODIS-Aqua AOD data at 550nm against corresponding AERONET data for the (a) Thessaloniki, (b) Athens and (c) Heraklion-Crete stations. The correlation coefficients (R), standard deviations of differences (SD) and bias metrics are given in each case.

Similarly, good, and even better, results are also obtained by attempting comparisons between the higher resolution MODIS data and those from AERONET, although also in this case a systematic overestimation is found by MODIS, especially in the lower AOD range of values (smaller than 0.3).

European Union
European Social Fund
OPERATIONAL PROGRAMME
EDUCATION AND LIFELONG LEARNING
investing in knowledge society
MINISTRY OF EDUCATION & RELIGIOUS AFFAIRS
MANAGING AUTHORITY
NSRF 2007-2013
programme for development
EUROPEAN SOCIAL FUND
Co-financed by Greece and the European Union

The comparison shows the limitations of satellite derived products of aerosol optical properties, but the results are encouraging given the different nature of the two types of data, i.e. satellite and ground based, especially given that the latter refer to specific locations while the former are representative of surface areas of a few hundred squared kilometers.

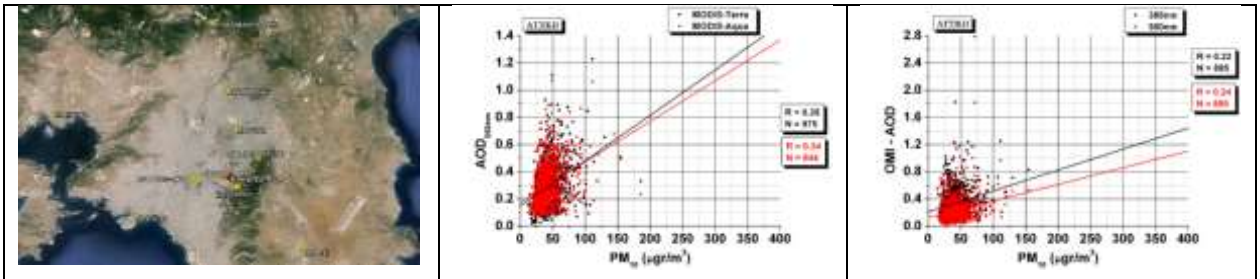

(a) (b) (c)

Figure B8: Scatterplot comparison between satellite AOD data and surface PM_{10} data averaged from measurements taken from 10 stations in Attica (a). The comparison for MODIS-Terra and MODIS-Aqua is in (b) and that for OMI-Aura in (c) AOD.

Finally, a comparison was also made between the high-resolution MODIS and OMI AOD data and surface PM_{10} measurements from 10 stations in Athens. The results (Fig. B8) reveal a relatively poor agreement between the two types of data, which is slightly better for MODIS (R values of 0.34-0.35) than OMI (R=0.22-0.24). This poor agreement is explained by the different nature of two types of data, since the satellite ones refer to the entire atmospheric column, while the PM measurements are representative of the particulate matter of the surface layer only. This proves the difficulty in using satellite AOD as proxy of surface PM_{10} data, and vice-versa. This is valid only under specific conditions in which the major part of aerosol matter is confined in the surface layer.

European Union
European Social Fund
OPERATIONAL PROGRAMME
EDUCATION AND LIFELONG LEARNING
investing in knowledge society
MINISTRY OF EDUCATION & RELIGIOUS AFFAIRS
MANAGING AUTHORITY
NSRF 2007-2013
programme for development
EUROPEAN SOCIAL FUND
Co-financed by Greece and the European Union

B. References

Gkikas, A., Hatzianastassiou, N., Mihalopoulos, N., Katsoulis, V., Kazadzis, S., Pey, J., Querol, X., and Torres, O.: The regime of intense desert dust episodes in the Mediterranean based on contemporary satellite observations and ground measurements, Atmos. Chem. Phys., 13, 12135-12154, doi:10.5194/acp-13-12135-2013, 2013.

Intergovernmental Panel on Climate Change (IPCC): Climate Change 2007: The physical science basis. Summary for policymakers report, 21 pp., Paris, 2007.

Levy, R.C., Remer, L.A., Kleidman, R.G., Mattoo, S., Ichoku, C., Kahn, R., and Eck, T. F.: Global evaluation of the Collection 5 MODIS dark-target aerosol products over land, Atmos. Chem. Phys., 10, 10399-10420, doi:10.5194/acp-10-10399-2010, 2010.

Petrenko, M., Ichoku, C., and Leptoukh, G.: Multi-sensor Aerosol Products Sampling System (MAPSS), Atmos. Meas. Tech. Discuss., 5, 909-945, doi:10.5194/amtd-5-909-2012, 2012.

European Union
European Social Fund
OPERATIONAL PROGRAMME
EDUCATION AND LIFELONG LEARNING
investing in knowledge society
MINISTRY OF EDUCATION & RELIGIOUS AFFAIRS
MANAGING AUTHORITY
NSRF 2007-2013
programme for development
EUROPEAN SOCIAL FUND
Co-financed by Greece and the European Union

C. Global run of the radiative transfer model FORTH model with aerosol data from CALIOP aerosol and cloud data from ISCCP

C1. The radiative transfer model

The vertical profile of aerosol direct radiative effect is computed using a deterministic spectral radiative transfer model (Hatzianastassiou et al., 2007) developed from a radiative-convective model (Vardavas and Carver, 1984). The model computations are performed on a monthly, 2.5°x2.5° resolutions, for 118 wavelengths ranging from 0.20 μm to 1 μm and at 10 intervals between 1 and 10 μm. For each wavelength and spectral interval, a set of monochromatic radiative flux transfer equations is solved for an absorbing/multiple-scattering atmosphere using the delta-Eddington method.

The radiative transfer model is taking into account the scattering and absorption of solar radiation by clouds (low, middle, high), aerosols, and the reflection from the Earth's surface. In the ultraviolet-visible part of the spectral range the model considers Rayleigh scattering and ozone absorption, while in the near-infrared it takes into account absorption by water vapor, carbon dioxide, and methane.

C2 Input data

The aerosol data used in this study come from space-borne retrievals from CALIOP (Cloud-Aerosol Lidar with Orthogonal Polarisation) lidar onboard CALIPSO (Cloud-Aerosol Lidar and Infrared Pathfinder Satellite Observation), which was launched in April 2006 and has been making measurements since June 2006. CALIOP has been designed in order to provide curtain-like views of the vertical distribution of aerosols (Winker et al., 2013). For our analysis, we have used CALIOP Level 2 Version 3.01 products for a 3-year long period (2007-2009). The vertical resolution of CALIOP layer data is 30 m up to the altitude of 8.2 km and 60 m higher altitudes up to 20.2 km. The

European Union
European Social Fund
OPERATIONAL PROGRAMME
EDUCATION AND LIFELONG LEARNING
investing in knowledge society
MINISTRY OF EDUCATION & RELIGIOUS AFFAIRS
MANAGING AUTHORITY
NSRF 2007-2013
EUROPEAN SOCIAL FUND
Co-financed by Greece and the European Union

horizontal resolution is 5 km, although some layers were detected at coarser horizontal resolution. The data that were used are freely available at the CALIPSO website (https://eosweb.larc.nasa.gov/project/
calipso/calipso table).

CALIOP is a two-wavelength and polarization-sensitive elastic backscatter lidar on board CALIPSO and its main advantage is its operation on of two wavelengths, at 532 nm and 1064 nm. The use of two wavelengths enables the identification of the dimensions of the target, whereon laser beam is backscattered (Winker et al., 2009). CALIPSO lidar is designed to detect up to 8 overlapping layers of aerosols, subject to the extinction that the laser beam undergoes within each layer. In order to facilitate the aerosol input to our radiation transfer model, we redistributed the vertical aerosol profile into forty layers, similarly with the vertical resolution of the model.

C3 Model results

C3.1 Aerosol direct radiative effect at surface

According to our model results, under all-sky conditions, atmospheric aerosols cause cooling of the Earth's surface, through scattering and absorption of the downwelling solar radiation. In Fig. C1, the mean annual (2007–2009) direct aerosol effect (DRE) at the Earth's surface is presented. As we can see, the cooling effect is more pronounced in continental areas with greater aerosol load, consisting by both natural and anthropogenic particles. The strongest surface cooling (up to −15.4 W m^{-2}) is observed in the Arabian desert and the Indian sub-continent. Aerosols cause strong cooling of the surface also over northern Africa (arid and semi-arid Sahara and Sahel regions), large portion of the southern Africa and eastern China. The average surface cooling in land areas is −1.37 W m^{-2}. In the oceans, the aerosol effect is smaller (average value −0.63 W m^{-2}), mainly due to the generally low aerosol load, except in the tropical North Atlantic Ocean (cooling up to −5 W m^{-2} locally), where extensive desert dust outflows

European Union
European Social Fund
OPERATIONAL PROGRAMME
EDUCATION AND LIFELONG LEARNING
investing in knowledge society
MINISTRY OF EDUCATION & RELIGIOUS AFFAIRS
MANAGING AUTHORITY
NSRF 2007-2013
EUROPEAN SOCIAL FUND
Co-financed by Greece and the European Union

from Sahara are observed (Remer et al., 2008; Winker et al., 2013) and the northern Indian ocean (mainly the Arabian sea) due to transport of aerosols from South and South-western Asia.

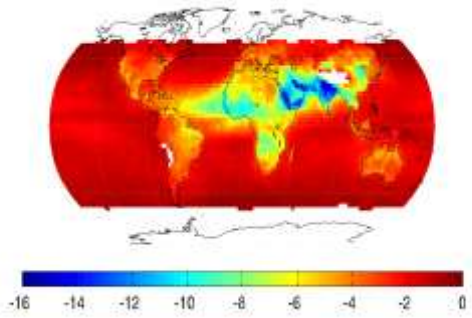

Fig. C1. Mean annual (2007–2009) global distribution of aerosol direct radiative effect (in Wm^{-2}) on the Earth's surface

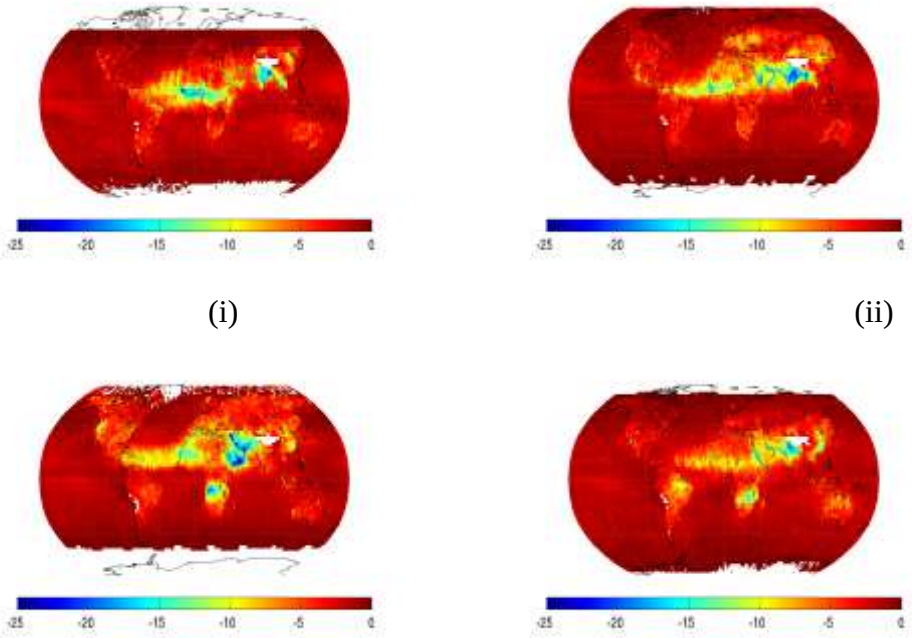

Fig. C2. Mean Seasonal (2007–2009) global distribution of aerosol direct radiative effect (in Wm^{-2}) on the Earth's surface. The mid-seasonal months of January, April, July, and October correspond to (i), (ii), (iii) and (v) subplots.

European Union
European Social Fund
OPERATIONAL PROGRAMME
EDUCATION AND LIFELONG LEARNING
investing in knowledge society
MINISTRY OF EDUCATION & RELIGIOUS AFFAIRS
MANAGING AUTHORITY
NSRF 2007-2013
EUROPEAN SOCIAL FUND
Co-financed by Greece and the European Union

The seasonal variation of the DRE (Fig. C2) is in agreement with the AOD intra-annual cycle, with larger aerosol effect above regions and in months with greater aerosol load. Characteristically, during the austral winter and spring, in southern Africa biomass burning aerosols produced by wildfires cause a strong cooling effect (up to −20 Wm^{-2}, locally). The seasonal biomass burning results also in a greater surface cooling during austral spring in South America, mainly in Amazon region (Remer et al., 2008). A clear seasonal cycle is observed also in the Arabian Peninsula with larger aerosol effect in summer and lower in winter and fall, in agreement with the seasonal variation of the desert dust activity which is greater during summer compared to winter (Prospero et al., 2002).

Setting in the radiative transfer model cloud amount equal to zero, we have obtained the aerosol DRE under clear-sky conditions. Our model results indicates an increasing of the aerosol effect, up to 8 W m^{-2} locally, depending mainly on the cloudiness of each region. Under clear sky conditions the mean annual global values of DRE_{surf} over land and ocean are −2.23 Wm^{-2} and −1.25 Wm^{-2}, respectively.

C3.2 Aerosol direct radiative effect in the atmosphere

C3.2.1 Columnar results

The mean annual and seasonal distribution of the total (columnar) aerosol effect within the atmosphere (DRE_{atm}), or equivalently the aerosol effect on atmospheric absorption, are presented in Fig. C3 and C4, respectively. As we can see, aerosols cause an increase of the atmospheric absorption. The enhancement of absorbed solar radiation is converted into heat (Hatzianastassiou et al., 2007). Thus, the DRE_{atm} is of opposite sign to the DRE_{surf} (Sec. C3.1) (I.e. aerosols warm the atmosphere). This heating effect is strongest in the same regions with largest (negative) surface DRE. More specifically the DRE_{atm} is stronger (up to 14.1 Wm^{-2}) over regions where the aerosol load consists

European Union
European Social Fund
OPERATIONAL PROGRAMME
EDUCATION AND LIFELONG LEARNING
investing in knowledge society
MINISTRY OF EDUCATION & RELIGIOUS AFFAIRS
MANAGING AUTHORITY
NSRF 2007-2013
EUROPEAN SOCIAL FUND
Co-financed by Greece and the European Union

mainly of absorbing particles (desert dust or soot) and generally high surface albedo, such as the Saharan and Arabian deserts and the Indian subcontinent. The mean annual all-sky DRE_{atm} above land is 2.67 Wm^{-2}, while above ocean is much lower (0.30 Wm^{-2}) first due to the highest AOD above continental areas and second due to the fact that major sources of highly absorbing aerosol particles are located in the continents. Under clear-sky conditions the corresponding values are 3.05 Wm^{-2} (land) and 0.37 Wm^{-2} (ocean).

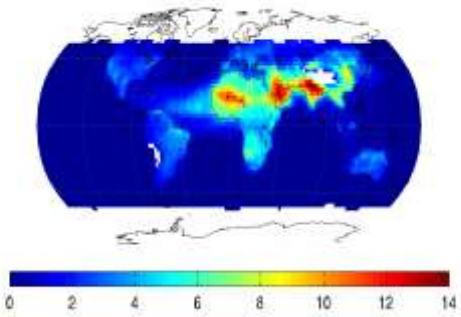

Fig. C3. Mean annual (2007–2009) global distribution of aerosol direct radiative effect (in Wm^{-2}) within the atmosphere

European Union
European Social Fund
OPERATIONAL PROGRAMME
EDUCATION AND LIFELONG LEARNING
investing in knowledge society
MINISTRY OF EDUCATION & RELIGIOUS AFFAIRS
MANAGING AUTHORITY
NSRF 2007-2013
programme for development
EUROPEAN SOCIAL FUND
Co-financed by Greece and the European Union

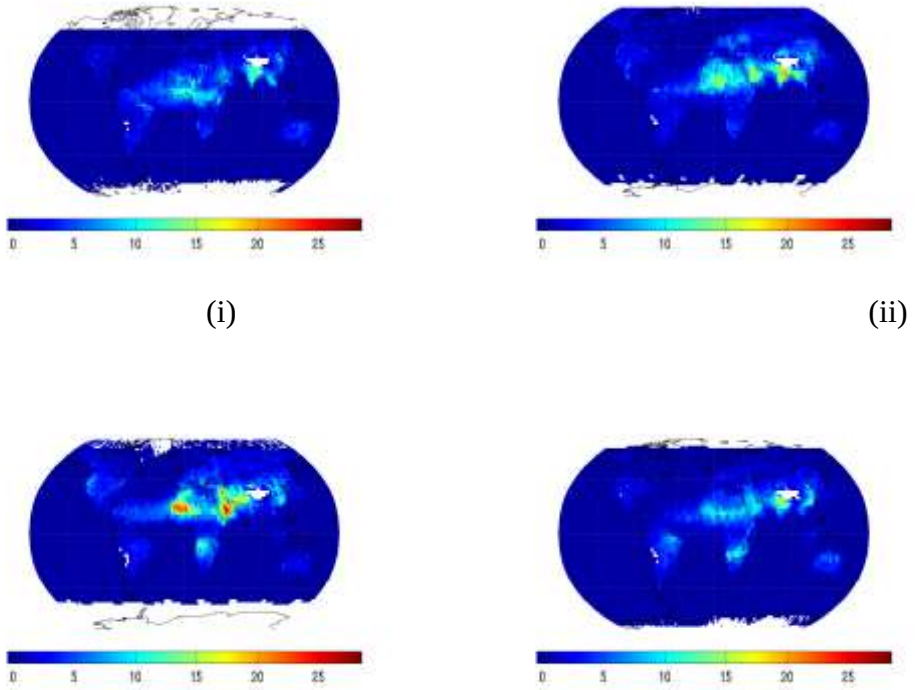

(i) (ii)

(iii) (iv)

Fig. C4. Mean Seasonal (2007–2009) global distribution of aerosol direct radiative effect (in Wm^{-2}) within the atmosphere

C3.2.2 DRE and Heating rates profile

The aforementioned columnar results of the aerosol effect on the atmospheric absorption does not provide the whole picture of the aerosol effect within the atmosphere. Because of the importance of this effect on atmospheric stability, we make use of the detailed vertical profile of the DRE_{atm}. From the vertical profile of the DRE and using the fist thermodynamic law and the hydrostatic equilibrium we calculate the atmospheric heating rates profile:

European Union
European Social Fund
OPERATIONAL PROGRAMME
EDUCATION AND LIFELONG LEARNING
investing in knowledge society
MINISTRY OF EDUCATION & RELIGIOUS AFFAIRS
MANAGING AUTHORITY
NSRF 2007-2013
programme for development
EUROPEAN SOCIAL FUND
Co-financed by Greece and the European Union

$$\frac{\partial T}{\partial t} = \frac{g}{c_p}\frac{\Delta F}{\Delta P}$$

where $\frac{\partial T}{\partial t}$ is the heating rate (given in K day^{-1}), g is the gravitational acceleration, c_p the specific heat capacity of air at constant air pressure (1006 J Kg^{-1} K^{-1}) and P is the atmospheric pressure. The calculated heating rates express the initial tendency of the atmosphere to warm up, without any feedback and are proportional to the aerosol absorption of solar radiation.

In Fig. C5 the aerosol effect on the atmospheric absorption, as well as the resulting heating rates are presented. The results are averaged for each latitude (top) and longitude (bottom) in order to have some insight regarding their geographical variation. The first conclusion to be drawn from Fig. C5 is that the aerosol DREs depend strongly on altitude and are collocated with areas of large aerosol mass. Therefore, the aerosol heating effects are stronger in the lower parts of the atmosphere, where the aerosol load is greater, resulting in an increase of the atmospheric stability. The strongest DRE (up to 0.27 Wm^{-2}, resulting to heating rates up to 0.1 K day^{-1}) is observed in the latitudes between 20° and 30° N because of the Saharan and Arabian Deserts (both sources of strongly absorbing mineral particles). Moreover, the aerosol effect in these regions extends to greater heights, due to the strong vertical extent of desert dust, mainly during summer (Winker et al., 2013). In the Southern Hemisphere the aerosol effect, and consequently heating rates, are much lower than in the Northern due to the fewer aerosol sources. A secondary maximum in the zonal distribution of the DRE is observed in the austral sub-tropical latitudes (20° - 30° S). This is due to the dust particles originating from southern African arid and semi-arid regions such as Kalahari Desert, as well as smoke from savanna biomass burning processes during the austral winter (dry season). The longitudinally averaged profile of the aerosol DRE_{atm} reveals stronger effects on the eastern hemisphere compared to the western. In Fig. C5b, four zones with high aerosol effect are detected. The first one, between 10°W and 50°E, with aerosol

European Union
European Social Fund
OPERATIONAL PROGRAMME
EDUCATION AND LIFELONG LEARNING
investing in knowledge society
MINISTRY OF EDUCATION & RELIGIOUS AFFAIRS
MANAGING AUTHORITY
NSRF 2007-2013
EUROPEAN SOCIAL FUND
Co-financed by Greece and the European Union

effect on atmospheric absorption and heating rates reaching values up to 0.25 W m^{-2} and 0.1 K day^{-1} is associated with the presence of desert dust aerosol originating mainly from Saharan and Arabian deserts. The second one (around 80°E) can be attributed with aerosol sources in the Indian sub-continent (mainly biomass burning and anthropogenic aerosol particles). The anthropogenic pollution in the Far-East (and more specifically in China) is mainly associated with the third zone (105°E-115°E), while the fourth (40°W-70°W) corresponds to South America. Between 145°E and 120°W the aerosol effects are negligible due to the mostly clean atmosphere in the Pacific Ocean.

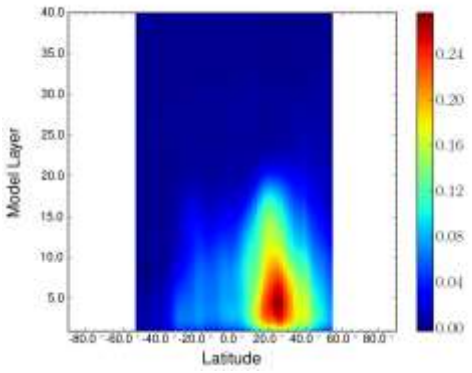

(a-i)

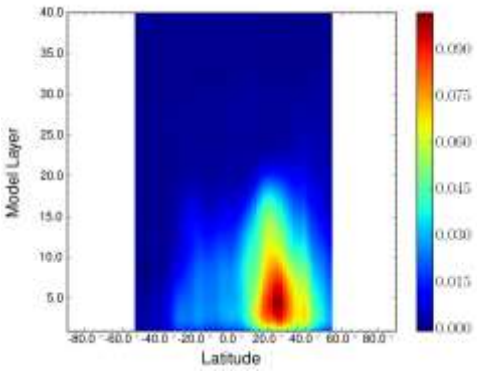

(a-ii)

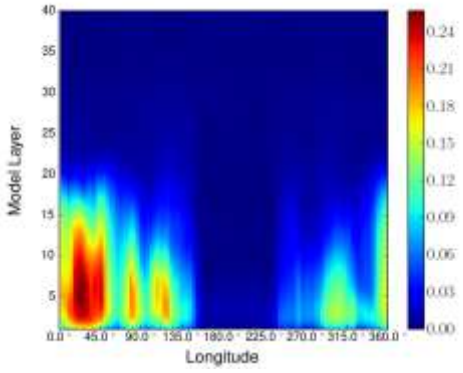

(b-i)

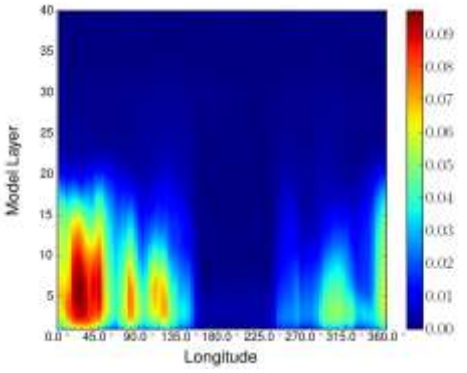

(b-ii)

Fig. C5. Mean annual (2007–2009) zonally (a) and meridionally (b) averaged profile of: (i) aerosol effect on atmospheric absorption (in W m^{-2}) and (ii) heating rates (in K day^{-1}).

European Union
European Social Fund
OPERATIONAL PROGRAMME
EDUCATION AND LIFELONG LEARNING
investing in knowledge society
MINISTRY OF EDUCATION & RELIGIOUS AFFAIRS
MANAGING AUTHORITY
NSRF 2007-2013
EUROPEAN SOCIAL FUND
Co-financed by Greece and the European Union

C3.3 Aerosol direct radiative effect at the top of atmosphere

In Fig. C6 we present the geographical distribution of the aerosol effect on the Top Of the Atmosphere (TOA). Negative values correspond to a decrease of the net incoming solar radiation or, equivalently, to an increase of the planetary albedo, which results in planetary cooling. In contrast, positive values correspond to an aerosol-induced planetary heating effect. The aerosol DRE on TOA is the sum of the DREs on the Earth's surface and within the atmosphere. As shown in Fig. C6, on the Top of Atmosphere, aerosol DRE ranges between -6.9 (planetary cooling) and 5.2 W m^{-2} (planetary heating effect). In most areas, due to the fact that aerosol surface cooling is more pronounced than the warming effect within the atmosphere, the overall DRE on TOA is of negative sign. The aerosol DRE at TOA is of positive sign in the regions characterized by both absorbing aerosol and large albedo values (Johnson et al., 2008). Larger planetary heating effect is observed above northern Africa and the Arabian Peninsula. This is due to the large surface albedo of the Saharan and Arabian deserts, which results in multiple scattering between aerosols and the ground, and also the presence of significant amount of absorbing desert dust particles (Hatzianastassiou et al., 2004). Smaller planetary warming is observed also in other parts of Asia, such as above southern China.

In contrast, the greatest planetary cooling effect is observed over the tropical North Atlantic Ocean, the Red and the Arabian seas and also over the Persian Gulf, indicating a strong cooling effect at TOA of the advected desert dust. The different sign of the DRE between adjacent areas (such as the northern Africa and the tropical North Atlantic Ocean) with the same type of aerosols reveals the very important role of the surface albedo in the determination of the DRE at TOA.

European Union
European Social Fund
OPERATIONAL PROGRAMME
EDUCATION AND LIFELONG LEARNING
investing in knowledge society
MINISTRY OF EDUCATION & RELIGIOUS AFFAIRS
MANAGING AUTHORITY
NSRF 2007-2013
programme for development
EUROPEAN SOCIAL FUND
Co-financed by Greece and the European Union

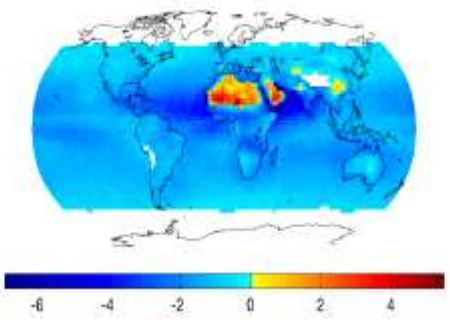

Fig. C6. Mean annual (2007–2009) global distribution of aerosol direct radiative effect (in Wm^{-2}) at the Top Of Atmosphere (TOA)

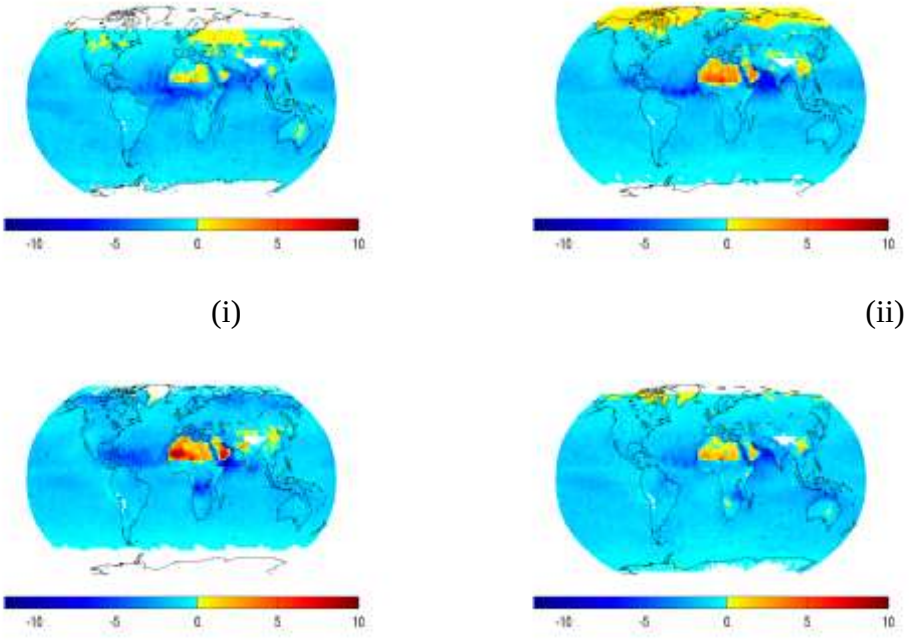

Fig. C7. Mean seasonal (2007–2009) global distribution of aerosol direct radiative effect (in Wm^{-2}) at the Top Of Atmosphere (TOA)

The geographical distribution of the aerosol effect at TOA during the mid-seasonal months is presented in Fig. C7. As we can see in this figure, a planetary heating effect (up to 2 Wm^{-2}) is observed above snow and ice covered regions such as the Arctic

European Union
European Social Fund
OPERATIONAL PROGRAMME
EDUCATION AND LIFELONG LEARNING
investing in knowledge society
MINISTRY OF EDUCATION & RELIGIOUS AFFAIRS
MANAGING AUTHORITY
NSRF 2007-2013
EUROPEAN SOCIAL FUND
Co-financed by Greece and the European Union

during April and most part of Russia during January. This, mainly for the case of the Arctic, is very important because of the climatic sensitivity of these regions (Stocker et al., 2013). Also the intra-annual variation of the DRE reveals that over the Arabian and Saharan deserts the aerosol induced planetary heating effect is much more pronounced in July (up to 10 W m^{-2}). Our model results at TOA reveal a mean annual increase of the atmospheric albedo around −0.41 W m^{-2}.

C4 Forcing efficiency

The aerosol radiative forcing efficiency (ARFE) (in W m^{-2}) at the Surface, within the Atmosphere and at TOA was calculated dividing the corresponding DRE by the columnar CALIOP AOD. The ARFEs are calculated under both all-sky and clear-sky conditions (setting cloud amount = 0), and their mean annual (2007–2009) geographical distributions are presented in Fig. C8. At the earth's surface, the aerosol forcing efficiency is stronger (more negative values, up to -100 Wm^{-2}) in regions with aerosol load consisting mainly of absorbing aerosols and generally low surface albedo, such as the tropical north Atlantic Ocean (where absorbing desert dust particles are advected from the Sahara), the southern and the eastern Asia. This indicates that an increase of aerosol absorptivity or a decrease of surface albedo leads to an increase of surface cooling. Within the atmosphere, the aerosol forcing efficiency is larger primarily where absorbing aerosols are observed and secondarily above highly reflective regions. The greatest forcing efficiency (80 Wm^{-2}) is observed above the Sahara Desert. More absorbing aerosols induce greater atmospheric heating effect, as shown also in Sec. C3. At TOA the forcing efficiency is driven mainly by the surface albedo. An increase of the albedo is causing less negative or more positive efficiency. Consequently, above highly reflective regions, the planetary cooling is reduced and in certain regions with absorbing aerosols, such as Saharan desert, the TOA ARFE becomes positive indicating aerosol-induced planetary warming. The presence of clouds results in a decrease of the aerosol forcing efficiency, in terms of absolute values. Therefore, we note a decrease in both the aerosol-induced surface cooling and the atmospheric heating. At the TOA

European Union
European Social Fund
OPERATIONAL PROGRAMME
EDUCATION AND LIFELONG LEARNING
investing in knowledge society
MINISTRY OF EDUCATION & RELIGIOUS AFFAIRS
MANAGING AUTHORITY
NSRF 2007-2013
programme for development
EUROPEAN SOCIAL FUND
Co-financed by Greece and the European Union

the aerosol cooling effects are decreasing, leading even to a change of DRE sign in certain regions, such as China (from -20 W m^{-2} to 5 W m^{-2}).

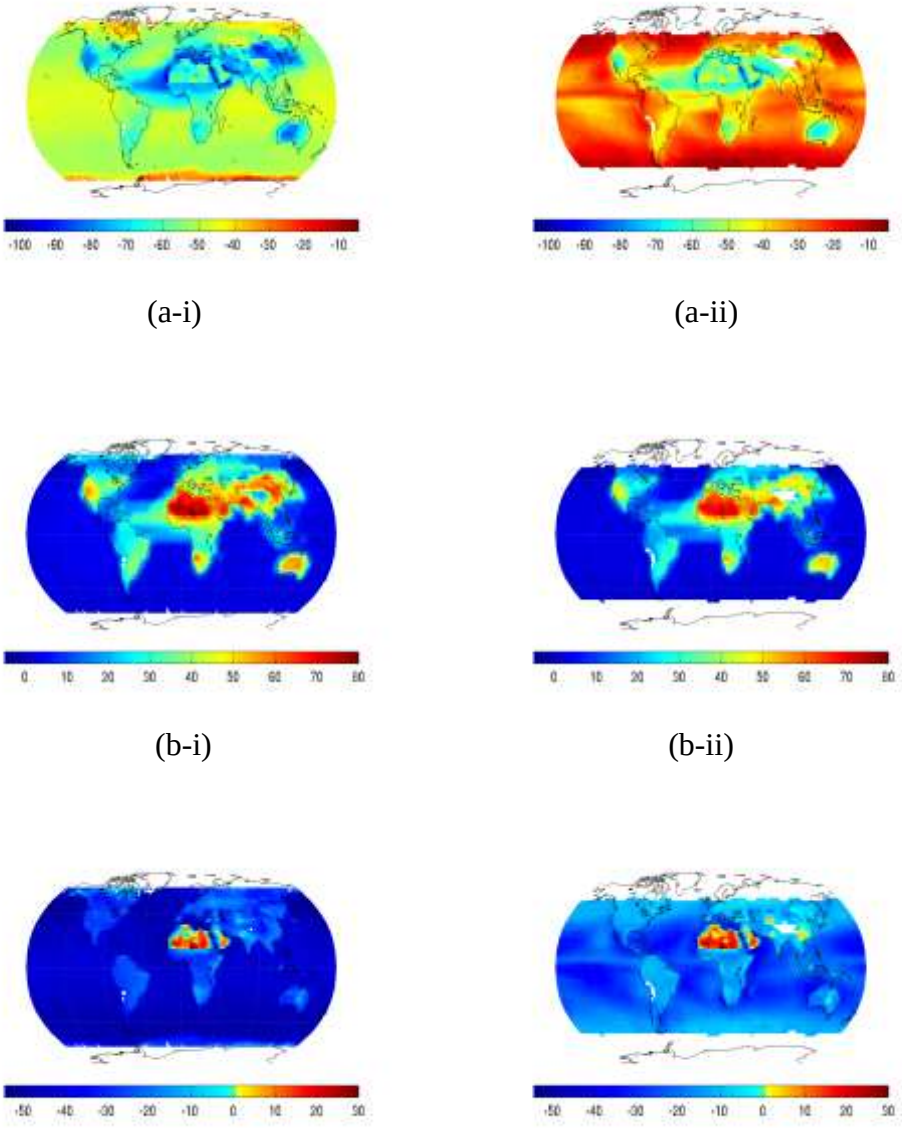

(a-i) (a-ii)

(b-i) (b-ii)

(c-i) (c-ii)

Fig. C8. Mean annual (2007–2009) global distribution of aerosol forcing efficiency at the surface (top row), the atmospheric column (middle row) and the TOA (bottom row). Both clear-sky (left column) and all-sky (right column) are presented.

European Union
European Social Fund
OPERATIONAL PROGRAMME
EDUCATION AND LIFELONG LEARNING
investing in knowledge society
MINISTRY OF EDUCATION & RELIGIOUS AFFAIRS
MANAGING AUTHORITY
NSRF 2007-2013
EUROPEAN SOCIAL FUND
Co-financed by Greece and the European Union

C5 References

Hatzianastassiou, N., Katsoulis, B., and Vardavas, I. (2004). Sensitivity analysis of aerosol direct radiative forcing in ultraviolet–visible wavelengths and consequences for the heat budget, Tellus B, 56, 368–381

Hatzianastassiou, N., Matsoukas, C., Drakakis, E., Stackhouse Jr, P., Koepke, P., Fotiadi, A., Pavlakis, K., and Vardavas, I. (2007). The direct effect of aerosols on solar radiation based on satellite observations, reanalysis datasets, and spectral aerosol optical properties from Global Aerosol Data Set (GADS), Atmospheric Chemistry and Physics, 7, 2585–2599

Johnson, B. T., Heese, B., McFarlane, S. A., Chazette, P., Jones, A., and Bellouin, N. (2008). Vertical distribution and radiative effects of mineral dust and biomass burning aerosol over West Africa during DABEX, J. Geophys. Res., 113, D00C12, doi:10.1029/2008JD009848

Prospero, J. M., Ginoux, P., Torres, O., Nicholson, S. E., and Gill, T. E. (2002). Environmental characterization of global sources of atmospheric soil dust derived from the NIMBUS7 TOMS absorbing aerosol product, Rev, REVIEWS OF GEOPHYSICS, 40, 1002

Remer, L. A., Kleidman, R. G., Levy, R. C., Kaufman, Y. J., et al., (2008). Global aerosol climatology from the MODIS satellite sensors, J. Geophys. Res., 113

Stocker, D. Q. et al.. (2013). Climate change 2013: The physical science basis, Working Group I Contribution to the Fifth Assessment Report of the Intergovernmental Panel on Climate Change, Summary for Policy-makers, IPCC

Vardavas I., Carver J. H. (1984). Solar and terrestrial parameterizations for radiative convective models. Planetary and Space Science 32, 1307–1325

Winker, D. M., Vaughan, M. A., Omar, A., Hu, Y., Powell, K. A., Liu, Z., Hunt, W. H., and Young, S. A. (2009). Overview of the CALIPSO Mission and CALIOP Data Processing Algorithms, J. Atmos. Ocean. Technol., 26, 2310–2323, doi:10.1175/2009JTECHA1281.1

European Union
European Social Fund
OPERATIONAL PROGRAMME
EDUCATION AND LIFELONG LEARNING
investing in knowledge society
MINISTRY OF EDUCATION & RELIGIOUS AFFAIRS
MANAGING AUTHORITY
NSRF 2007-2013
programme for development
EUROPEAN SOCIAL FUND
Co-financed by Greece and the European Union

Winker, D., Tackett, J., Getzewich, B., Liu, Z., Vaughan, M., and Rogers, R. (2013): The global 3-D distribution of tropospheric aerosols as characterized by CALIOP, Atmospheric Chemistry and Physics, 13, 3345–3361

European Union
European Social Fund
OPERATIONAL PROGRAMME
EDUCATION AND LIFELONG LEARNING
investing in knowledge society
MINISTRY OF EDUCATION & RELIGIOUS AFFAIRS
MANAGING AUTHORITY
NSRF 2007-2013
programme for development
EUROPEAN SOCIAL FUND
Co-financed by Greece and the European Union

D. Development and Integration of Anthropogenic and Biogenic Gridded Emission Inventories for the European Continent and Greece during the Thales June – July 2012 period

D1. Introduction

This deliverable report briefly documents the anthropogenic and biogenic emission inventories, which constitute a basic component of any successful air quality modeling study. These inventories are provided as input to a Chemical Transport Model (CTM) such as PMCAMx [Environ, 2004]. Part of our involvement in the Thales project was the creation and integration of detailed biogenic and anthropogenic emission inventories into a single merged inventory. This inventory is specific to the modelling domain (European continent and Greece) and contains both anthropogenic and biogenic emissions from various sources. Emissions of gases (CO, NO, NH_4, etc.), as well as particulate matter emissions (organic and elemental carbon, sea salt aerosols etc.) are included in the model input. All emission inventory constituents are built in accordance with the SAPRC 99 chemical mechanism. Temporal resolution of the emissions data is one hour.

A variety of anthropogenic emission sources are identified in the related inventories including industrial, domestic, agricultural and traffic. Since anthropogenic emissions are provided as yearly values, time splitting the data was necessary in order to estimate hourly fluxes for the given time period (Schaap et al., 2008).

Three different datasets are combined in order to produce the biogenic emissions. The majority of the gas emissions from ecosystems are produced by implementation of the MEGAN (Model of Emissions of Gases and Aerosols from Nature) code (Guenther et al., 2006). Marine aerosols comprise the largest natural source of aerosols globally. Since sea surface covers a considerable portion of the domain, we used a marine aerosol

European Union
European Social Fund
OPERATIONAL PROGRAMME
EDUCATION AND LIFELONG LEARNING
investing in knowledge society
MINISTRY OF EDUCATION & RELIGIOUS AFFAIRS
MANAGING AUTHORITY
NSRF 2007-2013
programme for development
EUROPEAN SOCIAL FUND
Co-financed by Greece and the European Union

model. We also adopted wildfire biogenic emissions inventory for a specific time period. The time span of the emission inventories is from June 5 to July 31 2012.

In the following sections we will provide a detailed description of the processing tasks implemented on the pre-described datasets including a presentation of the final database.

D1.1 Description of work

A short description of the original inventories used in the present report is provided below:

- Anthropogenic emissions inventories :
    - A high resolution gridded European emissions database which from hereinafter will be referenced as **GEMS** (Global and regional Earth-system Monitoring using Satellite and in-situ data). This inventory was provided by TNO (Denier van der Gon, TNO, private communication). All gas emissions inputs are provided from GEMS dataset for referance year 2003 as well as off-shore emission from year 2004 [Visschedijk et al., 2007].
    - A Pan-European Carbonaceous aerosol inventory [EUCAARI deliverable D42, 2009]. This inventory was provided by TNO (Denier van der Gon, TNO, private communication) and hereinafter will be referenced as **EC/OC**. Particle mass of Elemental Carbon (EC) and Organic Carbon (OC) originate from the Pan-European Carbonaceous Aerosol Inventory for referance year 2005.
- Biogenic emissions inventories:

European Union
European Social Fund
OPERATIONAL PROGRAMME
EDUCATION AND LIFELONG LEARNING
investing in knowledge society
MINISTRY OF EDUCATION & RELIGIOUS AFFAIRS
MANAGING AUTHORITY
NSRF 2007-2013
EUROPEAN SOCIAL FUND
Co-financed by Greece and the European Union

- Gas emissions produced by plant canopies are modeled by the implementation of the MEGAN v2.4 code [Guenther et al., 2006]. The produced dataset will be referenced as **MEGAN**. MEGAN inputs include the leaf area index, the plant functional type and the emission factors. Weather data input for MEGAN is provided from WRF.

- Marine aerosol emissions were produced by implementation of code that was developed in-house for the specific need. The developed code is based on previously published work (Monahan et al., 1986; Smith and Harrison, 1998; Geever et al., 2005; Cavalli et al., 2004; O'Dowd et al., 2008). The code and the related dataset will be referenced hereinafter as **MARINE**. This model estimates mass flaxes for both accumulation and coarse mode, including the organic aerosol fraction. Chlorophyll-a concentrations and wind speed data from WRF are used as input for the marine aerosol model.

- A fire emissions inventory was created for the time period of Jun – July 2012 and hereinafter will be referenced as **FIRES**. The raw uncrossed daily fire emissions were produced by the IS4FIRES system (Sofiev et al., 2009) and are available online via http://is4fires.fmi.fi/.

The final product of the described work is the production of detailed emission datasets. These datasets are exported into files with specific structure that meets the PMCAMx input requirements. Emissions of particulate matter were size resolved into 8 size bins (Table DI). These size bins are compatible to PMCAMx-2008, with particle diameters ranging from 0.039 μm to10 μm.

European Union
European Social Fund
OPERATIONAL PROGRAMME
EDUCATION AND LIFELONG LEARNING
investing in knowledge society
MINISTRY OF EDUCATION & RELIGIOUS AFFAIRS
MANAGING AUTHORITY
NSRF 2007-2013
EUROPEAN SOCIAL FUND
Co-financed by Greece and the European Union

Table DI: PMCAMx size bin ranges

Size Bin	Diameters range (μm)
1	0.039063 – 0.078125
2	0.078125 – 0.15625
3	0.15625 – 0.3125
4	0.3125 – 0.625
5	0.625 – 1.25
6	1.25 – 2.5
7	2.5 – 5.0
8	5.0 – 10.0

D1.1.1 The PMCAMx grid

In all cases the final datasets are registered on the chosen PMCAMx grid (Figure D1). This grid spans the European continent with the following key parameters:

Geographical coordinate system:	*Polar stereographic*.
SW grid corner (latitude/longitude):	*34.2459° / -27.5284°*
Number of rows:	*162*
Number of columns:	*150*
True latitude:	*60.0°*
Standard longitude:	*-32.0°*
Cell dimensions:	*36.0 km × 36.0 km*

European Union
European Social Fund
OPERATIONAL PROGRAMME
EDUCATION AND LIFELONG LEARNING
investing in knowledge society
MINISTRY OF EDUCATION & RELIGIOUS AFFAIRS
MANAGING AUTHORITY
NSRF 2007-2013
EUROPEAN SOCIAL FUND
Co-financed by Greece and the European Union

Figure D1. The PMCAMx grid area

Additionally, a higher spatial resolution grid of the Greek region was also created (Figure D2.). For the specific grid the key parameters are:

Geographical coordinate system:	*Polar stereographic*.
SW grid corner (latitude/longitude):	*39.8593° / 17.5937°*
Number of rows:	*104*
Number of columns:	*128*
True latitude:	*60.0°*
Standard longitude:	*-32.0°*
Cell dimensions:	*9.0 km × 9.0 km*

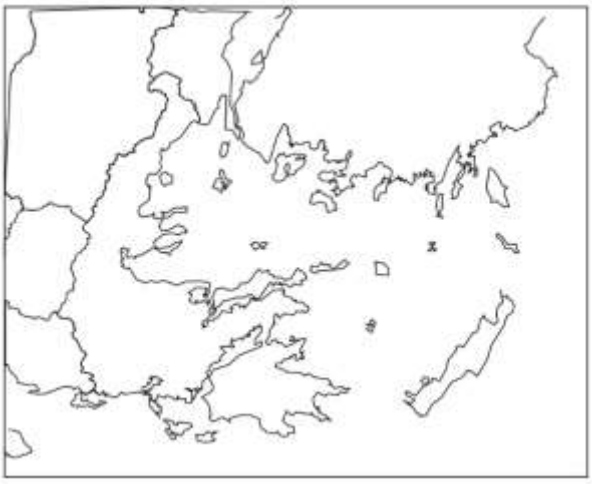

Figure D2. The PMCAMx nested grid area

D1.1.2 The essential inventory processes

The final gridded hourly emissions are built specifically for the selected time periods of June - July 2012. Since each individual database presents its own challenges, we have developed a generalized framework to cope with the various inconsistencies. For each database we followed a number of generalized steps. These basic steps are mentioned below. However in many cases we had to perform various intermediate tasks not explicitly stated here:

1. Pre-process tasks: These tasks are performed on the original inventory file. During the pre-process we perform the following jobs:
    - *Identification of the various data files that compose the original inventory.*
    - *Identification of the database records and determination of the total data population.*
    - *File and data integrity tests.*
    - *Development of the automated access code.*
    - *Mass conservation tests*

European Union
European Social Fund
OPERATIONAL PROGRAMME
EDUCATION AND LIFELONG LEARNING
investing in knowledge society
MINISTRY OF EDUCATION & RELIGIOUS AFFAIRS
MANAGING AUTHORITY
NSRF 2007-2013
EUROPEAN SOCIAL FUND
Co-financed by Greece and the European Union

- *Identification of the original grid and determination of the grid characteristics. If needed, registration of the data on the original grid.*
- *Data and export into suitable intermediate files.*

2. Main-process tasks A : This step is necessary in order to register the data into the PMCAMx grid. This step is performed once for each inventory.

   Creation of the registration guide that describes the mapping of the original grid to the PMCAMx grid. For this purpose we used an algorithm developed in-house and based on the Monte Carlo method.

   Verification of the mapping.

3. Main-process tasks B :

   - *Data registration.*
   - *Time splitting of the data in order to produce hourly emission values.*
   - *Chemical species data splitting (if needed).*
   - *Mass conservation tests.*
   - *The final data consists of species records compatible with PMCAMx input. All the data are provided as:* ***moles cell^{-1} hour^{-1}*** *for gases and as* ***g cell^{-1} hour^{-1}*** *for particulate matter. These data are exported into either binary or ASCII files suitable for easy data access. These files form the final database of each inventory.*

4. Post-process tasks: The above tasks are repeated for each inventory. Then the final datasets produced by steps 1–3 are post-processed.

   - *Database merging and exporting into the final ASCII files. These files form the final merged database.*
   - *Analysis of the total mass fluxes of the final data to be used for reference.*
   - *Creation of the final data files suitable for direct input to PMCAMx.*

Step 1 is applicable to the anthropogenic and FIRES inventories. Since no emissions data were available for the terrestrial ecosystems and the marine aerosol emissions, we produce our own emission inventories (MARINE and MEGAN). These inventories

European Union
European Social Fund
OPERATIONAL PROGRAMME
EDUCATION AND LIFELONG LEARNING
investing in knowledge society
MINISTRY OF EDUCATION & RELIGIOUS AFFAIRS
MANAGING AUTHORITY
NSRF 2007-2013
programme for development
EUROPEAN SOCIAL FUND
Co-financed by Greece and the European Union

were then processed according to steps 2 - 3. Finally all biogenic and anthropogenic inventories were processed according to step 4.

D2. Anthropogenic Emissions

The original emissions are provided as yearly values further categorized by source and by country and are gridded on a 1/8º×1/16º resolution of approximately 7 km×7 km. The emission sources included in the initial inventory are number coded (1-10). A summary of the available sources is listed here:

1. Public electricity and other energy transformation GEMS/ECOC
2. Small combustion plants GEMS/ECOC
   21. Residential wood combustion ECOC
   22. Residential coal combustion ECOC
3. Industrial combustion and process with contact GEMS/ECOC
4. Industrial process emission GEMS/ECOC
5. Fossil fuel production and fugitive emissions GEMS/ECOC
6. Solvent and product use GEMS/ECOC
7. Road transport GEMS
   71. Road transport gasoline ECOC
   72. Road transport diesel ECOC
   73. Road transport LPG ECOC
   75. Road transport non-exhaust (tire, break etc.) ECOC
8. Other (non-road) transport and mobile machinery GEMS/ECOC
9. Waste disposal GEMS/ECOC
10. Agriculture GEMS/ECOC

– International shipping GEMS (provided separately)

Anthropogenic emissions were either described as area emissions (emission rate for the total cell area) or point emissions (emission rate at a specific location). Anthropogenic

European Union
European Social Fund
OPERATIONAL PROGRAMME
EDUCATION AND LIFELONG LEARNING
investing in knowledge society
MINISTRY OF EDUCATION & RELIGIOUS AFFAIRS
MANAGING AUTHORITY
NSRF 2007-2013
programme for development
EUROPEAN SOCIAL FUND
Co-financed by Greece and the European Union

emissions were updated to decrease SO_2 emissions by 50% for the Megalopoli and Ptolemaida (Greece) power plants in order to account for the Greek economic recession that impacted year 2012.

D3. Inventories integration

For the specific research needs, we integrated the PMCAMx gridded hourly emissions, originating from GEMS, EC/OC, MEGAN, MARINE and FIRES, to deliver the final datasets. These datasets were provided as input to the PMCAMx model. A summary of all emission inventories for all the chemical components during June - July 2012 are presented in Table DII (master grid) and Table DIII (nested grid). Illustrative examples of the 24-hour average emission values distributions for elemental carbon (EC) (tons/cell) for a given day of July can be found in Figures D3a-b. According to table II, EC emissions are attributed to the EC/OC and FIRES inventories. We also provide an example of the Na emissions (Figure D4). In this case, Na emissions are from the MARINE inventory.

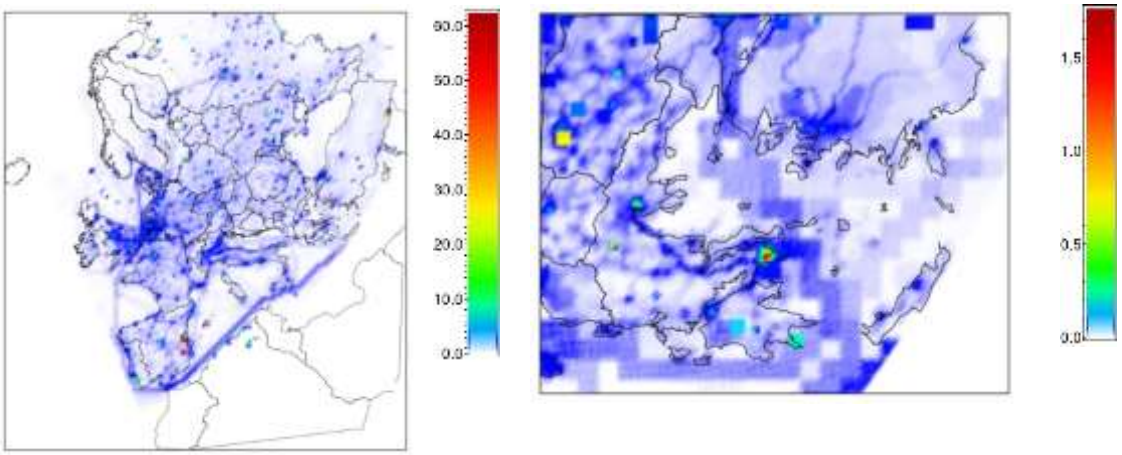

(a) **(b)**

Figure D3 a,b. EC/OC and FIRES inventories for size bins 1 to 8, 24-hour total emissions (tons/cell) of EC during July 1st 2012. (a) master grid European emissions of area and point sources. (b) nested grid emissions of area only sources.

European Union
European Social Fund
OPERATIONAL PROGRAMME
EDUCATION AND LIFELONG LEARNING
investing in knowledge society
MINISTRY OF EDUCATION & RELIGIOUS AFFAIRS
MANAGING AUTHORITY
NSRF 2007-2013
EUROPEAN SOCIAL FUND
Co-financed by Greece and the European Union

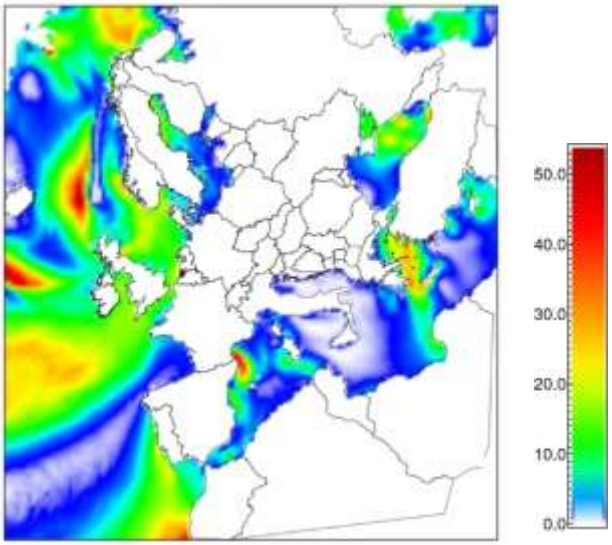

Figure D4. 24-hour total MARINE Na emissions for size bins 1-8, (tons/cell) during July 1st 2012.

European Union
European Social Fund
OPERATIONAL PROGRAMME
EDUCATION AND LIFELONG LEARNING
investing in knowledge society
MINISTRY OF EDUCATION & RELIGIOUS AFFAIRS
MANAGING AUTHORITY
NSRF 2007-2013
programme for development
EUROPEAN SOCIAL FUND
Co-financed by Greece and the European Union

Table DII. Emissions mass totals (ktons) for the European domain, from June 5 to July 31, 2012

	Emission Inventories					
Species[1]	**GEMS**	**EC/OC**	**MEGAN**	**MARINE**	**FIRES**	**Total**
CO	6512,80	–	1694,71	–	7950,38	16157,89
NH3	1001,17	–	–	–	118,41	1119,58
ALK1	144,24	–	8,80	–	–	153,04
ALK2	278,69	–	3,01	–	–	281,70
ALK3	236,05	–	202,53	–	–	438,59
ALK4	443,96	–	4,52	–	–	448,48
ALK5	494,67	–	23,80	–	–	518,47
OLE1	136,16	–	440,95	–	–	577,11
OLE2	70,43	–	149,36	–	–	219,79
ARO1	202,49	–	10,34	–	–	212,82
ARO2	167,57	–	13,67	–	–	181,24
ETHE	110,00	–	367,19	–	–	477,19
MEK	54,53	–	2,85	–	–	57,38
PROD	52,97	–	0,00	–	–	52,97
HCHO	42,65	–	82,13	–	109,99	234,77
CCHO	1,37	–	161,65	–	–	163,03
RCHO	30,92	–	7,21	–	–	38,13
MEOH	0,38	–	2693,16	–	–	2693,54
NO	2639,74	–	98,75	–	225,66	2964,15
NO2	139,39	–	–	–	–	139,39
SO2	2927,38	–	–	–	33,83	2961,21
SO3	59,78	–	–	–	–	59,78
ISOP	–	–	5297,66	–	–	5297,66
TERP	–	–	1593,94	–	–	1593,94
ACET	–	–	395,51	–	–	395,51
CH4	–	–	98,38	–	–	98,38
COOH	–	–	53,55	–	–	53,55
CO2H	–	–	54,75	–	–	54,75
BALD	–	–	0,58	–	–	0,58
RC2H	–	–	4,75	–	–	4,75
PEC	–	105,51	–	–	166,58	272,09
POC	–	140,93	–	21,22	523,02	685,17
PNO3	–	–	–	–	74,42	74,42
PNH4	–	–	–	–	11,74	11,74
PSO4	71,72	–	–	540,65	161,25	773,62
NA	–	–	–	2067,97	–	2067,97
PCL	–	–	–	3716,94	–	3716,94
CRST	–	94,12	–	432,52	136,33	662,97

[1]All species names are according to SAPRC99 and PMCAMx-2008 terminology

European Union
European Social Fund
OPERATIONAL PROGRAMME
EDUCATION AND LIFELONG LEARNING
investing in knowledge society
MINISTRY OF EDUCATION & RELIGIOUS AFFAIRS
MANAGING AUTHORITY
NSRF 2007-2013
EUROPEAN SOCIAL FUND
Co-financed by Greece and the European Union

Table DIII. Emissions mass totals (ktons) for the Greek nested grid, from June 5 to July 31, 2012

	Emission Inventories					
Species[1]	**GEMS**	**EC/OC**	**MEGAN**	**MARINE**	**FIRES**	**Total**
CO	332,969	–	102,840	–	425,747	861,556
NH3	37,431	–	–	–	6,341	43,771
ALK1	4,923	–	0,534	–	–	5,457
ALK2	12,060	–	0,183	–	–	12,242
ALK3	9,103	–	13,229	–	–	22,332
ALK4	16,262	–	0,274	–	–	16,536
ALK5	16,021	–	1,299	–	–	17,320
OLE1	7,140	–	26,758	–	–	33,898
OLE2	3,360	–	9,052	–	–	12,412
ARO1	13,207	–	0,627	–	–	13,834
ARO2	10,579	–	0,645	–	–	11,224
ETHE	6,217	–	22,282	–	–	28,499
MEK	1,302	–	0,173	–	–	1,475
PROD	1,257	–	0,000	–	–	1,257
HCHO	2,538	–	4,984	–	5,890	13,411
CCHO	0,052	–	10,559	–	–	10,611
RCHO	1,694	–	0,438	–	–	2,131
MEOH	0,014	–	153,052	–	–	153,066
NO	136,436	–	6,285	–	12,084	154,805
NO2	7,636	–	–	–	–	7,636
SO2	248,558	–	–	–	1,812	250,370
SO3	5,109	–	–	–	–	5,109
ISOP	–	–	407,204	–	–	407,204
TERP	–	–	78,373	–	–	78,373
ACET	–	–	22,957	–	–	22,957
CH4	–	–	5,495	–	–	5,495
COOH	–	–	3,250	–	–	3,250
CO2H	–	–	3,322	–	–	3,322
BALD	–	–	0,035	–	–	0,035
RC2H	–	–	0,288	–	–	0,288
PEC	–	6,022	–	–	8,920	14,943
POC	–	10,580	–	0,040	28,008	38,627
PNO3	–	–	–	–	3,985	3,985
PNH4	–	–	–	–	0,629	0,629
PSO4	6,129	–	–	21,580	8,635	36,344
NA	–	–	–	82,542	–	82,542
PCL	–	–	–	148,361	–	148,361
CRST	–	7,200	–	17,264	7,300	31,765

[1]All species names are according to SAPRC99 and PMCAMx-2008 terminology

European Union
European Social Fund
OPERATIONAL PROGRAMME
EDUCATION AND LIFELONG LEARNING
investing in knowledge society
MINISTRY OF EDUCATION & RELIGIOUS AFFAIRS
MANAGING AUTHORITY
NSRF 2007-2013
EUROPEAN SOCIAL FUND
Co-financed by Greece and the European Union

D4 References

Cavalli F., Facchini M. C., Decesari S., Mircea M., Emblico L., Fuzzi S., Ceburnis D., Yoon Y. J., O' Dowd C. D., Putaud J. P., and Dell'Acqua A., (2004), "Advances in characterization of size resolved organic matter in marine aerosol over the North Atlantic", J. Geophys. Res., vol. 109, D24215, doi: 10.1029/2004JD005137.

Environ, (2004). "User's guide to the comprehensive air quality model with extensions (CAMx)", version 4.10 s, report, ENVIRON Int. Corp., Novato, Calif. (available at http://www.camx.com).

EUCAARI deliverable D42, (2009), "D42 Pan – European Carbonaceous aerosol inventory", EUCAARI Deliverable Report, Netherlands, TNO Built Environment and Geosciences.

Geever, M., O'Dowd C. D., van Ekeren S., Flanagan R., Nilsson D. E., de Leeuw G., Rannik Ü., (2005), "Sub-Micron Sea-Spray Fluxes", Geophys. Res. Letts., vol. 32, doi: 10.1029/2005GL023081.

Guenther G., Karl T., Harlay P., Wiedinmyer C., Palmer P. I., and Geron C., (2006), "Estimates of global terrestrial isoprene emissions using MEGAN (Model of Emissions of Gases and Aerosols from Nataure)", Atmos Chem. Phys, vol. 6, pp. 3181 – 3210.

Monahan E. C., Spiel D. E. and Davidson K. L., (1986). "A model of marine aerosol generation via whitecaps and wave disruption, in oceanic whitecaps and their role in Air-Sea exchange", edited by E.C. Monahan and G. Mac Niocaill, pp. 167-174, D. Reidel, Norwell, Mass.

European Union
European Social Fund

OPERATIONAL PROGRAMME
EDUCATION AND LIFELONG LEARNING
investing in knowledge society
MINISTRY OF EDUCATION & RELIGIOUS AFFAIRS
MANAGING AUTHORITY

NSRF 2007-2013
programme for development
EUROPEAN SOCIAL FUND

Co-financed by Greece and the European Union

O'Dowd C.D., Langmann B., Varghese S., Scannell C., Ceburnis D., and Facchini M. C., (2008), "A Combined Organic-Inorganic Sea-Spray Source Function", Geophys. Res. Letts., vol. 35, L01801, doi:10.1029/2007GL030331.

Schaap M, Timmermans R. M. A., Sauter F. J., Roemer M., Velders G. J. M., Boersen G. A. C., Beck J. P.,Builtjes P. J. H., (2008), "The LOTOS-EUROS model: description, validation and latest developments", Int J. of Environment and Pollution, vol. 32, pp. 270-289.

Smith M. H. and Harrison N. M., (1998), "The sea spray generation function", J. Aer. Science. vol. 29, pp. S189–S190.

Sofiev, M., Vankevich, R., Lotjonen, M., Prank, M., Petukhov, V., Ermakova, T., Koskinen, J., and Kukkonen, J, (2009), "An operational system for the assimilation of the satellite information on wild-land fires for the needs of air quality modelling and forecasting", Atmos. Chem. Phys., 9, pp. 6833-6847, doi:10.5194/acp-9-6833-2009

Visschedijk A. J. H., Zandveld P. and Denier van der Gon, H. A .C. (2007), "TNO Report 2007 A-R0233/B: A high resolution gridded European emission database for the EU integrated project GEMS", Netherlands, Organization for Applied Scientific Research.

European Union
European Social Fund
OPERATIONAL PROGRAMME
EDUCATION AND LIFELONG LEARNING
investing in knowledge society
MINISTRY OF EDUCATION & RELIGIOUS AFFAIRS
MANAGING AUTHORITY
NSRF 2007-2013
programme for development
EUROPEAN SOCIAL FUND
Co-financed by Greece and the European Union

E. Estimation of key aerosol optical properties using data from a CTM model.

E1. Introduction

Aerosols affect Earth's climate by altering its atmospheric radiative properties. Predicting the net effect of aerosols on climate is a complicated task, since aerosol concentrations and chemical composition exhibit high spatial and temporal variability. Furthermore, aerosol climate interactions are diverse, including both direct interactions of particles with radiation and indirect, through modifications on cloud size, albedo and lifetime. In this report, we will focus on the interaction of aerosols with light. Even this subset of the larger problem is a challenging task (Kehnert et al. 2014). Scattering and absorption of light by particles is controlled by their size, shape, chemical composition and mixing state (Pilinis and Pandis, 1995; Pilinis and Li, 1998; Bond and Bergstrom, 2006). Real world aerosols exhibit diverse mass size distributions, morphologies and chemical compositions, depending on their initial emission sources and the various interactions with the atmospheric gases and other particulate matter, that undergo during their lifetime in the atmosphere.

Chemical Transport Models (CTMs) are often used to simulate the aerosol dynamics and provide realistic predictions of the aerosol evolution and spatial distribution (Aan de Brugh et al. 2011; Fountoukis et al. 2011). Concentration predictions provided by CTMs can be used in order to calculate the aerosol optical properties (AOP). These optical properties include the aerosol scattering and absorption coefficients, the aerosol single scattering albedo (SSA) and the asymmetry parameter. The exact approach followed in order to calculate critical AOPs depends on the CTM characteristics and on the scope of the study. Since CTMs output a large amount of data, the needed AOPs estimations impose a substantial computational burden.

In this report we used the newly developed code, AtmOptC, that is capable of providing spectral AOPs predictions that are critical to simulations of aerosol forcing, and can be used to post process CTMs output. AtmOptC is capable of performing a vast amount

European Union
European Social Fund
OPERATIONAL PROGRAMME
EDUCATION AND LIFELONG LEARNING
investing in knowledge society
MINISTRY OF EDUCATION & RELIGIOUS AFFAIRS
MANAGING AUTHORITY
NSRF 2007-2013
programme for development
EUROPEAN SOCIAL FUND
Co-financed by Greece and the European Union

of Mie theory calculations, in order to provide both spatial and temporal high resolution estimates of aerosol optical properties. AtmOptc supports calculations of various BC mixing states. AtmOptC integrates Mie calculations of homogeneous and multilayered spheres at the core of the code and does not use pre-calculated AOP estimates. Therefore, AtmOptC can provide accurate estimates of AOPs accounting for variable size distributions and chemical compositions.

In section D2, we will provide a detailed description of the AtmOptC optical model, and the simulation scheme. In section 3, we present an overview of the delivered output. The final optical properties inventory over the European region covers the period from June 5 to July 31, 2012.

E2. Simulation

E2.1 The AtmOptC aerosol optical model

AtmOptC, is utilized to predict AOPs from CTM output data. AtmOptC input accepts chemical and size resolved PM mass concentrations. It uses a segmentational approach to the input mass size distributions. Size distributions are divided into an arbitrary number of discrete size bins. In this case AtmOptC can be set up to match the predefined size bins of PMCAMx-2008 CTM model. AtmOptC is designed to handle chemical concentrations of organics, BC, sulfate, nitrate, ammonium, chlorine, sodium, water, and crustal material. At the core of the AtmOptC code, the aerosol scattering (Q_{sc}), absorption (Q_{abs}) efficiencies and the asymmetry parameter (g) are calculated using Mie theory. Calculations are performed using the aerosol chemical and mass concentrations for each size bin of a specific cell at a specific layer of the PM data provided by the CTM. Additionally, AtmOptC provides spectral estimates of the scattering (b_{sc}), absorption (b_{abs}) coefficient and the asymmetry parameter (g) at an arbitrary number of discrete wavelengths. The final delivered inventory incorporates optical calculations at 13 wavelengths (λ = 0.2, 0.3, 0.44, 0.55, 0.65, 0.80, 1.0, 1.2, 1.5, 2.0, 2.5, 3.0 and 4.0 μm).

European Union
European Social Fund
OPERATIONAL PROGRAMME
EDUCATION AND LIFELONG LEARNING
investing in knowledge society
MINISTRY OF EDUCATION & RELIGIOUS AFFAIRS
MANAGING AUTHORITY
NSRF 2007-2013
EUROPEAN SOCIAL FUND
Co-financed by Greece and the European Union

Let $b_{opt}(\lambda)$ be the optical coefficient at a given wavelength (λ) of either the scattering (b_{sct}) or absorption (b_{abs}) coefficient and Q_{opt} the related optical efficiency of a single particle (Q_{sc} or Q_{abs}). Assuming an internal mixture of spheres and a total number of K size bins, the optical coefficient for all size bins (j = 1,.., K) is calculated according to:

$$b_{opt}(\lambda) = \sum_{j=1}^{K} b_{opt,j}(\lambda) = \sum_{j=1}^{K} \frac{\pi D_{m,j^2}}{4} N_j Q_{opt,j}(a_j(\lambda), m_j) \quad \text{E2.1.1}$$

$b_{opt,j}(\lambda)$ being the scattering or absorption coefficient of the monodisperse aerosol of the j-th size bin. N_j is the aerosol particles number concentration at each size bin and m_j is the effective complex refraction index (CRI) of the homogeneous sphere. $D_{m,j}$ is the mean diameter of each size bin. The size parameter, $a_j(\lambda)$, in eq. E2.1.1, describes the relative size of the particle to the incoming radiation wl:

$$a_j(\lambda) = \frac{\pi D_{m,j}}{\lambda} \quad \text{E2.1.2}$$

In the case of the core – shell particles, the m_j in eq. E2.1.1 and E2.1.2 can be substituted by the array of values $\{m_{core,j}, m_{cell,j}\}$ for the core and cell refractive indices. Additionally, $D_{m,j}$ in eq. 2.1.1 and 2.1.2 can be substituted by the array $\{D_{core,j}, D_{cell,j}\}$, restricted according to $D_{core,j} + D_{cell,j} = D_{m,j}$, for the core and cell diameters. To perform the necessary Mie calculations, AtmOptC incorporates the SCATTNLAY routine of Peña and Pal, (2009) at the core of the AtmOptC code, capable of providing the Q_{opt} and g quantities of both homogeneous and multilayered spheres.

The asymmetry of the total aerosol distribution is calculated as the weighted mean value of the asymmetries, g_j, of the size bin j spherical particles, with the $b_{sct,j}$ acting as weights (Andrews et al., 2008):

$$g(\lambda) = \sum_{j=1}^{K} b_{sct,j}(\lambda) g_j(\lambda) / \sum_{j=1}^{K} b_{sct,j}(\lambda) \quad \text{E2.1.3}$$

Let $c_{l,j}$ be the aerosol mass concentration of species l (l = 1,…,L) of the j-specific size bin with mean diameter $D_{m,j}$. Since the distribution of the mass concentration, $c_{l,j}$, of species l (l = 1,…,L) within the j size bin is unknown, we assume that all particles, within the specific size bin, have a diameter equal to $D_{m,j}$. For an internal mixture of aerosol particles, the number concentration N_j at size bin j, is estimated according to:

European Union
European Social Fund
OPERATIONAL PROGRAMME
EDUCATION AND LIFELONG LEARNING
investing in knowledge society
MINISTRY OF EDUCATION & RELIGIOUS AFFAIRS
MANAGING AUTHORITY
NSRF 2007-2013
EUROPEAN SOCIAL FUND
Co-financed by Greece and the European Union

$$N_j = \frac{6c_{tot,j}}{\pi p_{m,j} D_{m,j^3}} \qquad \text{E2.1.4}$$

$p_{m,j}$ being the mean density of the single particle, calculated from the densities, p_l, of each chemical component l and $c_{tot,j}$ being the total mass concentration of all chemicals, at size bin j.

For a total of L aerosol chemical species with known densities p_l, and wavelength dependent complex refractive indices $m_l(\lambda)$, the homogeneous sphere complex refractive index, is calculated using two different EMA methods. We either use the simple volume-weighted average of the refractive indices (Pilinis and Pandis, 1995), or the Maxwell-Garnett method (Schuster et al., 2005; Chylek et al., 2000). The former is used when calculating the CRI of a homogeneous sphere, consisting of a mixture of the various inorganics and secondary organic aerosol (SOA), while the latter is only utilized in the case of BC addition in the medium (Kahnert et al. 2012).

Table-EI summarizes the assumed spectral CRI for all the chemical components. The specific CRIs were chosen after reviewing the available literature, based on the data availability and field of application. BC is the most important light absorption component, having a high imaginary part of the CRI. Various values of CRI_{BC} are reported in literature (Bond et al., 2013). In the case of CRI_{BC} we choose to adopt the wavelength independent value of 1.95-0.79i, hypothesized by Bond and Bergstrom (2006), which has been shown to improve agreement with atmospheric absorption observations (Stier et al., 2007). Atmospheric organic carbon (OC) particulate matter originates from SOA formation and a mixture of primary sources, including both anthropogenic and wildfires. It is known that OC emitted by biomass burning, exhibits moderate absorption (Arola et al., 2011). Since the origin of the OC masses is not tracked by PMCAMx, we assume OC to be non-absorbing. An investigation of the brown carbon contribution to aerosol absorption is out of the scope of this report. According to Table – DI, crustal (CRST) material also exhibits some absorption.

European Union
European Social Fund
OPERATIONAL PROGRAMME
EDUCATION AND LIFELONG LEARNING
investing in knowledge society
MINISTRY OF EDUCATION & RELIGIOUS AFFAIRS
MANAGING AUTHORITY
NSRF 2007-2013
EUROPEAN SOCIAL FUND
Co-financed by Greece and the European Union

AtmOptC supports calculations of aerosol optical properties for an internal mixture of particles. For this case, AtmOptC models the BC, as either homogeneous spheres (HS) or core – shell (CS) spheres, consisting of a pure BC core. The final inventory includes results from these two BC mixing states

Table-EI. Assumed complex refractive indices per aerosol chemical component.

Chemical Component	Real RI at 550 nm	Imaginary RI at 550 nm	Comment/Reference
SO_4, NH_4	1.53	$1.0x10^{-7}$	Ammonium sulfate /GEISA-2011 and GACP[1]
NO_3	1.556	$1.1x10^{-9}$	Ammonium nitrate /GACP dataset
Cl and Na	1.5	$1.0x10^{-8}$	Sea salt/GACP dataset
OC	1.5	0.	Constant value independent of wl
BC	1.95	0.790	Soot / Bond and Bergstrom, 2006
CRST	1.53	$5.5\ x10^{-3}$	Minerals / OPAC, GEISA-2011 database
Water	1.33	$1.96\ x10^{-9}$	Seinfeld and Pandis, 1998

[1]GACP (Global Aerosol Climatology Project, NASA) datasets available from http://gacp.giss.nasa.gov/data_sets/.

.

E3. Inventory of Aerosol optical properties

In this section, we will review the calculated optical properties that form the final delivered datasets. A summary of the datasets included in the final inventory is provided in Table EII. The final inventory covers a period of 56 days and incorporates optical

European Union
European Social Fund
OPERATIONAL PROGRAMME
EDUCATION AND LIFELONG LEARNING
investing in knowledge society
MINISTRY OF EDUCATION & RELIGIOUS AFFAIRS
MANAGING AUTHORITY
NSRF 2007-2013
EUROPEAN SOCIAL FUND
Co-financed by Greece and the European Union

data from both HS and CS mixing sates. PMCAMx was set up to run at 14 vertical layers, reaching a maximum height of approx. 6000 m and with a horizontal resolution of 150×160 cells. The temporal resolution of the provided data is 1 hour. Figure E1 presents results of the AtmOptC code application for a single hour and day.

Table-EII. Summary of the final inventory (June 5 to July 31, 2012)

Dataset	Units	Dataset Dimensions	Notes
Scattering Coef. ($b_{sct,}$)	m^{-1}	150×162 cells, 14 layers, 13 wl, 24 hours, 56 days, 2 BC mixing sates (HS and CS)	Each file contains 14 layers and is specific to a day, hour, wl and BC mixing state
Absorption Coef. ($b_{abs,}$)	m^{-1}	150×162 cells, 14 layers, 13 wl, 24 hours, 56 days, 2 BC mixing sates (HS and CS)	Each file contains 14 layers and is specific to a day, hour, wl and BC mixing state
AOD	–	150×162 cells, 13 wl, 24 hours, 56 days, 2 BC mixing sates (HS and CS)	AOD accounting all layers. Each file is for a specific day, hour, wl and BC mixing state
Layer heights (h)	m	150×162 cells, 14 layers, 24 hours, 56 days	Thickness of each layer. Each file is for a specific day and hour
VSRM flag (fl_{VSRM})	–	150×162 cells, 14 layers, 24 hours, 56 days	fl_{VSRM} = 0 : VSRM code not active. fl_{VSRM} = 1 : VSRM code active. Each file is for a specific day and hour

European Union
European Social Fund
OPERATIONAL PROGRAMME
EDUCATION AND LIFELONG LEARNING
investing in knowledge society
MINISTRY OF EDUCATION & RELIGIOUS AFFAIRS
MANAGING AUTHORITY
NSRF 2007-2013
EUROPEAN SOCIAL FUND
Co-financed by Greece and the European Union

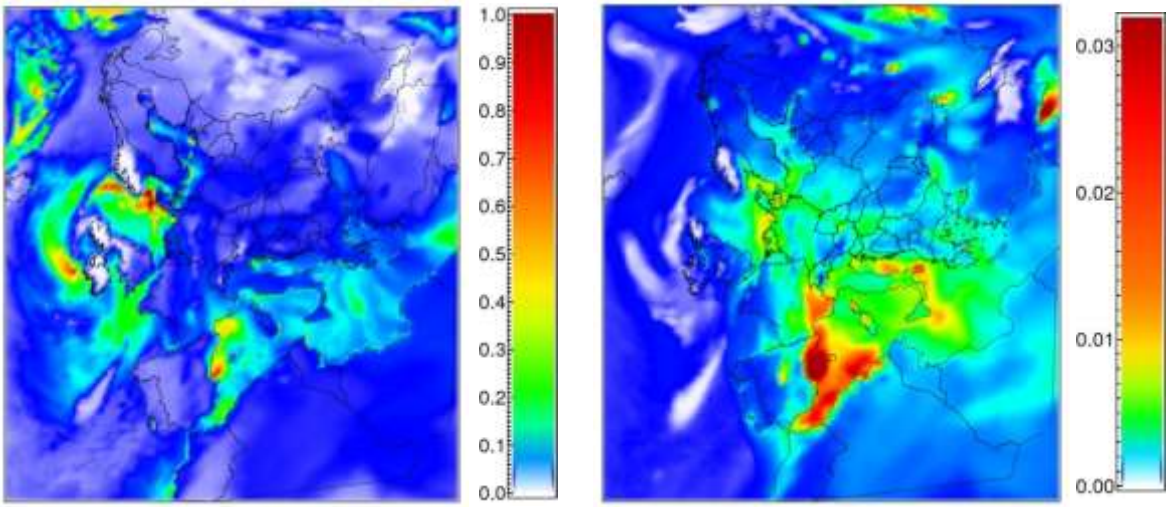

(a) **(b)**

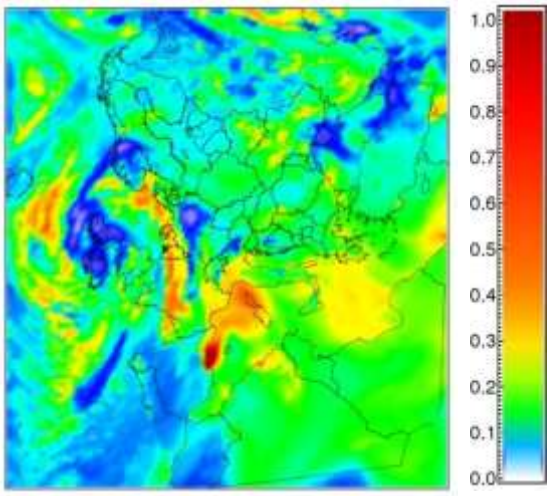

(c)

Fig. E1. Aerosol optical properties (550 nm) of homogeneous spheres, during June 21 at 12:00 for the assumed PMCAMx grid. (a) Scattering coefficient at ground layer ($\times 10^{-3}$ m^{-1}). (a) Absorption coefficient at ground layer ($\times 10^{-3}$ m^{-1}). (c) AOD**.**

European Union
European Social Fund
OPERATIONAL PROGRAMME
EDUCATION AND LIFELONG LEARNING
investing in knowledge society
MINISTRY OF EDUCATION & RELIGIOUS AFFAIRS
MANAGING AUTHORITY
NSRF 2007-2013
EUROPEAN SOCIAL FUND
Co-financed by Greece and the European Union

E. References

Aan de Brugh, J. M. J., Schaap, M., Vignati, E., Dentener, F., Kahnert, M., Sofiev, M., Huijnen, V., and Krol, M. C., (2011), "The European aerosol budget in 2006", Atmos. Chem. Phys., 11, 1117-1139, doi:10.5194/acp-11-1117-2011

Andrews, E., et al. (2006), "Comparison of methods for deriving aerosol asymmetry parameter", J. Geophys. Res., 111, D05S04, doi:10.1029/2004JD005734.

Arola, A., Schuster, G., Myhre, G., Kazadzis, S., Dey, S., and Tripathi, S. N., (2011) "Inferring absorbing organic carbon content from AERONET data", Atmos. Chem. Phys., 11, 215-225, doi:10.5194/acp-11-215-2011

Bond, T. C., et al. (2013), "Bounding the role of black carbon in the climate system: A scientific assessment", J. Geophys. Res. Atmos., 118, 5380–5552, doi:10.1002/jgrd.50171.

Bond T. C. and Bergstrom R.W., (2006), "Light absorption by carbonaceous particles: An investigative review," Aerosol Sci. Technol. 40, 27–67.

Chylek P., Videen G., Geldart D. J. W., Dobbie J. S., and Tso H. C. W., "Effective medium approximations forheterogeneous particles," in Light Scattering by Nonspherical Particles, M. I. Mishchenko, J. W. Hovenier, and L. D. Travis, eds. Academic Press, 2000, pp. 274–308.

Fountoukis, C., P.N. Racherla, H.D. van der Gon, P. Polymeneas, P. Haralabidis, C. Pilinis and S.N. Pandis, (2011), "Evaluation of a three-dimensional chemical transport model (PMCAMx) in the European domain during the EUCAARI May 2008 campaign", Atmos. Chem. Phys., vol. 11, p. 10331–10347, doi:10.5194/acp-11-10331-2011.

Kahnert,M. T. Nousiainen, H. Lindqvist, and M. Ebert, (2012) "Optical properties of light absorbing carbon aggregates mixed with sulfate: assessment of different model geometries for climate forcing calculations," Opt. Express 20, 10042–10058.

Kahnert M., Nousiainen T., Lindqvist H., (2014), "Review: Model particles in atmospheric optics", Journal of Quantitative Spectroscopy & Radiative Transfer (JQSRT) (0022-4073).

European Union
European Social Fund

OPERATIONAL PROGRAMME
EDUCATION AND LIFELONG LEARNING
investing in knowledge society
MINISTRY OF EDUCATION & RELIGIOUS AFFAIRS
MANAGING AUTHORITY

NSRF 2007-2013
programme for development
EUROPEAN SOCIAL FUND

Co-financed by Greece and the European Union

Peña O. and Pal U., (2009), “Scattering of electromagnetic radiation by a multilayered sphere”, Computer Phys. Com., 180, pp. 2348–2354, doi:10.1016/j.cpc.2009.07.010

Pilinis C. and Pandis S. N., (1995), “Physical, Chemical and Optical Properties of Atmospheric Aerosols”, The handbook of Environmental Chemistry, Airborn Particulate Matter, Springer, pp. 99 – 124

Pilinis C. and Li X., (1998), “Particle shape and internal inhomogeneity effects in the optical properties of tropospheric aerosols of relevance to climate forcing”, J. Geophys. Res., 103, pp. 3789–3800

Schuster, G. L., O. Dubovik, B. N. Holben, and E. E. Clothiaux, (2005),” Inferring black carbon content and specific absorption from Aerosol Robotic Network (AERONET) aerosol retrievals”, J. Geophys. Res., 110, D10S17, doi:10.1029/2004JD004548

Stier, P., Seinfeld, J. H., Kinne, S., and Boucher O., (2007), “Aerosol absorption and radiative forcing”, Atmos. Chem. Phys., 7, 5237-5261, doi:10.5194/acp-7-5237-2007

European Union
European Social Fund
OPERATIONAL PROGRAMME
EDUCATION AND LIFELONG LEARNING
investing in knowledge society
MINISTRY OF EDUCATION & RELIGIOUS AFFAIRS
MANAGING AUTHORITY
NSRF 2007-2013
programme for development
EUROPEAN SOCIAL FUND
Co-financed by Greece and the European Union

F. Aerosol radiative effects over Europe from the FORTH radiation transfer model with AtmOptC aerosol optical properties

This subsection presents the results of the second run of FORTH radiative model. We used the output of PMCAMx and AtmOptC (described above) as input to FORTH, in order to derive the radiation fluxes for June and July of 2012. The region of interest is Europe, the spatial resolution is 36 km x 36 km and the temporal resolution is hourly. The aerosol optical depth and therefore the aerosol direct radiative forcing, exhibit significant hourly and daily variability due to effects such as wildfires and synoptic conditions. Some indicative daily-averaged or hourly maps of AOD and DRE are presented below.

F1. Aerosol optical properties by AtmOptC As shown in Fig. F1, over the region of interest the aerosol optical depth (AOD) has values up to 0.30. The largest AOD values are observed over the coastal areas of eastern and northeastern Spain. In general, large values reaching or exceeding 0.20 are seen over the southern areas of the central Mediterranean basin, the industrialized areas of Balkans, the Po valley, the southern Iberian Peninsula, as well as southeastern Turkey, along the border with Syria. AOD reaching 0.15-0.17 is observed over Western Europe and Ukraine. We should note that cautions should be exercised for results over northern Africa, because PMCAMx does not employ desert dust emissions and therefore the AOD there is expected to be underestimated. The same holds for all other regions where dust transport is common at the time of study, e.g. over the western Mediterranean.

The single-scattering albedo (SSA) over our region ranges between 0.84 and 1 (Fig. F2). The largest SSA values (scattering aerosol) are seen primarily over the Atlantic Ocean (due to the presence of marine aerosols) and secondarily over extended parts of western and northern Europe. The smallest SSA (absorbing aerosol) are noted over the western Mediterranean, parts of eastern and southern Iberian Peninsula, southeastern Turkey, Italy, the Balkans, as well as over urban/industrial centers of Eastern Europe.

European Union
European Social Fund
OPERATIONAL PROGRAMME
EDUCATION AND LIFELONG LEARNING
investing in knowledge society
MINISTRY OF EDUCATION & RELIGIOUS AFFAIRS
MANAGING AUTHORITY
NSRF 2007-2013
programme for development
EUROPEAN SOCIAL FUND
Co-financed by Greece and the European Union

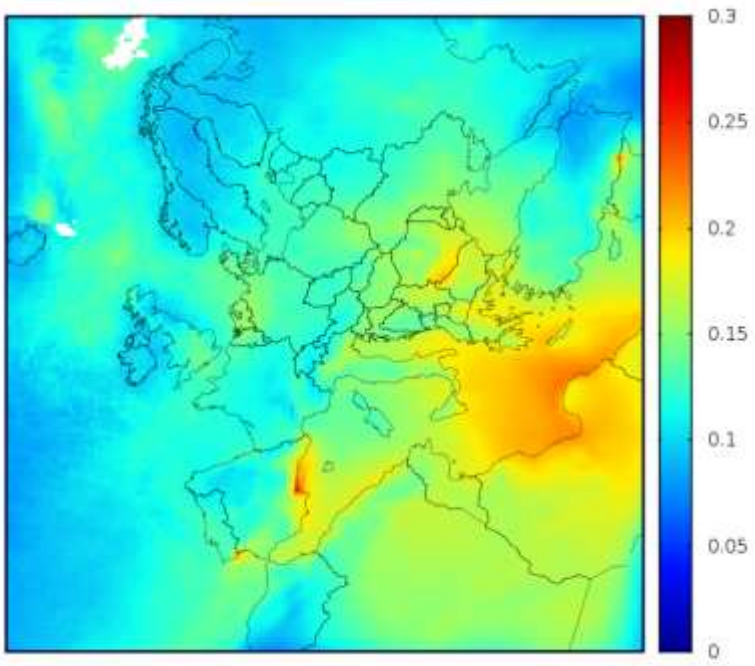

Fig. F1: Average optical depth daily values from AtmOptC between 5/6 and 30/7/2012

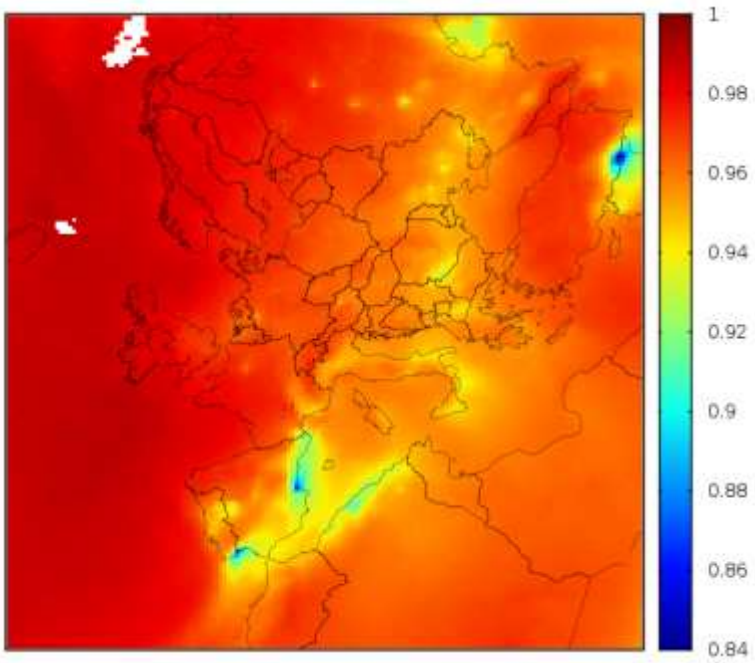

Fig. F2: Average aerosol single-scattering albedo daily values from AtmOptC between 5/6 and 30/7/2012

European Union
European Social Fund
OPERATIONAL PROGRAMME
EDUCATION AND LIFELONG LEARNING
investing in knowledge society
MINISTRY OF EDUCATION & RELIGIOUS AFFAIRS
MANAGING AUTHORITY
NSRF 2007-2013
EUROPEAN SOCIAL FUND
Co-financed by Greece and the European Union

The aforementioned results are produced by AtmOptC, when run in the homogeneous spheres mode, assuming internal mixing for the aerosol and expected to overestimate absorption. AtmOptC also produced data for the core-shell (non-homogeneous) scenario, which was expected to decrease the absorption coefficient. However, the difference between the core-shell and homogeneous spheres scenarios is very small (cf. Fig. F2 and Fig. F3), so we will report only the homogeneous spheres results in this report.

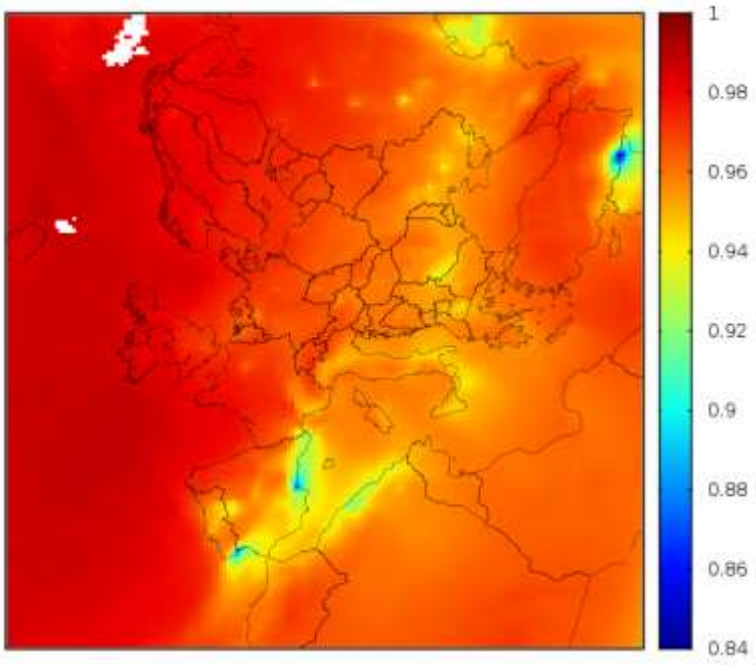

Fig. F3: Average aerosol single-scattering albedo daily values from AtmOptC between 5/6 and 30/7/2012, derived from the core-shell algorithm. In contrast, Fig. 2 show results from the homogeneous spheres algorithm

F2 Results from the FORTH radiation transfer model

F2.1 Average daily values

AOD from AtmOptC (presented in the previous paragraph) were used from FORTH. The hourly radiation fluxes output were average for the whole period of interest (June

European Union
European Social Fund
OPERATIONAL PROGRAMME
EDUCATION AND LIFELONG LEARNING
investing in knowledge society
MINISTRY OF EDUCATION & RELIGIOUS AFFAIRS
MANAGING AUTHORITY
NSRF 2007-2013
EUROPEAN SOCIAL FUND
Co-financed by Greece and the European Union

and July 2012) and presented in the following figures. Areas with missing data or unsatisfactory temporal coverage are shown with white in all maps. In Fig. F4 we show the average of daily values of direct radiative effect (DRE) at the surface DRE_{surf}. The surface cooling is stronger over areas with larger aerosol load, like the central and west Mediterranean basin, the Balkans and the western Black Sea. The largest DRE values are observed over the eastern coast of Spain (local values down to -50 Wm^{-2}). Also, DRE_{surf} takes large (absolute) values over regions of continental Europe with a predominance of absorbing aerosol.

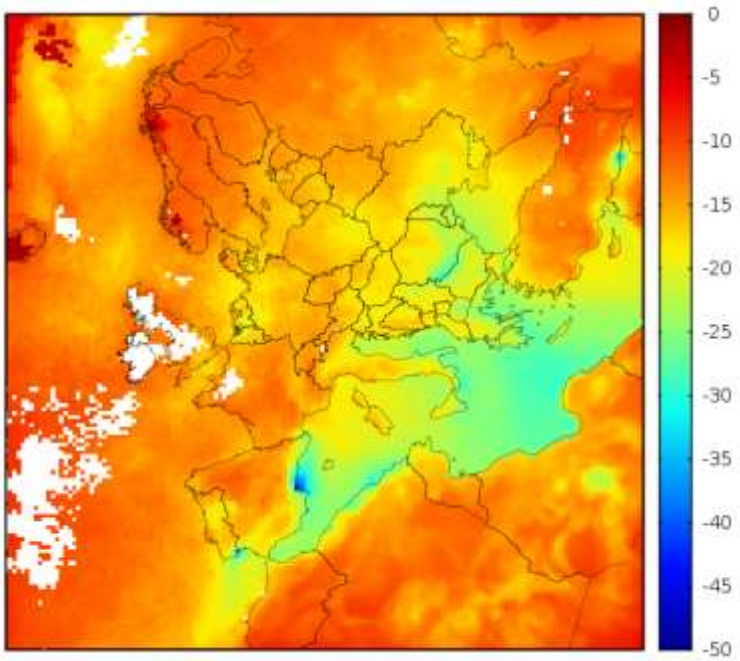

Fig. F4: Average daily values of the DRE at the surface. Output of FORTH in Wm^{-2} between 5/6 and 30/7/2012

Fig. F5 shows a map with the long-term average of DRE daily values inside the atmospheric column (DRE_{atm}). The results are the sum of the local DRE over the model's 28 vertical layers. We generally observe that the strongest DRE on the atmospheric absorption is located over the same regions as the surface cooling. Consequently, the largest DRE_{atm} values (locally up to 35 Wm^{-2}) are found over areas with large aerosol load, especially one of absorbing aerosol. In contrast, over ocean

European Union
European Social Fund
OPERATIONAL PROGRAMME
EDUCATION AND LIFELONG LEARNING
investing in knowledge society
MINISTRY OF EDUCATION & RELIGIOUS AFFAIRS
MANAGING AUTHORITY
NSRF 2007-2013
programme for development
EUROPEAN SOCIAL FUND
Co-financed by Greece and the European Union

areas or areas with weak absorption (e.g. Scandinavia) with small loads of primarily scattering aerosol, DRE_{atm} takes small values (< 5 Wm^{-2}).

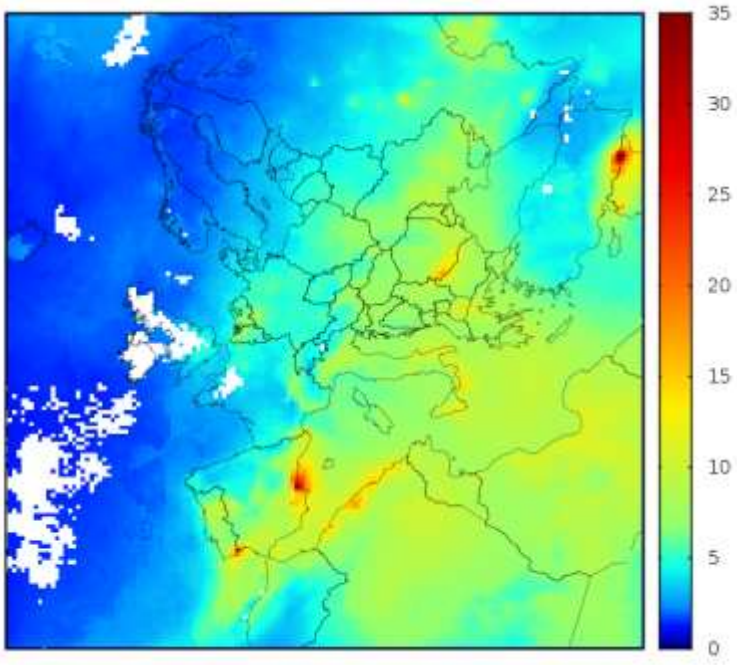

Fig. F5: Average daily values of the DRE inside the atmospheric column. Output of FORTH in Wm^{-2} between 5/6 and 30/7/2012

At the top of the atmosphere (TOA) during June and July 2012, aerosols cause cooling almost over the whole examined area, i.e. they increase the planetary albedo. Exceptions are seen at snow- or ice-covered areas in Scandinavia, as well as over areas of Iceland and Greenland (weak warming <5 Wm^{-2}). This behavior highlights the significance of multiple scattering between the ground and the aerosol layers. The observed planetary cooling is a result of the larger negative surface DRE than the positive atmospheric DRE (Fig. F6). The largest cooling occurs over regions with small albedo coinciding with large load of scattering particles. More specifically the aerosol cooling over the Mediterranean (especially the central part) reaches -25 Wm^{-2}, while over the North and the Norwegian Seas DRE_{TOA} can take values as low as -15 and -20 Wm^{-2}. Over the continent the DRE_{TOA} is clearly less pronounced and ranges between -7 and -12 Wm^{-2}. Over the Iberian Peninsula and southeastern Turkey, DRE_{TOA} is even

European Union
European Social Fund
OPERATIONAL PROGRAMME
EDUCATION AND LIFELONG LEARNING
investing in knowledge society
MINISTRY OF EDUCATION & RELIGIOUS AFFAIRS
MANAGING AUTHORITY
NSRF 2007-2013
EUROPEAN SOCIAL FUND
Co-financed by Greece and the European Union

weaker, due to absorbing aerosol warming the atmosphere and almost negating the surface cooling.

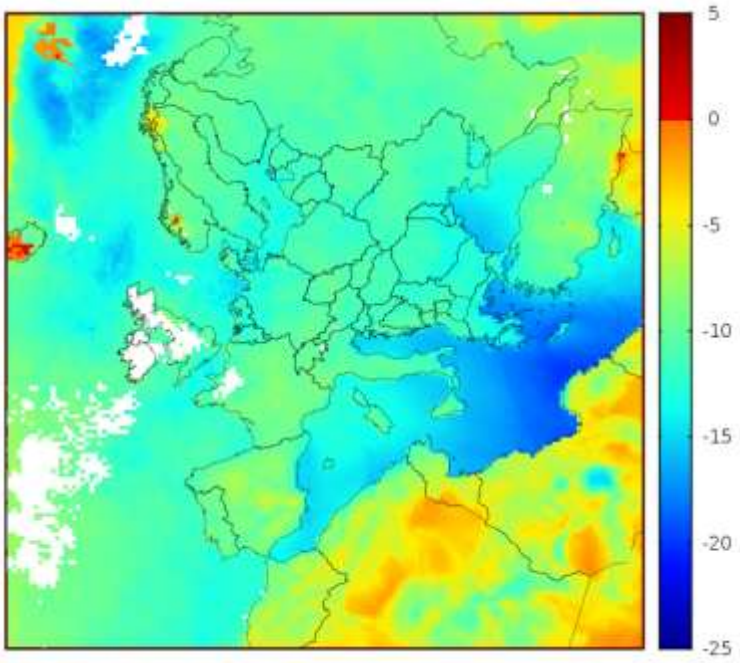

Fig. F6: Average daily values of the DRE at the top of the atmosphere. Output of FORTH in Wm^{-2} between 5/6 and 30/7/2012.

F2.2 Diurnal variability of the direct radiative aerosol effect

The hourly DRE values from the FORTH model were averaged and their 24h variability was calculated for the examined time period. Indicative results for DRE_{surf}, DRE_{atm} and DRE_{TOA}, for hours 4, 8, 12, 16, 20 και 24 UTC are presented in Figs. F7-F9. The direct radiative effect is expectedly stronger during hours with a large solar height, reflecting the primary role of incoming radiation at the top of the atmosphere. During morning and afternoon hours and especially near dawn and dusk DREs are small. However if they are expressed as percentages of the incoming solar radiation at TOA, they become larger than the noon values. The averaged diurnal variability of the AOD is generally small (not shown) and therefore its role in our results is limited.

European Union
European Social Fund
OPERATIONAL PROGRAMME
EDUCATION AND LIFELONG LEARNING
investing in knowledge society
MINISTRY OF EDUCATION & RELIGIOUS AFFAIRS
MANAGING AUTHORITY
NSRF 2007-2013
EUROPEAN SOCIAL FUND
Co-financed by Greece and the European Union

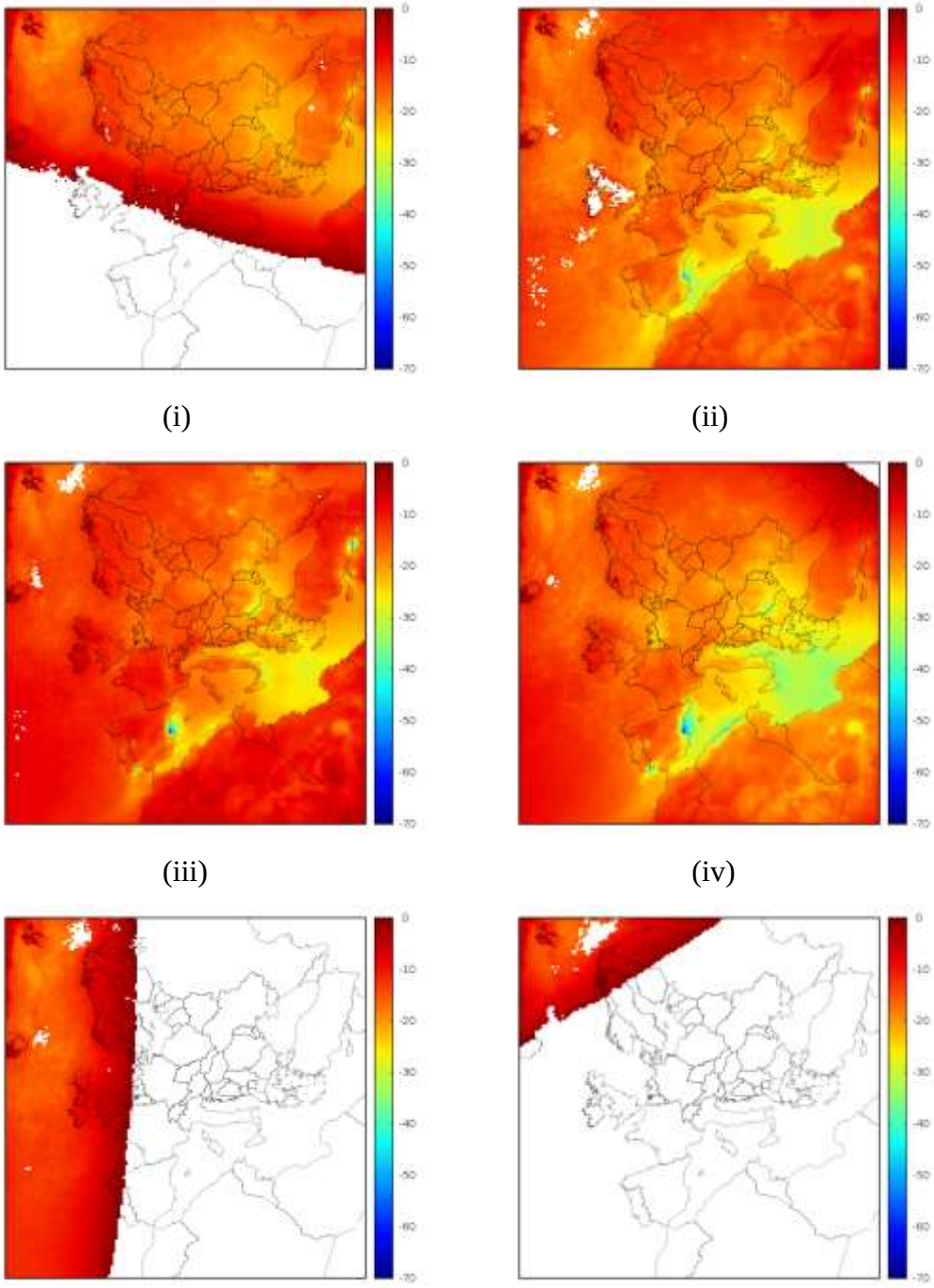

Fig. F7: Average hourly DRE at the surface (in W/m^2) for the period between 5/6 and 30/7 2012. The results shown correspond to (i) 4 UTC, (ii) 8 UTC, (iii) 12 UTC, (iv) 16 UTC, (v) 20 UTC and (vi) 24 UTC.

European Union
European Social Fund
OPERATIONAL PROGRAMME
EDUCATION AND LIFELONG LEARNING
investing in knowledge society
MINISTRY OF EDUCATION & RELIGIOUS AFFAIRS
MANAGING AUTHORITY
NSRF 2007-2013
EUROPEAN SOCIAL FUND
Co-financed by Greece and the European Union

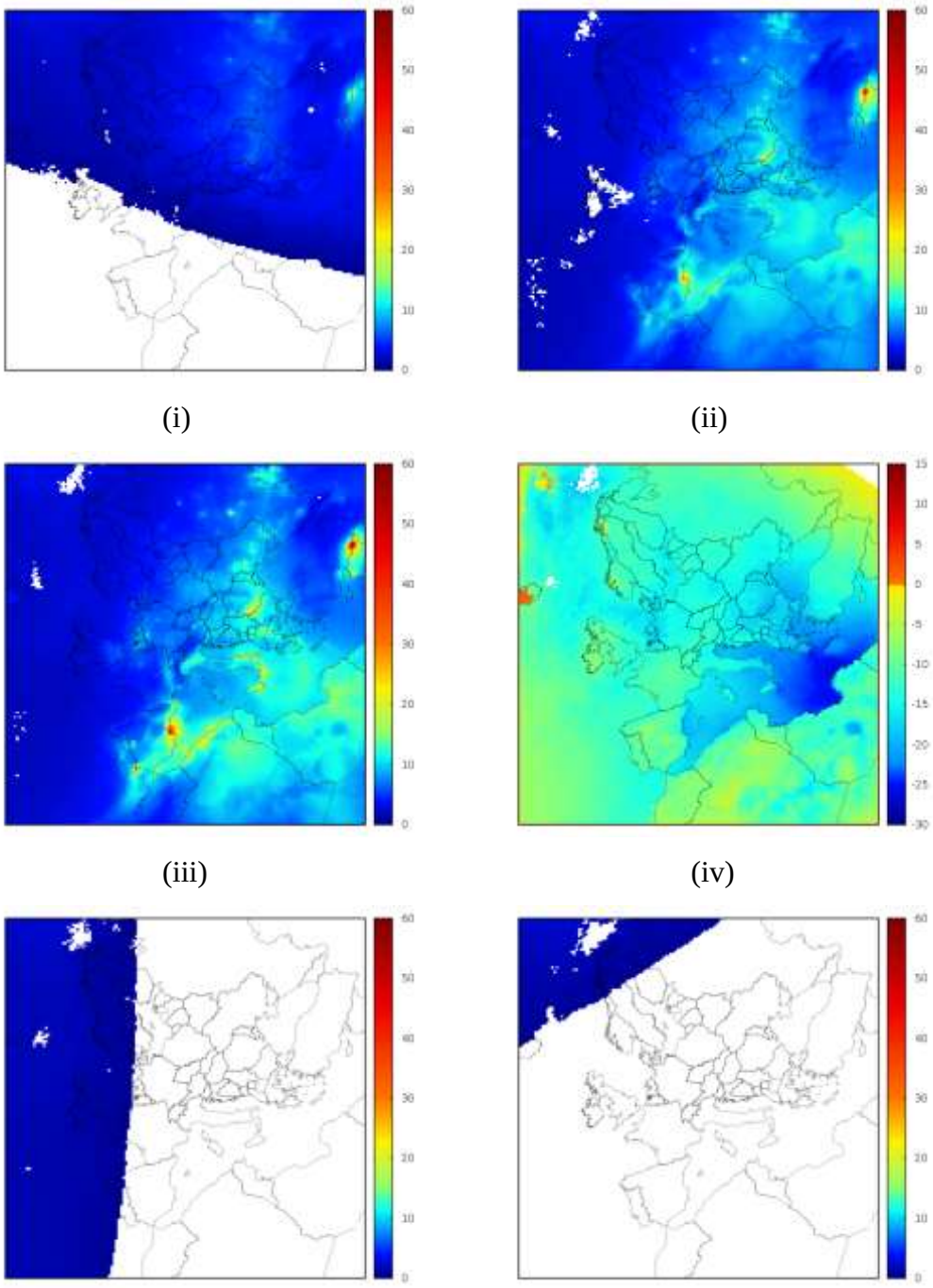

Fig. F8: Average hourly DRE in the atmospheric column (in W/m^2) for the period between 5/6 and 30/7 2012. The results shown correspond to (i) 4 UTC, (ii) 8 UTC, (iii) 12 UTC, (iv) 16 UTC, (v) 20 UTC and (vi) 24 UTC.

European Union
European Social Fund
OPERATIONAL PROGRAMME
EDUCATION AND LIFELONG LEARNING
investing in knowledge society
MINISTRY OF EDUCATION & RELIGIOUS AFFAIRS
MANAGING AUTHORITY
NSRF 2007-2013
programme for development
EUROPEAN SOCIAL FUND
Co-financed by Greece and the European Union

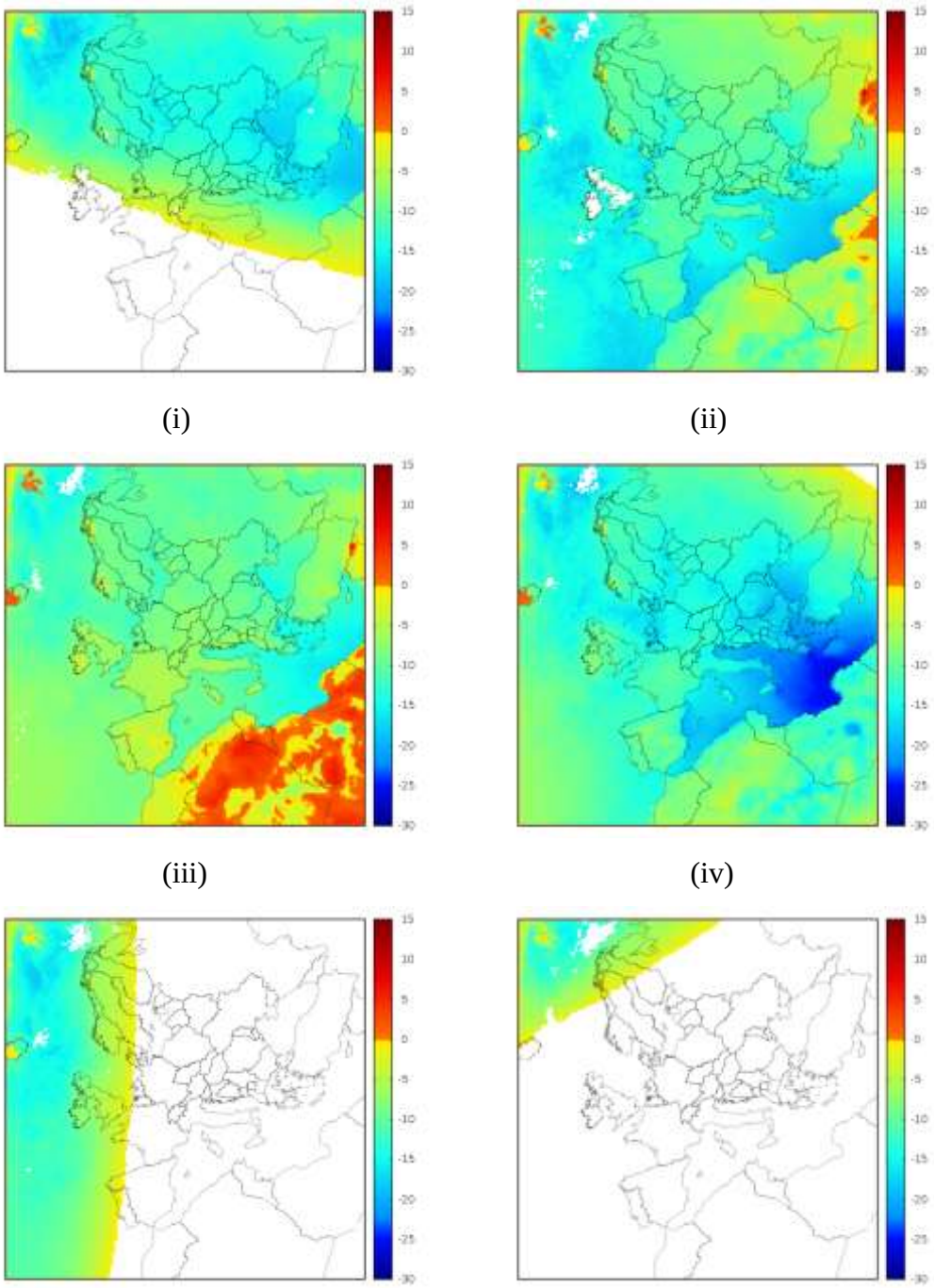

(i) (ii)

(iii) (iv)

(v) (vi)

Fig. F9: Average hourly DRE at the TOA (in W/m^2) for the period between 5/6 and 30/7 2012. The results shown correspond to (i) 4 UTC, (ii) 8 UTC, (iii) 12 UTC, (iv) 16 UTC, (v) 20 UTC and (vi) 24 UTC.

European Union
European Social Fund
OPERATIONAL PROGRAMME
EDUCATION AND LIFELONG LEARNING
investing in knowledge society
MINISTRY OF EDUCATION & RELIGIOUS AFFAIRS
MANAGING AUTHORITY
NSRF 2007-2013
programme for development
EUROPEAN SOCIAL FUND
Co-financed by Greece and the European Union

CONTRACT OBLIGATIONS-DELIVERABLES

According to the agreement with the Greek government, the success of the program is partially measured by the following criteria (δείκτες):

1. Number of researchers participating in this program = 20
2. Number of researchers from abroad =1
3. Number of publications/ presentations = 10
4. Number of Ph.D. dissertations = 2

We have satisfied all of the above. Specifically:

1. *Number of researchers participating in this program*

In this program participated the following Professors/Researchers:

- C. Pilinis (University of the Aegean)
- O. Kalantzi (University of the Aegean)
- C. Matsoukas (University of the Aegean)
- G. Biskos (University of the Aegean)
- S. Pandis (FORTH/ICE-HT -University of Patras)
- S. Andronopoulos (N.C.S.R. "Demokritos")
- K. Eleftheriadis (N.C.S.R. "Demokritos")
- E. Gerasopoulos (NOA)
- N. Mihalopoulos (NOA-University of Crete)
- P. Papagiannakopoulos (University of Crete)
- E. Stephanou (University of Crete)
- I. Vardavas (University of Crete)
- N. Hatzianastassiou (University of Ioannina)

In addition, two Postdocs contributed substantially to the program. Their names are

- A. Gkikas (University of Ioannina)
- P. Charalampidis (University of the Aegean)

Finally, a number of graduate (both Ph. D. and MS) students actively participated in this project. Specifically:

- M. B. Korras-Carraca (University of the Aegean)
- S. Bezantakos (University of the Aegean)
- M. Tsiflikiotou (University of Patras)
- K. Florou (University of Patras)
- M. Psichoudaki (University of Patras)
- J. Stavroulas (University of Crete)
- L. Fourtziou (University of Crete)

2. *Number of researchers from abroad*

- A. Nenes (Georgia Tech. USA)

European Union
European Social Fund
OPERATIONAL PROGRAMME
EDUCATION AND LIFELONG LEARNING
investing in knowledge society
MINISTRY OF EDUCATION & RELIGIOUS AFFAIRS
MANAGING AUTHORITY
NSRF 2007-2013
programme for development
EUROPEAN SOCIAL FUND
Co-financed by Greece and the European Union

3. *Number of publications/ presentations*

This program is highly successful in terms of publications. Three articles have been prepared and published in important scientific journals:

- V. Pappas, N. Hatzianastassiou, C. Papadimas, C. Matsoukas, S. Kinne, and I. Vardavas, "Evaluation of spatio-temporal variability of Hamburg Aerosol Climatology against aerosol datasets from MODIS and CALIOP", *Atmos. Chem. Phys.*, 13, 8381–8399, 2013, doi:10.5194/acp-13-8381-2013.
- A. Gkikas, E. E. Houssos, C. J. Lolis, A. Bartzokas, N. Mihalopoulos and N. Hatzianastassiou, "Atmospheric circulation evolution related to desert-dust episodes over the Mediterranean", Q.J.R. Meteorol. Soc. (2014) DOI:10.1002/qj.2466
- M. B. Korras-Carraca, N. Hatzianastassiou, C. Matsoukas, A. Gkikas, and C. D. Papadimas, "The regime of aerosol asymmetry parameter over Europe, Mediterranean and Middle East based on MODIS satellite data: evaluation against surface AERONET measurements", *Atmos. Chem. Phys.* (in print)

In addition, a number of articles have been prepared and presented in major conferences:

- Kalli K. Florou, Michael Pikridas, and Spyros N. Pandis, "Wintertime Air Pollution and the Greek Financial Crisis", EGU, Vienna, Austria, April 2013.
- Evangelia Kostenidou, Christos Kaltsonoudis, and Spyros Pandis "Chemical characterization of ambient submicron aerosol during summer 2 012 in Patras, Greece", EGU, Vienna, Austria, April 2013.
- Christos Kaltsonoudis, Kalliopi Florou, Evangelia Kostenidou, and Spyros Pandis "Temporal Variability of VOCs and Organic Particulate Matter in the Eastern Mediterranean", EGU, Vienna, Austria, April 2013.
- E. Diapouli, V. Vasilatou, S. Vratolis , M. Gini , D. Saraga, Th. Maggos , K. Eleftheriadis, "Effect of the extensive use of fireplaces on carbonaceous particle concentration levels in Athens, Greece", European Aerosol Conference, Prague, Czech Republic, September 2013.
- Charalampidis P. E., Pilinis C., Fountoukis C., Panagiotopoulou A. and S. N. Pandis, "Predictions of aerosol extinction coefficients over Greece by means of a new modular software system", EAC 2013, Prague Czech Republic, September, 2013.
- S. Bezantakos, E. Konstenidou, A. Bougiatioti, K. Eleftheriadis, N. Mihalopoulos, A. Nenes, S. Pandis, G. Biskos, "Chemical Composition and Hygroscopic Properties of Ultrafine Aerosol Particles in the Atmosphere over an Urban Background Site in Patras, Greece", European Aerosol Conference, Granada, Spain, September 2012.
- D. Siakavaras, C. Samara, A. Kelessis, G. Biskos "Characteristics of Local and Regional Nucleation Events at an Urban Background Site during Summer Period in Thessaloniki, Greece", EAC 2013, Prague Czech Republic, September, 2013.

- S. Bezantakos, E. Kostenidou, K. Florou, A. Bougiatioti, K. Elefteriadis, N. Mihalopoulos, A. Nenes, S. Pandis, G. Biskos, “Hygroscopic Properties and Mixing state of Ultrafine Aerosol Particles over two Urban Background Sites”, EAC 2013, Prague Czech Republic, September, 2013.
- S. Bezantakos, A. Bougiatioti, I. Stavroulas, K. Eleftheriadis, N. Mihalopoulos, A. Nenes, G. Biskos, “Hygroscopic Properties and Mixing State of Ultrafine Aerosol Particles over the Eastern Mediterranean Background Site of Finokalia”, EAC 2013, Prague Czech Republic, September, 2013.
- S. Vratolis, M. Gini, D. Siakavaras, S. Bezantakos, I. Stavroulas, N. Kalivitis, E. Kostenidou, E. Louvaris, G. Biskos, N. Mihalopoulos, S. Pandis, C. Pilinis, K. Eleftheriadis, “Particle Number Size Distribution Statistics at Urban and Suburban Background and Remote Sites in Greece during Summer”, EAC 2013, Prague Czech Republic, September, 2013.
- M. Korras-Carraca, V. Pappas, C. Matsoukas, N. Hatzianastassiou and I. Vardavas, “Aerosol effect on atmospheric heating rates on global scale using vertically resolved satellite aerosol data”, RMetS Student Conference 2013, Reading, UK, September, 2013.
- Vasileios Pappas, Nikos Hatzianastassiou, Christos Matsoukas, and Ilias Vardavas, “Aerosol effect on atmospheric heating rates in the Mediterranean region using vertically resolved satellite aerosol data”, EGU, Vienna, Austria, April 2013.
- Antonis Gkikas, Nikos Hatzianastassiou, Nikos Mihalopoulos, Vasilis Katsoulis, Stelios Kazadzis, Jorge Pey, Xavier Querol, and Omar Torres “A satellite based algorithm for identifying dust episodes: the regime of episodes in the Mediterranean basin and evaluation against surface measurements”, EGU, Vienna, Austria, April 2013.
- Liakakou E., Stavroulas J., Roukounakis N., Psiloglou V., Fourtziou L., Paraskevopoulou D., Sciare J., Gerasopoulos E., Mihalopoulos N. “Black carbon measurements during winter 2013-2014 in Athens and intercomparison between different techniques”, EGU2014, Vienna, Austria.
- Gerasopoulos, E., E. Liakakou, V. Psiloglou, J. Stavroulas, L., Fourtziou, N. Roukounakis, M. Lianou, N, Kappos, P. Zarmpas, H. Kambezidis, J. Sciare, N. Mihalopoulos, “Smog events over Athens during winter 2013-2014: Pollution measurements and chemical characterization”, EGU2014, Vienna, Austria.
- Gkikas A., N. Hatzianastassiou and N. Mihalopoulos “Characterization of intense aerosol episodes in the Mediterranean basin from satellite observations”, EGU2014, Vienna, Austria.
- Korras-Carraca M. B., V. Pappas, C. Matsoukas, N. Hatzianastassiou and I. Vardavas, “Global profiles of the direct aerosol effect using vertically resolved aerosol data”, EGU2014, Vienna, Austria.
- Pappas V., Hatzianastassiou N., Matsoukas C., Vardavas I. “Sensitivity of the atmospheric heating/cooling rate profile to the vertical distribution of aerosols”, COMECAP 2014, Heraklion, Greece.

European Union
European Social Fund
OPERATIONAL PROGRAMME
EDUCATION AND LIFELONG LEARNING
investing in knowledge society
MINISTRY OF EDUCATION & RELIGIOUS AFFAIRS
MANAGING AUTHORITY
NSRF 2007-2013
programme for development
EUROPEAN SOCIAL FUND
Co-financed by Greece and the European Union

- Korras-Carraca M. B., Pappas V., Matsoukas C., Hatzianastassiou N., Vardavas I. "Aerosol effect on atmospheric heating rate profiles using vertically resolved satellite aerosol data", COMECAP 2014, Heraklion, Greece.

3. *Number of Ph.D. dissertations*

- M. Psichoudaki, *"Atmospheric Organic Aerosol-Water Interractions"*, Department of Chemical Engineering, University of Patras, April 2014.
- S. Bezantakos, *"Physicochemical Properties of Atmospheric Aerosol Particles over Suburban and Remote Locations and Development of Techniques for the Improvement of their Determination Methods"*, Department of Environment, University of the Aegean, (accepted by the committee, exam date pending).
- M. B. Korras-Carraca, *"Aerosol effect on the radiative energy budget from in situ and satellite measurements"*, Department of Environment, University of the Aegean, (accepted by the committee, exam date pending).

As a result of this project, a number of significant databases has been produced. These databases are available to the scientific community upon request. Tables 1 and 2 depict the complete set of instruments used during the measurement campaigns and the scientist responsible for the corresponding databases. These campaigns, as well as, the resulting databases correspond to Activities 3-5. Similarly, Table 3 depicts the available modeling databases and the corresponding scientist for them. These databases are the result of Activity 6.

Finally, there is an Activity 7, which is, basically, the evaluation of the performance of this project. This activity will start upon the completion of all other activities, including this final report.

European Union
European Social Fund
OPERATIONAL PROGRAMME
EDUCATION AND LIFELONG LEARNING
investing in knowledge society
MINISTRY OF EDUCATION & RELIGIOUS AFFAIRS
MANAGING AUTHORITY
NSRF 2007-2013
EUROPEAN SOCIAL FUND
Co-financed by Greece and the European Union

Table 2: Instruments Engaged for the Summer 2012 Field Campaign

ATHENS SUMMER 2012				
Instrument	**Group**	**Dates**	**Notes**	**Person Responsible for Data (Name – email)**
PM10 & PM2.5 Sampler	Demokritos	Continuously	One 24-h gravimetric PM10 measurements. One 24-h filter for inorganics.	K. Eleftheriadis elefther@ipta.demokritos.gr
Nephelometer	Demokritos	Continuously	ECOTECH 3 wavelength, PM10, dry.	K. Eleftheriadis elefther@ipta.demokritos.gr
SMPS	Demokritos	Continuously	7-400 nm (TSI)	K. Eleftheriadis elefther@ipta.demokritos.gr
OPC	Demokritos	Continuously	0.25-2.5 μm (Grimm)	K. Eleftheriadis elefther@ipta.demokritos.gr
EC/OC	Demokritos	Continuously	No quartz filter sampling needed for EC/OC	K. Eleftheriadis elefther@ipta.demokritos.gr
Aethalometer	Demokritos	Continuously		K. Eleftheriadis elefther@ipta.demokritos.gr
PTRMS	Patras	2/7-22/7		Spyros Pandis spyros@chemeng.upatras.gr
HR-AMS	Patras	2/7-22/7		Spyros Pandis spyros@chemeng.upatras.gr
HTDMA-CCNC	Demokritos/GIT	2/7-22/7		George Biskos biskos@aegean.gr
O3 Analyzer	PERPA	Continuously		PERPA
NOx Analyzer	PERPA	Continuously		PERPA
SO2 Analyzer	PERPA	Continuously		PERPA
ADDED BY NOA FOR PENTELI STATION				
Optical scattering	NOA	1/6/ - 3/10 2012, available also before and after	Radiance Research Integrated Nephelometer M903 (Συντελεστής σκέδασης στα 530 nm)	Gerasopoulos Evangelos egera@noa.gr
PM2.5, PM2.5-10	NOA	1/6/ - 30/9 2012	Dichotomous Partisol+ 2025 Sequential Air Sampler (16.7 lpm)	Gerasopoulos Evangelos egera@noa.gr
Ozone	NOA	1/6/ - 30/9 2012	THERMO (hourly avg from 5min measurements)	Gerasopoulos Evangelos egera@noa.gr

European Union
European Social Fund
OPERATIONAL PROGRAMME
EDUCATION AND LIFELONG LEARNING
investing in knowledge society
MINISTRY OF EDUCATION & RELIGIOUS AFFAIRS
MANAGING AUTHORITY
NSRF 2007-2013
EUROPEAN SOCIAL FUND
Co-financed by Greece and the European Union

Thessaloniki (Eptapyrgio)				
Instrument	**Group**	**Dates**	**Notes**	**Person Responsible for Data (Name – email)**
Nephelometer	Aegean	Continuously		George Biskos biskos@aegean.gr
SMPS	Aegean	9/6 - 22/7		George Biskos biskos@aegean.gr
O3 Analyzer	Municipality Thess.	Permanent		Municipality Thess.
NOx Analyzer	Municipality Thess.	Permanent		Municipality Thess.
SO2 Analyzer	Municipality Thess.	Permanent		Municipality Thess.
PATRAS (IEXMH)				
Instrument	**Group**	**Dates**	**Notes**	**Person Responsible for Data (Name – email)**
PM2.5 Sampler	Patras	8/6-22/7	Daily average composition of PM2.5	Spyros Pandis spyros@chemeng.upatras.gr
MAAP	Patras	Continuously		Spyros Pandis spyros@chemeng.upatras.gr
SMPS	Patras	Continuously		Spyros Pandis spyros@chemeng.upatras.gr
OPC	Patras	Continuously		Spyros Pandis spyros@chemeng.upatras.gr
PTRMS	Patras	8/6-29/6		Spyros Pandis spyros@chemeng.upatras.gr
HR-AMS	Patras	8/6-29/6		Spyros Pandis spyros@chemeng.upatras.gr
HTDMA-CCNC	Demokritos/GIT	8/6-29/6		George Biskos biskos@aegean.gr
O_3 Analyzer	Patras	Continuously		Spyros Pandis spyros@chemeng.upatras.gr
NOx Analyzer	Patras	Continuously		Spyros Pandis spyros@chemeng.upatras.gr
SO_2 Analyzer	Patras	Continuously		Spyros Pandis spyros@chemeng.upatras.gr
NH_3 Analyzer	Patras	Continuously		Spyros Pandis spyros@chemeng.upatras.gr

European Union
European Social Fund
OPERATIONAL PROGRAMME
EDUCATION AND LIFELONG LEARNING
investing in knowledge society
MINISTRY OF EDUCATION & RELIGIOUS AFFAIRS
MANAGING AUTHORITY
NSRF 2007-2013
programme for development
EUROPEAN SOCIAL FUND
Co-financed by Greece and the European Union

PATRAS (STATION AT CENTER)				
Instrument	**Group**	**Dates**	**Notes**	**Person Responsible for Data (Name – email)**
PM2.5 Sampler	Patras	8/6-22/7	Daily average composition of PM2.5	Spyros Pandis spyros@chemeng.upatras.gr
SMPS	Aegean	8/6-22/7		Spyros Pandis spyros@chemeng.upatras.gr
Nephelometer	Patras	8/6-22/7		Spyros Pandis spyros@chemeng.upatras.gr
FINOKALIA				
Instrument	**Group**	**Dates**	**Notes**	**Person Responsible for Data (Name – email)**
PM1 & PM10 Sampler	Crete	Continuously	PM1: Quartz filter, 24-h (or 12-h) sampling, from 8/6 – 17/7. After 17/7, 48-hr sampling, i.e., one per week.	Mihalopoulos Nikos mihalo@uoc.gr
			PM10: Quartz filter, 24-hr sampling.	Mihalopoulos Nikos mihalo@uoc.gr
PILS (PM1,	Crete	Continuously 8/6 – 17/7,	One measurement every 20 min.	Mihalopoulos Nikos mihalo@uoc.gr
anions sampling)		After 17/7,		Mihalopoulos Nikos mihalo@uoc.gr
		10 days per month		Mihalopoulos Nikos mihalo@uoc.gr
Nephelometer	Crete	Continuously		Mihalopoulos Nikos mihalo@uoc.gr
SMPS	Crete	Continuously		Mihalopoulos Nikos mihalo@uoc.gr
OPC	Aegean	8/6-1/10	0.75-25 μm (Grimm)	Mihalopoulos Nikos mihalo@uoc.gr
mini AMS	FORTH	Continuously		Mihalopoulos Nikos mihalo@uoc.gr
HTDMA-CCNC	Demokritos/GIT	22/7- 1/10		George Biskos biskos@aegean.gr
Aethalometer	Crete	Continuously		Mihalopoulos Nikos mihalo@uoc.gr
O3 Analyzer	Crete	Continuously		Mihalopoulos Nikos mihalo@uoc.gr
NOx Analyzer	Crete	Continuously		Mihalopoulos Nikos mihalo@uoc.gr

European Union
European Social Fund
OPERATIONAL PROGRAMME
EDUCATION AND LIFELONG LEARNING
investing in knowledge society
MINISTRY OF EDUCATION & RELIGIOUS AFFAIRS
MANAGING AUTHORITY
NSRF 2007-2013
programme for development
EUROPEAN SOCIAL FUND
Co-financed by Greece and the European Union

NEO, Messinia				
Instrument	**Group**	**Dates**	**Notes**	**Person Responsible for Data (Name – email)**
Sampler (PM10)	NOA	8/6-22/8	1 every 24 hours (quartz)	Gerasopoulos Evangelos egera@noa.gr
DMPS	Stockholm Uni.	Continuously	dry, PM10	Gerasopoulos Evangelos egera@noa.gr
Soot Photometer	Stockholm Uni.	Continuously	1w, PM10	Gerasopoulos Evangelos egera@noa.gr
O3 Analyzer	NOA/Crete	Continuously		Gerasopoulos Evangelos egera@noa.gr

European Union
European Social Fund
OPERATIONAL PROGRAMME
EDUCATION AND LIFELONG LEARNING
investing in knowledge society
MINISTRY OF EDUCATION & RELIGIOUS AFFAIRS
MANAGING AUTHORITY
NSRF 2007-2013
EUROPEAN SOCIAL FUND
Co-financed by Greece and the European Union

Table 2: Instruments Engaged for the Winter 2013 Field Campaign

1. Athens (Demokritos)

Instrument	Operating Group	Dates	Notes	Person Responsible for Data (Name – email)
PMcourse & PM2.5 Sampler	Demokritos	Continuously	Two every 24 hours for each sampler. Gravimetric PM10 & PM2.5 measurements. Times: 8:00 and 18:00, to be in parallel with Pendeli and Crete. (PTFE)	K. Eleftheriadis elefther@ipta.demokritos.gr
PM10	Demokritos		4 every 24 hours (quartz) Times: 6:00, 12:00, 18:00, 24:00 (sequential sampler)	K. Eleftheriadis elefther@ipta.demokritos.gr
Nephelometer	Demokritos	Continuously	ECOTECH 3 wavelength, PM10, dry.	K. Eleftheriadis elefther@ipta.demokritos.gr
SMPS+ Thermodenuder	Demokritos	Continuously	7-400 nm (TSI) Temperatures: 30, 120, and 250 °C.	K. Eleftheriadis elefther@ipta.demokritos.gr
OPC	Demokritos	Continuously	0.25-2.5 μm (Grimm)	K. Eleftheriadis elefther@ipta.demokritos.gr
EC/OC	Demokritos	Continuously	No quartz filter sampling needed for EC/OC. (sample every 3 hours)	K. Eleftheriadis elefther@ipta.demokritos.gr
Aethalometer	Demokritos	Continuously	PM2.5.	K. Eleftheriadis elefther@ipta.demokritos.gr
ACSM	Crete	Continuously	PM1, time resolution of 35min, flow rate 1.36 cc/sec 53.34 cm x 49.53 cm x 86.36 cm , 64 kg Power 300W	Mihalopoulos Nikos mihalo@uoc.gr
PILS	Crete	Continuously	flow rate IC 1ml/min MSA, air flow 16.7lt/min for cations	Mihalopoulos Nikos mihalo@uoc.gr
O3 Analyzer	PERPA	Continuously		PERPA

European Union
European Social Fund
OPERATIONAL PROGRAMME
EDUCATION AND LIFELONG LEARNING
investing in knowledge society
MINISTRY OF EDUCATION & RELIGIOUS AFFAIRS
MANAGING AUTHORITY
NSRF 2007-2013
EUROPEAN SOCIAL FUND
Co-financed by Greece and the European Union

NOx Analyzer	PERPA	Continuously		PERPA
SO2 Analyzer	PERPA	Continuously		PERPA
Meteorological Data	Demokritos	Continuously	Wind Speed/Direction, Temperature, RH	K. Eleftheriadis eleftheр@ipta.demokritos.gr

2. Athens (NOA Thisseio)

Instrument	Operating Group	Dates	Notes	Person Responsible for Data (Name – email)
PM10 & PM2.5 Sampler	NOA	Continuously	4 every 24 hours. (quartz for ions and OC/EC) Times: 0:00-6:00, 6:00-12:00, 12:00-18:00, 18:00-24:00. Location: roof or next to the room	Gerasopoulos Evangelos egera@noa.gr
PM2.5 high volume sampler (TISCH)	Patras		1 every 24 hours (quartz for organic speciation) Location: roof	Spyros Pandis spyros@chemeng.upatras.gr
FTIR filters	Patras		4 every 24 hours (quartz) Times: 0:00-6:00, 6:00-12:00, 12:00-18:00, 18:00-24:00. Location: room	Spyros Pandis spyros@chemeng.upatras.gr
PTRMS	Patras	Continuously	Location: van	Spyros Pandis spyros@chemeng.upatras.gr
HR-AMS + Thermodenuder	Patras	Continuously	Location: van (this is the same Thermodenuder that will be used upstream of SMPS1 – see below for temperatures).	Spyros Pandis spyros@chemeng.upatras.gr
SMPS (with water-based CPC) + Thermodenuder		Continuously	Temperatures: 20, 40, 60, 100, 150, 200, and 300 °C. Location: van	Spyros Pandis spyros@chemeng.upatras.gr
O_3 Analyzer	Patras	Continuously	Location: room	Spyros Pandis spyros@chemeng.upatras.gr
NOx Analyzer	Patras	Continuously	Location: room	Spyros Pandis spyros@chemeng.upatras.gr
CO Analyzer	Patras	Continuously	Location: room	Spyros Pandis spyros@chemeng.upatras.gr

MAAP (with PM2.5 head and drier)	Patras	Continuously	Absorption EC Location: room	Spyros Pandis spyros@chemeng.upatras.gr
CCN-SMPS (with water-based CPC)	Patras	Continuously	Location: room	Spyros Pandis spyros@chemeng.upatras.gr
TEOM	Patras	Continuously	PM2.5 and PM10	Spyros Pandis spyros@chemeng.upatras.gr
HTDMA	Demokritos	Continuously	Growth factors at 85% RH. Dry diameters: ,,,, nm.	George Biskos biskos@aegean.gr
Lidar (EMORAL ESA's Mobile Raman Lidar)	NOA		depolarization – Raman lidar, capable of detecting polar and cross-polar signal at 355nm, total linear polarized signal at 532nm and nitrogen's Raman return at 387nm. Level 1: backscatter signals at 355 and 532 nm, Level 2: backscatter, extinction and depolarization vertical profiles. Location: opening in front of the central building.	Gerasopoulos Evangelos egera@noa.gr
Ceiliometer	NOA		Vaisala CL31, attenuated backscatter coefficient from 70 m up to 7.5 km. Selectable spatial resolution of 5 or 10 m and temporal resolution of 2 s to 120 s. Location: close to the Meteo station.	Gerasopoulos Evangelos egera@noa.gr
Meteorological data	NOA	Continuously	Wind Speed/Direction, Temperature, RH.	Gerasopoulos Evangelos egera@noa.gr

European Union
European Social Fund
OPERATIONAL PROGRAMME
EDUCATION AND LIFELONG LEARNING
investing in knowledge society
MINISTRY OF EDUCATION & RELIGIOUS AFFAIRS
MANAGING AUTHORITY
NSRF 2007-2013
programme for development
EUROPEAN SOCIAL FUND
Co-financed by Greece and the European Union

			Location: 100 m from the station.	

3. Athens (NOA-Penteli)

Instrument	Operating Group	Dates	Notes	Person Responsible for Data (Name – email)
Sampler (PM10 & PM2.5)	NOA	Continuously	2 every 24 hours (PM2,5 and PM10-2,5 quartz) Times: 8:00 and 18:00h	Gerasopoulos Evangelos egera@noa.gr
Nephelometer	NOA	Continuously	(1 wavelength)	Gerasopoulos Evangelos egera@noa.gr
PSAP	NOA	Continuously	(3 wavelengths)	Gerasopoulos Evangelos egera@noa.gr, Mihalopoulos Nikos mihalo@uoc.gr
Meteorological station (actinometric)	NOA	Continuously		Gerasopoulos Evangelos egera@noa.gr

4. Messinia (NEO)

Instrument	Operating Group	Dates	Notes	Person Responsible for Data (Name – email)
Sampler (PM10)	NOA	10/1-10/2	1 every 24 hours (quartz)	Gerasopoulos Evangelos egera@noa.gr
DMPS	Stockholm Uni.	Continuously	dry, PM10	Gerasopoulos Evangelos egera@noa.gr
Soot Photometer	Stockholm Uni.	Continuously	1w, PM10	Gerasopoulos Evangelos egera@noa.gr
O3 Analyzer	NOA/Crete	Continuously		Gerasopoulos Evangelos egera@noa.gr

5. Thessaloniki (Eptapyrgio)

Instrument	Operating Group	Dates	Notes	Person Responsible for Data (Name – email)
SMPS	Aegean	Continuously		George Biskos biskos@aegean.gr
O3 Analyzer	Municipality Thess.	Permanent		Municipality Thess.
NOx Analyzer	Municipality Thess.	Permanent		Municipality Thess.
SO2 Analyzer	Municipality Thess.	Permanent		Municipality Thess.

6. Patras (Station at the center)

Instrument	Operating Group	Dates	Notes	Person Responsible for Data (Name – email)
PM2.5 Sampler (SASS)	Patras	Continuously	2 quartz + 2 PTFE filters per 24 hours	Spyros Pandis spyros@chemeng.upatras.gr
SMPS (butanol-based CPC)	Patras	Continuously		Spyros Pandis spyros@chemeng.upatras.gr
Nephelometer	Patras	Continuously		Spyros Pandis spyros@chemeng.upatras.gr

7. Crete (Finokalia)

Instrument	Operating Group	Dates	Notes	Person Responsible for Data (Name – email)
PM1 & PM10 Sampler	Crete	Continuously	1 every 24 hours for PM10, twice a week for PM1	Mihalopoulos Nikos mihalo@uoc.gr
Nephelometer	Crete	Continuously		Mihalopoulos Nikos mihalo@uoc.gr
SMPS (butanol-based CPC)	Crete	Continuously		Mihalopoulos Nikos mihalo@uoc.gr
OPC	Aegean	Continuously	0.75-25 μm (Grimm)	Mihalopoulos Nikos mihalo@uoc.gr
Aethalometer	Crete	Continuously		Mihalopoulos Nikos mihalo@uoc.gr
O3 Analyzer	Crete	Continuously		Mihalopoulos Nikos mihalo@uoc.gr
NOx Analyzer	Crete	Continuously		Mihalopoulos Nikos mihalo@uoc.gr

European Union
European Social Fund
OPERATIONAL PROGRAMME
EDUCATION AND LIFELONG LEARNING
investing in knowledge society
MINISTRY OF EDUCATION & RELIGIOUS AFFAIRS
MANAGING AUTHORITY
NSRF 2007-2013
programme for development
EUROPEAN SOCIAL FUND
Co-financed by Greece and the European Union

8. Crete (Station at Heraclion city center)

Instrument	Operating Group	Dates	Notes	Person Responsible for Data (Name – email)
TSP, PM sampler	ECPL	Continuously	2 every 24 hours (quartz) Times: 8:00 and 18:00. (20 m above ground)	Mihalopoulos Nikos mihalo@uoc.gr
Nephelometer	ECPL	Continuously		Mihalopoulos Nikos mihalo@uoc.gr

PM Samplers

Instrument	Operating Group	Dates	Notes	Person Responsible for Data (Name – email)
2. Athens (Thisseio)	NOA	PM10 & PM2.5 Sampler	4 every 24 hours. (quartz for ions and OC/EC) Times: 0:00-6:00, 6:00-12:00, 12:00-18:00, 18:00-24:00. Location: roof or next to the room	Gerasopoulos Evangelos egera@noa.gr
	Patras	FTIR filters	4 every 24 hours (quartz) Times: 0:00-6:00, 6:00-12:00, 12:00-18:00, 18:00-24:00. Location: room	Spyros Pandis spyros@chemeng.upatras.gr
3. Athens (Penteli)	NOA	Sampler (PM10 & PM2.5)	2 every 24 hours (PM2,5 and PM10-2,5 quartz) Times: 8:00 and 18:00	Gerasopoulos Evangelos egera@noa.gr
4. Messinia Sampler	NOA	(PM10)	1 every 24 hours (quartz)	Gerasopoulos Evangelos egera@noa.gr
6. Patras (Center)	Patras	PM2.5 Sampler (SASS)	2 quartz + 2 PTFE filters per 24 hours	Spyros Pandis spyros@chemeng.upatras.gr
7. Crete (Finokalia)	Crete	PM1 & PM10 Sampler	1 every 24 hours for PM10, twice a week for PM1	Mihalopoulos Nikos mihalo@uoc.gr
8. Crete (Heraklion city center)	ECPL	Specify type of sampler	2 every 24 hours (quartz) Times: 8:00 and 18:00. (20 m above ground)	Mihalopoulos Nikos mihalo@uoc.gr

European Union
European Social Fund
OPERATIONAL PROGRAMME
EDUCATION AND LIFELONG LEARNING
investing in knowledge society
MINISTRY OF EDUCATION & RELIGIOUS AFFAIRS
MANAGING AUTHORITY
NSRF 2007-2013
EUROPEAN SOCIAL FUND
Co-financed by Greece and the European Union

Table 3: Models and Spatial Data employed in the THALES program

Model	Operating Group	Dates	Notes	Person Responsible for Data (Name – email)
Emissions Inventory	Univ. of the Aegean Univ. of Patras	June 5, 2012 to July 31 2012	Emissions inventory of anthropogenic and biogenic sources. Final inventory is produced by a combination of data sources. Anthropogenic emissions are from the GEMS and EC/OC inventories. Biogenic emissions are from the MARINE model (sea salt emissions), the MEGAN model (plant canopy emissions) and the FIRES (active fires inventory). The inventory includes gridded (master grid) emissions over Europe of 36 km ×36 km spatial resolution. Nested emissions are of 9 km×9 km resolution over the Greek region. Temporal resolution is 1 hour. The final inventory consists of gas species that are compatible to SAPRC99 mechanism and	Spyros Pandis spyros@chemeng.upatras.gr

European Union
European Social Fund
OPERATIONAL PROGRAMME
EDUCATION AND LIFELONG LEARNING
investing in knowledge society
MINISTRY OF EDUCATION & RELIGIOUS AFFAIRS
MANAGING AUTHORITY
NSRF 2007-2013
EUROPEAN SOCIAL FUND
Co-financed by Greece and the European Union

			particulate species including sulfate, nitrate, ammonium, sodium, chloride, potassium, calcium, elemental carbon, and primary organics.	
WRF	Univ. of Patras	June 5, 2012 to July 31 2012	Meteorological model. WRF is driven by static geographical data and dynamic meteorological data (near real-time and historical data generated by the Global Forecast System (1˚×1˚). 27 vertical sigma-p layers up to 0.1 bars were used. The WRF run were reinitialized every 3 days. Output of the model includes horizontal wind components, vertical diffusivity, temperature, pressure, water vapor, clouds and rainfall. Spatial resolution is 36 km×36 km.	Spyros Pandis spyros@chemeng.upatras.gr
PMCAMx	Univ. of Patras	June 5, 2012 to July 31 2012	CTM model that provides the chemically- and size- resolved aerosol distributions and vertical mass profiles. PMCAMx describes the processes of horizontal and vertical advection, horizontal and vertical dispersion, wet and dry deposition, and gas-phase chemistry. It dynamically tracks the size evolution of the aerosol mass across 10 size sections spanning from 40 nm to 40 μm. The	Spyros Pandis spyros@chemeng.upatras.gr

European Union
European Social Fund
OPERATIONAL PROGRAMME
EDUCATION AND LIFELONG LEARNING
investing in knowledge society
MINISTRY OF EDUCATION & RELIGIOUS AFFAIRS
MANAGING AUTHORITY
NSRF 2007-2013
EUROPEAN SOCIAL FUND
Co-financed by Greece and the European Union

			aerosol species modeled include sulfate, nitrate, ammonium, sodium, chloride, potassium, calcium, magnesium, elemental carbon, primary and secondary organics. The chemical mechanism used in the gas-phase chemistry is based on the SAPRC99 mechanism.	
AtmOptC	Univ. of the Aegean	June 5, 2012 to July 31 2012	Aerosol optical properties model. Post-processor of the PMCAMx data. Calculations performed for an internal mixture of either homogeneous spheres or core-shell spheres. The model output includes estimates the vertical distributions of aerosol scattering and absorption coefficients, the asymmetry parameter, and the aerosol AOD. Optical properties are calculated for 13 distinct wavelengths ranging from 0.2 to 4 μm. Resolution is 36 km×36 km over the European region.	Christos Matsoukas matsoukas@aegean.gr Christodoulos Pilinis xpil@aegean.gr
FORTH radiation transfer model with	Univ. of the Aegean	2007 - 2009	The FORTH radiation transfer model works with the delta-Eddington two-stream algorithm. Cloud data were provided by ISCCP, aerosol	Christos Matsoukas matsoukas@aegean.gr

CALIOP aerosol vertical profiles			data by CALIOP and a variety of ancillary input by reanalyses. The output includes: Radiation fluxes at the top of the atmosphere, inside the atmospheric column, at the surface Aerosol radiative effect at the top of the atmosphere, inside the atmospheric column, at the surface Heating rates and the aerosol effect in the atmospheric column Global coverage, spatial resolution: 1º×1º, temporal resolution: monthly	
FORTH radiation transfer model with aerosol vertical profiles from AtmOpt	Univ. of the Aegean	June 5, 2012 to July 31 2012	The FORTH radiation transfer model works with the delta-Eddington two-stream algorithm. Aerosol data were provided by AtmOptC and atmospheric state data by WRF. The output includes: Radiation fluxes at the top of the atmosphere, inside the atmospheric column, at the surface	Christos Matsoukas matsoukas@aegean.gr

			Aerosol radiative effect at the top of the atmosphere, inside the atmospheric column, at the surface Heating rates and the aerosol effect in the atmospheric column European coverage, spatial resolution: 36 km×36 km, temporal resolution: hourly	
MODIS-Terra	Univ. of Ioannina	March 1, 2000 to January 20, 2014	Aerosol optical depth at 550nm, global coverage, spatial resolution: 1° x 1° and 10km x 10km, temporal resolution: daily Aerosol fine mode fraction, global coverage, spatial resolution: 1° x 1° and 10km x 10km, temporal resolution: daily Aerosol Ångström Exponent, global coverage, spatial resolution: 1° x 1° and 10km x 10km, temporal resolution: daily	Nikos Hatzianastassiou nhatzian@cc.uoi.gr

MODIS-Aqua	Univ. of Ioannina	July 4, 2002 to September 2, 2013	Aerosol optical depth at 550nm, global coverage, spatial resolution: 1° x 1° and 10km x 10km, temporal resolution: daily Aerosol fine mode fraction, global coverage, spatial resolution: 1° x 1° and 10km x 10km, temporal resolution: daily Aerosol Ångström Exponent, global coverage, spatial resolution: 1° x 1° and 10km x 10km, temporal resolution: daily	Nikos Hatzianastassiou nhatzian@cc.uoi.gr
OMI-Aura	Univ. of Ioannina	October 1, 2004 to December 14, 2013	Aerosol optical depth at 500nm, global coverage, spatial resolution: 1° x 1° and 13km x 24km, temporal resolution: daily Aerosol optical depth at 388nm, global coverage, spatial resolution: 1° x 1° and 13km x 24km, temporal resolution: daily Aerosol absorption optical depth at 500nm, global coverage, spatial resolution: 1° x 1° and 13km x 24km, temporal resolution: daily	Nikos Hatzianastassiou nhatzian@cc.uoi.gr

European Union
European Social Fund
OPERATIONAL PROGRAMME
EDUCATION AND LIFELONG LEARNING
investing in knowledge society
MINISTRY OF EDUCATION & RELIGIOUS AFFAIRS
MANAGING AUTHORITY
NSRF 2007-2013
EUROPEAN SOCIAL FUND
Co-financed by Greece and the European Union

			Aerosol absorption optical depth at 388nm, global coverage, spatial resolution: 1° x 1° and 13km x 24km, temporal resolution: daily Aerosol single scattering albedo, global coverage, spatial resolution: 1° x 1° and 13km x 24km, temporal resolution: daily Aerosol Index, global coverage, spatial resolution: 1° x 1° and 13km x 24km, temporal resolution: daily	
CALIOP	Univ. of Ioannina	July 1, 2006 to October 31, 2011	Aerosol optical depth at 532nm, global coverage, spatial resolution: 1° x 1°, temporal resolution: daily	Nikos Hatzianastassiou nhatzian@cc.uoi.gr
AERONET	Univ. of Ioannina	Variable depending on the station	Aerosol optical depth at 500nm, for 7 stations in Greece (Athens, Thessaloniki, Heraklion, Epanomi, Sindos, Xanthi, Kolimbari), temporal resolution: daily	Nikos Hatzianastassiou nhatzian@cc.uoi.gr

European Union
European Social Fund
OPERATIONAL PROGRAMME
EDUCATION AND LIFELONG LEARNING
investing in knowledge society
MINISTRY OF EDUCATION & RELIGIOUS AFFAIRS
MANAGING AUTHORITY
NSRF 2007-2013
EUROPEAN SOCIAL FUND
Co-financed by Greece and the European Union